Research for Development

Enkui Duan · Mian Long *Editors*

Life Science in Space: Experiments on Board the SJ-10 Recoverable Satellite

Science Press Beijing

Springer

Research for Development

The series Research for Development serves as a vehicle for the presentation and dissemination of complex research and multidisciplinary projects. The published work is dedicated to fostering a high degree of innovation and to the sophisticated demonstration of new techniques or methods.

The aim of the Research for Development series is to promote well-balanced sustainable growth. This might take the form of measurable social and economic outcomes, in addition to environmental benefits, or improved efficiency in the use of resources; it might also involve an original mix of intervention schemes.

Research for Development focuses on the following topics and disciplines:

Urban regeneration and infrastructure, Info-mobility, transport, and logistics, Environment and the land, Cultural heritage and landscape, Energy, Innovation in processes and technologies, Applications of chemistry, materials, and nanotechnologies, Material science and biotechnology solutions, Physics results and related applications and aerospace, Ongoing training and continuing education.

Fondazione Politecnico di Milano collaborates as a special co-partner in this series by suggesting themes and evaluating proposals for new volumes. Research for Development addresses researchers, advanced graduate students, and policy and decision-makers around the world in government, industry, and civil society.

THE SERIES IS INDEXED IN SCOPUS

More information about this series at http://www.springer.com/series/13084

Enkui Duan · Mian Long
Editors

Life Science in Space: Experiments on Board the SJ-10 Recoverable Satellite

Science Press
Beijing

Springer

Editors
Enkui Duan
Institute of Zoology
Chinese Academy of Sciences
Beijing, China

Mian Long
Institute of Mechanics
Chinese Academy of Sciences
Beijing, China

ISSN 2198-7300 ISSN 2198-7319 (electronic)
Research for Development
ISBN 978-981-13-6324-5 ISBN 978-981-13-6325-2 (eBook)
https://doi.org/10.1007/978-981-13-6325-2

Jointly published with Science Press
The print edition is not for sale in China. Customers from China please order the print book from: Science Press.
ISBN of the China edition: 978-7-03-062078-1

This Springer imprint is published by the registered company Springer Nature Singapore Pte Ltd.
The registered company address is: 152 Beach Road, #21-01/04 Gateway East, Singapore 189721, Singapore

The two books “Physical Science under Microgravity: Experiments on Board the SJ-10 Recoverable Satellite” and “Life Science in Space: Experiments on Board the SJ-10 Recoverable Satellite” are organized under the guidance of the Chief Scientist of SJ-10 satellite mission, Professor Wenrui Hu.

Foreword

The SJ-10 recoverable microgravity experimental satellite, the 24th recoverable satellite of China, was successfully launched on April 6, 2016 completely for the experiments of microgravity physics and space biology. The recoverable capsule was landed safely on the ground after 12 days of the launch and the experiments of cool combustion and fluid physics onboard the un-recoverable capsule continued for another week afterward. Scientific purpose of the SJ-10 mission is to promote the scientific research in the space microgravity environment by operating the satellite at lower earth orbit. There are totally 28 space experiments, including 18 experiments in the field of microgravity physics (microgravity fluid physics 6, microgravity combustion 4, and space materials science 8) and 10 experiments in the field of space biology (radiation biology 3, gravitational biology 3, and space biotechnology 4). The SJ-10 Mission was arranged as one of the four scientific satellites by the space science program of the Chinese Academy of Sciences in the "12th Five-Years-Plan" period (2010–2015).

Microgravity experiments for a long period, which could be performed only in the space infrastructures such as space station, space shuttle, and satellite, are essential for the development of microgravity science and space life science. The recoverable satellite is a useful and efficient tool for space experiments in the microgravity environment, and such kind of satellites have been launched first for remote sensing observation for many years, and then for microgravity experiments since the late 1980s in China. Many space experiments have been also arranged in China Manned Space Engineering Program consisting of the spaceships Shenzhou mission since the late 1990s, the space laboratory mission at the present time, and then the space station mission in the near future.

China National Space Administration (CNSA) organized an expert group for the microgravity research in the early twenty-first century, and seven panels were established under the expert group: microgravity fluid physics, microgravity combustion, space material sciences, space fundamental physics, radiation biology, gravitational biology, and space biotechnology. The program of SJ-8 recoverable satellite launched on September 9, 2006 was arranged jointly by CNSA and Chinese Academy of Sciences (CAS); the recoverable capsule was used for the

breeding experiments as the main mission and the un-recoverable capsule was used for the microgravity research (The results of microgravity research of SJ-8 satellite were published in a special issue of Microgravity Science and Technology, vol. 20, number 2, August 2008). The program of a microgravity satellite was originally organized by CNSA in the middle of 2000s. Ten experiments of microgravity science and ten experiments of space life science were selected from more than 200 applications in late 2004 and early 2005. The mission proposals of space experiments (including two cooperation experiments in collaboration with French Space Agency and one with Europe Space Agency) were reviewed in October 2005. The engineering proposal of satellite platform was reviewed in May 2006 by CNSA. Then, the demonstration working group on "recoverable satellite of scientific experiments for space environment utilization" was formally organized, and the mission was determined as SJ-10. Unfortunately, the demonstrative phase was stopped after 1 year due to the reform of CNSA, and re-started when the government of China determined to move the national management of scientific satellite from CNSA to CAS in 2011. The re-started demonstration phase was completed at the end of 2012, and the engineering phase of program SJ-10 started since the beginning of 2013. According to the schedule, the satellites were purposed to be launched at the end of 2015, but it was delayed for 4 months.

A grant for research on the space experiments of SJ-10 missions was founded jointly by National Nature Science Foundation of China (NSFC) the CAS in 2017. This grant supports the analysis of the space experiments, and the results are summarized mainly in the present two books: Physical Science under Microgravity: Experiments on Board the SJ-10 Recoverable Satellite edited by Professors W. R. Hu and Q. Kang; and Life Science in Space: Experiments on Board the SJ-10 Recoverable Satellite edited by Professors E. K. Duan and M. Long. The first book contains the results of fluid physics, combustion, and materials science, and the second book consists of the radiation biology, gravitational biology, and biological technology and biological facility studies.

I am grateful to the authors of these books for their respective contributions, to the book editors and mission organizers for their outstanding works, to Drs. Jian Li and June Tang of Springer and Y. F. Niu of Science Press of Beijing for their kind assistance in publishing the books. Many thanks are due to Chinese Academy of Sciences, National Space Center of CAS and National Nature Science Foundation of China for their great supports.

Beijing, China

Wen-Rui Hu
Chief scientist of SJ-10 mission

Contents

Introduction to Results of Life Sciences from SJ-10 Recoverable Satellite

Enkui Duan and Mian Long

Abstract Space life science and biotechnology is to conduct the biological and biotechnological experiments of various species in space by utilizing the space hardware in the space vehicle, in which the effect of microgravity and space radiation on biological activities is a crucial issue in this field. The experiments conducted in a Shijian-10 (shortly, SJ-10) recoverable satellite mission are segregated into two groups. One is physical science under microgravity, consisting of eleven experiments. Another is space life science, being composed of ten experiments. In space life science, three categories are defined as radiation biology (Chaps. 3, 4 and 5), gravitational biology (Chaps. 6, 7 and 8), and biotechnology (Chaps. 9, 10, 11 and 12). Meanwhile, the system design and flight results of the SJ-10 satellite (Chap. 2) and the related techniques, space hardware and ground-based devices are described (Chaps. 13 and 14). In this chapter, the summaries of this book including the introduction to SJ-10 recoverable satellite and ten space life science projects as well as the scientific issues and Chinese scientific advances in the field of radiation biology, gravitational biology and space biotechnology in the past 15 years are addressed briefly.

1 Introduction to SJ-10 Recoverable Satellite

Specialized microgravity and radiation in space induce numerous alterations in physical and biological processes such as the lack of buoyant convection and the boss loss. While a body of evidences has been obtained from those ground-based studies using space environment stimulating platforms, quite a few investigations have been conducted in real space. To further elucidate the underlying mechanisms in the above

E. Duan (✉)
Institute of Zoology, Chinese Academy of Sciences, Beijing 100101, China
e-mail: duane@ioz.ac.cn

M. Long (✉)
Institute of Mechanics, Chinese Academy of Sciences, Beijing 100190, China
e-mail: mlong@imech.ac.cn

E. Duan and M. Long (eds.), *Life Science in Space: Experiments on Board the SJ-10 Recoverable Satellite*, Research for Development,
https://doi.org/10.1007/978-981-13-6325-2_1

processes, a Shijian-10 (shortly, SJ-10) recoverable satellite is designed to conduct the experiments in space and collect the relevant data directly from the mission. At the end of December, 2012, the SJ-10 satellite project has been approved by Chinese Academy of Sciences (CAS). After 40-month technical and scientific preparations, the satellite is launched on April 6, 2016 and recovered back to the Earth on April 18, 2016 successfully. All the samples and specimen have been sent immediately back to the respective laboratories for further studies. This SJ-10 satellite project consists of six systems of Satellite, Rocket Vehicle, Launching, Monitoring and Recovery, Ground Supporting, and Scientific Application. Prof. Wenrui Hu from Institute of Mechanics, CAS serves as the chief scientist, Prof. Bochang Tang from China Academy of Space Technology (CAST) serves as the chief engineer, and Prof. Hejun Yin from the Headquarter of CAS serves as the chief commander and Profs. Ji Wu and Xin Meng from National Space Science Center, CAS serve as the executive and deputy commanders, respectively, of the SJ-10 satellite.

2 Introduction to Ten Space Life Science Projects

Space life science and biotechnology is to conduct the biological and biotechnological experiments of various species in space by utilizing the space hardware in the space vehicle, in which the effect of microgravity and space radiation on biological activities is a crucial issue in this field. The experiments conducted in SJ-10 satellite mission are segregated into two groups. One is physical science under microgravity, consisting of eleven experiments. Another is space life science, being composed of ten experiments. In space life science, three categories are defined as radiation biology, gravitational biology, and biotechnology. In the category of radiation biology, three scientific issues are intended to be addressed in systems biology in space radiation (Dr. Yeqing Sun from Dalian Maritime University), effect of space environment on genome stability (Dr. Haiying Hang from Institute of Biophysics, CAS), and effect of space environment on silkworm development and gene mutation (Dr. Yongping Huang from Shanghai Institutes for Biological Sciences, CAS). In the category of gravitational biology, three issues are focused on effect of gravity on plant growth at molecular level (Dr. Weiming Cai from Shanghai Institutes for Biological Sciences, CAS), flowering in space (Dr. Huiqiong Zheng from Shanghai Institutes for Biological Sciences, CAS), and biomechanics of mass transportation on cell-cell interactions under microgravity (Dr. Mian Long from Institute of Mechanics, CAS). In the category of space biotechnology, four projects are designed to elucidate the maintaining and directed differentiation of hematopoietic stem cells under microgravity (Dr. Yong Zhao from Institute of Zoology, CAS), three-dimensional cell culture and tissue restoration of neural stem cells under microgravity (Dr. Jianwu Dai from Institute of Genetics and Developmental Biology, CAS), mouse early embryo development under microgravity (Dr. Enkui Duan from Institute of Zoology, CAS), and osteogenic differentiation of human mesenchymal stem cells under microgravity (Dr. Jinfu Wang from Zhejiang University). Meanwhile, the related techniques,

space hardware and ground-based devices are developed by Shanghai Institute of Technical Physics, CAS (Dr. Tao Zhang), National Space Science Center, CAS (Dr. Yuanda Jiang), and Institute of Mechanics, CAS (Dr. Shujin Sun), respectively. All the payloads work well in space to guarantee the success of the SJ-10 mission.

3 Scientific Issues Addressed

The aforementioned projects attempt, from the viewpoint of space life science and biotechnology, to unravel the sensing and transduction mechanisms of various species under microgravity and space radiation and to develop the novel techniques in stem cell differentiation and embryonic development. Scientific issues are mainly focused on understanding the effect of space environment on evolution of terrestrial life and on the impact of space environment on physiological homeostasis of organisms. Three specific aims are: (1) How do the terrestrial lives sense microgravity and/or space radiation signaling and what are the underlying transduction pathways? (2) How do the organisms adapt themselves to the microgravity and/or space radiation environment? (3) How are the microgravity and/or space radiation resources utilized to promote the perspective of space life science and the development of space biotechnology? The outcomes of these projects would provide the fundamental understandings, propose new concepts, new ideas, and new methodology, and establish the integrated platforms in ground- or space-based studies for space life science and biotechnology. Expected results are to develop numerical simulation platforms and biologically-specific techniques and to further the understandings in sensation and transduction of microgravity and space radiation signaling for plant or animal cells or in tissue histogenesis. The related issues and aims are briefed individually as below (Hu et al. 2014).

3.1 Radiation Biology

The first project in this category, entitled *Molecular biology mechanism of space radiation mutagenesis*, aims (i) to analyze the sequence information of genome methylation and transposon change caused by space radiation and explore the molecular mechanisms of space radiation induced genomic instability; and (ii) to study the proteomics profiles of model organisms caused by different radiation qualities, mine the molecular mechanisms of functional proteins, and to establish the biological systems that evaluate radiation qualities (Wang et al. 2008). Plant and animal model organisms are located at three distinct radiation environments inside the satellite. By monitoring three tissue equivalent detector devices, the space radiation parameters such as absorbed dose, absorbed dose rate, linear energy transfer value, and dose equivalent are detected. The biological materials irradiated by different kinds of particles that belong to the same satellite orbit are then harvested and recovered. System

biology analyses such as genome epigenetic scanning and proteomic approaches are conducted to obtain information of biological changes under different radiation qualities and to correlate biological effects with different radiation parameters.

The second project entitled *Roles of space radiation on genomic DNA and its genetic effects*, attempts to elucidate the roles of space radiation on genomic DNA and its genetic effects in the real space environment in two aspects: (i) Space radiation and genomic stability. Genomic stability of wild type and radiation-sensitive mouse cells and fruit flies is investigated in pre- and post-flight or at different time points during the spaceflight. Quantitative parameters of space radiation of genome and its genetic effects are then obtained in the real space environment. (ii) Gene expression profiles and sensitive response genes to space radiation. Gene expression profiles are obtained from the above mouse cells and of fruit flies. Novel and sensitive biological molecules are identified as space radiation markers. This work provides novel information for developing evaluation methods for the risk factors and protection tools against space radiation (Wang et al. 2011; Cui et al. 2010).

The third project, entitled *Effects of space environment on silkworm embryo development and mechanism of mutation*, applies the selected silkworm embryos to pursue the following contents: (i) gene expression pattern of embryo under real space environment; (ii) proteome of silkworm embryo; (iii) mutation discovery and functional analysis; and (iv) embryo development and its characterization. Systematic approaches of the embryo development design and multiple sampling throughout the entire developmental stages are performed under space environment. Multiple platforms of gene expression, proteomics, and functional genomics, are employed to unravel the development characteristics of silkworm in space and to find out the possible mutations through molecular approaches (Miao et al. 2005).

3.2 Gravitational Biology

The first project in this category, entitled *Biological effects and the signal transduction of microgravity stimulation in plants*, focuses on elucidating the effects of microgravity (weightless) environment in space on plant growth and the molecular mechanisms underlined in two specific aims: (i) whether plant's sensation of the weight loss is also mediated by statoliths or other mechanisms; and (ii) whether there are any differences in transduction cascades between weight loss and gravitropic signaling. The hypothesis that the rigidity of the supporting tissue (i.e., the cell wall in plant) is regulated by microgravity is tested to understand how space microgravity affects the rigidity of plant cell wall and the metabolism of plant cell wall, which in turn manipulates the growth of plants (Hu et al. 2005; Cui et al. 2005).

The second project, entitled *Biomechanics of mass transport of cell interactions under microgravity*, attempts (i) to develop a novel space cell culture hardware consisting of precisely controlled flow chamber and gas exchange system and to investigate the mass transport mechanisms in cell growth and cell-cell interactions under microgravity; and (ii) to distinguish the direct responses of cells from those indirect

responses via the varied mass transport conditions induced by gravity changes. New data sets on the metabolism, proliferation, apoptosis, differentiation, and cytoskeleton of osteoblasts and mesenchymal stem cells are collected under well-defined mass transfer. This work provides an insight into quantifying the direct cellular responses in space, revealing the effects of gravity on cell-cell interactions, elucidating the mechanisms of cell growth and differentiation in space, and overcoming the methodological bottlenecks of space cell biology studies (Sun et al. 2008; Long et al. 2011; Li et al. 2018).

The third project, entitled *Photoperiod-controlling flowering of Arabidopsis and rice in microgravity*, aims at deciphering how space microgravity regulates the transportation of flowering signals from leaf to shoot apex at molecular level. Using transgenic *Arabidopsis thaliana* and rice plants (expressing FT or Hd 3a gene with the reporter genes GFP or GUS), living fluorescence imaging technique is developed to determine the induction of FT and Hd3a gene expression and floral initiation in shoot apex under long-day and short-day photoperiod condition under space microgravity or in normal gravity on the ground. This work sheds light on regulating mechanisms of photoperiod controlled flowering in both *Arabidopsis thaliana* and rice by microgravity (Zheng and Staehelin 2011; Wei et al. 2010).

3.3 Space Biotechnology

The first two projects, entitled *Three-dimensional cell culture of neural and hematopoietic stem cells in space*, share the same hardware in SJ-10 satellite. They aim to understand whether microgravity environment is suitable for the self- renewal and differentiation of hematopoietic or neural stem cells. Three-dimensional cell culture of hematopoietic stem cells and neural stem cells is conducted in space. With microscopic detection, image transmission, and gene/protein analysis through the recovered samples, the effects of microgravity on the self-renewal/differentiation of two types of stem cells are tested to reveal the characteristics of growth and differentiation of these 3D cultured stem cells under microgravity. The outcomes are crucial in regenerative medicine for treatment of various blood diseases and neural injury, respectively (Cui et al. 2008; Chen et al. 2007).

The third project, entitled *Development of mouse early embryos in space*, attempts (i) to determine whether early mammalian embryo can develop in outer space or not; (ii) to observe the developmental process during space flight by transmitted images of the embryo from the satellite to the ground; and (iii) to investigate a potential molecular mechanism of the early embryo development in space. Using mouse early embryos, the 2-cell or 4-cell stage mouse embryos are cultured in a specialized hardware and the morphological alterations at various developmental stages (4-cell, 8-cell, early morula, compacted morula, blastocyst and hatched blastocyst) of early embryos are monitored by optical microscopy in space. Molecular mechanisms are further tested using recovered fixed embryos. This work furthers the understanding

in the beginning of mammalian life and the entire process of reproduction in space (Lei et al. 2011; Ning et al. 2015).

The fourth project, entitled *Potential and molecular mechanism of osteogenic differentiation from human bone mesenchymal stem cells*, aims to examine the potential mechanisms of osteogenic differentiation from human bone mesenchymal stem cells (hBMSCs) in space microgravity in the three aspects: (i) to develop a specialized space hardware and techniques for the osteogenic differentiation of hBMSCs under space microgravity; (ii) to elucidate the capacity of the osteogenic differentiation potential of hBMSCs in space and to identify the effects of space microgravity on osteogenic differentiation of hBMSCs; and (iii) to analyze the underlying signaling pathways and the protein expression in the osteogenic differentiation of hBMSCs in space. This work provides an insight into how space microgravity affects the osteogenic differentiation of hBMSCs through specific signaling pathways and what the molecular mechanisms and the roles of these key molecules are in osteogenic differentiation of hBMSCs under space microgravity (Pan et al. 2008; Shi et al. 2010).

4 Summaries of This Book

This book consists of fourteen chapters, dealing with both scientific and technical advances from SJ-10 satellite mission and also summarizing the recent progresses in the related fields from the worldwide community of space life sciences and biotechnology. Briefly, the book attempts to address the key issues such as (1) how space radiation regulates the biological activities and effects of model organisms (mammalian cells, *Drosophila*, *C. elegans* and silkworm), (2) how space microgravity defines the biological responses and flowering mechanisms of higher plants (*Oryza sativa*, *Arabidopsis thaliana*), (3) what the biomechanical principles of mass transfer under microgravity are in the cell growth (endothelial cells and mesenchymal stem cells), (4) how microgravity governs the early embryonic development of mammalian animal (murine), and (5) whether microgravity environment is able to promote the technologies of directed differentiation and three-dimensional growth of stem cells (hemopoietic, neural, and mesenchymal). Specifically, chapter "Introduction to Results of Life Sciences from SJ-10 Recoverable Satellite" introduces the overview of space life sciences and biotechnology in SJ-10 recoverable satellite. Chapter "System Design and Flight Results of China SJ-10 Recoverable Microgravity Experimental Satellite" introduces the system design and flight performance of SJ-10 satellite. Chapters "Space Radiation Systems Biology Research in SJ-10 Satellite" to "Effects of the Space Environment on Silkworm Development Time" explore space radiation effects. Chapters "Plant Adaptation to Microgravity Environment and Growth of Plant Cells in Altered Gravity Conditions" to "Flowering of Arabidopsis and Rice in Space" exploit gravitational biology effects. Chapters "The Maintaining and Directed Differentiation of Hematopoietic Stem Cells Under Microgravity" to "Effects of Space Microgravity on the Trans-differentiation Between Osteogenesis and Adipogenesis of Human Marrow-Derived Mesenchymal Stem Cells" decipher

space biotechnology. Chapters "Facilities and Techniques of Space Life Science" and "Study on Bone Marrow Box, Radiation Gene Box and Integrated Electrical Control Boxes" elaborate the related techniques and hardware. Together with informative protocols, procedures, figures/tables, and colorful images, this book could serve as the reference for senior undergraduates and graduates in space life sciences and biotechnology, or help to the scientists, scholars, engineers, administrative officers, and enthusiast in the related fields. The contents of this book would provide the space-based data in understanding the life activities and growth mechanisms under microgravity and space radiation and promote the technical bases in solving the bottleneck issues in experimental study of space life science and technical development of biotechnology.

5 Acknowledgements to All the Contributors

The authors are grateful for all the individuals and institutions to implement the SJ-10 recoverable satellite. They are (but not limited to) Prof. Hejun Yin from Headquarter of CAS and Prof. Ji Wu from National Space Science Center, CAS for their leaderships in this Space Science Strategic Project, CAS, Prof. Wenrui Hu as the chief scientist and Prof. Bochang Tang as the chief engineer, Prof. Xin Meng as the deputy commander, and Profs. Qi Kang and Chengguang Huang as the chief engineer and the commander of Scientific Application system, respectively. The authors also acknowledge all the colleagues, experts, engineers, administrators, and participants from the six systems of Satellite, Rocket Vehicle, Launching, Monitoring and Recovery, Ground Supporting, and Scientific Application for the SJ-10 satellite mission.

The authors are grateful to the substantial contributions from Drs. Xiaohua Lei (Institute of Zoology, CAS) and Shujin Sun (Institute of Mechanics, CAS) for technical editing.

All the ten SJ-10 space life science projects are supported by the Strategic Priority Research Program of the Chinese Academy of Sciences (Grant No. XDA04020000) and United funding from National Natural Science Foundation of China and Chinese Academy of Sciences.

References

Chen B, Lin H, Wang J et al (2007) Homogeneous osteogenesis and bone regeneration by demineralized bone matrix loading with bone morphogenetic protein-2. Biomaterials 28(6):1027

Cui D, Neill SJ, Tang Z et al (2005) Gibberellin-regulated XET is differentially induced by auxin in rice leaf sheath bases during gravitropic bending. J Exp Botany 56:1327

Cui M, Huang YL, Zhao Y et al (2008) FoxO3a transcription factor mediates cell death in HIV-1 infected macrophages. J Immunol 180(2):898

Cui P, Lin Q, Xin C et al (2010) Hydroxyurea-induced global transcriptional suppression in mouse ES cells. Carcinogenesis 31(9):1661

Hu WR, Zhao JF, Long M et al (2014) Space program SJ-10 of microgravity research. Microgravity Sci Technol 26(3):159–169

Hu XY, Neill S, Tang ZC et al (2005) Nitric oxide mediates gravitropic bending in soybean roots. Plant Physiol 137:663

Lei XH, Ning LN, Cao YJ et al (2011) NASA-approved rotary bioreactor enhances proliferation of human epidermal stem cells and supports formation of 3D epidermis-like structure. PLoS ONE 6(11):e26603

Li N, Wang CZ, Sun SJ et al (2018) Microgravity-induced alterations of inflammation-related mechanotransduction in endothelial cells on board SJ-10 satellite. Front Physiol 9:1

Long M, Sato M, Lim CT et al (2011) Advances in experiments and modeling in micro- and nanobiomechanics: a mini review. Cell Mol Bioeng 4(3):327

Miao XX, Xu SJ, Li MH et al (2005) Simple sequence repeat-based consensus linkage map of Bombyx mori. Proc Natl Acad Sci USA 102(45):16303–16308

Ning LN, Lei XH, Cao YJ et al (2015) Effect of short-term hypergravity treatment on mouse 2-cell embryo development. Microgravity Sci Technol 27:465–471

Pan Z, Yang J, Guo C et al (2008) Effects of hindlimb unloading on *ex vivo* growth and osteogenic/adipogenic potentials of bone marrow-derived mesenchymal stem cells in rats. Stem Cells Dev 17:795

Shi DY, Peng S, Wang JF (2010) Effects of microgravity modeled by large gradient high magnetic field on the osteogenic initiation of human mesenchymal stem cells. Stem Cell Rev Rep 6:567

Sun SJ, Gao YX, Shu NJ et al (2008) A novel counter sheet-flow sandwich cell culture system to unravel cellular responses in space. Microgravity Sci Tech 20(2):115

Wang W, Gu DP, Zheng Q et al (2008) Leaf proteomic analysis of three rice heritable mutants after seed space flight. Adv Space Res 42:1066

Wang Y, An L, Jiang Y et al (2011) Effects of simulated microgravity on embryonic stem cells. PLoS ONE 6(12):e29214

Wei N, Tan C, Qi B et al (2010) Changes in gravitational forces induce the modification of *Arabidopsis thaliana* silique pedicel positioning. J Exp Bot 61:3874

Zheng HQ, Staehelin LA (2011) Protein storage vacuoles are transformed into lytic vacuoles in root meristematic cells of germinating seedlings by multiple, cell type-specific mechanisms. Plant Physiol 155(4):2023

System Design and Flight Results of China SJ-10 Recoverable Microgravity Experimental Satellite

Huiguang Zhao, Jiawen Qiu and Ying Wang

Abstract China recoverable satellite is a multi-utility, mid-scale satellite with the capability of capsule recovery. Twenty-five recoverable satellites have been developed successfully ever since 1970s. SJ-10 recoverable microgravity experimental satellite (SJ-10 satellite) is the 25th recoverable satellite in China recoverable satellite series and also the first China space microgravity experiment satellite. The main mission of SJ-10 satellites to carry out experimental researches on microgravity science and space life science by means of satellite space flight and capsule recovery. The experiments cover six disciplines, including microgravity fluid physics, microgravity combustion, space materials science, space radiation effect, biological effects of gravity, and space biotechnology. In order to satisfy the requirements of space experiments as well as under the constraints of schedule, funds and others, the new approach of satellite engineering development is promoted and carried out during the process of satellite development. The mission of SJ-10 satellite has been carried out successfully in 2016, and the flight results show that the satellite has absolute advantages in many aspects, such as the ability of recovery, better microgravity level and others. In this chapter, the technical characteristics and mission execution results of the recoverable satellite SJ-10 satellite are summarized. The further development ideas and the improvements of service performances of China recoverable satellite are also discussed briefly.

This chapter is simultaneously published in "Physical Science under Microgravity: Experiments on Board the SJ-10 Recoverable Satellite" and "Life Science in Space: Experiments on Board the SJ-10 Recoverable Satellite". The editors feel that this chapter would be useful to the different audiences of both books to better understand the system design and flight test results of SJ-10 recoverable microgravity experimental satellite.

H. Zhao (✉) · J. Qiu · Y. Wang
China Academy of Space Technology, Beijing, China
e-mail: zhaohuiguang@spacechina.com

E. Duan and M. Long (eds.), *Life Science in Space: Experiments on Board the SJ-10 Recoverable Satellite*, Research for Development,
https://doi.org/10.1007/978-981-13-6325-2_2

Abbreviations

CCSDS	Consultative Committee for Space Data Systems
DC	Direct Current
D-S theory	Dempster-Shafer evidence theory
FIR	Finite Impulse Response
FMEA	Failure Mode and Effects Analysis
g	Gravity
ISO	International Organization for Standardization
ISS	International Space Station
mg	Milli gravity
N	Newton
SA76	The U.S. Standard Atmosphere 1976
SJ-10 satellite	SJ-10 recoverable microgravity experimental satellite
TTC	Tracking, telemetry and command

1 Introduction

China recoverable satellite is a multiutility, mid-scale satellite with the capability of capsule recovery. Twenty-five recoverable satellites have been developed successfully ever since 1970s. SJ-10 satellite is the 25th recoverable satellite in China recoverable satellite series and also the first China space microgravity experiment satellite. The main mission of SJ-10 satellite is to carry out experimental researches on microgravity science and space life science by means of satellite space flight and capsule recovery. The experiments cover six disciplines, including microgravity fluid physics, microgravity combustion, space materials science, space radiation effect, biological effects of gravity, and space biotechnology. This Space Project was included in Strategic Priority Research Program of Chinese Academy of Sciences during the end of twelfth five-year plan. In September 2012, the scientific goals and payload configuration were reviewed and 28 experiments were confirmed. The SJ-10 satellite was approved officially and the engineering development was started at the end of 2012.

To satisfy the requirements of on-orbit experiments and sample recovery, the system design of SJ-10 satellite was upgraded significantly based on previous platform status. The performances such as microgravity level and data services, payload thermal control, remote-control ability for on-orbit experimental operation and prelaunch operation for life samples mounting into satellite, were all improved greatly. Many aspects have gained significant breakthrough, playing a major role in on-orbit experiments of SJ-10 satellite.

In order to be more efficient under the constraints of schedule, funds and others, the new approach of satellite engineering development was promoted and carried out during the process of satellite development. We tailored the ordinary satellite

development process by means of reducing the initial system validations, adding the special and necessary validations, and breaking through the product assurance method of reusing the product to reduce the cost and shorten the development cycle. The product quality was ensured simultaneously. The mission of SJ-10 satellite has been carried out successfully in 2016, and the flight results show that the satellite has absolute advantages in many aspects, such as the ability of recovery, better microgravity level and others.

With the progress of science and technology, the pace of human exploration and utilization of space will be deepened. Future space science experiments, research and application of space environment utilization will have broad prospects. China recoverable satellite can be used as a customized platform with better performances for the research and development of space environmental utilization. This chapter summarizes the technical characteristics and mission execution results of the SJ-10 satellite, and further discusses the development ideas and approaches of the satellite system technology in view of the future applications of scientific experiments and others.

2 Development of Foreign and Domestic Platform

2.1 Brief Introduction

Different from the methods of drop tower, drop tube, sounding rocket and parabolic flight of aircraft, the method of orbital flight of spacecraft can provide high-level and longer time of microgravity environment. The comprehensive environment of microgravity and space radiation provide better space science research conditions. Various types of spacecraft have become important platforms for space science research. At present, the recoverable satellites and manned space stations are the best platforms for scientific application.

As a kind of experimental platform with high-precision and long duration microgravity, the prominent characteristics of the recoverable satellites are as follows: (1) Experimental samples can be returned to the ground; (2) Based on the orbital operation mode of unmanned spacecraft, the microgravity level of the experimental platform is higher, meeting the high microgravity level requirements of many experimental projects. (3) A satellite platform can provide customized service support for on-orbit parallel experiment tasks of multi-experiment projects, and has high adaptability. (4) Satellite engineering has a high cost-effectiveness ratio and is supposed to meet the needs of both fundamental science research and commercial applications at a low cost.

2.2 Development of Foreign Platform

In the international space research field, the main spacecrafts used to support space microgravity science, life science experiments and new technology experiments are the Russian unmanned recoverable satellites and the International Space Station.

After more than 40 years of development, Russia's recoverable satellite spectrum has evolved into two series, namely Foton and Bion series. In many space flights and return missions of the Foton/Foton-M and Bion/Bion-M satellites, a large number of space science experiments from the United States, Europe, Russia, Japan and other countries have been carried out, and fruitful scientific achievements have been obtained.

Foton was developed in 1983–1999, and 12 satellites have been successfully launched. It carried out a large number of experiments in the semiconductor and optical materials, biological engineering, cell biology, molecular structure, crystal culture, and fluid physics.

After 2000, Russia upgraded the Foton satellite and formed a new generation of Foton-M recoverable satellite. The technical upgrade of the Foton satellite platform mainly includes: enhancing the energy supply capability of the payload and the tele-operation capability of on-orbit experimental payloads, and improving the thermal control system. From 2002 to 2015, Foton-M recoverable satellites have carried out 4 missions. The main technical parameters of Foton-M satellite are as follows:

- **Orbit**: circular orbit, altitude 205–550 km;
- **Inclination**: 62.8°–64.9°;
- **Mass**: 6500 kg;
- **Payload mass**: 650 kg (max);
- **Power for load**: 500 W (normal), 700 W (peak);
- **No. of experiments**: 21 (Foton-M3);
- **Microgravity level**: 10^{-5} to 10^{-6} g_0;
- **Landing speed (vertical)**: $\leq$5 m/s;
- **Lifespan**: 12–44 days.

Bion serial recoverable satellite has successfully completed 11 launches from 1973 to 1996. In recent years, Russia upgraded the Bion series satellite platform and formed Bion-M recoverable satellite platform. Major improvements include the enhanced payload return capability and better power supply with solar cells. The Bion-M series completed its first flight in 2013. The main technical parameters of Bion-M satellite are as follows:

- **Orbit**: circular orbit, altitude 205–550 km;
- **Inclination**: 64.9°;
- **Mass**: 6300 kg;
- **Payload mass inside cabin**: 650 kg (max);
- **Payload mass outside**: 250 kg (max);
- **Power for Load**: 550 W;
- **No. of experiments**: 19;

- **Microgravity level**: 10^{-5} to 10^{-6} g_0;
- **Landing speed (vertical)**: $\leq$5 m/s;
- **Lifespan**: 30 days (6 months with solar array).

The International Space Station (ISS) is a large-scale, manned orbital space experiment platform. Its outstanding feature is that it can support space science experimental projects with long-term orbital microgravity environment requirements, and the experiments can be carried out under manned conditions, therefore it is suitable for many highly complex experiments which cannot be automatically controlled. Since ISS establishment and application, a large number of space science experiments and research projects has been completed in many disciplines, including materials, biology, medicine and other new technologies. Relatively inadequate is that, for scientific experiments with very high microgravity levels, it is necessary to develop and install ultra-quiet isolation platforms on the basis of cabins.

2.3 Development of Domestic Platform

At present, there are two types of spacecraft in China, namely the recoverable satellite and Shenzhou manned spacecraft, which can support the development of space microgravity scientific experiments. The Chinese Space Station is under construction, which will gradually provide more and more comprehensive space science experimental services. In view of the experimental requirements of space life science and microgravity science, both the recoverable satellite and Shenzhou spacecraft need to improve and enhance their technical capability and economy.

The key technology upgrades should include improving the payload return capability, and providing better microgravity level, radiation experimental conditions and other platform service performance. The payload capability of the recoverable satellite can only be improved by layout optimization because of the limited volume of the recovery capsule. The Shenzhou spacecraft and the Chinese Space Station project obviously have more enhanced downward return capability of the experimental payload, especially in the future. In terms of micro-gravity level, China's recoverable satellite running on-orbit has good rigidity, and there is no flutter disturbance of low-frequency from large flexible body. A better micro-gravity level can be obtained by adopting appropriate orbit height and restraining the vibration of moving parts on the satellite. For the space station, in order to obtain higher microgravity level, it is necessary to develop an ultra-quiet and vibration suppression device to isolate the various environmental disturbances of the space station. For the improvement of radiation conditions, except for the configuration of environmental data measurement function, all the radiation test conditions without shielding can only be provided by installing the payload outside the cabin. In terms of engineering economy, the total cost of the recoverable satellite project can be reduced by using reusable technologies.

The research and development of China's recoverable satellites began in the 1970s. Up to the SJ-10 satellite mission, 25 recoverable satellites have been successfully

developed, forming a series of reliable and mature recoverable satellites. These satellite missions are mainly used in remote sensing and space science experiments. The main technical parameters of the satellite are as follows:

- **Orbit**: 260 × 340 km;
- **Inclination**: 63°;
- **Mass**: 3600 kg;
- **Payload mass**: 250 kg (recovered), 300 kg (not recovered);
- **Power for payload**: 350 W;
- **Microgravity level**: 10^{-3} to 10^{-5} g_0;
- **Landing speed (Vertical)**: $\leq$13 m/s;
- **Lifespan**: 15–30 days.

3 Object of System Design

SJ-10 satellite is China's first microgravity science experimental satellite with return function, and the system design goal includes:

- Improving microgravity level in an all-round way to reach the best level of similar spacecraft in the world;
- To provide flexible and efficient operation control and management for multiple payloads on-orbit experiments. Payloads on board satellite supported by satellite-ground links can respond quickly to scientific experimental instructions on the ground, less than 1–2 flight tracks;
- To provide excellent environmental protection conditions for all types of experimental payloads, and to support large power consumption, heat recovery of the experimental load to carry out in-orbit test;
- Low-cost design of the system can be used as commercial microgravity experimental platform to promote the application.

4 System Design

4.1 Characteristics and Difficulties Analysis

SJ-10 satellite is a new type of recoverable satellite which is developed on the basis of Chinese traditional satellite platform with comprehensive adaptability improvement. The new space mission requires new technologies to achieve greater capability under low cost constraints. It brings new difficulties and challenges throughout satellite development:

(1) The system design is difficult. From the launch of SJ-8 satellite in 2006 to now, SJ-10 satellite is the only recoverable satellite in this decade. Almost

all on-board electric products need to be upgraded comprehensively, and all subsystem programs need to be redesigned except for structure and recovery subsystem. Especially for electronic system, the information architecture needs to be redesigned to adapt to the mission requirements of multiple payloads.

(2) Payload design and validation is difficult. SJ-10 satellite will support 28 scientific experiments (19 equipment included) with various types and quantity of payloads. Each payload is an individualized equipment with different scientific objective. Besides, the environmental condition, installation and layout, experiment process and time sequence control for each payload are also different. All of these differences increase the complexity of payload system, and therefore, the difficulties of information management, on-orbit experiment process design, fault isolation, system integration and verification arise significantly.

(3) The requirement of microgravity level is much higher than before. SJ-10 satellite is China's first space microgravity scientific experiment satellite, which is required to have the world-class leading microgravity level so as to support high-level experimental projects. One of the design goals is to realize an order of magnitude higher than the previous platform, which is a great challenge and need to improve the overall system design.

(4) The budget is limited. SJ-10 satellite devotes to build low-cost and affordable microgravity platform, and the cost is strictly controlled from the beginning of the project. From the system scheme to product, every design step must reduce cost through system optimization in the premise of guarantee of reliability.

4.2 System Composition and Architecture

SJ-10 satellite is composed of 11 subsystems, including payload, power supply and distribution, control, propulsion, telemetry and control, engineering parameter measurement, on-board data handling, structure, thermal control, antenna, and recovery subsystem (Fig. 1).

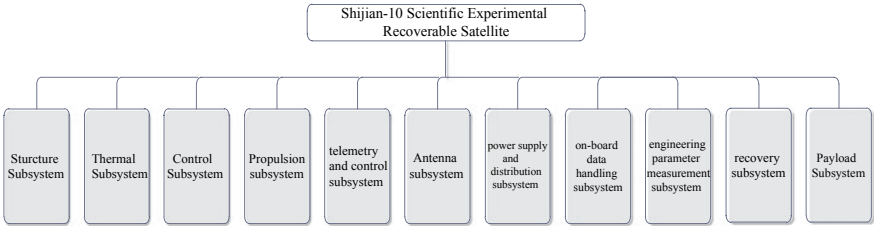

Fig. 1 System composition and architecture

4.3 System Technical Characteristics

- **Total weight**: not more than 3600 kg
- **Recoverable/unrecoverable payload carrying capacity**: 236 kg/279 kg
- **Satellite lifetime**: 20 days, reentry module returns in 12 days
- **Quasi-steady microgravity level**: 10^{-6} g
- **Micro-vibration level**: better than 1.5 mg, transient peak 7 mg
- **Power supply capacity for payload**: long-term 350 W, short-term 500 W
- **Recoverable/unrecoverable payload temperature**: 22 ± 2 °C/8–22 °C
- **Scientific demand adjustment time**: 1–2 orbits
- **Data download rate**: 150/300 Mbps
- **Experimental sample disposal time before launch**: 5 h
- **Pressure in sealed cabin**: 40–60 kPa
- **Attitude stabilization**: ≤0.03°/s (3σ)
- **Attitude pointing accuracy**: ≤3°(3σ)
- **Landing speed of reentry module**: not more than 13 m/s.

4.4 Orbit Design

Inclination Design: The orbit inclination is designed close to the latitude of reentry module landing area to increase the number of return windows and improve the emergency return disposal capacity. Besides, it can reduce the lateral error of landing point caused by the low accuracy of orbit measurement and control for low orbit satellite. Due to the latitude of Siziwangqi landing area, the orbit inclination is chosen as about 43°.

Orbit altitude design: The altitude is selected mainly considering the requirement of returning maneuver. An over high orbit leads to a long return voyage, and the landing accuracy is difficult to guarantee for ballistic return. But a very low orbit cannot meet the requirements of microgravity, and the satellite lifetime and obit measurement and control accuracy cannot be guaranteed. The orbit altitude is chosen as about 250 km finally, and the orbit parameters are designed as follows:

- **Altitude**: 256 km
- **Eccentricity**: 0
- **Inclination**: 42.893°.

4.5 System Configuration and Layout Design

The configuration of SJ-10 is a combination of cylinder and cone, with a height of 5144 mm, a maximum diameter of 2200 mm, and a shell as the main bearing structure, as shown in Fig. 2. The satellite consists of reentry module and instrument module,

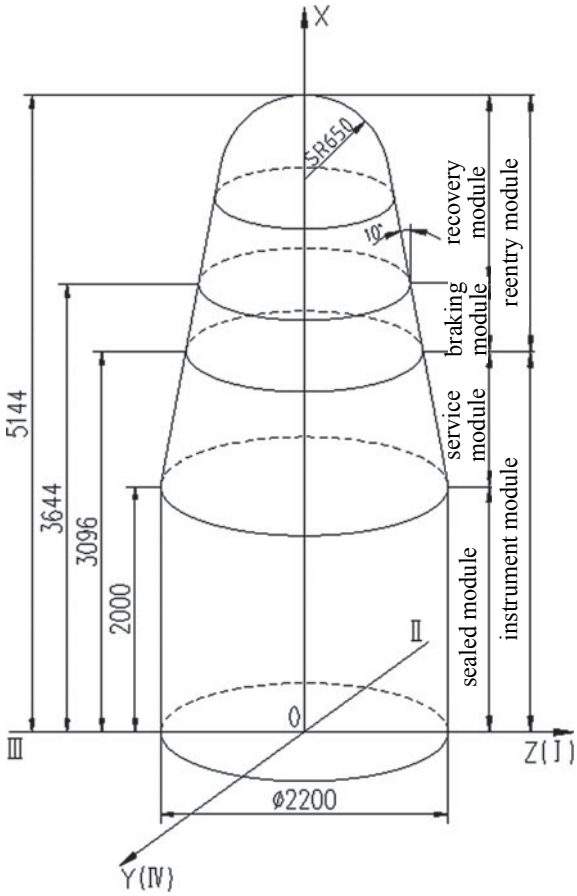

Fig. 2 Satellite configuration

in which the reentry module is composed of braking module and recovery module, and the instrument module is composed of sealed module and service module.

Recoverable life science payloads are installed in recovery module, and those physical science payloads unrecoverable are installed in sealed module, which provides pressure environment for experiments. The braking module has a braking system, which mainly provides power for the return, and the service module has service equipment.

4.6 Flight Procedure

SJ-10 flight process can be divided into four stages, that is, launch, on orbit, return and reentry and landing, as shown in Fig. 3 and specified below.

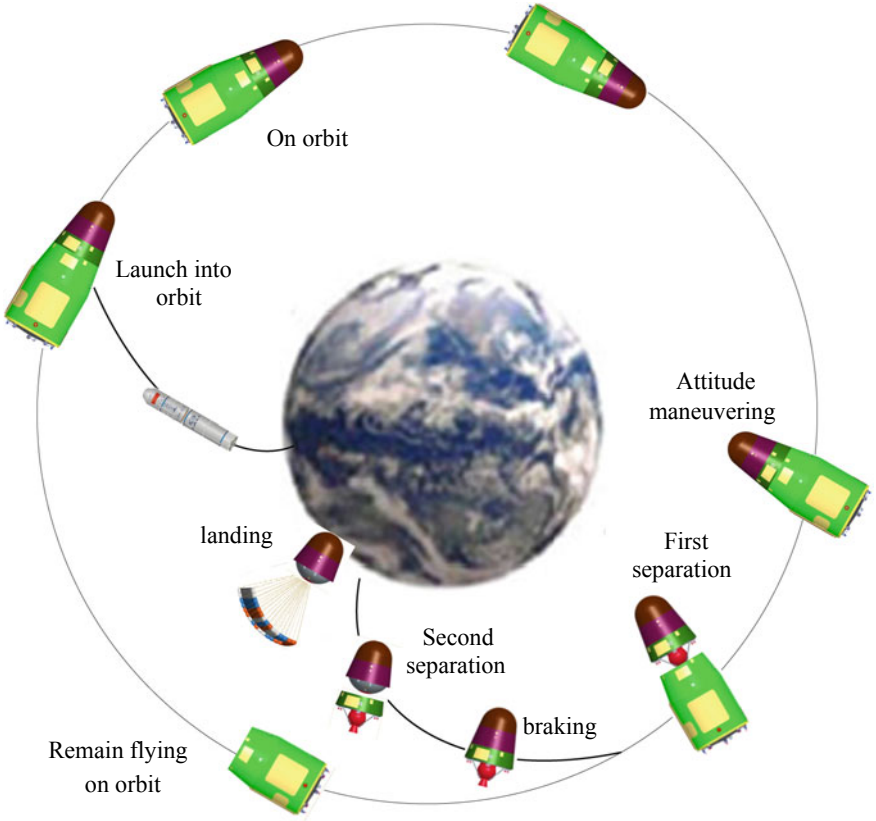

Fig. 3 Flight procedure of satellite

Launch: Launching satellite into orbit under the support of launch site system, telemetry and control system, and rocket system.
On orbit: After launching, carrying out experiments on the orbit.
Return and reentry: Attitude maneuvering before return, reentry module separation from the instrument module, firing the braking engines, recovery module separation from braking module, and recovery module reentry.
Landing: Recovery module reentry, opening the umbrella, and safe landing.

4.7 Scientific Experiment Flow Design

SJ-10 has 28 scientific experiments, 19 in recovery module and 9 in sealed module. Some projects have high power consumption, some generate large amounts of data, and two combustion payloads may produce a large number of exhaust gas needed

to be exhausted outside of the module. All of these need special considerations in payload experimental time sequence design:

(1) Experimental time sequence must meet the requirements of scientific experiments;
(2) Projects with high power consumption should be scheduled non-simultaneously, in order to lower requirements for thermal control;
(3) Projects needed to exhaust gas should not be carried out simultaneously to simplify gas pipeline design and control;
(4) Carrying out experiments with large amounts of data should consider peak load shifting to guarantee data download in time.

Experimental time sequences for sealed module projects and recovery module projects are as shown in Fig. 4.

4.8 Design of the Micro-gravity Environment

Some payloads are so sensitive to microgravity environment that they would be affected by acceleration even down to 10^{-7} g. Improving the microgravity environment faces the following difficulties: (1) The structure and configuration of the recoverable satellite imposes restrictions on the improvement of the microgravity environment; (2) As ballistic reentry is adopted for recoverable satellite, and the orbit altitude cannot be too high. So it is difficult to reduce the atmosphere drag force; (3) There are lots of moving parts on the satellites that deteriorates the microgravity environment, especially the pumps, valves, stepper motor and others (Fig. 5). The system solutions need to be optimized to improve the microgravity environment over one order of magnitude.

Microgravity environment is composed of quasi-steady acceleration, oscillatory acceleration and transient acceleration. The methods of eliminating or reducing these three kinds of acceleration are different. It is necessary to optimize and synthesize them from the system level based on the effect and cost of the corresponding measures. Methods adopted for reducing the microgravity acceleration is shown in Table 1.

4.8.1 Improvement of the Quasi-steady Micro-gravity Environment

Quasi-steady acceleration represents the microgravity varies little over long time period, typically with frequency lower than 0.1 Hz. Quasi-steady acceleration exists mainly due to rotation of the satellite, the gradient of the earth gravitational field and drag of the atmosphere. Additionally, the recoverable satellite uses thrusters for attitude control. Quasi-steady acceleration of the satellite will be disturbed transiently while the thrusters work.

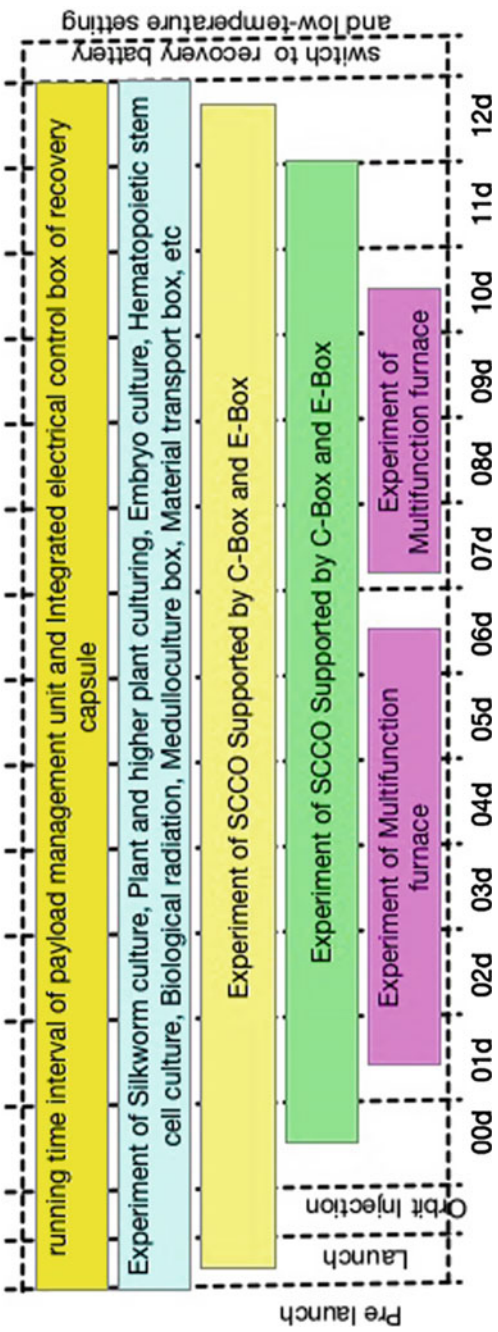

Fig. 4 Scientific experiment flow of recovery module load

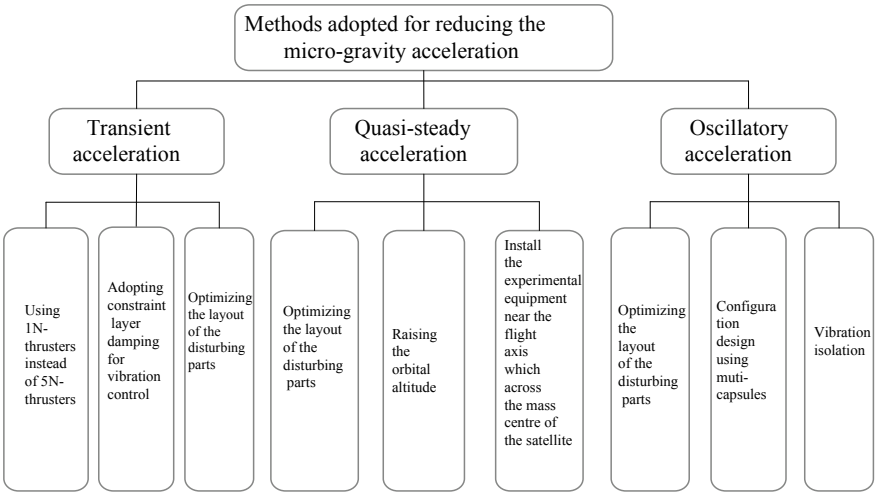

Fig. 5 Keep of the micro-gravity environment

Table 1 Methods adopted for reducing the microgravity acceleration

Quasi-steady acceleration	Oscillatory acceleration	Transient acceleration
Raising the orbital altitude	Optimizing the layout of the disturbing parts	Using 1N-thrusters instead of 5N-thrusters
Install the experimental equipment near the flight axis which across the mass center of the satellite	Configuration design using multi-capsules	Optimizing the layout of the disturbing parts
Using 1N-thrusters instead of 5N-thrusters	Vibration isolation	Adopting constraint layer damping for vibration control
Shut off sensitive experiments during certain period when the microgravity environment deteriorates		

(1) **Measures to reduce the atmosphere drag force**

The atmosphere drag force which depend on the atmospheric density and the ratio between windward area and mass of the satellite acts on the center of mass of the recoverable satellite. The area-mass ratio of the satellite has already reached 0.0011 m^2/kg and is difficult to further minimize. The atmospheric density is the function of orbital height. So, reduction of the atmosphere drag force can be realized by raising the orbit of the satellite. The aerodynamic acceleration caused by the atmosphere drag can be expressed as follow (Curtis 2005).

$$|\vec{g}_{s1}| = \left|\frac{\vec{F}_k}{m}\right| = \frac{0.5C_D A\rho V^2}{m} \tag{1}$$

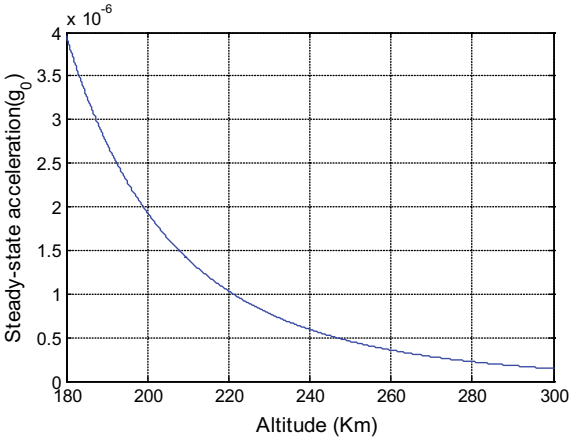

Fig. 6 Quasi-steady acceleration induced by atmosphere drag

in which $\vec{F}_k$ is the atmosphere drag force, A is the windward area of the satellite, ρ is the density of atmosphere, V is the velocity of the spacecraft with respect to the atmosphere, C_D is the aerodynamic drag coefficient, m is the mass of the recoverable satellite.

Using the typical atmosphere model SA76, the quasi-steady acceleration induced by atmosphere drag is presented in Fig. 6, in which it can be clearly seen that the acceleration reduces rapidly from 180 to 250 km.

(2) **Measures to reduce the tidal force**

The rest of major contributions to the quasi-steady acceleration are the tidal force and the rotation of the satellite, which acts on the satellite except for the mass center. For any position on the spacecraft deviated from center of mass, there exists quasi-steady acceleration caused by tidal force and the rotation of the satellite, which can be expressed as follows (Sidi 1997):

$$\begin{aligned} |\vec{g}_{s2x}| &\approx \frac{3\Omega^2 xy}{R} = \frac{3 \times 0.0012^2 \times 1.1 \times 1.1}{6{,}378{,}137} \approx 0 \\ \left|\vec{g}_{s2y}\right| &\approx 3\Omega^2 y = 3 \times 0.0012^2 \times 1.1 = 4.6 \times 10^{-7}\ g_0 \\ |\vec{g}_{s2z}| &\approx -\Omega^2 z = 0.0012^2 \times 1.1 = 1.5 \times 10^{-7}\ g_0 \end{aligned} \tag{2}$$

in which Ω is the average rotation velocity of the spacecraft, which is equal to the rotation velocity around the center of the earth. The main parameters that affect the tidal force are y and z, which represent the distance between the analyzed location and flying axis on y and z respectively. The nearer the payload installed to the flying axis, the smaller the tidal force is.

(3) **Measures to reduce the disturbance on the quasi-steady acceleration from propulsion system**

Transient disturbance on the quasi-steady acceleration of the traditional recoverable satellite of China was caused by the propulsion system, which contains one orbital control thruster (20N) and twelve attitude control thrusters (5N). All the thrusters were installed on the bottom of the recoverable satellite. In order to lower the transient disturbance from propulsion system, 5N-thrusters were replaced by 1N-thrusters.

The acceleration induced by 1N-thrusters can be calculated as follows (Sidi 1997):

$$\begin{aligned} |\vec{g}_{t1z}| &= \left| \frac{d\vec{\omega}_z}{dt} \times \vec{r} + \vec{\omega}_z \times (\vec{\omega}_z \times \vec{r}) \right| \leq 7.34 \times 10^{-5}\ g_0 \\ |\vec{g}_{t1y}| &= \left| \frac{d\vec{\omega}_y}{dt} \times \vec{r} + \vec{\omega}_y \times (\vec{\omega}_y \times \vec{r}) \right| \leq 1.46 \times 10^{-4}\ g_0 \\ |\vec{g}_{t1x}| &= \left| \frac{d\vec{\omega}_x}{dt} \times \vec{r} + \vec{\omega}_x \times (\vec{\omega}_x \times \vec{r}) \right| \leq 9.82 \times 10^{-5}\ g_0 \end{aligned} \tag{3}$$

in which $\vec{g}_{t1x}$, $\vec{g}_{t1y}$ and $\vec{g}_{t1z}$ represents the acceleration along x-, y- and z-axis respectively, $\vec{\omega}_x$, $\vec{\omega}_y$ and $\vec{\omega}_z$ are the angular velocity about x-, y- and z-axis respectively.

It has to be noted that the recoverable satellite is considered as a rigid-body in the above evaluation of the acceleration. The above results are the angular acceleration of the satellite generated by the propulsion system. Disturbance on the quasi-steady acceleration also depends on the actual wave of the thrust, duration of the thrust and interval between two adjacent thrusts.

The 20N-thruster which is installed along the x-axis was used for orbital control. The acceleration disturbance caused by orbit control will reach 10^{-4} g_0 magnitude level. During the 15-day on-orbit mission of the recoverable satellite, the 20N-thruster only worked for very short period, during which sensitive experiments were shut off.

4.8.2 Improvement of the Oscillatory Environment

Oscillatory accelerations represent microgravity which is periodic in nature with a characteristic frequency. The characteristic frequency of oscillatory acceleration on the recoverable satellite is in the sub-Hertz to hundreds of Hertz range. The source of oscillatory accelerations on the recoverable satellite includes pumps of the fluid loop, air fans for the thermal control and the infrared earth sensor. It has to be noted that the payloads for carrying out space experiments may also contain several disturbance sources which could deteriorate the microgravity environment.

The ground vibration measurement tests show that disturbance from infrared earth sensor is negligible compared to pumps and air fans. Acceleration caused by the pumps of the fluid loop is below 500 mg (milli gravity) at the location where the pump is installed, with frequencies of 146 and 292 Hz. Acceleration caused by the air fan is about 70 mg at the location where it is installed.

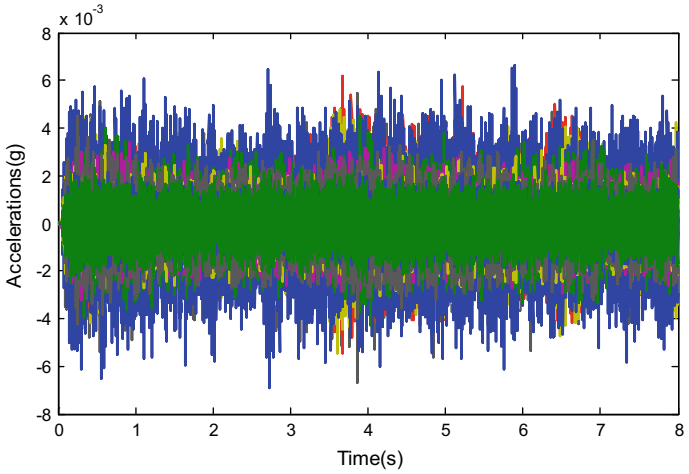

Fig. 7 Comparison of acceleration disturbance caused by fluid loop pump before and after vibration reduction

Therefore, primary measures for reducing the oscillatory acceleration is to carry out vibration isolation for the pumps. The pumps are installed far from the payloads. After translating over several mechanical joints, the oscillatory acceleration induced by the pumps can be reduced by more than two orders of magnitude. Figure 7 shows the comparison of acceleration disturbance caused by fluid loop pump before and after vibration reduction of connected structures.

4.8.3 Improvement of the Transient Acceleration Environment

Transient acceleration has wide range of exciting frequency and usually lasts for less than 1 s. The source of transient acceleration disturbance in recoverable satellite includes electric relay movement, valve movement, jet thrusters and others. Using low force thrusters and optimizing layout of disturbance source can improve the transient acceleration environment. In addition, constrained damping approach is used for thrusters' mounting bracket to decrease the wide band vibration. All the thrusters of recoverable satellite are installed on lower bottom which consists of shell structure. For the shell structure, installing constrained damping layer on it is an effective method of suppressing vibration. The constrained damping layer consists of 0.3 mm damping layer and 2 mm restraint layer, which can reduce transient vibration speed of payload installation site to about 50%.

4.9 High Payload-to-Total-Weight Ratio Design

The main structure of SJ-10 satellite inherited from traditional reentry design. 28 experiments were performed in 19 installations—515 kg total—where 19 of them required recovery. SJ-10 satellite is the first recoverable satellite that applied fluid circuit system. The large amount of payloads, heavy weight, large equipment volume and irregularity and high assembly requirements bring difficulties to payload bay design. The high payload-to-total-weight ratio is realized by system design in not only structure, configuration and layout optimizations, but also system function optimization, sequence optimization, effective energy management and precise control of the center of mass. The design outline mainly includes:

(1) Top level optimization. The functions of each segment of the satellite are optimized. Deorbiting and recovery system is kept in minimum scope. 400 kg from retrorockets is thus removed since required total impulse halved. Only one monopropellant system is installed instead of traditional configuration of one monopropellant system plus one cool gas system, reducing 30 kg from the propulsion system.
(2) Effective energy management. Batteries are used for energy supply on SJ-10 satellite instead of solar panels. The power of the reentry capsule is supplied by Li-Thionyl chloride batteries in the sealed capsule instead of Silver-Zinc batteries that only have lower specific energy, removing 140 kg from batteries. The power supply bus is in parallel. All subsystems share one batch of batteries while payloads share another. Power waste is well avoided by compensations between each subsystem through the bus instead of independent power supply on each subsystem.
(3) Structure lessening design. Structure lessening is realized by material selection, optimization and crafting improvement: (1) Material selection. Materials are selected for different applications so that the material matches functional requirements. Crucial bearing parts are made of titanium for high strength and specific stiffness. The seal capsule is made of 5A06 for good mechanical property, weldable and corruption resistance. Skin is made of 2A12 for high strength and heat resistance. Bearing frames apply 2A14 for high strength. Mounting brackets are magnesium alloy for light weight. (2) Optimization. Optimization is performed by analysis software and mathematical tools. The instrument disk and the twin platform, for example, loss 20% weight through topology configuration optimizations. (3) Crafting improvement. Dead weight is reduced by manufacturing improvement. For instance, solder consumption is reduced by laser welding.
(4) Effective space utilization configuration. Optimizations are conducted on recovery capsule: (1) Separation design. Payload and functional equipment are separated, avoiding coupling and connections of cables or pipelines. (2) Conformal design of payload bay within recovery capsule. The payload combination is conformal with the capsule, increasing space utilization. (3) Some of the payload instrument is deformed in order to further improve space utilization.

(5) Precise control of center of mass. The spinning reentry lays strict requirement on mass property of the recovery capsule. 1 mm precision of lateral center of mass without counter mass is acquired by model-based automatic configuration and detailed design in capsule structure, instrument arrangement and pipeline layout.

The payload-to-total-weight ratio of SJ-10 satellite was improved to 15.3% (3370 kg gross weight with 515 kg payloads) by applying these systematic designs.

4.10 Temperature Control System Design of the Payload of Recovery Capsule

Payloads to carry out on-orbit experiments need the platform of satellite to provide the appropriate temperature environment. This is because the recovery capsule surface of satellite is wrapped with a thick layer of ablative heat protection structure and the heat produced in the high-power load working process cannot dissipate effectively, which becomes a technical bottleneck that it hinders the traditional return satellite to support the high power load experiment.

SJ-10 satellite is facing a more serious situation: there are 11 scientific loads arranged in the recovery capsule, and the average power is about 400 W, which is 10 times of heat consumption of the traditional return type satellite recovery capsule. In addition, unlike the traditional return type satellite, the SJ-10 satellite recovery capsule continues to operate within 3 h after loads unblocking, re-entry into the atmosphere, and landing. The ambient temperature of the load equipment continues to rise, which brings a lot of pressures to thermal and energy of recovery capsule.

In order to solve the thermal control problems in the on-orbit and return phase of the recovery capsule, the system takes into account the factors such as satellite load management, energy management and thermal control management. A scheme was proposed to manage the heat energy inside the recovery capsule with the single-phase fluid circuit as the core subsystem. The details are as follows:

Two cold plate of approximately 1 m in diameter was installed for recovery capsule which is used to collect heat of the experimental load. The mechanical pump drives the fluid circuit to transfer heat to the radiator on the surface of sealed cabin, and to dissipate the heat into the cryogenic space. The fluid circuit is divided into internal circulation and external circulation. The thermal control unit adjusts the opening of thermostatic valve according to the set temperature, and controls the flow proportion of internal circulation to the external circulation to realize the precise control on the load temperature. With the above technical scheme, the on-orbit data shows that the temperature of recovery capsule can be controlled at 22 ± 2 °C.

4.11 Design of Multi-payload Space Laboratory Management System

There are many kinds of payloads onboard satellite, such as microgravity fluid physics, microgravity combustion, space material science, space material science, space radiation effect, microgravity biological effect and space biotechnology. The working pattern is diverse and the timing control is complex. According to the on-orbit experimental results of the payload experimental device, scientists need to adjust experimental parameters flexibly and quickly to plan new test requirements. It takes one to two orbital cycles to transform the new experimental requirements proposed by scientists into uplink instruction injection for satellites. The fault isolation problem of the experimental device is also a key issue. For multi-payload parallel experiment tasks, any individual failure or abnormal problem of the experimental payload must not affect the rest of the experimental payloads, including the safe operation of the satellite platform. Parallel experiments with multiple payloads may lead to resource constraints such as high heat consumption and large amount of data in specific time periods, and thus it is necessary to optimize the experimental timing.

The main controller is payload manager for recovery and sealed capsule. It is made of 11 recovery capsule load test device and 8 sealed capsule load test device that is independent of each other but also can be interactive information collection and distribution of space experimental control system. Payload system and 19 payload test devices are combined to form the distribution of space experimental control system by the configuration of payload support subsystem (as seen in Fig. 8 and specified below).

(1) By the reference of SIOS standard published by CCSDS, for the different needs of the payload, payload subsystem configured data bus architecture and a variety of special communication interface to meet the stand-alone load control requirements and data management requirements.
(2) Using master-slave system bus architecture, see Fig. 9 for topology. The character includes: RS485 bus bases physical layer and UART serial communication link layer protocol, supports automatic identification for site address, and customizes high-reliability application layer protocol. Low speed data management is realized for 11 test devices in recovery capsule and 8 test devices in sealed capsule, and also, cost and development cycle is reduced because of the easy of protocol realization.
(3) Payload support subsystem uses a variety of interfaces (RS422, LVDS and others) to achieve low- and high-speed data acquisition and storage functions.
(4) Data merging and data multiplexing function of adaptive low- and high-speed data seamless switching are realized. The sealed capsule payload manager receives the LVDS high-speed image data and the RS422 low-speed real-time engineering parameters of each load in the cabin, and then packs the data to the storage unit. After the satellite enters, RS422 real-time engineering parameters of the recovery capsule and sealed capsule, and the LVDS playback data

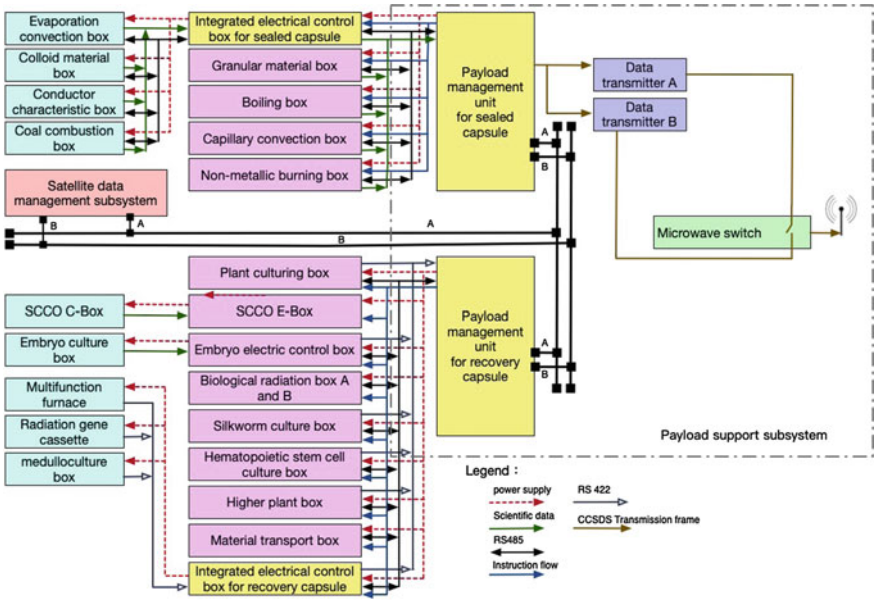

Fig. 8 Distributed control system of payload

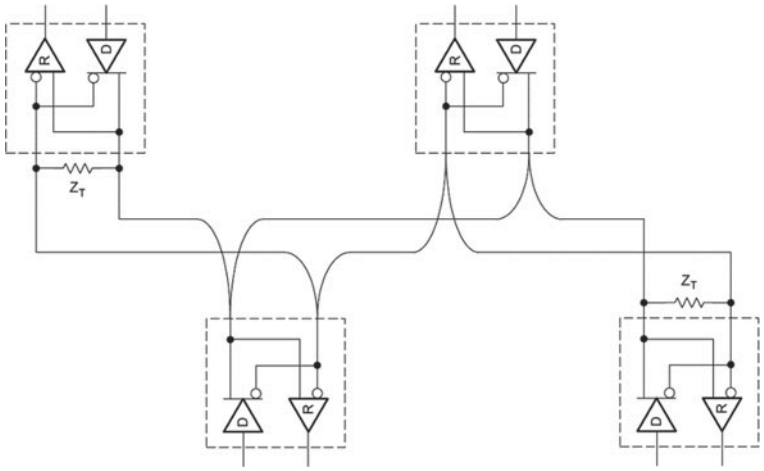

Fig. 9 Low cost master-slave system bus architecture

input from the large-capacity storage unit are multiplexed. Finally, LDPC code is transmitted to the digital transmission transmitter.

(5) The on-orbit health management and fault isolation are realized. The load manager acquire important engineering parameters for critical product in real time, according to the default or injection judgment on-orbit to perform automatic judgment, so that products can achieve automatic shutdown and fault isolation abnormal condition.

(6) Rapid adjustment of scientific experiment processing and parameters in orbit is achieved. In order to ensure that the experimental devices fulfill the scientific objects and even find more unknown physical phenomenon, SJ-10 satellite perform on-orbit autonomous management by event table from payload manager. Firstly, the simulation and analysis of the power and energy consumption of the multi-load simultaneous working mode under various complex conditions are carried out. Under the condition of satisfying the safety of the whole power supply, the flight process is designed according to each scientific target demand and in-orbit configuration requirement. At the same time, the rapid generation, transmission and confirmation strategy of the dedicated configuration instruction is realized by using the terrestrial network, which satisfies all the requirements of quick setting and parameter adjustment of all 28 scientific experiments in the limited transit time of the satellite. The configuration period is optimized from 4 tracks to 1–2 track.

By designing a distributed load control system which is independent and efficient with the reclaiming payload manager of recoverable module and sealed module as the hub, it can solve the problem of complex time sequence control, fault isolation and scientific demand change. The on-orbit implementation satisfies all the requirements of fast reconstruction and parameter adjustment that related to 28 scientific experiments. The configuration period is optimized from 4–8 tracks to 1–2 track (1.5–3 h).

4.12 Aerospace Products Reuse Technology

SJ-10 satellite project propose strict limit to development costs. The most efficient technical means of cutting the cost is making use of recovery products from other retrievable spacecraft. This is the first project of China which use large scale of recovery products and of high risk. No experience can be used for reference. We have great challenges on product state assessment and product assurance. The solution of assuring adaptability and reliability of recovery products is to propose the principle of using, assess the healthy state, and innovate product assurance mode and state management by classification.

Technical program:
Carding reuse principle: by carding product state and proposing reuse guiding ideology, we summarize and refine the technology adaptability principles, entirely assess the state principle, and minimize change principle and full test principle.

In aspect of assessing the healthy state of recovery products: we make use of complete machine test data as the main criterion, and at the mean time lead into biographical analysis as another important criterion. Combining the two criterions, we get the final assessment result and employ the healthy assessment method which is based on D-S theory and test data analysis. Product biographical analysis makes use of reliability budget, expert assess and empirical formula. We assess the influence on product healthy state from design, technological level, test experience and storage experience.

In order to analyze the machine healthy state, we first define key parameter by analyzing the test data of key parameter from first assembly to reuse, and get the belief function and finally the assess results which can guide choose and state control of the following products.

In aspect of product state control: we perform the category management according to assess results. Environment test must be carried out, according to the recovery product from former retrievable satellite, for analyzing the reason of property drift, periodic inspection, multiple test to assure product state. For the good state product, the emphasis is interpreting the uniformity of test data, ensuring that the test result is stable. For the product which does not need to rewrite the software, environment test can be cancelled by making use of the like products to confirm the state as a side witness.

In aspect of product assurance: assurance methods such as replacing the component independent management with complete machine management, reusing software specific analysis, and performing technology materials specific check can be used. Making special provisions to software, component, craftwork, material, data pack, file management and security, all these provision can make sure the reuse product meet the reuse requirements.

SJ-10 satellite is the first spacecraft of China which makes great scale use of recovery aerospace product on platform. Reuse rate of information system is 70% which save cost as high as 7.6%. Through this practice, we get a new method and technical norms of reusing the recovery products, and make a benefit attempt for the future reusable spacecraft.

4.13 Low Cost Design

On the one hand, the demand of low-cost system development comes from the pressure of funding constraints; on the other hand, from the development process of spacecraft, reducing the cost is the eternal theme of spacecraft development, especially for spacecraft with respect to the space microgravity scientific experiments.

The cost is of great significance to improve the market competitiveness and enhance the vitality of the spacecraft itself.

Technical approach of SJ-10 low-cost development includes.

4.13.1 Product Reuse

The most effective way to reduce costs is product reuse. SJ-10 used seven devices from the previous satellites to complete information management functions. List of equipment is shown in Table 2.

4.13.2 System Integration of Products Among Fields and Systems

In order to realize the cost control, SJ-10 satellite have chosen the products from many fields, such as recoverable satellite, manned spacecraft, transmission remote sensing, deep space exploration and small satellite platform. Through the design and optimization of electronic system architecture and information system architecture, a good solution comes out for the problem of multi-system products compatible matching and system integration testing.

4.13.3 Using Commercial Modules and Components

For module parts, in order to reduce development costs, satellite non-critical equipment selected commercial products, such as sealed cabin convection fan 4414F/2 from Ebmpapst company as the core component for convection in sealed cabin. On the above basis, secondary development is performed for electronic control module. To ensure the products meet the requirements of in orbit working, performance test,

Table 2 List of equipment

No.	Product	Function	Quantity
1	Remote control demodulator	Demodulation and distribution of direct remote command and injection data	1
2	Telecontrol central control acquisition unit	Framing and modulation of satellite LLC data	1
3	Landing search beacon	Data providing	1
4	Pulse transponder (band C)	Signal tracking providing in return leg	1
5	CTU	Center of satellite data management	1
6	RTUa	Indirect command source	1
7	RTUb	Indirect command source	1

mechanical and thermal environmental testing and EMC test are performed to ensure the products meet the launch and in-orbit requirements.

For components parts, most of the payload used industrial-grade components and modules, and even commercial-grade products. By checking the working principle and design scheme of payloads, system level characteristic analysis and FMEA analysis of each load, critical products and key module of each product are identified, and the functional redundancy, especially the heterogeneous functional redundancy design is emphasized. Moreover, we formulate the criteria of low-grade components and modules within the product: the product of critical items should use quality components that has strict accordance with the overall satellite product assurance requirements, the products of non-critical are graded according to the failure severity of functional unites, the non-single-point failure can use low-level components and modules, and the single-point failure should use components and modules that has passed the upgraded screening or stricter test assessment. In addition, system test syllabus and rules are developed to ensure the test coverage of product redundant design. As a result of in-orbit operation, low-level components and modules did not appear to clap, working in good condition.

4.13.4 Development Procedure Optimization

Development process of SJ-10 satellite is carried out a number of optimization to simplify the system work, shorten the development cycle, reduce system risk and reduce the repeated work. Also, these acts will provide significant contribution for system development costs reducing. Optimization of development technical process is mainly reflected in the following aspects.

(1) There is no structural model and thermal control model in preliminary design phase. The satellite mechanical and thermal control system design directly goes into critical design phase by the means of design and simulation, recheck and recalculation, virtual test, and others.
(2) Parallel work is taken through manufacturing, assembly, testing and others according to the characteristics of four modules of the satellite. At the same time, technological approaches about satellite fast manufacturing, assembly and testing are explored to compress the development cycle and save the money.
(3) Optimize work order, save the money of crafts development and reduce AIT projects.

According to the approaches above, total cost is reduced by 15%.

5 Evaluation of Flight Test Results

The flight test results are evaluated by the implementation of system technical indexes, the assessment of microgravity level condition and the conduct situation of in-orbit scientific experiments.

5.1 Evaluation of System Technical Characteristics

The comparison of key technical indexes are shown in Table 3. All the functional performance parameters satisfy the task requirements.

5.2 Evaluation of Microgravity Environment

On-orbit evaluation of microgravity environment was carried out based on the on-orbit measured microgravity data. Qualifications of SJ-10 micro gravity admeasuring apparatus are illustrated in Table 4.

5.2.1 On-orbit Evaluation of the Quasi-steady Microgravity Environment

There are two microgravity sensors which are made up of quartz accelerometers installed on the satellite. One is installed in the re-entry capsule and the other is installed in the sealed capsule.

Although quartz flexibleness accelerometer of microgravity admeasuring apparatus can measure the DC component (the frequency of acceleration is 0 Hz), the offset and resolution of microgravity admeasuring apparatus cannot satisfy the requirement for measurement of quasi-steady acceleration on satellite. Then quasi-steady acceleration caused by atmospheric drag and tidal force can be got from analytic technique. Considering that the analytical error of atmospheric drag and tidal force is small, which cannot cause greater impact to the evaluation of quasi-steady microgravity environment, the theoretical analysis results can explain the order of quasi-steady microgravity.

At the same time, because satellite attitude control thrust is big and the quasi-steady microgravity fluctuation of recoverable satellite mainly depends on the turbulence of attitude control thrusters, the evaluation focus of quasi-steady microgravity is to evaluate the low-frequency turbulence of attitude control thrusters.

In the process of SJ-10 satellite attitude maneuver, the attitude angular velocity is about 0.5°/sand the microgravity sensors are installed about 2.5 m away from

Table 3 Satisfaction situation of system technical indexes

Content	Flight test result	Technical index	Compare result
The weight of whole satellite	3368 kg	≤3600 kg	Satisfied
Carrying capacity of return payload	236 kg	236 kg	Satisfied
Carrying capacity of non-return payload	279 kg	279 kg	Satisfied
Flight time of re-entry capsule	12 days and 14.5 h	≥12 days	Superior to index
Flight time in orbit	8 days	≥3 days	Superior to index
Quasi-steady acceleration	Reaches 10^{-6} g order	Superior to 10^{-3} g	Superior to index
Micro vibration level	Superior to 1.5 mg for long-term, 7 mg for transient peak	–	–
Power supply capacity for payload	350 W for long-term, 500 W for short-term	320 W for long-term, 450 W for short-term	Superior to index
Payload temperature in re-entry capsule	20.6–23.6 °C	5–35 °C	Superior to index
Payload temperature in sealed cabin	8–22 °C	0–35 °C	Superior to index
Experimental sample handling time before launch	5 h before launch	24 h before launch	Superior to index
Response time of in-orbit adjustment for scientific demand	1–2 orbits	4 orbits	Superior to index
Re-entry capsule searching time	40 min	≤3 h	Superior to index
Sealed cabin pressure	47.55–55.6 kPa	40–60 kPa	Superior to index
Scientific data download rate	300/150 Mpbs optional	150 Mpbs	Superior to index
Satellite attitude stabilization	≤0.01°/s (3σ)	<0.03°/s (3σ)	Superior to index
Attitude pointing precision	≤2° (3σ)	<3° (3σ)	Superior to index
Landing accuracy	39 km from landing site in southwest	Landing ellipse: 190 × 110 km	Superior to index
Landing velocity	12.5 m/s	≤13 m/s	Superior to index

Table 4 Qualifications of microgravity admeasuring apparatus

Item	Qualification
Measuring range	(1) X1: (−250 to +250) mg (2) X2, Y, Z: (−20 to +20) mg
Resolution	(1) Wide range: ≤35 μg (2) Narrow range: ≤narrow

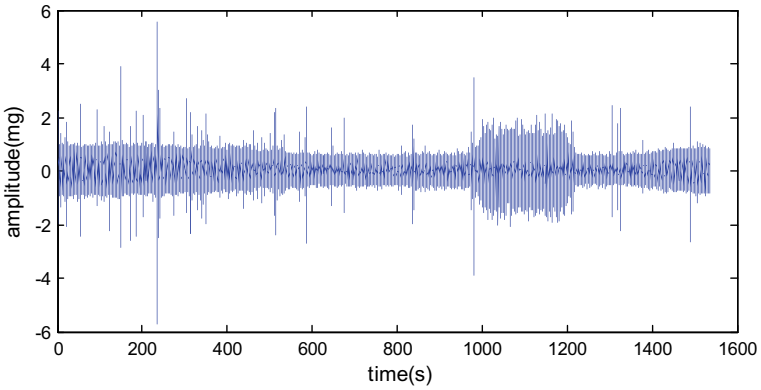

Fig. 10 Time course of microgravity measurement in the process of attitude maneuver

barycenter, the centrifugal acceleration of this position can be calculated theoretically below:

$$\omega^2 r = 2.5 \times (0.5/57.3)^2 = 1.9 \times 10^{-5}\ \mathrm{g} \tag{5}$$

In the process of attitude maneuver, the results of microgravity measurements are shown in the Fig. 10.

Making use of FIR low pass filter to process the signal in Fig. 10, the window function is KASIER, the cut-off frequency of pass band is 0.1 Hz, and the attenuation of pass band is less than 1 dB. Given that the cut-off frequency of stop band is 0.2 Hz and the attenuation of stop band is more than 80 dB, the vibration acceleration in the process of attitude maneuver after filtering is shown in Fig. 11. It is obviously that the quasi-steady acceleration in the process of attitude maneuver changes about 1.75 $\times$ 10^{-5} g, which is in agreement with the theoretical analysis.

When attitude control thrusters are implementing attitude maintenance, the quasi-steady turbulence caused by air injection can be extracted by low pass filter. Figure 12 intercepts the biggest influence of quasi-steady microgravity level caused by attitude control thrusters when on-orbit. Five jumps in the Fig. 12 are transient jumps caused by attitude control thrusters. It is clear that, when attitude control thrusters are working, their influence to the quasi-steady microgravity ranges from 10^{-6} to 10^{-5} g.

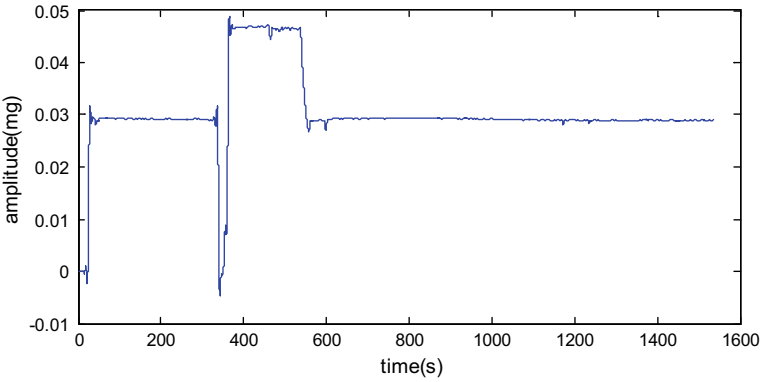

Fig. 11 Time course of microgravity measurement after filtering in the process of attitude maneuver

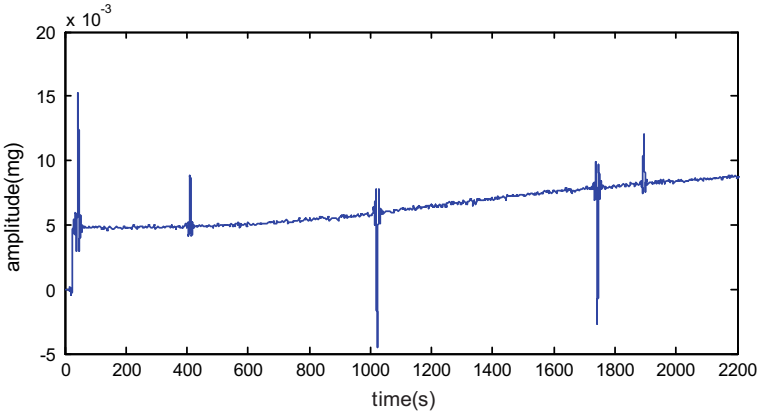

Fig. 12 Jumps of quasi-steady microgravity caused by attitude control thrusters

5.2.2 Micro Vibration Environment On-orbit Evaluation

(1) **Influence of fluid loop pump**

As mentioned before, fluid loop pump has the greatest impact on micro vibration environment of satellite platform. Here we focus on the on-orbit micro vibration evaluation result of fluid loop pump.

When the satellite is on-orbit operating, we take shutting down action to fluid loop pump, and then analyze the time-domain curve before and after shutting down. The results are shown in Figs. 13 and 14. From the comparison, after the fluid loop is closed, two peaks near 146 and 292 Hz are disappeared, implying that the influence of fluid loop pump mainly concentrates upon 146 and 292 Hz which is consistent with the result of ground experiment (Fig. 15).

Making use of band pass filter to process these data and extracting the components near 146 and 292 Hz (Figs. 16 and 17), we can see that the greatest influence of fluid loop pump is about 0.6 mg on recovery capsule and about 0.7 mg on sealed module. Moreover, through on-orbit data analysis, the micro vibration peak value caused by fluid loop pump changes with angle of temperature-control valve and speed of fluid, but the frequency remains stable. In summary, the greatest impact of fluid loop pump is less than 2 mg under different operating mode.

(2) **Influence of other equipment**

For the source of disturbance that generates small amplitude of vibration, it is difficult to extract the frequency-amplitude information through the measured data which has

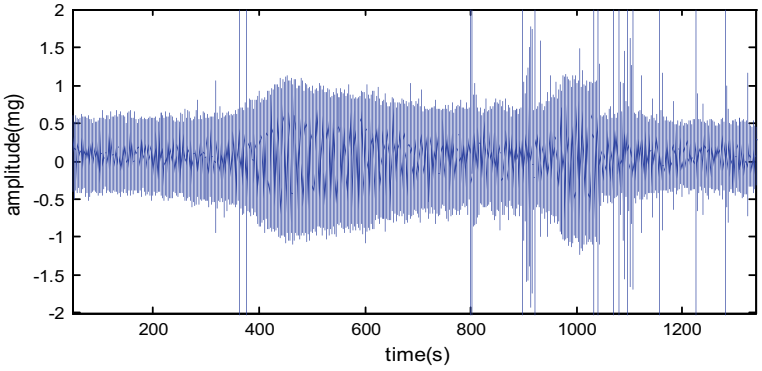

Fig. 13 Directly collected curve before and after fluid loop pumps shut down (X direction)

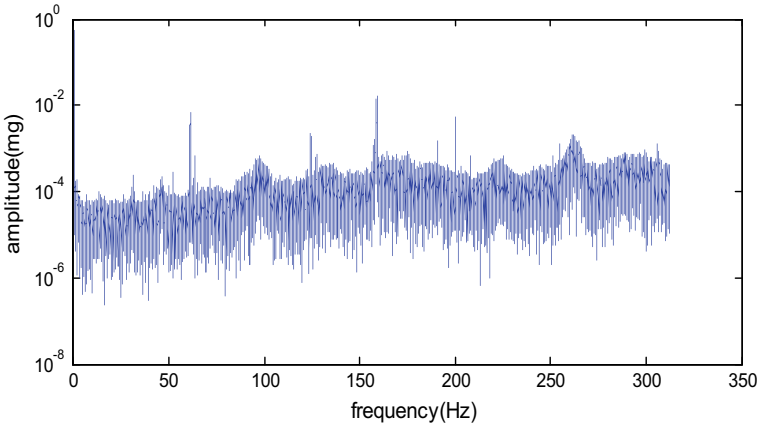

Fig. 14 Amplitude frequency diagram after fluid loop pumps shut down (X direction)

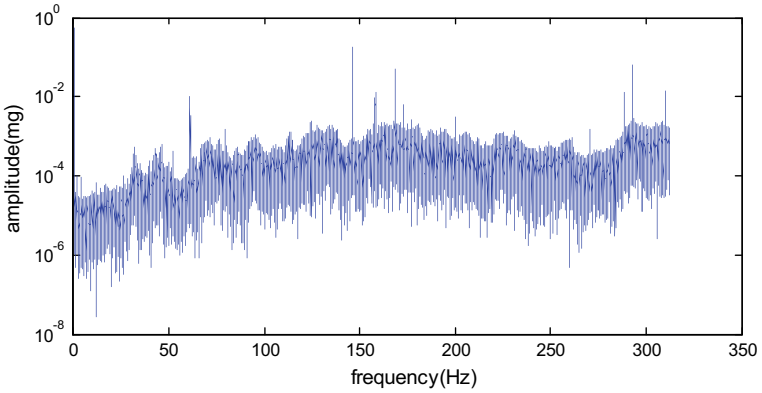

Fig. 15 Amplitude frequency diagram before fluid loop pumps shut down (X direction)

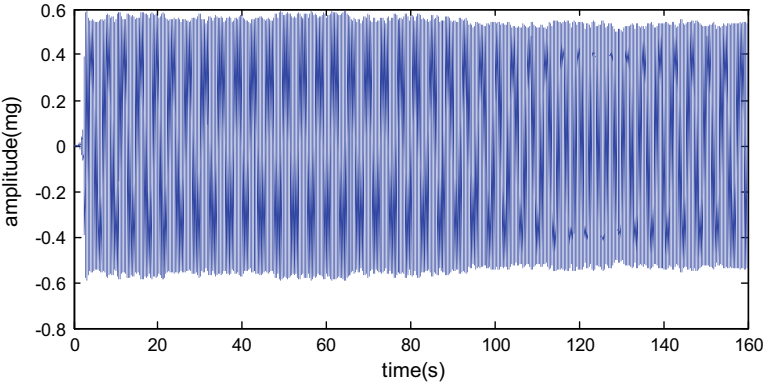

Fig. 16 Influence of fluid loop pump on recovery capsule (Y direction near 146 Hz after filtering)

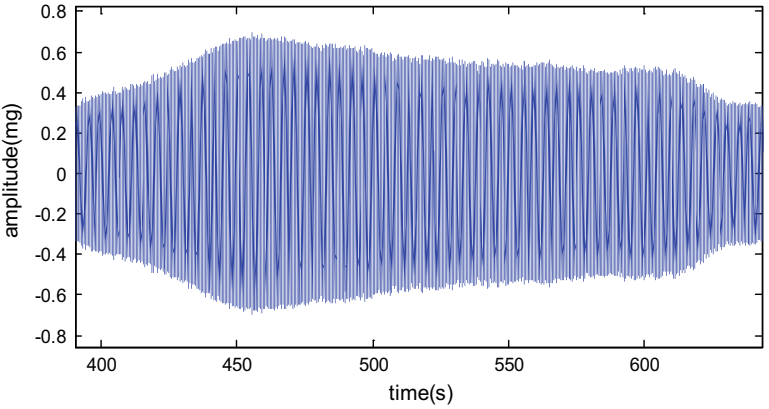

Fig. 17 Influence of fluid loop pump on sealed module (X direction near 146 Hz after filtering)

Table 5 Micro vibration environment influenced by equipment on the SJ-10 platform

	Infrared earth sensor	Gyro	Pump	Air fan
X	About 0.3 mg	About 0.05 mg	0.2–1.8 mg	0.3 mg
Y	About 0.2 mg	About 0.05 mg	0.3–2 mg	0.25 mg
Z	About 0.25 mg	About 0.05 mg	0.4–2 mg	0.08 mg

massive noises. Thus, we measured the microgravity acceleration of each disturbance source one by one with payloads stop working.

With each disturbance source working alone, oscillatory vibration of temperature control valve, spinning top and fan can be measured respectively though special experiment of microgravity. With the analysis results, the influence of these devices can be excluded from the data measured on orbit, and therefore, further extraction of the micro vibration disturbance of other equipment can be obtained. Table 5 shows that micro vibration environment influenced by equipment on the SJ-10 satellite platform.

5.2.3 Evaluation of Transient Vibration on Orbit

Transient vibration is caused by relays, dynamos and others, which usually last for less than 1 s. The peak value of transient vibration can be measured directly.

Typical transient vibration on orbit can be seen in Fig. 18. According to measurement data, maximum value of transient acceleration is approximately 30 or 40 mg in respective sealed or reentry modules, in which most transient vibration is less than 10 mg except for very few peaks. The maximum transient acceleration are coursed by certain movements such as pump turning on/off. Sensitive experiments were shut off when these movements showed up.

5.2.4 Evaluation of Microgravity Environment

Microgravity level of SJ-10 satellite can be seen in Table 6. Flight results showed that quasi-steady microgravity level of SJ-10 satellite was about 10^{-6} g, micro vibration acceleration influenced by equipment was about 2×10^{-3} g, and transient micro vibration was less than 40 mg.

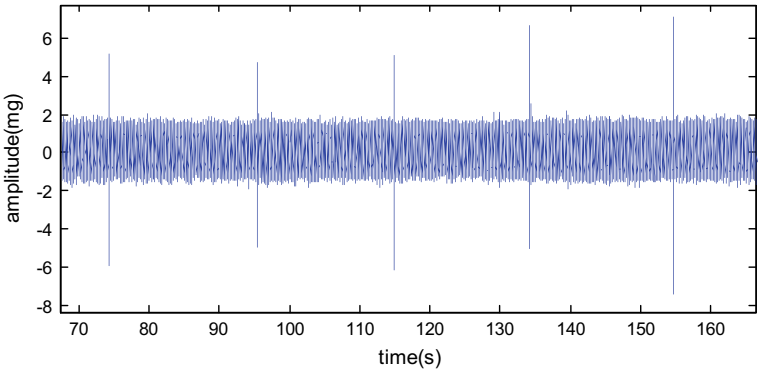

Fig. 18 Curve of measured micro vibration on orbit

Table 6 Microgravity environment of SJ-10 satellite

	Sealed module	Re-entry module
Platform micro vibration environment (0.1–300 Hz)	Approximately 0.6–2 mg frequency of peak value (approximately 146 Hz)	Approximately 0.4–2 mg frequency of peak value (approximately 146 Hz)
Transient micro vibration environment	10^{-3} to 3×10^{-2} g	10^{-3} to 4×10^{-2} g
Quasi steady state microgravity environment (0–0.1 Hz)	Orbit control: ≈1 mg	
	Attitude adjustment: better than 4×10^{-5} g	
	Quiet state: 10^{-6} g; Centroid; 10^{-7} to 10^{-6} g	
	Quasi steady state microgravity influenced by attitude adjustment thruster: 10^{-6} to 10^{-5} g	

5.3 Evaluation of In-orbit Scientific Experiments

The scientific experiments carried out on-orbit are summarized as follows:

- Microgravity experiments: Among 67 samples and 78 experiment stations, 430 experiments are successful out of total 478 experiments, and the cumulative experiment time is 740 h. The success rate of the experiments is 98.2%, the success rate of the experiment station is 100%, and the success rate of the samples is 77%.
- Space life experiment: Among 28 samples and 90 culture mediums, the cumulative test is 3064 h for all the 11 experiments. The process and recovery success rate of the samples is 100%.

The payloads successfully implemented 28 scientific experiments in accordance with the experiment process, and a lot of scientific experiment data and clear images and video of experiment process were obtained. A number of experiments presented groundbreaking scientific results: the results of liquid evaporation and phrase change heat transfer in microgravity were measured for the first time, and mam-

malian embryo development was first realized in space. With the future research on the ground, these 28 scientific experiments will continue to bring a large number of scientific and technological achievements with independent intellectual property rights.

6 Future Development Outlook of China Recoverable Satellite

Based on the experience of 25 China recoverable satellite missions, we can summarize several service requirements needed to be enhanced in foregoing China recoverable satellite platform. These items and its technical roads can be generalized as follow:

(a) More recoverable payloads with more chances for orbit access

For scientists, it is still difficult to get a chance to carry out space experiment up to now. The payload mass for recovery and orbit running is still limited. The China recoverable satellite can only provide about 300 kg payloads for recovery and 250 kg payloads is unable to recover. Next, we can enlarge the recovery module to improve its return capability based on the principle of aerodynamic similarity. At the same time, we are considering the satellite to adopt modular design and shelf storage to provide shuttle bus space mission services for scientists.

(b) Better performance and service for space experiments

Space science experiments using recoverable satellite require, in particular, better microgravity levels and radiation conditions. At the same time, it requires the platform to provide convenient and sufficient service capability for instruction, data and communication. Good microgravity levels need to consider the overall performance of quasi stationary and micro vibration frequencies. So in order to construct better microgravity environment, the ways will include the selection of orbit altitude, smaller drag area along the direction of flight, and disturbance reduction of moving parts dwell on satellite platform. If necessary, active or passive vibration isolation measures should be taken to ensure that some bands have ultra clean micro-vibration environment. Satellite platform already have several technical means to ensure adequate instructions, data, power supply and other services for experimental projects, which can fully meet this demand.

(c) Lower cost

Space science experiments using spacecraft space flight methods are still a costly means. Recoverable satellites are relatively inexpensive compared to space stations, but current costs still need to be further improved greatly. The main solution is to carry out comprehensive low-cost design, development and testing. In particular, the whole satellite should adopt the technologies, such as non-destructive recovery and reuse technology, low-cost materials and structural technology, and high-integration,

commercial devices used on-board electric systems. And it is also required to consider using the global business aerospace TTC network and the internet based experimental control to carry out the satellite operation.

7 Conclusion

Focusing on high performance and low cost system design, several key technologies such as high microgravity level security, high load ratio system design, thermal control technologies for high thermal consumption loads, space experiment management for multi-loads, massive reuse of aerospace products, low cost system development were studied and solved in SJ-10 satellite. The satellite performance was greatly improved, and the cost was well controlled. The in-orbit flight test shows that the technical indexes of the satellite meet the scientific experiment requirements very well. The satellite can provide a high performance, high reliability and low-cost space experiment platform for domestic and foreign scientific and engineering users, and has broad application prospects.

Acknowledgements We credit numerous people who made the SJ-10 satellite a success. During the development of the satellite, we have done a lot of design and integration verification work, and here we would like to thank my team of designers particularly. It was their hard work over the past few years for supporting and ensuring the successful implementation of China's first microgravity scientific satellite mission. System designer, Ying Wang and her partners overcame many difficult problems. Our eleven sub-system chief designers also did great favors to success of the mission. As general directors, I and Jiawen Qiu thanks them from our heart. We also want to give our great thanks to Bochang Tang, our project engineering chief designer and our project office partners. Everybody did his best to our mission success. Thank them all sincerely.

References

Curtis HD (2005) Orbital mechanics for engineering students, 1st edn. Elsevier Butterworth-Heinemann, Oxford

Sidi MJ (1997) Spacecraft dynamics and control: a practical engineering approach. Cambridge University Press, London

Space Radiation Systems Biology Research in SJ-10 Satellite

Yeqing Sun, Wei Wang, Meng Zhang, Lei Zhao, Dong Mi, Binquan Zhang, Dazhuang Zhou and Shenyi Zhang

Abstract Space radiation biology is one of the important parts of space biology, mainly focusing on the mechanisms of biological effects and genetic variations in organisms induced by space radiation. Space radiation biological effects cannot be described by a simple dose-effects relationship due to the complexity of space radiation environment. The diversity of space radiation induced biological mechanisms and the uncertainty of the synergetic interaction between space radiation and microgravity should be considered from the views of multidimensional and systematic ways. The system biology approaches should be used to study the relationships between the space radiation qualities and the space radiation induced biological effects, which are to find the main mechanisms and the key stressors to induce the mutagenic effects. This study investigates the space radiation qualities and the corresponding biological effects with the aid of SJ-10 satellite. The approaches of data mining and system biology are used to analyze these datasets. In the experiment, biological materials (*O. sativa* seeds, *A. thaliana* seeds and *C. elegans*) were located in three different bio-radiation boxes to obtain three distinct radiation environments inside the satellite. The absorbed dose, absorbed dose rate, linear energy transfer, and dose equivalent were measured with the use of active and passive radiation detectors. The biological samples irradiated by the space radiation within the satellite were harvested. After recovery of the satellite, by applying phenotypic and physio-

Y. Sun (✉) · W. Wang · M. Zhang · L. Zhao
Institute of Environmental Systems Biology, College of Environmental Science and Engineering, Dalian Maritime University, Dalian, Liaoning, People's Republic of China
e-mail: yqsun@dlmu.edu.cn

D. Mi
Department of Physics, Dalian Maritime University, Dalian, Liaoning, People's Republic of China

B. Zhang · D. Zhou · S. Zhang
National Space Science Center, Chinese Academy of Sciences, Beijing, People's Republic of China

E. Duan and M. Long (eds.), *Life Science in Space: Experiments on Board the SJ-10 Recoverable Satellite*, Research for Development,
https://doi.org/10.1007/978-981-13-6325-2_3

logical analysis as well as system biology analysis such as genome epigenetic and proteomic scanning to biological samples. The biological changes under different radiation qualities will be analyzed and relevancy between biological effects and radiation parameters will be studied.

Abbreviations

AFLP	Amplified fragment length polymorphism
ANOVA	Analysis of variance
BRB	Bio-radiation boxes
ced-1	Cell death abnormality protein 1
CR-39	Columbia Resin #39
DDR	DNA damage response
DE	Differentially expressed
DSB	DNA double-strand breaks
dys-1	Dystrophin-1
GCRs	Galactic cosmic rays
GO	Gene Ontology
HIMAC	Heavy Ion Medical Accelerator in Chiba
HZE	High charge and high energy heavy ions
IQR	Inter Quantile Range
LEO	Low earth orbit
LET	Linear energy transfer
pgm	Phosphoglucomutase
PIN2	Auxin efflux carrier component 2
rad-51	DNA recombination and repair protein
RF	Random forest
SAA	South Atlantic anomaly
SEPs	Solar energetic particles
SITEL	Silicon Telescope
SNDE	Slow Neutron Dose Equivalent
SVM	Support vector machine
TEs	Transposable elements
TLD	Thermoluminescent dosimeters
ttg	Transducin/WD40 repeat-like superfamily protein
unc-54	Myosin-4

1 Introduction

Space radiation biology is one of the important parts of space biology, mainly focusing on the mechanisms of biological effects and genetic variations in organisms induced by space radiation. The main sources of space radiation in low earth orbit (LEO) include galactic cosmic rays (GCRs), solar energetic particles (SEPs), geomagnetic trapped belts, and albedo particles (Chancellor et al. 2014). GCRs originate from space outside the Solar System where high energetic particles are involved. GCR particles consist of 98% baryons and 2% electrons, and the baryonic component is composed of 85% protons, 14% alpha particles and 1% heavy ions (Lebel et al. 2011). High charge and high energy heavy ions are termed as HZEs. Although the fluxes of HZE particles in GCR are low their contribution to the radiation dose equivalent is high compared to those from other types of radiations, because their radiation quality factors are large due to their high linear energy transfer (LET) (Hada et al. 2007). In addition, HZE particles are difficult to be shielded due to their long range. Therefore, HZE particles are considered as the main factors to induce the biological effects in LEO.

SEPs emitted by the Sun are mainly protons with the energy ranges from 10 to 1000 MeV. SEPs are observed as random events, and the occurrence frequency and intensity of SPEs are related to the solar-cycle phase, typically high in the peak years of the solar activity (Cucinotta et al. 2013). The geomagnetic trapped belts or radiation belts, also called Van Allen belts, are the main regions of the bounded energetic particles originated from the interactions of GCRs and SEPs with the Earth's magnetic fields and the atmosphere, including the inner belt and outer belt. The inner belt is formed mainly by protons, while the outer belt is mainly consisted by electrons. The radiation belts extend over a region from 200 km to about 75,000 km around the geomagnetic equator. Of special importance for LEO is the so-called South Atlantic anomaly (SAA) where the radiation belt extends down to 200 km, which is due to an 11° inclination of the Earth's magnetic dipole axis from the rotation axis. The radiation received is remarkably increased when spacecrafts pass through the SAA. Albedo particles are mainly protons and neutrons scattered from the Earth's atmosphere.

All the primary radiation particles from different sources can produce a variety of secondary particles, such as secondary heavy ions, light ions, neutrons and gamma rays. Through nuclear reactions and bremsstrahlung when they pass through the material of spacecraft and the instruments and equipment inside the spacecraft (Cucinotta et al. 2011). In general, these complex particles in spacecraft can firstly induce the biological damage of genetic material, such as DNA double-strand breaks (DSB), gene mutations (Bessou et al. 1998) and chromosomal aberrations (George et al. 2001), then cause the cellular dysfunction and even cell inactivation, which can lead to a series of pathogenic risks, including carcinogenesis (Durante and Cucinotta 2008), degenerative tissue effects [such as cataracts (Cucinotta et al. 2001), heart disease (Preston et al. 2003), acute radiation syndromes (Durante 2014)] and the damage to the central nervous system (Cucinotta et al. 2014). Therefore, space radiation are

generally considered to be one of the most important risk factors in space environment (Durante and Cucinotta 2008), and the potential for adverse health effects of radiation will limit further development of long-duration space missions (Cucinotta et al. 2013).

2 Foundations of This Research

In early time, the dry seeds were mainly used to study the biological effects and their mechanisms induced by space radiation; and the phenotypes of plants grown from the carried dry seeds were observed after recoverable satellites or spacecrafts were landed from space flight. With the development of the experimental methods and equipments, the biological effects induced by space environment in some model animals, e.g., chromosomal aberration, functional genomics and its methylation were also investigated in our lab. These studies indicated that the anti-stress mechanism can be activated by space radiation, and cause a series of biological effects in model organisms. In addition, the biological effects can also be affected by the persistent microgravity environment, suggesting that the biological effects and mechanisms induced by the space environment are very complicated.

We have sent 50 varieties of seeds of *Oryza sativa* (L.) on board recoverable satellites (e.g., "JB-1", "20th and 21th recoverable satellites") and spacecrafts (e.g., "Shenzhou-3", "Shenzhou-4", and "Shenzhou-6") since 1996. After landing from spaceflight, the seeds of *O. sativa* (L.) were planted standard in the laboratory and field, and then the phenotype variations, cytological effects, the characteristics of genomic mutations, and the change of protein profiling and genomic methylation were further studied from the levels of phenotype, cytology and molecule, etc.

For example, we have found that the mutation rates of phenotype in ten varieties of *O. sativa* (L.) after boarding Shenzhou-3 flight were significantly increased, which showed that different varieties of *O. sativa* (L.) have different sensitivities to space radiation environment. Furthermore, we have researched the phenotype variations of plant height, effective spike number and leaf color in the second generation of *O. sativa* (L.) carried in Shenzhou-3, and the results showed that the mutation rate ranged from 0.05 to 0.52% (Yu et al. 2007), which indicates that space radiation can induce a large widely variations in phenotypic characters. In addition, the inheritable effects could also be observed in these results. In order to compare the difference between the biological effects induced by space radiation and γ-rays, we have investigated the induced effects in the 24 varieties of var. *japonica* and var. *indica* of *O. sativa* (L.) with different maturation periods, which were exposed in Shenzhou-4 spacecrafts and γ-rays simulated in the ground, respectively. In the level of plant height and ripening rate, the result showed that the biological effects caused by space radiation in different varieties of var. *japonica* were equivalent to the mutagenic effect induced by 10–50 Gy γ-rays, and the characters of stimulated effects were obviously observed in the different varieties of *O. sativa* (L.) (Wang et al. 2006; Wei et al. 2006b; Xu. 2000). Furthermore, most of the varieties insensitive to γ-rays were also not sensitive to

space radiation either, while half of the varieties sensitive to space radiation were also sensitive to γ-rays. The phenotypic results of second generation mutation indicated that space and γ-ray radiations could also induce the mutations in plant height and heading stage, while there was a significant difference in mutation frequency of phenotypes between them (Wei et al. 2006b). All these results indicated that the mutation mechanisms of space radiation were different from those of γ-rays in the ground due to the differences in particle type and energy, radiation dose and dose rate, etc. between two kinds of radiation conditions.

To study the mutagenic effects and mechanisms of space radiation, we put dry seeds of *Zea mays* (L), heterozygous for Lw_1/lw_1 alleles (The mutation of Lw_1 gene will lead to yellow stripes on leaves, which can be used as an indicator of mutagenic effects of space radiation.), sandwiched biostack between nuclear track detectors aboard "JB-1" satellite for 15 days (Mei et al. 1998). After landing, the radiation doses and the corresponding mutations of morphology and molecule were detected, and the results showed that the radiation dose and dose-rate, measured by LiF detector, were 2.656 mGy and 0.177 mGy/d respectively. And, the flux of radiation particles with $Z \geq 3$ was 29/cm^2, and the average LET was about 0.5 keV/μm, which means that the majority particles penetrated the shielding of the satellite are high energy protons (Mei et al. 1998). In addition, the results also showed that the phenotypic mutations of yellow stripes were associated with the hit numbers of radiation particles in the *Z. mays* (L), while further study is needed for a better understanding of the nature mechanisms (Mei et al. 1998).

Furthermore, we have studied the phenotypic mutation, chromosomal aberration and mitotic index of root tip meristem in 9 varieties of *O. sativa* (L.), which were exposed in "20th recoverable satellite" for 21 days. And the same variety seeds were irradiated with the same radiation dose as spaceflight (2 mGy) but different LETs by Heavy Ion Medical Accelerator in Chiba (HIMAC). The results showed that the mutagenic effects on the above indexes caused by space radiation were significantly higher than those of Iron ions radiations (500 keV/μm), Neon ions radiations (31 keV/μm) and Carbon ions radiations (13.3 keV/μm) (Wei et al. 2006a). Similarly, the chromosomal aberration and mitotic index in different varieties of *O. sativa* (L.) experienced in Shenzhou-4 were also significantly higher than those of the treatment in the ground (Wei et al. 2007), which suggests that space environment can stimulate the processes of mitosis and halt the cell division at metaphase. And, the chromosome aberration of *O. sativa* (L.) in the space environment was higher than those of γ-rays and heavy ions radiations in the ground (Wei et al. 2006a), which indicates that the mutation mechanisms induced by different kinds of radiation might be different.

To reveal the genetic variation mechanisms of *O. sativa* (L.) induced by space radiation environment on the levels of phenotype and cell, we have found some differentially expressed genes in the stable mutants of *O. sativa* (L.) (e.g. 972-4), in which some can also be identified as new resistance genes (Li et al. 2004; Zhang et al. 2011). In addition, the method of amplified fragment length polymorphism (AFLP) was used to analyze the characteristics of genome mutations of *O. sativa* (L.) after Shenzhou-3 spaceflight. In the second generation mutation of *O. sativa*

(L.) experienced Shenzhou-3 mission, we have found that the genome mutation rate ranged from 1.7 to 6.2% in the 479 polymorphism loci (Yu et al. 2007). We compared the characteristics of the genome mutations in the three different mutants induced by spaceflight and other 11 cultivars of *O. sativa* (L.) and found that the mutated sites in the three mutations were 75.9, 84.9 and 100% in the polymorphic regions of interspecific genome, indicating that there was a preference in the presence of genome for the mutation effects induced by space radiation. That is, there are "hot spot" regions in the genomic mutations caused by space radiation (Li et al. 2007).

We analyzed the protein expression profiles of *O. sativa* (L.) experienced "JB-1 satellites", "Shenzhou-6 spacecraft", and "20th and 21th recoverable satellites", for investigation of protein expression profiles of rice plants after spaceflights and the hereditary capacity in the offspring plants, clustering and principal component analysis were performed to summarize and compare the protein expression variations between the space samples and their corresponding ground controls in different spaceflights and in 1st and 2nd generations. Results indicated that protein expression profiles were changed after seed space environment exposures onboard the satellite or space craft, but there were variations in the degree of difference in different types of flights: the longer the flight duration lasted, which meant that rice seeds were affected by space radiation environment heavier, the greater differences existed in protein expression profiles. Distribution of biological processes of differentially expressed proteins indicated that physiological and biochemical changes of rice cells were induced by space environment. The biological processes impacted in 1st generation plants after flights were nucleic acid metabolic process, light reaction, proteolysis, defense response to fungus, response to stress with amino acid and derivative metabolism. Alterations of protein expression profiles in 1st generation would resume or recover in the corresponding 2nd generation plants; the degree of recovery was associated with the sensitivity of the rice variety to environment. Changes of proteins involving in biological processes such as cell wall organization, nucleic acid metabolic process, proteolysis, RNA-dependent DNA replication, amino acid and derivative metabolism, pentose-phosphate shunt, response to stress tended to recover in 2nd generation plants; while seed maturation, protein folding, glycolysis, lipid biosynthetic process, glycogen biosynthetic process and tricarboxylic acid cycle related proteins only differentially expressed in 2nd generation plants. Therefore, the biological effects of space environment could be reflected in protein expression level (Ma et al. 2007; Wang et al. 2008).

To analyze the relationship between the genomic and epigenetic changes, we analyzed the genomic methylation in *O. sativa* (L.), which have been exposed in the spaceflight and heavy ions simulated radiation on the ground. The results showed that space flight and heavy ion simulated radiation could cause the changes of genetic methylation in genomic DNA, and the changes of methylation were more pronounced in the contemporary phenotypic variants (Shi et al. 2009, 2014b). The special sites could also be observed in the changed regions of methylation (Shi et al. 2009, 2014b). Most importantly, the polymorphisms in DNA methylation caused by space flight and heavy ionization radiation were associated with the polymorphisms of their corresponding genomic sequences. That is, a higher degree of methylation will lead

to a higher change of the corresponding genomic mutations. However, determination of the sequences of the polymorphic sites showed that the distribution of the site of methylation changes was significantly different from those of genomic changes. For example, the changes of methylation were occurred in the coding region, while the changes of the genomic sequence were occurred in the repetitive sequence region. Further studies focused on the corresponding gene expressions of the methylation changes in the coding region of genome, and the results showed that the expressions of the nucleotide metabolism, molecular chaperone family and heat shock protein related genes were changed, which preliminary revealed that methylation changes induced by space environment may be associated to genome instability (Shi et al. 2014a).

The similar results can be found in the studies of Ou et al., which also showed that the genomic methylation and the expressions of the corresponding gene were changed in *O. sativa* (L.) after spaceflight. The expression of 6 transposable elements (TEs) and 11 genes were also identified, and the changes of the DNA methylation of TEs were generally occurred at the CG and CNG sites, whereas the changes of the DNA methylation of other genes were generally occurred only at the CNG sites (Ou et al. 2009). Our studies also indicated that the carbon ion radiations can induce the polymorphism changes of DNA methylation in *O. sativa* (L.), the level of DNA demethylation was significantly higher than that of DNA methylation, and the changes of the DNA methylation were general in the CNG sites (Zhao et al. 2016a).

These results give rise to a new question that why such a significant biological effects were induced by the extremely low dose (mGy order of magnitude) of space radiation in the LEO. It is still unclear that whether it is caused by the hit of HZE or the persistence of microgravity in space. To study the synergistic effect of space radiation and microgravity on organisms, dauer larvae of *Caenorhabditis elegans* (L), including *dys-1* (dystrophin-1) mutant, *ced-1* (cell death abnormality protein 1) mutant, and wild-type, were divided into nine groups and put into the special SIMBOX devices in Shenzhou-8, and they were exposed to three different conditions: spaceflight, spaceflight control (in a 1 × g centrifugal device), and ground control. During 7 h after the landing of the re-entry vehicle, the mRNA (Gao et al. 2015a) and miRNA (Xu et al. 2014) expression profiles were performed enrichment analyses by distribution characteristics, biological processes and signal pathways, with particular attention given to DNA damage response (DDR) processes (Xu et al. 2014). The results showed that the spaceflight synergistic environment increased the quantity and significance of differentially expressed genes and miRNAs than space radiation environment in wild-type *C. elegans* (L). And compared the *dys-1* mutant and *ced-1* mutant with the wild-type, we found that the limited transcriptional differences were detected between the microgravity and non-microgravity environments in the gravity-sensing defective *dys-1* mutants, and the radiation-sensing mutant *ced-1* had an enhanced radiation response. Results indicated that, microgravity, depending on gravity sensor, enhanced the DNA damage response in the presence of space radiation, and probably play a vital role on DDR during short-duration spaceflight (Gao et al. 2015b).

In brief, the previous results have indicated that space radiation and microgravity environment are the main stress factors to cause the biological effects in the model plants and animals. And the mutagenic effects including phenotypic variations and cytological effects are associated with genomic mutations in the regions of "hot spots", transcriptome and proteomic changes, indicating the changes were involved with epigenetic regulations.

3 Significance of This Research

It can be seen from the above discussions that the space radiation biological effects cannot be described by a simple dose-effects relationship due to the complexity of space radiation environment, the diversity of space radiation induced biological mechanisms, and the uncertainty of the synergetic interaction between space radiation and microgravity, etc., and should be considered from the perspective of multidimensional and systematic views of point. Firstly the qualitative and quantitative analysis of the space radiation quality on bio-samples should be analyzed to obtain the data for incentives analysis. Secondly, the biological effects induced by space environment will be detected on molecular, cellular and phenotypic levels, but whether it can lead to damage or repair, depends on complex organisms function of molecular network regulation. Therefore, the biological mechanism of space radiation induced effects is very complex, which is involved in different levels and dimensions. And then, the system biology approaches should be used to study the relationships between the space radiation qualities and the space radiation induced biological effects, which are to find the main mechanisms and the key stressors to induce the mutagenic effects. In addition, this will also contribute to discover the space environment sensitive biomarkers to provide the basic data for further space radiation risk assessment and early risk warning in the long-term space missions.

This study investigates the space radiation qualities and the corresponding biological effects with the aid of SJ-10 satellite by integrating the space radiation detection technology. The approaches of data mining and system biology are used to analyze these datasets from the point of genetics and epigenetics, reveal the space radiation environment of biological genetic variation and damage mechanisms. Therefore, the following description includes two main aspects: "project design and implementation" and "progress of the research on space radiation systems biology". And the first one will be depicted in detail on "project design", "selection of space radiation detectors and model organisms", and "manufacture of bio-radiation box". The later one will be composed of "methods and results of space radiation measurements", "space radiation induced biological effects", and "analysis for space radiation systems biology researches".

4 Project Design and Implementation

4.1 Project Design

The research of this project focuses on the space radiation systems biology, as shown in Fig. 1. The various integration of radiation measurement unit and model organism unit results in three different bio-radiation boxes (BRB). They could provide comprehensive information of the space radiation environment and the corresponding biological effects at different levels, which could be quantitatively analyzed. Data integration and the corresponding analysis of systems biology are carried out so as to systematically describe the mechanisms of the biological effects of space radiation and its relationship with the space radiation quality.

4.2 Selection of Space Radiation Detectors and Model Organisms

4.2.1 Selection of Space Radiation Detectors

In order to measure the space radiation completely received by the model organisms, the space radiation measurement module for this research is combined of active detectors and passive detectors, which are listed in Table 1. The active detectors

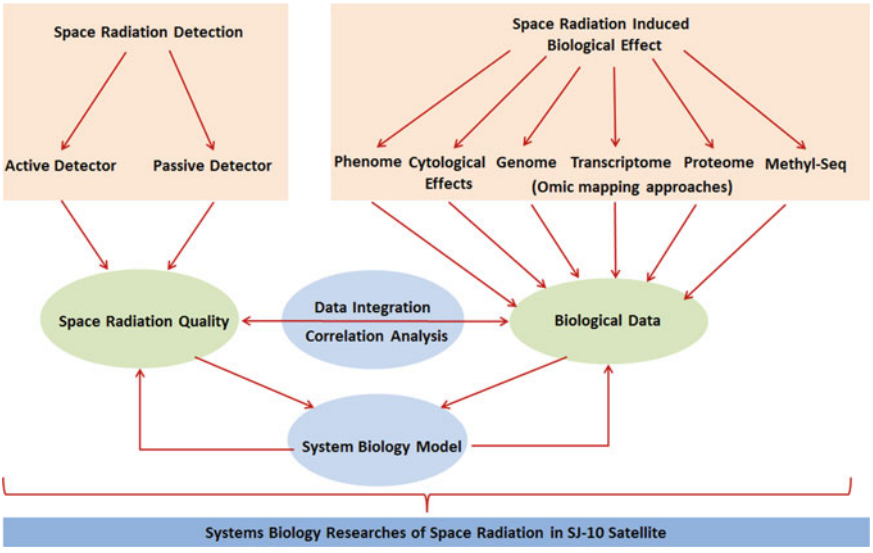

Fig. 1 Framework of the research on space radiation systems biology

Table 1 Space radiation detection modules and its function used in this project

Space radiation detection modules		Types of radiation measured	LET (keV/μm)	Dose	Dose equivalent	Flux
Passive detectors	TLD	Proton, electron, X-ray	/	√	/	/
	CR-39	High LET radiation	≥5	√	√	√
Active detectors	SITEL	Proton and heavy ions	0.1–230	√	√	√
	SNDE	Neutron with energy from 0.025 eV to 10 MeV	/	/	√	√

Note The symbol of "√" indicates that the detector have such a function, while the symbol of "/" indicates that the detector do not yet have such a function

include the Slow Neutron Dose Equivalent (SNDE) detector and the Silicon Telescope (SITEL). The SNDE detector is designed to measure the radiation equivalent dose rate of neutrons in space, with the ^{3}He gas proportional counter. In order to moderate the fast neutrons, the ^{3}He counter is in the center of a polyethylene sphere with a diameter of 15 cm. The SNDE detector could measure the neutron dose equivalent rate in the range of 1 μSv/h–10 mSv/h. The SITEL detector consists of two silicon semiconductor detectors, which have a thickness of 300 μm and a diameter of 26 mm. From the energy loss of the particles in the silicon detector, the LET values of the particles could be calculated. The detected LET spectrum is from dosimeters (TLD) and Columbia Resin #39 (CR-39) plastic nuclear track detectors. In order to accurately and comprehensively measure the radiation quality for radiation received by the model organisms, the TLD and CR-39 detectors were placed together with the organisms.

4.2.2 Selection of Model Organisms

O. sativa var. *japonica* (L), *Arabidopsis thaliana* (L) (*col*) and *C. elegans* (L) were selected in this research by considering the different mechanisms of space radiation biological effects between inter-species (model plant and animal), and monocotyledon and dicotyledons. Because of the different genetic background of each variety in the same species, six varieties of *O. sativa* var. *japonica* (L) seeds were carried on SJ-10 satellite, including Nipponbare, Koshihikari, Zhenzhuhong, Dongnong416 (DN416), Dongnong423 (DN423) and 433. In addition, the seeds of the wild type of *A. thaliana* (L) (*col*) and 3 mutants were also carried on SJ-10 satellite for studying the different mechanisms of biological effects induced by radiation and microgravity, as shown in Table 2.

Table 2 Cultivars of model varieties and their functions selected in this study

No.	Varieties	Cultivars	Characteristic
1	*O. sativa* var. *japonica* (L)	Nipponbare	Model variety of *O. sativa* var. *japonica* (L)
2		Koshihikari	Sensitive to space environment
3		Zhenzhuhong	Sluggish to space environment
4		Dongnong 416	Sluggish to space environment
5		Dongnong 423	Sensitive to space environment
6		433	Compact panicle varieties
7	*Arabidopsis thaliana* (L)	Columbia (*col*)	Model varieties of *Arabidopsis thaliana* (L)
8		PIN2 mutant	Mutant of auxin transport protein, which affects to the mechanism of plant response to gravity
9		*pgm* mutant	Lack mutant of starch grains, which affects to the gravitropism of the root
10		*ttg* mutant	Mutant of the blocked anthocyanin synthesis

Fresh seeds were harvested in 2015 for spaceflight and ground-control, and 200 main spikes were selected for each variety. Three copies of seeds were taken from each of the main spike to detect the germination rate and purity identification, where the following conditions should be required: the germination rate was greater than 98%, while the purity identification that was detected by the AFLP molecular marker should be less than 1%. These seeds which meet the above conditions were randomly divided into 6 copies: three copies for ground-control, three copies for spaceflight. And ground-control and spaceflight copies were placed into the BRB-A, -B, and -C, respectively.

To further compare the mechanism difference of space radiation biological effects in the model animal, N2 (wild-type) strain, two microgravity perception mutant strains (*dys-1*: anti-muscle atrophy protein defect, *unc-54*: Myosin-4, myosin heavy chain structural defect) and two radiation perception mutant strains (*ced-1*: apoptotic defect, *rad-51*: DNA damage repair defect) were selected and carried on SJ-10 satellite, as shown in Table 3. More details about the cultivation, propagation, synchronization for *C. elegans* (L) can be found in our previous publications (Gao et al. 2015a, b, c; Xu et al. 2014).

Table 3 Strains of *C. elegans* (L) and their functions selected in this study

No.	ID.	Strains of *C. elegans* (L)	Function
1	N2	Wild type	Model variety
2	LS292	*dys-1*	Anti-muscle atrophy defect
3	AM141	*unc-54*	Myosin heavy chain structural defect
4	MT4930	*ced-1*	Apoptotic defect
5	VC1873	*rad-51*	DNA damage repair defect

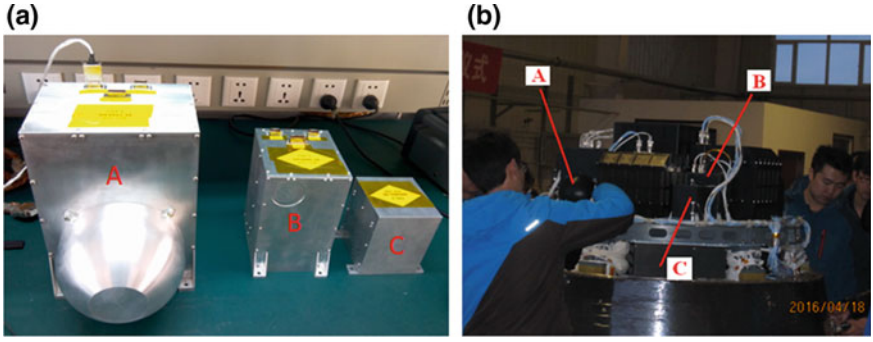

Fig. 2 The BRB and their corresponding arrangement in the satellite

4.3 Manufacture of BRB

The hardware of this research consists of three payloads, i.e., BRB-A, -B and -C, as shown in Fig. 2a. The surface material of the BRBs is aluminum, which has an average thickness of 2.5 mm. In each BRB, both the space radiation measurement module and the model organism module are included.

4.3.1 Space Radiation Detection Module

The radiation measurement module in each bio-radiation box is a combination of different radiation detectors, as shown in Table 4. The passive detectors, TLD and CR-39, are placed within each of the three BRBs. In the BRB-A, the measurement unit also includes both SNDE and SITEL active detectors. Only the SITEL active detector is in the BRB-B, and there is no active detector in BRB-C.

Table 4 Arrangement of the radiation detectors in BRBs

Radiation detectors	Passive detectors	Active detectors	
	TLD+CR-39	SITEL	SNDE
Bio-radiation box A	√	√	√
Bio-radiation box B	√	√	/
Bio-radiation box C	√	/	/

Note The symbol of "√" indicates that the bio-radiation box have such detectors, while the symbol of "/" indicates that the bio-radiation box do not yet have such detectors

4.3.2 Model Organisms Culture Modules

There are three types of model organism units: the sandwich-like biostacks (Fig. 3a, b), the seed bags and the *C. elegans* (L) container (Fig. 3c, d). Biostacks and seed bags are placed within each BRB. The *C. elegans* (L) container is placed only in the BRB-C. The biostacks are designed to provide the radiation information of heavy ions which hit the plant seeds. In the biostacks, the plant seeds are reserved in the organic material and fixed using non-toxic glue. Above the plant seeds are two layers of CR-39 detector, which could measure the heavy ions that hit the seeds. In each biostack, besides CR-39 detector, there are also four TLD detectors, of which two are TLD-600s and two TLD-700s. During the experiment, a total number of 576 rice seeds and a number of 4800 *A. thaliana* (L) seeds are in the biostacks. In the seed bags, there are different varieties of rice seeds, as well as radiation detectors of TLD and CR-39. The *C. elegans* (L) container is divided into eight small rooms. Each room contains a different type of *C. elegans* (L). Above the rooms there are four CR-39 detectors.

After the matching test under rigorous quality control, the model organisms were placed in the respective model organism unit of the BRB-A, -B and -C. The BRBs were then installed in re-entry capsule of SJ-10 satellite. The look direction of BRB-A, -B and -C is -Y Axis, -Z axis and +X axis of the satellite respectively (Fig. 3b). The altitude of SJ-10's orbit is 252 km and the inclination angle is 42°. After the flight on orbit of 12.5 days, the three boxes including the radiation measurement modules and the model organism modules were returned to the laboratories. From the radiation measurement modules, space radiation quantities such as LET spectrum, radiation absorbed dose, dose equivalent, et al. could be achieved. The contributions to the radiation qualities from different types of particles (protons, heavy ions and neutrons, etc.) were also studied. The biological phenotype, functional genome, genome methylation, and proteome of the model organisms would be fully analyzed.

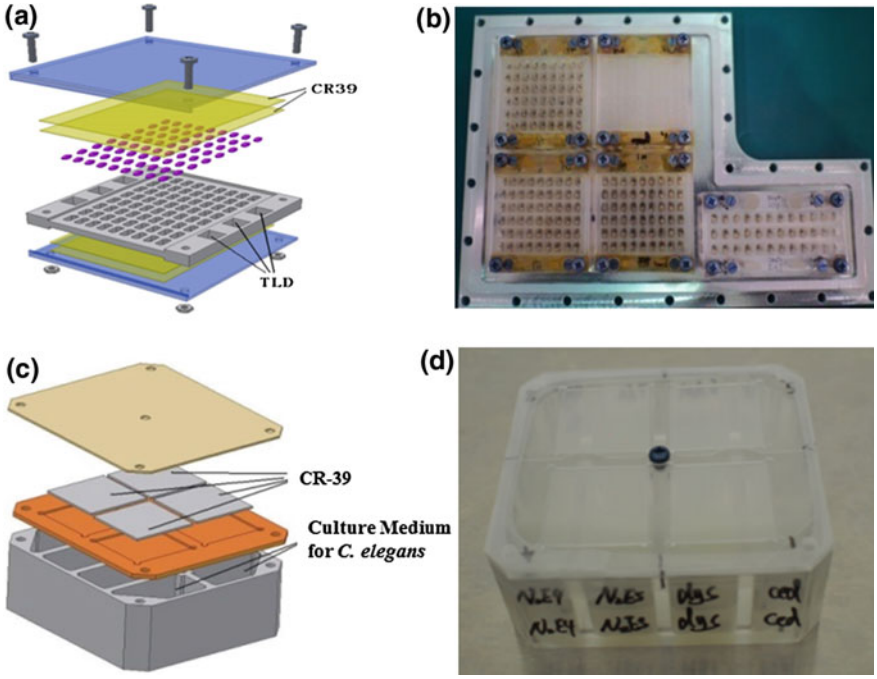

Fig. 3 The biostack (**a**, **b**) and the *C. elegans* (L) container (**c**, **d**)

5 Progress of the Research on Space Radiation Systems Biology

5.1 Methods and Results of Space Radiation Measurements

5.1.1 LET Methods of Space Radiation Detection

The LET values of the GCR heavy ions, the radiation physical quantities and the radiation spectrum have not been accurately measured in previous studies of space biological effects. The CR-39 nuclear track detectors in this research of SJ-10 and LET methods were used for the first time to achieve these measurements. These results would be useful for quantitatively studying of the relationships between the biological effects and LET values.

Detailed approaches to the LET spectrum of CR-39 detectors in radiation measurements can be found in the related papers (O'Sullivan et al. 1999; Reitz et al. 2009; Zhou 2012; Zhou et al. 2006a, b, 2007, 2008, 2009, 2010, 2011). The key processes of the LET spectrum method include: design of the CR-39 detector stack, LET calibrations with the heavy ions and protons generated by accelerators, space radiation exposure of the detector stack, detector stack recovery and chemical etch-

ing, microscopic scan and identification of the nuclear tracks and data acquisition, data analysis and processing, accurate calculation of the LET value for each particle event and the generating of differential/integral LET spectrum. The HZE particles can be obtained from the coincident tracks during the scan, and the distance between the HZE particle and the biological sample can also be accurately measured.

5.1.2 Preliminary Results of Space Radiation Measured in SJ-10

According to the number of GCR heavy ions hitting on the seeds of *O. sativa* (L), the total of 576 seeds in the biostacks is divided into nine groups, and the seed number of each group is shown in Fig. 4a. Result shows that, among the 576 rice seeds, about 9.9% of rice seeds were not hit by heavy ions. About 18.2% of the seeds were hit once, 23.1% of the seeds were hit twice, and about 48.8% of the seeds were hit no less than three times. It's also found that there are seven rice seeds, each of which is hit by eight heavy ions.

Figure 4b shows the LET spectrum measured by SITEL and CR-39 detectors. The LET spectrum obtained is in the range from 0.1 to 1700 keV/μm. The LET spectrum of 10–230 keV/um from the SITEL active detector agrees well with those from CR-39 passive detectors. The results has been published on "Journal of Geophysical Research: Space Physics" (Zhou et al. 2018). In addition, the radiation absorbed dose rate and dose equivalent rate were 0.072 mGy/d and 0.162 mSv/d, respectively, which were lower than the absorbed dose rate of 0.2–0.3 mGy/d and dose equivalent rate of 0.4–0.6 mSv/d on the international space station. This is mainly due to the fact that the fluxes of the Galactic cosmic rays and the radiation belt particles are decreased in the orbit of SJ-10, compared to those for the International Space Station (orbit altitude: 370 km/403 km).

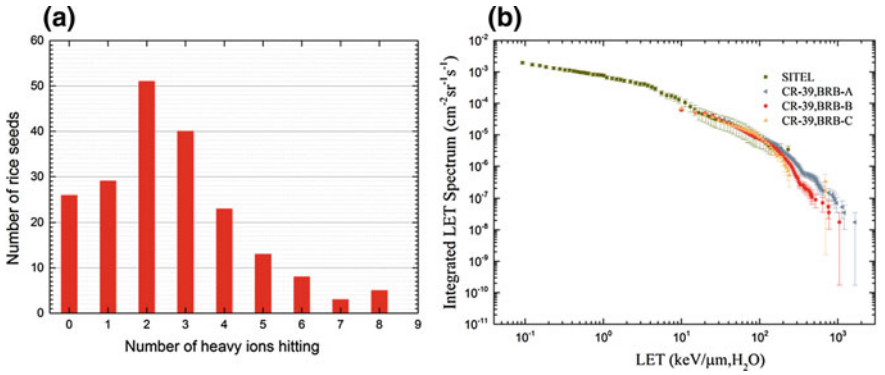

Fig. 4 **a** The distribution of the rice seed numbers according to the number of heavy ions hitting on the seeds; **b** the LET spectrums achieved from the SITEL and CR-39 detectors in the BRBs

5.2 *Biological Effects Induced by Space Radiation*

5.2.1 Biological Effects in Different Varieties of *O. sativa* (L)

In order to observe the biological effects induced by space radiation on *O. sativa* (L) at different growth stages, different varieties of *O. sativa* (L) seeds from seed packets undergone SJ-10 flight, including Nipponbare, Koshihikari, Zhenzhuhong, DN416 and DN423 were grown in the artificial climate room after spaceflight. The deionized water was used at 25 °C for 4 days to measure the germination rate. The Yoshida medium was used for rice cultivation in artificial climate chamber (25 °C, 12 h light, 60% relative humidity, 3000 lx of the light intensity) till the three-leaf stage for further studies. And these biosamples were used to analyze the changes of phenotype, antioxidant enzyme systems and the expressions of genes and proteins. For example, as the phenotype of the Nipponbare of *O. sativa* var. *japonica* (L), the results showed that there was no significant change in seed germination after spaceflight ($p > 0.05$). But, the heights of the seedlings in spaceflight were higher than those in ground-control. And the heights of seedlings were higher significantly than those of the ground-control group after the fourth day ($p < 0.05$), as shown in Fig. 5, indicating that spaceflight has stimulation effect to the height of seedling stage of *O. sativa* (L).

In addition, the phenotypes of the *O. sativa* (L) were observed from the four-leaf stage to the mature stage when growing in the fields. The seeds from seed packets undergone SJ-10 flight were firstly sprouted at 25 °C after 48 h for germination, and

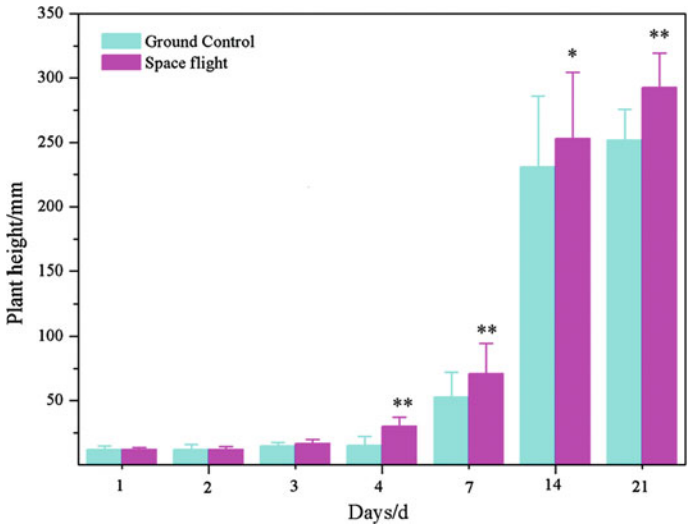

Fig. 5 The dynamic curve of the height of the rice induced by spaceflight in SJ-10 satellite. The data was depicted in the mean ± standard deviation

then planted in special discs. Finally, the seedlings were transplanted to the field on May 30th, 2016. DN416 and DN423 were planted in Wu Chang, and Nipponbare, Koshihikari and Zhenzhuhong were planted in Dong Gang, Dandong. More than 500 seeds of each varieties of *O. sativa* (L) were cultivated in the field.

The results showed that the germination rate of the six varieties of *O. sativa* (L) seeds was not significantly changed ($p > 0.05$). Thirty plants were randomly selected, and the plant heights of *O. sativa* (L) and Fv/Fm of photosynthesis parameters were measured at four-leaf stage. The results showed that the height of Nipponbare and DN416 in the spaceflight group were lower than those of in ground control, indicating the inhibition of growing. The plant heights of Koshihikari, Zhenzhuhong and DN423 in spaceflight group were higher than those of in ground control, indicating the stimulation of growing. And the Fv/Fm of photosynthetic parameters was changed in different varieties, suggesting the stimulation and inhibition effects were both existed in this study. The stimulation and inhibition phenomenon still existed on the height of plant and photosynthetic parameters at heading stage. The phenotype, including the number of tillers and effective tillers, the height of plant, the length of spike and awn, the number of grain, immature grain and filled grains, the rate of filled grains and the shape of spikes etc., were also measured at mature stage on Nipponbare, Koshihikari, Zhenzhuhong and 433. These results indicated that, except for the number of filled grains and the rate of filled grains, the other phenotypes were mainly inhibited. In addition, the contrary phenotypic changes between the seedlings and the field plants might be due to the different culture environments and growing stages.

All these results demonstrated that the influence of the phenotypic traits induced by spaceflight is persistent, and related to the growth stage of *O. sativa* (L): the stimulation effect at three-leaf stage, the coexistence of the stimulation and inhibition effects from the four-leaf stage to the heading stage and the growth inhibition effects at mature stage. Further, the cytological effects, such as the chromosome aberration and mitotic index, should also be observed. And the sequencing of the genome, methylation of DNA, and transcriptome, combining with proteomic researches will be detected in further work to explore molecular basis of these changes. The seeds of *O. sativa* (L) that were hit by HZE were chosen for the analysis of biological effects in the further work too.

The seeds of contemporary rice were tested for successive generations. On the phenotypic level, it was found that the number of tillers and effective tillers in the F1 generation of rice was significantly reduced, while the length and grain number of spike presented both growth stimulation and physiological inhibition between different varieties. At the same time, we also found a small number of contemporary suspected phenotypic mutant strains, such as the next generation of rice with the mutation of plant height and mature period showed stable inheritance, as shown in Fig. 6. The mutation of the rice growth period in the spaceflight seed showed that the next generation showed the characteristic of early-maturing mutation. The hereditable changes in phenotypic level can clear shown mutagenesis effect of the spaceflight mutation on rice genetic, and mutation frequency of offspring was obviously higher than that of contemporary. The genome instability cause by the space

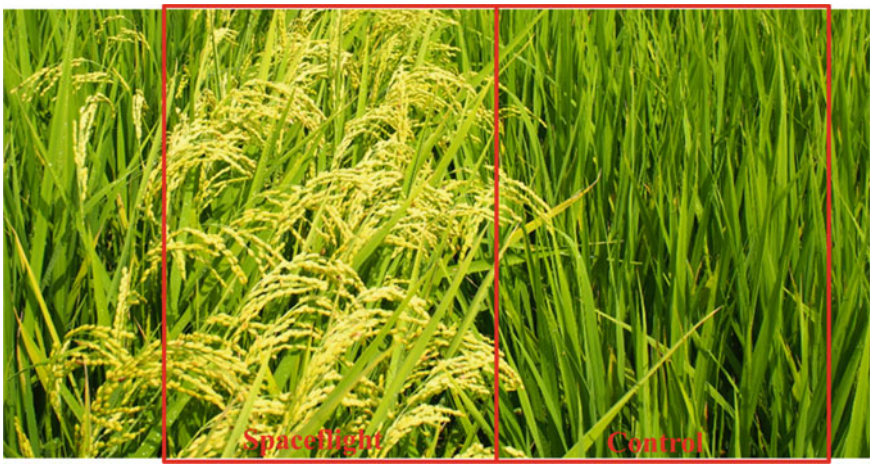

Fig. 6 The hereditable early-maturing mutation of rice seeds offspring after spaceflight

environment was strong evidence of radiation effects. It lays a foundation for the discovery of the biological effect mechanism of space radiation from the molecular level.

5.2.2 Biological Effects in Different Strains of *C. elegans* (L)

After landing to the ground, the survival ability, reproduction ability and locomotion ability were followed during life-cycle for five strains of *C. elegans* (L). Furthermore, by comparing the proteomic changes of the microgravity or radiation defect mutants with that of the wild type *C. elegans* (L) under the conditions of spaceflight and ground, the regulated functions induced by space environment, including the longevity, oviposition, muscle contraction, DNA damage repair process, etc., the mechanism and regulation pathway of the synergistic effects between microgravity and radiation are analyzed in detail.

For the protein profiles, a total of 5,000 *C. elegans* (L) were used as one sample to extract total protein, and then the protein profiles were analyzed by LC-MS/MS. And three experimental replicates were conducted for each treatment. The results showed that a total of 24,407 peptides and 3,343 proteins were identified. The intensities of 3343 proteins were plotted into clustered heat maps, as shown in Fig. 7a. It is obvious to find that the expression patterns were divided into two clusters for the treatments of ground control and space flight, indicating that the proteome of the wild type *C. elegans* (L) was significantly changed after spaceflight. In addition, we selected the differentially expressed proteins by the filtering conditions of the fold-change (spaceflight/ground control), which is greater than 2 or less than 0.5 with $p < 0.05$ (Significant B analysis). The results showed that a total of 175 proteins

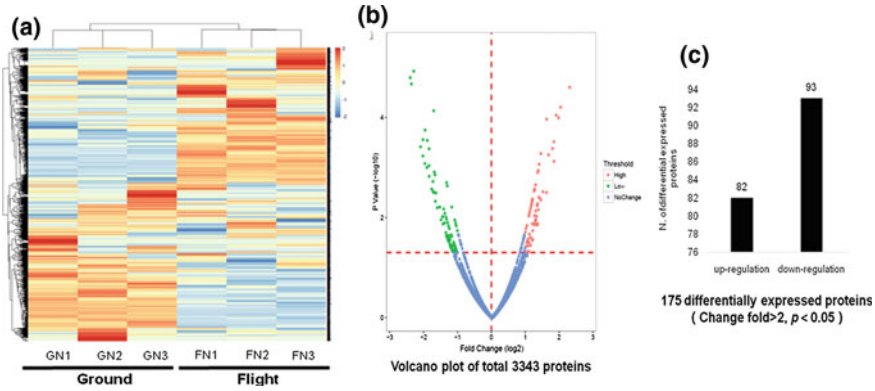

Fig. 7 Protein expression profiles of *wild-type C. elegans* (L) in SJ-10 satellite

were identified as significant changes, in which 82 proteins were up-regulated and 93 proteins were down-regulated, respectively (Fig. 7b, c). The regulated pathways will be further analyzed and discussed for the synergetic biological effects induced by space radiations and microgravity.

5.3 Systems Biological Analysis of Space Radiation Effects

The spaceflight environment can significantly induce the biological responses on the levels of genes and proteins, which are acquired from "omics" technologies, including genomics, transcriptomics, proteomics, etc. At present, "omics" technology is now extensively used to mine potential biomarkers in space biology researches. The characteristics of "omics" datasets obtained directly after spaceflight are always much smaller than the features to be investigated, which can be termed as small samples with big data.

In such cases, the key question is how to mine the sensitive biomarkers of space radiation environment from the high-throughput data. Currently, at least two different strategies can be adopted to deal with this situation (Von Heydebreck et al. 2004). One strategy attempts to use relevant biological knowledge to reduce the set of genes to a manageable number, while the other ignores the dependencies between genes and analyses the data gene-by-gene. In order to select the special genes involved in the biological responses (DNA damage responses, apoptotic gene expression, and miRNAs expression, etc.) of spaceflight environments for Shenzhou-8 mission, our previous studies mainly focused on the first strategy (Gao et al. 2015a, b). By integrated analysis of miRNA and mRNA, we have found that microgravity probably enhanced the biological responses in the presence of space radiation, and suggested a possible synergistic interaction between space radiation and microgravity (Gao et al. 2015a, b; Xu et al. 2014). However, we do not know what kinds of genes are

important and should be studied due to the lack of understanding of the function or pathway of these genes.

Different techniques have been proposed and implemented to select the differentially expressed (DE) genes based on the second strategy (Mutch et al. 2002). Historically, the first method used to identify DE genes was the "fold change", which is performed through a simple fold change cutoff, typically between 1.8 and 3.0 (Aittokallio et al. 2003; Tarca et al. 2006). However, the choice of threshold has a certain degree of arbitrariness, which may give rise to both false negative and false positive results (Mutch et al. 2002). We have ever used the traditional method of fold change to detect the DE genes in the microarray datasets in our previous studies, while the defects in this method are obvious. For example, some genes with small fold-change may have important biological functions, such as transcription factors (Aittokallio et al. 2003; Mutch et al. 2002; Tarca et al. 2006). In addition, the traditional method does not consider the background noise and variability of microarray datasets (Mutch et al. 2002).

In order to overcome the deficiency of the "fold change", the feature selection techniques have been proposed to meet the challenges of biomarkers screening (Saeys et al. 2007). These techniques can be divided into three categories: filter methods, wrapper methods and embedded methods. Each of them possesses advantages as well as disadvantages. Briefly, the filter methods [such as Inter Quantile Range (IQR) (Cordero et al. 2007), *t*-test (Jafari and Azuaje 2006), analysis of variance (ANOVA) (Nadon and Shoemaker 2002), Wilcoxon rank sum (Thomas et al. 2001), etc.] identify the relevance of features by looking only at the intrinsic properties of the data, i.e., the method of "gene-by-gene", which are computationally simple, fast and independent of the classification algorithm (Saeys et al. 2007). However, the main flaws of filter methods are that they ignore the feature dependencies, which may lead to worse classification performance. Wrapper methods [such as sequential search (Inza et al. 2004), genetic algorithms (Ooi and Tan 2003), etc.] embed the model hypothesis search within the feature subset search, while the common drawback of these methods is that they all have a higher risk of over-fitting and computational cost than filter

Fig. 8 Overlapping features based on the feature sets generated by IQR and ANOVA algorithms, reprinted from ref. Zhao et al. (2016b), copyright 2016, with permission from Mutation Research/Fundamental and Molecular Mechanisms of Mutagenesis

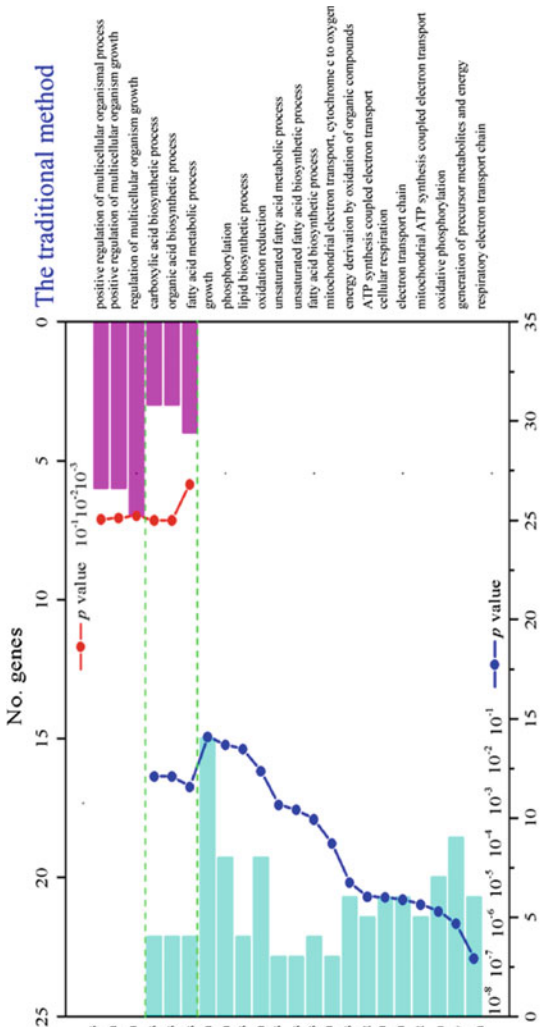

Fig. 9 Biological process of differential expression genes obtained from the traditional method of fold change and the present method of IQR and ANOVA, reprinted from ref. Zhao et al. (2016b), copyright 2016, with permission from Mutation Research/Fundamental and Molecular Mechanisms of Mutagenesis. Differential expression genes were annotated by GO using DAVID software, GO terms with computed *P* values less than 0.05 were considered as significantly enriched

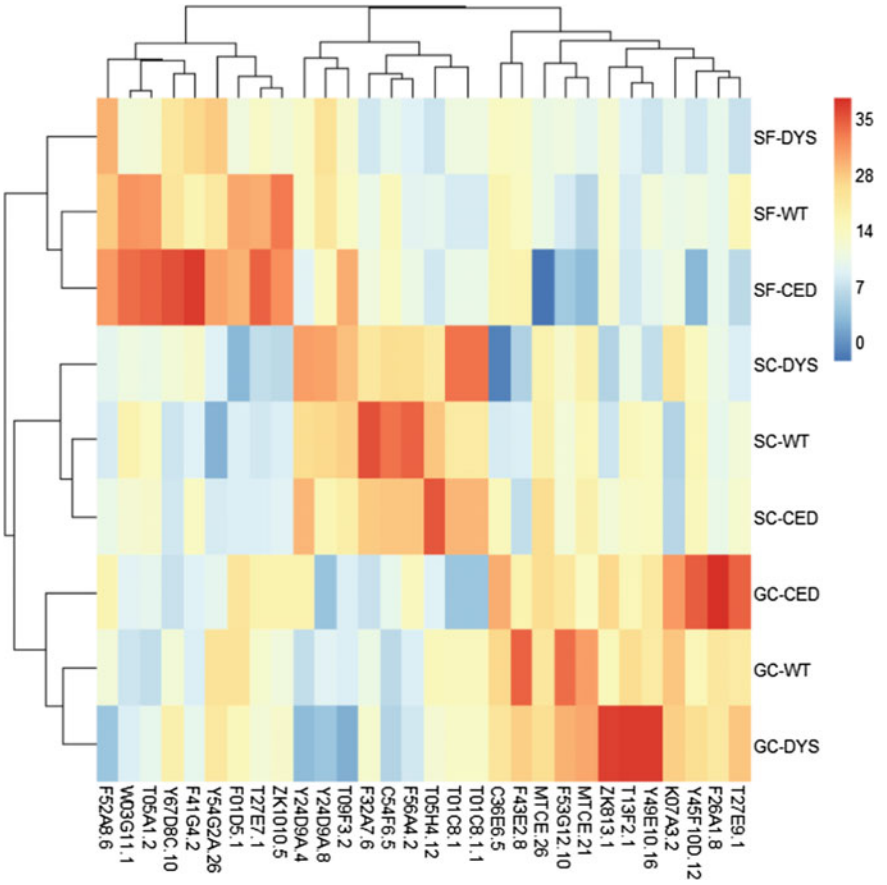

Fig. 10 Heat map of the top 30 ranking based on random forest algorithm, reprinted from ref. Zhao et al. (2016b), copyright 2016, with permission from Mutation Research/Fundamental and Molecular Mechanisms of Mutagenesis

techniques (Saeys et al. 2007). In addition, the embedded methods (such as Random forest (RF) (Diaz-Uriarte and de Andres 2006), Support vector machine (SVM) (Guyon et al. 2002) take an optimal subset of features to build into the classifier construction, while at the same time being far less computationally intensive than wrapper methods (Saeys et al. 2007).

To identify the potential biomarkers associated with space flight, a combined algorithm, which integrates the feature selection techniques, was used to deal with the microarray datasets of *C. elegans* (L) obtained in the Shenzhou-8 mission (Zhao et al. 2016b). A total of 86 DE genes in responses to space synthetic environment or space radiation environment were identified by two filter methods (IQR and ANOVA algorithms) (Fig. 8). Compared with the ground control treatment, this algorithm can select more functional genes in responses to spaceflight environment. Gene Ontology

(GO) annotation and functional enrichment analyses indicated that these DE genes mainly related to oxidative phosphorylation (Fig. 9), suggesting that the combined use of these algorithms may make the feature selection more reliable and robust. Furthermore, the results of RF algorithm and clustering analysis (Fig. 10) showed that 17 genes can be regarded as potential biomarkers associated with spaceflight due to their high sensitivity to space flight environment. And the synergetic biological effects are likely to exist between space radiation and microgravity.

The combined algorithm, which integrates the feature selection techniques, will be used to analyze the high-throughput profiles of *O. sativa* (L) and *C. elegans* (L) experienced SJ-10 flight to select the biomarkers, which can reflect the space radiation environment. And these results will be compared with the previous conclusions obtained from the Shenzhou-8 mission to confirm the space radiation sensitive biomarkers. Based on these, the correlation analysis between space radiation qualities and the corresponding sensitive biomarkers will be further conducted to mine the key factors or main mechanism of the biological effects induced by space radiation. And the systems biology model will be established for space radiation risk assessment and early risk warning, as shown in Fig. 10.

6 Conclusions

Based on the comprehensive review to the research background, foundation, and significance, this project was designed and implemented by putting the space radiation detectors and model organisms into three BRBs inside the SJ-10 satellite. The space radiation quantities and LET spectra were precisely measured, and the biological effects for *O. sativa* (L) and *C. elegans* (L) were observed after landing to the ground. The further in-depth studies will focus on the system biology approaches, which will be used to mine the biomarkers sensitive to the space radiation and the key factors or main mechanisms of the biological effects induced by space radiation.

Acknowledgements This research was supported by the Strategic Priority Research Program on Space Science of the Chinese Academy of Sciences (grant No. XDA04020202-12 and XDA04020412) and by the National Natural Science Foundation of China (grant No. 31770918). We would like to thank the National Laboratory of Heavy Ion Accelerator, Lanzhou, and the National Key Laboratory for Metrology and Calibration Techniques, China Institute of Atomic Energy, who provided support on the calibration of the radiation detectors. We are grateful to Mr. Guan S. H. in Harbin Institute of Technology and Yang Y. K. in Dandong Yalu River Cereals Industry Corporation for the preparations of *O. sativa* (L) and field plantations. Mr. Yang J., Ms. Luo Y. J., Wu D., and Yuan S., in the Institute of Environmental Systems Biology, Dalian Maritime University, are also acknowledged for their work in this research project and/or this manuscript.

References

Aittokallio T, Kurki M, Nevalainen O et al (2003) Computational strategies for analyzing data in gene expression microarray experiments. J Bioinform Comput Biol 01(03):541–586

Bessou C, Giugia J-B, Franks CJ et al (1998) Mutations in the Caenorhabditis elegans dystrophin-like gene dys-1 lead to hyperactivity and suggest a link with cholinergic transmission. Neurogenetics 2(1):61–72

Chancellor J, Scott G, Sutton J (2014) Space radiation: the number one risk to astronaut health beyond low earth orbit. Life 4(3):491

Cordero F, Botta M, Calogero RA (2007) Microarray data analysis and mining approaches. Brief Funct Genomics 6(4):265–281

Cucinotta FA, Manuel FK, Jones J et al (2001) Space radiation and cataracts in astronauts. Radiat Res 156(5):460–466

Cucinotta FA, Plante I, Ponomarev AL et al (2011) Nuclear interactions in heavy ion transport and event-based risk models. Radiat Prot Dosim 143(2–4):384–390

Cucinotta FA, Kim M-HY, Chappell LJ (2013) Space radiation cancer risk projections and uncertainties-2012. In: NASA technical report-217375

Cucinotta FA, Alp M, Sulzman FM et al (2014) Space radiation risks to the central nervous system. Life Sci Space Res 2:54–69

Diaz-Uriarte R, de Andres SA (2006) Gene selection and classification of microarray data using random forest. BMC Bioinform 7(1):3

Durante M (2014) Space radiation protection: destination Mars. Life Sci Space Res 1:2–9

Durante M, Cucinotta FA (2008) Heavy ion carcinogenesis and human space exploration. Nat Rev Cancer 8(6):465–472

Gao Y, Li S, Xu D et al (2015a) Changes in apoptotic microRNA and mRNA expression profiling in Caenorhabditis elegans during the Shenzhou-8 mission. J Radiat Res 56(6):872–882

Gao Y, Xu D, Zhao L et al (2015b) Effects of microgravity on DNA damage response in Caenorhabditis elegans during Shenzhou-8 spaceflight. Int J Radiat Biol 91(7):531–539

Gao Y, Zhao L, Mi D et al (2015c) Distribution of differentially expressed gene loci induced by spaceflight environments in Caenorhabditis elegans. Space Med Med Eng 28(3):157–162 (in Chinese)

George K, Durante M, Wu H et al (2001) Chromosome aberrations in the blood lymphocytes of astronauts after space flight. Radiat Res 156(6):731–738

Guyon I, Weston J, Barnhill S et al (2002) Gene selection for cancer classification using support vector machines. Mach Learn 46(1–3):389–422

Hada M, Cucinotta FA, Gonda SR et al (2007) mBAND analysis of chromosomal aberrations in human epithelial cells exposed to low-and high-LET radiation. Radiat Res 168(1):98–105

Inza I, Larranaga P, Blanco R et al (2004) Filter versus wrapper gene selection approaches in DNA microarray domains. Artif Intell Med 31(2):91–103

Jafari P, Azuaje F (2006) An assessment of recently published gene expression data analyses: reporting experimental design and statistical factors. BMC Med Inform Decis Mak 6:27

Lebel EA, Rusek A, Sivertz MB et al (2011) Analyses of the secondary particle radiation and the DNA damage it causes to human keratinocytes. J Radiat Res 52(6):685–693

Li CY, Yang Q, Wang XF et al (2004) Function of newly cloned pi-hit-1 gene is associated with rice blast resistance. High Technol Lett 14(10):21–26 (in Chinese)

Li Y, Liu M, Cheng Z et al (2007) Space environment induced mutations prefer to occur at polymorphic sites of rice genomes. Adv Space Res 40(4):523–527

Ma Y, Cheng Z, Wang W et al (2007) Proteomic analysis of high yield rice variety mutated from spaceflight. Adv Space Res 40(4):535–539

Mei M, Qiu Y, Sun Y et al (1998) Morphological and molecular changes of maize plants after seeds been flown on recoverable satellite. Adv Space Res 22(12):1691–1697

Mutch DM, Berger A, Mansourian R et al (2002) The limit fold change model: a practical approach for selecting differentially expressed genes from microarray data. BMC Bioinform 3(1):1–11

Nadon R, Shoemaker J (2002) Statistical issues with microarrays: processing and analysis. Trends Genet 18(5):265–271
Ooi CH, Tan P (2003) Genetic algorithms applied to multi-class prediction for the analysis of gene expression data. Bioinformatics 19(1):37–44
O'Sullivan D, Zhou D, Heinrich W et al (1999) Cosmic rays and dosimetry at aviation altitudes. Radiat Meas 31(1):579–584
Ou X, Long L, Zhang Y et al (2009) Spaceflight induces both transient and heritable alterations in DNA methylation and gene expression in rice (Oryza sativa L.). Mutat Res/Fundam Mol Mech Mutagen 662(1–2):44–53
Preston DL, Shimizu Y, Pierce DA et al (2003) Studies of mortality of atomic bomb survivors. Report 13: Solid cancer and noncancer disease mortality: 1950–1997. Radiat Res 160(4):381–407
Reitz G, Berger T, Bilski P et al (2009) Astronaut's organ doses inferred from measurements in a human phantom outside the International Space Station. Radiat Res 171(2):225–235
Saeys Y, Inza I, Larranaga P (2007) A review of feature selection techniques in bioinformatics. Bioinformatics 23(19):2507–2517
Shi JM, Huang L, Li WJ et al (2009) DNA methylation alterations on rice seeds and seedlings induced by low-dose heavy ion irradiation. Acta Laser Biol Sin 18(5):641–646 (in Chinese)
Shi J, Lu W, Sun Y (2014a) Comparison of space flight and heavy ion radiation induced genomic/epigenomic mutations in rice (Oryza sativa). Life Sci Space Res 1:74–79
Shi JM, Sun YQ, Sun ZW et al (2014b) DNA methylation changes on cytidine deaminase gene of rice induced by space flight. J Nucl Agric Sci 28(7):1149–1154 (in Chinese)
Tarca AL, Romero R, Draghici S (2006) Analysis of microarray experiments of gene expression profiling. Am J Obstet Gynecol 195(2):373–388
Thomas JG, Olson JM, Tapscott SJ et al (2001) An efficient and robust statistical modeling approach to discover differentially expressed genes using genomic expression profiles. Genome Res 11(7):1227–1236
Von Heydebreck A, Huber W, Gentleman R (2004) Differential expression with the Bioconductor project. In: Encyclopedia of genetics, genomics, proteomics and bioinformatics. Wiley, pp 1–15
Wang JM, Xu JL, Wei LJ et al (2006) Mutagenic differences of space environment and ground γ-irradiation in rice. Acta Agron Sin 32(7):1006–1010 (in Chinese)
Wang W, Gu DP, Zheng Q et al (2008) Leaf proteomic analysis of three rice heritable mutants after seed space flight. Adv Space Res 42(6):1066–1071
Wei LJ, Yang Q, Xia HM et al (2006a) Analysis of cytogenetic damage in rice seeds induced by energetic heavy ions on-ground and after spaceflight. J Radiat Res 47(3–4):273–278
Wei LJ, Wang JM, Yang Q et al (2006b) A comparative study on mutagenic effects of space flight and γ-rays irradiation in rice. Sci Agric Sin 39(7):1306–1312 (in Chinese)
Wei LJ, Qian Y, Yang Q et al (2007) Cytological effects of space environment on different genotype of rice. J Beijing Inst Technol 16(2):220–225
Xu JL (2000) Biological effects of space mutagenic factors on different genotypic Japonica rice. Acta Agric Nucleatae Sin 14(1):56–60 (in Chinese)
Xu D, Gao Y, Huang L et al (2014) Changes in miRNA expression profile of space-flown Caenorhabditis elegans during Shenzhou-8 mission. Life Sci Space Res 1:44–52
Yu X, Wu H, Wei LJ et al (2007) Characteristics of phenotype and genetic mutations in rice after spaceflight. Adv Space Res 40(4):528–534
Zhang M, Liang SJ, Chen ZL et al (2011) Function analysis of space flight rice pi-hit-1 gene promoter. J Biol 28(2):1–4 (in Chinese)
Zhao Q, Wang W, Zhang M et al (2016a) DNA methylations of rice seeds induced by heavy ion radiation. Acta Agric Nucleatae Sin 30(9):1665–1671 (in Chinese)
Zhao L, Gao Y, Mi D et al (2016b) Mining potential biomarkers associated with space flight in Caenorhabditis elegans experienced Shenzhou-8 mission with multiple feature selection techniques. Mutat Res/Fund Mol M 791:27–34
Zhou D (2012) CR-39 Plastic nuclear track detectors in physics research. Nova Science Publishers Inc., New York, pp 1–17

Zhou D, O'sullivan D, Flood E (2006a) Radiation field of cosmic rays measured at aviation altitudes by CR-39 detectors. Adv Space Res 37(6):1218–1222

Zhou D, O'Sullivan D, Semones E et al (2006b) Charge spectra of cosmic ray nuclei measured with CR-39 detectors in low earth orbit. Instrum Methods Phys Res Sect A Accel Spectrometers Detect Assoc Equip 564(1):262–266

Zhou D, Semones E, Weyland M et al (2007) LET calibration for CR-39 detectors in different oxygen environments. Radiat Meas 42(9):1499–1506

Zhou D, O'Sullivan D, Semones E et al (2008) Radiation dosimetry for high LET particles in low Earth orbit. Acta Astronaut 63(7–10):855–864

Zhou D, Semones E, Gaza R et al (2009) Radiation measured with different dosimeters during STS-121 space mission. Acta Astronaut 64(4):437–447

Zhou D, Semones E, Guetersloh S et al (2010) The experimental and simulated LET spectrum and charge spectrum from CR-39 detectors exposed to irons near CRaTER at BNL. Radiat Meas 45(8):916–922

Zhou D, O'Sullivan D, Semones E et al (2011) Radiation of cosmic rays measured on the international space station. In: International cosmic ray conference, p 102

Effects of Space Environment on Genome Stability

Lili An, Yingjun Fan, Changqing Li, Fanlei Ran, Yuanda Jiang, Yaqing Liu, Xingzhu Cui and Haiying Hang

Abstract Because of the development of spacecraft design and life-support technologies, people can be sent farther in space and kept there longer. The characteristics of the space environment include the space radiation, microgravity, temperature extremes, high vacuum, space debris and ionospheric plasma etc. Among them, the two major challenges associated with spaceflight are the biological effects of space radiation and microgravity. DNA, the genetic material, is a kind of important biologic molecule. The maintenance of the stability of genomic DNA affects many cellular events, which prevents diverse human diseases. DNA can accumulate numerous lesions which is the underlying hallmark of cancer, aging and many other diseases. It is well known that many environmental factors can affect the integrity of DNA molecules. Thus, it is important to investigate the effects of space environment on the maintenance of genomic stability. In this work, we investigated "Roles of space radiation on genomic DNA and its genetic effects" on board the SJ-10 recoverable microgravity experimental satellite (SJ-10 satellite), using the wild type and corresponding radiation sensitive mutant mammalian cells and fruit flies models created by our team.

L. An · Y. Fan · C. Li · H. Hang (✉)
Key Laboratory for Protein and Peptide Pharmaceuticals, National Laboratory of Biomacromolecules, Institute of Biophysics, Chinese Academy of Sciences, Beijing, China
e-mail: hh91@sun5.ibp.ac.cn

F. Ran
Key Laboratory of Pathogenic Fungi and Mycotoxins of Fujian Province, Key Laboratory of Biopesticide and Chemical Biology of Education Ministry, School of Life Sciences, Fujian Agriculture and Forestry University, Fuzhou 350002, China

Y. Jiang
Center for Space Science and Applied Research, Chinese Academy of Sciences, Beijing, China

Y. Liu · X. Cui
Institute of High Energy Physics, Chinese Academy of Sciences, Beijing, China

E. Duan and M. Long (eds.), *Life Science in Space: Experiments on Board the SJ-10 Recoverable Satellite*, Research for Development,
https://doi.org/10.1007/978-981-13-6325-2_4

Abbreviations

DEGs	Differentially expressed genes
DSB	DNA double strand break
ESA	European Space Agency
GCRs	Galactic comics rays
HIRFL	Heavy Ions Research Facility in Lanzhou
HR	Homologous recombination
Hu	Hydroxyurea
ISS	International Space Station
LET	Linear energy transfer
mESCs	Mouse embryonic stem cells
NASA	National Aeronautics and Space Administration
NHEJ	Nonhomologous end joining
PBL	Peripheral blood lymphocytes
RAD	Radiation detector
RWV	Rotating wall vessel bioreactor
SJ-10 satellite	SJ-10 recoverable microgravity experimental satellite
SMG	Simulated microgravity
SRGDB	Space Radiation on Genomic DNA and its genetic effects Box

1 Background

1.1 Effects of Space Environment on Genomic Stability of Mammalian Cells

1.1.1 Effects of Real Space Environment on Genomic Stability of Mammalian Cells

Physiological Effects of Microgravity: When the objects in an aircraft do the same circular motion together with the aircraft, the gravitational force acts as a centripetal force and the centrifugal force is in balance with the gravitation of the earth. That is, the aircraft cabin objects are in weightlessness. Since the orbit of the satellite is elliptical, its gravity is not absolutely zero. The acceleration of gravity on Earth is 9.8 m/s^2 (g). The acceleration of gravity of spacecraft on the orbit is probably equivalent to 10^{-3} to 10^{-6} g (the equivalent of one-thousandth to one millionth of that on the earth's surface), which is known as microgravity (Qiu 1994).

Spaceflight can result in a number of health problems, many of which are associated with the physiological stress response to microgravity. These adverse effects include space motion sickness, spatial disorientation, shift of the venous fluid to upper body, reduced plasma volume (about 17%) and total blood volume (about

10%), decreased vasoconstrictor response, loss of bone mineral density, reduced calf muscle volume, etc. (Macdougall and Moore 2010).

Characteristics of Space Radiation: There are two kinds of space radiation, primary space radiation and secondary radiation. Galactic cosmic rays, solar particles and trapped particles from geomagnetic fields are the source of primary space radiation. Galactic cosmic rays that are from outside our solar system consist of three high energy particles, such as protons, α-particles and heavy particles. Solar particles are mainly composed of protons and electrons, which come from solar flares and solar winds. They have high energy so that even one solar particle events probably leads to death for the astronauts at the space environment without shielding (Sihver et al. 2015). The primary components of geomagnetically trapped particles are protons and electrons. The secondary radiation, which consists of protons, neutrons and heavy ions, is produced by nuclear reaction when primary space radiation enters spacecraft hulls or bodies (Cucinotta and Durante 2006; Ohnishi 2005; Thirsk et al. 2009).

The biological effects of space radiation on astronauts are the key factor considered in spaceflight. The option of shielding materials is the main method to decrease the health risk for astronauts. However, spacecraft wall now does not have the sufficient resisting power to protect astronauts from penetrating of rays except the solar proton events (Wilson et al. 1995). Polyethylene, the more effective shielding material, just reduces 35% galactic cosmic rays (Cucinotta and Durante 2006). As a result, astronauts in the spacecraft mainly receive high-energy proton, electrons, heavy ions, X-rays, gamma rays and neutrons. The average dose a person receives on earth is 2 mSv/year. By contrast, astronauts received 1 mSv/day for STS and 0.3 mSv/day for MIR (Thomson 1999). High-energy heavy ions have high ionization power that makes them the main contributor to the risk to the health of astronauts, in spite of their low hit frequency (Cucinotta and Durante 2006). While on the earth, most natural radiation is low-linear-energy-transfer radiation, such as X-rays. Since high-energy heavy ions in space was burn up when they entered the earth's atmosphere. Thus, it's key to study the biology effects of the high-energy heavy ions (Delp et al. 2016).

Biological Effects of Space Radiation: Space radiation can lead to a lot of biological effects. Many researchers have carried out a number of studies from the point of view of human health for long-term stay in space. It has been reported that space radiation have a great impact on the astronauts' eyes, such as light flashes and cataracts. Light flashes were observed by astronauts on Apollo and subsequent Skylab, space shuttle, and Mir missions (Bidoli et al. 2000; Pinsky et al. 1975; Pinsky and Thompson 1974). Cucinotta et al. reported that relatively low doses of space radiation may increase the risk for cataracts. The Jones team's results also show that astronauts have a higher incidence of cataracts (Cucinotta et al. 2001; Jones et al. 2007).

Ohnishi and his colleagues used the TdT post-labeling assay to detect DNA strand breaks induced by space radiation and found that after 40 days' staying in the Russian Mir space station, HeLa cells had a significant increase in DNA damage compared with the ground control sample, while the DNA damage was lower of the cells on the U.S. Space Shuttle for 9 days; They also found that accumulation of p53 (an

important DNA damage response molecule) in the skin and muscle tissue of rats after space flight (Ohnishi et al. 1999, 2003).

Effects of Combined Exposure to Microgravity, Radiation, and Other Space Environment on Mammalian Cells: Because of the heavy costs and the limited access to space flight, it is hard to perform elegant experiments to investigate the effects of separated space environment factors on mammalian cells. In the Japanese "Kibo" facility in the ISS, the Japan Aerospace Exploration Agency has performed five life science experiments since 2009, and two additional experiments are currently in progress. The first life science experiment in space was the "Rad Gene" project, which utilized two human cultured lymphoblastoid cell lines expression either mutated p53 gene or parental wild-type p53 gene. They detected space radiation-induced DNA double strand break (DSB) by observing γ-H2AX foci, p53-dependent gene expression during space flight as well as after space flight and the adaptive response in the two cell lines after exposure to space radiation. In this project, they used the centrifuge which provided the 1 × g level for the growth of the cells on the ISS. Thus, they can investigate the difference effects between microgravity alone and the other flight-associated stresses (Ohnishi 2016).

German scientists designed the space experiment "Cellular Response to Radiation in Space" on the ISS. This experiment was planned to be performed in the Biolab which is located in the European laboratory module Columbus. To investigate the effects of combined exposure to space environment, they will use the centrifuge to provide the 1 gravity and the Promethium-147 radiation source to provide an artificial radiation source on the ISS. In this project, human embryonic kidney cells stably transfected with reported genes will be seeded on ground in multiwall plate units, transported to the ISS, and irradiated by Promethium-147 radiation source after an adaptation period at 0 × g and 1 × g. After different incubation periods, the cells will be fixed and the evaluation of the fluorescence signals will be performed after the transport back to Earth (Hellweg et al. 2015). However, these two space projects can only detect the effects of combined exposure to space environment after the return of the samples. They could not provide the real-time results on the ISS.

1.1.2 Effects of Simulated Space Environment on Genomic Stability of Mammalian Cells

Devices for the Simulation of the Biological Effects of Microgravity: At present, people are studying the biological effects of simulated microgravity (SMG) by using the clinostat devices. A large number of experimental results show that the clinostat can be a good simulation of microgravity on the biological effects of cells (Klement et al. 2004; Zeng and Liu 2007). For an organism on clinostat, the gravity acting on the organism will continuously change direction with the rotating of the clinostat constantly. As to the response time to gravity, each organism has its threshold. The direction of the gravity vector is constantly changing and the time spent in each direction is extremely short (less than the threshold of the organism) so that the

organism will not feel the force of gravity. This will produce a biological phenomenon similar to the effect of microgravity environment (Jiang et al. 2008). The diversity of biology determines that different bioreactors need different designs for different research objects. At present, the clinostat or rotary bioreactor mainly include the following (Long 2014). (1) Clinostat mainly used to study the plant's perception, conduction and response of gravity. (2) Rotating wall vessel bioreactor (RWV): This bioreactor is currently used extensively in studying the perception, conduction and response of animal cells or tissues to gravity. The Rotating Cell Culture System invented by National Aeronautics and Space Administration (NASA) is the most commonly used in RWV systems (Yuge et al. 2003). (3) Rotating wall perfusion vessel bioreactor: It can solve the problems of nutrient supply and material exchange, and is currently used in the fields of regenerative medicine and tissue engineering.

Effects of Simulated Microgravity on Genomic Stability of Mammalian Cells: Previously, our lab found that SMG alone was unable to induce increased DNA damage in wild type mouse embryonic stem cells (mESCs) (Wang et al. 2011). Degan et al. reported that exposure of freshly drawn lymphocytes and lymphoblastoid cells to SMG for 24 or 72 h is not significantly associated with the induction of DNA damage (Degan et al. 2005). However, Kumari et al. reported that the exposure of human lymphocytes to SMG for 7 days significantly increased the level of DNA damage (Kumari et al. 2009). Roberts et al. also observed that human retinal pigment epithelial cells exposed to SMG for 24 h suffered from significant damage in the form of single-stranded DNA breaks when compared with control cells (Roberts et al. 2006). It seems that the effect of SMG on DNA damage varies among different types of cells and depends on the time length of microgravity exposure. Maybe, SMG is a weak stress on cellular DNA and the final effects of SMG on DNA damage are determined by both the length of SMG exposure time and DNA damage response status of the cell. The efficiency of the DNA damage response system varies depending on the cell type and genetic background. Consistent with this, our lab observed significant SMG-induced DNA damage in Rad9$^{-/-}$ mESCs, which was extremely sensitive to DNA damage agents such as UV light, gamma rays and hydroxyurea, but not in their corresponding wild type cells (Li et al. 2015).

Nowadays, little is known about the mechanism of the effects of SMG on DNA damage and DNA damage response. Some evidences indicate that SMG may affect the expression of the genes involved in DNA damage response. Kumari et al. reported that exposure of human lymphocytes to simulated microgravity decreased the expression of DNA repair genes (Kumari et al. 2009). Zhao et al. also observed that exposure of BL6-10 melanoma cells to simulated microgravity down-regulated the expression of 10 DNA repair genes and inhibited the molecules involved in the DNA-damage response, such as p53, PCNA, ATM/ATR and Chk1/2 (Zhao et al. 2016).

Heavy Ions Accelerators, the Facilities Used in Ground-Based Space Radiation Research: Heavy ion radiation contributes largely to the biological effects of space radiation. High-energy heavy ions in space were burn up when they enter the earth's atmosphere. Thus, our knowledge of the biological effects of high-energy heavy ions is almost exclusively derived from the heavy ions accelerators. There are

more than 30 large scale heavy ions accelerators. The main heavy ions accelerators overseas are the Brookhaven National Laboratory—Relativistic Heavy Ion Collider in the United States, the RIKEN—Radioactive Isotope Beam Factory in Japan, the MSU—Facility for Rare Isotope Beams in the United States, the National Large Heavy Ion Accelerator-SPIRAL2 in France and the FAIR in Europe which is under construction. In China, there are the BRIF in Beijing and the Heavy Ions Research Facility in Lanzhou (HIRFL) being operation and High Intensity heavy-ion Accelerator Facility which will be built in Huizhou. HIRFL is the largest scale heavy-ion accelerator facility with the most ion species and the highest ion energy in China at present. Its main parameters have reached international advanced level. HIRFL is composed of Electron Cyclotron Resonance ion source, sector focused cyclotron, separated sector cyclotron, radioactive ion beam lines RIBLL1 and RIBLL2, cooler storage rings CSRm and CSRe, and many terminals. HIRFL can accelerate all ion species and provide high quality stable beams and radioactive beams with many ion species and broad energy ranges (Durante et al. 2007; Xia et al. 2016).

Heavy Ions Radiation Causes Clustered DNA Damage: X-rays and γ-rays are the most studied radiation on the ground which belongs to the low-linear energy transfer (LET) radiation. However, high-energy heavy ions belong to the high-LET radiation. Low-LET radiation deposits its energy uniformly within cells which mainly produces simple DNA damage (Goodhead 1994). While high-LET radiation deposit its energy in a very small distance along the track of the traversing particle which led to clustered DNA damage. Clustered DNA damage include two or more closely spaced individual lesions, including abasic sites, base damages (oxidized purines or pyrimidines), DNA single strand breaks and DSBs, within one or two turns of the DNA helix, caused by traversal of a single-radiation track (Sutherland et al. 2001). The complexity and yield of radiation-induced clustered DNA damage increases with increasing ionizing density of the radiation (Goodhead 2006).

Nowadays, two methods were used to detect the clustered DNA damage. One is the in vitro gel electrophoresis assays which could sensitively quantify the DNA lesions (Sutherland et al. 2003). The other is the immunostaining assay using 53BP1, XRCC1 and hOGG1 as surrogate markers for clustered DNA damage (Asaithamby et al. 2011). Each method has its advantage and limitations and the combination of these two assays will be more precisely in estimating the amount of clustered DNA damage.

Compared with the simple DNA lesion, the clustered DNA damages are more difficult to repair which lead to elevated relative biological effectiveness as to various biological end points (Asaithamby et al. 2011; Durante et al. 2008). It has been reported that ATM and ATR (two important kinase in DSB repair) are differentially regulated concerning low- and high-LET radiation (Saha et al. 2013). Nonhomologous end joining (NHEJ) and homologous recombination (HR) are the major two pathways in DSB repairing. HR participates in the DSB repair during S and G2 phase, while NHEJ throughout all cell cycles. However, compared with low-LET radiation induced DSBs, NHEJ was less efficient in repairing high-LET radiation induced DSBs (Wang et al. 2010). It has been shown that some NHEJ and HR factors such

as Artemis (Sridharan et al. 2012) and Rad51 (Zafar et al. 2010) may play important roles in the repair of clustered DNA damage. However, the precise mechanisms of NHEJ and HR to the repair of clustered DNA lesions are still unknown. The existence of DSBs is closely related to the chromosome aberration. There is evidence that heavy-ions induce a high fraction of complex-type exchanges, and possibly unique chromosome rearrangements (Ritter and Durante 2010).

Effects of Heavy Ions Radiation and Simulated Microgravity on Genomic Stability of Mammalian Cells: Mosesso P. et al. reported that SMG could increase X-ray radiation-induced chromosome abbreviation in human lymphocytes (Mosesso et al. 2001). Mognato M et al. irradiated human peripheral blood lymphocytes with 0–3 Gy X-ray or γ-ray, then the cells were treated under SMG or 1G for 24 h. They found that SMG treatment significantly increase radiation-induced hypoxanthine guanine phosphoribosyl-transferase mutation (Mognato and Celotti 2005). In their following work, they irradiated human peripheral blood lymphocytes with 5 Gy γ-ray, then the cells were treated under SMG or 1G for different time. The results indicated that SMG treatment delayed the repair of radiation-induced DNA DSBs and increased the apoptosis of irradiated cells significantly (Mognato et al. 2009). Dang et al also reported that simulated microgravity increased heavy ion radiation-induced apoptosis in human B lymphoblasts (Dang et al. 2014). In our previous work, we found that SMG alone could not increase DNA damage in wild type mESC. While it could delay the repair of DNA DSBs induced by radiation (Wang et al. 2011). Girardi et al analyzed miRNA expression profile of human peripheral blood lymphocytes (PBL) incubated for 4 and 24 h in normal gravity (1 × g) and in SMG after irradiation with 0.2 and 2 Gy of γ-rays. The results show that MMG alters miRNA expression signature of irradiated PBL by decreasing the number of radio-responsive miRNAs. Gene Ontology analysis reports that the biological category of "Response to DNA damage" is enriched when PBL are incubated in 1 g but not in SMG. They provide evidence that modeled microgravity can affects the DNA-damage response to ion radiation in human PBL (Girardi et al. 2012).

1.2 Effects of Space Environment on Genomic Stability of Drosophila melanogaster

1.2.1 Fruit Fly (*Drosophila melanogaster*), a Classic and Powerful Model Organism

Fruit fly (*Drosophila melanogaster*), a kind of cute insect, has been one of the most remarkable organism since the beginning of last century. Working on these little animals, Thomas Hunt Morgan's lab at Columbia University successfully generated various mutants including the famous white-eyed fly among the wild type red-eyed individuals. Then, they analyzed the mutant characteristics of thousands of fruit flies and studied their inheritance. Based on the stunning results, Morgan and his

students developed the concepts, and provided the proof for the chromosomal theory of heredity, genetic linkage, chromosomal crossing over and non-disjunction. These discoveries formed the basis of the modern science of genetics. According to this contribution, Dr. Morgan was awarded the Nobel Prize in Physiology or Medicine in 1933.

Soon after, Fruit fly became one of the scientists' favorite animals and the first organism used for genetic analysis. Fruit fly has a lots of advantages for the scientists: short life cycle (about ten days from embryo to adult fly at 25 °C), production of large number of offspring (a female lays about 100 eggs per day), ease and cheapness of culture and maintenance, less space for large-scale breeding experiments (only 3 mm long of each adult fly), and a low number of chromosomes (four pairs of chromosomes).

Mutant flies with defects of several thousand genes have been produced continuously for a century, so *Drosophila* is genetically best-known of all eukaryotic organisms and one of the most widely used model organisms in diverse biological research especially with the rapid development of molecular biology. Its significance was recognized when three developmental biologists, Ed Lewis, Christiane Nusslein-Volhard and Eric Wieschaus, won the Nobel Prize in medicine or physiology for their discovery in late 1970s of the important genetic mechanisms which control early embryonic development in *Drosophlia melanogaster* in 1995. Nussleln-Volhard and Wieschaus identified and classified a small number of genes playing key role in determining the body plan and the formation of body segments. Lewis investigated how these genes control the further development of individual body segments into specialized organs. These genes are highly conserved from *Drosophlia* to mammals, therefore the principles found in the fruit fly, apply also to higher organisms including human, which will be benefit of explaining and treatment of congenital malformations.

The third time of *Drosophila* as biological stardom is in year 2000, when the sequencing of *Drosophila* genome has been completed and released. A survey in 2001 showed that 50% of fly protein sequences have mammalian analogues, and 75% of known human disease genes have an identifiable match in the genetic code of fruit flies (Reiter et al. 2001). Moreover, accumulating studies demonstrate that most signaling pathways that series biochemical reactions responding to various signal molecules from outside of cells in human are revolutionarily conserved in flies. Taking together, *Drosophila* is one of the most valuable organisms in biological research. This has led to a new paradigm for understanding how human disease genes function—we can analyze their partners in the simpler organism. For many years, *Drosophila* have been used to test the mutagenic properties of environmental toxicants and as a model to understand how organisms respond to a changing environment.

Fruit fly is the pioneer of universe exploration that it's the first animal sent to the space. In 1947, Fruit flies traveled as high as 108 km in the American Rocket V-2 and returned to the Earth safely. Afterwards, *Drosophila* becomes the most frequent passenger on the satellite, parabolic flights, space shuttle and space station as a model for investigating the effects of spaceflight factors on organisms.

1.2.2 Genetic Changes of *Drosophila* Affected by Spaceflight Factors

Research was focused on the genetic changes of *Drosophila* caused by space effect factors after flight in the earlier period. Wildtype strain D-32 flies were cultured under suitable condition in various space crafts and orbital station. The progeny from these flies showed an increase in the rate of visible mutations for *y*, *ct*, *w* and *vg* loci over those observed in the earth control (Dubinin et al. 1973; IaL et al. 1975; Dubinin et al. 1977). In addition, earlier oocyte stage presented an increased sensitivity to spaceflight factors as according to the frequency of both dominant and recessive lethal (Dubinin et al. 1973; Kogan and Chzhan 1980; Kogan and Tia 1981). Then, wild type and a radiation-sensitive strain mei-41 were used in later experiments. The frequencies of recessive lethal mutations in flight groups were 2 and 3 times higher for wild type Canton-S and mei-41 strains, respectively, than those in ground control groups (Hara 1994; Ikenaga et al. 1998). Furthermore, a significant increase in the frequency of nondisjunction and loss of chromosomes during meiosis in *Drosophila* females was observed (Vaulina et al. 1981). On the other hand, spaceflight conditions increased the frequencies of non-disjunctions, breaks and mitotic recombination in chromosomes in males (Filatova et al. 1984).

1.2.3 Visible Phenotype of *Drosophila* Responding to the Spaceflight Factors

Serial experiments have been done in different space shuttles, and several interesting differences between in-flight and the parallel ground controls were observed: (1) There was an increase in oocyte production and size. (2) There was a significant decrease in the number of larvae hatched from the embryonic cuticles in microgravity. (3) The majority of embryos were normally fertilized and at late stages of development, except in the space-flown containers in microgravity where a percentage of earlier stage embryos were recovered showing alterations in the deposition of yolk. (4) In correspondence with these results, at least 25% of the living embryos recovered from space failed to develop into adults. (5) Studies of the larval cuticles and those of the late embryos indicate the existence of alterations in the anterior, head and thoracic regions of the animals. (6) There was a delay in the development into adults of the embryos and larvae that had been subjected to microgravity and recovered from the space shuttle at the end of the flight. (7) Adult males emerged from the recovered embryos showed a slight shortening in life span and accelerated aging of the microgravity exposed male flies since they exhibited a significant decrease in mating ability and a consistently lower negative geotaxis response. (8) By repeatedly video-recording, very marked increase in the locomotor activity of the fruit flies in space. It seems that fruit flies are able to sense and respond to the absence of gravity and cosmic radiation, changing several developmental processes even in very short spaceflights (Vernós et al. 1989; Marco and González 1992; Benguría et al. 1996).

1.2.4 Transcription Profile Changes of *Drosophila* Responding to Spaceflight Factors

With rapid developed sequencing technology, the whole genome and RNA sequencing are widely used in various studies including space science. Genome-wide transcriptional profiling shows that reducing gravity levels during *Drosophila* metamorphosis in the ISS causes important alterations in gene expression: a large set of differentially expressed genes (DEGs) are observed compared to controls. Gene ontology analysis of them shows they are genes that affect respiratory activity, developmental processes and stress-related changes (Herranz et al. 2010).

A recent paper demonstrates results in the creation of the third generation of fruit fly (third-stage larvae) during the 44.5-day space flight [Foton-M4 satellite (2014, Russia)], then the fourth generation on Earth and the fifth generation again in conditions of the 12-day space flight (2014, in the Russian Segment of the ISS). The species preserves fertility despite a number of changes in the level of expression and content of cytoskeletal proteins, which are the key components of the cleavage spindle and the contractile ring of cells. The results of transcriptome screening and space analysis of cytoskeletal proteins show that the exposure to weightless conditions leads to the increased transcription of metabolic genes, cuticle components and the decreased transcription of genes involved in morphogenesis, cell differentiation, cytoskeletal organization and genes associated with the plasma membrane. "Subsequent" exposure to the microgravity for 12 days resulted in an even more significant increase/decrease in the transcription of the same genes. On the contrary, the transition from the microgravity conditions to the gravity of Earth leads to the increased transcription of genes whose products are involved in the morphogenesis, cytoskeletal organization, motility of cells and transcription regulation, and to the decreased transcription of cuticle genes and proteolytic processes (Ogneva et al. 2016).

1.3 Research Progress of Space Radiation Detector

Radiation is the greatest risk of the astronauts' health. Measurements of the high energy particles fluxes of the space environment, is of great importance for the safety of space engineering purposes. The long term in suit observation of the elements is space radiation and their effect on genome will provide the evidence on how the radioactive particles affect the health of the astronaut. Meanwhile, the obtained fluxes data will also be used to determine the effects of space radiation on other payloads.

The space radiation detector in Rad Gene Box was designed to obtain the high quality space radiation data, which is of great importance to the radiation gene box experiment on-board SJ-10 satellite.

1.3.1 Developing Situation and Tendency at Home and Abroad

There are three sources for radiation particle, the trapped particles by geomagnetic field, the solar particle events and the Galactic cosmic rays. The magnetically trapped radiation mainly consists of protons and electrons. Based on the large amounts of data obtained by satellites, the Vette group from NASA had developed the AP1–AP8 proton models (Vette 1991) to describe the protons in energy range 0.1–400 MeV, while the other particles models besides proton is only conservative estimate based on inadequate experiments' data. As order of magnitude difference had been found between the prediction of AP8 model and the derived data, there is still much work to be done. There are two main energy eruption phenomena of the Sun, i.e., the solar wind and the solar energetic particles. The solar wind is a continuous flow of ionized plasma from the sun's corona, which is consisted of high flux, low energy protons and equivalent electrons. While the solar energetic particles are the high speed energetic particles emitted from corona during an active events, which is mainly high energy protons. The galactic comics rays (GCRs) are consisted by low flux and high energy particles. The flux of GCRs particles is modulated by the solar active period. When the sun in the solar maximum, the GCRs particle flux decreased and vice versa. All the exist models of space radiation is based on the statistical analysis of the measured values of past satellites. For a given spacecraft with specified orbitals, the radioactive parameters should be derived by measurement of instrument onboard the spacecraft.

The semiconductor and scintillator detectors are usually applied in charge particles measurement, while the detectors are classified as heavy ions detector, high energy proton spectrometer and high energy electron spectrometer. In 1992, the NASA small-class explorer mission SAMPEX (Baker et al. 1993) had measured the energy, composition and charge states of heavy ions from He to Ni in energy range of 10 MeV to several hundred MeV, protons of 20–300 MeV and electrons of 1–30 MeV were also derived in a long-term measurement. The Energetic Particle Sensors (Fennelly 2011) flown on the Geostationary Operational Environmental Satellites (Rodriguez et al. 2014) have measured the proton fluxes in the energy range 0.8–700 MeV, He-ion fluxes between 4 and 3400 MeV and electron in the energy range 0.6–4 MeV. The DOSTEL of German, RRMD-III of Japan and Charge Particle Detectors of NASA which were operated as classical ΔE-E telescopes were installed on the ISS to detect the charge particles.

Base on the results of the Charge Particle Detector on board the Oersted satellite (Leonov et al. 2005) which was launched in 1999 by European Space Agency (ESA), the flux of energetic protons is of an order of magnitude higher than the AP-8 predictions (Leonov et al. 2005). The ICARE instrument onboard the Argentinean satellite SAC-C (Boatella et al. 2009) in 2000 and IDP spectrometer onboard the France DEMETER satellite (Sauvaud et al. 2006) have obtained the electron and proton fluxes at the low polar orbit. The ESA SREM monitors onboard PROBA and INTEGRAL (Evans et al. 2008) have derived the radiation level at different location. The data of EPT onboard PROBA-V show electron, proton and helium flux increases during SEP events.

With development of technology, the detector adopt in the space mission have evolved from proportional counter which can only measure the flux specified particles to a detector with comprehensive ability to derive energy, flux, direction and variety of the particles.

1.3.2 Performance Comparison with the Existing Instruments

It has become a conventional means to research the space environment by measuring flux of charge particles. Over the past few decades, a batch of particle detectors have been launched and operated at space including the MARIA-2 instrument on the Mir station of USSR, the PET instrument on SAMPEX of USA, the IDP instrument on DEMETER of France, the LAZIO-SIRAD instrument on ISS of Italian, the TES instrument on COMPOSS-2 of Russia, the ARINA instrument on RESURS-DK2 of Russia. Several satellites in home were also equipped with the charge particle detector, such as FY-1, FY-2, ZY-1and SJ-10. The results of charge particle detector provided data to validated the space radiation model, which can also be used to study the particle flux variation linked to human activities and natural phenomena like earthquakes, volcano eruptions etc. Meanwhile, the results can also be used to find the correlation between electronic parts' fault and the space environment. Miniaturization and modularization has become a direction in particle detector design. As shown in Table 1, the Standard Radiation Environment Monitor (SREM) is such a standard instrument which had been widely used on ESA satellites such as STRV-1, INTEGRAL\ROSETTA, PROVA-1, GIOVE-B, Herschel, Planck and GAIA. The lower limits of SJ-10 satellite RAD for electron, proton and helium ion are sub MeV, several MeV and dozens of MeV, respectively, while the corresponding upper limits is several MeV, 200 and 300 MeV (Liu et al. 2015), which is comparable with the advance instruments aboard.

1.3.3 Detection Approaches Comparison with the Existing Instruments

Conventionally, the silicon is chosen as active sensor in the charge particle detection. Both single layer silicon and telescope structure with multi-layer silicon was adapted. In some case, the scintillator calorimeter was utilized. Normally, a thin layer of aluminum foil was install in front of the detector to prevent photons and low energy particles. The comparison of technical approaches of SJ-10 satellite RAD to other instruments was shown in Table 2. To identify the four type of radiation, a classical ΔE-E telescope architecture was adapted. To reduce the mass, Volume and power of the instrument, we chose the composed semiconductor detector instead of scintillation detectors as calorimeter. Without using the photomultipliers, the stability of the signal was also improved.

Table 1 The comparison goals and performance of SJ-10 satellite RAD with other particle detector

Instrument	Launching time	Performance	Goals
SAC-C/ICARE	2000.11	Electron: 0.25–1.5 MeV Proton: 10–30 MeV Helium ion: >70 MeV	Measure the space radiation and it effects
INTEGRAL/SREM	2002.10	Electron: 0.55–2.3 MeV Proton: 11–120 MeV Heavy ion: 150–185 MeV/n	Continually measures electron and proton fluxes along the orbit and provide alert information to the spacecraft and payload, support in tracing the spacecraft anomalies
DEMTER/IDP	2004.6	Electron: 70–2500 keV	Systematically study the electromagnetic waves linked to human activities and natural phenomena like earthquakes, volcano eruptions, atmospheric and magnetic storms Study the related ionospheric changes, and the related precipitation of particles from the radiation belts
RESURS/ARINA	2005.09	Electron: 3–30 MeV Proton: 30–100 MeV	Monitor the bursts of high-energy charged particles as earthquake precursors
PROBA-V/EPT	2013.5	Electron: 0.5–20 MeV Proton: 9.5–248 MeV Helium ion: 36–1000 MeV	Perform the absolute measurements required for scientific studies
SJ-10 satellite/RAD	2016.04	Electron: 0.5–10 MeV Proton: 5–200 MeV HELIUM ion: 30–300 MeV	Derive the flux of charge particles which have effect on the tissue

2 The Experiment "Roles of Space Radiation on Genomic DNA and Its Genetic Effects" Onboard the SJ-10 Satellite

The recoverable satellite is a very useful tool for space microgravity experiments. China's first recoverable satellite was launched in 1975 and 23 recoverable satellites have been launched and recovered successfully since then. The 24th recoverable satellite is designed specially for microgravity experiments of microgravity physics as well as space life science, which was named as SJ-10 satellite program. Scientific

Table 2 The comparison of technical approaches of SJ-10 satellite RAD to other instruments

Instrument	Launching time	Technical approaches
SAC-C/ICARE	2000.11	① Low energy detector: 500 μm Si (single mode) ② Medium energy detector: 150 μm Si/6 mm Si–Li (single mode and coincidence modes) ③ Medium energy detector: 500 μm Si/500 μm Si (ingle mode and coincidence modes)
INTEGRAL/SREM	2002.10	① Single Si diode D3, 0.7 mm Al window ② Two Si diodes arrange in a telescope configuration, 2 mm Al window, 1.7 mm Al and 0.7 mm Ta separate the diodes
DEMTER/IDP	2004.6	1 mm Implanted Si with active area of 490 mm^2, 6 μm Al window
RESURS/ARINA	2005.09	Multi-layer scintillation detectors were used as coupling trigger detector, Calorimeter and Anti coincidence detector
PROBA-V/EPT	2013.5	All detectors have a thickness of 375 μm, silicon diode detector, classical ΔE-E telescope ① S1/S3 sensor with diameter of 3.5 mm/35 mm serve as ΔE detector ② S2 sensor with diameter of 20 mm serve E detector, ③ 200 μm aluminum foil as front window
SJ-10 satellite/RAD	2016.04	Classical ΔE-E telescope ① 80 μm Silicon diode as ΔE detector ② Two layers of CZT with thickness of 3 mm as E detector ③ 100 μm aluminum foil as front window

purpose of the program is to promote the scientific research in the space microgravity environment by operation of recoverable satellite at low Earth orbit for 2 weeks. There are 6 experiments of fluid physics, 3 of combustion and 8 of materials science in the field of physical science, 3 experiments of radiation biology, 3 of gravitational biology and 4 of biotechnology in the field of life science (Hu et al. 2014). "Roles of space radiation on genomic DNA and its genetic effects" is one of the experiments in this program which is in the field of radiation biology. This experiment was performed in the payload of the "*The space radiation on genomic DNA and its genetic effects box (SRGDB)*" onboard the SJ-10 satellite.

2.1 Purpose of the Space Experiment

In this study, we used wild type *mRad9*$^{+/+}$ mESCs and *mRad9*$^{-/-}$ mESCs as the models. After onboard the SJ-10 satellite for 1 day and 5 days, the cells were fixed in RNAlater. After the recovery of the SJ-10 satellite, the cells were harvested and the RNA were extracted for high throughput RNA sequencing analysis. This design

concerns the following three aspects. (1) We will perform the experiment both on board the SJ-10 satellite and on the ground using the same payload. Thus, we could know the effects of space environment (including microgravity and space radiation) on the mESCs. (2) We used both wild type mESCs and *mRad9*$^{-/-}$ mESCs as the models. Rad9 plays important roles in DNA damage response. *mRad9*$^{-/-}$ mESCs demonstrated a remarkable increase in spontaneous chromosome aberrations and hypoxanthine-guanine phosphoribosyltransferase mutations, and were extremely sensitive to DNA damage agents such as UV light, gamma rays and hydroxyurea relative to wild type mESCs. Thus, we expected to observe more significant effects of space environment in *mRad9*$^{-/-}$ mESCs than that in wild type mESCs. (3) In previous work, it was found that simulated microgravity could delay the repair of DNA double strand breaks induced by radiation, and there was no significant difference in DNA damage between the simulated microgravity group and the 1 × g group at Day 1 and Day 5 to the wild type mouse cells. In contrast, there were significantly more DNA damage in the radiation sensitive mouse cells under the simulated microgravity than 1 g gravity on Day 1 but not on Day 5. We wonder whether this was also the case in the real space environment. Therefore, we detected the effects of space environment on board the SJ-10 satellite on both Day 1 and Day 5.

Although a radiation sensitive mutant *mei-41* was used for studying the effects of cosmic radiation, there have been no deep and detailed investigations, such as the genomics and transcriptomics analysis. And the recent gene expression profile was only generated from the wild type flies. In SJ-10 Satellite, we will explore the effects of space environment factors on genomic stability of *Drosophila melanogaster*. We are also aimed to find some novel radiation sensitive genes by comparison the genomics and transcriptomics between the control and mutant flies in the satellite and on the ground. *Drosophila* RecQ5 (dRecQ5) functions in vivo in homologous recombination-mediated DSB repair, which is similar to RecQ5 in mammals. We generated null alleles of *dRecQ5* and the mutant animals are homozygous viable, but with growth retardation during development. The mutants are sensitive to both exogenous DSB-inducing treatment, such as gamma-irradiation, and endogenously induced DSBs by I-SceI endonuclease. In the absence of dRecQ5, single strand annealing-mediated DSB repair is compromised with compensatory increases in either inter-homologous gene conversion, or NHEJ when inter-chromosomal homologous sequence is unavailable. Loss of function of dRecQ5 also leads to genome instability in loss of heterozygosity assays (Chen et al. 2010). Thus, in this mission, *RecQ5* null mutant and the control flies are used.

Using the wild type and corresponding radiation sensitive mutant mammalian cells and fruit flies models created by our team, it is expected to study the effects of space radiation on genomic stability and to discover novel sensitive biological molecules as space radiation markers, which will be useful for developing sensitive detecting methods of the biological effects of space radiation in the future.

2.2 Space Experimental Projects

2.2.1 Mouse Cells Culture

Two kinds of mouse cells will be cultured for 1 day and 5 days, respectively, and then be fixed and harvested for the following analysis. From the comparison with the experimental results on the ground, gene expression profiles and the sensitive response genes to space radiation will be obtained. The experimental conditions are as follows:

Samples: two kind of mouse cells;
The culture area: ϕ75 mm;
The volume of each culture container: 50 ml;
The temperature at launching and on orbit: 37$\pm$1 °C;
The temperature after fixed: 8$\pm$2 °C;
Atmospheric pressure: 100 kPa;
The composition of the gas: air (5% CO_2).

2.2.2 Fruit Fly Culture

Fruit flies models will be cultured on orbit and recovered for the following-up analysis. From the comparison with the experimental results on the ground. The influence of the space radiation to gene expressions of the fruit flies will be obtained. The experimental conditions are as follows:

Samples: the wild type and radiation sensitive mutant pupas at early age of fruit flies;
The volume of each culture container: ϕ35 mm $\times$ 80 mm;
The temperature at launching and on orbit: 18–27 °C;
Atmospheric pressure: 100 kPa;
The composition of the gas: local air-proof, air.

2.3 Principle and Structure of the Experimental Facility

Based on the scientific objectives of the experiment and the technical constraints of the SJ-10 satellite, the device of SRGDB is mainly composed of four mouse cells culture devices, four fruit fly culture containers, three temperature controllers, two fluid reservoirs, two injection pumps, a liquid distributor, an electronic driver controller and a three-segment air-proof payload body. The internal layout and structure of the SRGDB is shown in Fig. 1a. To satisfy the experiment conditions in a microgravity environment, the pressure inside the air-proof capsule is nominally 100 kPa, while the external pressure of the device is about 0.01 MPa. The outer envelope size of the payload is 300 $\times$ 300 $\times$ 320 mm^3; with a weight of 22 kg; average power

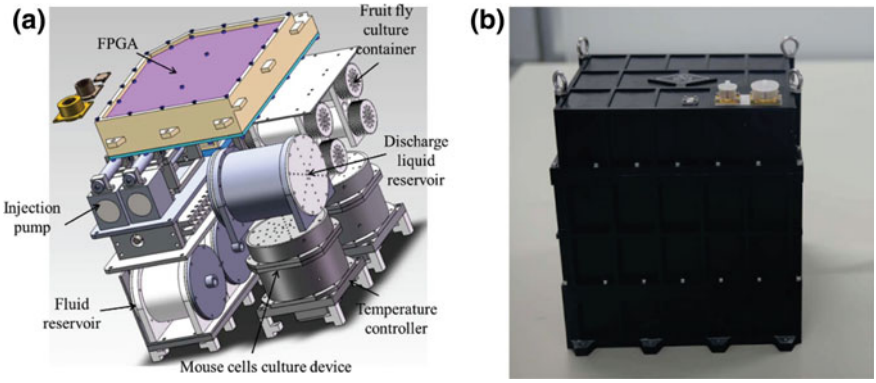

Fig. 1 **a** The internal layout and structure of the SRGDB. **b** Payload

consumption of 23.5 W; and peak power consumption of 40 W. The payload body, which is made by aluminium alloy with a black anodized surface, consists of a floor, and a middle piece and an upper cover. The flanges of the two sides of the middle piece are inset with wire threads and labyrinth grooves. The structure parts are made from integrally machining and fixed by GB70 M4 sockets. The thin wall is 3 mm, the flange is 12 mm and the floor is 10 mm. There are two cable ports on the upper cover. The appearance of the payload is shown in Fig. 1b.

2.3.1 Mouse Cells Culture Device

The four mouse cells culture devices, which have a inner diameter of 80 mm; a depth of 12 mm; and a volume of 50 ml, are divided into two groups. The mouse cells culture device is mainly composed of a cells culture plate, an upper cover, a demarcation plate, a rolling film and a hollow connector (Fig. 2). The cells culture plate, which is embedded in the bottom case, has the diameter of 75 mm and the depth of 1 mm. A basin-size rolling film, which is made of flexible material, is fixed in the middle of the device. The culture plate and a rolling film constitute a cells culture container, and mouse cells adhere to the culture plate. A demarcation plate, which has small holes to allow liquid flowing, is placed up the cells culture plate to give an isolation between the rolling film and cells. In order to accomplish liquid replacement in the microgravity environment, the upper cover of the mouse cells culture device, which has vent holes, associates with the rolling film are able to achieve a volumetric change of the cells culture container. When the liquid flow into the device through the hollow connector, the rolling film turns up and the air is exhausted from the vent holes. Well, when the liquid is discharged, the rolling film turns down and the air is inhaled into the device. The volume change between the rolling film turns up and down is 95% of the actual liquid capacity.

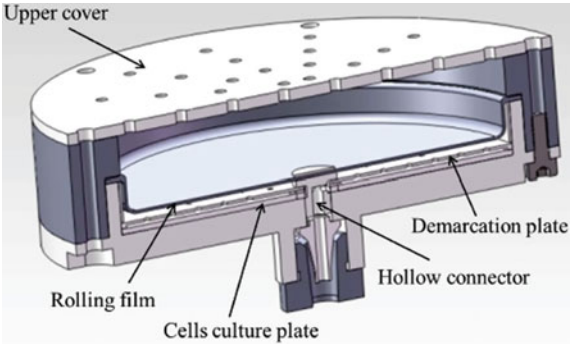

Fig. 2 Model structure of mouse cells culture device

2.3.2 Double Unit Folded Temperature Controller

The schematic of the folded temperature controller is shown in Fig. 3. Its major components include a bottom heat transfer plate, a upper heat transfer plate, adiabatic pillars, a semiconductor temperature control tablet, a temperature sensor, and resistance heating films. The shell of the temperature controller is made of thermal insulation material.

The bottom heat transfer plate is fixed on the floor of the payload box by adiabatic pillars. A semiconductor temperature control tablet is inserted tightly in the gap between the bottom heat transfer plate and the floor of the payload box, and thermally conductive silica gel is painted on the both sides of the temperature control tablet to increase the heat transfer efficiency. The temperature sensor is embedded in a hole reserved in the bottom heat transfer plate. Resistance heating films are pasted on the side of the upper heat transfer plate, functioning as an auxiliary heater.

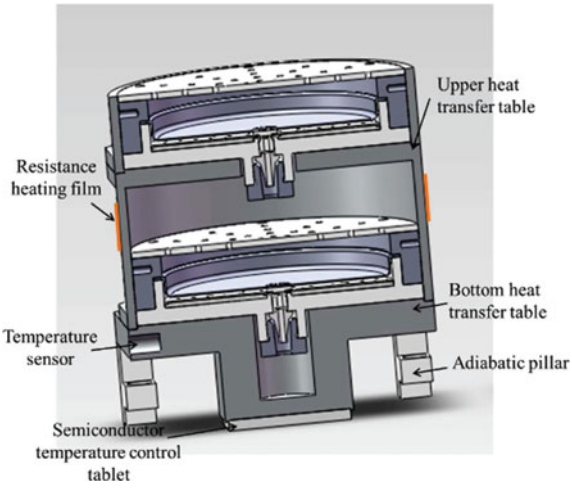

Fig. 3 Model structure of temperature controller

The two mouse cells culture devices start to work before launching. At the cells culture process, the semiconductor temperature control tablet and resistance heating films operate simultaneously to insure temperature consistent in two cells culture devices. The setting temperature is 37 ± 1 °C. When the cells are fixed, resistance heating films stop to heating and the temperature control tablet switches to refrigeration. The cells are storing in a low temperature 8 ± 2 °C environment. The power dissipation of the heating up and preservation process is 4–6 W, and the power dissipation of the cooling and low temperature preservation process is 3–7 W. The temperature controller in the fluid reservoir is similar to that in the cells culture device, but without auxiliary heaters.

2.3.3 Cells Culture Liquid Transportation and Control Unit

Each cells culture device has an injecting pump. The injection pump consists of a needle syringe, a step motor and screw. The stroke of the injection is dominated by a micro switch, and the full stroke is 5 ml. The total amount of injected liquid is managed accurately by setting the open times of the micro switch. The rolling speed of the step motor is restrained to prevent a damage from liquid shearing force to the cells.

A liquid distributor composes of cam groups is designed to manage the liquid. The cam groups with different angles press the liquid pipelines accordingly. When the gap of the cam meets the pipeline, the pipeline expands by its elasticity. In other conditions, the cam restrains liquid flowing by pressing the pipeline. The cam groups are tandem drive by a motor and a drive shaft. The positions of the cam groups are given by a magnet code disc, which has a positioning accuracy of ±1 °C, on the extremity of the shaft. The gaps of the cam groups arrange successively in order of a circle to meets the experimental requirements.

2.3.4 Fruit Fly Culture Container

The cultural conditions for fruit fly is distinct from that for mouse cells, so the fruit fly culture container is designed with a air-proof structure and isolated from the cell culture devices. The fruit fly culture containers have a volume ϕ35 mm × 80 mm. The fruit fly culture container is made up with a sealed cap, a middle piece of the container, one food baffle, supports and a sealed ring (Fig. 4). All the components in the fruit fly culture container are made by Makrolon which is pervious to light, and assembled before launching. To provide a rest for the fruit fly in the microgravity environment, there is superficial thread on the inside wall of the middle piece of the container. The food for the fruit fly is filled in a trough in one cap, and covered with a poriferous food baffle. The fruit fly can acquire the food revealed from the poriferous food baffle.

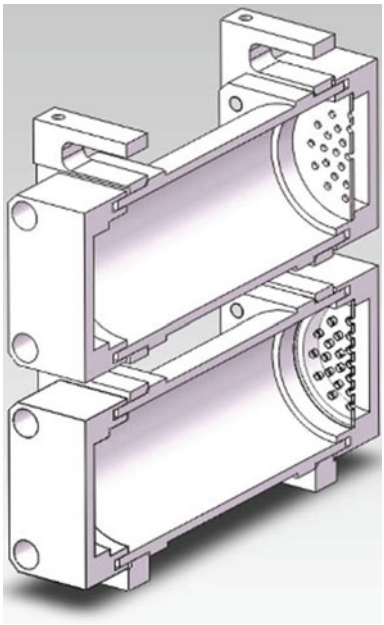

Fig. 4 Model structure of the fruit fly culture container

2.4 System Design of the Space Radiation Detector

The space radiation detector in Rad Gene Box was composed by the Sensor, the Processing electronic and the cable. Please see "Radiation detector of 14.1.2.3.3" for detailed information about the composition and working principle for the space radiation detector. The conceptual design of the instrument was verified by Monte Carlo simulation basing on Geant4 tools package. As shown in Fig. 5, different kinds of particle can be easily identified by the energies deposited in the three detectors.

2.5 The Matching Experiments of MESCs

2.5.1 Identification of the Culture Condition of Mouse Cells in the SRGDB

In the payload "Space Radiation on Genomic DNA and its genetic effects Box" (SRGDB), we used the wild type and corresponding radiation sensitive mutant mammalian cells and fruit fly models. The mESCs should be cultured in an atmosphere of 95% air/5% CO_2 at 37 °C while the fruit flies should be kept in a normal atmosphere at 18–27 °C. According to the original design of the SRGDB, both the cell culture device and the fruit fly culture container can exchange gases with the inner

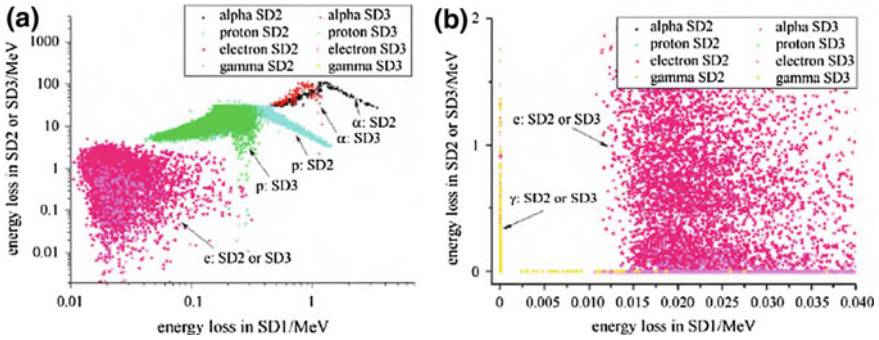

Fig. 5 Particle identification capability of the space radiation detector derived from simulation. The left figure show the differences of energies deposited in the three detectors of the instrument by charge particles. The right figure show the differences of energies deposited in the three detectors by the γ-ray and electrons. With the fluxes derived by the space radiation detector, the radiation dosage of the biological tissue can be deduced, which will provide the data for further research

environment of SRGDB. Thus, we first tried to culture the mESCs under normal atmosphere.

Hydroxyethyl piperazine ethanesulfonic acid (HEPES) is widely used in cell culture. Compared to bicarbonate buffers, it is better at maintaining physiological pH despite changes in carbon dioxide concentration. Therefore, we tested the growth of mESCs under normal atmosphere in the medium containing HEPES. The wild type mESCs were seeded in five 60 mm dishes which were designated as 1#, 2#, 3#, 4# and 5#, and were cultured in the CO_2 incubator for 18 h to achieve adhesion. Then the cells were treated as mentioned below: 1#, the cells cultured in CO_2 incubator without HEPES; 2#, the cells cultured without HEPES at 37 °C and saturated humidity under normal atmosphere; 3#, the cells cultured with 10 mM HEPES at 37 °C and saturated humidity under normal atmosphere; 4#, the cells cultured with 20 mM HEPES at 37 °C and saturated humidity under normal atmosphere; 5#, the cells cultured with 50 mM HEPES at 37 °C and saturated humidity under normal atmosphere. Twenty-four hours after the treatment, the cells were observed under a light microscope and photographed. As shown in Fig. 6, the cells grew well with 50 mM HEPES when cultured at 37 °C and saturated humidity under normal atmosphere for 1 day. However, as the culture time prolonged to 5 days, the cells could not survive with 50 mM HEPES under normal atmosphere. Therefore, we failed to culture the mESCs under normal atmosphere.

Finally, we changed the design of the SRGDB. (1) We changed the fruit fly culture container as an air-proof structure and isolated it from the cell culture devices. (2) Before we sealed the SRGDB, we placed the SRGDB in a CO_2 incubator with 95% air and 5% CO_2 for 30 min. Thus, the inner environment of SRGDB was the same as that of the CO_2 incubator.

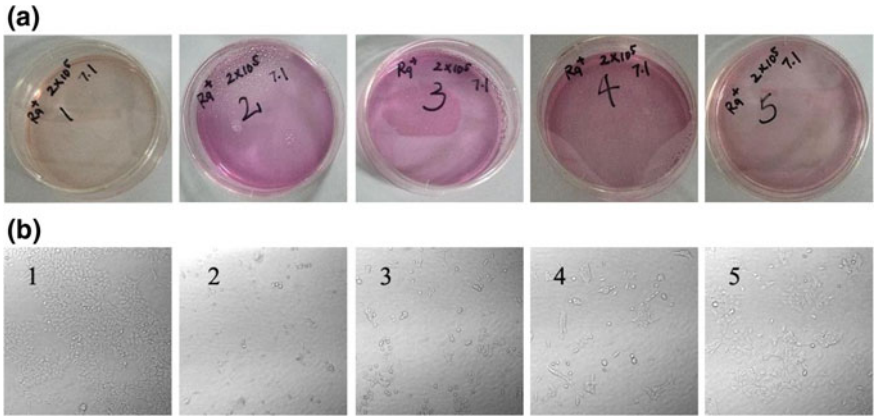

Fig. 6 The growth of mES cells cultured in different concentrations of HEPES. 1#, the cells cultured in CO_2 incubator without HEPES; 2#, the cells cultured without HEPES at 37 °C and saturated humidity under normal atmosphere; 3#, the cells cultured with 10 mM HEPES at 37 °C and saturated humidity under normal atmosphere; 4#, the cells cultured with 20 mM HEPES at 37 °C and saturated humidity under normal atmosphere; 5#, the cells cultured with 50 mM HEPES at 37 °C and saturated humidity under normal atmosphere

2.5.2 Successful Culture of MESCs in the Cell Culture Device of SRGDB

As shown in Fig. 3, the cell culture device is mainly composed of a cell culture plate, an upper cover, a demarcation plate, a rolling film and a hollow connector. First of all, the cells were seeded on the culture plate which was placed in a 10 cm culture dish and cultured in a CO_2 incubator. After adhesion, the culture plate was assembled with the other components into the cell culture device under aseptic conditions. Then 50 ml medium was injected into the cell culture device without bubble. The cell culture device was placed in the CO_2 incubator before it was installed into the SRGDB. To achieve this, we solved the following problems.

Selection of Suitable Cell Culture Plate: We compared two kinds of culture plates which were made of polycarbonate and polystyrene. As shown in Fig. 7, the status of the cells cultured on the plate of polystyrene was much better than those cultured on the plate of polycarbonate. Thus, we chosed the plate of polystyrene in this work.

Selection of the Suitable Sterilization Method for the Components of the Cell Culture Device: The components of the cell culture device can be sterilized with high-pressure saturated steam except the culture plate. Thus, we tried different methods for the sterilization of the culture plate. At first, we used UV radiation combined with alcohol soaking. Both sides of the culture plates were exposed to UV at 880 $\mu W/cm^2$ for 10 min, then the plate was soaked into alcohol (75%) overnight. Finally, the plates were dried in the ultra-clean bench before use. However, the pollution rate of the plates was over 50%, which was unacceptable. Then we tried another

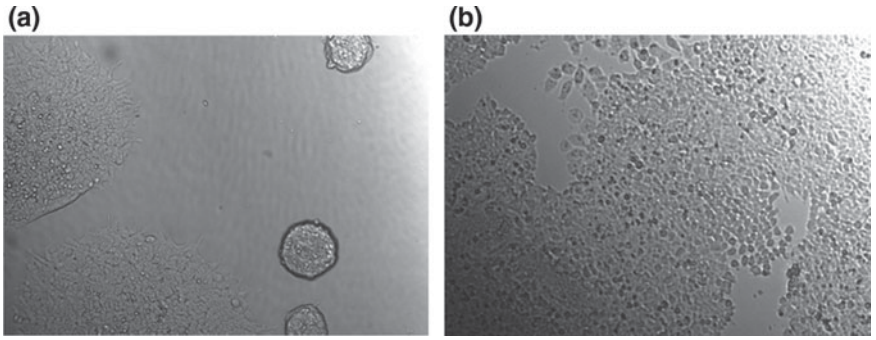

Fig. 7 The growth of cells on different materials. **a** The cells cultured on the plate of polycarbonate; **b** the cells cultured on the plate of polystyrene

method. One piece of the culture plate was placed in a cell culture dish with 100 mm × 20 mm style. Such dishes were sealed in a plastic bag with 20/sleeve and irradiated with 25 kGy gamma-ray before use. Using this method, the pollution rate of the plates was zero and the cells grew well on these plates.

Identification of the Suitable Cell Number for Seeding on the Cell Culture Plate: As to *mRad9*$^{+/+}$ mESCs, we seeded 10^6 cells for 1 day's culture and 2×10^5 cells for 5 days' culture. As to *mRad9*$^{-/-}$ mESCs, we seeded 10^6 cells for 1 day's culture and 4×10^5 cells for 5 days' culture.

2.5.3 Examination of the Effects of the Remaining Medium on the Preservation of the Cells in RNAlater

In our plan, after 1 day and 5 days' culture, the medium will be discharged, while the RNAlater will be injected. Then the cells will be preserved in the RNAlater for RNA and DNA extraction after the recovery of the satellite. However, as mentioned above, the volume change between the rolling film turns up and down is 95% of the actual liquid capacity. Therefore, there will be a certain amount of remaining medium in the RANlater after the fixation of the cells. Thus, we detected the effects of different amount of remaining medium on the preservation of the cells in RNAlater.

We preserved the cells in RNAlater with 5, 10, 15 and 20% medium and stored at 8 °C for 14 days. Then the cells were lysed with Trizol and RNA was extracted. It showed that even the quantity of the RNA extracted from the cells preserved in the RNAlater with 20% medium was good enough for further RNA sequencing analysis.

2.5.4 Identification of the Best Work Flow of the Assembly of the SRGDB Before the Launch of the Satellite

In the SRGDB, the cell culture device, fruit fly culture containers, fluid reservoirs, the injection pumps, the liquid distributor and the tubes etc. all need to be installed under aseptic conditions before the launch of the SJ-10 satellite. First of all, we identified the suitable length of each tube and the best work flow of assembly of the SRGDB (Fig. 8). Then, according to this work flow, we performed the matching experiments again and again. As shown in Fig. 9, both *mRad9*$^{+/+}$ and *mRad9*$^{-/-}$ mESCs cultured for 1 day and 5 days grew well in the payload of SRGDB.

2.6 The Matching Experiments of Fruit Flies

2.6.1 Optimization of Medium Supply and Light

The diameter of each medium baffle and distance between baffles were optimized to adapt the requirement of fruit flies and satellite flight. Flies grow in the condition of 12 h light per day supplied by light-emitting diode light.

2.6.2 Mechanical Examination

To ensure that the fly culture container and the fly medium are fixed well and the flies can survive during the launch, flight and return of the satellite, containers with medium and flies at different developmental stage including eggs, larvae, pupae and adults, were examined for vibration, concussion and hypergravity at higher level than actual situation. The flies were cultured in the containers afterwards for designed time. The adult flies were alive and the others at different developmental stage could developed to later stage until adults. The containers were intact, and the medium baffles and medium were fixed well.

2.6.3 Viability of Fruit Fly in Different Air

Because the whole SRGDB contains air with 5% carbon dioxide, we try culture the flies in this condition at 25 °C and 12 h light per day, however adult flies died in 3–5 days (Fig. 10a). Then we tried to culture flies in the sealed culture container with about 50 ml of normal air. Flies could be alive until 8 days that couldn't meet the travel time of the satellite (Fig. 10b). The adult flies might die of Oxygen consumption and carbon dioxide increase due to movement. Then we tried late 3rd instar larvae and early pupae in sealed culture container. Both could survive more than 14 days, but the eclosion rate of larvae is lower than pupae.

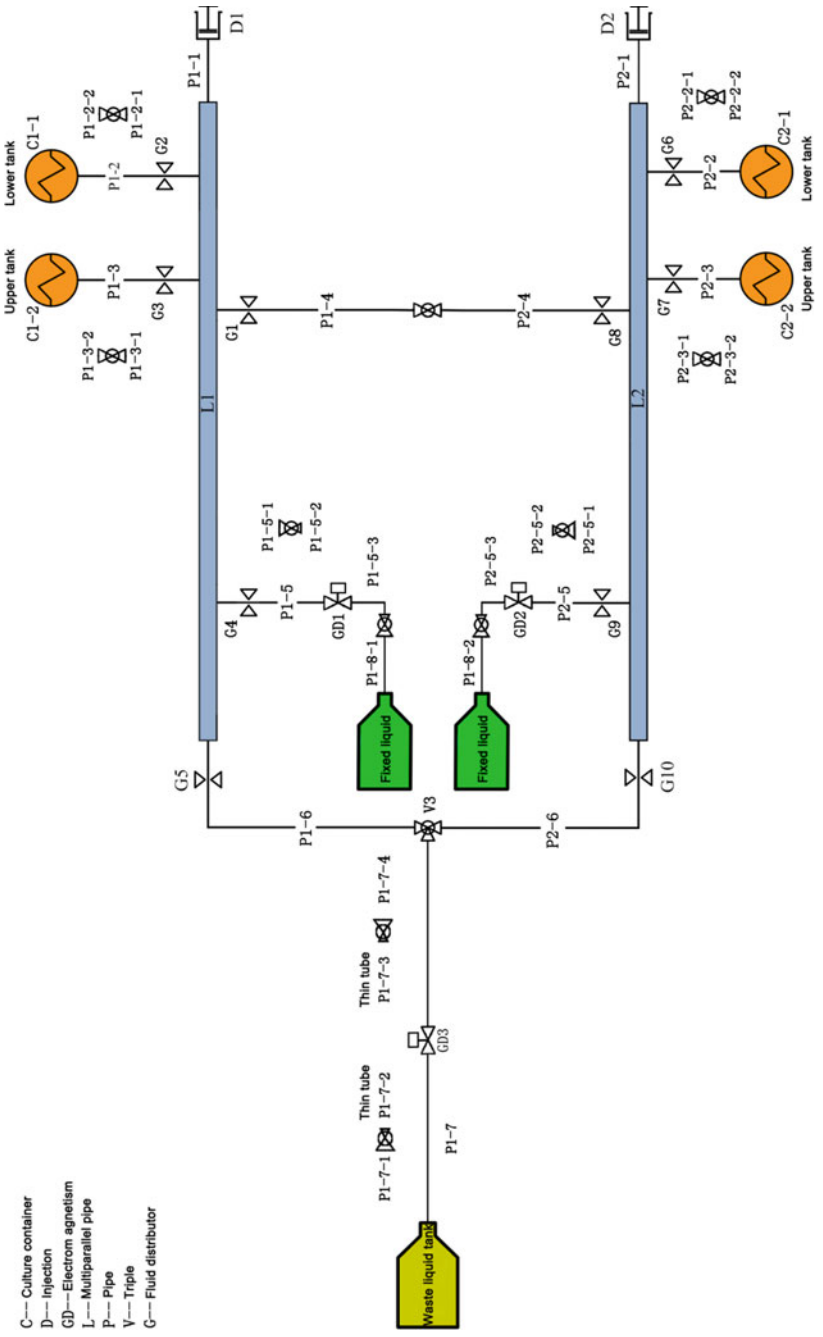

Fig. 8 Schematic diagram of the SRGDB system

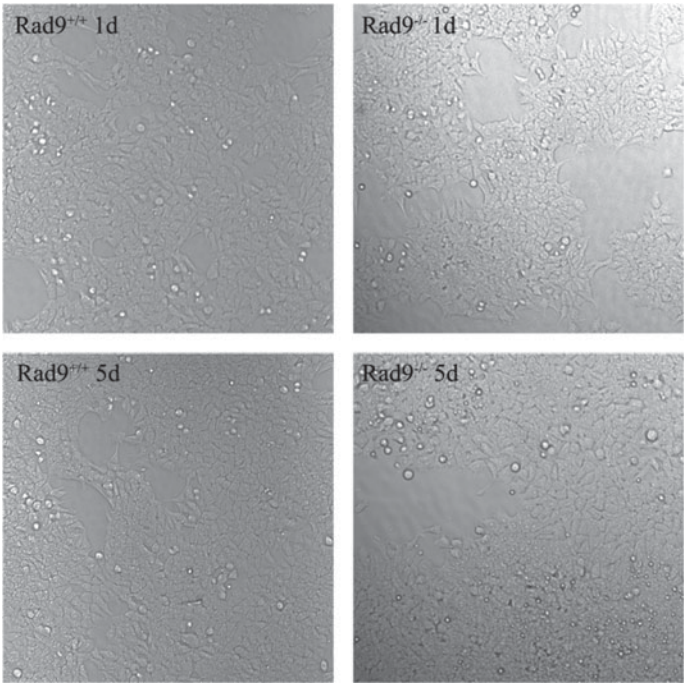

Fig. 9 The growth state of mES cells was obtained by matching test

2.6.4 Optimization of Assembly

Only male flies were used to minimize the oxygen consumption. According to the experiments mentioned above, pupae was chosen for the assembly. Three pupae per container is the maxim after serial tests. The optimized procedure is that late 3rd instar larvae are prepared one day before assembly for puparation and the strong early pupae are installed in the culture container when assembly.

2.7 The Flight Experiment

2.7.1 The Procedure of the Flight Experiment

Preparation works

Prepare Gelatin-coated Culture Plates: The sterilized culture plate in the culture plate was emerged in 0.1% gelatin for 30 min. Then the gelatin was discharged and the plate was dried in the ultra-clean bench. The culture dish with gelatin-coated plate was placed in the CO_2 incubator before use.

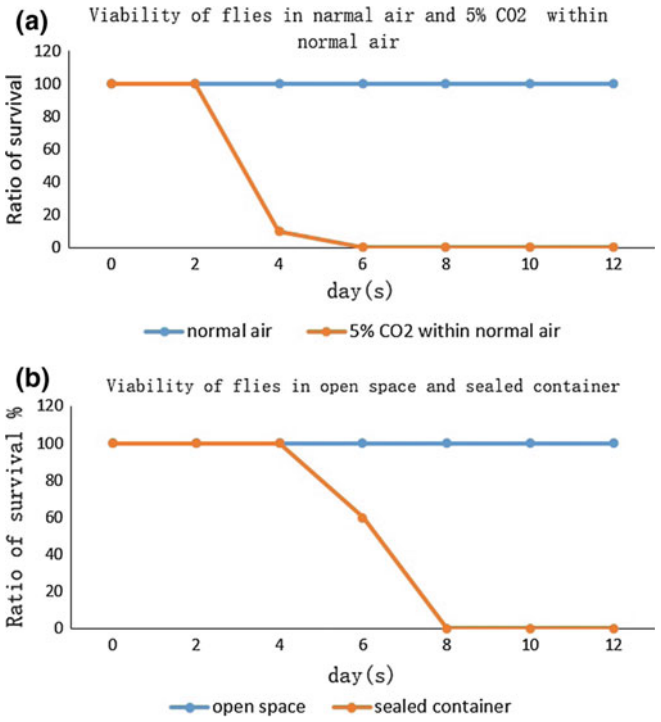

Fig. 10 Viability of fruit fly in different air. **a** Normal air and 5% CO_2 within normal air. **b** Open space and sealed container

Preparation of the Items for Assembling of the Cell Culture Devices: The top part of the container, the middle part of the container, the bottom part of the container, the demarcation plate, the rolling film, the screws, the syringe, and the tubes (P1-3-2, 27 cm, for cell culture device 1#; P1-2-2, 32 cm, for cell culture device 2#; P2-3-2, 21 cm, for cell culture device 3#; P2-2-2, 32 cm, for cell culture device 4#) were sterilized with high-pressure saturated steam.

Preparation of the Items for Assembling of the Tubes to the Fluid Distributor: The following 6 tubes were connected to multiparallel pipe 1 in order from left to right, P2-6 (20 cm), P2-5-1 (20 cm), P2-4 (15 cm), P2-3-1 (26 cm), P2-2-1 (26 cm) and P2-1 (35 cm). The following 6 tubes were connected to multiparallel pipe 2 in order from left to right, P1-6 (20 cm), P1-5-1 (20 cm), P1-3-1 (20 cm), P1-2-1 (20 cm), P1-4 (15 cm), P1-1 (35 cm). The two multiparallel pipes connected with the tubes mentioned above, the two-way joints, the scissors and the tweezers were sterilized with high-pressure saturated steam.

Preparation of the Items for Assembling of the Tubes to the Electromagnetic Valve: The tubes connected to the electromagnetic valve were thinner than the other tubes. The following tubes were needed, P1-5-2 (17 cm, thin, connected with a two

way joint with variable diameter), P2-5-2 (17 cm, thin, connected with a two way joint with variable diameter), P1-5-3 (10 cm, thin, connected with a two way joint with variable diameter), P2-5-3 (11 cm, thin, connected with a two way joint with variable diameter), P1-7-3 (thin, 10 cm)-two way joint with variable diameter-P1-7-4 (normal, 9 cm)-three way joint and P1-7-2 (thin, 20 cm). These tubes, two syringes, a scissor, a tweezer, the screws and the wrenches were sterilized with high-pressure saturated steam.

Preparation of the Items for Assembling of the Waste Liquid Tank: Install the inner part, the outer part and the rolling film of the waste liquid tank. Connect the tube (P1-7-1, 29 cm) to the waste liquid tank. The assembled waste liquid tank, a syringe and the binder clips were sterilized with high-pressure saturated steam.

Preparation of the Items for Assembling of the Fixed Liquid Tanks: Install the inner part, the outer parter and the rolling film of the fixed liquid tanks. Connect the tube (P1-8-1, 10 cm) to the fixed liquid tank 1# and the tube (P1-8-2, 20 cm) to the fixed liquid tank 2#. The assembled fixed liquid tanks, a syringe, the three-way joints and the binder clips were sterilized with high-pressure saturated steam.

Preparation of Other Items: The bottles with ultra-pure water, the syringes, the gauze, the screws, tubes, tweezers, etc were sterilized with high-pressure saturated steam.

Assembling of SRGDB Before the Launch of the Recoverable SJ-10 Satellite
The overall work flow of assembly of SRGDB before the launch of the SJ-10 satellite was shown in Fig. 11. (a) Seeding of the cells on the culture plate; (b) assembly of the culture plates into the cell culture device; (c) Fixation of the cell culture device on the lower part of the payload body; (d) Assembly of the middle part of SRGDB; (e) Connection of the tubes of the middle part and the lower part of SRGDB; (f) Detection of the circuit parameters; (g) Sealing of the lower part and the middle part of the payload; (h) Weighing of the payload; (i) Placing SRGDB in the CO_2 incubator; (j) Sealing of the upper part and the middle part of the payload. Then SRGDB was transferred to the launch tower and installed into the satellite.

Seeding of the Cells on the Culture Plate: About 55 h before the launch of the SJ-10 satellite, 10^6 *mRad9*$^{+/+}$ mESCs, 2×10^5 *mRad9*$^{+/+}$ mESCs, 10^6 *mRad9*$^{-/-}$ mESCs, 2×10^5 *mRad9*$^{-/-}$ mESCs, were seeded on the gelatin-coated culture plates for 1 day's culture, 5 days' culture, 1 day's culture and 5 days' culture, respectively (Fig. 11a). The cells were cultured in a CO_2 incubator with an atmosphere of 95% air/5% CO_2 at 37 °C.

Assembling of the Culture Plates into the Cell Culture Device: One day after the seeding of the cells (about 31 h before the launch of the SJ-10 satellite), the culture plates were installed into the cell culture device (Fig. 11b). In short, the culture plate was placed in the bottom part of the container. About 7 ml of the medium was added to avoid drying of the cells. The demarcation plate was assembled in the bottom part of the container carefully to avoid the bubbles. Then the rolling film, the middle part of the container and the tube mentioned in "Preparation of the items for assembling

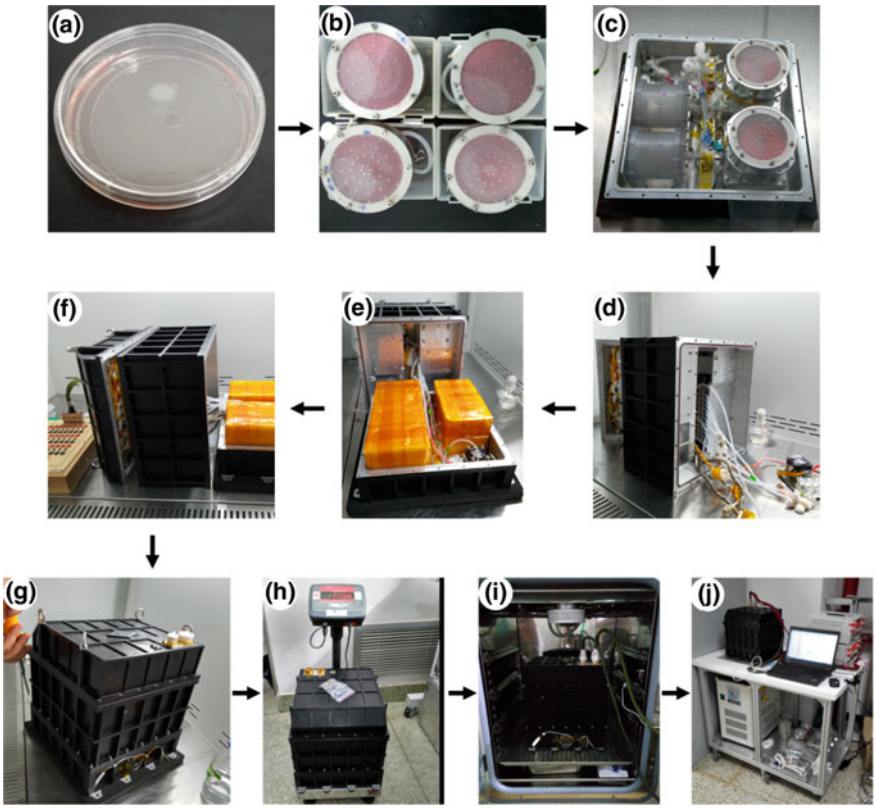

Fig. 11 The assembly flow chart of radiation gene box. **a** Seeding of the cells on the culture plate; **b** assembly of the culture plates into the cell culture device; **c** fixation of the cell culture device on the lower part of the payload body; **d** assembly of the middle part of SRGDB; **e** connection of the tubes of the middle part and the lower part of SRGDB; **f** detection of the circuit parameters; **g** sealing of the lower part and the middle part of the payload; **h** weighing of the payload; **i** placing SRGDB in the CO_2 incubator; **j** sealing of the upper part and the middle part of the payload

of the cell culture devices" was installed. About 45 ml medium was injected into the culture device through the tube and the gas were extracted. At last, the tube was sealed and the upper part of the container was assembled. After assembling, the four culture devices were placed in a CO_2 incubator with an atmosphere of 95% air/5% CO_2 at 37 °C for about 5 h.

Testing the Electromagnetic Valves: About 2 h before the assembling of SRGDB, give power to the SRGDB and connect thin tubes to the electromagnetic valves. Inject 75% alcohol, ultra-pure water and gas in turn to sterilize the inner of the electromagnetic valves and ensure that they can work well.

Preparation of the Ultra-clean Bench: About 1 h before the assembling of SRGDB, open the ultra-clean bench. All the following operations will be performed in the ultra-clean bench.

Fixation of the Cell Culture Devices in the Lower Part of the Payload Body: About 26 h before the launch of the SJ-10 satellite, the four cell culture devices were installed in the lower part of the payload body with the temperature controller (Fig. 11c). This operation needed about 1 h. After assembling, the four cell culture devices together with the lower part of the payload body was placed in a CO_2 incubator with an atmosphere of 95% air/5% CO_2 at 37 °C.

Assembling of the Middle Part of SRGDB: Assembling of the middle part of SRGDB (Fig. 11d) needed about 2 h. It contains the following 8 procedures, (1) testing the impermeability of the waste liquid tank, (2) installing the tubes of the fluid distributor, (3) installing the tubes of the electromagnetic valves, (4) fixation of the waste liquid tank in the middle part of SRGDB, (5) fixation of the fluid distributor in the middle part of SRGDB, (6) connection of the tubes of the fluid distributor and the electromagnetic valves, (7) fixation of the fly culture containers in the middle part of SRGDB, (8) assembling of the injecting pump in the middle part of SRGDB.

Testing the Impermeability of the Waste Liquid Tank: Inject 50 ml sterilized ultra-pure water into the waste liquid tank through the tube (P1-7-1) and seal the tube. The waste liquid tank was than placed in the ultra-clean bench to test if there was any water leak.

Installing the Tubes of the Fluid Distributor: Open the gate of the fluid distributor in order and insert the tubes connected to the two multiparallel pipes (see "Preparation of the items for assembling of the tubes to the fluid distributor") through the gate. That is, P2-6 in gate 10, P2-5-1 in gate 9, P2-4 in gate 8, P2-3-1 in gate 7, P2-2-1 in gate 6, P1-6 in gate 5, P1-5-1 in gate 4, P1-3-1 in gate 3, P1-2-1 in gate 2 and P1-4 in gate 1. Then P1-4, P2-4, P1-3-1, P1-2-1, P2-3-1 and P2-2-1 were connected with a two-way joint, respectively.

Installing the Tubes of the Electromagnetic Valves: Connect the prepared tubes (see 13.3.7.1.1.4) with the 3 electromagnetic valves. That is, P1-5-2 with gate 1 of electromagnetic valve 1#, P1-5-3 with gate 2 of electromagnetic valve 1#, P2-5-2 with gate 1 of electromagnetic valve 2#, P2-5-3 with gate 2 of electromagnetic valve 2#, P1-7-3 with gate 1 of electromagnetic valve 3# and P1-7-2 with gate 2 of electromagnetic valve 3#. Then P1-7-3 and P1-7-2 were fixed to the electromagnetic valve 3# with screws to avoid their drop.

Fixation of the Waste Liquid Tank in the Middle Part of SRGDB: Draw out the ultra-pure water from the waste liquid tank (see "Testing the Impermeability of the Waste Lquid Tank"), connect P1-7-1 with a two way joint with variable diameter and fix the waste liquid tank in the middle part of SRGDB with screws.

Fixation of the Fluid Distributor in the Middle Part of SRGDB with Screws.

Connection of the Tubes of the Fluid Distributor and the Electromagnetic Valves: Connect P1-5-1 (gate 4 of the fluid distributor) with P1-5-2 (gate 1 of electromagnetic valve 1#), P2-5-1 (gate 9 of the fluid distributor) with P2-5-2 (gate 1 of electromag-

netic valve 2#) and P1-6 (gate 5 of the fluid distributor) as well as P2-6 (gate 10 of the fluid distributor) with P1-7-3 (gate 1 of electromagnetic valve 3#).

Fixation of the Fly Culture Containers in the Middle Part of SRGDB with Screws.

Assembling of the Injecting Pump in the Middle Part of SRGDB: The needle syringe 1# (5 ml) was connected with the tube P1-1 (see "Preparation of the items for assembling of the tubes to the fluid distributor") and fixed to the liquid transportation and control unit with screws. The needle syringe 2# (5 ml) was connected with the tube P2-1 (see "Preparation of the items for assembling of the tubes to the fluid distributor") and fixed to the liquid transportation and control unit with screws.

Connection of the Lower part and the Middle Part of SRGDB: Connection of the lower part and the middle part of SRGDB (Fig. 11e.) needed about 1.5 h. It contains the following 6 procedures, (1) fixation of the fixed liquid tanks in the lower part of SRGDB, (2) connection of the tubes of the middle part and the lower part of SRGDB, (3) adjust the temperature of the CO_2 incubator, (4) fixation of the electromagnetic valves, (5) connection of the wire terminals, (6) add the foam box for heat preservation.

Fixation of the Fixed Liquid Tanks in the Lower Part of SRGDB: Inject 164 ml RNAlater into the fixed liquid tank 1# through the tube P1-8-1. Inject 164 ml RNAlater into the fixed liquid tank 2# through the tube P1-8-2. The two fixed liquid tanks were installed in the lower part of SRGDB with screws.

Connection of the Tubes of the Middle Part and the Lower Part of SRGDB: Connect the tube P1-3-2 (cell culture device 1#) with the tube P1-3-1 (gate 3), the tube P1-2-2 (cell culture device 2#) with the tube P1-2-1 (gate 2), the tube P2-3-2 (cell culture device 3#) with the tube P2-3-1 (gate 7), the tube P2-2-2 (cell culture device 4#) with the tube P2-2-1 (gate 6), the tube P1-8-1 (fixed liquid tank 1#) with the tube P1-5-3 (gate 2 of electromagnetic valve 1#) and the tube P1-8-2 (fixed liquid tank 2#) with the tube P2-5-3 (gate 2 of electromagnetic valve 2#).

Adjust the Temperature of the CO_2 Incubator to 25 °C.

Fixation of the Electromagnetic Valves: Take off the tube P1-5-3 from gate 2 of electromagnetic valve 1# and inject sterilized ultra-pure water from P1-5-3 to make sure the space in the tube from the fixed liquid tank 1# to the gate 2 of electromagnetic valve 1# was full of water to avoid the blockage of the tube by the crystallization of RNAlater. Then the tube P1-5-3 was connected to the gate 2 of electromagnetic valve 1# again. After that, the tubes P1-5-2 and P1-5-3 were fixed to the electromagnetic valve 1# with screws to avoid their drop. Take off the tube P2-5-3 from gate 2 of electromagnetic valve 2# and inject sterilized ultra-pure water from P2-5-3 to make sure the space in the tube from the fixed liquid tank 2# to the gate 2 of electromagnetic valve 2# was full of water to avoid the blockage of the tube by the crystallization of RNAlater. Then the tube P2-5-3 was connected to the gate 2 of electromagnetic valve 2# again. After that, the tubes P2-5-2 and P2-5-3 were fixed to the electromagnetic valve 2# with screws to avoid their drop. At last, the three electromagnetic valves were fixed to the lower part of SRGDB with screws.

Connection of the Wire Terminals.

Add the Foam Box on the Cell Culture Devices and the Fixed Liquid Tanks for Heat Preservation.

Detection of the Circuit Parameters: Detection of the circuit parameters (Fig. 11f) needed about 15 min.

Sealing of the Lower Part and the Middle Part of SRGDB: Sealing of the lower part and the middle part of SRGDB (Fig. 11g) needed about 1 h. It contains the following 3 procedures, (1) discharging the gas in the tube from cell culture device to the liquid distributor, (2) connection of the tubes of the electromagnetic valve and the waste liquid tank, (3) sealing of the lower part and the middle part of SRGDB.

Discharging the Gas in the Tube from Cell Culture Device to the Liquid Distributor: To avoid the effects of the gas in the tube between the cell culture devices and the gate of the liquid distributor on our experiment on board the satellite, we discharged the gas in the tube on this line. The tube P1-7-2 (gate 2 of electromagnetic valve 3#) was placed in a sterilized tube. Then 5 ml of medium was bumped out from each cell culture device and flowed out through P1-7-2 into the sterilized tube. This process was controlled by the liquid Transportation and Control Unit, which was to make sure the space in the tube from the cell culture devices to the gate of the liquid distributor was full of medium.

Connection of the Tubes of the Electromagnetic Valve and the Waste Liquid Tank: Connect the tube P1-7-1 (waste liquid tank) with the tube P1-7-2 (gate 2 of electromagnetic valve 3#).

Sealing of the Lower Part and the Middle Part of SRGDB: Seal the lower part and the middle part of SRGDB with screws.

Weighing of the Payload (Fig. 11h).

Placing SRGDB in the CO_2 Incubator: To ensure that the atmosphere inside the SRGDB was the same as that in the CO_2 incubator (95% air/5% CO_2), we placed the SRGDB in the CO_2 incubator with the upper part open for 30 min (Fig. 11i). The temperature inside the CO_2 incubator was about 25 °C (see 13.3.7.1.2.3) to maintain the survival of the fruit flies, while the temperature of the cell culture devices were heated to 37 °C by the temperature controller of the SRGDB to maintain the survival of the cells.

Sealing of the Upper Part and the Middle Part of the Payload: Seal the upper part and the middle part of the payload with screws as soon as possible (Fig. 11j). Then SRGDB was transferred to the launch tower and installed into the satellite.

2.7.2 The Results of the Space Radiation Detector

The space radiation detector in Rad Gene Box, onboard SJ-10 satellite, reached the orbit on Apr 6, 2016 with the orbit parameters: the height of 233–277 km and inclination of 43°. The measurement was conducted continuously between Apr 6 and Apr 18. The instrument worked properly during the whole process, no invalid data

Table 3 The fluxes of γ-ray, electronic, proton and Helium in different energy range obtained by the space radiation detector

Electron-1 (0.5–1 MeV)	81,612
Electron-2 (1–2 MeV)	864
Electron-3 (2–10 MeV)	2553
Gamma (0.5–2 MeV)	5,953,956
Proton-1 (5–7 MeV)	1236
Proton-2 (7–10 MeV)	430
Proton-3 (10–15 MeV)	328
Proton-4 (15–35 MeV)	9812
Proton-5 (35–50 MeV)	230
Proton-6 (50–85 MeV)	398
Proton-7 (85–150 MeV)	831
Proton-8 (150–200 MeV)	1506
Alpha1 (30–60 MeV)	38
Alpha2 (60–130 MeV)	770
Alpha3 (130–300 MeV)	220

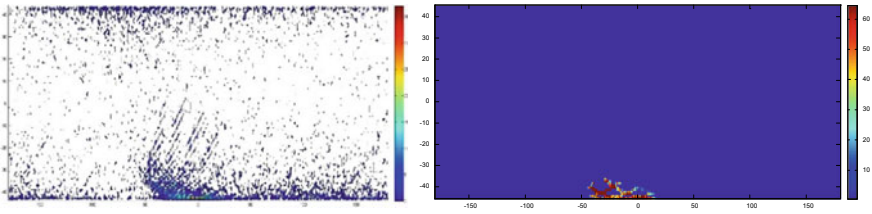

Fig. 12 The comparison of the Proton fluxes derived by the space radiation detector and the AP8 Model, which shown a good agreement between each other

was found in the engineering parameters and scientific data. The radiation particle fluxes in Rad Gene Box of γ-ray, electronic, proton and Helium were obtained, as shown in Table 3.

The predictions of electron and proton fluxes by AE-8 and AP-8 were derived with the orbit parameter of the SJ-10 satellite. The measuring results are in good accordance with the predictions. As shown in Figs. 12 and 13. It demonstrate the correctness of the instrument design.

2.7.3 The Results of mESCs

After the return of the satellite, the culture plates were taken out of the cell culture device, washed with PBS and observed under the microscope. As shown in Fig. 14, the mESCs grew well on the culture plates during the flight and could be used for the following experiments. As for the control group, after the return of the satellite, we

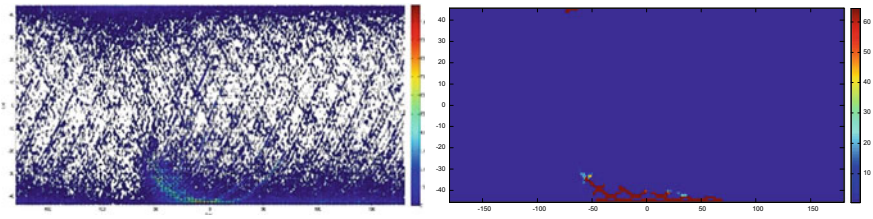

Fig. 13 The comparison of the electron fluxes derived by the space radiation detector and the AE8 Model, which shown a good agreement between each other

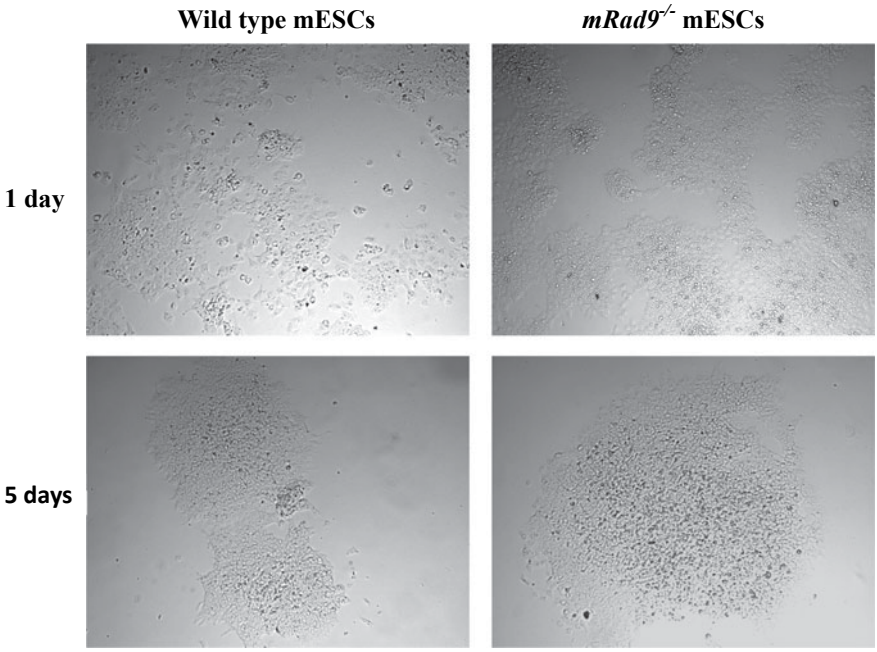

Fig. 14 The mESCs grew well on the culture plates during the flight

performed the experiments of wild type *mRad9*$^{+/+}$ mESCs and *mRad9*$^{-/-}$ mESCs on the ground using the same payload and the same procedure as the experiments performed onboard SJ-10 satellite.

The cells on the culture plates were lysed with Trizol. Some of the samples were sent to Berry Genomics Co, Ltd. for RNA extraction and subsequent RNA-sequence analysis. The RNA extracted from the samples was with good quality and could be used for high throughput RNA sequencing analysis.

After data quality evaluation, we identified the DEGs using a threshold of fold change ≥ 2, FDR < 0.05. We had 8 samples in total and identified 12 sets of DEGs which could be clustered into 3 groups concerning the comparison of space/ground,

wildtype *mRad9*$^{+/+}$ mESCs/*mRad9*$^{-/-}$ mESCs, and 1 day's culture/5 days' culture respectively.

As for the comparison of space and ground, there are 372 genes up-regulated and 674 genes down-regulated in wild type *mRad9*$^{+/+}$ mESCs cultured for 1 day, 710 genes up-regulated and 987 genes down-regulated in wild type *mRad9*$^{+/+}$ mESCs cultured for 5 days, 92 genes up-regulated and 311 genes down-regulated in wild type *mRad9*$^{-/-}$ mESCs cultured for 1 day, and 91 genes up-regulated and 380 genes down-regulated in *mRad9*$^{-/-}$ mESCs cultured for 5 days. As for the comparison of wild type *mRad9*$^{+/+}$ mESCs and *mRad9*$^{-/-}$ mESCs, there are 1110 genes up-regulated and 596 genes down-regulated in the samples cultured for 1 day in space, 286 genes up-regulated and 291 genes down-regulated in the samples cultured for 5 days in space, 527 genes up-regulated and 190 genes down-regulated in the samples cultured for 1 day on the ground, and 778 genes up-regulated and 444 genes down-regulated in the samples cultured for 5 days on the ground. As for the comparison of 1 day's culture and 5 days' culture, there are 458 genes up-regulated and 288 genes down-regulated in wildtype *mRad9*$^{+/+}$ mESCs cultured in space, 96 genes up-regulated and 213 genes down-regulated in *mRad9*$^{-/-}$ mESCs cultured in space, 476 genes up-regulated and 571 genes down-regulated in wild type *mRad9*$^{+/+}$ mESCs cultured on the ground, 32 genes up-regulated and 31 genes down-regulated in *mRad9*$^{-/-}$ mESCs cultured on the ground.

In general, space flight made more genes down-regulated than up-regulated in either wild type *mRad9*$^{+/+}$ mESCs or *mRad9*$^{-/-}$ mESCs. In our previous work, we reported that hydroxyurea (Hu, a genotoxic agent) induced global transcriptional suppression in wild type *mRad9*$^{+/+}$ mESCs (Cui et al. 2010). It seems that like Hu treatment, space flight is also suppressive in global gene expression. However, the mechanism needs further investigation. Since it has been well studied that *mRad9*$^{-/-}$ mESCs are more sensitive to DNA damage agents such as UV light, gamma rays and hydroxyurea than wildtype *mRad9*$^{+/+}$ mESCs, we expected more significant alternation of the gene expression profile in *mRad9*$^{-/-}$ mESCs than that in wild type *mRad9*$^{+/+}$ mESCs. Contrary to our expectations, the alternation of space flight induced global gene expression was weaker in *mRad9*$^{-/-}$ mESCs than that in wild type *mRad9*$^{+/+}$ mESCs. This phenomenon is novel and deserves further investigation.

2.7.4 The Results of Fruit Flies

Late 3rd instar male larvae were prepared one day before assembly for pupation and the strong early pupae were installed in the culture container when assembly (Fig. 15). All pupae developed in to adult flies in the condition of space environment, lower Oxygen and higher carbon dioxide (Fig. 16).

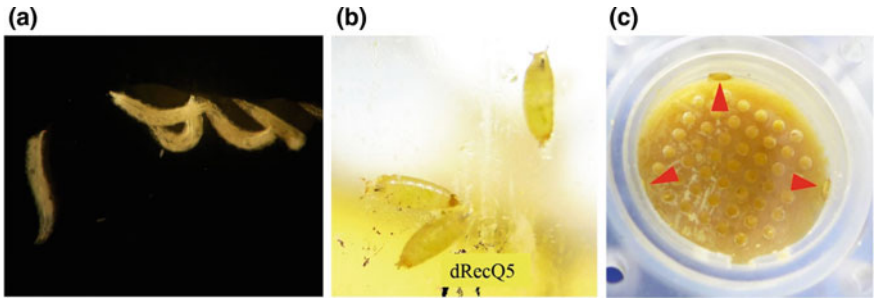

Fig. 15 Preparation of assembly. **a** Late 3rd instar male larvae. **b** Pupation. **c** Installation in culture container. Arrow head indicates the pupae

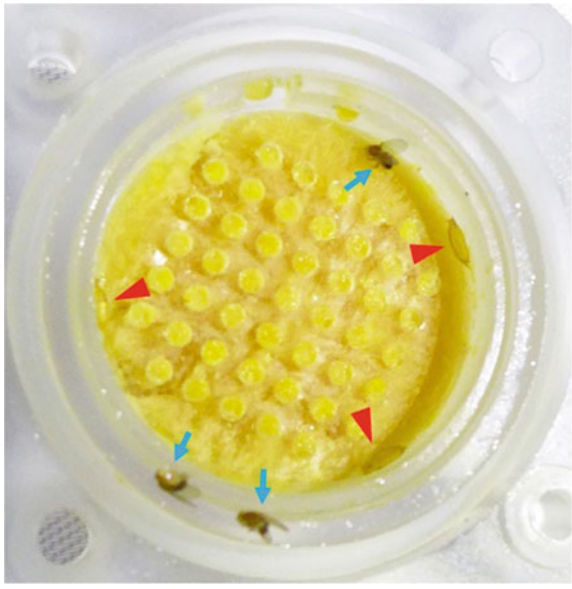

Fig. 16 Pupae developed to adult flies during satellite flight. Arrow head indicates empty pupal exuviate, and arrow indicates enclosed adult fly

Acknowledgements This work was supported by the grants from "Strategic Priority Research Program" of the Chinese Academy of Sciences (Grant No. XDA04020202-13 and XDA04020413) and National Natural Science Foundation of China (U1738112).

References

Asaithamby A, Hu B, Chen DJ (2011) Unrepaired clustered DNA lesions induce chromosome breakage in human cells. Proc Natl Acad Sci USA 108(20):8293–8298

Baker DN, Mason GM, Figueroa O et al (1993) An overview of the solar anomalous, and magnetospheric particle explorer (SAMPEX) mission. IEEE Trans Geosci Remote Sens 31(3):531–541

Benguría A, Grande E, Juan ED et al (1996) Microgravity effects on Drosophila melanogaster behavior and aging. Implications of the IML-2 experiment. J Biotechnol 47 (2–3):191–201
Bidoli V, Casolino M, Pascale MD et al (2000) Study of cosmic rays and light flashes on board Space Station MIR: the SilEye experiment
Boatella C, Hubert G, Ecoffet R et al (2009) ICARE on-board SAC-C: more than 8 years of SEU and MCU. Anal Predict 57(4):369–374
Chen Y, Wen D, Yu Z et al (2010) Drosophila RecQ5 is required for efficient SSA repair and suppression of LOH in vivo. Protein Cell 1(5):478–490
Cucinotta FA, Durante M (2006) Cancer risk from exposure to galactic cosmic rays: implications for space exploration by human beings. Lancet Oncol 7(5):431–435
Cucinotta FA, Manuel FK, Jones J et al (2001) Space radiation and cataracts in astronauts. Radiat Res 156(1):460–466
Cui P, Lin QC, Han L et al (2010) Hydroxyurea-induced global transcriptional suppression in mouse ES cells. Carcinogenesis 31(9):1661–1668
Dang B, Yang Y, Zhang E et al (2014) Simulated microgravity increases heavy ion radiation-induced apoptosis in human B lymphoblasts. Life Sci 97(2):123–128
Degan P, Sancandi M, Zunino A et al (2005) Exposure of human lymphocytes and lymphoblastoid cells to simulated microgravity strongly affects energy metabolism and DNA repair. J Cell Biochem 94(3):460–469
Delp MD, Charvat JM, Limoli CL et al (2016) Apollo lunar astronauts show higher cardiovascular disease mortality: possible deep space radiation effects on the vascular endothelium. Sci Rep 6:29901
Dubinin NP, Glembotsky YL, Vaulina EN et al (1973) Effects of space flight factors on Drosophila. Life Sci Space Res 11:163–165
Dubinin NP, Glembotsky YL, Vaulina EN et al (1977) Biological experiments on the orbital station Salyut 4. Life Sci Space Res 15:267–272
Durante M, Cucinotta FA (2008) Heavy ion carcinogenesis and human space exploration. Nat Rev Cancer 8:7
Durante M, Kraft G, O'Neill P et al (2007) Preparatory study of a ground-based space radiobiology program in Europe. Adv Space Res 39(2007):1082–1086
Evans HDR, Bühler P, Hajdas W et al (2008) Results from the ESA SREM monitors and comparison with existing radiation belt models. Adv Space Res 42(9):1527–1537
Fennelly J (2011) The energetic particle telescope (EPT) concept and performances. Proc SPIE Int Soc Opt Eng 8148(1):231–242
Filatova LP, Vaulina EN, Tia G (1984) Frequency of chromosome recombination, nondisjunction and breaks in Drosophila melanogaster males exposed during space flight. Genetika 19(12):2008–2013
Girardi C, Pittà CD, Casara S et al (2012) Analysis of miRNA and mRNA expression profiles highlights alterations in ionizing radiation response of human lymphocytes under modeled microgravity. PLoS ONE 7(2):723–727
Glembotskiĭ I, Vaulina EN, Pal'mbakh LR et al (1975) Genetic effects in Drosophila caused by space flight factors in "Kosmos-573". Genetika 11(7):70–77
Goodhead DT (1994) Initial events in the cellular effects of ionizing radiations: clustered damage in DNA. Int J Radiat Biol 65(1):7–17(11)
Goodhead DT (2006) Energy deposition stochastics and track structure: what about the target? Radiat Prot Dosimetry 122(1–4):3–15
Hara R (1994) Genetic effects of cosmic radiation in Drosophila melanogaster. Biol Sci Space 8(1):12–22
Hellweg CE, Shahana D, Astrid A et al (2015) Space experiment "cellular responses to radiation in space (CellRad)": hardware and biological system tests. Life Sci Space Res 7:73–89
Herranz R, Benguría A, Laván DA et al (2010) Spaceflight-related suboptimal conditions can accentuate the altered gravity response of Drosophila transcriptome. Mol Ecol 19(19):4255–4264

Hu WR, Zhao JF, Long M et al (2014) Space program SJ-10 of microgravity research. Microgravity Sci Technol 26:159–169
Ikenaga M, Yoshikawa I, Kojo M et al (1998) Mutations induced in Drosophila during space flight. Biol Sci Space 11(4):346–350
Jiang YD, Li WN, Wang LF et al (2008) Several new type of clinostats. Space Med Med Eng 21(4):368–371
Jones JA, Mccarten M, Manuel K et al (2007) Cataract formation mechanisms and risk in aviation and space crews. Aviat Space Environ Med 78(4 Suppl):56–66
Klement BJ, Young QM, George BJ et al (2004) Skeletal tissue growth, differentiation and mineralization in the NASA Rotating Wall Vessel. Bone 34(3):487–498
Kogan IG, Chzhan TI (1980) Effect of dynamic factors of space flight on the mutagenic effect of radiation. I. Occurrence of dominant lethal mutations during Drosophila melanogaster oogenesis. Genetika 16(4):650–655
Kogan IG, Tia G (1981) [Effect of the dynamic factors of space flight on the mutagenic effect of radiation. II. Development of recessive lethals and loss of X-chromosomes in Drosophila melanogaster oocytes]. Genetika 17(3):455–459
Kumari R, Singh KP, DuMond Jr JW (2009) Simulated microgravity decreases DNA repair capacity and induces DNA damage in human lymphocytes. J Cell Biochem 107(4):723–731
Leonov A, Cyamukungu M, Cabrera J et al (2005) Fluxes of energetic protons and electrons measured on board the Oersted satellite. Ann Geophys 23(9):2975–2982
Li N, An L, Hang H (2015) Increased sensitivity of DNA damage response-deficient cells to stimulated microgravity-induced DNA lesions. PLoS ONE 10(4):e0125236
Liu Y, Wang H, Cui X et al (2015) Physical design and Monte Carlo simulations of a space radiation detector onboard the SJ-IO satellite. Chin Phys C 39(1):54–59
Long M (2014) How to stimulate a space microgravity environment or effect on Earth from the viewpoint of responses of space cell growth to micro-gravity (in Chinese). Chin Sci Bull (Chin Ver) 59(20):2004–2015
Macdougall H, Moore ST (2010) The journey to Mars: physiological effects and operational consequences of long-duration microgravity exposure. J Cosmol
Marco R, González J (1992) Microgravity effects on Drosophila melanogaster development and aging: comparative analysis of the results of the Fly experiment in the Biokosmos 9 biosatellite flight. Adv Space Res Off J Comm Space Res 12(1):157–166
Mognato M, Celotti L (2005) Modeled microgravity affects cell survival and HPRT mutant frequency, but not the expression of DNA repair genes in human lymphocytes irradiated with ionising radiation. Mutat Res/Fundam Mol Mech Mutagen 578(1–2):417–429
Mognato M, Girardi C, Fabris S et al (2009) DNA repair in modeled microgravity: double strand break rejoining activity in human lymphocytes irradiated with γ-rays. Mutat Res/Fundam Mol Mech Mutagen 663(1–2):32–39
Mosesso P, Schuber M, Seibt D et al (2001) X-ray-induced chromosome aberrations in human lymphocytes in vitro are potentiated under simulated microgravity conditions (Clinostat). Phys Med 17 Suppl 1(1):264–266
Ogneva IV, Belyakin SN, Sarantseva SV (2016) The development of Drosophila melanogaster under different duration space flight and subsequent adaptation to earth gravity. PLoS ONE 11(11)
Ohnishi T (2005) The biological effects of space radiation during long stays in space. Biol Sci Space 18(4):201–205
Ohnishi T (2016) Life science experiments performed in space in the ISS/Kibo facility and future research plans. J Radiat Res 57 (S1):rrw020
Ohnishi T, Takahashi A, Ohnishi K et al (1999) DNA damage formation and p53 accumulation in mammalian cells exposed to the space environment. Biol Sci Space 13(2):82–87
Ohnishi T, Ohnishi K, Takahashi A et al (2003) Detection of DNA damage induced by space radiation in Mir and space shuttle. J Radiat Res 43 Suppl (4):S133-S136

Pinsky LS, Thompson LF (1974) Light flashes observed by astronauts on Apollo 11 through Apollo 17. Science 183(4128):957–959
Pinsky LS, Osborne WZ, Hoffman RA et al (1975) Light flashes observed by astronauts on skylab 4. Science 188(4191):928–930
Qiu S (1994) Microgravity and biology. Bull Biol 8:18–20
Reiter LT, Potocki L, Chien S et al (2001) A systematic analysis of human disease-associated gene sequences in Drosophila melanogaster. Genome Res 11(6):1114–1125
Ritter S, Durante M (2010) Heavy-ion induced chromosomal aberrations: a review. Mutat Res 701(1):38–46
Roberts JE, Kukielczak BM, Chignell CF et al (2006) Simulated microgravity induced damage in human retinal pigment epithelial cells. Mol Vis 12(12):633–638
Rodriguez JV, Krosschell JC, Green JC (2014) Intercalibration of GOES 8–15 solar proton detectors. Space Weather Int J Res Appl 12(1):92–109
Saha J, Wang M, Cucinotta FA (2013) Investigation of switch from ATM to ATR signaling at the sites of DNA damage induced by low and high LET radiation. DNA Repair 12(12):1143–1151
Sauvaud JA, Moreau T, Maggiolo R et al (2006) High-energy electron detection onboard DEMETER: the IDP spectrometer, description and first results on the inner belt. Planet Space Sci 54(5):502–511
Sihver L, Ploc O, Puchalska M et al (2015) Radiation environment at aviation altitudes and in space. Radiat Prot Dosimetry 164(4):477–483
Sridharan DM, Whalen MK, Almendrala D et al (2012) Increased Artemis levels confer radioresistance to both high and low LET radiation exposures. Radiat Oncol 7(1):1–12
Sutherland BM, Bennett PV, Schenk H et al (2001) Clustered DNA damages induced by high and low LET radiation, including heavy ions. PM: Int J Devoted Appl Phys Med Biol Off J Ital Assoc Biomed Phys (AIFB) 17(Suppl 1):202–204
Sutherland BM, Georgakilas AG, Bennett PV et al (2003) Quantifying clustered DNA damage induction and repair by gel electrophoresis, electronic imaging and number average length analysis. Mutat Res/Fundam Mol Mech Mutagen 531(1–2):93–107
Thirsk R, Kuipers A, Mukai C et al (2009) The space-flight environment: the International Space Station and beyond. Can Med Assoc J 180(12):1216–1220
Thomson I (1999) EVA dosimetry in manned spacecraft. Mutat Res 430(2):203–209
Vaulina EN, Anikeeva ID, Kostina LN et al (1981) The role of weightlessness in the genetic damage from preflight gamma-irradiation of organisms in experiments aboard the Salyut 6 orbital station. Adv Space Res 1(14):163–169
Vernós I, González-Jurado J, Calleja M et al (1989) Microgravity effects on the oogenesis and development of embryos of Drosophila melanogaster laid in the Spaceshuttle during the Biorack experiment (ESA). Int J Dev Biol 33(2):213–226
Vette JI (1991) The AE-8 trapped electron model environment. Nasa Sti/recon technical report N 92
Wang H, Zhang X, Wang P et al (2010) Characteristics of DNA-binding proteins determine the biological sensitivity to high-linear energy transfer radiation. Nucleic Acids Res 38(10):3245–3251
Wang Y, An L, Jiang Y et al (2011) Effects of simulated microgravity on embryonic stem cells. PLoS ONE 6(12):e29214
Wilson JW, Thibeault SA, Cucinotta FA et al (1995) Issues in protection from galactic cosmic rays. Radiat Environ Biophys 34(4):217–222
Xia JW, Zhan WL, Wei BW et al (2016) Heavy ions research facility in Lanzhou (HIRFL). Chin J 61(4–5):467
Yuge L, Hide I, Kumagai T et al (2003) Cell differentiation and p38MARK cascade are inhibited in human osteoblasts cultured in a three-dimensional clinostat. Vitr Cell Dev Biol Anim 39(1–2):89–97
Zafar F, Seidler SB, Kronenberg A et al (2010) Homologous recombination contributes to the repair of DNA double-strand breaks induced by high-energy iron ions. Radiat Res 173(1):27–39

Zeng Y, Liu X (2007) Experimental technologies for imposing mechanical force on cells. Space Med Med Eng 20(3):227–234

Zhao T, Tang X, Umeshappa CS et al (2016) Simulated microgravity promotes cell apoptosis through suppressing Uev1A/TICAM/TRAF/NF-κB-regulated anti-apoptosis and p 53/PCNA- and ATM/ATR-Chk1/2-controlled DNA-damage response pathways. J Cell Biochem 117 (9)

Effects of the Space Environment on Silkworm Development Time

Zulian Liu, Zhiqian Li, Peng Shang, Yongping Huang and Anjiang Tan

Abstract As aviation technology has developed, there has been more emphasis on exploitation and utilization of the space frontier. The lepidopteran insect *Bombyx mori* has advantages, including small body size, light weight, short life cycle, and well-characterized genetics, when used as a model for biological investigations in space compared with other animals. In preparation for experiments in space, we carried out a simulation experiment, and the number of embryos and the culture temperature and humidity were optimized. The silkworm incubator was launched with China's SJ-10 recoverable microgravity experimental satellite and was in orbit for 12 days and 15 h in 2016. The embryos were cultured in space. Images of the silkworm embryos were obtained during flight. The embryos cultured in space hatched properly after returning to the ground, but silkworm larva obtained from cultures grown on the SJ-10 satellite grew more rapidly than the ground control group. Analyses of subsequent generations and genome, transcriptome, and proteome analyses are ongoing.

Abbreviations

BmNPV	*B. mori* nuclear polyhedrosis virus
cDNA	Coding DNA
CRISPR	Clustered regularly interspaced short palindromic repeats
ISS	International Space Station
mRNA	Messenger RNA
RNAi	RNA interference
TALENs	Transcription activator-like effector nucleases

Z. Liu · Z. Li · Y. Huang · A. Tan (✉)
Key Laboratory of Insect Developmental and Evolutionary Biology, Center for Excellence in Molecular Plant Sciences, Shanghai Institute of Plant Physiology and Ecology, Chinese Academy of Sciences, Shanghai 200032, China
e-mail: ajtan01@sibs.ac.cn

P. Shang
Faculty of Life Sciences, Northwestern Polytechnical University, Xi'an 710072, China

E. Duan and M. Long (eds.), *Life Science in Space: Experiments on Board the SJ-10 Recoverable Satellite*, Research for Development,
https://doi.org/10.1007/978-981-13-6325-2_5

ZFNs Zinc finger nucleases
ZFP Zinc finger proteins

1 Silkworms Are Ideal Subjects for Life-Science Research in Space

1.1 Silkworms Are of Economic Importance

The silkworm, *Bombyx mori*, is an economically important insect due to its ability to produce silk. These insects originated in China and have been raised in the region for thousands of years. Each silkworm larva eats 20–25 g of fresh mulberry leaves during its life and produces approximately 0.2–1 g of silk with a length of 700–1500 m. Thus, the conversion efficiency of leaves to silk is approximately 5%. The silk gland, which is the tissue that biosynthesizes and secretes the silk, is formed at the embryonic stage but grows very slowly during the first four larval stages. The gland has three parts: the anterior silk gland, the middle silk gland, and the posterior silk gland. In the fifth (and final) instar, the silk gland grows rapidly, and the worms begin to spin and form a cocoon at the end of the larval stage. During the fifth larval instar, high levels of polyploidization result in an increase in the production of silk thousands of times higher relative to levels in the fourth instar. Due to the long history of sericulture in China, silk is widely used in the textile industry, in medicine, and in military applications.

1.1.1 The Silkworm as the Lepidopteran Model Insect

The silkworm is also an important model lepidopteran insect. The genome of the silkworm was first sequenced in 2004, and sequences of 40 different silkworm strains were reported in 2006 (Xia et al. 2004, 2009). This genomic information enabled many post-genomic studies. In 2000, Tamura and his colleagues used the *piggyBac* transposon to insert one reporter gene into the silkworm genome, successfully establishing the transgene system in the silkworm (Tamura et al. 2000). Genome editing tools such as zinc-finger nucleases (ZFNs), transcription activator-like effector nucleases (TALENs), and clustered regularly interspaced short palindromic repeats (CRISPR)/Cas9 systems provide us with more choices for loss-of-function analysis in the silkworm (Wang et al. 2013a, b, 2014b). The fact that these tools have been successfully used in silkworm genome editing means that the silkworm is considered the model insect for Lepidoptera.

1.2 The Lifespan of the Silkworm

The silkworm life cycle has four stages: embryo, larva, pupa, and adult. In each stage, the morphology of the silkworm is different. The embryo stage lasts approximately 10 days before hatching into the larval stage. Larvae eat fresh mulberry leaves continuously. The larval stage lasts approximately 18 days. During this stage, the insect normally moults four times; at each moulting, the body becomes slightly yellower and the skin becomes tighter. The larva then stops eating, and when the gut is empty, it enters the wandering stage, indicating that the insect is preparing to enter the pupal phase of the lifecycle. The silkworm encloses itself in a cocoon made of raw silk produced by the salivary glands; building the cocoon takes approximately 2 days. The final moult from larva to pupa takes place within the cocoon, which provides a vital layer of protection during the vulnerable, almost motionless pupal state. The silkworm pupal stage lasts 10 days. At the end of the pupal stage, the insect releases proteolytic enzymes that make a hole in the cocoon so that it can emerge as an adult moth. The female moth produces approximately 300–500 eggs after mating. The entire lifespan of the silkworm is approximately 40–50 days and depends on temperature.

1.3 Suitability of the Silkworm for Space Flight

A large number of scientists are now focused on space-based life science research. In comparison to other model animals, the silkworm has certain advantages for space flight-based research. First, the volume of the silkworm embryo is small, and embryos do not need to be fed during short space flights. Second, the silkworm embryo stage is short, lasting approximately 10 days. Third, differentiation, diapause, metamorphosis, and genetic characteristics of silkworms are well understood (Kotani et al. 2002). The embryos can be maintained in the diapause state for at least two years by controlling the storage temperature (Furusawa et al. 1982). Fourth, radiation of silkworm eggs is an efficient strategy for generating mutations, so the effects of a range of doses of radiation on these insects are understood (Furusawa et al. 2001; Henneberry and Sullivan 1963; Kotani et al. 2002). Most importantly, space research using the silkworm has and will provide insights expected to improve silk production and sericulture.

2 Space Flight History of the Silkworm

2.1 Silkworm Studies in Space Conducted by Researchers Worldwide

In 1997, researchers from the Department of Applied Biology at Kyoto Institute of Technology loaded silkworm eggs onto to the US space shuttle Atlantis (STS-84) with the goal of investigating the effects of cosmic radiation and microgravity on embryogenesis and post-embryonic development in *Bombyx* eggs. Insects in two different developmental stages were studied during the 9-day flight: eggs from the early stage after oviposition and diapause-terminated eggs (Furusawa et al. 2001). Approximately 85% of the eggs in space and in the ground-based control experiments matured; approximately 56% of eggs in the flight group and 43% of eggs in the ground control group hatched. Researchers also found that silkworms in the flight group had morphological disorders, such as segmental fusion of the 4th and 5th segments, and the percent of individuals with abnormal crescent marking was significantly higher than in the control group. It was assumed that the higher rate of abnormalities in the space-based samples than in the ground-based controls was caused by microgravity rather than the influence of cosmic rays, as there was no significant difference in the absorbed dose of radiation between the normal and abnormal larvae that were hatched from the eggs that had been in space (Shimada et al. 1986). These results show that the silkworm could be a useful model to investigate the biological effects of microgravity and cosmic rays on insect development (Kotani et al. 2002).

A series of experiments on silkworms were conducted aboard the Columbia space shuttle on the STS-107 mission. For STS-107, a series of miniature habitats were developed by BioServe Space Technologies, and the BioServe's Commercial Generic Bioprocessing Apparatus was loaded with three developmental silkworm larvae in the growth phase, two larvae in the wandering stage, and three pupae that were expected to eclose during flight. The instruments enabled strict control of temperature and humidity (it was necessary to keep the food moist). In the flight group, the three larvae grew normally despite the fact that the food was not fixed because of the weightlessness in the space environment. One of the wandering-stage larval insects successfully spun a cocoon in the flight vehicle, and the other died before cocooning. One of the pupae eclosed on the first day during the flight, whereas the second pupa eclosed on the seventh day of the mission, and the third pupa had not eclosed by the end of the mission. In the ground control group, one of the wandering larva cocooned on the eighth day of the mission, and the other wandering larva had begun cocooning but did not complete it before the end of the mission. One of the pupae started eclosion on the first day, and the other two moths had emerged by the end of the mission. The wide range of developmental timelines observed between the flight and ground units was attributed to the difficulty in determining the ages of the larvae and pupae at loading (Carla and Goulart 2004).

Scientists in the Japanese 'Kibo' facility in the International Space Station (ISS) (Furusawa et al. 2001) and the European Space Agency (Ohnishi 2016) performed

experiments on the silkworm. The Japan Aerospace Exploration Agency took *B. mori* eggs to the International Space Station(ISS) and studied the insects for 3 months with the aim of examining the biological effects of cosmic rays. A black-striped strain (P^S/P^S) and a normally marked strain ($+^p/+^p$) were crossed, and heterozygous silkworm eggs ($P^S/+^p$) were obtained. When heterozygous silkworm eggs ($P^S/+^p$) were exposed to heavy ion particles of carbon, neon, or iron in ground-based experiments, white spots were present on the backs at the fifth instar (Toshiharu Furusawa et al. 2009). In the larvae of the heterozygous silkworm eggs maintained in the ISS that hatched when returned to the ground, no mutants were detected in the first generation. Surprisingly, larvae from the second and third generations had white spots. These results suggest that space radiation affects primordial germ cells during embryonic development (Ohnishi 2016).

2.2 *Space Flight Studies of Silkworm Performed by Chinese Researchers*

To explore the impact of the space environment on the development of the silkworm, China used several return satellites to carry 12 batches of silkworm eggs into space. The first time silkworm eggs were sent to space in a Chinese recoverable satellite was in 1988, but the silkworm eggs were dehydrated upon return to the ground because the satellite lacked a biological protection cabinet (Gui et al. 2001). Two batches of silkworm experiments resulted in no data due to the failure of the satellite launches, and another six batches of silkworm eggs died after returning to the ground due to high capsule temperature.

In October 1990, silkworm eggs spent 8 days in space on a recoverable satellite. The goal of this space experiment was to study the effect of microgravity on the development and heredity of silkworm eggs. Another objective was to determine whether mutation induced in space might improve silkworm cocoon yield or silk quality (Shi et al. 1994). After being returned to the ground, the embryonic development of the silkworms was analysed and compared to eggs maintained on the ground. A number of interesting observations were made. First, the embryonic development of the silkworms was completed normally in the flight environment, but the mean lifespan of silkworms that had been in space was shorter than that of the ground control group. Second, the hatching rate of stagnant hybrid eggs was unaffected by the time in space, but that of the purebred eggs decreased. Third, the development of the silkworm eggs that had been in space was more rapid than the control group: the larval stage was shortened by a mean of 7 days, and eggs hatched a mean of 1 day sooner than ground controls. Fourth, the mean body weight of silkworm larvae was not significantly altered by flight, but the rate of digestion and absorption, the transformation rate of silk, the r-glutathione activity of the midgut, and the activity of GTPase in the silk gland were increased. Finally, the quality of the silk produced by the silkworms was also improved by space flight. None of these effects were observed

when silkworms were sent into space at the diapause stage. These results showed that the silkworm could complete normal embryonic development in microgravity. Moreover, this experiment suggested that new varieties of silkworm that produce better quality or more silk can be cultivated in a special space environment (Shi et al. 1994).

After these experiments, Chinese scientists used a Russian biosatellite to explore the biological effects of space microgravity and cosmic radiation on silkworm eggs. The biosatellite was launched into orbit on 29 December 1992 and returned to the ground on 10 January 1993 (Shi et al. 1995; Zhuang et al. 1995); the total flight time was 12 days. The temperature in the satellite capsule was between 20 and 26 °C. The dose of flight radiation was 1.849 mGy, and the daily dose was 0.154 mGy. The silkworm eggs were divided into two groups: a space flight group and a ground control group. The volume of the container carried by the satellite was $45 \times 75 \times 150\ mm^3$, and it was divided into four small cabins to carry larval stage insects, cocoons, pupae, and eggs. There were four (2♂, 2♀ line: H1 × jia90) wandering stage larvae for investigation of the behaviour of silk production, cocooning, and pupation. The goal of sending the four cocoons (2♂, 2♀ line: 54A) was to study pupation. There were eight pupae (4♂, 4♀ line: 54A) to investigate mating, oviposition, fertilization, and other adult behaviours. Finally, there were six kinds of diapaused silkworm eggs of different strains to allow investigation of the influence of genetic variation during flight. The results showed that the silkworm could complete silk spinning, cocooning, pupation, moth, mating, oviposition, fertilization, embryo formation, embryo development, and larval hatching stages during the space flight. It was of utmost importance that the variation of the pupae and the trimester were found in the recovered samples. Thus, the mutations induced in space were inherited upon subculture. Moreover, these characteristics were not observed in the ground control group (Shi et al. 1998).

A Chinese satellite that launched on 27 September 2005 and returned on 15 October of the same year carried another experiment into space. In this experiment, the total time in space was 18 days (Wu et al. 2005). This experiment showed that space travel had a negative impact on embryos. Variations in cocoon and egg colour were observed in the next generation of those embryos that survived. This confirmed that time in space could cause genetic variation in offspring.

To explore gene expression in silkworm embryos under space conditions, we sent embryos into space on the SJ-10 satellite in 2016. The results of this experiment will be discussed in detail in Sect. 4.

In 2016, China sent the Tiangong-2 space station into space and conducted many scientific experiments, including a silkworm culture experiment. This experiment was designed to observe (1) the cocoon stage, (2) the development of silkworm chrysalis, (3) the pupae, (4) the moth's movement in space and the process of mating, and (5) the oviposition status of female moths after mating. Five larvae are expected to spin cocoons, which is important progress in space experiments. When the spacecraft returns to Earth, the research team will observe whether the "space silkworm" silk spinning behaviour is different from the behaviour of ground silkworms and whether these changes can improve silkworm breeding technology.

3 Silkworm Research Platforms

3.1 Silkworm Genomic Sequence

The draft genome sequence of *B. mori* was simultaneously released by scientists from China and Japan in 2004 (Mita et al. 2004; Xia et al. 2004, 2014). The estimated silkworm genome size is 428.7 Mb; 18,510 genes were identified. The silkworm genome databases—SilkDB (China) and KAIKObase (Japan)—were established and are updated independently. These are important bioinformatic resources for the scientific community (Duan et al. 2010; Shimomura et al. 2009; Wang et al. 2005). In 2007, with the combination of nine-fold-coverage whole-genome sequencing data, fosmid and BAC sequencing data, and full-length coding DNA (cDNA) sequencing data, a 432-Mb more complete genome sequence was achieved (International Silkworm Genome 2008). Furthermore, to reveal the secrets of domestication of *B. mori* from the wild silkworm, *B. mandarina*, a single-base-pair-resolution silkworm genetic variation map was constructed from 29 phenotypically and geographically diverse domesticated strains and 11 wild varieties (Xia et al. 2009).

In addition to the general silkworm genome sequence, scientists have also explored other detailed genomic information, including microsatellite DNA (Prasad et al. 2005), microRNA expression (Liu et al. 2010), segmental duplication (Zhao et al. 2013), Z chromosome genes (Arunkumar et al. 2009), and expressed genes in wild silkmoths (Arunkumar et al. 2008). Illumina high-throughput bisulfite sequencing revealed that 0.11% of all genomic cytosines are methylcytosines that mainly occur in CG dinucleotides (Xiang et al. 2010); the level of methylation is much lower than in plants and mammals. Methylation in silkworms is positively correlated with the expression of corresponding genes (Xiang et al. 2010). In 2013, researchers created 21 full-length cDNA libraries derived from 14 tissues and performed full sequencing by primer walking to obtain a full-length sequence for 11,104 cDNAs, which enabled researchers to annotate the silkworm genome more accurately (Suetsugu et al. 2013). Despite this progress, compared with organisms such as *Drosophila*, information is lacking for the silkworm. In particular, information on functional small RNAs, including piRNAs and lncRNAs, is needed, and additional sequencing should be performed to make the genomic blueprint of silkworms more comprehensive and complete.

3.2 Silkworm Transcriptomic Research

3.2.1 Transcriptome Analysis in Insects

With the advent of the post-genome era, technologies to study transcriptomes, proteomes, and metabolomes have been developed and have been widely used in biological studies (Lockhart and Winzeler 2000). The genetic central dogma demonstrated

that genetic information is precisely transferred from the DNA to protein by the messenger RNA (mRNA). Therefore, mRNA is considered to be a "bridge" for biological information transfer between DNA and proteins, and the identification of all expressed genes and their transcriptional levels is collectively referred to as transcriptomic analysis (Costa et al. 2010). A transcriptome is the sum of all RNA transcribed in a specific tissue or cell at a developmental stage or functional state, including mRNA and non-coding RNA (Costa et al. 2010; Wang et al. 2009).

In the mid-1990s, two transcriptomics research methods emerged almost simultaneously: DNA microarray technology (Lockhart et al. 1996) and serial analysis of gene expression (Velculescu et al. 1995), which are based on northern hybridization and expressed sequence tag analysis, respectively. Next-generation DNA sequencing technology, also known as high-throughput sequencing, has also been applied in transcriptomic analysis (Ansorge 2009; Rusk and Kiermer 2008; Schuster 2008).

3.2.2 Transcriptomic Analysis in the Silkworm

The silkworm is a heteromorphic insect, and different subsets of genes are expressed in different feeding stages and in the moulting period. High-throughput sequencing has been used to analyse differential gene expression in different stages, and these data will help us to understand the gene transcription profile throughout the developmental process.

Using high-throughput paired-end RNA sequencing, Li et al. explored the genes specifically expressed in different developmental stages (Li et al. 2012). Around the same time, Shao et al. identified 320 novel genes and identified thousands of alternative splicing and 58 trans-splicing events at different developmental stages and different tissues using Illumina sequencing technology (Shao et al. 2012).

In 2014, Kiuchi et al. performed deep sequencing (RNA-seq) of silkworm embryos and identified 157 transcripts that are expressed in significantly different amounts in female and male embryos (Kiuchi et al. 2014). Among these differentially expressed transcripts, they found one transcript that is highly expressed in females at all stages of embryogenesis but not in male embryos. This transcript is expressed from the W chromosome and is a precursor of a female-specific piRNA. On the basis of this work, they performed clustering analysis of sexually biased transcripts and divided them into 10 groups according to their expression patterns (Kawamoto et al. 2015). Parthenogenetic reproduction can be either obligate or facultative. There are complex variations between species of silkworm (Kellner et al. 2013), and parthenogenesis occasionally occurs in the domesticated silkworm. Liu et al. investigated the gene expression profile in silkworms undergoing thermal parthenogenesis and found that differentially expressed genes are mainly involved in reproduction, chorion formation, female gamete generation, and cell development pathways (Liu et al. 2015).

How silkworms respond to the environment is of great interest. Ogata et al. analysed the expression of drug resistance-related genes in silkworm fat body cells cultured in medium and harvested from silkworms grown under natural conditions. The comparison of transcriptomes in natural conditions and in cultured tissues revealed

that fewer genes represent a larger portion of the transcriptome in the natural fat body than the cultured fat body (Ogata et al. 2012). In 2014, researchers constructed four digital gene expression libraries from the silkworm fat body of females and males to analyse the effects of temperature. After constant high-temperature treatment, there were significant changes in gene expression in the fat body, especially in binding, catalytic, cellular, and metabolic processes (Wang et al. 2014a). Nie et al. analysed gene expression in neonatal larvae after hyperthermia-induced seizures in the contractile silkworm and found that the most common differentially expressed genes were up-regulated and that these genes encoded heat shock proteins (Nie et al. 2014).

Host-pathogen interactions are complex processes, and understanding these interactions is critical to the silk industry. Fungal infections induce a variety of responses in silkworms. To obtain an overview of the interaction between silkworm and an entomopathogenic fungus, Hou et al. identified a subset of genes in silkworm larvae that exhibit altered expression in response to *Beauveria bassiana* infection. These genes are involved in many biological processes, such as defence and response to pathogens, signal transduction, phagocytosis, regulation of gene expression, RNA splicing, biosynthesis and metabolism, and protein transport (Hou et al. 2014). In 2015, Wang et al. performed transcriptomic profiling of the brains of healthy silkworm larvae and larvae infected with *B. mori* nuclear polyhedrosis virus (BmNPV). The transcriptional level changes observed in the BmNPV-infected brain samples provided new clues regarding the molecular mechanisms that underlie BmNPV infection (Wang et al. 2015).

3.2.3 Problems and Future Development of Transcriptomic Research

Compared with traditional sequencing, next-generation sequencing technology has several advantages, including high throughput, high sequencing speed, and low cost. There are shortcomings, however. First, the sequence length obtained using next-generation sequencing is usually short, which makes efficient assembly challenging. Second, although useful for studying tissue-specific gene expression, the technique is not suitable for single-cell gene expression studies (Wolf 2013). Third, transcripts of overlapping genes encoded on different chains are not effectively distinguished, which makes it difficult to annotate genes because next-generation sequencing analyses single-stranded mRNAs. Fourth, the mRNA is only an intermediate in the gene expression process, and mRNA level changes are not necessarily reflective of protein level changes. Finally, next-generation sequencing technology is essentially PCR-based sequencing, and some mismatch incorporation occurs during the PCR process, which adversely impacts the accuracy of next-generation sequencing (Wolf 2013).

3.3 Development of Transgenic Silkworms and Applications

Germline transformation in silkworms was first achieved using a *piggyBac* transposon-derived vector (Tamura et al. 2000). The *piggyBac* transposase randomly recognizes the sequence TTAA in the genome and integrates the foreign expression cassette that this site (Uchino et al. 2008). Other transgenic elements, including the Minos transposase (Uchino et al. 2007), ψ31 integrase (Long et al. 2013), and FLP recombinase (Long et al. 2012), have also been demonstrated to mediate genetic transformation in silkworms.

With the ability to generate transgenic silkworms, researchers have developed many genetic tools for silkworm reverse genetics research. The binary GAL4-UAS gene expression system was established to explore gene functions (Kimoto et al. 2014; Kobayashi et al. 2011; Sakai et al. 2016; Tan et al. 2005; Tsubota et al. 2014) and has been used to reveal the roles of small RNAs (Ling et al. 2015). Techniques for transient expression in specific tissues (i.e., the epidermis) have also been applied to explore certain gene functions (Yoda et al. 2014). Many tissue, sex, and stage-specific promoters have been identified by the transgenic expression of marker genes (Deng et al. 2013; Xu et al. 2015), and these will greatly benefit future research. As the silk gland from silkworms are a highly effective protein production biofactory, specific promoters have been used to engineer the expression of foreign proteins in the silk glands of transgenic silkworms (Tatematsu et al. 2010; Wang et al. 2013a).

As an insect with economic importance, efficient systems to separate the male individuals from females, which will enable higher silk yields, are desired. Transgenic platforms have been used to allow genetic sexing using a W chromosome-linked transgene and a transgene-based female-specific lethality system (Tan et al. 2013; Ma et al. 2013). Also of economic importance is the development of methods to engineer resistance to viral infection, particularly BmNPV. With the combination of transgenics and the RNA interference (RNAi) system, researchers have generated transgenic silkworms that are more resistant to different viruses than wild-type insects (Ito et al. 2008; Subbaiah et al. 2013; Zhang et al. 2014; Zhou et al. 2014).

After almost two decades of development, the transgenic platform in silkworms has proven its power in both fundamental and applied research. Work in silkworms has also been horizontally transferred to pest species in the lepidopteran order. Some improvements could be made, such as the establishment of a genome-scale gene RNAi (shRNA) library and the application of an enhancer trap system to identify more expression regulatory elements for accurate and specific gene expression control.

3.4 Genome Editing Techniques for Silkworms

During the first decade of the 21st century, genome editing tools began to be established in various organisms, including the silkworm. The first generation genome editing methods are ZFNs and TALENs, which are based on the combination of

domains that bind specifically to a particular DNA sequence (the zinc finger proteins and TALEs, respectively) and a non-specific DNA-cleaving nuclease. The first successful targeted mutagenesis in the silkworm was of the epidermal colour marker gene *BmBLOS2* using ZFNs (Takasu et al. 2010; Daimon et al. 2014). Subsequently, the application of TALEN-mediated gene disruption was also achieved in the *BmBLOS2* gene (Ma et al. 2012; Sajwan et al. 2013; Takasu et al. 2013, 2016b); this gene has become the ideal target for testing new genome engineering techniques. In addition to its use in gene depletion for functional research (Daimon et al. 2015), the TALEN system has been applied to mediate precise genetic transformation (Nakade et al. 2014; Takasu et al. 2016a; Wang et al. 2014a, b), to transform the silkworm silk gland into a highly efficient bioreactor (Ma et al. 2014b), and for genetic sexing (Xu et al. 2014).

More recently, the newly emerged tour de force genome editing tool, the CRISPR/Cas9 system, was established in silkworms (Wang et al. 2013a, b). The CRISPR/Cas9 system enables multiplex targeted mutation, large genomic fragment deletion, and heritable mutagenesis in silkworm cells and in vivo (Li et al. 2015; Liu et al. 2014; Ma et al. 2014a; Wei et al. 2014; Xu et al. 2016; Zhang et al. 2015). Researchers have also tried to enhance gene targeting by knocking out factors in the non-homologous end joining pathway; this will facilitate the application of homologous recombination-mediated gene insertion in silkworm individuals (Zhu et al. 2015). A highly efficient virus-inducible CRISPR/Cas9 system was also established in silkworm cells, which suggested the possibility of a CRISPR/Cas9-based anti-virus strategy (Dong et al. 2016). Finally, U6 promoter-mediated N20NGG-type sgRNA expression for gene disruption in vitro and in vivo, which is different from that in mammals, has expanded the targetable engineering sites in the silkworm genome (Zeng et al. 2016).

As nuclease-based genome-editing techniques have demonstrated great potential in silkworm research, further studies should be performed to enhance and improve these methods. There are still some issues to address, such as finding ways to reduce off-target effects, expanding the target range and realizing CRISPR-mediated gene insertion, and achieving specific mutations and single-nucleotide correction. Genome editing techniques optimized and validated in the silkworm will also find application in genetic control of lepidopteran pests. The CRISPR-based platform has already been established in mosquitoes (Gantz et al. 2015; Hammond et al. 2016).

4 SJ-10 Satellite Experiment

4.1 The Silkworm Incubator, SJY102-10/Z01-1, Used Aboard the SJ-10 Satellite

Based on our research goals and comprehensive consideration of the conditions aboard the SJ-10 satellite platform, we developed an incubator to study the influ-

Fig. 1 The silkworm incubator used aboard the SJ-10 satellite

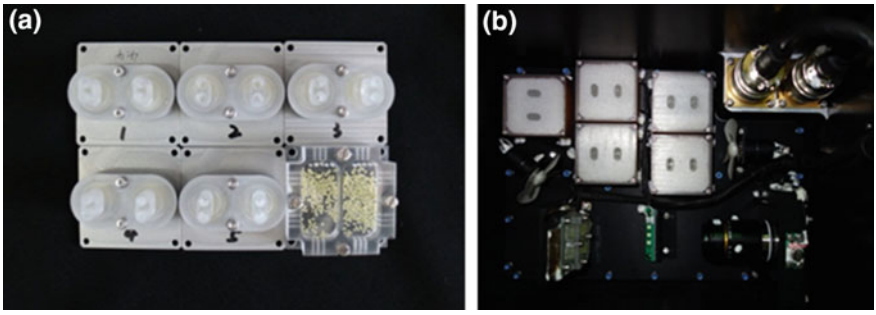

Fig. 2 **a** Silkworm embryos in the incubator. **b** The culture units installed in the silkworm incubator

ence of the space environment on silkworm embryonic development (Fig. 1). This system allowed the culture of silkworm eggs in space for 12 days and 15 h of flight, providing full control of temperature and enabling continuous monitoring of environmental conditions (Fig. 2). Biological samples were collected and stored during the cultivation process within the incubator.

Considering the effects of the space environment, we carried out a simulation experiment on the ground before launching. The number of embryos and the culture temperature and humidity were optimized in the ground simulation (Fig. 3). Loading of the silkworm incubator with embryos was completed on April 4, 2016, and installation and tower trans-shipment work was completed on April 5, 2016. The satellite was launched on April 6, and the incubator was retrieved on April 18, 2016.

The silkworm incubator was used for the in-orbit experiment, and there were five units in the incubator. The culture temperature was 21 °C, but the temperature was changed to 4 °C every two days in one unit during the entire culture process. Digital

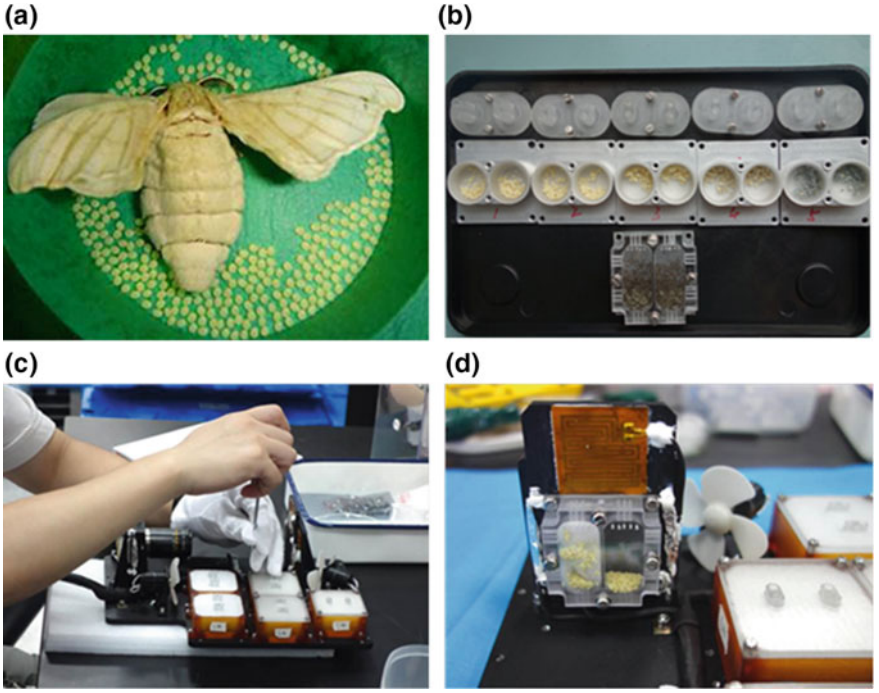

Fig. 3 Silkworm embryo collection and sample loading. **a** Collection of the embryos. **b** Image of the incubator after the simulation experiment on the ground. **c** The cryogenic fixation of samples. **d** The transparent unit enables digital images to be taken during culture

Fig. 4 Images of the silkworm embryonic development in space. **a** Image captured aboard the SJ-10 satellite on day 1 after launch. **b** Image captured after 6 days in orbit. **c** Image captured in the SJ-10 satellite on the final day in orbit

images of the silkworm embryos were obtained every day during flight (Fig. 4). After flight, the silkworm embryos were retrieved. All remained in good condition.

4.2 Studies of Silkworm Development in Space

4.2.1 Goals of the Silkworm Study Performed Onboard the SJ-10 Satellite

The space environment is significantly different from that on the earth with lower temperatures, higher radiation levels, vacuum characteristics, long-term microgravity, and weaker magnetic fields than on earth. We expected to find developmental differences between embryos that had been in space compared to ground-based controls that might be observed in subsequent generations. A goal is to identify genes that play dominant roles in the regulation of these processes. These experiments are continuing.

4.2.2 Study of Silkworm Phenotypes

The study of growth, development, ageing, and death of the silkworm may result in lessons that can be extrapolated to other organisms and even human beings. The silkworm is an animal model for radiation dose biometrics and basal metabolic resistance to external environment disturbances. In silkworms that had been aboard the satellite and in ground controls, a number of physiological indexes were measured, including embryonic development rate, hatching rate, larval digestion and absorption, larval weight, larval developmental period, total lipid droplets in larval haemolymph, protein concentration in larval haemolymph, larval mid-gut esterase activity, larval fat mass, soluble protein and total lipid droplet concentrations, juvenile hormone and ecdysone levels, silkworm cocoon yield, silk quality, silk gland GPTase activity, glutathione S-transferase activity, mating behaviour and oviposition.

4.2.3 Analysis of the Genome, Genes, and Non-coding RNA Expression

The rapid development of sequencing technology and silkworm genomics has made possible the study of differences in the genomes and transcriptomes of flight group s and ground control groups. We are performing whole genome re-sequencing, transcriptome and proteome analysis and using other methods to carry out correlation analyses of the flight group and the ground control group. We are also working to identify the differentially expressed genes and non-coding RNAs. We are eager to identify genetic variations and explore the candidate genes responsible for certain traits. We also want to perform long-chain non-coding RNA sequencing, circular RNA sequencing, and small RNA sequencing and plan to use whole-genome bisulfite sequencing techniques to study DNA methylation and mRNA and miRNA methylation, as well as transcription factor binding site methylation.

4.2.4 Functional Validation of Certain Space-Responsible Candidate Genes

Based on the cultivation of silkworm embryos in the SJ-10 satellite, a single environment of microgravity, heavy ions, protons, and neutrons was established to simulate the space environment. This will allow further study of the effects of the space environment on the gene expression and protein expression characteristics of the silkworm. Using the latest genome-editing technologies, such as CRISPR/Cas9 and TALENs, we are also trying to explore the functional and molecular mechanisms of space environment-sensitive genes.

4.3 Preliminary Research Results

After incubation in the space environment, the hatching rate of the silkworm embryos was not significantly different from that of the ground control group. The larvae in both the ground control group and the SJ-10 satellite group were reared on fresh mulberry leaves at 25 °C. In the larval stage, the development time of SJ-10 satellite group silkworms after 15 days was significantly shorter than that of the ground animals after 18 days. Furthermore, the flight group showed precocious wandering behaviour and earlier larval-pupal transition by 3 days relative to the ground-based controls (Figs. 5 and 6). No significant changes in larval or pupal body sizes or pupal development time were observed between the SJ-10 satellite group and the ground group. In the adult stage, the SJ-10 satellite group silkworms mated normally, and the oviposition rate did not differ significantly from that of the ground control. The next generation has begun breeding. Other data still need further analysis.

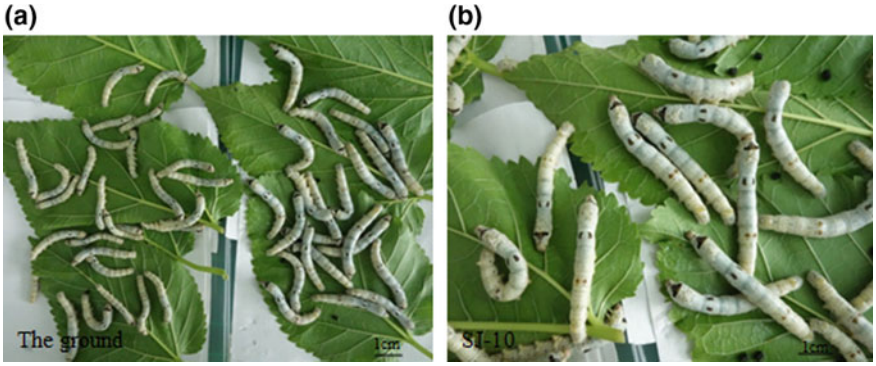

Fig. 5 The flight group made an earlier larval to pupal transition than the ground group. Photographs of **a** the ground group and **b** the SJ-10 satellite group captured on the same day. The ground group consisted of day 2 larvae at the fifth instar, and the SJ-10 satellite group consisted of day 5 larvae at the fifth instar

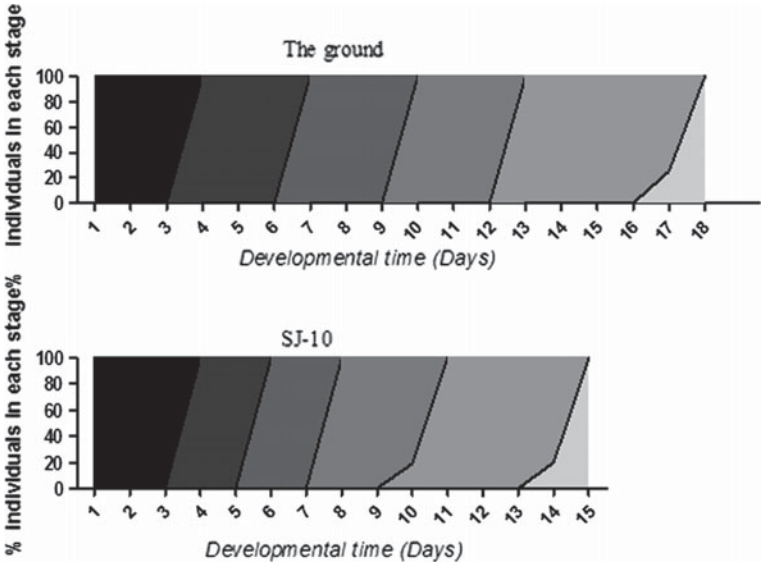

Fig. 6 The percentage of individuals in each stage of larval development in the ground group (**top panel**) and the SJ-10 satellite group (**bottom panel**)

5 Discussion and Prospective

Over the more than a half century that humans have been in space, valuable and meaningful data have been obtained on effects of space on various organisms, and these studies have laid the foundation for the future exploration and development of space. However, many problems and challenges remain. Firstly, satellites are typically built one at a time and at huge expense, making it expensive to launch and maintain satellite-based experiments. The time frame of an experiment is limited, and there is very little opportunity for reproducibility, so results obtained may not be reliable. Secondly, due to hardware limitations and the fact that satellites are not manned means that experiments cannot be performed on large organisms and complex life science experiments are not possible. Finally, the time in space experiment is limited. Therefore, a large number of ground-based simulations of space conditions are needed.

In the space environment, there are many factors, including weightlessness, strong ionizing radiation, and sub-magnetic field, that could alter physiological and biochemical functions during silkworm development. Our study of the influence of space on the development and genetic variation of the silkworm provided important data for the development of silkworm breeding, and it also provided a theoretical basis for exploring new breeding methods.

China is a major location for sericulture and is the homeland of silk; silkworms have been bred in captivity for thousands of years in China. The silkworm is an

important economic insect, and the silk industry is an ecologically sound component of China's economic strategy. At the present, there are more than 10 million farmers in China involved in the silkworm industry, and the sericulture areas are spread over 26 provinces, with a total of more than 800,000 ha of mulberry gardens. In 2011, cocoon production was approximately 800,000 tons, with Chinese silk production accounting for more than 75% of total world production. China is the center of the world silk industry, and the Chinese silk accounts for 50% of the world export trade. The output value of the silk industry is more than 160 billion yuan. The silkworm also contains valuable proteins and is a good germplasm resource.

In recent years, Chinese scientists have used space technology in an effort to enhance crop mutagenesis and to select new traits. The application of space mutagenesis technology to silkworms will lead to characterization of new silkworm mutant lines that will be beneficial to silkworm researchers and in industrial applications. The silk industry has played an important role in solving the problem of rural surplus labor, maintaining social stability. Using the space environment for systematic research on the silkworm thus has not only important theoretical significance but also economic value.

Interestingly, studies suggest that silkworms may be an ideal high-nutrition food for astronauts that can be grown efficiently in a controlled system like a space station. Studies of the nutritional composition, maturity time, and processing of these insects demonstrate that the silkworm can be used as a source of protein for astronaut recipes. Life-support technology is important for long-term viability of a manned space program, such as a lunar base, a space laboratory, or a space station. Five or six silkworm pupae are equivalent to an egg in terms of nutrition value. Based on weight, the content of protein in a silkworm chrysalis is much higher than that of eggs, and the amino acid content is also several times higher than pork, lamb, eggs, or milk by weight. The proteins produced by silkworm can be harvested in a short time, and silkworms do not need water and so do not produce waste water. In brief, the silkworm is an ideal protein source for astronauts in the space.

Acknowledgements This work was supported by grants from the Strategic Priority Research Program of Chinese Academy of Sciences (XDA04020414) and National Science Foundation of China (U1738110).

References

Ansorge WJ (2009) Next-generation DNA sequencing techniques. Nat Biotechnol 25:195–203

Arunkumar KP, Tomar A et al (2008) WildSilkbase: an EST database of wild silkmoths. BMC Genom 9:338

Arunkumar KP, Mita K et al (2009) The silkworm Z chromosome is enriched in testis-specific genes. Genetics 182:493–501

Carla V, Goulart SW et al (2004) Performance of the STARS life sciences habitats in space flight and ground controls. In: 34th international conference on environmental systems (ICES)

Costa V, Angelini C et al (2010) Uncovering the complexity of transcriptomes with RNA-Seq. J Biomed Biotechnol 2010:853916

Daimon T, Kiuchi T et al (2014) Recent progress in genome engineering techniques in the silkworm, Bombyx mori. Dev Growth Differ 56:14–25
Daimon T, Uchibori M et al (2015) Knockout silkworms reveal a dispensable role for juvenile hormones in holometabolous life cycle. Proc Natl Acad Sci USA 112:E4226–4235
Deng D, Xu H et al (2013) The promoter of Bmlp3 gene can direct fat body-specific expression in the transgenic silkworm, Bombyx mori. Transgenic Res 22:1055–1063
Dong ZQ, Chen TT et al (2016) Establishment of a highly efficient virus-inducible CRISPR/Cas9 system in insect cells. Antiviral Res 130:50–57
Duan J, Li R et al (2010) SilkDB v2.0: a platform for silkworm (Bombyx mori) genome biology. Nucleic Acids Res 38:D453–456
Furusawa T, Shikata M et al (1982) Temperature dependent sorbitol utilization in diapaus eggs of the silkworm. J Comp Physiol B Biochem Syst Environ 147:21–26
Furusawa T, Kotani E et al (2001) Embryonic development in the eggs of the silkworm, Bombyx mori, exposed to the space environment. Biol Sci Space 15(Suppl):S177–182
Gantz VM, Jasinskiene N et al (2015) Highly efficient Cas9-mediated gene drive for population modification of the malaria vector mosquito Anopheles stephensi. Proc Natl Acad Sci USA 112:E6736–6743
Gui ZZ et al (2001) Research status of Bombyx mori carrying. Jiangsu Seric 1:11–18
Hammond A, Galizi R et al (2016) A CRISPR-Cas9 gene drive system targeting female reproduction in the malaria mosquito vector Anopheles gambiae. Nat Biotechnol 34:78–83
Henneberry TJ, Sullivan WN (1963) Effect of gamma-radiation on eggs of the silkworm. Nature 200:1121–1122
Hou C, Qin G et al (2014) Transcriptome analysis of silkworm, Bombyx mori, during early response to Beauveria bassiana challenges. PLoS ONE 9:e91189
International Silkworm Genome C (2008) The genome of a lepidopteran model insect, the silkworm Bombyx mori. Insect Biochem Mol Biol 38:1036–1045
Ito K, Kidokoro K et al (2008) Deletion of a gene encoding an amino acid transporter in the midgut membrane causes resistance to a Bombyx parvo-like virus. Proc Natl Acad Sci USA 105:7523–7527
Kawamoto M, Koga H et al (2015) Sexually biased transcripts at early embryonic stages of the silkworm depend on the sex chromosome constitution. Gene 560:50–56
Kellner K, Seal JN et al (2013) Sex at the margins: parthenogenesis vs. facultative and obligate sex in a Neotropical ant. J Evol Biol 26:108–117
Kimoto M, Tsubota T et al (2014) Hox transcription factor Antp regulates sericin-1 gene expression in the terminal differentiated silk gland of Bombyx mori. Dev Biol 386:64–71
Kiuchi T, Koga H et al (2014) A single female-specific piRNA is the primary determiner of sex in the silkworm. Nature 509–633
Kobayashi I, Kojima K et al (2011) An efficient binary system for gene expression in the silkworm, Bombyx mori, using GAL4 variants. Arch Insect Biochem Physiol 76:195–210
Kotani E, Furusawa T et al (2002) Somatic mutation in larvae of the silkworm, Bombyx mori, induced by heavy ion irradiation to diapause eggs. J Radiat Res 43(Suppl):S193–198
Li Y, Wang G et al (2012) Transcriptome analysis of the silkworm (Bombyx mori) by high-throughput RNA sequencing. PLoS ONE 7:e43713
Li Z, You L et al (2015) Ectopic expression of ecdysone oxidase impairs tissue degeneration in Bombyx mori. Proc Biol Sci/R Soc 282:20150513
Ling L, Ge X et al (2015) MiR-2 family targets awd and fng to regulate wing morphogenesis in Bombyx mori. RNA Biol 12:742–748
Liu S, Li D et al (2010) MicroRNAs of Bombyx mori identified by Solexa sequencing. BMC Genom 11:148
Liu Y, Ma S et al (2014) Highly efficient multiplex targeted mutagenesis and genomic structure variation in Bombyx mori cells using CRISPR/Cas9. Insect Biochem Mol Biol 49:35–42
Liu P, Wang Y et al (2015) Transcriptome analysis of thermal parthenogenesis of the domesticated silkworm. PLoS ONE 10:e0135215

Lockhart DJ, Winzeler EA (2000) Genomics, gene expression and DNA arrays. Nature 405:827–836
Lockhart DJ, Dong H et al (1996) Expression monitoring by hybridization to high-density oligonucleotide arrays. Nat Biotechnol 14:1675–1680
Long DP, Zhao AC et al (2012) FLP recombinase-mediated site-specific recombination in silkworm, Bombyx mori. PloS ONE 7:e40150
Long D, Zhao A et al (2013) In vivo site-specific integration of transgene in silkworm via PhiC31 integrase-mediated cassette exchange. Insect Biochem Mol Biol 43:997–1008
Ma S, Zhang S et al (2012) Highly efficient and specific genome editing in silkworm using custom TALENs. PLoS ONE 7:e45035
Ma S, Wang X et al (2013) Genetic marking of sex using a W chromosome-linked transgene. Insect Biochem Mol Biol 43:1079–1086
Ma S, Chang J et al (2014a) CRISPR/Cas9 mediated multiplex genome editing and heritable mutagenesis of BmKu70 in Bombyx mori. Sci Rep 4:4489
Ma S, Shi R et al (2014b) Genome editing of BmFib-H gene provides an empty Bombyx mori silk gland for a highly efficient bioreactor. Sci Rep 4:6867
Mita K, Kasahara M et al (2004) The genome sequence of silkworm, Bombyx mori. DNA Res Int J Rapid Publ Rep Genes Genomes 11:27–35
Nakade S, Tsubota T et al (2014) Microhomology-mediated end-joining-dependent integration of donor DNA in cells and animals using TALENs and CRISPR/Cas9. Nat Commun 5:5560
Nie H, Liu C et al (2014) Transcriptome analysis of neonatal larvae after hyperthermia-induced seizures in the contractile silkworm, Bombyx mori. PLoS One 9:e113214
Ogata N, Yokoyama T et al (2012) Transcriptome responses of insect fat body cells to tissue culture environment. PLoS ONE 7:e34940
Ohnishi T (2016) Life science experiments performed in space in the ISS/Kibo facility and future research plans. J Radiat Res 57(Suppl 1):i41–i46
Prasad MD, Muthulakshmi M et al (2005) SilkSatDb: a microsatellite database of the silkworm, Bombyx mori. Nucleic Acids Res 33:D403–406
Rusk N, Kiermer V (2008) Primer: sequencing—the next generation. Nat Methods 5:15
Sajwan S, Takasu Y et al (2013) Efficient disruption of endogenous Bombyx gene by TAL effector nucleases. Insect Biochem Mol Biol 43:17–23
Sakai H, Sumitani M et al (2016) Transgenic expression of the piRNA-resistant masculinizer gene induces female-specific lethality and partial female-to-male sex reversal in the silkworm, Bombyx mori. PLoS Genet 12:e1006203
Schuster SC (2008) Next-generation sequencing transforms today's biology. Nat Methods 5:16–18
Shao W, Zhao QY et al (2012) Alternative splicing and trans-splicing events revealed by analysis of the Bombyx mori transcriptome. RNA 18:1395–1407
Shi ZZ, Zhuang ZD et al (1994) Experimental studies of silkworm eggs onboard recoverable satellite. Space Med Med Eng 7 Suppl:s23–s28
Shi ZZ, Zhuang ZD et al (1995) Flight experiment of silkworm onboard russian biosatellite. Space Med Med Eng 8:220–224
Shi ZZ, Zhuang D et al (1998) Space flight experiment on Chinese silkworm on board the Russian 10th Biosatellite. Adv Space Res 21:1145–1150
Shimada T, Ebinuma H et al (1986) Expression of homeotic genes in Bombyx mori estimated from asymmetry of dorsal closure in mutantnormal mossics. J Exp Zool 240:335–342
Shimomura M, Minami H et al (2009) KAIKObase: an integrated silkworm genome database and data mining tool. BMC Genom 10:486
Subbaiah EV, Royer C et al (2013) Engineering silkworms for resistance to baculovirus through multigene RNA interference. Genetics 193:63–75
Suetsugu Y, Futahashi R et al (2013) Large scale full-length cDNA sequencing reveals a unique genomic landscape in a lepidopteran model insect, Bombyx mori. Genes Genomes Genet 3:1481–1492
Takasu Y, Kobayashi I et al (2010) Targeted mutagenesis in the silkworm Bombyx mori using zinc finger nuclease mRNA injection. Insect Biochem Mol Biol 40:759–765

Takasu Y, Sajwan S et al (2013) Efficient TALEN construction for Bombyx mori gene targeting. PLoS ONE 8:e73458
Takasu Y, Kobayashi I et al (2016a) Precise genome editing in the silkworm Bombyx mori using TALENs and ds- and ssDNA donors—a practical approach. Insect Biochem Mol Biol 78:29–38
Takasu Y, Tamura T et al (2016b) Targeted Mutagenesis in Bombyx mori using TALENs. Methods Mol Biol 1338:127–142
Tamura T, Thibert C et al (2000) Germline transformation of the silkworm Bombyx mori L. using a piggyBac transposon-derived vector. Nat Biotechnol 18:81–84
Tan A, Tanaka H et al (2005) Precocious metamorphosis in transgenic silkworms overexpressing juvenile hormone esterase. Proc Natl Acad Sci USA 102:11751–11756
Tan AJ, Fu GL et al (2013) Transgene-based, female-specific lethality system for genetic sexing of the silkworm, Bombyx mori. Proc Natl Acad Sci USA 110:6766–6770
Tatematsu K, Kobayashi I et al (2010) Construction of a binary transgenic gene expression system for recombinant protein production in the middle silk gland of the silkworm Bombyx mori. Transgenic Res 19:473–487
Toshiharu Furusawa KN, Ichida Masatoshi, Nagaoka Sumiharu et al (2009) Introduction to the proposed Space Experiments Aboard the ISS using the silkworm, Bombyx mori. Biol Sci Space 23:61–69
Tsubota T, Uchino K et al (2014) Establishment of transgenic silkworms expressing GAL4 specifically in the haemocyte oenocytoid cells. Insect Mol Biol 23:165–174
Uchino K, Imamura M et al (2007) Germ line transformation of the silkworm, Bombyx mori, using the transposable element Minos. Mol Genet Genomics MGG 277:213–220
Uchino K, Sezutsu H et al (2008) Construction of a piggyBac-based enhancer trap system for the analysis of gene function in silkworm Bombyx mori. Insect Biochem Mol Biol 38:1165–1173
Velculescu VE, Zhang L et al (1995) Serial analysis of gene expression. Science 270:484–487
Wang J, Xia Q et al (2005) SilkDB: a knowledgebase for silkworm biology and genomics. Nucleic Acids Res 33:D399–402
Wang Z, Gerstein M et al (2009) RNA-Seq: a revolutionary tool for transcriptomics. Nat Rev Genet 10:57–63
Wang F, Xu H et al (2013a) An optimized sericin-1 expression system for mass-producing recombinant proteins in the middle silk glands of transgenic silkworms. Transgenic Res 22:925–938
Wang Y, Li Z et al (2013b) The CRISPR/Cas system mediates efficient genome engineering in Bombyx mori. Cell Res 23:1414–1416
Wang H, Fang Y et al (2014a) Transcriptome analysis of the Bombyx mori fat body after constant high temperature treatment shows differences between the sexes. Mol Biol Rep 41:6039–6049
Wang Y, Tan A et al (2014b) Site-specific, TALENs-mediated transformation of Bombyx mori. Insect Biochem Mol Biol 55:26–30
Wang G, Zhang J et al (2015) Transcriptome analysis of the brain of the silkworm Bombyx mori infected with Bombyx mori nucleopolyhedrovirus: a new insight into the molecular mechanism of enhanced locomotor activity induced by viral infection. J Invertebr Pathol 128:37–43
Wei W, Xin H et al (2014) Heritable genome editing with CRISPR/Cas9 in the silkworm, Bombyx mori. PloS ONE 9:e101210
Wolf JB (2013) Principles of transcriptome analysis and gene expression quantification: an RNA-seq tutorial. Mol Ecol Resour 13:559–572
Wu FQ et al (2005) Growth and development of later generation silkworm after the eggs carrying by satellite. In: Summary of the national crop biotechnology and mutagenesis technology symposium, p 222
Xia Q, Zhou Z et al (2004) A draft sequence for the genome of the domesticated silkworm (Bombyx mori). Science 306:1937–1940
Xia Q, Guo Y et al (2009) Complete resequencing of 40 genomes reveals domestication events and genes in silkworm (Bombyx). Science 326:433–436
Xia Q, Li S et al (2014) Advances in silkworm studies accelerated by the genome sequencing of Bombyx mori. Annu Rev Entomol 59:513–536

Xiang H, Zhu J et al (2010) Single base-resolution methylome of the silkworm reveals a sparse epigenomic map. Nat Biotechnol 28:516–520
Xu J, Wang Y et al (2014) Transcription activator-like effector nuclease (TALEN)-mediated female-specific sterility in the silkworm, Bombyx mori. Insect Mol Biol 23:800–807
Xu J, Bi H et al (2015) Transgenic characterization of two testis-specific promoters in the silkworm, Bombyx mori. Insect Mol Biol 24:183–190
Xu J, Zhan S et al (2016) Sexually dimorphic traits in the silkworm, Bombyx mori, are regulated by doublesex. Insect Biochem Mol Biol 80:42–51
Yoda S, Yamaguchi J et al (2014) The transcription factor Apontic-like controls diverse colouration pattern in caterpillars. Nat Commun 5:4936
Zeng B, Zhan S et al (2016) Expansion of CRISPR targeting sites in Bombyx mori. Insect Biochem Mol Biol 72:31–40
Zhang P, Wang J et al (2014) Resistance of transgenic silkworm to BmNPV could be improved by silencing ie-1 and lef-1 genes. Gene Ther 21:81–88
Zhang Z, Aslam AF et al (2015) Functional analysis of Bombyx Wnt1 during embryogenesis using the CRISPR/Cas9 system. J Insect Physiol 79:73–79
Zhao Q, Zhu Z et al (2013) Segmental duplications in the silkworm genome. BMC Genom 14:521
Zhou F, Chen RT et al (2014) piggyBac transposon-derived targeting shRNA interference against the Bombyx mori nucleopolyhedrovirus (BmNPV). Mol Biol Rep 41:8247–8254
Zhu L, Mon H et al (2015) CRISPR/Cas9-mediated knockout of factors in non-homologous end joining pathway enhances gene targeting in silkworm cells. Sci Rep 5:18103
Zhuang DH et al (1995) A preliminary report on experiments in the silkworm (Bombyx mori l.) on board a recoverable satellite. Sci Seric 21:135–138

Plant Adaptation to Microgravity Environment and Growth of Plant Cells in Altered Gravity Conditions

Weiming Cai, Haiying Chen, Jing Jin, Peipei Xu, Ting Bi, Qijun Xie, Xiaochen Pang and Jinbo Hu

Abstract This paper introduces one of the plant biology experiments, "Biological effects and the signal transduction of microgravity stimulation in plants", carried out on the SJ-10 recoverable microgravity experimental satellite (SJ-10 satellite). The experimental equipment, experimental process and some results of follow-up analysis are described. When the *Arabidopsis* seedlings returned to the ground after 11 days of microgravity, their leaf area was larger than that of the ground control. The whole genome methylation analysis was also performed by using the *Arabidopsis* seedlings chemically fixed with RNAlater in space after 60 h of growth under microgravity environment. The results demonstrated that the epigenetic differences in *Arabidopsis* seedlings exposed to microgravity. The *Arabidopsis* genome exhibits lower methylation levels in the CHG, CHH and CpG contexts under microgravity conditions. Microgravity stimulation was related to altered methylation of a number of genes, including DNA methylation-associated genes, hormone signaling related genes, cell wall modification genes and transposable elements (TEs). Relatively unstable DNA methylation of TEs was responsible for the induction of active transposons. These observations suggest that DNA demethylation within TEs may change the function exertion of transposons in response to microgravity conditions. In order to further understand the relationship between plant growth, epigenetic changes and plant adaptation to microgravity environment, the biological effects of gravity on plant cells and seedlings based on data obtained from both ground-based research and space experiments on board the Chinese satellite "SJ-10" and the Chinese spaceship "Shenzhou-8" are discussed in this chapter. The data demonstrate the impact of direction and intensity changes of gravity on cell wall metabolism during plant gravitropism and on cells in the state of weightlessness. It is assumed that the maintenance of cell shape requires a balance between cell wall rigidity and cell turgor. When the cell turgor is greater than the rigidity, the balance is broken and may lead to increasing cell volume. Therefore, changes in gravity may affect cell growth by

W. Cai (✉) · H. Chen · J. Jin · P. Xu · T. Bi · Q. Xie · X. Pang · J. Hu
Laboratory of Photosynthesis and Environment, CAS Center for Excellence in Molecular Plant Sciences, Shanghai Institute of Plant Physiology and Ecology, Chinese Academy of Sciences, No. 300 Fenglin Road, Shanghai 200032, China
e-mail: wmcai@sibs.ac.cn

E. Duan and M. Long (eds.), *Life Science in Space: Experiments on Board the SJ-10 Recoverable Satellite*, Research for Development,
https://doi.org/10.1007/978-981-13-6325-2_6

influencing the balance between cell wall rigidity and cell turgor. As a result, the supporting tissue system of plants is weakened in the process of adapting to the microgravity environment, leading to the disruption of the mechanical balance in cells, which may further affect the plant growth and development. In summary, the results of these investigations are beneficial for understanding the mechanism of plant adaptation to microgravity and improve strategies to allow plants to adapt to space.

Abbreviations

ABA	Abscisic acid
ARFs	Auxin response factors
AMR	Altered methylation-related
BRs	Brassinosteroids
CDS	Coding sequences
DMRs	Differentially methylated regions
GO	Gene ontology
NO	Nitric oxide
RAR	Radio-adaptive response
SJ-10 satellite	SJ-10 recoverable microgravity experimental satellite
TEs	Transposable elements
TFs	Transcription factors

1 Introduction

After life evolved from aquatic to terrestrial life, it is adapted to a constant gravitational force on Earth, and biological processes in organisms have evolved under this natural constant. Animals can move to forage for food and water in different places within their living space, whereas plants root into a fixed place to grow; thus, it is important for plants to expand to gain sufficient living space.

Plants extend themselves in various ways. Some climbing plants evolved suckers, tendrils and other organs, and with the help of these special organs, foliage can be fully extended to conduct photosynthesis.

In the process of natural evolution, however, most plants developed a stem and root system that allows them to grow upward into the air and downward into the soil, respectively. This system is a masterpiece of nature. Plants growing on Earth have always endured gravity presented in a constant direction and magnitude. Most plants have evolved with the characteristics of gravitropism. Therefore, plant growth is closely related to the effects of gravity.

With the development of science and technology, human activities have expanded to outer space, which is a microgravity or zero gravity environment. Plants will be

significantly influenced when taken into outer space. This scientific problem is one that needs to be continuously explored.

This review will discuss the adaptation of plant to microgravity environment and the influence of gravity on plant growth, and is based on the results of studies of plant gravitropism and microgravity effects.

2 Results of Space and Ground-Based Experiments

2.1 The Hardware and Procedures of the Experiment on the SJ-10 Satellite

The hardware used in the space experiment was designed and constructed by Shanghai Institution of Technical Physics (Fig. 1a, b) (Xu et al. 2016). The equipment included two cultivation units, a canal system and a pump support system. The polysulfone chambers were in the cultivation units. They had windows that were covered by a gas-permeable membrane. The chambers were connected to the fixative unit by tube connectors. The air temperature near the incubator averaged approximately 23 °C. The average relative humidity near the incubator was approximately 25%, and the microgravity level was estimated to be approximately 10^{-3} to 10^{-4} g during the unified flight phase (Xu et al. 2018).

After growth for 60 h under microgravity conditions, seedlings were fixed with RNAlater. They were harvested approximately 4 h after landing, stored at 4 °C, and transported to our laboratory for further assays. Samples of the 1 × g ground controls in cultivation unit 1 were also fixed in RNAlater at the same time as the in-space samples (Fig. 1d). Seedling DNA was extracted and used for methylome analysis. RNAlater was added to the culture chambers on board SJ-10 satellite and on the ground to halt cellular activities in space and preserve the DNA methylome profile.

2.2 Growth of Arabidopsis *Seedlings Under Microgravity Conditions on Board the SJ-10 Satellite*

One culture chamber was installed in cultivation unit 2. The seedlings in this culture chamber grew for 11 days under microgravity conditions. They were alive and were recovered with the satellite at the end of the flight. 4 *Arabidopsis* seedlings (Col-0) grown in space were obtained. These seedlings were photographed immediately on removal from the satellite and used for the measurement of leaf area. Their first and second true leaves were partially expanded at that time. We compared the areas of these 8 true leaves with those of the leaves at the same leaf position of control *Arabidopsis* seedlings grown on the ground (Xu et al. 2018). The results show that

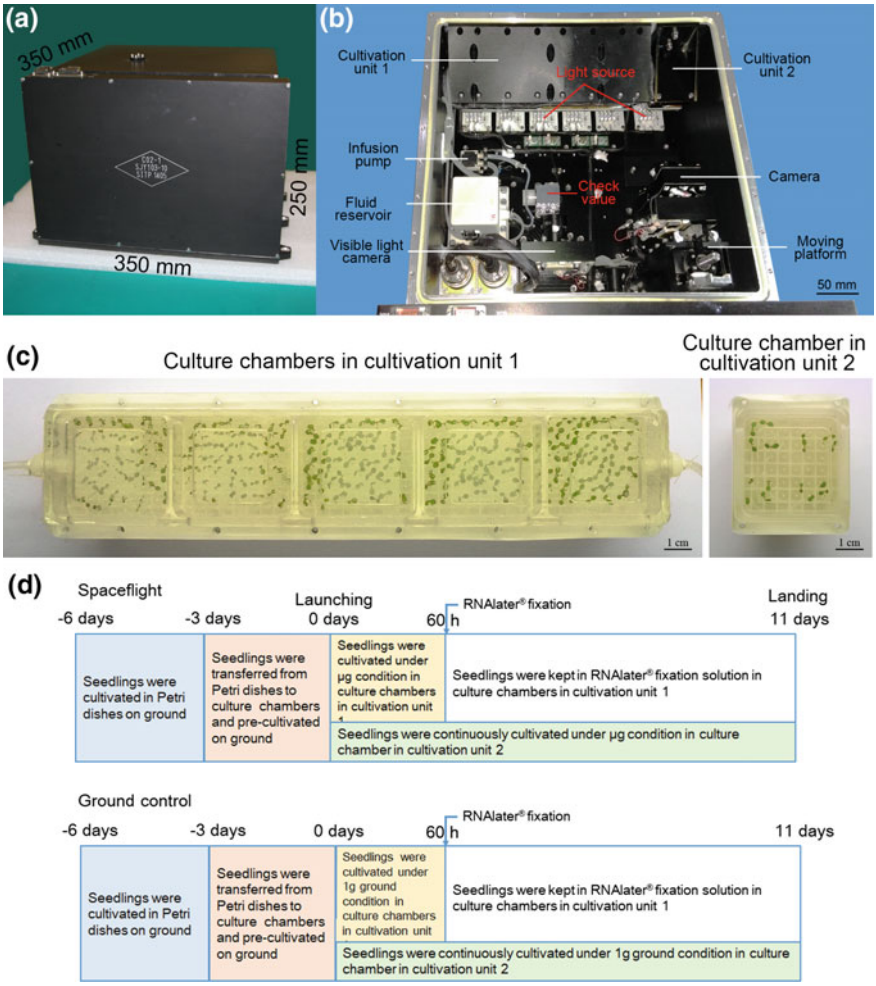

Fig. 1 Hardware and experimental procedures used in the experiment on board the SJ-10 satellite. **a** The hardware used in the spaceflight experiment. The equipment functioned as a housing for the culture chambers. **b** Distribution of internal components of the hardware. The hardware includes culture chambers, a pump support system, a canal system and a fixative unit connected to the culture chambers. **c** *Arabidopsis* seedlings were grown in culture chambers during the space experiment. **d** Schematic view of the *Arabidopsis* seedlings on board the SJ-10 satellite during spaceflight and on the ground. *Arabidopsis* seedlings in culture chambers were transferred from Petri dishes 3 days before launching. Seedlings in culture chambers installed in cultivation unit 1 were grown for 60 h under microgravity conditions and fixed in space using RNAlater. The seedlings in the culture chamber installed in cultivation unit 2 grew for 11 days under microgravity; after this time, they were still alive and returned with the satellite. The g-profile during SJ-10 satellite in orbit is described in the references (Hu et al. 2017; Wang et al. 2016). The g-profile during launch was as follows: the first-level maximum static overload was 4.8 × g in flight for 150 s; the second-level maximum static overload was 6.0 × g in flight for 180 s (Reprinted from Xu et al. 2018.)

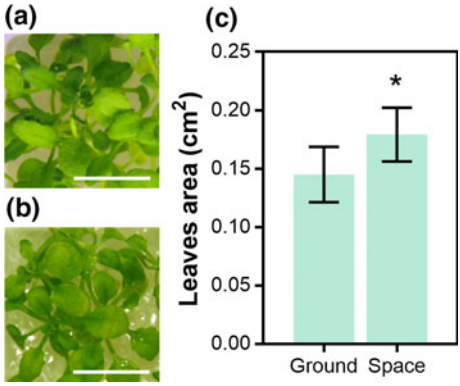

Fig. 2 Comparison of the phenotypes of *Arabidopsis* seedlings grown under microgravity and on the ground. **a** Seedlings that served as ground control samples. **b** Seedlings that returned to earth with the satellite after growth under microgravity for 11 days. The experimental procedure was the same as described in Fig. 1d. The leaf area was measured using ImageJ. Bar = 1 cm (in figure **a**, **b**). **c** The data shown are the mean values obtained for 8 leaves (n = 8); the vertical bars represent the standard deviation. Asterisks indicate a statistically significant difference ($p < 0.05$) between spaceflight and control samples using Student's two-tailed *t* test (Reprinted from Xu et al. 2018.)

the leaves of the seedlings grown in microgravity were larger than those of the ground control samples (Fig. 2).

2.3 Variation of Global DNA Methylation Patterns of Arabidopsis *Seedlings Under Microgravity Conditions*

Single-base-resolution methylome analysis was conducted using *Arabidopsis* (Col-0) seedlings that had been grown for 60 h under microgravity conditions (Xu et al. 2018). The DNA methylation profiles at the whole-genome level were determined. Analysis of the read intensity around the annotated genes revealed lower DNA methylation levels under microgravity conditions (Fig. 3). Because euchromatin and heterochromatic genomic regions such as coding sequences and repetitive sequence regions display different DNA methylation patterns, we further evaluated the detailed methylation patterns within genes, including coding sequences (CDS) and non-coding areas. The results showed that CpG sites had the highest methylation levels and that CHH sites had the lowest methylation levels in each gene region (Fig. 3a–c). In the CpG context, CpG methylation in the 5′ UTR and 3′ UTR regions was lower than that in coding regions, and the 5′ UTR methylation level was much lower than that in the 1500-bp upstream region and in the 3′ UTR (Fig. 3c). The CHG context appeared to be quite different from the CpG context, with much higher methylation levels in 1500-bp upstream regions and 5′ UTR regions, and CDS displayed the lowest methylation level (Fig. 3a). However, the CHH context showed higher methylation levels in the

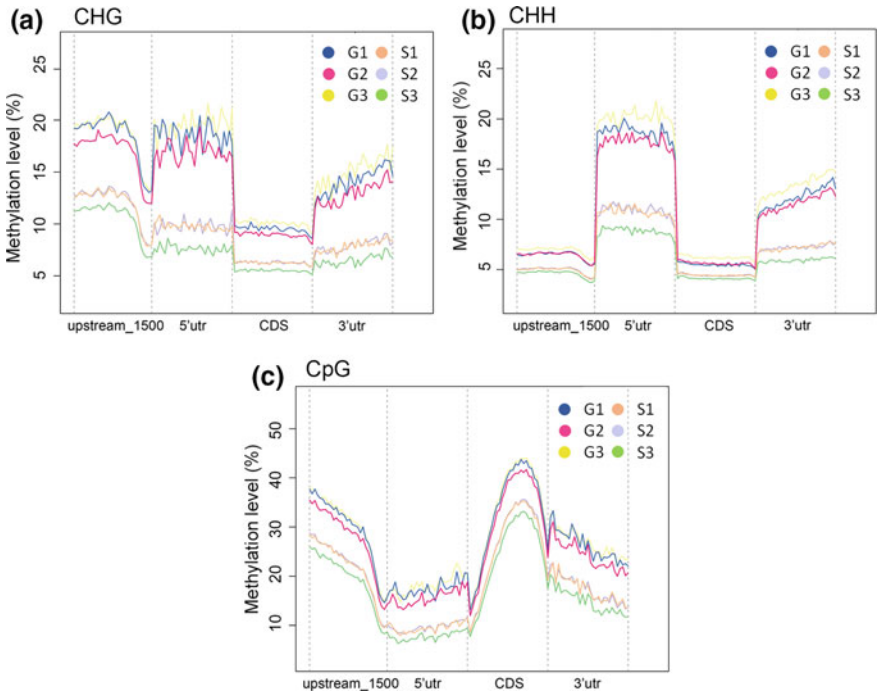

Fig. 3 DNA methylation patterns in various genomic regions. **a**–**c** Distribution of the DNA methylation levels in the CHG (**a**), CHH (**b**) and CpG (**c**) contexts among various gene regions, including the promoter, 5′ UTR, gene body and 3′ UTR in ground controls (G1, G2, G3) and in plants maintained under microgravity conditions (S1, S2, S3) (Reprinted from Xu et al. 2018.)

5′ UTR and 3′ UTR regions and lower methylation levels in the 1500-bp upstream region and CDS sites (Fig. 3b).

Cytosine methyltransferases and demethylases are involved in a number of biological functions and play important roles in the maintenance of genomic methylation (Penterman et al. 2007). We examined all of these genes to determine whether there were any changes in their DNA methylation levels under microgravity to investigate possible altered methylation patterns in methyltransferase- and demethylase-related genes in response to microgravity conditions. The results indicate that exposure of the plants to microgravity was accompanied by alterations in the DNA methylation patterns of specific genes (Table 1).

The results of this SJ-10 satellite experiment demonstrated that lower methylation levels in the CHG, CHH and CpG contexts in the *Arabidopsis* genome tended to occur under microgravity conditions (Fig. 3). However, this does not mean that all gene patterns were hypomethylated. As the results in Tables 1, 2 and 3 show, methylation-related genes (*AGO2*, *DME*, *DMT1* and *APE1*), transcription factor genes (*MYB65, MYB74, BHLH35, BHLH81, BHLH131, BZIP68, GATA26, NAC081, NAC100, NAC105, WRKY7* and *WRKY19*) and hormone-related genes (*ARF3, IAA9*

Table 1 Methylation-related genes which showed altered methylation levels in *Arabidopsis* grown in microgravity compared with the control grown under 1 × g ($p < 0.05$) (Reprinted from Xu et al. 2018.)

Gene name	Locus	Annotation	Diff. Methy (S-G)
Protein argonaute			
AGO2	AT1G31280	Exon 3 of 3	0.213
		Exon 3 of 3	0.173315
AGO8	AT5G21030	Exon 5 of 21	−0.29709
		Exon 6 of 21	−0.36424
AGO10	AT5G43810	Exon 20 of 20	−0.2002
		Promoter-TSS	−0.22464
		TTS	−0.37014
DNA (cytosine-5)-methyltransferase			
CMT3	AT1G69770	Exon 7 of 21	−0.36427
S-adenosyl-L-methionine-dependent methyltransferases superfamily protein			
DRM3	AT3G17310	Intron 6 of 9	−0.35597
SNF2 domain-containing protein			
CLSY1	AT3G42670	TTS	−0.20012
CLSY2	AT5G20420	TTS	0.190565
CLSY4	AT3G24340	Exon 3 of 3	−0.28239
Histone-lysine N-methyltransferase			
SUVH3	AT1G73100	TTS	−0.37213
SUVH4	AT5G13960	Intron 12 of 14	−0.25522
SUVH5	AT2G35160	Exon 3 of 3	−0.39782
		Exon 3 of 3	−0.57018
		Exon 3 of 3	−0.40895
SUVH6	AT2G22740	Exon 2 of 2	−0.4596
RNA-binding (RRM/RBD/RNP motifs) family protein			
ROS3	AT5G58130	Exon 4 of 4	−0.29129
Transcriptional activator			
DME	AT5G04560	Exon 11 of 18	0.182532
DNA (cytosine-5)-methyltransferas			
DMT1	AT5G49160	Exon 2 of 12	0.286685
Acclimation of photosynthesis to environment			
APE1	AT5G38660	Intron 5 of 12	0.333855
Tetraspanin			
TET14	AT2G01960	TTS	−0.31082

Table 2 Transcription factor genes that showed altered methylation level in Arabidopsis grown in microgravity ($p < 0.05$) (Reprinted from Xu et al. 2018.)

Gene name	Locus	Annotation	Diff. Methy (S-G)
MYB35	AT3G28470	Promoter-TSS	−0.393009
MYB3R5	AT5G02320	TTS	0.363732
		Exon 8 of 9	−0.377741
MYB65	AT3G11440	Exon 3 of 4	0.548274
MYB74	AT4G05100	Promoter-TSS	0.401997
BHLH28	AT5G46830	Promoter-TSS	−0.145863
BHLH35	AT5G57150	TTS	0.220791
BHLH41	AT5G56960	TTS	−0.153077
BHLH66	AT2G24260	TTS	−0.435487
BHLH81	AT4G09180	Intron 3 of 4	0.394391
BHLH95	AT1G49770	Promoter-TSS	−0.204263
BHLH123	AT3G20640	TTS	−0.319919
BHLH131	AT4G38070	TTS	0.296181
BHLH140	AT5G01310	Exon 3 of 6	−0.189424
BHLH144	AT1G29950	Exon 4 of 5	−0.316130
BZIP16	AT2G35530	Exon 5 of 13	−0.515903
BZIP28	AT3G10800	TTS	−0.489383
BZIP30	AT2G21230	TTS	−0.36030
BZIP63	AT5G28770	Promoter-TSS	−0.318241
BZIP68	AT1G32150	Exon 9 of 13	0.263631
GATA	AT3G25660	Intron 3 of 8	0.186431
GATA10	AT1G08000	TTS	0.229709
GATA14	AT3G45170	Exon 2 of 2	−0.200013
	AT3G45170	TTS	0.170634
GATA26	AT4G17570	Exon 3 of 8	0.281708
NAC008	AT1G25580	Exon 4 of 6	−0.348574
NAC023	AT1G60280	TTS	−0.236220
NAC039	AT2G24430	TTS	−0.236220
NAC043	AT2G46770	Promoter-TSS	−0.236220
NAC069	AT4G01550	Promoter-TSS	−0.236220
NAC081	AT5G08790	Promoter-TSS	0.268681
NAC100	AT5G61430	Promoter-TSS	0.268681
NAC105	AT5G66300	Promoter-TSS	0.268681
		Exon 1 of 3	0.268681

(continued)

Table 2 (continued)

Gene name	Locus	Annotation	Diff. Methy (S-G)
WRKY1	AT2G04880	TTS	−0.408020
WRKY7	AT4G24240	Intron 11 of 14	0.292929
WRKY19	AT4G12020	Intron 4 of 5	0.270506
WRKY20	AT4G26640	Exon 3 of 6	−0.499226
	AT4G26640	Promoter-TSS	−0.548767
WRKY74	AT5G28650	Promoter-TSS	−0.434246

Table 3 Hormone related genes that showed altered methylation level in Arabidopsis grown in microgravity ($p < 0.05$) (Reprinted from Xu et al. 2018.)

Gene name	Locus	Annotation	Diff. Methy (S-G)
Auxin response factor			
ARF1	AT1G59750	Exon 5 of 15	−0.50845
		Exon 6 of 15	−0.53716
		Exon 13 of 15	0.260059
ARF2	AT5G62000	Exon 12 of 16	−0.51619
		Exon 13 of 16	−0.65464
		Exon 15 of 16	0.26779
ARF3	AT2G33860	Intron 5 of 9	0.30883
ARF4	AT5G60450	Exon 10 of 12	−0.34222
		Exon 10 of 12	−0.38993
		Intron 5 of 11	0.317819
ARF5	AT1G19850	TTS	−0.32076
ARF6	AT1G30330	Exon 13 of 14	−0.48895
ARF6	AT1G30330	Exon 14 of 14	−0.28162
ARF8	AT5G37020	Intron 4 of 13	−0.25235
ARF19	AT1G19220	Exon 8 of 12	−0.32607
ARF21	AT1G34410	Intron 3 of 13	−0.36508
ARF22	AT1G34390	Exon 3 of 14	−0.130253
Auxin signaling F-box			
AFB2	AT3G26810	Exon 3 of 3	0.26723
AFB5	AT5G49980	Exon 2 of 3	−0.20794
TIR	AT1G72930	TTS	0.190826
Auxin-responsive protein			

(continued)

Table 3 (continued)

Gene name	Locus	Annotation	Diff. Methy (S-G)
IAA9	AT5G65670	Exon 3 of 6	0.204658
		Intron 2 of 5	0.18341
IAA33	AT5G57420	TTS	0.580797
Indole-3-acetaldehyde oxidase			
AAO1	AT5G20960	Exon 2 of 10	0.237555
AAO2	AT3G43600	Exon 2 of 9	−0.49537
		Exon 2 of 9	0.535264
		Exon 5 of 9	−0.32953
Auxin transport protein			
BIG	AT3G02260	Exon 4 of 14	0.230049
		Exon 4 of 14	0.281997
		Exon 4 of 14	0.279249
		Exon 8 of 14	−0.52414
		Exon 12 of 14	0.283206
Brassinosteroid insensitive 1-associated receptor kinase			
BAK1	AT4G33430	Intron 9 of 10	−0.40569
		Exon 10 of 12	0.187463
ABA deficient			
ABA3	AT1G16540	Promoter-TSS	0.211757
		Promoter-TSS	−0.30194
		Exon 6 of 21	−0.3429
		Exon 9 of 21	0.263019
Ethylene-insensitive protein			
EIN2	AT5G03280	Exon 7 of 8	0.303509
EIN3	AT3G20770	Exon 2 of 2	−0.42091
		Exon 2 of 2	0.048629
Ethylene-responsive transcription factor			
ERF11	AT1G28370	TTS	−0.36503
		TTS	−0.30229
ERF094	AT1G06160	Promoter-TSS	0.257507
Ethylene response sensor			
ERS1	AT2G40940	TTS	−0.31638

and *IAA33*) were all hypermethylated. Some genes, including *MYB3R5, GATA14, ARF1, ARF2, ARF4, AAO2, BIG, BAK1, ABA* and others, displayed more than two regions with opposite methylation patterns. The actual changes in the expression of these genes will require further experimental verification. Our results cannot be simply interpreted as indicating that the methylation of DNA is inhibited by microgravity, thereby contributing to hypomethylation of the *Arabidopsis* genome.

2.4 Altered Methylation Profiles of Functional Genes in Response to Microgravity Conditions

We used GO enrichment to categorize the genes that showed alterations in their methylation patterns under microgravity conditions to perform an in-depth analysis of the functional categories of genes (Xu et al. 2018). In the CHG context in the category of biological processes, altered methylation-related (AMR) genes were enriched for cell wall related processes, carbohydrate metabolic processes, defense response and nitrogen compound transport (Fig. 4a). Changes in these biological processes were also shown in transcriptomic studies in several previous plant spaceflight experiments (Jin et al. 2015; Johnson et al. 2017). Changes in cell wall related processes and defense response were consistently detected, although the results of various spaceflight experiments differ for a variety of reasons (Johnson et al. 2017). This suggests that the weakening of the plant cell wall that occurs under microgravity may be regulated at the level of DNA methylation. Changes in metabolism-associated AMR genes, including carbohydrate metabolic processes and nitrogen compound transport, suggested that energy metabolism might be regulated in response to the microgravity environment.

In the CHH context in the category of biological processes, AMR genes for metabolic processes, cellular metabolic processes, biosynthetic processes, signaling transduction, oxidation-reduction processes and lipid biosynthesis were enriched (Fig. 4b). Here, we found the lipid biosynthesis AMR genes. Lipid biosynthesis has been implicated in gravity responses in *Arabidopsis* and is likely involved in adjusting the polarity of cells (Briarty and Maher 2004). Oxidation-reduction process AMR genes were also identified. Gravity sensing in plant cells involves signals related to oxidative stress. Regarding cellular components such as cell, intracellular, organelle, plasma membrane and cell periphery, AMR genes were enriched.

In the CpG context in the category of biological processes, AMR genes for mRNA transport, mRNA export from the nucleus, microtubule-based movement, telomere maintenance in response to DNA damage, regulation of telomere maintenance and inositol phosphate phosphorylation were enriched (Fig. 4c). Here, we found DNA damage and regulation of telomere maintenance AMR genes, supporting this assumption. Because space radiation can cause damage to DNA directly, the radio-adaptive response (RAR) of *Arabidopsis* root growth is modulated under microgravity conditions, and DNA damage repair in RAR is regulated by microgravity (Paul and

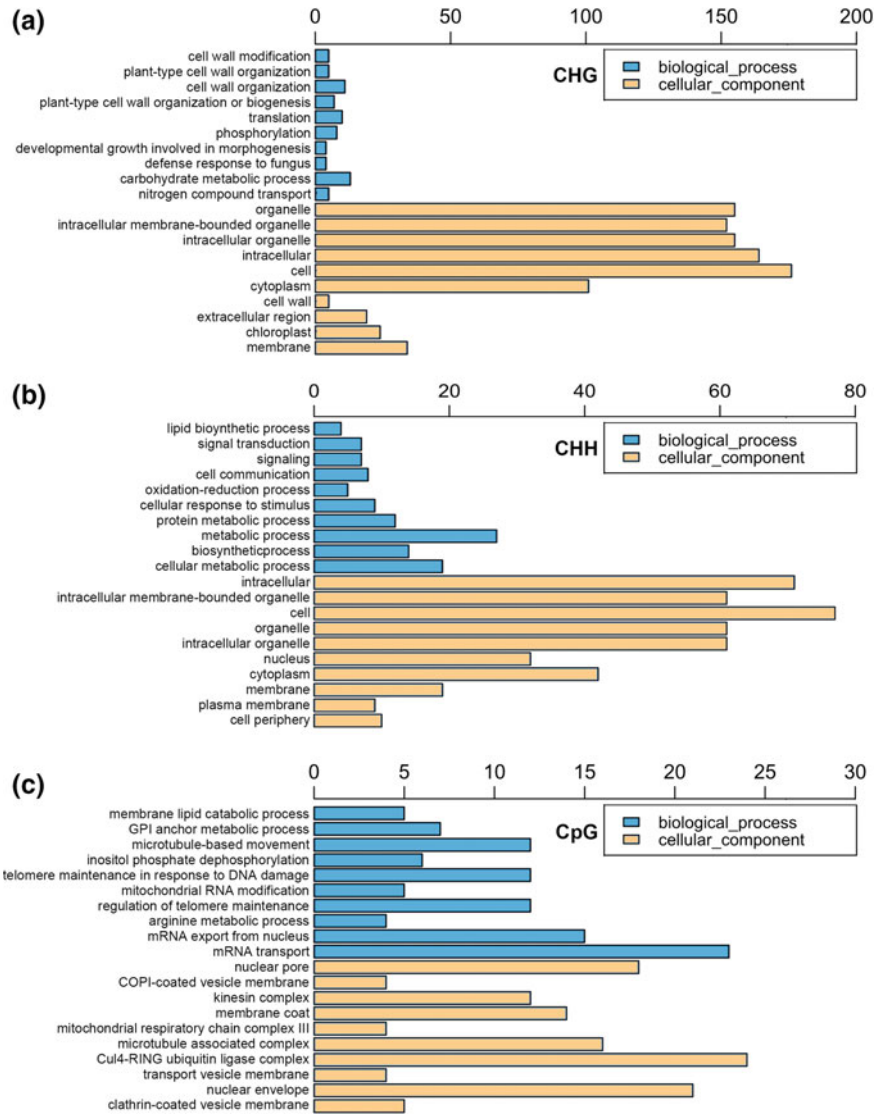

Fig. 4 GO term enrichment network of genes with altered methylation levels in the *Arabidopsis* genome. **a**–**c** GO term enrichment analysis of altered gene methylation patterns in the CHG (**a**), CHH (**b**) and CpG (**c**) contexts under microgravity conditions was conducted. The bar represents the number of genes in the test set belonging to each GO category. Only the top 10 GO terms are listed ($p < 0.05$) (Reprinted from Xu et al. 2018.)

Ferl 2015). Inositol phosphate signaling has also been shown to occur in response to microgravity conditions (Kriegs et al. 2006). For cellular components, AMR genes for the functional categories of Cul4-RING ubiquitin ligase complex, nuclear envelope, and nuclear pore were enriched.

2.5 *Numerous TE Genes Are Hypomethylated Under Microgravity Conditions*

Under microgravity conditions, many differentially methylated TEs were demethylated (Xu et al. 2018). The methylation patterns of the CHG, CHH, CpG contexts in the TE regions and methylation levels in the 1-kb upstream and downstream regions were demonstrated (Fig. 5a). TEs presented lower methylation levels in the CHG, CHH and CpG contexts in spaceflight samples. The results showed that a large proportion of the TEs in these contexts are differentially methylated and that hypomethylation of TE sites was likely the result of the induction of active TEs. Previous research has shown that mobilization and silencing of transposable elements (TEs) are often accompanied by disruption of DNA methylation (Hashida et al. 2006). TEs can affect the size of the genome, create insertions and other mutations, and influence gene expression patterns. Therefore, the change of TEs methylation in microgravity environment should be paid more attention to.

2.6 *Changed Methylation Profiles of TEs of Different Lengths in Response to Microgravity Conditions*

That the length of TEs can affect their methylation levels has been shown by previous research (Xing et al. 2015). To further identify the association between methylation status and TE length in *Arabidopsis*, TEs were divided into three groups: a 1st group with lengths shorter than 500 bp, a 2nd group with lengths ranging from 500 bp to 2000 bp; and a 3rd group with lengths of more than 2000 bp. Compared with the ground controls (G1, G2, G3), the 1st group of TEs showed a striking decrease in CHG and CHH methylation levels under microgravity conditions (S1, S2, S3) (Fig. 5b). The 2nd group showed a marginal decrease in the CHG and CHH methylation contexts (Fig. 5c). The 3rd group showed a decrease in the CHG context but no decrease in the CHH or CpG methylation contexts under microgravity conditions (Fig. 5d). TE methylation levels can influence transposon expression in response to environmental stress (Dowen et al. 2012). We propose that demethylation of TEs plays an important role under microgravity conditions (Xu et al. 2018).

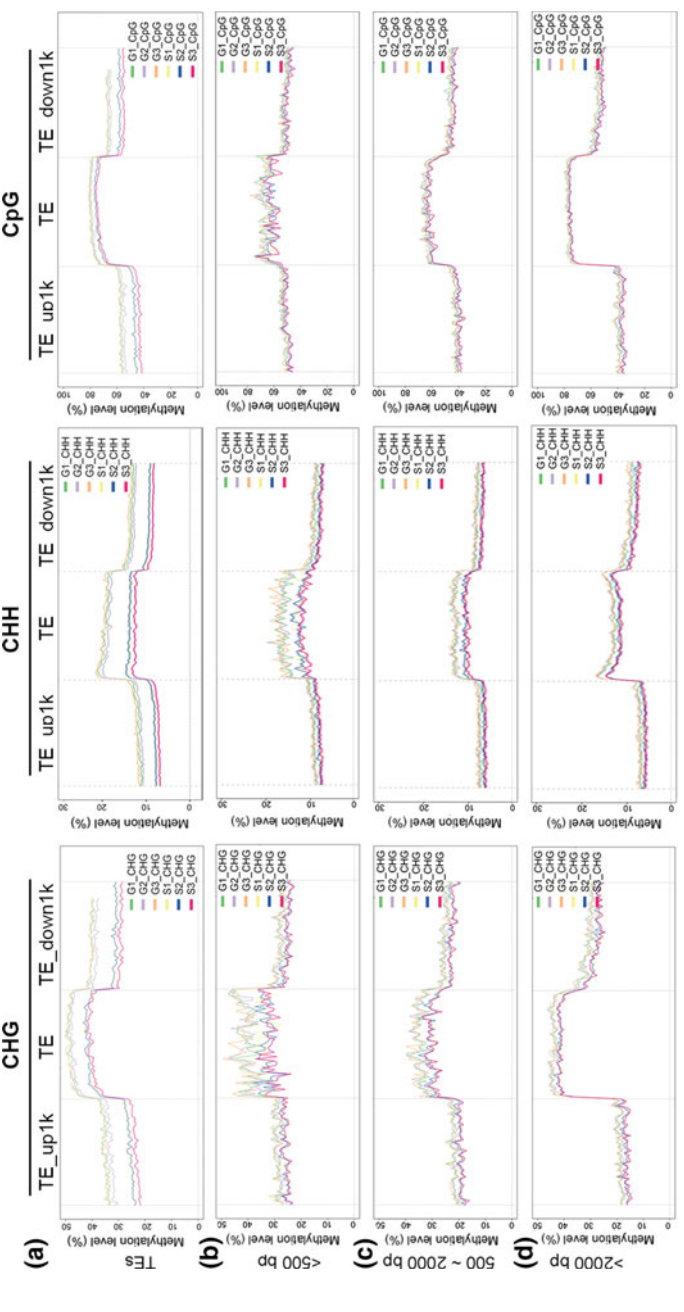

Fig. 5 Methylation patterns of TEs and different types of TEs with different lengths in the *Arabidopsis* genome. **a** Methylation patterns of TEs. The distribution of the methylation read density for all TEs in the *Arabidopsis* genome between ground controls (G1, G2, G3) and under microgravity conditions (S1, S2, S3) is shown. The *x*-axis represents the TE body and its 1-kb upstream and downstream regions. The *y*-axis indicates the average methylation level. Three types of methylation patterns, CHG, CHH and CpG, are shown in the figure. **b–d** Methylation patterns of TEs with different lengths. Methylation patterns of TEs with different lengths in ground controls (G1, G2, G3) and in plants grown under microgravity conditions (S1, S2, S3). TEs were divided into quintiles based on their lengths: the 1st quintile is the shortest, and the 3rd quintile represents TEs of the longest length. The read density distribution for TEs with lengths of **a** less than 500 bp, **b** 500–2,000 bp, and **c** more than 2,000 bp within the *Arabidopsis* genome is shown. Three types of methylation patterns, CHG, CHH and CpG, are shown in each figure (Reprinted from Xu et al. 2018.)

2.7 The Important Biological Processes Involved in Changes in DNA Methylation in Response to Microgravity Spaceflight

The DMRs in flight seedlings and ground controls were analyzed to identify the potential influence of microgravity spaceflight on the methylation level of the whole genome (Xu et al. 2018). KEGG pathway enrichment analysis was conducted to determine the molecular functions of these DMR-related genes.

In the CpG context, they were mainly assigned to pathways associated with metabolism related processes (such as sulfur metabolism, terpenoid backbone metabolism, N-glycan biosynthesis, butanoate metabolism and beta-alanine metabolism), ABC transporters, nucleotide excision repair, protein procession in the ER and endocytosis (Fig. 6c). In the previous spaceflight experiments, many of the pathways identified here have also been found in the studies of transcriptomic analysis under microgravity (Jin et al. 2015; Johnson et al. 2017). In the CHG context, these genes were mainly assigned to pathways associated with metabolism (starch and sucrose metabolism, phenylalanine biosynthesis, purine metabolism, glutathione metabolism, amino sugar and nucleotide sugar metabolism), proteasomes, ribosomes and phagosomes (Fig. 6a), whereas in the CHH context they were assigned to pathways related to metabolic pathways, biosynthesis of secondary metabolites, phenylpropanoid biosynthesis and ribosomes (Fig. 6b). In the CpG context, they were mainly assigned to pathways associated with metabolism related processes (such as sulfur metabolism, terpenoid backbone metabolism, N-glycan biosynthesis, butanoate metabolism and beta-alanine metabolism), ABC transporters, nucleotide excision repair, protein procession in the ER and endocytosis (Fig. 6c). In the previous spaceflight experiments, many of the pathways identified here have also been found in the studies of transcriptomic analysis under microgravity (Jin et al. 2015; Johnson et al. 2017).

Methylation alterations in genes encoding transcription factors (TFs) was also further characterized (Xu et al. 2018). The PlantTFDB predicts that the *Arabidopsis* genome contains more than 2200 TFs. Approximately 36 TF genes showed altered methylation levels during microgravity spaceflight. These included bHLH, bZIP, GATA, WRKY and NAC members (Table 2). That the expression of many TF genes is altered under microgravity was demonstrated by previous spaceflight experiments (Correll et al. 2013; Jin et al. 2015). For example, an NAC TF gene, *ANAC104/XND1* (At5g64530), was up regulated under microgravity conditions in the TROPI-2 project (Correll et al. 2013). *ANAC104/XND1* regulates the synthesis of tracheal element secondary walls and can affect plant height and the length of tracheal elements in stems and hypocotyls (Zhao et al. 2008). Another NAC TF gene, *NAC1* (NAC domain-containing protein 21/22, At1g56010), was down regulated under microgravity (Correll et al. 2013). *NAC1* encodes a transcription factor that is induced by auxin and mediates auxin signaling to promote lateral root development (Xie et al. 2002). Alteration of the expression of auxin related and cell wall related genes under microgravity is closely related to plant adaptation to microgravity. Therefore, it is

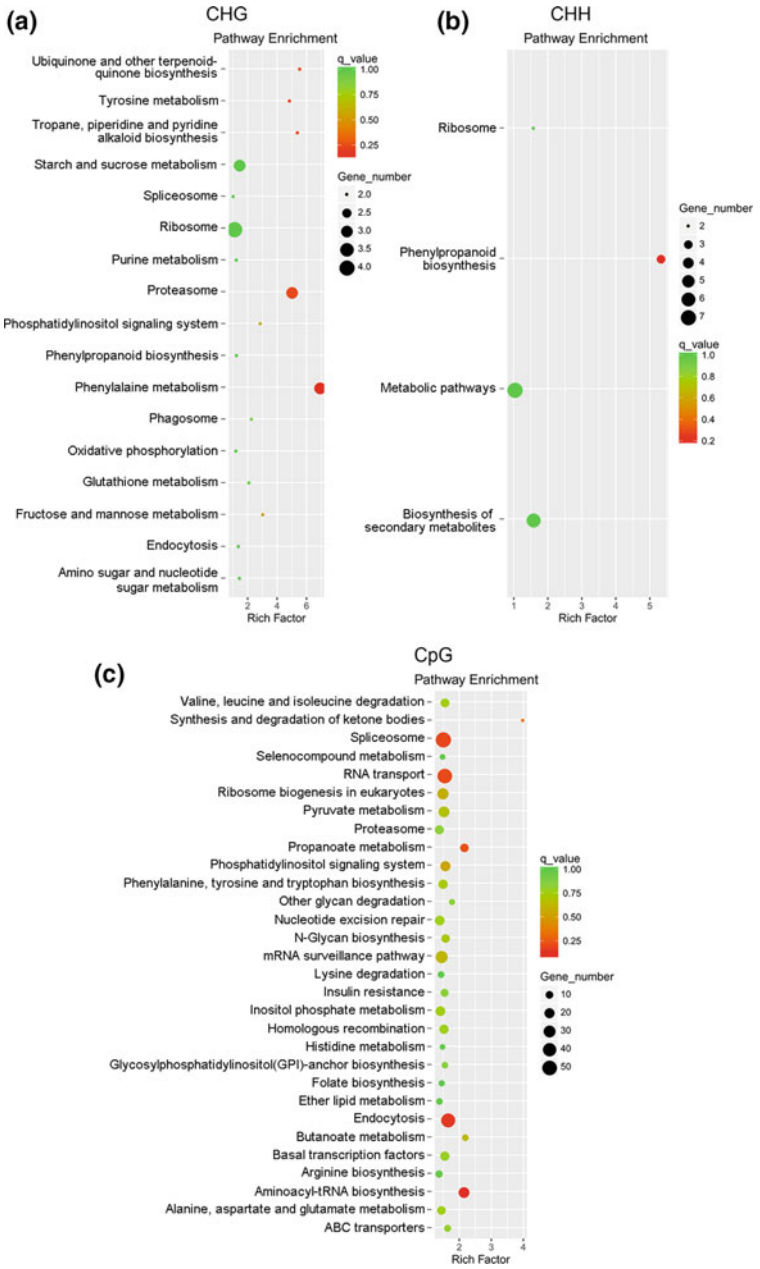

Fig. 6 Pathway analysis of genes that showed altered methylation. **a–c** KEGG pathway enrichment analysis of CHG (**a**), CHH (**b**) and CpG (**c**) differentially methylated genes in the *Arabidopsis* genome in plants grown under microgravity conditions and ground controls was performed. The size of the circle represents the gene numbers, and the color represents the *q* value (Reprinted from Xu et al. 2018.)

proposed that the possible differential methylation of genes encoding TFs may also contribute to the adaptation of plants to microgravity.

Abundant DMRs were found to be involved in the "Signaling" pathway. The observed alterations in the methylation of genes involved in hormone signaling pathways were functionally characterized. Genes involved in hormone signaling pathways, including auxin, ABA (abscisic acid), ethylene and BRs (brassinosteroids), were also differentially methylated (Table 3).

Notably, several auxin related genes whose DNA methylation was changed under microgravity have been identified, including the genes encoding auxin responsive factors (ARF1-6, ARF8, ARF19, ARF21 and ARF22), auxin signaling F-box proteins (TIR1, AFB2 and AFB5), auxin responsive proteins (IAA9 and IAA33), transport protein (BIG) and indole-3-acetaldehyde oxidases (AAO1 and AAO2). *TIR1* encodes an auxin receptor that mediates auxin-regulated transcription. The observation of altered *TIR1* methylation levels implies that microgravity affects auxin signaling in plants (Dharmasiri et al. 2005). Aux/IAA proteins are short-lived transcription factors that function as repressors of early auxin response genes (Goh et al. 2012). Repression is thought to result from the interaction of the repressors with auxin response factors (ARFs). Formation of heterodimers with ARF proteins may alter the ability of these proteins to modulate the expression of genes involved in the early auxin response. The decreased methylation level of *ARF* genes and the increased methylation level of the *IAA9* and *IAA33* genes may contribute to an increased auxin response. The gravimorphogenesis of plant organs was changed due to the effects of microgravity on the polar transport of auxin (Yamazaki et al. 2016). *BIG* encodes a membrane-associated protein and is required for auxin transport. We found that *BIG* was hypermethylated in space; thus, microgravity might inhibit auxin transport by increasing *BIG* methylation. Based on these results, we concluded that microgravity affects auxin-related processes at the levels of perception, signaling, transport and biosynthesis (Yamaguchi and Komeda 2013). The data imply that the effects of microgravity on auxin-related processes observed in previous spaceflight experiments may be related to changes in DNA methylation levels. In addition, altered methylation levels of the *EIN2* and *EIN3* genes, which play important roles in the ethylene signaling pathway, were detected. Alterations in the methylation of the ethylene responsive transcription factor genes *ERF11* and *ERF094* were also involved in the response to microgravity. Moreover, the methylation levels of the genes involved in ABA biosynthesis (*ABA3*) and brassinosteroid insensitive1 associated receptor kinase (BAK1) were also decreased.

Alterations in the methylation of genes related to cell wall were also identified. Hypergravity has been shown to up regulate cell wall rigidity in stems and roots (Martzivanou and Hampp 2003). However, plant cell wall rigidity is lower under microgravity conditions than on ground conditions (Hoson 2014). The thickness of cell walls decreased in response to the microgravity stimulus. The space-grown plants also contained xyloglucan and 1,3,1,4-β-glucans with lower molecular masses resulting from increases in xyloglucan-degrading and 1,3,1,4-b-glucanase activities. These results show that increasing plant cell wall rigidity via modification of the metabolism of cell wall constituents is an important step in gravity resistance. The

results shown in Table 4 indicate that numerous genes related to cell wall biosynthesis, such as the gene encoding the cellulose synthase catalytic subunit, callose synthase genes and cell wall expansion-related genes such as xyloglucan endotransglucosylase, beta-galactosidase and beta-glucosidase, displayed altered methylation levels.

That altered cell shape occurs as a result of cell wall perturbation under microgravity have been shown in previous space experiments (Johnson et al. 2017). This phenomenon may also be associated with changes in the expression of auxin-related

Table 4 Cell wall related genes that showed altered methylation level in Arabidopsis grown in microgravity compared with that grown under 1 × g control ($p < 0.05$) (Reprinted from Xu et al. 2018.)

Gene name	Locus	Annotation	Diff. Methy (S-G)
Root meristem growth factor			
RGF3	AT2G04025	TTS	0.210603
RGF4	AT3G30350	Promoter-TSS	0.273889
Cellulose synthase A catalytic subunit			
CESA1	AT4G32410	Exon 10 of 14	−0.41712
CESA5	AT5G09870	Exon 5 of 13	−0.321
CESA6	AT5G64740	Exon 10 of 13	−0.20271
		Exon 13 of 13	0.192504
CESA8	AT4G18780	Exon 6 of 12	−0.33978
		Exon 6 of 12	−0.25971
CESA9	AT2G21770	Intron 5 of 12	−0.37932
Callose synthase			
CALS1	AT1G05570	Exon 41 of 44	−0.41977
CALS3	AT5G13000	Exon 33 of 44	0.20095
		Exon 40 of 44	−0.35827
		Exon 43 of 44	−0.38991
		Intron 22 of 42	−0.23397
		Intron 26 of 42	−0.45092
CALS6	AT3G59100	Intron 16 of 41	−0.3966
CALS7	AT1G06490	Exon 23 of 42	0.348981
		Intron 19 of 41	−0.27468
CALS8	AT3G14570	Exon 27 of 42	−0.33138
CALS9	AT3G07160	Exon 3 of 50	−0.44072
		Exon 35 of 50	0.201205
		Intron 35 of 49	0.059917
		Intron 41 of 49	−0.38041
CALS10	AT2G36850	Intron 5 of 49	−0.35113
		Intron 34 of 49	0.378681

(continued)

Table 4 (continued)

Gene name	Locus	Annotation	Diff. Methy (S-G)
		Intron 44 of 49	−0.44741
CALS12	AT4G03550	Exon 2 of 5	−0.22841
		Exon 2 of 5	0.306824
		Intron 2 of 4	0.34053
Xyloglucan endotransglucosylase/hydrolase			
XTH10	AT2G14620	Exon 4 of 4	0.323687
XTH17	AT1G65310	Promoter-TSS	0.24495
Pectinesterase/pectinesterase inhibitor			
PME14	AT2G36700	Exon 3 of 5	0.280889
PME19	AT1G11590	TTS	−0.32367
		Exon 2 of 3	0.245865
PME42	AT4G03930	Promoter-TSS	−0.19401
PME48	AT5G07410	TTS	0.246784
PME49	AT5G07420	Promoter-TSS	0.206408
PME51	AT5G09760	TTS	−0.34578
Starch synthase			
SS1	AT5G24300	Exon 2 of 16	−0.1843
SS2	AT3G01180	Exon 8 of 8	0.219161
SS4	AT4G18240	Exon 12 of 16	−0.39843
		TTS	0.18302
Beta-galactosidase			
BGAL5	AT1G45130	Intron 11 of 16	0.265369
BGAL9	AT2G32810	TTS	0.311635
BGAL12	AT4G26140	Intron 15 of 16	0.527798
BGAL15	AT1G31740	Promoter-TSS	−0.20524
BGAL16	AT1G77410	Exon 15 of 19	−0.26202
		TTS	−0.21557
Beta-glucosidase			
BGLU24	AT5G28510	TTS	0.380285
BGLU42	AT5G36890	Promoter-TSS	0.130545
BGLU45	AT1G61810	TTS	−0.16838

genes under microgravity because the main effect of auxin is to relax the cell wall, thereby increasing cell growth. Growth induced by auxin is achieved by increasing the plasticity of the cell wall. During spaceflight, alterations in the methylation of cell wall-related genes were identified (Table 4). Changes in the expression of this category of genes in microgravity were also observed in several previous spaceflight experiments (Johnson et al. 2017). Figure 2 shows that the leaf growth of *Arabidopsis* seedlings was enhanced under microgravity. The most immediate effect that plants experience under space conditions is weightlessness. This is an environment that terrestrial plants have never encountered. Therefore, the most direct adaptive response of plants is the weakening of mechanical support tissue under microgravity (Hoson et al. 2014). First, the rigidity of the plant cell wall decreases under microgravity conditions (Hoson et al. 2014; Johnson et al. 2017). As a result, the expression of cell wall genes is altered (Johnson et al. 2017). Regulation of these gene expression changes may be related to changes in the DNA methylation level in plant cells. We found changes in the DNA methylation levels of genes encoding transcription factors and certain genes associated with cell wall metabolism. Based on these results, the phenotypic acceleration of seedling growth under microgravity may be related to changes in the DNA methylome, in the expression of auxin-related genes and cell-wall-related genes, and in cell wall rigidity. The results suggest that adjustment of cell wall rigidity by modification of the metabolism of the cell wall is an important mechanism through which plants adapt to changes in gravity. These inferences are supported by the results of previous space experiments in which it was demonstrated that increased plasticity of the cell wall enhanced the growth of the hypocotyl of *Arabidopsis*, rice coleoptile and flower stems of *Arabidopsis* under microgravity conditions (Hoson et al. 2014).

2.8 The Process of Plant Gravitropism

Early in the 19th century, it was discovered that plant organs grew under the guidance of gravity. The root of the plant always grows in the direction of gravity, whereas the shoot penetrates the soil upward to allow the stems and leaves to expand in space. Through this process, plants can survive by gaining access to sunlight, nutrients and water resources. Because of the negative gravitropism of stem growth, plant fruits and seeds can grow away from the harm of the damp ground environment, thereby avoiding decay. Plants can grow using negative gravitropism and resist lodging after undergoing storms.

There are 4 stages of plant gravitropism: 1. Perception Stage, whereby a plant senses gravistimulation; 2. Transduction Stage, whereby a plant converts the biophysical signal into a biochemical signal; 3. Transmission Stage, whereby a signal is conducted from the sensing area to the bending area; and 4. Reaction Stage, whereby asymmetric growth (elongation) of the elongation region occurs, leading to a change in growth direction (Fig. 7) (Perbal and Driss-Ecole 2003; Sievers 1991).

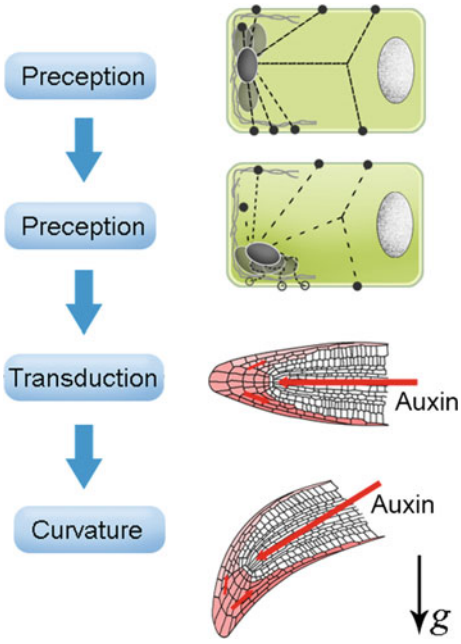

Fig. 7 The stages of plant gravitropism growth. (Reprinted from Perbal and Driss-Ecole 2003)

Several hypotheses have been proposed to explain the mechanism of gravity direction sensing by a plant. The starch-statolith hypothesis has been experimentally supported in many plants (Cai et al. 1997; Perbal and Driss-Ecole 2003; Sievers 1991). Plant organs detect gravity through a sensitive area, such as a root cap, which is in the very tip of the root and composed of several layers of cells, young stem tissue or other components such as internode, hypocotyl and inflorescence, which have not lost the abilities of growth. Typically, amyloplasts in the columella cells in the root cap can deposit along the direction of gravity, guiding the direction of root growth. These amyloplasts are designated statoliths, and the cells containing the statoliths are called statocytes. Statocytes are also found in plant stems, which are cortical cells. Sack et al. demonstrated that the gravity response of the starchless mutant *pgm* is much weaker than the wild type—there were no statoliths in the root cap cells of the *pgm* mutant (Kiss and Sack 1989). However, a *pgm* mutant with no statoliths still had very weak gravitropism (Caspar and Pickard 1989). This result implies that the plant has other mechanisms of detecting gravity in addition to statoliths.

After sensing the gravity signal, the second step is to convert the biophysical signal into a biochemical signal. When the plants are stimulated by gravity change, the amyloplasts shift, changing the exerting force between the cytoskeleton and the statoliths or the pressure of statoliths deposited in the endoplasmic reticulum (Cai et al. 1997; Perbal and Driss-Ecole 2003; Sievers 1991). In addition, ion channels on cell membranes are activated. The concentration of intracellular calcium ions, reactive oxygen species, proton concentration and other signal molecules appear to

respond (Belyavskaya 1992; Bourgeade and Boyer 1994; Joo et al. 2001; Strohm et al. 2012), which results in Ca^{2+}, IP_3, and H^+ gradients (Hejnowicz et al. 1998), as well as leading to a rearrangement of auxin transporters (e.g., PIN3 protein) (Strohm et al. 2012). Auxin is transported polarly.

After the gravity signal is converted from the physical signal to the chemical signal in the root cap, the third stage occurs. Auxin is transported to the organ elongation region asymmetrically. This model is the Cholodny-Went model (Thimann 1992). Auxin is the main carrier of this signal transmission process. Auxin-resistant1, *aux1*, which fails to input auxin into cells, leads to an agravitropic phenotype (Marchant et al. 1999). Mutants that lack auxin transport proteins, such as PIN proteins, exhibit a decrease in gravitropism to varying degrees (Chen et al. 1998; Luschnig et al. 1998). The concentration gradient of auxin in the organ elongation region caused by asymmetric auxin transport leads to asymmetric gravitropic growth. That is, the fourth stage—asymmetric growth bending.

2.9 Asymmetric Growth Caused by Plant Gravitropism Curvature

Auxin is synthesized in the aerial part of the plant (although a low amount is also synthesized in the root tip) (Ljung et al. 2001), is transported to the underground part of the root tip through PIN1 proteins in the vascular tissue, is transported back to the basal part of the stem under the guidance of PIN3 and PIN7 proteins, and then is transversely transported back to the vascular bundles through the endodermis of the elongation and mature zones (Adamowski and Friml 2015; Band et al. 2014; Swarup and Bennett 2003). In the elongation zone, auxin enhances the activity of the P-type H^+ pump in the plasma membrane within a few minutes, increases the excretion of H^+, decreases the cell wall pH, increases cell wall remodeling factor activity, enhances the elasticity of the cell wall and facilitates the enlargement of the protoplast (Hager and Le Blanc 2003). Of course, asymmetric auxin concentrations on both sides will lead to asymmetric growth.

For example, when the root is subjected to gravistimulation (changing the growth direction by 90°), auxin is preferentially transported to the lower elongation zone of the root, forming a concentration gradient of auxin in this region, making the cell grow longer on the up side than that on the down side, thus prompting the root to bend downwards (Fig. 8) (Strohm et al. 2012).

The asymmetric distribution of auxin triggers a series of follow-up cascade reactions, such as triggering the asymmetric distribution of signaling molecules such as nitric oxide (NO) (Fig. 9) (Hu et al. 2005). Such reactions may additionally mediate symmetric growth.

A rice shoot base was used to study plant gravitropism (Fig. 10) (Cui et al. 2005). Asymmetric distribution of gibberellin has also been formed during the formation of the asymmetric auxin gradient (Fig. 11) (Cui et al. 2005). The formation of a

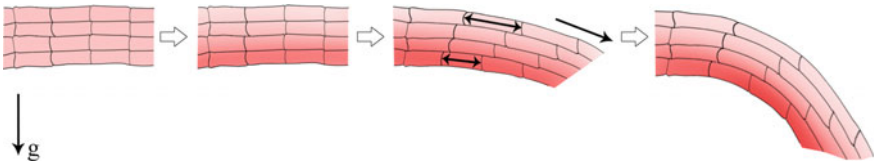

Fig. 8 The asymmetric growth of a plant root during gravitropism (Reprinted from Strohm et al. 2012.)

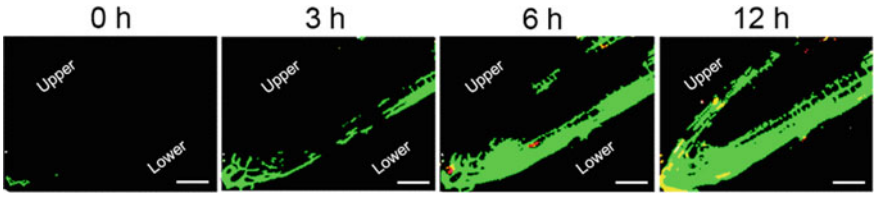

Fig. 9 Nitric oxide mediates gravitropic bending in soybean roots. Gravistimulation induces the rapid accumulation of NO required for gravitropism in soybean roots. Gravistimulation induces asymmetric NO accumulation. Soybean roots were loaded with DAF-2DA and gravistimulated by orientating the roots horizontally. The fluorescence intensity of dissected root tips was observed at the indicated times by confocal fluorescence microscopy. Experiments were repeated at least five times with similar results (Reprinted from Hu et al. 2005.)

GA gradient may be related to the asymmetric metabolism of gibberellin on both sides of the elongation zone. Differential expressions of genes linked to gibberellin metabolism in the up and down sides were observed (Fig. 12) (Cui et al. 2005; Hu et al. 2013; Shan et al. 2014).

In studies of gravitropism of rice shoot bases, the results from the analysis of the microarray data showed that an important part of the asymmetric transcript is involved in the metabolism and modification of the cell wall material (Fig. 13) (Hu et al. 2013). A proteomic analysis also found a variety of proteins that were involved in the asymmetric distribution in cell wall metabolism. In studies of *XET* (encoding xyloglucan glycosyltransferase) and *EXP* (encoding expansin), these genes were found to be highly expressed in the cells located on the side where the cell elongates faster (Figs. 14 and 15) (Cui et al. 2005; Hu et al. 2007). XET is involved in plant tissue softening by decomposing xyloglucan, the main component of cell wall hemicellulose polysaccharides. EXP is also a protein that exists in the plant cell wall and plays an important role in the growth of plant cells and the maturation of fruit. These results indicate that the relaxation of the cell wall facilitates the development of gravitropic bending. There has also been a series of reports of the changes in the cell wall responding to gravistimulation (Strohm et al. 2012).

The effect of aquaporin was also observed while studying cell wall changes during gravitropism. Aquaporin exists in the cytoplasmic membrane, the vacuole membrane and other locations and is involved in water transportation. For example, an aquaporin located in rice cytoplasmic membranes named OsRWC3 has a higher abundance in

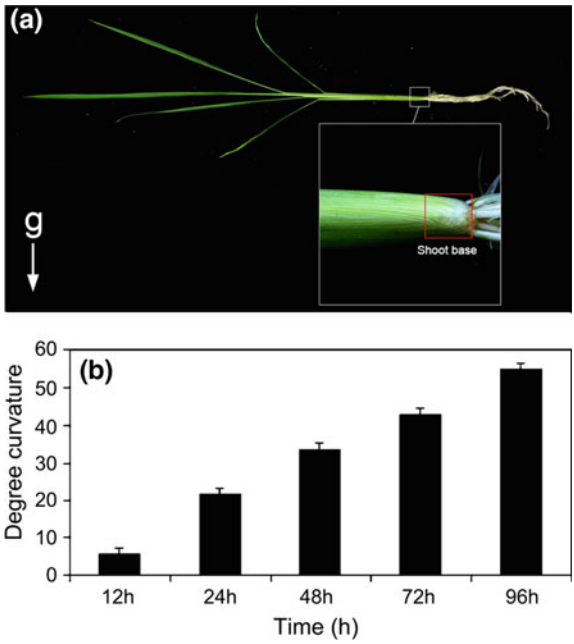

Fig. 10 Graviresponses of rice seedling following horizontal orientation. **a** Graviresponding rice seedlings used for analyses. All experiments were performed using 3–4-week-old seedlings. The arrow indicates the bending rice shoot base. 'g' shows the gravity vector. **b** After gravistimulation for the indicated times, the curvature of rice shoot base was determined (n = 8, mean ± SD) (Reprinted from Cui et al. 2005.)

the faster elongated side of the rice shoot base. Its gene expression level is also higher on the faster growth side (Fig. 16) (Hu et al. 2007).

The expressions of the genes mentioned above, such as *XET*, *EXP*, and *OsRWC3*, are related to the regulation of gibberellin during gravitropism (Hu et al. 2009).

The asymmetric transport of auxin, the distribution of gibberellin, the relaxation of cell walls and the expression of related genes in water transport are all involved in the asymmetric growth of the gravitropism response.

2.10 The Model of Plant Cell Growth

The asymmetric growth of a plant cell is determined by a series of molecular processes.

In the elongation region of the organ where the gravitropic bending occurs, the shape of the plant cell is maintained by a balance between cell wall rigidity and turgor pressure produced by intracellular vacuoles (Fig. 17) (Cai et al. 2016). To elongate, a cell must loosen its cell wall by reducing cell wall rigidity and then by increasing

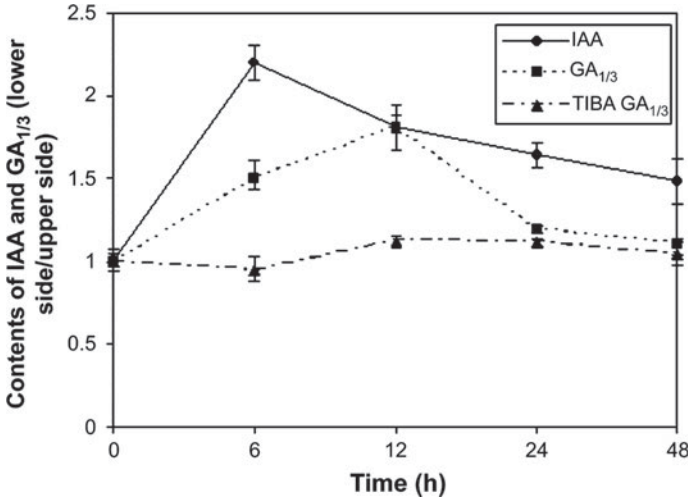

Fig. 11 Gravity-induced asymmetric accumulation of IAA and GAs in rice shoot bases and the effects of TIBA on GA asymmetric accumulation. Rice seedlings were grown in the absence or presence of TIBA (30 μM) and gravistimulated by rotating their pots 90°. After gravistimulation for the indicated times, the bending portions of the shoot bases were removed and bisected with a razor blade into upper and lower flanks. IAA and $GA_{1/3}$ were extracted and concentrations determined by ELISA. The ratio of hormone content (lower/upper flanks) is shown. Values are the means (± SDs) from three replicate experiments with at least eight seedlings per replicate (Reprinted from Cui et al. 2005.)

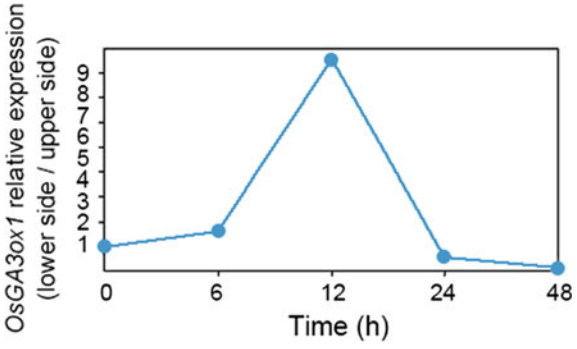

Fig. 12 The effects of gravistimulation and TIBA on *OsGA3ox1* expression in rice shoot bases. The rice seedlings were grown in the absence or presence of TIBA (30 μM) and gravistimulated for the indicated times. RNA was extracted from shoot base flanks after gravistimulation. RT-PCR was used to analyze *OsGA3ox1* expression in the lower and upper shoot base flanks (Reprinted from Cui et al. 2005.)

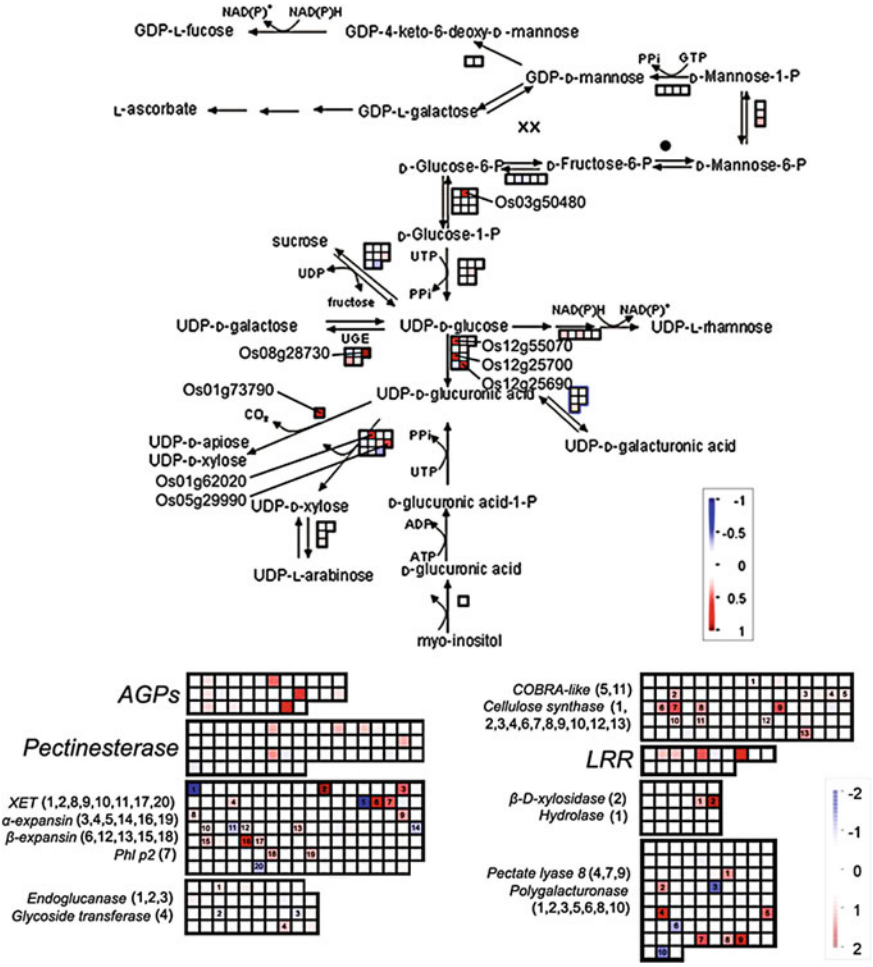

Fig. 13 Changes in the transcripts of cell wall precursors and cell wall protein-related pathways between the lower and upper half flanks at 6 h after gravistimulation. MapMan output was used to illustrate the significant transcriptional changes across the cell wall tissue precursors and cell wall proteins at 6 h after reorientation. The reported values are log transformed ratios of transcripts in the lower flank to the upper flank. Each transcript is indicated as being up-regulated (red square; increase in the ratio of the lower to upper transcript values) or down-regulated (blue square; decrease in ratio of the lower to upper transcript values). Squares arranged in rows and columns represent individual transcripts at a single time point in the process. The individual square in a given area has the same color as the guide bar in the same column. A filled circle indicates that no transcript was detected in the process. Significantly changed transcripts in each process are marked with a series of numbers (Reprinted from Hu et al. 2013.)

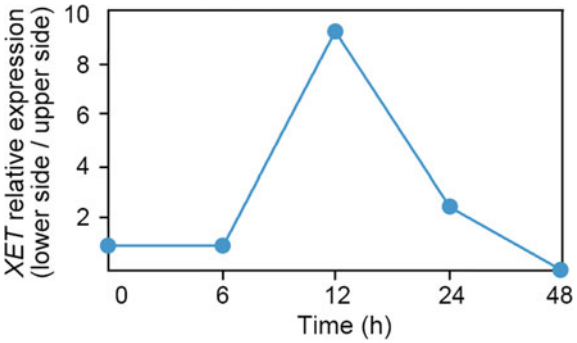

Fig. 14 The effect of gravistimulation on *XET* expression in rice shoot bases. RNA was extracted from the shoot base flanks at 0, 6, 12, 24, or 48 h after gravistimulation. RT-PCR was used to analyze *XET* expression in the lower and upper shoot base flanks (Reprinted from Cui et al. 2005.)

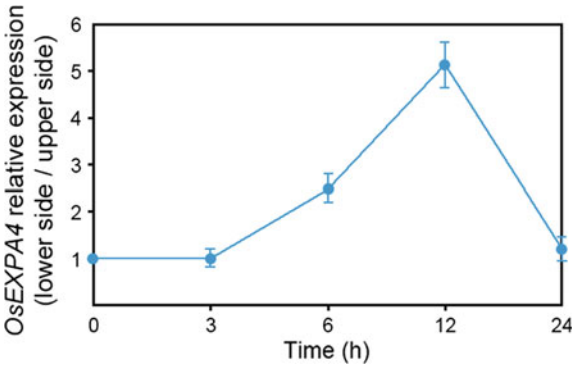

Fig. 15 Gravistimulation induces asymmetric *OsEXPA4* expression in rice shoot bases. RNA was extracted from leaf sheath halves at 0, 3, 6, 12 or 24 h after gravistimulation, and RT–PCR was used to analyze *OsEXPA4* expression in the lower and upper shoot base flanks. Relative quantification data represent the mean values (±SDs) of three replicates (Reprinted from Hu et al. 2007, copyright 2007, with permission from Physiologia Plantarum.)

intracellular turgor pressure. It is necessary to make the cell wall more flexible to enhance the metabolism of the primary wall (Cui et al. 2005; Hu et al. 2007; Hu et al. 2013) and to increase the transport of water into the intracellular vacuoles at the same time. This equilibrium process in the elongation zone on both sides of the cell causes gravitropic bending.

It was also observed that the osmotic potential in the cells on both sides of the rice shoot base were also asymmetric (Fig. 18) (Hu et al. 2007). This asymmetry of osmotic potential is maintained by glucose metabolism and other cellular processes (Hu et al. 2007; Hu et al. 2009).

The capacity of water transport among different aquaporins is different. Water channel activity of AQP, PgTIP1, OsPIP2;7, OsPIP2;3, OsTIP3;2, OsTIP;2,

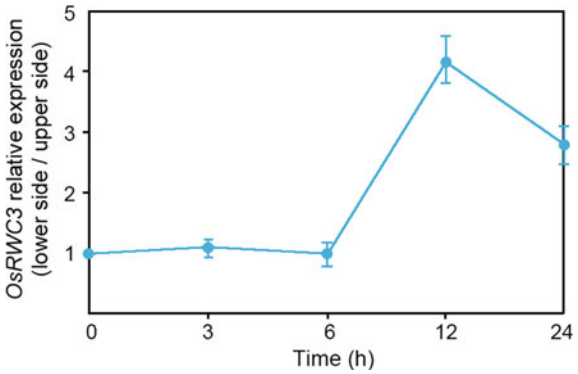

Fig. 16 *OsRWC3* expression in the upper and lower flanks of transgenic rice shoot bases during gravitropic bending. After gravistimulation, the bending segments of rice shoot bases were removed and bisected with a razor blade into the upper and lower flanks. RNA was extracted from shoot base flanks at 0, 3, 6, 12 or 24 h after gravistimulation and used to analyze *OsRWC3* expression in the upper and lower shoot base flanks. Relative quantification data represent the mean values (±SDs) of three replicates (Reprinted from Hu et al. 2009.)

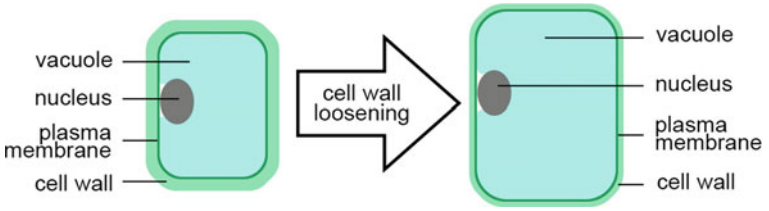

Fig. 17 The relationship between the cell wall, the vacuole and the growth of a plant cell during gravitropism

Fig. 18 The osmotic potential of rice shoot bases during gravistimulation. Values are the means ±SDs from three replicates with at least five seedlings per replicate (Reprinted from Hu et al. 2007.)

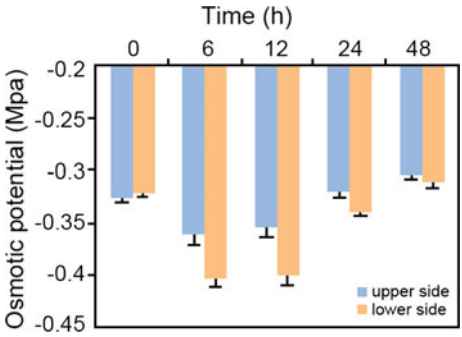

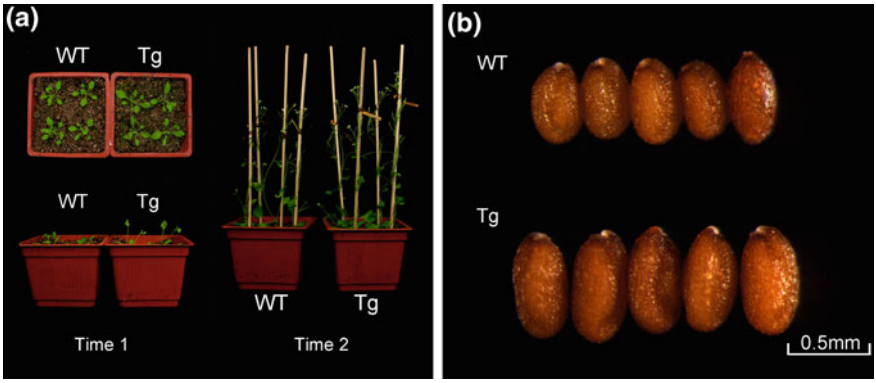

Fig. 19 Phenotypic and molecular characterization of *PgTIP1* over-expressing *Arabidopsis* plants. **a** Wild type and transgenic Arabidopsis thaliana at time 1 and time 2. Time 1 is the bolting time and time 2 is 10 days after time 1. **b** Mature dried seeds from wild type and transgenic Arabidopsis plants. (Bar = 0.5 mm) (Reprinted from Chen et al. 2010.)

OsTIP1;2 and OsTIP1;1 were compared. The results showed that the activity of PgTIP1 was not only higher than that of three OsTIPs, but also higher than that of two OsPIPs (Li 2008). When an aquaporin with higher water permeability was introduced into plant cells, some cells in the transgenic plant were enlarged (Fig. 19) (Chen et al. 2010; Lin et al. 2007). These observations support the hypothesis that the balance between cell wall rigidity and turgor pressure determine the degree of plant cell growth.

2.11 The Effect of Microgravity on Plant Cells

Research using rice cell culture (grown on N6 medium containing 2 mg/L 2,4-D and hormone free N6 medium) was carried out on board the Chinese spacecraft "Shenzhou 8" (Jin et al. 2014). Rice cells were cultured for approximately 324 h and then fixated in space under microgravity conditions. Microarray analysis was carried out on samples that returned to Earth. The data revealed that there was a significant effect of microgravity on rice cells at the transcriptional level (Fig. 20) (Jin et al. 2015), and only the results in cell wall changes are discussed here.

From the calli grown on N6 medium containing 2,4-D under microgravity, we identified 8 transcripts related to cell wall formation (Table 5) (Jin et al. 2018). Among these 8 transcripts, 3 of the down-regulated transcripts corresponded to endoglucanases (LOC Os01g21070, LOC Os04g57860) related to cell wall degradation and the pectinesterase-1 precursor (LOC Os01g57854). Two endoglucanases (LOC Os01g21070, LOC Os04g57860) were down-regulated under F-μg versus both G-1 g and F-1 g. Five of the up-regulated transcripts corresponded to proteins involved in primary cell wall modification (xyloglucan endotransglucosy-

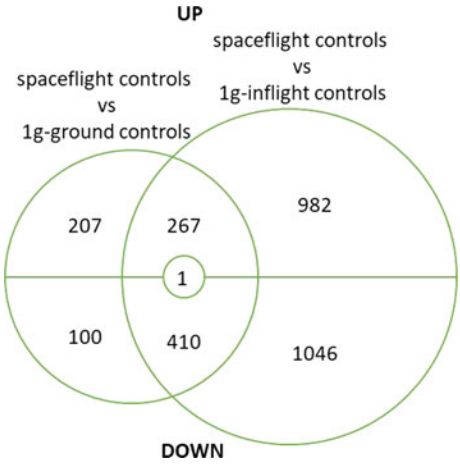

Fig. 20 The overlap of the differentially expressed probe sets (up- and down-regulated) under spaceflight controls, 1g-inflight controls and 1g-ground controls in rice calli experiments (calli grown on hormone free N6 medium) in the SIMBOX on "Shenzhou 8" (Reprinted from Jin et al. 2015, copyright 2015, with permission from Microgravity—Science and Technology.)

lase/hydrolase protein 23 (OsXTH23, LOC Os06g48200), beta-expansin 1a precursor (LOC Os03g01270)), cell wall degradation (polygalacturonase (PG) (LOC Os08g44020)), the cell wall structure (fasciclin-like arabinogalactan protein 8 (FLA8), LOC Os01g62380) and hemicellulose synthesis through glycosyltransferases (LOC Os03g48610). The changed levels of these cell wall loosening and cell wall precursor synthesis-related genes under F-μg may contribute to microgravity by affecting cell wall relaxation and extension.

The experimental results show that exogenous 2,4-D in the culture influenced the effects of the spaceflight experiments on the rice calli. The results indicated that for many aspects, e.g., most of the MR genes related to glycolysis and most of the MR transcript factors (TFs), the reaction trend induced under microgravity in these two types of rice calli was indeed different, and opposite trends were observed in some cases. However, the effect of microgravity on the cell wall were consistent in both callus types (Jin et al. 2015). The trends in the changes of cell wall metabolism were similar across groups of rice calli cultured without 2,4-D under microgravity (Jin et al. 2015). In rice calli cultured without 2,4-D under microgravity conditions, nine transcripts related to cell wall metabolism and modification were found. Two of the transcripts were down-regulated, and they were involved in secondary wall metabolism (cellulose synthase: LOC Os02g49332, LOC Os04g35020). Seven transcripts were up-regulated, and they were proteins associated with cell wall loosening (lipoprotein A-like double-psi beta-barrel-containing, LOC Os04g44780), proteins related to the modification of the primary cell wall (xyloglucan endotransglycosylase LOC Os06g48200, α expansin precursor protein 20 LOC Os06g41700), and proteins involved in the cell structure (AGPs, LOC Os08g38270, LOC Os08g23180, LOC

Table 5 Differentially expressed transcripts of cell wall genes in calli grown on N6 medium containing 2,4-D under microgravity (Reprinted from Jin et al. 2018, copyright 2018, with permission from Microgravity—Science and Technology.)

Probe set ID	Locus name	Annotation	Fold change	
			F-μg versus G-1g	F-μg versus F-1g
osaffx.13411.1.s1 at	LOC Os03g48610	Protein transferase, transferring glycosyl groups	2.877	2.454
os.42475.1.s2 at	LOC Os01g62380	Fasciclin-like arabinogalactan protein 8 precursor	2.449	3.860
os.28032.1.a1 at	LOC Os01g21070	Endoglucanase 1 precursor	0.281	0.165
os.50125.1.s1 at	LOC Os04g57860	Endoglucanase precursor	0.087	0.373
os.50320.1.s1 at	LOC Os08g44020	Protein lyase	2.858	4.093
os.22839.1.s2 at	LOC Os06g48200	Xyloglucan endotransgluco-sylase/hydrolase protein 23 precursor	2.296	2.146
os.9312.1.s1 at	LOC Os03g01270	Beta-expansin 1a precursor	3.041	2.070
os.27505.1.s1 at	LOC Os01g57854	Pectinesterase-1 precursor	0.054	0.248

Os06g30920, LRR, LOC Os06g49100). Cell wall loosening and greater cell elongation in rice coleoptiles under microgravity were also reported by Hoson et al. (2002a, b, 2004, 2014). The size of the callus cultures was also enhanced under microgravity compared to the 1-g controls (Fengler et al. 2015).

The results obtained from previous spaceflight experiments in which research was conducted on the transcriptome of *Arabidopsis* are inconsistent across many aspects due to the differences in experimental design and the diverse hardware used (Fengler et al. 2015; Johnson et al. 2017). In particular, analysis of individual plant organs or entire seedlings indicated organ-specific changes in response to spaceflight (Paul et al. 2012). However, cell wall remodelling and stress response results were similar in three BRIC-16 experiments (Johnson et al. 2017). Rice calli cultured with 2,4-D and hormone-free cultures represented two types of tissue with different physiological states. A transcriptome study showed that there are many differences between habituated cells and their original state (Pischke et al. 2006). The fact that cells behave differently under microgravity could be due to the following two reasons:

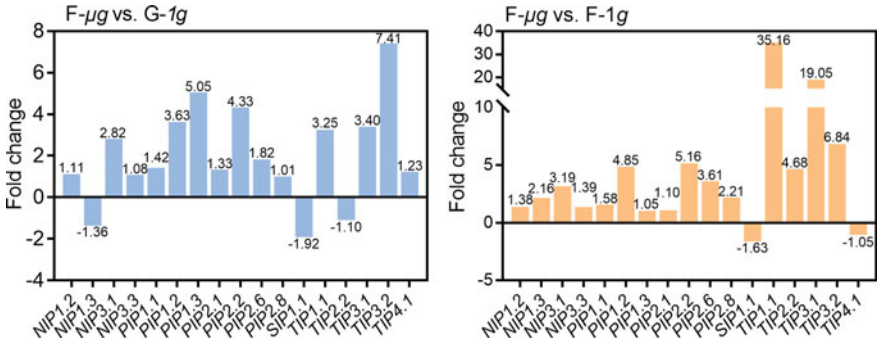

Fig. 21 Differentially expressed transcripts of OsPIPs, OsTIPs and OsNIPs in rice calli under F-μg versus both G-1g and F-1g (Reprinted from Jin et al. 2018, copyright 2018, with permission from Microgravity—Science and Technology.)

the presence of 2,4-D may affect plant cell responses to microgravity stimulation, and habituated cells with a different physiological status may also respond differently to microgravity. We present the integrated results of these two types of callus under microgravity treatment and also emphasize and discuss the consistency of the results of the effects of microgravity on the metabolism and modification of the cell wall of rice calli. The results of cell wall loosening and higher cell elongation in rice coleoptiles in microgravity were also reported by Hoson et al. (2002a, b, 2004, 2014).

With the international space station running, the study of microgravity effects on plant growth and morphogenesis has become more in-depth, and the effects of microgravity are becoming more specified. As plant stem and root elongation is promoted and lateral extension is inhibited, an auto morphogenesis phenomenon appeared. The emergence of these changes is related to the effects of microgravity on the cell wall (Hoson et al. 2014).

According to the results of the analysis from gene chip data (http://www.ebi.ac.uk/arrayexpress, E-MTAB-2518, http://www.ncbi.nlm.nih.gov/geo, GSE78839) obtained by the space flight experiment (Fengler et al. 2015; Jin et al. 2015), gene expression levels of plasma membrane aquaporins (PIPs) and tonoplast aquaporins TIPs in *Arabidopsis* and rice cells grown under microgravity conditions were generally up-regulated.

Gravity causes changes in the expression of water channel genes during plant gravitropism (Hu et al. 2007). We analysed the transcripts of OsPIPs, OsTIPs and OsNIPs, i.e., genes of the aquaporin gene family (Fig. 21), most of which were up-regulated under F-μg versus both G-1g and F-1g (the fold change was greater than or equal to 2). The false discovery rate (*p)* of changes in the expression of three genes, *PIP1.3* (LOC Os02g57720), *TIP3.2* (LOC Os04g44570) and *NIP3.1* (LOC Os10g36924), under F-μg versus both G-1g and F-1g was lower than 0.05. (Jin et al. 2018). Therefore, in the case of microgravity, there was a new balance between cell wall rigidity and cell turgor pressure.

The involvement of cortical microtubules in growth stimulation in space was demonstrated (Hoson et al. 2004). The cortical microtubules lead to cell wall changes probably through signal transduction and transduction processes in plant gravity resistance (Hoson et al. 2014). All of these factors together create the effects of microgravity on cell growth.

3 Conclusion

The growth of terrestrial plants that evolved from the sea is guided by gravity presented in a constant direction and magnitude on Earth. Plants developed a set of mechanisms of gravity resistance during evolution, and plants lost the stable and reliable signal of gravity in microgravity conditions when they were brought to orbital flight in space. Plants lose gravity's guide to growth and do not need to fight against gravity to survive under microgravity environment. As a result, it not only loses the gravitropism, but also leads to the weakening of the supporting tissue system in the body. This adaptation is reflected in the epigenetic, transcriptome, metabolism, morphological structure and other levels. As discussed earlier in this article, the loosening of the cell wall may be regarded as the adaptation of plants in microgravity due to the disuse of the support system. Numerous genes related to cell wall biosynthesis, such as the gene encoding the cellulose synthase catalytic subunit, callose synthase genes and cell wall expansion-related genes such as xyloglucan endotransglucosylase, beta-galactosidase and beta-glucosidase, displayed altered methylation levels under microgravity. The breaking of the balance of mechanical forces within the cell, could be explained by the effects of microgravity on plant cell wall extensibility, aquaporin gene expression, and the new balance between cell wall rigidity and cell turgor pressure will be established under microgravity conditions. The balance of mechanical forces inside the cells was broken and reconstructed under microgravity, which resulted in the changes of cell growth and organ growth, and then affected the growth and development of plants.

Acknowledgements We thank Drs. Hu Xiangyang, Cui Dayong, Lin Wuling, Hu Liwei, Mei Zhiling and Shan Chi for their work in our laboratory that contributed to this review. This work was supported by the Strategic Priority Research Program of the Chinese Academy of Sciences (Grant Nos. XDA04020202-15 and XDA04020415), the National Natural Science Foundation of China (Grant Nos. U1738107, 31570859, 31500236 and 31600684) and the China Manned Space Flight Technology Project. The projects were coordinated by Institute of Mechanics (Chinese Academy of Sciences), National Space Science Center (Chinese Academy of Sciences) and The Technology and Engineering Center for Space Utilization (Chinese Academy of Sciences). Shanghai Institute of Technical Physics (Chinese Academy of Sciences) provided spaceflight equipment.

References

Adamowski M, Friml J (2015) PIN-dependent auxin transport: action, regulation, and evolution. Plant Cell 27:20–32

Band LR, Wells DM, Fozard JA et al (2014) Systems analysis of auxin transport in the *Arabidopsis* root apex. Plant Cell 26:862–875

Belyavskaya NA (1992) The function of calcium in plant graviperception. Adv Space Res 12:83–91

Bourgeade P, Boyer N (1994) Plasma-membrane H+-Atpase activity in response to mechanical stimulation of *Bryonia-Dioica* internodes. Plant Physiol Biochem 32:661–668

Briarty LG, Maher EP (2004) Reserve utilization in seeds of *Arabidopsis thaliana* germinating in microgravity. Int J Plant Sci 165:545–551

Cai WM, Braun M, Sievers A (1997) Displacement of statoliths in *Chara* rhizoids during horizontal rotation on clinostats. Shi yan sheng wu xue bao 30:147–155

Cai WM, Jin J, Chen HY (2016) Effects of gravity on growth of plant cells. Chin J Space Sci 36(4):552–556

Caspar T, Pickard BG (1989) Gravitropism in a starchless mutant of *Arabidopsis*—implications for the starch-statolith theory of gravity sensing. Planta 177:185–197

Chen R, Hilson P, Sedbrook J et al (1998) The *Arabidopsis thaliana AGRAVITROPIC 1* gene encodes a component of the polar-auxin-transport efflux carrier. Proc Natl Acad Sci USA 95:15112–15117

Chen HY, Ying L, Jin J et al (2010) Determining the transcriptional regulation pattern of *PgTIP1* in transgenic Arabidopsis thaliana by constructing gene. Adv Biosci Biotechnol 1:384–390

Correll MJ, Pyle TP, Millar KD et al (2013) Transcriptome analyses of *Arabidopsis thaliana* seedlings grown in space: implications for gravity-responsive genes. Planta 238:519–533

Cui DY, Neill SJ, Tang ZC et al (2005) Gibberellin-regulated XET is differentially induced by auxin in rice leaf sheath bases during gravitropic bending. J Exp Bot 56:1327–1334

Dharmasiri N, Dharmasiri S, Estelle M (2005) The F-box protein TIR1 is an auxin receptor. Nature 435:441–445

Dowen RH, Pelizzola M, Schmitz RJ et al (2012) Widespread dynamic DNA methylation in response to biotic stress. Proc Natl Acad Sci USA 109:E2183–2191

Fengler S, Spirer I, Neef M et al (2015) A whole-genome microarray study of *Arabidopsis thaliana* semisolid callus cultures exposed to microgravity and nonmicrogravity related spaceflight conditions for 5 days on board of Shenzhou 8. Biomed Res Int 2015:547495

Goh T, Kasahara H, Mimura T et al (2012) Multiple AUX/IAA-ARF modules regulate lateral root formation: the role of *Arabidopsis* SHY2/IAA3-mediated auxin signalling. Philos Trans R Soc B 367:1461–1468

Hager JW, Le Blanc JC (2003) High-performance liquid chromatography-tandem mass spectrometry with a new quadrupole/linear ion trap instrument. J Chromatogr A 1020:3–9

Hashida SN, Uchiyama T, Martin C et al (2006) The temperature-dependent change in methylation of the Antirrhinum transposon Tam3 is controlled by the activity of its transposase. Plant Cell 18:104–118

Hejnowicz Z, Sondag C, Alt W et al (1998) Temporal course of graviperception in intermittently stimulated cress roots. Plant Cell Environ 21:1293–1300

Hoson T (2014) Plant growth and morphogenesis under different gravity conditions: relevance to plant life in space. Life (Basel) 4:205–216

Hoson T, Soga K, Mori R et al (2002a) Stimulation of elongation growth and cell wall loosening in rice coleoptiles under microgravity conditions in space. Plant Cell Physiol 43:1067–1071

Hoson T, Soga K, Wakabayashi K et al (2002b) Growth and cell wall changes in rice roots under microgravity conditions in space. Uchu Seibutsu Kagaku 16:171–172

Hoson T, Soga K, Mori R et al (2004) Cell wall changes involved in the automorphic curvature of rice coleoptiles under microgravity conditions in space. J Plant Res 117:449–455

Hoson T, Soga K, Wakabayashi K et al (2014) Growth stimulation in inflorescences of an *Arabidopsis* tubulin mutant under microgravity conditions in space. Plant Biol (Stuttg) 16(Suppl 1):91–96

Hu X, Neill SJ, Tang Z et al (2005) Nitric oxide mediates gravitropic bending in soybean roots. Plant Physiol 137:663–670
Hu LW, Cui DY, Neill S et al (2007) OsEXPA4 and OsRWC3 are involved in asymmetric growth during gravitropic bending of rice leaf sheath bases. Physiol Plantarum 130:560–571
Hu LW, Cui DY, Zang AP et al (2009) Auxin-regulated OsRGP1 and OsSuS are involved in gravitropic bending of rice shoot bases. Fen Zi Xi Bao Sheng Wu Xue Bao 42:27–34
Hu LW, Mei ZL, Zang AP et al (2013) Microarray analyses and comparisons of upper or lower flanks of rice shoot base preceding gravitropic bending. PLoS ONE 8:e74646
Hu WR, Tang BC, Kang Q (2017) Progress of microgravity experimental satellite SJ-10. Aeron Aero Open Access J 1:125–127
Jin J, Chen HY, Cai WM (2014) Growth of rice cells in Shenzhou 8 under microgravity and transcriptome analysis. Manned Spacefl 5(20):481–490
Jin J, Chen HY, Cai WM (2015) Transcriptome analysis of *Oryza sativa* calli under microgravity. Microgravity Sci Technol 27:437–453
Jin J, Chen H, Cai W (2018) Transcriptomic analysis reveals the effects of microgravity on Rice calli on board the Chinese spaceship Shenzhou 8. Microgravity Sci Technol 4:1–10
Johnson CM, Subramanian A, Pattathil S et al (2017) Comparative transcriptomics indicate changes in cell wall organization and stress response in seedlings during spaceflight. Am J Bot 104:1219–1231
Joo JH, Bae YS, Lee JS (2001) Role of auxin-induced reactive oxygen species in root gravitropism. Plant Physiol 126:1055–1060
Kiss JZ, Sack FD (1989) Reduced gravitropic sensitivity in roots of a starch-deficient mutant of *Nicotiana sylvestris*. Planta 180:123–130
Kriegs B, Theisen R, Schnabl H (2006) Inositol 1,4,5-trisphosphate and Ran expression during simulated and real microgravity. Protoplasma 229:163–174
Li GW (2008) Study on the functions of rice aquaporins and their response to various abiotic stresses. Institute of plant physiology and ecology, SIBS, CAS, Shanghai
Lin W, Peng Y, Li G et al (2007) Isolation and functional characterization of PgTIP1, a hormone-autotrophic cells-specific tonoplast aquaporin in ginseng. J Exp Bot 58:947–956
Ljung K, Bhalerao RP, Sandberg G (2001) Sites and homeostatic control of auxin biosynthesis in *Arabidopsis* during vegetative growth. Plant J 28:465–474
Luschnig C, Gaxiola RA, Grisafi P et al (1998) EIR1, a root-specific protein involved in auxin transport, is required for gravitropism in *Arabidopsis thaliana*. Gene Dev 12:2175–2187
Marchant A, Kargul J, May ST et al (1999) AUX1 regulates root gravitropism in *Arabidopsis* by facilitating auxin uptake within root apical tissues. EMBO J 18:2066–2073
Martzivanou M, Hampp R (2003) Hyper-gravity effects on the *Arabidopsis* transcriptome. Physiol Plant 118:221–231
Paul AL, Ferl RJ (2015) Spaceflight exploration in plant gravitational biology. Methods Mol Biol 1309:285–305
Paul AL, Zupanska AK, Ostrow DT et al (2012) Spaceflight transcriptomes: unique responses to a novel environment. Astrobiology 12:40–56
Penterman J, Zilberman D, Huh JH et al (2007) DNA demethylation in the *Arabidopsis* genome. P Natl Acad Sci USA 104:6752–6757
Perbal G, Driss-Ecole D (2003) Mechanotransduction in gravisensing cells. Trends Plant Sci 8:498–504
Pischke MS, Huttlin EL, Hegeman AD et al (2006) A transcriptome-based characterization of habituation in plant tissue culture. Plant Physiol 140:1255–1278
Shan C, Mei ZL, Duan JL et al (2014) OsGA2ox5, a Gibberellin metabolism enzyme, Is involved in plant growth, the root gravity response and salt stress. PloS ONE 9
Sievers A (1991) Gravity sensing mechanisms in plant cells. ASGSB Bull 4:43–50
Strohm AK, Baldwin KL, Masson PH (2012) Multiple roles for membrane-associated protein trafficking and signaling in gravitropism. Front Plant Sci 3:274
Swarup R, Bennett M (2003) Auxin transport: the fountain of life in plants? Dev Cell 5:824–826

Thimann KV (1992) The cholodny-went "theory". Plant Mol Biol Report 10(2):103–104
Wang Y, Zhao H, Zhang Y et al (2016) Establishing and evaluation of the microgravity level in the SJ-10 recoverable satellite. Aerosp China 4:3–13
Xie Q, Guo HS, Dallman G et al (2002) SINAT5 promotes ubiquitin-related degradation of NAC1 to attenuate auxin signals. Nature 419:167–170
Xing MQ, Zhang YJ, Zhou SR et al (2015) Global analysis reveals the crucial roles of DNA methylation during Rice seed development. Plant Physiol 168:1417–1432
Xu ZC, Zhang T, Zheng WB et al (2016) Design of plant incubator under microgravity environment. Chin J Space Sci 36:556–570
Xu PP, Chen HY, Jin J et al (2018) Single-base resolution methylome analysis shows epigenetic changes in *Arabidopsis* seedlings exposed to microgravity spaceflight conditions on board the SJ-10 recoverable satellite. Npj Microgravity 4:556–570
Yamaguchi N, Komeda Y (2013) The role of CORYMBOSA1/BIG and auxin in the growth of *Arabidopsis* pedicel and internode. Plant Sci 209:64–74
Yamazaki C, Fujii N, Miyazawa Y et al (2016) The gravity-induced re-localization of auxin efflux carrier CsPIN1 in cucumber seedlings: spaceflight experiments for immunohistochemical microscopy. Npj Microgravity 2:16030
Zhao C, Avci U, Grant EH et al (2008) XND1, a member of the NAC domain family in *Arabidopsis thaliana*, negatively regulates lignocellulose synthesis and programmed cell death in xylem. Plant J 53:425–436

Cell Growth and Differentiation Under Microgravity

Shujin Sun, Chengzhi Wang, Ning Li, Dongyuan Lü, Qin Chen and Mian Long

Abstract The mechano-biological coupling mechanism of cell response to altered gravity is crucial to understand physiological changes of astronauts in space microgravity environment and to develop relevant countermeasures. To address this issue, a novel space cell culture hardware mainly consisting of precisely controlled flow chamber and gas exchange unit is developed as an experimental payload in SJ-10 recoverable microgravity experimental satellite. Endothelial cells (ECs) and mesenchymal stem cells (MSCs) are cultured in the hardware during the SJ-10 mission, and recovered samples are analysed elaboratively. The results indicate that microgravity can suppress cellular metabolism. MSCs cultured with hepatic inducing medium are preferential in hepatic differentiation at long-term duration under microgravity. Both ECs and MSCs are regulated by microgravity and respond differentially in initiating cytoskeletal remodeling, or dysregulating signaling pathways relevant to cell adhesion, or directing hepatic differentiation.

Abbreviations

ALB	Albumin
ANOVA	Analysis of variance
CCD	Charge-coupled device
CCL5	C-C motif chemokine ligand 5
CYP450	Cytochrome P450
ECM	Extracellular matrix
ECs	Endothelial cells
eNOS	Endothelial nitric oxide synthase
F-actin	Actin filaments

S. Sun · C. Wang · N. Li · D. Lü · Q. Chen · M. Long (✉)
Key Laboratory of Microgravity (National Microgravity Laboratory), Center for Biomechanics and Bioengineering and Beijing Key Laboratory of Engineered Construction and Mechanobiology, Institute of Mechanics, Chinese Academy of Sciences, Beijing, China
e-mail: mlong@imech.ac.cn

E. Duan and M. Long (eds.), *Life Science in Space: Experiments on Board the SJ-10 Recoverable Satellite*, Research for Development,
https://doi.org/10.1007/978-981-13-6325-2_7

HUVEC	Human umbilical vein endothelial cells
ICAM-1	Intercellular adhesion molecule-1
IF	Immunofluorescence
IGFBP-2	Insulin-like growth factor binding protein 2
IL-1 R4	Interleukin 1 receptor 4
IL-8	Interleukin 8
mAbs	Monoclonal antibodies
MCP-1	Monocyte chemotactic protein 1
PDGF-AA	Platelet-derived growth factor AA
p-FAK	Phospho-focal adhesion kinase
PI3K	Phosphoinositide 3-kinase
rBMSCs	Rat bone marrow mesenchymal stem cells
SCCS	Space cell culture system
VCAM-1	Vascular cell adhesion molecule-1

1 Introduction

Physiological adaptation of astronauts to the microgravity environment is complicated, requiring an integrative perspective to fully understand the mechanisms involved. Responses of mammalian cells to gravity alteration remains fundamental to the issue, which also helps to elucidate the role that the gravity has played in the evolution of life on our planet. To date, it is still unclear if a single mammal cell could sense the gravity change or not, if the cell sensation is direct or indirect, how the gravity signals are transmitted or transduced into the cells, and what the underlying mechanisms are in regulating cell-cell or cell-surface interactions under microgravity (Bizzarri et al. 2014, 2015). The reasoning lies in the two aspects, at least. On one hand, the scarcity of flight opportunities in space makes it difficult to unravel these mechanisms under real microgravity condition. On the other hand, the experimental techniques in space cell biology are not well developed and standardized as those in laboratory on ground to collect the repeatable, reliable data. Thus, in the project of SJ-10 satellite (Hu et al. 2014; Li et al. 2018; Lü et al. 2019) we focus on both the scientific issues and technology upgrading to take full advantage of the limited and expensive space missions.

Various types of space cell culture devices have been developed since Russian scientists performed space cell biology experiments in 1960s (Krikorian 1996; Buravkova 2010; Freed and Vunjak-Novakovic 2002; Vandendriesche et al. 2004; Sun et al. 2008; Harada-Sukeno et al. 2009; Bizzarri et al. 2014, 2015; Kim et al. 2015). Those earlier space experiments have reported the inconsistent or even conflicting data mainly due to the technical difficulties in controlling cell culture conditions (Buravkova 2010; Bizzarri et al. 2015). Although the use of specialized devices with environmental control has improved the mission success rate of space cell growth, the absence of adequate analytical procedures for cell biology cannot ensure

the quality of data collected in spacecraft. Before the spacecraft possesses the capacity to do the on-site analyses for various behaviors of cellular responses in space, most of biological samples have to be analyzed off-line after recovering to laboratories on ground. At the current stage, the techniques of on-orbit environmental control for cell culture and sample preservation outweigh other considerations.

Technically, mammal cell growth in space requires the well-controlled nutrient supply, mass transport, and mechanical stimulation, as well as the defined temperature and pH value, since the disappearance of buoyant convection and sedimentation in space remarkably alters the processes of nutrient supply and mass transport as compared to those in conventional laboratories on ground. Thus, space cell biology experiments call for the specialized hardware to quantify the consistency between the two data sets from space mission and ground control, especially on the basis of very limited space mission opportunities. This work attempts to develop a novel space cell culture hardware mainly consisting of precisely controlled flow chamber and gas exchange unit and to investigate the cell growth and stem cell differentiation under microgravity. The specific aims are to collect the data on the metabolism, proliferation, apoptosis, differentiation, and cytoskeletal remodeling of human endothelial cells and rat bone mesenchymal stem cells. These new techniques and the related biological data are expected to reveal the effects of gravity on cell-cell interactions, to elucidate the underlying mechanisms of cell growth and differentiation in space, and to overcome the methodological bottlenecks of space cell biology research.

2 Scientific Issues

Cells may sense gravity change through different mechanisms. It is hypothesized that the cells possess the specialized structures or elements for gravity perception (*direct mechanism*) or are affected by the change in physical features of gravity-dependent microenvironment (*indirect mechanism*), or both mechanisms work cooperatively (Bizzarri et al. 2014, 2015). To address the issue, it is required to accumulate the ample data for characterizing the effects of nutrient supply, mass transport, and mechanical environment on the cells under microgravity. These types of data are very sparse and diverse at present, leading to the difficulty for comparing the data out of various labs.

Physiologically, the long-term exposure of astronauts to space condition induces typical alterations in bone loss, muscle atrophy, cardiovascular deconditioning, impairment of pulmonary function, and immune response (Bizzarri et al. 2014, 2015). Meanwhile, embryonic development and histogenesis could also be regulated by microgravity. At cellular level, their responses, as the basic element of life, are vital in space life sciences as well as space physiology and medicine. Thus, it is crucial to elucidate the mechano-biological coupling of the cells about how altered gravity regulates their biological responses. To do so, those cell types sensitive to mechanical stimulation are preferentially considered.

Endothelial cells (ECs) lining the inner surface of blood vessels play a critical role in maintaining vascular integrity, tissue homeostasis, and regulating local blood flow and other physiological processes. ECs are sensitive to mechanical forces including shear stress, tensile stretch, and mechanical compression (Byfield et al. 2009; Chancellor et al. 2010; Wang et al. 2014) as well as hypergravity and microgravity (Maier et al. 2015). For example, the altered EC morphology, cell membrane permeability and senescence are first documented by spaceflight experiments on cultured endothelium (Maier et al. 2015). Unfortunately, it is still unclear how the cells grow, line up, and vascularize in space. Here a human umbilical vein cell line, EA.hy926, is applied to investigate cell growth under microgravity.

Bone marrow mesenchymal stem cells (BMSCs), as a typical type of somatic stem cells, can differentiate into osteoblasts, chondrocytes, and adipocytes (Li et al. 2013). In the past decades, BMSCs have attracted much attention as a well-defined model in elucidating bone loss mechanism under microgravity and as a potential candidate in resisting bone loss since bone is a constantly renewed organ involving the interplay of various bone cells (Burger and Klein-Nulend 1998; Ulbrich et al. 2014). In fact, BMSCs possess wide plasticity to transdifferentiate into the cells of other germlayer. For instance, hepatocytes are derived from the endoderm, and the liver is an organ not bearing body weight specifically and not stimulated by mechanical forces frequently (Ayatollahi et al. 2010). It is unclear if the BMSC transdifferentiation to hepatocytes is also influenced by microgravity. Here the effects of microgravity on hepatocyte differentiation of rat BMSCs are investigated and the outcomes are significant for understanding the mechanism of stem cell responses to gravity change.

3 Hardware Development

The space experiment presented here is defined as one of ten life science payloads in SJ-10 recoverable satellite launched on 6th April and recovered on 18th April, 2016. The following supporting resource conditions are distributed from the satellite hub to this hardware: 365 × 285 × 250 mm in maximum geometry size, 17 W in average power, cabin vacuum environment, and heat conduction from installation plane with water circulation.

A space cell culture system (SCCS) is developed in-house upon the above supporting resources. All experimental modules are designed to be enclosed in an air-sealed box within an atmospheric pressure sensor used to monitor air leakage. To provide the basic conditions for mammal cell culture and the specific support for microgravity effect test, the SCCS system is composed of six modules of cell culture, liquid supply, temperature control, environmental monitoring, micro-image capture, and electrical control (Fig. 1).

The cell culture module (Fig. 2) is the core unit of the system. Six culture chambers are lined in parallel and connected with silicone tubes. For a single chamber, a cell culture plastic slide (Permanox® slide, 25 × 75 cm, Nunc) is used and sealed by a silicone gasket with an effective culture area of 12 cm^2 and the inner height of 1 mm

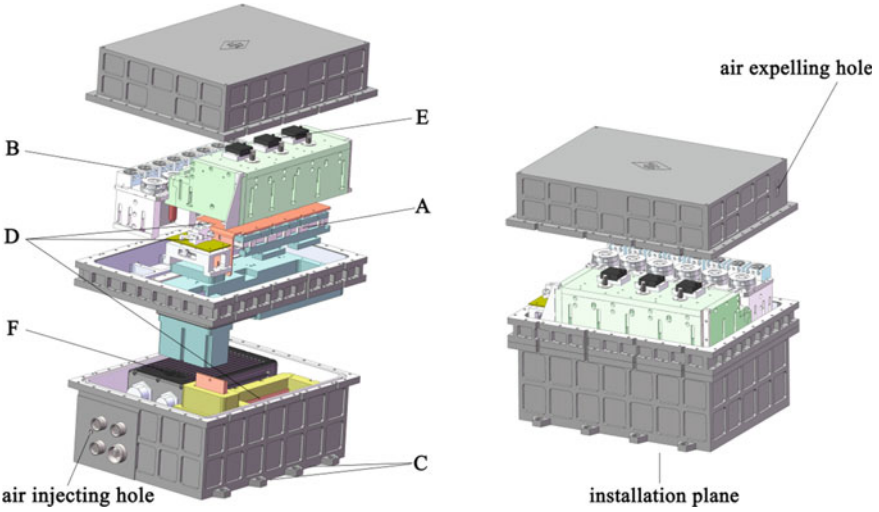

Fig. 1 Overview of the hardware mounted on SJ-10 satellite from the exploded (*left*) and assembled (*right*) view before the box is closed. It consists of six modules of cell culture (*A*), liquid supply (*B*), temperature control (*C*), environmental monitoring (*D*), micro-image capture (*E*), and electrical control (*F*)

(thereupon the medium volume of ~1.2 ml). The inlet of each chamber is coupled with a de-bubble unit that is specially designed to trap small bubbles in the liquid circuit (Sun et al. 2019). The silicone tube between the pump and chamber inlet is used as a gas exchanger for O_2 and CO_2 exchange in medium (Sun et al. 2019).

The liquid supply module (Fig. 2) is composed of a set of micro-peristaltic pumps and multi-channel pinch valves. The pumps and valves work upon manufacturers' instruction and in house-reprogramed codes. The module functions in supplying fresh medium, collecting culture supernatant, and fixing grown cells. To provide sufficient nutrient supply and mass transport and, meantime, avoid interference of flow shear when the medium flows through the chamber, the flow rate is estimated on the geometry of the chamber and the rate of cell glucose and oxygen consumption. Here we applied a flow rate of 0.3 ml/min and a wall shear stress of 1.05×10^{-3} Pa, which meets the nutrient demand of the cells but does not impair significantly the cell growth and behaviors.

The temperature control module (Fig. 2) governs two separated zones, *that is*, the culture zone that encloses all chambers and maintains the temperature at 36 ± 1 °C, and the medium storage zone that keeps the temperature at 4–10 °C. Semiconductor chilling plates fixed on the bottom of the box are used to manipulate the respective temperatures, in which the heating side faces to the former and the cooling side faces to the latter. Heat flux is conducted to the satellite platform through the installation plane wherein a circulating water cooling system is furnished (*cf.* Fig. 1). It takes about 2 h to reach from room temperature (20–25 °C) to the ones required.

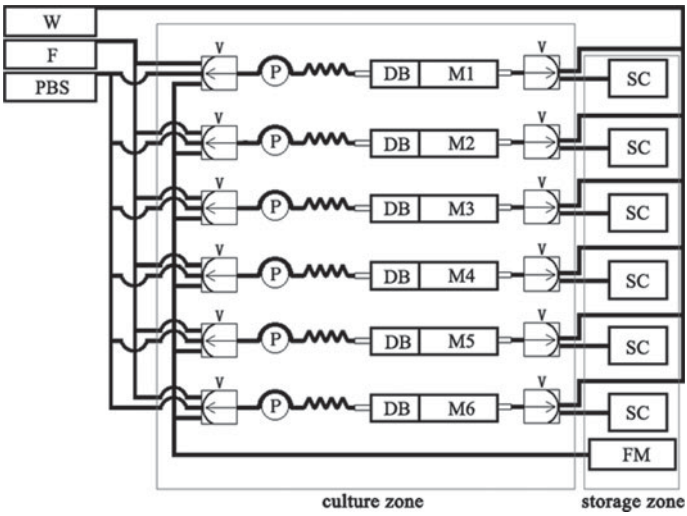

Fig. 2 Schematic of flow network of the SCCS. *M1–M6*, chambers of cell culture module; *DB*, de-bubble unit; *P*, micro-peristaltic pump; *V*, multi-channel pinch valve; *SC*, culture supernatant collection bag; *FM*, fresh medium storage bag; *PBS*, phosphate-buffered saline; *F*, fixing agent; *W*, waste collection bag. The *wave line* denotes the gas exchanger

The environmental monitoring module (Fig. 2) includes an atmospheric pressure sensor, two photoelectric pH sensors, and nine temperature sensors. The pressure sensor records pressure data within the box for judging if the vacuum seal fails. The pH sensors monitor the pH values of medium supplied for the cells. The temperature sensors monitor the temperatures of nine preset points in the box, in which three are set at the culture zone, two are placed at the medium storage zone, and the other four are located next to those pumps and valves of liquid supply module and to the chilling plates.

The micro-image capture module (Fig. 2) consists of three sets of CCD camera and microscopic lens, which are fixed on the top and bottom at three specific culture chambers, together with optical alignment. The images of cellular morphology in three chambers are captured automatically every 3 h using the image grabbing card integrated into the electrical control module.

The electrical control module (Fig. 2) is designed and constructed for implementing entire experimental procedure and operating all actuators with programmed software. It is also responsible for data transfer between the experimental device and the SJ-10 payload data manager center.

All the modules are assembled together into the box and the resulted hardware has been tested systematically to assure its reliability and robustness. These tests includes stress screening, vibration, impact, acceleration, thermal cycling, thermal vacuum, aging, reliability life, pressure leak, biocompatibility, comprehensive performance matching, and electromagnetic compatibility.

4 Materials and Methods

4.1 Cell-Culture Procedure

Human endothelial cell line EA.hy926 obtained from China Infrastructure of Cell Line Resource (Beijing, China) is cultured in Endothelial Cell Medium (Sciencell Research Laboratories, Carlsbad, CA) and incubated at 37 °C in a humidified incubator supplemented with supplemented with 5% carbon dioxide (CO_2).

Rat BMSCs or rBMSCs are isolated from 3- to 4-week-old male SpragueeDawley (SD) rats (Vital River Laboratory Animal Technology Company, Beijing, China). Briefly, the animal is sacrificed by cervical dislocation and the femur and tibia are collected. The bone marrow is flushed out, and the collected cell suspension is added into the MSC culture medium composed of DMEM/F12 medium (Gibco, USA) supplemented with 15% fetal bovine serum and 1% NEAA, 1% glutamine, 1% sodium pyruvate and 1% penicillin-streptomycin in a T-25 flask or 12-well plastic plate. Adherent cells are then maintained in a humidified, 95% air and 5% CO_2, 37 °C incubator by refreshing the medium every two or three days. When grown to 85–90% confluence, the cells are rinsed in Ca^{2+}- and Mg^{2+}-free PBS and then detached using 0.25% trypsin-EDTA for 1 min. This procedure is repeated three or four times to collect rBMSCs at ~90% purity. Collected rBMSCs are identified as described previously (Li et al. 2013).

Thirty hours prior to the launching, the two types of cells are detached using 0.25% trypsin-EDTA separately. Then the cell suspension is injected, respectively, into the chambers with 5×10^5 cells per chamber. Four chambers (M1–M4) are seeded with EA.hy926 cells, and two chambers (M5, M6) are seeded with rBMSCs. The chambers are placed incubator for 12 h to reach firm adhesion and then transferred into clean bench. The medium in the four chambers with EA.hy926 cells is removed and the individual chambers are re-filled with fresh medium to wash out the unattached cells and to eliminate air bubbles. The two chambers with rBMSCs undergo same washing procedure but replaced with hepatocyte induction medium, i.e., MSC culture medium supplemented with 20 ng/ml HGF and 10 ng/ml EGF.

After medium replacement and bubble elimination, the culture chambers are mounted in the culture zone of SCCS. Then the box is sealed and temperature control is initiated. Once these operations are completed, the air in the box is replaced by pre-mixed 95% air and 5% CO_2 through the air injecting and expelling holes embedded in the box wall (*cf.* Fig. 1).

4.2 Flight Mission Procedure

Eight hours before launching, the SCCS hardware is assembled onto the preset platform of the SJ-10 satellite and the temperature control module keeps running until taking off. At the moment the satellite enters orbit for half an hour, the programmed

procedure is initiated. This time point is defined as the starting time ($t = 0$) of space experiment in orbit. In brief, images of cultured cells are captured every 3 h. Cells in the chamber M1, M3 or M5 are fixed at $t = 72$ h (3 d) and meanwhile the supernatant in each chamber is collected individually and preserved in the medium storage zone. The medium in chambers M2, M4 and M6 is refreshed every 48 h and the supernatant in each chamber is also preserved as above. Cells in the chamber M2, M4 or M6 are fixed at $t = 240$ h (10 d), after which the temperature of culture zone is lowered to <20 °C till the satellite is recovered. Along the entire procedure in orbit, all captured images and environmental parameters are downloaded to the data acquisition system on ground and also backed up to an internal storage unit of the SJ-10 payload data manager center. These images and parameters are checked timely during the entire mission to make sure that the system works as designed. After running in orbit for 12 days, the satellite is recovered to the ground. All cell and medium samples are taken out and transported at 4–10 °C to the laboratory within 18 h.

The ground control experiments are performed four times independently following the same procedure by the same SCCS hardware in order to have identical preflight and postflight conditions.

4.2.1 Cell Metabolism Analysis

Once all samples are transported to the laboratory, the supernatants are stored at −70 °C immediately until test. Glucose consumption and L-lactate production are tested by commercially available glucose (Huaxingbio, Beijing, China) and L-lactate (BioAssay Systems, Hayward, CA) kits following the manufacturers' protocols, respectively.

4.2.2 Immunofluorescence (IF) Staining

Alexa Fluor® 594-conjugated rabbit anti-β-actin (13E5), Alexa Fluor® 555-conjugated rabbit anti-α-tubulin (11H10) and Alexa Fluor® 647-conjugated rabbit anti-vimentin (D21H3) monoclonal antibodies (mAbs) are purchased from Cell Signaling Technology (Danvers, MA). Alexa Fluor® 647-conjugated mouse anti-intercellular adhesion molecule-1 (ICAM-1, HCD54) mAbs are obtained from BioLegend (San Diego, CA). Alexa Fluor® 647-conjugated rabbit anti-vascular cell adhesion molecule-1 (VCAM-1, EPR5047) and anti-NF-κB p65 (clone E370), Alexa Fluor® 488-conjugated mouse anti-β1-integrin (12G10), phycoerythrin (PE)-conjugated mouse anti-CD44 (F10-44-2), mouse anti-Rac-1 (0.T.127), anti-phospho-focal adhesion kinase (p-FAK, Tyr397, M121) and anti-RhoA (1B12) mAbs, as well as mouse anti-Cdc42, rabbit anti-albumin (ALB) and anti-cytochrome P450 (CYP450) polyclonal antibodies (pAbs), DyLight® 594-conjugated donkey anti-rabbit and Alexa Fluor® 488-conjugated goat anti-rabbit and donkey anti-mouse secondary pAbs are all from Abcam (Cambridge, UK). For immunostaining, EA.hy926 or rBMSC cells are incubated successively in IF blocking buffer (1% BSA in DPBS),

primary Abs (10 μg/ml in blocking buffer) and secondary Abs (5 μg/ml in blocking buffer) for 1 h at 37 °C. The images of stained cells are collected using a confocal laser-scanning microscope (Zeiss LSM710, Germany) with a 63 × oil immersion objective.

5 Results and Discussions

Data hereinafter for space samples of EA.hy926 cells come from the culture chambers M1 and M4 and those for rBMSCs are derived from the chambers M5 and M6. Those samples from the chambers M2 and M3 are not included further analysis mainly due to incomplete cell fixation even though the related in-orbit images for cell growth are available.

5.1 Cell Metabolism

To test the possible energy metabolism deficiency caused by spaceflight, the glucose (Fig. 3a–b) and L-lactate (Fig. 3c–d) concentrations from the supernatants under different conditions are quantified. Here glucose concentration for the EA.hy926 cells and rBMSCs cultured for 3 days in space is increased additional 129% and 47%, respectively, compared with ground control (Fig. 3a–b). This is consistent with our previous findings in earlier space experiment where a distinct trophoblastic tumor cell line (JAR) yields slightly higher values in space on different flow condition (Long et al. 2009). By contrast, lactate production for the EA.hy926 cells and rBMSCs cultured for 3 days is respectively reduced to 16 and 0.4% in space compared to ground control (Fig. 3c–d). The significant differences of glucose and L-lactate metabolism are disappeared between EA.hy926 cells cultured for 10 days in space and on ground (Fig. 3a, c), while those for rBMSCs are reduced (Fig. 3b, d) possibly attributed to the slowed growth associated with long-term contact inhibition (Everding et al. 2000; Hung and Terman 2011). These first-hand results suggest that space microgravity can suppress energy metabolism with lower glucose consumption and lesser lactate production, which is in agreement with previous study (Chakraborty et al. 2018). Due to insufficient reduplicated space samples from these experiments with limited resources, it requires further replicated studies to reassure the hypothesis in the future.

5.2 Cell Morphology

The morphology of the two types of the cells exposed to microgravity is monitored and compared with those on ground. It is indicated that the shape of EA.hy926 cells

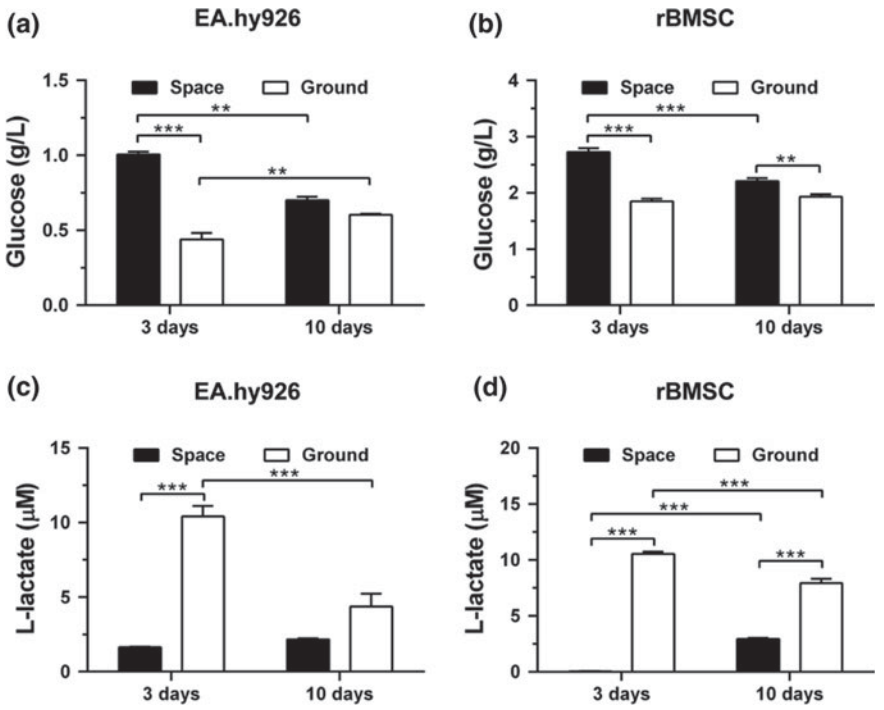

Fig. 3 Glucose (**a**–**b**) and L-lactate (**c**–**d**) concentrations of EA.hy926 cells (**a**, **c**) and rBMSCs (**b**, **d**) for 3 and 10 days cultured in space (*closed bars*) and on ground (*open bars*). Data are presented as the mean ± SEM of one experiment in space and 2–4 independent experiments on ground, both of which are performed in technical triplicate and analyzed with two-way ANOVA followed by Holm-Sidak test. *, $P < 0.05$; **, $P < 0.01$; ***, $P < 0.001$ (Reproduced from Li et al. 2018.)

cultured in space or on ground shows no significant difference. These endothelial cells present typical cobblestone shape at day 3 and are slighted elongated at day 10 (Fig. 4a–d). While the altered EC morphology is documented by previous spaceflight experiments on the cultured endothelium, it should also be noticed that those data is derived from human umbilical vein endothelial cells (HUVEC) cultured on microcarrier beads (Kapitonova et al. 2012, 2013). Regardless of different types of ECs used, other factors may also be involved in these differences between the observations here and those in the literatures, including the material and curvature of the carrier. We observe neither the grooved nor the tube-like structures formed by EA.hy926 cells on the entire culture substrate as those previous studies in microgravity effect simulation using clinostats (Grimm et al. 2009; Ma et al. 2014), showing that the ECs may respond differently to real space microgravity and clinostat culture.

On the other hand, the shape of rBMSCs cultured in space or on ground is also similar. In the hepatocyte induction medium, these mesenchymal stem cells present long and narrow shape at day 3 and are slighted elongated at day 10 (Fig. 4e–h). Intriguingly at day 10, the cells tend to form a visible plate-like structure (i.e., the hepato-

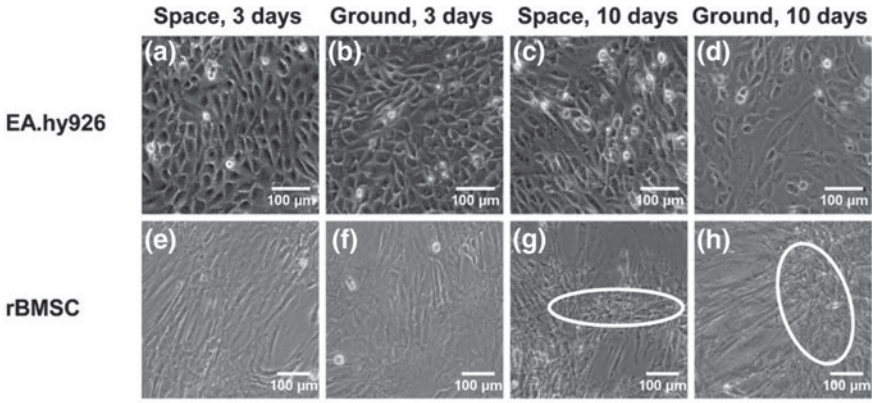

Fig. 4 Morphology of EA.hy926 cells and rBMSCs cultured in space or on ground. Presented are the optical images of EA.hy926 cells cultured for three (**a**–**b**) or ten (**c**–**d**) days in space (**a**, **c**) and ground (**b**, **d**) or rBMSCs cultured in hepatocyte induction medium for three (**e**–**f**) or ten (**g**–**h**) days in space (**e**, **g**) and ground (**f**, **h**), with a 10× objective. *Ellipses* indicate the plate-like structure for rBMSCs at day 10 (**g**–**h**)

cytes are arranged in a radial, plate-like pattern) in space than on ground (Fig. 4g–h), suggesting the possible effects of microgravity on directing the hepatocyte-like morphology from rBMSCs that has not been observed previously. Taken together, these results indicate that both EA.hy926 cells and rBMSCs grow normally under microgravity environment and no significant difference in cell morphology is observed using optical microscopy.

5.3 Cytoskeletal Remodeling

It is known that the cells in space usually undergo cytoskeletal remodeling (van Loon 2009; Long et al. 2015). Here we further test the observations by staining three key components, actin, tubulin and vimentin. Typical confocal analysis at day 3 indicates that the EA.hy926 cells cultured in space tend to disassemble their actin fibers and redistribute the disperse actin proteins at the periphery of the cells near the plasma membrane (Fig. 5a). By contrast, the actins are distributed over the entire cells on ground and no stress fibers are visible (Fig. 5b). The reorganization of actin including markedly reduced amount (Carlsson et al. 2003), depolymerization of actin filaments (F-actin) and clustering of the stress fibers at the cellular membrane (Infanger et al. 2007; Grenon et al. 2013) are known to be regulated by simulated microgravity effect on ground, but no direct evidences are reported for ECs under real space microgravity. Interestingly, HUVECs exposed to hypergravity of 3.5 × g for 96 h tend to accumulate actin fibers around the nucleus, but not at the periphery of the cells, although the total amount of actin proteins remains the same (Versari

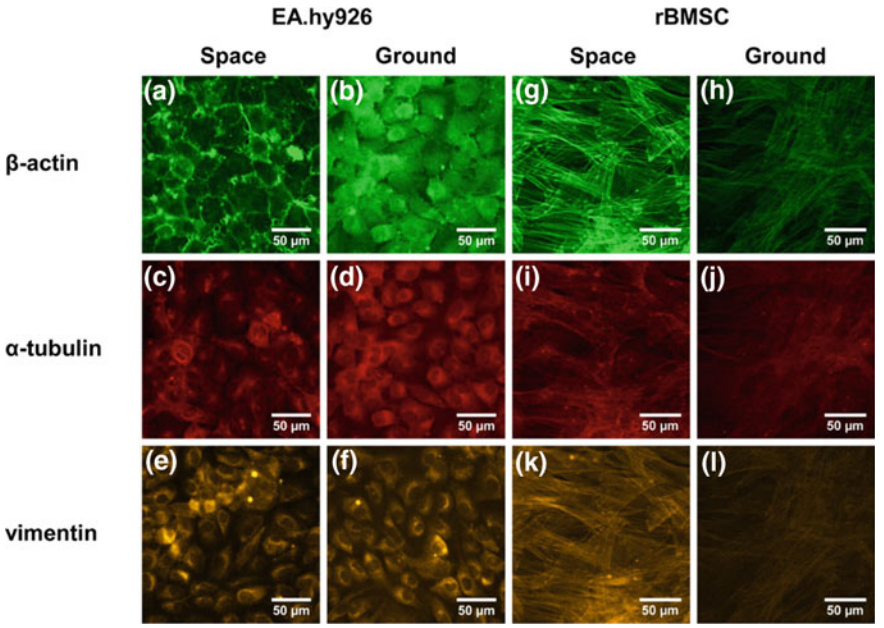

Fig. 5 Cytoskeletal remodeling of EA.hy926 cells and rBMSCs in space or on ground. Presented are the typical confocal images of β-actin (**a**–**b**, **g**–**h**), α-tubulin (**e**–**f**, **i**–**j**) and vimentin (**e**–**f**, **k**–**l**) in the two types of the cells cultured for three days in space (**a**, **c**, **e**, **g**, **i**, **k**) or on ground (**b**, **d**, **f**, **h**, **j**, **l**) for EA.hy926 cells (**a**–**f**) and rBMSCs (**g**–**l**). Bar = 50 μm

et al. 2007). Thus, our results corroborate the actin disassembly in space or clinostat culture for ECs and other types of cells (Maier et al. 2015).

Existing evidences indicate that those HUVECs re-adapted by subsequent passages after spaceflight exhibit the persisting changes in the organization of microtubules and form prominent bundles that occupies the peripheral cytoplasm (Kapitonova et al. 2012). The total amount of tubulin is also significantly reduced in the cytoplasm of these cells compared to ground control. Here we find that 3-day culture in space leads to a dramatic decrease in the amount of microtubules for EA.hy926 cells (Fig. 5c–d), which is consistent with the observations from previous spaceflight (Kapitonova et al. 2012) and clinostat culture studies (Buravkova et al. 2018) for HUVECs. More importantly, the enhanced mRNA-encoding actin and tubulin are observed in the exosomes collected from the supernatant of EA.hy926 cells cultured for 10 days in space, which may contribute to the disorganization of F-actin and microtubules in the cell body (Li et al. 2018).

Intermediate filaments such as vimentin contribute to maintain the structural and mechanical stability of cells (Zhang et al. 2017; Zhou et al. 2018). It is known that the expression of vimentin is enhanced in chondrocytes and papillary thyroid carcinoma cells cultured in clinostats (Infanger et al. 2006; Aleshcheva et al. 2013). While the expression of vimentin in EA.hy926 cells remains unchanged after 3-day culture in

space compared to the ground control (Fig. 5e–f), the extended exposure to space microgravity for 10 days leads to a significant increase of vimentin, which possibly compensates the loss of mechanical stability caused by the disorganization of F-actin and microtubules (Li et al. 2018).

On the other hand, cytoskeletal remodeling in rBMSCs cultured in hepatocyte induction medium presents a distinct pattern. The total expression of actin is higher in space than on ground, similar to those observations using parabolic flight at gene level (Aleshcheva et al. 2015). Here intracellular stress fibers are well formed at high intensity for the cells cultured in space (Fig. 5g). By contrast, only a few stress fibers are visible for the cells on ground (Fig. 5h). In particular, the actin cytoskeleton of rBMSCs exhibits significant redistribution and reorganization under real microgravity, presumably attributed to the coordinated regulation of biomechanical (microgravity) and biochemical (hepatocyte induction) signaling. Moreover, microtubules are also known to be gravisensitive. Here the total amount of tubulin in rBMSCs is increased significantly in space compared to ground control (Fig. 5i–j), also consistent with those observations at gene level using parabolic flight (Aleshcheva et al. 2015). In immunofluorescence analysis, tubulin filaments in space appears to present more visible bundles. While the expression of vimentin remains similar with that of tubulin (Fig. 5k–l), the exposure to space microgravity for 3 days leads to a significant increase of vimentin expression, which is consistent with previous studies via clinostat (Aleshcheva et al. 2015; Ebnerasuly et al. 2017).

To our knowledge, this is the first evidence, at protein level, of cytoskeletal alteration in hepatic induction of rBMSCs under real microgravity. More interesting is the finding of microgravity-induced enhancement of actin stress fibers, which could be associated with the plate-like structure (*cf.* Fig. 4g). Noting that actin proteins could either lose the stress fibers, present the perinuclear localization, or remain unchanged in different space flown experiments (Vorselen et al. 2014; Chen et al. 2016), these controversial observations are presumably attributed to different cell types, distinct space hardware, or differential quantification and standardization of mechanical environment such as mass transport.

5.4 Cell Adhesion

Energy metabolism deficiency in ECs exposed to space microgravity is cascaded into significant suppression of genes associated with host defense in previous spaceflight studies (Wang et al. 2015; Chakraborty et al. 2018). Decreased expression of cellular adhesive molecules (Grenon et al. 2013) and reduced release of pro-inflammatory cytokines (Grimm et al. 2010; Griffoni et al. 2011; Grenon et al. 2013) are also documented on ECs using clinostats. Here 3-day culture of EA.hy926 cells in space significantly decreases the presence of ICAM-1 (Fig. 6a–b) and VCAM-1 (Fig. 6c–d), two ligands for β2 and α4 integrins respectively, indicating the impairment of leukocyte recruitment and transmigration during inflammation. Exposure to space microgravity for 10 days further suppresses the release of a few pro-inflammatory (IL-8, MCP-

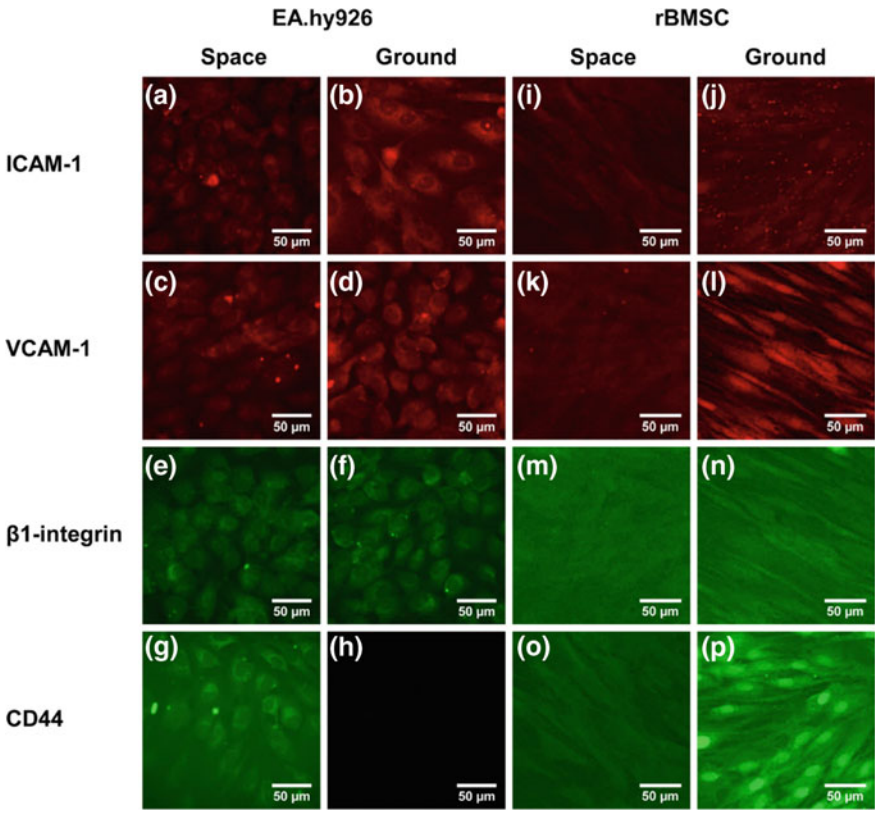

Fig. 6 Expression of adhesive molecules of EA.hy926 cells and rBMSCs in space or on ground. Presented are the typical confocal images of ICAM-1 (**a**–**b**, **i**–**j**), VCAM-1 (**c**–**d**, **k**–**l**), β1-integrin (**e**–**f**, **m**–**n**) and CD44 (**g**–**h**, **o**–**p**) on the surface of the two types of the cells cultured for three days in space (**a**, **c**, **e**, **g**, **i**, **k**, **m**, **o**) or on ground (**b**, **d**, **f**, **h**, **j**, **l**, **n**, **p**) for EA.hy926 cells (**a**–**h**) and rBMSCs (**i**–**p**). Bar = 50 μm

1, CCL5 and IL-1 R4) and pro-angiogenesis (Endoglin, IGFBP-2, PDGF-AA, and Pentraxin-3) cytokines in these ECs (Li et al. 2018). These data shed light on the suppressed host defenses and delayed wound healing faced by astronauts (Versari et al. 2013; Chakraborty et al. 2018).

Morphological alteration and cytoskeletal remodeling of cells in space are related to their anchorage onto the substrate via cellular adhesive molecules and extracellular matrix (ECM). β1-integrin and CD44 are two important adhesive molecules that interact with collagen I and hyaluronan (HA) in ECM, respectively, playing crucial roles in cell proliferation, angiogenesis and mechanotransduction (Savani et al. 2001; Provenzano and Keely 2011). Although the expression of β1-integrin on the surface of EA.hy926 cells after 3-day culture in space remains unchanged compared to the ground control (Fig. 6e–f), significantly reduction of collagen I is observed (Li et al.

2018), indicating the impairment of ECM/integrin/FAK pathway in space. Meanwhile, enhanced expression of CD44 is found in the presence of space microgravity (Fig. 6g–h), which is consistent with previous clinostat study in thyroid cancer cells (Grosse et al. 2012) and may lead to the augmented signals of Rho GTPases family (Bourguignon et al. 2006; Murray et al. 2014; Hyder et al. 2015).

Stem cell adhesion on substrate is also determined by the interactions between ECM proteins and transmembrane cellular adhesive molecules. Here it is indicated that, in the expression of several adhesive molecules for rBMSCs 3-day cultured in space, β1 integrin expression is significantly increased (Fig. 6m–n) but the expressions of ICAM-1 (Fig. 6i–j), VCAM-1 (Fig. 6k–l), and CD44 (Fig. 6o–p) are reduced at distinct degrees compared to those on ground. Thus, it is possible that the difference in ligand availability contributes to the differential regulation of distinct cell adhesion. For example, β1 integrin is the vital molecule in mesenchymal stem cells (Song et al. 2014) and hepatocytes (Speicher et al. 2014) and plays important roles in adhesion (Lee et al. 2004), mechanotransduction (Ode et al. 2011) and liver disease repairing (Aldridge et al. 2012). Here the enhanced expression of β1-integrin in space is found to be consistent with those observations derived from stimulated microgravity effect tests (Meyers et al. 2004). Since VCAM-1 expression in space is reduced and less β1-integrin-VCAM-1 pairs may be insufficient to support cell adhesion, one possible mechanism is that the extra β1-integrins could bind to other ligands to compensate the insufficiency. Collagen I is a candidate ligand since it binds to β1-integrin specifically and can be expressed in MSCs in ground-based stimulation (Meyers et al. 2004). This is critical especially for hepatic induction of rBMSCs since the reinforced β1-integrin signaling via VCAM-1 and/or collagen I binding could potentially favor hepatic differentiation (Popov et al. 2011; Bi et al. 2017).

5.5 Related Signaling Pathways

Cytoskeletal remodeling of cells in space is related to the regulation of underlying signaling molecules. Here the decreased collagen I expression (Li et al. 2018) leads to the impaired mechanotransduction through integrin-mediated signaling pathway and reduced tyrosine phosphorylation of FAK in EA.hy926 cells cultured in space (Fig. 7a–b), resulting in the depressed expression of phosphoinositide 3-kinase (PI3K) and endothelial nitric oxide synthase (eNOS) (Li et al. 2018) and down-regulation of the Rho GTPases family. RhoA, Rac-1 and Cdc42 are three Rho GTPases crucial for the rearrangement of cytoskeletal actin, tubulin and vimentin. Here spaceflight-induced increase of RhoA (Fig. 7c–d) is found in EA.hy926 cells cultured for 3 days, presumably associated with the enhanced expression of CD44 (*cf.* Fig. 6g–h). Meanwhile, 3-day culture in space does not affect Rac-1 expression in EA.hy926 cells (Fig. 7e–f) but reduces Cdc42 expression significantly (Fig. 7g–h). The decreased Cdc42 could result from the inhibition of ECM/integrin/FAK pathway (Li et al. 2018). The expression of NF-κB (nuclear factor kappa-light-chain-enhancer of activated B cells) is also quantified, and no significant difference is found between

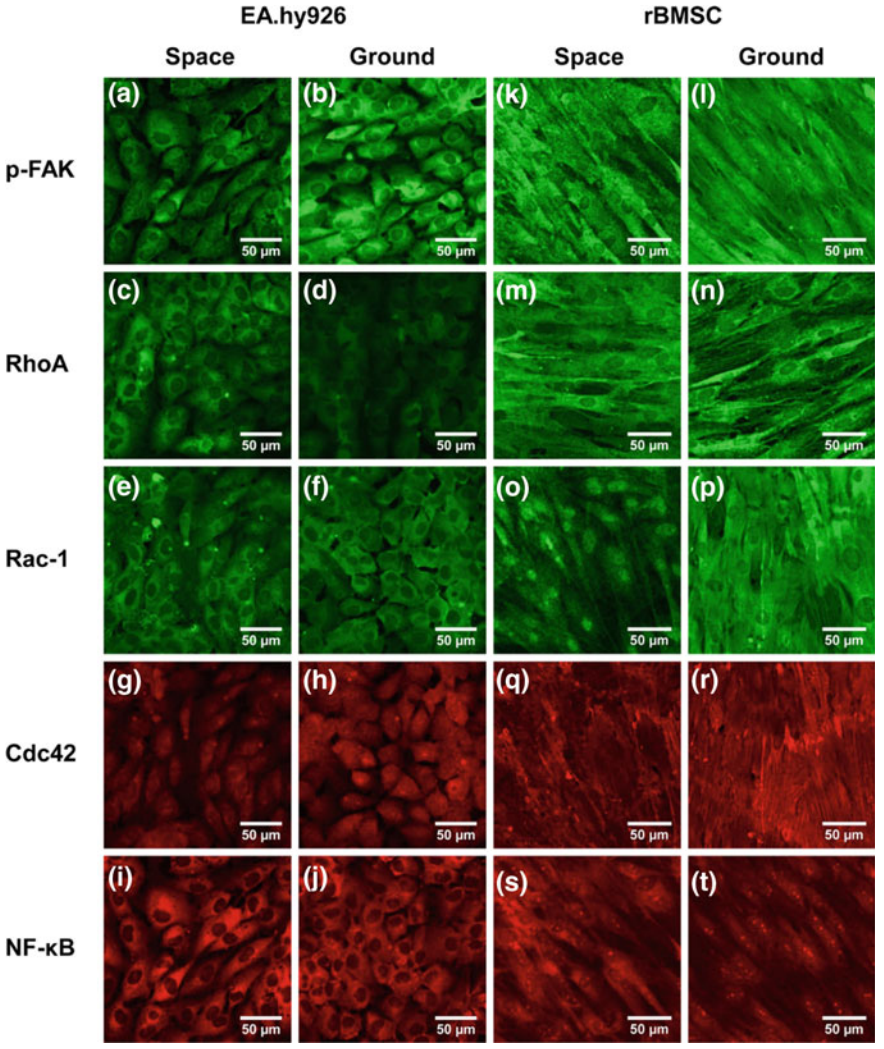

Fig. 7 Expression of signaling molecules of EA.hy926 cells and rBMSCs in space or on ground. Presented are the typical confocal images of p-FAK (**a**–**b**, **k**–**l**), RhoA (**c**–**d**, **m**–**n**), Rac-1 (**e**–**f**, **o**–**p**), Cdc42 (**g**–**h**, **q**–**r**) and NF-κB (**i**–**j**, **s**–**t**) in the two types of the cells cultured for three days in space (**a**, **c**, **e**, **g**, **i**, **k**, **m**, **o**, **q**, **s**) or on ground (**b**, **d**, **f**, **h**, **j**, **l**, **n**, **p**, **r**, **t**) for EA.hy926 cells (**a**–**j**) and rBMSCs (**k**–**t**). Bar = 50 μm

EA.hy926 cells cultured in space and on ground (Fig. 7i–j). These diverse regulations of distinct signaling molecules imply the complicated signaling network for ECs in space.

Abnormal regulations or functions of cellular cytoskeleton via cell adhesion alter cell phenotype. At early stage of the directed hepatic differentiation of rBMSCs for 3 days under microgravity, β1 integrin expression is upregulated, but autophosphorylation of adhesion-dependent kinase FAK (Fig. 7k–l) and expressions of Rho GTPases of Rho A (Fig. 7m–n) and Rac-1 (Fig. 7o–p) have no significant differences and Cdc42 has a slight decline (Fig. 7q–r), as compared to those on ground. At late stage of induced differentiation for 10 days, however, Rac-1 and Cdc 42 expressions are decreased and *p*-FAK and RhoA expressions are increased dramatically in space compared to ground control (*data not show*). NF-κB expression is significantly enhanced in space than that on ground at Day 3 but the difference between space and ground groups tends to reduce at Day 10 (Fig. 7s–t). Since hepatic differentiation of MSCs in space should result from the coupling of mechanical and chemical signaling, it is reasonably speculated that chemical induction plays major roles at early stage and mechanical factors work at late stage. To date, few studies are directed on hepatic differentiation of MSCs under space microgravity or ground-based simulation, and further studies are required to isolate the two distinct signaling mechanisms.

5.6 Hepatic Differentiation of RBMSCs

Directed differentiation of stem cells under microgravity is key for space reproductive biology and histogenesis. Here two typical biomarkers of hepatic differentiation are tested for rBMSCs cultured in hepatic induction medium. Interestingly, the cells yield fibroblast-like morphology and the expression of albumin (ALB) and cytochrome CYP450 enhances cell maturation and differentiation. ALB expression for the cells in space is higher at Day 10 than that at Day 3 (Fig. 8c and a) but is comparable between the two time points for the cells on ground (Fig. 8d and b). Specifically at the same point of Day 10, the expression is higher for the cells in space than that on ground (Fig. 8d). Similarly, CYP450 expression is higher in space at Day 10 (Fig. 8g and e) but comparable between Day 10 and Day 3 on ground (Fig. 8h and f). Also observed is the increased CYP450 expression at Day 3 in space compared to that on ground (Fig. 8e–f). These findings indicate that the differentiated cells present functional phenotype similar to those of hepatocytes (Choi et al. 2013). Collectively, these results suggest that rBMSCs are preferential in hepatic differentiation at long-term duration under microgravity. Actually, this is the first evidence for hepatic differentiation of rBMSCs under space microgravity. While liver is not a preferential candidate for gravity sensation, the observation that rBMSCs are more prone to hepatic differentiation under space microgravity than that under normal gravity is coincident with the theory of use and disuse. Elucidating the underlying mechanisms is helpful to understand the effects of gravity on stem cell differentiation.

In summary, we develop a novel SCCS system and elucidate the response of endothelial cells and mesenchymal stem cells to gravity alteration under real space microgravity environment in SJ-10 satellite. Our data indicate that space microgravity could suppress cellular metabolism. Both ECs and MSCs are regulated by

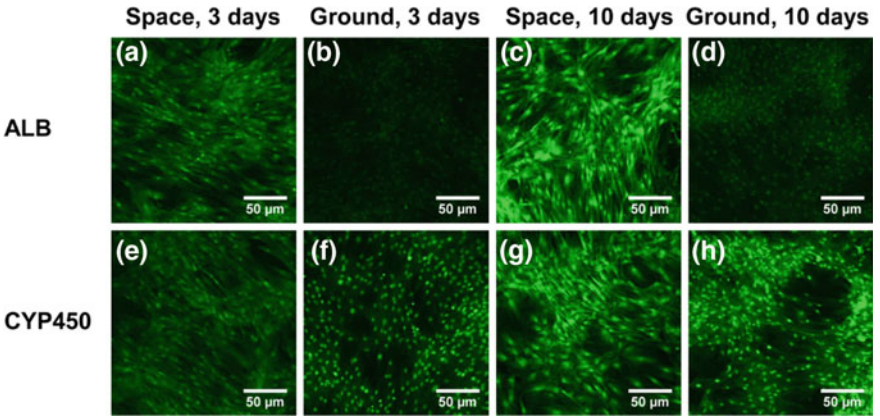

Fig. 8 Differentiation of rBMSCs to hepatocyte-like cells cultured in space or on ground. Hepatocyte biomarkers of ALB (**a**–**d**) and CYP450 (**e**–**h**) are stained in rBMSCs at day 3 (**a**, **b**, **e**, **f**) or 10 (**c**, **d**, **g**, **h**) in space (**a**, **c**, **e**, **g**) or on ground (**b**, **d**, **f**, **h**). Bar = 50 μm

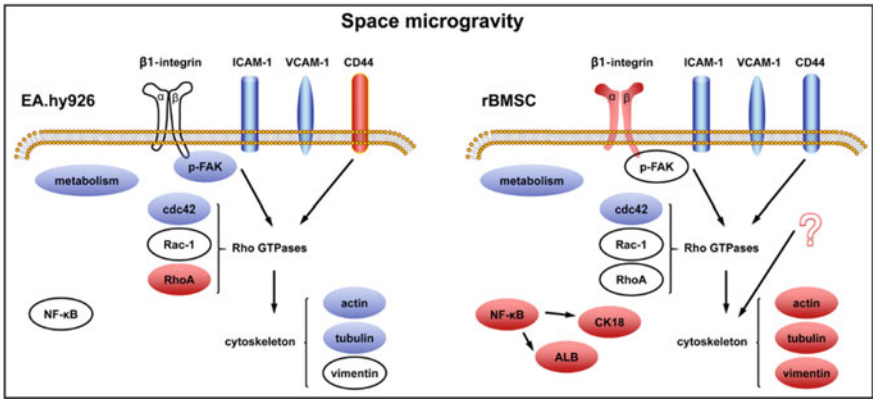

Fig. 9 Working model for the effects of space microgravity on EA.hy926 cells and rBMSCs at day 3. *Red*, *blue* and *white* icons represent up-, down-regulated and unchanged molecules, respectively

microgravity and respond differentially in initiating cytoskeletal remodeling, or dysregulating signaling pathways relevant to cell adhesion, or directing hepatic differentiation (Fig. 9). Since the space mission itself has inevitable limitations due to the well-known inconveniences such as the strictly-limited number of samples, the mechanical condition control, and the operational constrains, it is hard to unravel the underlying mechanism without more controllable or quantified mechanical and mass transport conditions. Nevertheless, this on-orbit experiment verifies the passive de-bubble technique and the effectiveness of designed medium supply patterns. These findings and techniques provide new potential bases for cell biology study under space microgravity.

Acknowledgements The authors are grateful to Lei Zhang, Jianquan Zhang, Zhongfang Deng, Xiang Li, Teng Xie, and Namei Du from Technology and Engineering Center for Space Utilization (CSU) of CAS for their helps in developing hardware and software. The authors also thank to Juan Chen and Yuxin Gao for their technical support, to Chen Zhang, Chunhua Luo, Fan Zhang and Lu Zheng for their assistance in biological tests, and to Shenbao Chen, Lüwen Zhou, Xiao Zhang, Yuzhen Bi, Bing Shangguan, Fan Zhang, and Hao Yang for their contributions to implement the space mission.

We are grateful to the staff members from National Space Science Center (NSSC) of CAS, China Academy of Space Technology (CAST), and China Aerospace Science and Technology Corporation (CASC) for their respective contributions to organization and administration for the payload system and for the satellite system of SJ-10 mission. We also thank the teams of other five systems of SJ-10 mission for their cooperation and support.

This work is supported by National Natural Science Foundation of China grants U1738115 and 31661143044, and Strategic Priority Research Program of CAS grants XDA04020202-17, XDA04020202-19, XDA04020416, XDA04073800, and QYZDJ-SSW-JSC018.

References

Aldridge V, Garg A, Davies N et al (2012) Human mesenchymal stem cells are recruited to injured liver in a β1-integrin and CD44 dependent manner. Hepatology 3:1063–1073

Aleshcheva G, Sahana J, Ma X et al (2013) Changes in morphology, gene expression and protein content in chondrocytes cultured on a random positioning machine. PLoS ONE 8:e79057

Aleshcheva G, Wehland M, Sahana J et al (2015) Moderate alterations of the cytoskeleton in human chondrocytes after short-term microgravity produced by parabolic flight maneuvers could be prevented by up-regulation of BMP-2 and SOX-9. FASEB J 6:2303–2314

Ayatollahi M, Kabir Salmani M, Soleimani M et al (2010) Expansion of human marrow derived mesenchymal stem cells and their transdifferentiation potential. Iran Red Crescent Med J 12(4):446–452

Bi H, Ming L, Cheng R et al (2017) Liver extracellular matrix promotes BM-MSCs hepatic differentiation and reversal of liver fibrosis through activation of integrin pathway. J Tissue Eng Regen Med 10:2685–2698

Bizzarri M, Cucina A, Palombo A et al (2014) Gravity sensing by cells: mechanisms and theoretical grounds. Rend Fis Acc Lincei 25(Suppl 1):S29–S38

Bizzarri M, Monici M, van Loon JJWA (2015) How Microgravity affects the biology of living systems. BioMed Res Int 2015(9):1–4

Bourguignon LY, Gilad E, Brightman A et al (2006) Hyaluronan-CD44 interaction with leukemia-associated RhoGEF and epidermal growth factor receptor promotes Rho/Ras co-activation, phospholipase C epsilon-Ca^{2+} signaling, and cytoskeleton modification in head and neck squamous cell carcinoma cells. J Biol Chem 281:14026–14040

Buravkova LB (2010) Problems of the gravitational physiology of a cell. Hum Physiol 36(7):746–753

Buravkova LB, Rudimov EG, Andreeva ER et al (2018) The ICAM-1 expression level determines the susceptibility of human endothelial cells to simulated microgravity. J Cell Biochem 119:2875–2885

Burger EH, Klein-Nulend J (1998) Microgravity and bone cell mechanosensitivity. Bone 22:127S–130S

Byfield FJ, Reen RK, Shentu TP et al (2009) Endothelial actin and cell stiffness is modulated by substrate stiffness in 2D and 3D. J Biomech 42:1114–1119

Carlsson SI, Bertilaccio MT, Ballabio E et al (2003) Endothelial stress by gravitational unloading: effects on cell growth and cytoskeletal organization. Biochim Biophys Acta 1642:173–179

Chakraborty N, Cheema A, Gautam A et al (2018) Gene-metabolite profile integration to understand the cause of spaceflight induced immunodeficiency. NPJ Microgravity 4:4
Chancellor TJ, Lee J, Thodeti CK et al (2010) Actomyosin tension exerted on the nucleus through nesprin-1 connections influences endothelial cell adhesion, migration, and cyclic strain-induced reorientation. Biophys J 99:115–123
Chen Z, Luo Q, Lin CC et al (2016) Simulated microgravity inhibits osteogenic differentiation of mesenchymal stem cells via depolymerizing F-actin to impede TAZ nuclear translocation. Sci Rep 6:30322
Choi SA, Choi HS, Kim KJ et al (2013) Isolation of canine mesenchymal stem cells from amniotic fluid and differentiation into hepatocyte-like cells. Vitro Cell Dev Biol Anim 1:42–51
Ebnerasuly F, Hajebrahimi Z, Tabaie SM et al (2017) Effect of simulated microgravity conditions on differentiation of adipose derived stem cells towards fibroblasts using connective tissue growth factor. Iran J Biotechnol 4:241–251
Everding B, Wilhelm S, Averesch S et al (2000) IFN-gamma-induced change in microtubule organization and alpha-tubulin expression during growth inhibition of lung squamous carcinoma cells. J Interferon Cytokine Res 20:983–990
Freed LE, Vunjak-Novakovic G (2002) Spaceflight bioreactor studies of cells and tissues. Adv Space Biol Med 8:177–195
Grenon SM, Jeanne M, Aguado-Zuniga J et al (2013) Effects of gravitational mechanical unloading in endothelial cells: association between caveolins, inflammation and adhesionmolecules. Sci Rep 3:1494
Griffoni C, Di Molfetta S, Fantozzi L et al (2011) Modification of proteins secreted by endothelial cells during modeled low gravity exposure. J Cell Biochem 112:265–272
Grimm D, Infanger M, Westphal K et al (2009) A delayed type of three-dimensional growth of human endothelial cells under simulated weightlessness. Tissue Eng Part A 15:2267–2275
Grimm D, Bauer J, Ulbrich C et al (2010) Different responsiveness of endothelial cells to vascular endothelial growth factor and basic fibroblast growth factor added to culture media under gravity and simulated microgravity. Tissue Eng Part A 16:1559–1573
Grosse J, Wehland M, Pietsch J et al (2012) Gravity-sensitive signaling drives 3-dimensional formation of multicellular thyroid cancer spheroids. FASEB J 26:5124–5140
Harada-Sukeno A, Kohno S, Nakao R et al (2009) "Myo Lab": a JAXA cell biology experiment in "Kibo (JEM)" of the international space station. Biol Sci Space 23(4):189–193
Hu WR, Zhao JF, Long M et al (2014) Space program SJ-10 of microgravity research. Microgravity Sci Technol 26:159–169
Hung RJ, Terman JR (2011) Extracellular inhibitors, repellents, and semaphorin/plexin/MICAL-mediated actin filament disassembly. Cytoskeleton (Hoboken) 68:415–433
Hyder CL, Kemppainen K, Isoniemi KO et al (2015) Sphingolipids inhibit vimentin-dependent cell migration. J Cell Sci 128:2057–2069
Infanger M, Kossmehl P, Shakibaei M et al (2006) Simulated weightlessness changes the cytoskeleton and extracellular matrix proteins in papillary thyroid carcinoma cells. Cell Tissue Res 324:267–277
Infanger M, Ulbrich C, Baatout S et al (2007) Modeled gravitational unloading induced downregulation of endothelin-1 in human endothelial cells. J Cell Biochem 101:1439–1455
Kapitonova MY, Muid S, Froemming GRA et al (2012) Real space flight travel is associated with ultrastructural changes, cytoskeletal disruption and premature senescence of HUVEC. Malays J Pathol 34(2):103–113
Kapitonova MY, Kuznetsov SL, Froemming GRA et al (2013) Effects of space mission factors on the morphology and function of endothelial cells. Bull Exp Biol Med 154(6):796–801
Kim YK, Park SH, Lee JH et al (2015) Design and performance of an automated bioreactor for cell culture experiments in a microgravity environment. J Astron Space Sci 32(1):81–89
Krikorian AD (1996) Strategies for "minimal growth maintenance" of cell cultures: a perspective on management for extended duration experimentation in the microgravity environment of a space station. Botanl Rev 62(1):41–108

Lee JW, Kim YH, Park KD (2004) Importance of integrin beta1-mediated cell adhesion on biodegradable polymers under serum depletion in mesenchymal stem cells and chondrocytes. Biomaterials 10:1901–1909
Li Z, Gong YX, Sun SJ et al (2013) Differential regulation of stiffness, topography, and dimension of substrates in rat mesenchymal stem cells. Biomaterials 34(31):7616–7625
Li N, Wang CZ, Sun SJ et al (2018) Microgravity-induced alterations of inflammation-related mechanotransduction in endothelial cells on board SJ-10 satellite. Front Physiol 9:1025
Long M, Sun SJ, Huo B et al (2009) Chapter 12: Biomechanics on cell responses to microgravity. In: Hu WR (ed) Advances in microgravity sciences. Transworld Research Network, Kerala, pp 215–233
Long M, Wang YR, Zheng HQ et al (2015) Mechano-biological coupling of cellular responses to microgravity. Microgravity Sci Technol 27:505–514
Lü DY, Sun SJ, Zhang F et al (2019) Microgravity-induced hepatogenic differentiation of rBMSCs on board SJ-10 satellite. FASEB J 33(3):4273–4286
Ma X, Sickmann A, Pietsch J et al (2014) Proteomic differences between microvascular endothelial cells and the EA.hy926 cell line forming three-dimensional structures. Proteomics 14:689–698
Maier JAM, Cialdai F, Monici M et al (2015) The impact of microgravity and hypergravity on endothelial cells. Bio Med Res Int 2015(9):434803
Meyers VE, Zayzafoon M, Gonda SR et al (2004) Modeled microgravity disrupts collagen I/integrin signaling during osteoblastic differentiation of human mesenchymal stem cells. J Cell Biochem 4:697–707
Murray ME, Mendez MG, Janmey PA (2014) Substrate stiffness regulates solubility of cellular vimentin. Mol Biol Cell 25:87–94
Ode A, Kopf J, Kurtz A et al (2011) CD73 and CD29 concurrently mediate the mechanically induced decrease of migratory capacity of mesenchymal stromal cells. Eur Cell Mater 22:26–42
Popov C, Radic T, Haasters F et al (2011) Integrins α2β1 and α11β1 regulate the survival of mesenchymal stem cells on collagen I. Cell Death Dis 2:e186
Provenzano PP, Keely PJ (2011) Mechanical signaling through the cytoskeleton regulates cell proliferation by coordinated focal adhesion and Rho GTPase signaling. J Cell Sci 124:1195–1205
Savani RC, Cao G, Pooler PM et al (2001) Differential involvement of the hyaluronan (HA) receptors CD44 and receptor for HA-mediated motility in endothelial cell function and angiogenesis. J Biol Chem 276:36770–36778
Song K, Huang M, Shi Q et al (2014) Cultivation and identification of rat bone marrow-derived mesenchymal stem cells. Mol Med Rep 2:755–760
Speicher T, Siegenthaler B, Bogorad RL et al (2014) Knockdown and knockout of β1-integrin in hepatocytes impairs liver regeneration through inhibition of growth factor signalling. Nat Commun 5:3862
Sun SJ, Gao YX, Shu NJ et al (2008) A novel counter sheet-flow sandwich cell culture system to mammalian cell growth in space. Microgravity Sci Technol 20:115–120
Sun SJ, Wang CZ, Bi YZ et al (2019) An integration design of gas exchange, bubble separation, and flow control in a space cell culture system on board the SJ-10 satellite. Rev Sci Instrum. https://doi.org/10.1063/1.5087770
Ulbrich C, Wehland M, Pietsch J et al (2014) The impact of simulated and real microgravity on bone cells and mesenchymal stem cells. BioMed Res Int 2014(9):928507
van Loon JJWA (2009) Mechanomics and physicomics in gravisensing. Microgravity Sci Technol 21:159–167
Vandendriesche D, Parrish J, Kirven-Brooks M et al (2004) Space station biological research project (SSBRP) cell culture unit (CCU) and incubator for international space station (ISS) cell culture experiments. J Gravit Physiol 11(1):93–103
Versari S, Villa A, Bradamante S et al (2007) Alterations of the actin cytoskeleton and increased nitric oxide synthesis are common features in human primary endothelial cell response to changes in gravity. Biochim Biophys Acta 1773(11):1645–1652

Versari S, Longinotti G, Barenghi L et al (2013) The challenging environment on board the International Space Station affects endothelial cell function by triggering oxidative stress through thioredoxin interacting protein overexpression: the ESA-SPHINX experiment. FASEB J 27:4466–4475

Vorselen D, Roos WH, MacKintosh FC et al (2014) The role of the cytoskeleton in sensing changes in gravity by nonspecialized cells. FASEB J 28(2):536–547

Wang JW, Lü DY, Mao DB et al (2014) Mechanomics: an emerging field between biology and biomechanics. Protein Cell 5(7):518–531

Wang CZ, Li N, Zhang C et al (2015) Effects of simulated microgravity on functions of neutrophil-like HL-60 cells. Microgravity Sci Technol 27:515–527

Zhang C, Zhou LW, Zhang F et al (2017) Mechanical remodeling of normally-sized mammalian cells under a gravity vector. FASEB J 31:802–813

Zhou LW, Zhang C, Zhang F et al (2018) Theoretical modeling of mechanical homeostasis of a mammalian cell under gravity-directed vector. Biomech Model Mechan 17:191–203

Flowering of Arabidopsis and Rice in Space

Huiqiong Zheng, Li Hua Wang and Jun Yan Xie

Abstract The reproductive success of plants is often dependent on their flowering time being adapted to the territorial environment, in which gravity remains constant. Whether plants can follow the same rule to determine their flowering time under microgravity in space is unknown. Here, a 12-day mission on orbiter Chinese SJ-10 recoverable microgravity experimental satellite (SJ-10 satellite) carried long-day-flowering *Arabidopsis thaliana* and short-day-flowering rice (*Oryza sativa*), and transgenic Arabidopsis plants engineered with a transgene composed of a heat shock-inducible promoter (HSP) linked to the green fluorescence protein (GFP) reporter gene and FLOWERING LOCUS T (FT) gene. The plants were used to examined FT gene expression patterns in space to address the effects of microgravity on flowering induction. In addition, application of GFP technique for FT visualization on the SJ-10 satellite in this study is also introduced. Finally, a comprehensive analysis of global gene expression of leaves of Arabidopsis and rice grown in space under a long-day (LD) and a short-day (SD) conditions, respectively, was carried out to understand effects of microgravity on photoperiodic flowering induction at molecular level. Our results showed that microgravity apparently down-regulated expression of GIGANTEA (GI), which is involved in circadian clock functions. Furthermore, possible key points of microgravity responses in the main photoperiod pathways, GI-CO-FT module in Arabidopsis or GI-Hd1-Hd3a module in rice, are also discussed with regard to potential future spaceflight experiment opportunities.

Abbreviations

BLSS	Bioregenerative life support system
CO	CONSTANS
DEGs	Differential expression genes

H. Zheng (✉) · L. H. Wang · J. Y. Xie
Institute of Plant Physiology, Institutes for Biological Sciences, Chinese Academy of Sciences, Shanghai 200032, China
e-mail: hqzheng@sippe.ac.cn

E. Duan and M. Long (eds.), *Life Science in Space: Experiments on Board the SJ-10 Recoverable Satellite*, Research for Development,
https://doi.org/10.1007/978-981-13-6325-2_8

FT	FLOWERING LOCUS T
GFP	Green fluorescence protein
GI	GIGANTEA
Hd1	Heading date 1
HSP	Heat shock-inducible promoter
ISS	International Space Station
LEDs	Light emitting diodes
LD	Long-day
PGB	Plant Growth Box
SD	Short-day
SJ-10 satellite	SJ-10 recoverable microgravity experimental satellite
WT	Wild-type

1 Introduction

Plants respond sensitively to many environmental stimuli, such as light, temperature, nutritional conditions and gravity. Among of these environmental signals, gravity is one that remains constant during plant lifetime. Removal of gravitational acceleration by spaceflight caused a wide range of morphogenesis and cellular and molecular changes in plants (Cogoli and Gmünder 1991; Hampp et al. 1997; Paul et al. 2013; Hoson 2014; De Micco et al. 2011; Zheng et al. 2015; Zheng 2018). For example, under microgravity conditions, plants exhibit spontaneous curvatures or changes in growth direction (Driss-Ecole et al. 2008; Soga et al. 2014), increased guttation (Wang et al. 2018), reduced growth and photosynthetic rate of wheat seedlings (Tripathy et al. 1996; Levinskikh et al. 2000), alteration in chloroplast morphology and chlorophyll a/b ratio in Brassica plants (Adamchuk et al. 1999; Jiao et al. 1999, 2004), and swollen mitochondria with an electron-dense matrix and well-developed cristae (Popova 2003). Changes that occur in the spaceflight environment at the genetic (DNA and RNA) and biochemical (protein) levels have recently been intensively studied. Informative results from several recent space flight experiments indicated that microgravity induced a wide range of alterations in gene expression and protein synthesis, including calcium-, lipid, and auxin-mediated signaling, the cell membrane biosynthesis, the total metabolism, responses to stress, and protein synthesis (Tan et al. 2011; Zheng et al. 2015; Zhang et al. 2015; Fengler et al. 2015). Expression of an Adh/GUS reporter gene in Arabidopsis indicated that spaceflight affected stress signal perception and transduction (Paul et al. 2001). The etiolated seedlings grown in space displayed significant changes in the expression of genes associated with drought stress, wounding, and calcium- and auxin-mediated signaling and cell wall development (Paul et al. 2012). In one of our pervious studies, comparison of the proteomic profiles of Arabidopsis callus growing under microgravity conditions with the controls on-board centrifuge (1 $\times$ g of the control) in the Chinese spacecraft SZ-8 flight indicated that significant differences were identified in the content of 45 proteins participating in a wide range of cellular processes, including general

responses to stresses, carbohydrate metabolism, protein synthesis and degradation, intracellular transport, signaling, and the biosynthesis of the cell membrane (Zhang et al. 2015). The expression of peroxidase and cell wall remodeling genes associated with root hair development was repressed under microgravity (Kwon et al. 2015). These results indicated the plasticity of plant growth and development in response to microgravity, and different tissues or organs might exhibit different responses to microgravity.

The life cycle of higher plants has three mutually distinct development stages: the embryogenetic, vegetative, and reproductive stages. Plants undergo a major physiological change when they transition from vegetative growth to reproductive development. The onset of reproductive development is a pivotal switch in the life of plants. Plant reproduction in the spaceflight environment is of great interest. Not only does it help us study fundamental questions regarding the role of gravity in normal development, but also higher plants could supply food and fiber, purify ambient air, and recycle human waste and water in a closed environmental life support system envisioned for long-duration spaceflight. Most of previous space experiments focused on response of plant vegetative stage to short-term microgravity (Kiss et al. 1998; Driss-Ecole et al. 2008; Kordyum 2014; Kordyum and Chapman 2017), but very little is known about the reproductive stage (Link et al. 2003; Merkys and Laurinavicius 1983; Musgrave et al. 1997). Plants frequently died in the transition from the vegetative to the reproductive stage in early attempts (Halstead and Dutcher 1987; Mashinsky et al. 1994). Even when Arabidopsis plants were pre-grown to the flowering stage on Earth and allowed to for seeds on orbit only 55% of seeds were fertile (27% aborted and 18% had non-viable embryos). The first successful complete plant life cycle under microgravity occurred in 1983 with *Arabidopsis thaliana* on board Salyut 7 (Merkys and Laurinavicius 1983). The second successful experiment was performed with *Brassica rapa* on board the Mir space station (Musgrave et al. 2000; Kuang et al. 2000). The seeds obtained in this experiment were healthy and viable, but less protein, fewer cotyledon cell, and aberrant deposition of starch grains. Wheat crop under the same environment on board Mir was failed to develop seeds (Strickland et al. 1997). These experiments indicated that ethylene concentration in the growth chambers was considered responsible for influence of plant reproduction. As international space station (ISS) was established, more long-term experiments on growing plant for a full life cycle were carried out in space. The first seed-to-seed experiment on board ISS was performed in the advanced astroculture plant growth unit, which could provide nutrients to the plant and control soil moisture, light, air temperature, humidity, ethylene, and CO_2 level (Link et al. 2003). Since then, advances in plant culture technology have led to more frequent successful seed set in space (Sychev et al. 2007; Link et al. 2014; Yano et al. 2013). However, seeds developed in space are still often of lower quality in comparison with control seeds formed in normal gravity conditions (De Micco et al. 2014; Link et al. 2014). Seeds produced in space exhibited delayed embryo development, alteration of storage reserves, delay in starch use in cotyledons and decreased cotyledon cell number (Kuang et al. 2000; Musgrave et al. 2000; Link et al. 2014). Flower development is crucial to ensure successful plant reproduction and seed yield. However,

most of information is available on final seed development in space (Kuang et al. 2000; Musgrave et al. 2000; Link et al. 2014), very little is known about the effects of microgravity on the transition from vegetative to reproductive stages. In the SJ-10 satellite experiment, we examined the effects of microgravity in space on the induction of flowering of two different photoperiodic response plants, *Arabidopsis thaliana* and rice. The molecular mechanisms that control the transition from vegetative growth to reproductive development under microgravity were also studied. Here, detail experimental designs and operations of the spaceflight experiment on the SJ-10 satellite to investigate plant flowering are introduced.

2 SJ-10 Satellite Space Experiment

2.1 Experimental Design

Arabidopsis thaliana and rice were used as plant materials in Chinese SJ-10 satellite (April 6–18, 2016) to investigate the effect of microgravity on the photoperiod controlling flowering induction. According to the response of plants to light during the induction of flowering, they can be classified as LD plants that induce flowering when day length exceeds a certain threshold, SD plants that flower when days are short and nights are long, and day neutral plants whose flowering is not dependent on the length of the day. *Arabidopsis thaliana* is LD plant, which floral transition is promoted under the LD (16 h light) condition in comparison with those under the SD (8 h light) condition. Rice is SD plant in which flowering is faster under SD (i.e., 8 h light) than that under the LD (i.e., 16 h light) condition.

To address the possibility that microgravity affect photoperiodic flowering and to assess whether the movement of FT from leaf to shoot apex under microgravity was different from the control on ground condition, we have designed an experiment by comparing LD flowering *Arabidopsis thaliana* and SD flowering rice on board SJ-10 satellite with their controls on ground. In addition, we used the advantages of heat shock (HS)-inducible gene switch and developed transgenic Arabidopsis containing the *HSP* gene promoter linked to the GFP reporter gene (*pHSP*:: *GFP*) and the FT gene (*pHSP*::*FT*). The expression of *pHSP*::*GFP* and *pHSP*::*FT* in Arabidopsis leaves were induced by half hour 37 °C heating under the SD condition and then expression of *GFP* in these leaves were monitored by a plant GFP imager. At the same time, time-lapse images also documented the effect of microgravity on the flowering induction of Arabidopsis and rice plants under a LD (16 h light/8 h dark) and a SD (8 h light/16 h dark) conditions, respectively (Fig. 1). After SJ-10 satellite returned to Earth, the Plant Growth Box (PGB) was unloaded and the root modules-grown plants were harvested approximately 4 h after landing. Samples from four different root modules were collected and fixed with fixation solution immediately and stored at 4 °C, and transported to the laboratory for analysis.

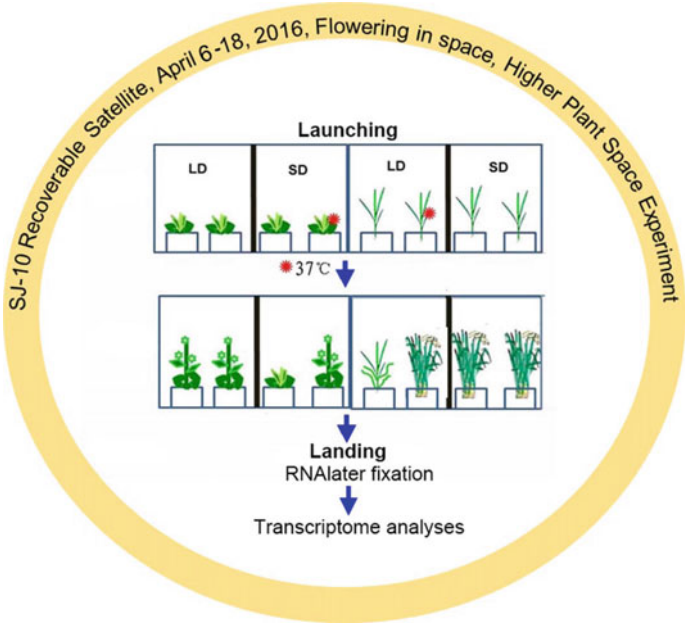

Fig. 1 Chinese SJ-10 satellite experimental setup. 15-day old *Arabidopsis thaliana* and 30-day old rice plants were loaded into sterile PGB approximately 24 h prior to launch on SJ-10 satellite. The PGB provided two photoperiodic conditions: LD (16 h light/8 h dark) and SD (16 h dark/8 h light) conditions. Arabidopsis "Columbia" was used as wild-type and transgenic plant expressing *pHSP*::*GFP* and *pHSP*::*FT* was also carried to observe in orbitor induction of *FT* in leaves by heating 37 °C for half hour (red asterisk indicates)

The PGB used for this experiment had a growing area of 0.013 m^2 and a height of 19 cm. It consisted of four different systems, including growth compartments, illumination system, photograph system, a temperature controlling system and a heater (Fig. 2). The growth compartments included four root modules and relate growth space. Seedlings of Arabidopsis and rice were set in the root modules containing commercially available vermiculite immersed by a medium containing macronutrient as described by Haughn and Sommerville (1986) in the PGB to investigate the effect of microgravity on the course from vegetative stage to reproductive stage and the flowering on the orbit. Illumination was provided by light banks of LED lamp (red: white, 1:2) on a 16-h photoperiod (LD) and an 8-h photoperiod (SD), respectively. Temperature and humidity were recorded every 1 min during flight. Light levels were also recorded with the same frequency. These data were used to set the ground control in a control growth chamber. Ethylene concentration in the growth chamber was regulated by a chemical regent (Zheng et al. 2008) for removal of virtually all released ethylene. Photographic equipments was used to record images of Arabidopsis and rice plants. Images were recorded by three automatic, preprogrammed cameras. Of two cameras were used for photographed plants under the LD

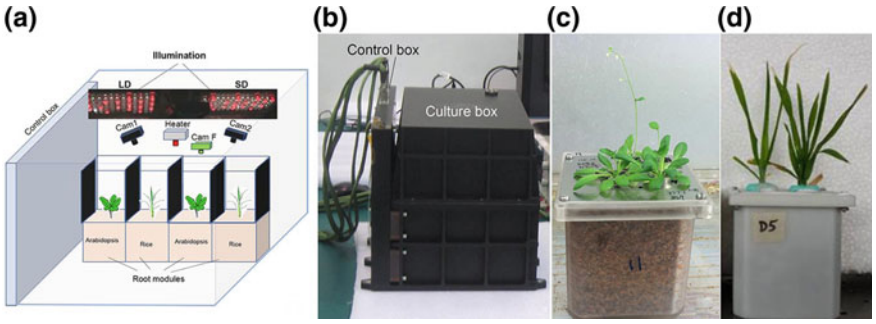

Fig. 2 The PGB was used in Chinese SJ-10 satellite. **a** The detail mechanical set up for the PGB, consisted of four growth modules including two root modules for Arabidopsis and two modules for rice; three cameras, two cameras were used for monitoring plant growth under the LD (cam 1) and the SD (cam 2) conditions, respectively; the other one was used to photograph GFP fluorescence (cam F); one heater was used to increase local temperature on leaves to activate the *HSP* promoter and induce expression of *FT* and *GFP* genes. **b** The PGB used in this experiment. **c** and **d** Two example experimental equipment, which were used as root modules to culture Arabidopsis and rice, respectively

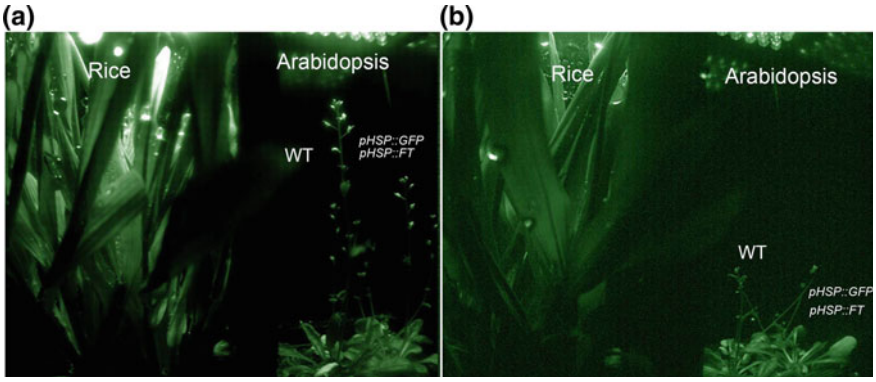

Fig. 3 Two representative images of plants grown the LD (**a**) and the SD (**b**) condition, respectively, on board the SJ-10 satellite. The images were transmitted from space cameras at day 10 after launching. The plants samples included rice wild-type, Arabidopsis wild-type (WT) and transgenic plants (*pHSP*::*GFP*; *pHSP*::*FT*)

and the SD conditions, respectively (Fig. 3). One was a GFP imager for GFP signal recorded. The photographs of plants were taken at 2-h intervals and 4 images every day for GFP signals. Temperature system was regulated by a control box to keep temperature and air movement in the box. A heater was designed to induce the *HSP* promoter controlling expression of *GFP* and *FT* genes by locally heating leaves to 37 °C for half hour.

This heating induced a local activation of the HSP promoter. We then monitored gene expression in the induced leaves with GFP imager camera (cam F) and devel-

opment of inflorescence shoot with cameras (cam 1 and cam 2, Fig. 2). Rice "d18h" was used as wild-type. The plants were grown in the PGB in space for about 12 days. Samples from the orbiter was harvested and fixation with RNAlater solution 4 h after landing, immediately stored at 4 °C, and transported to the laboratory for analysis.

2.2 Arabidopsis thaliana *Flowering in Space*

Flowering time in *Arabidopsis thaliana* is dependent on the length of the day with the LD (16 h light) in general promoting floral transition compared to the SD (8 h light). The phenomenon that plant flowering in response to day length is dubbed photoperiod response, which has been observed to be perceived in the leaves from which the long-distance signal called the florigen is transmitted to the shoot apex to induce flowering. The studies on florigen have been recently made tremendous progress due to identification of numerous genes involved in flowering regulation (reviewed by Jung et al. 2017). A protein called FT in Arabidopsis was proven to be established as florigen, which is contributing to the floral induction by acting as a long-distance signal between leaves and the shoot meristem. FT is genetically down-stream of CONSTANS (*CO*), which expression is under the control of the circadian clock with a phase of 24 h. The CO-FT module is conserved in both LD and SD plants (Srikanth and Schmid 2011). The FT protein act as a systemic inducer of flowering that is expressed in the companion cells of the phloem and exported to the phloem sieve elements in leaves from where it is transported to the shoot apex. This process includes at least three critical steps in florigen signaling: (1) exportation from companion cells to the sieve element; (2) transport from leaves to the shoot apex through phloem; (3) activation of its effector genes at the shoot apex that trigger subsequent flower development.

Gravity and light are two of most important environmental factors to regulate plant growth and development on earth. Effects of light on the regulation of plant flowering have been extensively studied (Putterill et al. 2004; Srikanth and Schmid 2011). However, gravity is permanent and always present in a constant direction and magnitude on earth, there is no way to eliminate the influence of gravity on plants on the surface of earth. Plants have utilized gravity as the most stable and reliable signal to direct their developmental processes. With the increased interest of plants in space, gravity cannot be ignored in studies of plant developmental processes, including plant flowering control. On board the Chinese SJ-10 satellite, the effects of microgravity on the flowering induction of LD Arabidopsis were investigated (Fig. 4). The FT protein act as a systemic inducer of flowering that is expressed in leaves from where it is transported to the shoot apex. To make sure we can induce expression of FT at the early time during flight, we generated *pHSP*::*FT*, *pHSP*::*GFP* fusion construct under control of the promoter of the HSP gene. We heated leaves of Arabidopsis plants grown under SD condition on SJ-10 satellite to 37 °C. This heating induced a local activation of the *HSP* promoter. We then monitored *GFP* gene expression in the induced leaves and compared the flowering time of the heating treated plants with

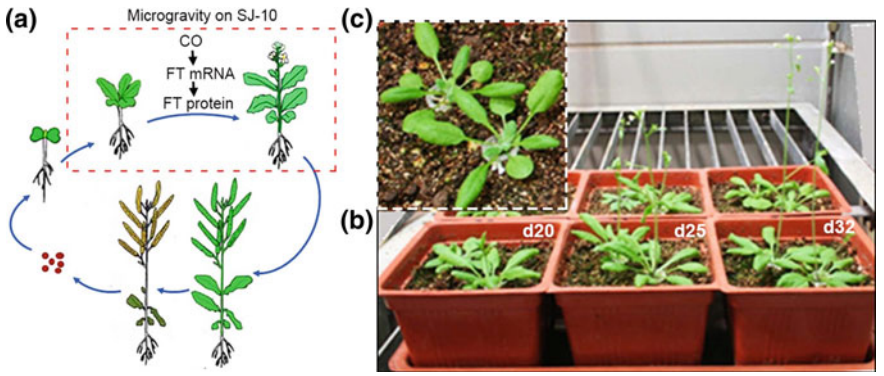

Fig. 4 Subsequent phases during life cycle of *Arabidopsis thaliana*. **a** Schematic diagram illustrating the phases those are more likely sensitive to microgravity. The framed region in red dotted line indicates that samples grown in space on board SJ-10 satellite and the Arabidopsis flowering time pathway could be modified under microgravity. **b** Preculture of Arabidopsis plants in green house for about 20 days before take-off. **c** Top view of 20-day old plants, which were used as samples in SJ-10 experiment. Seedlings at day 25 and day 32 after germination grown in green house on ground were also showed as controls to those grown in space

control (untreated plants) under the SD and LD both in space and on ground (Fig. 3). These results indicated that flowering time of plants grown in space was much longer than those on ground, and suggested that microgravity could affect movement of the FT protein from leaves to the shoot apex.

The evaluation of genome-wide patterns of native gene expression within Arabidopsis (wild-type) leaves grown under the LD and the SD condition, respectively, on board the SJ-10 satellite were preformed by comparing with their controls on ground with utilizing the Affymetrix Arabidopsis ATH1 genome array of 22,746 genes. 4432 genes in the LD plants and 2572 genes in the SD plants were observed to be differentially expressed between microgravity samples and their ground controls ($1 \times g$), of which 2959 and 1099 genes were specific to the LD and the SD condition, respectively (Fig. 5a). GO classification of differential expression genes (DEGs) indicated that the function of genes in response to light in chloroplast was apparently affected among the top 10 of GO term enrichments (Fig. 5b, c). Genes involved in controlling Arabidopsis flowering, including *GI*, *CCA1*, *LHY*, *PCC1*, *ELF4*, *BT3* and *ADG1*, were detected to alter expression under microgravity (Fig. 5d). According to these results, we proposed a model to address microgravity involved in Arabidopsis photoperiodic flowering pathway. In this model, microgravity inhibited expression of *GI*, which plays a key role in control of *FT* expression. In addition, microgravity enhanced expression of *CCA1* and *LHY*, which can regulate expression of *GI*.

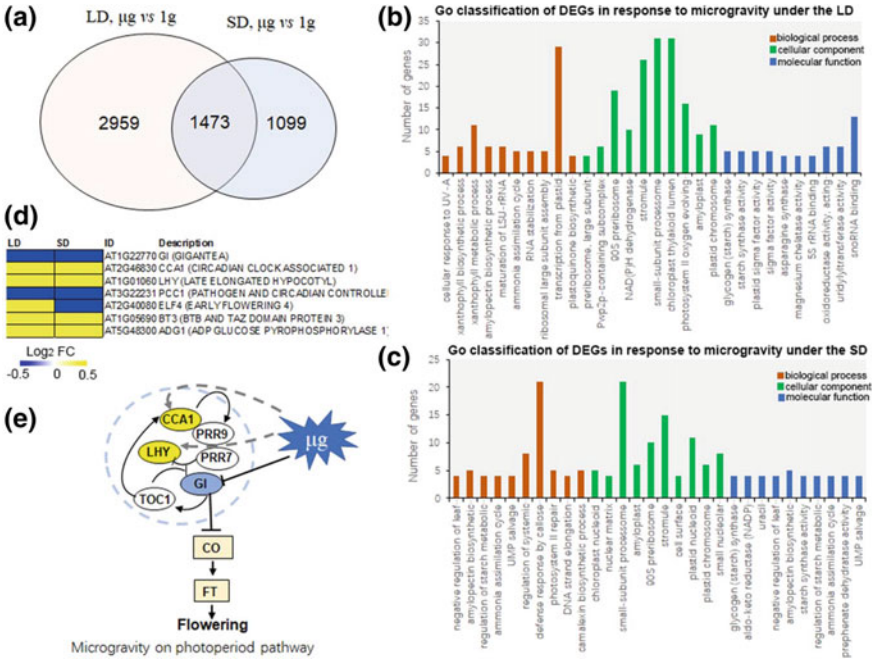

Fig. 5 Microgravity regulated genes in Arabidopsis leaves grown in space under different photoperiod conditions in comparison with their controls on ground. **a** Vennen diagram of transcriptome data. **b** and **c** GO classification of differential expression of genes (DEGs) of microgravity response genes under the LD and the SD conditions, respectively. **d** Expression profile of photoperiod controlling flowering under microgravity (μg) in comparison with their controls on ground (1 × g) under the LD and the SD conditions, respectively. Yellow indicates an increase in expression, blue indicates a decrease in expression. Scale bar shows $\log_2$ fold changes (FC). **e** Proposed model of the influence of microgravity involved in photoperiod pathway in Arabidopsis flowering controlling. In this model, microgravity inhibited expression of *GI*, which plays a key role in control of *FT* expression. In addition, microgravity enhanced expression *CCA1* and *LHY*, which can regulate expression of *GI*

2.3 *Rice Flowering in Space*

Like Arabidopsis, the life cycle of rice has also three mutually distinct developmental stages: the embryogenetic, vegetative, and reproductive stages (Fig. 6a). The vegetative stage can be further divided into the juvenile and adult phases. Importantly, plants can initiate flowering only during the adult phase, endogenous and environmental factors, which affect the change of juvenile-to-adult phase, are considered as key players in regulating plant development (Tanaka et al. 2011). Rice is a facultative SD plant, and molecular genetic studies have identified the major genes involved in SD flowering. Recent progress in genome analysis has provided a strategy for analyzing the genetic control of flowering in rice. Several studies have demonstrated that the structure of gene involved in the photoperiodic response of flowering in rice showed

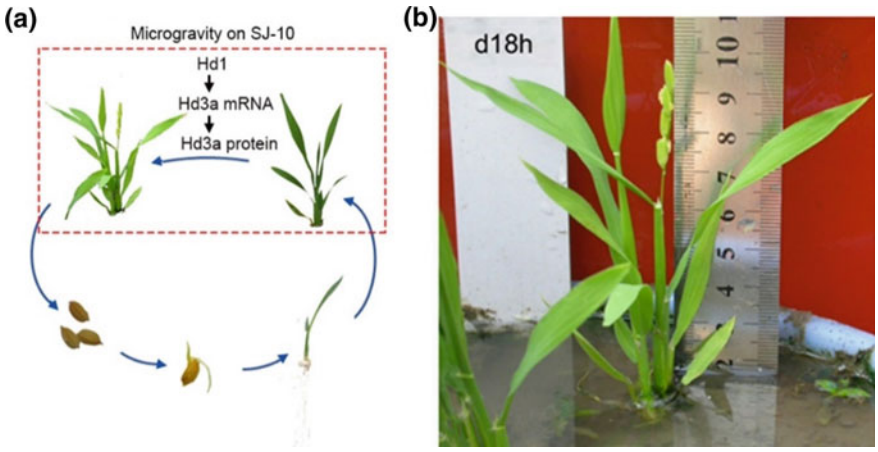

Fig. 6 Subsequent phases during life cycle of rice. **a** Schematic diagram illustrating the phases those are more likely sensitive to microgravity. The framed region in red dotted line indicated that samples grown in space on board SJ-10 satellite and the rice flowering time pathway which could be modified under microgravity. **b** Preculture of Arabidopsis plants in green house for about 30 days before take-off

remarkable similarity to those in Arabidopsis. For example, heading date 1 (*Hd1*), a major photoperiod sensitivity quantitative trait locus in rice, is closely related to the Arabidopsis flowering time gene *CO*. *Hd3a*, which was proven to be established as florigen, functions as *FT* in Arabidopsis.

On SJ-10 satellite space experiment, we focused on the transition vegetative-reproductive phase of rice. 30-day old seedlings were selected as samplers for space experiment (Fig. 5b). After grown in space on the SJ-10 satellite for about 12 days, the plants began flowering under the SD condition but not under the LD. Genome-wide patterns of gene expression within rice leaves grown under the LD and the SD condition, respectively, on board the SJ-10 satellite were preformed by the mapping of mRNAseq reads to the rice genome. Genes of very low aboundance were removed from the analysis, leaving a final number of 20,929 genes. 13,908 genes in the LD plants and 7136 genes in the SD plants were observed to be differentially expressed between microgravity (μg) samples and their ground controls (1 × g), of which 10,532 and 3760 genes were specific to the LD and the SD condition, respectively (Fig. 7a). GO classification of DEGs indicated that the genes function in regulated reproductive process were among the top 20 enrichment list (Fig. 7b, c). The expression of genes involved in controlling rice flowering, including *OsPhyB*, *OsGI*, *OsCOP1*, *OsFCA*, *Os FTL1*, *OsFTL2*, *OsFTL3*, WD domain, *OsFBO0* and *OsFBO9*, were altered under microgravity (Fig. 7d). According to these results, we proposed a model to address microgravity involved in rice photoperiodic flowering pathway. In this model, microgravity affected the signaling cascades of photoperiodic flowering of rice is indicated. Expression of *GI* and *OsPhyB* was down-regulated by microgravity. In addition, *OsCOP1* was also slightly down-regulated, but *RFT1* and

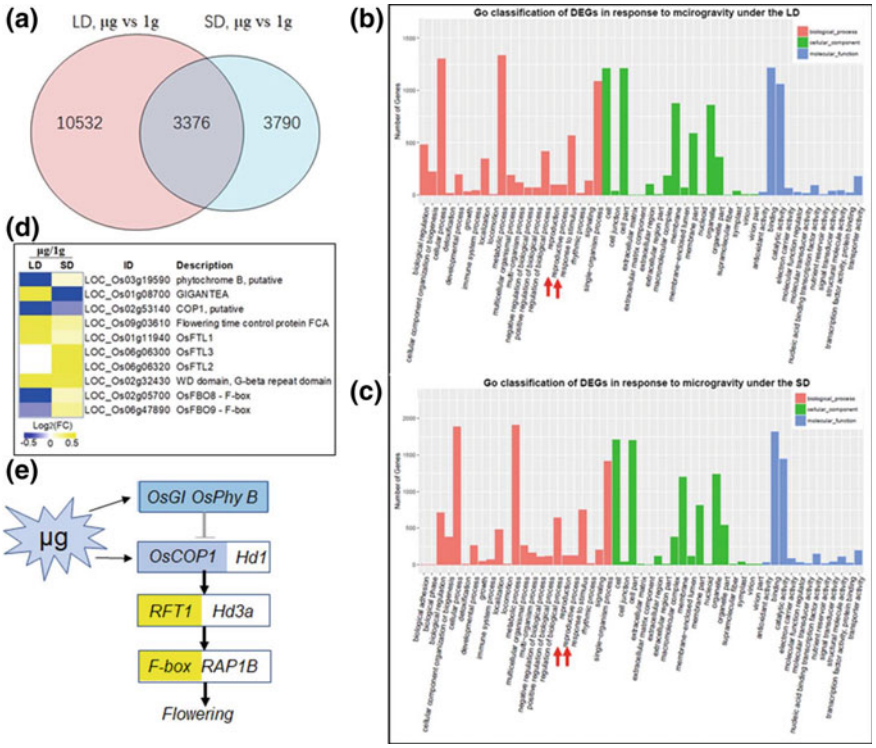

Fig. 7 Microgravity regulated genes in rice leaves grown in space under different photoperiod conditions in comparison with their controls on ground. **a** Vennen diagram of transcriptome data. **b** and **c** GO classification of differential expression of genes (DEGs) of microgravity response genes under the LD and the SD conditions, respectively. **d** Expression profile of photoperiod controlling flowering under microgravity (μg) in comparison with their controls on ground (1 × g) under the LD and the SD conditions, respectively. Yellow indicates an increase in expression, blue indicates a decrease in expression. Scale bar shows $\log_2$ fold changes (FC). **e** Proposed model of the influence of microgravity involved in photoperiod pathway in rice flowering controlling. In this model, microgravity affected the signaling cascades of photoperiodic flowering is indicated. Expression of *GI* and *phytochrome B* (*OsPhyB*) was down-regulated by microgravity. In addition, the expression of *OsCOP1* was also slightly down-regulated, but the expression of *RFT1* and F-box protein genes, such as *OsFBO8* and *OsFBO9*, were up-regulated to controlling rice flowering under microgravity

F-box protein genes, such as *OsFBO8* and *OsFBO9*, were up-regulated to controlling rice flowering under microgravity.

2.4 Application of GFP Technique for FT Visualization on the SJ-10 Satellite

The GFP camera in the PGB (Fig. 2) was the first generation of hardware designed to collect GFP expression data in real-time aboard a spaceflight experiment. A system of blue-light emitting diodes (LEDs) for excitation of GFP and a specially designed narrow band pass filter with a spectrum spread of λ 475/40 nm. Imaging is accomplished with a 10 mega pixel CMOS imager that can capture the leaves of seedlings grown in the CC in a 1280 × 1024 pixel image and these images then were transferred into on-board 3 mega pixel video chips before processing and storage on a local SD card. Telemetry was used to transmit GFP fluorescence images by issuing the commands to perform the functions of taking and downloading images from the ground controlling computer. In addition, the functions of imager and lighting can be modified by uploading commands.

One of the goals of our SJ-10 satellite experiment was to address specifically the possibility that microgravity affect photoperiod induced flowering and to assess whether the movement of FT from leaf to shoot apex under microgravity was similar to control terrestrial transformation of FT. Heat shock (HS)-inducible gene expression systems can respond to spatial information provided by localized heating, which is easy to handle in space experiment. On the SJ-10 satellite experiments, we used the advantages of HS-inducible gene switch and developed transgenic Arabidopsis containing the *HSP* gene promoter linked to the GFP reporter gene and the *FT* gene, respectively. The expression of *pHSP*::*GFP* and *pHSP*::*FT* were by locally heating Arabidopsis leaves grown in space at 37 °C for half hour under the SD condition (Fig. 8a, b). After the *HSP* promoter was activated by local heating the leaves, expression of FT gene was monitored by observed the GFP influorescence produced in the induced leaves through the GFP imager camera. The images downloaded from the SJ-10 satellite plants showed that a strong GFP influorescence appeared in the heating treated leaves (Fig. 8d) in comparison with those untreated leaves in the same condition (Fig. 8c). This confirmed that this heat shock system was effective to induce expression of goal genes (i.e., *GFP* and *FT*) and useful to monitor activation of genes under microgravity in space.

3 Conclusion and Outlook

One of the key developmental processes for plant produce seeds is the differentiation of the shoot apical meristem into a floral meristem. This process has been proven to be regulated by both endogenous and environmental factors. Gravity and light are considered as two of the most important environmental factors that control plant flowering development. In recent years, the studies on the effect of light on plant development have been tremendous progress due to identification of numerous genes involved in flowering regulation, but whether plants can follow the same rule to

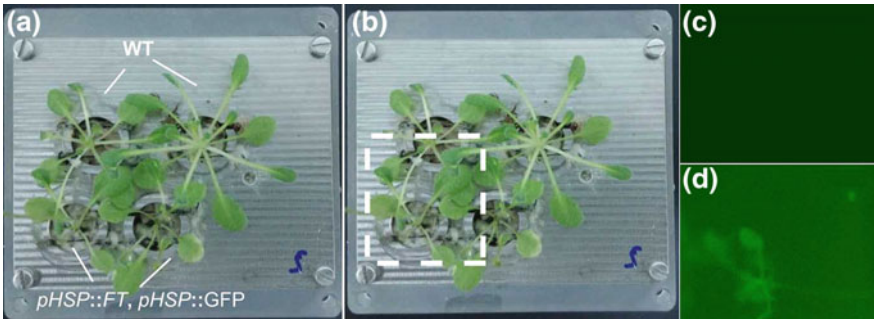

Fig. 8 Arabidopsis plants distribution in a root module and a representative fluorescence image of leaves before and after heating treated. **a** An example of the SJ-10 satellite plants distributed in a root module, including two wild-type (WT) plants and two transgenic plants, *pHSP*::*FT*, *pHSP*::*GFP*. **b** The framed region in dotted lines indicated the heating treated area. **c** The fluorescence image of the framed region before the heating treatment. **d** The fluorescence image of transgenic plants (*pHSP*::*FT*; *pHSP*::*GFP*) under the SD (8 h light/16 h dark) condition on board the SJ-10 satellite in the framed region 2 h after half hour 37 °C heating treatment

determine their flowering time under microgravity in space is unknown. Although numerous attempts have been made to grow a plant through a complete life cycle in space, apparently no published information exists concerning the flowering control of plant in space. In this study, we successfully grew two different type photoperiodic response model plants, the LD flowering Arabidopsis and the SD flowering rice in space on board SJ-10 satellite for 12 days. *FT* gene expression patterns in Arabidopsis leaves were also observed by a GFP imager. Finally, transcriptomes of Arabidopsis and rice response to microgravity under the LD and the SD conditions were obtained. Our results indicated that *GI* could be a key gene for both Arabidopsis and rice adaptation to microgravity in adjusting photoperiod pathways, GI-CO-FT module in Arabidopsis or GI-Hd1-Hd3a module in rice. As we know, this is the first time that examination of plant flowering control in space at molecular level.

In the future, long-term space experiments from successive generations and a systematic analysis of regulatory networks at the molecular level is needed to understand the mechanism of plant flowering control under microgravity condition in space. On board the Chinese space lab TG-2, we have extended to study the effect of microgravity on flowering control of Arabidopsis and rice, which were grown in space from seed to seed. The results will be reported in the future paper. The genes involved microgravity response identified in space experiments so far represent only a very small part of the plant genome and many other microgravity-responsive genes, including those in regulating plant flowering, will likely be identified in the future. For example, genes that control the activities of the pathways in the regulation of flowering timing in plants under microgravity will be very interested, because they will enable the manipulation of flowering time in crop species, which could have a major impact on the production of plants in bioregenerative life support system (BLSS). The energy using in plant cultivation on aboard spacecrafts such as space

shuttle and space station, and even the future space farm must rely on solar battery or fuel cell, which will be severely restricted on board long-term missions. How to increase of production efficiency of plant will be the most important task in setting up BLSS. A acceleration of flowering time in seed crops, such as rice and wheat, while prevention of bolting in vegetable plants, such as sugarbeet, many *Brassica* species, potato, spinach, and lettuce would significantly improve yield. Thus, control of flowering time by manipulation will be clearly an important biotechnological method to increase the productive of BLSS.

Acknowledgements The authors are indebted to Prof. W. R. Hu for suggestion in space experiment design and Prof. Tao Zhang's group for PGB construction. This work was supported by the National natural fund joint fund project (U1738106), the Strategic Pioneer Projects of CAS (XDA15013900), the National Natural Science Foundation of China (31670864), the China Manned Space Flight Technology project TG-2 and the National Science Foundation for Young Scientists of China (31500687).

References

Adamchuk NI, Mikhaylenko NF, Zolotareva EK et al (1999) Spaceflight effects on structural and some biochemical parameters of Brassica rapa photosynthetic apparatus. J Gravit Physiol 6:95–96

Cogoli A, Gmünder FK (1991) Gravity effects on single cells: techniques, findings and theory. Adv Space Biol Med 1:183–248

De Micco V, Arena C, Pignalosa D, Durante M (2011) Effects of sparsely and densely ionizing radiation on plants. Rad Env Biophy 50:1–19

De Micco V, De Pascale S, Paradiso R et al (2014) Microgravity effects on different stages of higher plant life cycle and completion of the seed-to-seed cycle. Plant Biology 16(suppl.1):31–38

Driss-Ecole D, Legue V, Carnero-Diaza E et al (2008) Gravisensitivity and automorphogenesis of lentil seedling roots grown on board the international space station. Physiol Plant 134:191–201

Fengler S, Spirer I, Neef M, Ecke M, Nieselt K, Hampp R (2015) A whole-genome microarray study of Arabidopsis thaliana semisolid callus cultures exposed to microgravity and nonmicrogravity related spaceflight conditions for 5 days on board of Shenzhou 8. BioMed Res Int Article ID 547495

Halstead TW, Dutcher FR (1987) Plants in space. Ann Rev Plant Physiol 38:317–345

Hampp R, Hoffmann E, Schönherr K et al (1997) Fusion and metabolism of plant cells as affected by microgravity. Planta 203:S42–53

Haughn GW, Sommerville C (1986) Sulfonylurea-resistant mutants of Arabidopsis thaliana. Mol Gen Gen 204:430–434

Hoson T (2014) Plant growth and morphogenesis under different gravity conditions: relevance to plant life in space. Life 4:205–216

Jiao S, Hilaire E, Paulsen AQ et al (1999) Ultrastructural observation of altered chloroplast morphology in space-grown *Brassica rapa* cotyledons. J Gravit Physiol 6:93–94

Jiao S, Hilaire E, Paulsen AQ et al (2004) *Brassica rapa* plants adapted to microgravity with reduced photosystem I and its photochemical activity. Physiol Plant 122:281–290

Jung C, Pillen K, Staiger D et al (2017) Editorial: recent advances in flowering time control. Front Plant Sci 7:2011

Kiss JZ, Katembe WJ, Edelmann RE (1998) Gravitropism and development of wild-type and starch-deficient mutants of Arabidopsis during spaceflight. Physiol Plant 102:493–502

Kordyum EL (2014) Plant cell gravisensitivity and adaptation to microgravity. Plant Biol 16(S1):79–90

Kordyum EL, Chapman DK (2017) Plants and microgravity: patterns of microgravity effects at the cellular and molecular levels. Cyt Gen 51:108–116
Kuang A, Xiao Y, Mcclure G et al (2000) Influence of microgravity on ultrastructure and storage reserves in seeds of *Brassica rapa* L. Ann Bot 85:851–859
Kwon T, Sparks JA, Nakashima J et al (2015) Transcriptional response of Arabidopsis seedlings during spaceflight reveals peroxidase and cell wall remodeling genes associated with root hair development. Amer J Bot 102:21–35
Levinskikh MA, Sychew VN, Derendyaeva TA et al (2000) Analysis of the spaceflight effects on growth and development of super dwarf wheat grown on the space station Mir. J Plant Physiol 156:522–529
Link BM, Durst SJ, Zhou W et al (2003) Seed-to-seed growth of Arabidopsis thaliana on the international space station. Adv Space Res 31:2237–2243
Link BM, Busse JS, Stankovic B (2014) Seed-to-seed-to-seed growth and development of Arabidopsis in microgravity. Astrobiology 14:866–875
Mashinsky A, Ivanova I, DerendyaevaT et al (1994) "From seed-to-seed" experiment with wheat plants under space-flight conditions. Adv Space Res 14:13–19
Merkys AL, Laurinavicius RS (1983) Complete cycle of individual development of *Arabidopsis thaliana* (L.) Heynh. Plants on board the Salyut-7 orbital station. Dokladi Akademii Nauk SSSR 271:509–512
Musgrave ME, Kuang A, Matthews SW (1997) Plant reproduction during spaceflight: importance of the gaseous environment. Planta 203:S177–S184
Musgrave ME, Kuang A, Xia Y et al (2000) Gravity independence of seed-to-seed cycling in *Brassica rapa*. Planta 210:400–406
Paul A-L, Daugherty CJ, Bihn EA et al (2001) Transgene expression patterns indicate that spaceflight affects stress signal perception and transduction in Arabidopsis. Plant Physiol 126:613–621
Paul A-L, Amalfitano CE, Ferlr J (2012) Plant growth strategies are remodeled by spaceflight. BMC Plant Biol 12:232
Paul A-L, Wheeler RM, Levine HG et al (2013) Fundamental plant biology enabled by the space shuttle. Amer J Bot 100:226–234
Popova AF (2003) Comparative characteristic of mitochondria ultrastructural organization in Chalorella cells under altered gravity conditions. Adv Space Res 31:2253–2259
Putterill J, Laurie R, Macknight R (2004) It's time to flower: the genetic control of flowering time. BioEssays 26:363–373
Soga K, Club B, Kurita A et al (2014) Growth and morphogenesis of Azui bean seedlings in space during SSAF2013 program. Biol Sci Space 28:6–11
Srikanth A, Schmid M (2011) Regulation of flowering time: all roads lead to rome. Cell Mol Life Sci 68:2013–2037
Strickland DT, Campbell WF, Salisbury FB et al (1997) Morphological assessment of reproductive structures of wheat grown on Mir. Gravit Space Biol Bull 11:14
Sychev VM, Levinskikh MA, Gostimsky SA, Bingham GE, Podolsky IG (2007) Space flight effects on consecutive generations of peas grown onboard the Russian segment of the international space station. Acta Astronaut 60:426–432
Tan C, Wang H, Zhang Y et al (2011) A proteomic approach to analyzing responses of Arabidopsis thaliana root cells to different gravitational conditions using an agravitropic mutant, *pin2* and its wild type. Proteome Sci 9:72
Tanaka N, Itoh H, Sentoku N et al (2011) The COP1 ortholog PPS regulates the juvenile-adult and vegetative-reproductive phase changes in rice. Plant Cell 23:2143–2154
Tripathy BC, Brown CS, Levine HG et al (1996) Growth and photosynthetic responses of wheat plants grown in space. Plant Physiol 110:801–806
Wang L, Han F, Zheng HQ (2018) Photoperiod-controlling guttation and growth of rice seedlings under microgravity on board Chinese spacelab TG-2. Microgravity Sci Tech. https://doi.org/10.1007/s12217-018-9644-3

Yano S, Kasahara H, Masuda D, Tanigaki F, Shimazu T, Suzuki H, Karahara I, Soga K, Hoson T, Tayama I, Tsuchiya Y, Kamisaka S (2013) Improvements in and actual performance of the plant experiment unit onboard Kibo, the Japanese experiment module on the international space station. Adv Space Res 51:780–788

Zhang Y, Wang L, Xie J et al (2015) Differential protein expression profiling of *Arabidopsis thaliana* callus under microgravity on board the Chinese SZ-8 spacecraft. Planta 241:475–488

Zheng HQ (2018) Flowering in space. Microgravity Sci Tech. https://doi.org/10.1007/s12217-018-9626-5

Zheng HQ, Wang H, Wei N et al (2008) Live imaging technique for studies of growth and development of Chinese cabbage under microgravity in a recoverable satellite (SJ-8). Microgravity Sci Tech 20:137–143

Zheng HQ, Han F, Le J (2015) Higher plants in space: microgravity perception, response, and adaptation. Microgravity Sci Tech 27:377–386

The Maintaining and Directed Differentiation of Hematopoietic Stem Cells Under Microgravity

Peng Wang, Juanjuan Qian, Hongling Tian and Yong Zhao

Abstract Hematopoietic stem cells (HSCs) are a major kind of pluripotent stem cells, which can give rise to all the other blood cells through the process of haematopoiesis and maintain the homeostasis of organism. HSCs are divided into three types based on their differentiation stage, including long-term self-renewing HSCs (LT-HSCs), short-term self-renewing HSCs (ST-HSCs) and multipotent progenitors (MPPs). These HSCs eventually differentiate into mature blood cells and immune cells after experiencing various common lymphoid progenitor (CLP) and common myeloid progenitor (CMP). The proliferation and differentiation of HSCs have been widely studied and revealed be controlled by various factors, molecules and transcription factors but litter is known about how microgravity affects HSCs. Our study was conducted in two flight programs, SJ-10 recoverable microgravity experimental satellite (SJ-10 satellite) program research and Tianzhou-1 cargo ship program, and mainly focuses on the maintaining and directed differentiation of hematopoietic stem cells. Our results revealed some new mechanisms for maintaining and directed differentiation under microgravity conditions, with the potential to boost immune system, and provide potential drugs for the prevention or treatment of immune system weakening in spaceflight.

Abbreviations

CBSC	Cord blood stem cells
CFU-G	Colony forming units-granulocyte
CFU-GM	Colony forming units-granulocyte macrophage
CFU-M	Colony forming units-macrophage
CLP	Common lymphoid progenitor
CMP	Common myeloid progenitor

P. Wang · J. Qian · H. Tian · Y. Zhao (✉)
State Key Laboratory of Membrane Biology, Institute of Zoology, Chinese Academy of Sciences, Beijing, China
e-mail: zhaoy@ioz.ac.cn

E. Duan and M. Long (eds.), *Life Science in Space: Experiments on Board the SJ-10 Recoverable Satellite*, Research for Development,
https://doi.org/10.1007/978-981-13-6325-2_9

DC	Dendritic cell
EP	Erythrocyte progenitor
GM-CSF	Granulocyte/monocyte colony-stimulating factor
GMP	Granulocyte/macrophage progenitor
GP	Granulocyteprogenitor
HSCs	Hematopoietic stem cells
HSPCs	Hematopoietic stem and progenitor cells
LT-HSCs	Long-term self-renewing HSCs
MacP	Macrophage progenitor
M-CSF	Macrophage-colony stimulating factor
MEP	Megakaryocyte/erythrocyte progenitor
MkP	Megakaryocyte progenitor
MPPs	Multipotent progenitors
NGS	Next-generation sequencing
NK	Natural killer
RBCM	Red blood cell mass
RWV	Rotating wall vessel
SJ-10 satellite	SJ-10 recoverable microgravity experimental satellite
SL-3	Spacelab 3
SLS-1	Splace lab Life Science 1
ST-HSCs	Short-term self-renewing HSCs
STS-40	Space Shuttle Orbiter Columbia
WBC	White blood cell

1 Introduction

Since the beginning of space travel, a number of reports regarding the deleterious effects of spaceflight on the human health emerge in endlessly. Life during spaceflight includes multiple stressed factors, such as microgravity, radiation, loss of light-dark cycle and confinement. Among all these factors, microgravity (between 10^{-3} and 10^{-5} g) exposure is the most important and stable factor reportedly affected human physiological and psychological functions (Grigor'ev 2007; Wichman 2005). It is clear from the last 50 years of space research that a series of changes occurred in human blood, including anemia, thrombocytopenia, a reduction in the numbers and suppressive function of lymphocytes, and structural abnormalities of the red blood cells (Davis et al. 1996; Blaber et al. 2010) during and post spaceflight. In recent years, the effects of microgravity on immune function have received more and more attentions, and have been investigated through analysis of blood leukocytes obtained from astronauts5, cells secured from space-flown mice and rats (Kraemer et al. 2004; Hwang et al. 2015) and in vitro cell culture (Paulsen et al. 2015). The composite data from International Space Station, Skylab and Shuttle flight suggest that deregulated immune-cell–mediated cytokine secretion is a major mechanism of spaceflight-associated immune dysfunction (Taylor et al. 1997; Tauber et al. 2017;

Hughes-Fulford et al. 2015; Stowe et al. 2011; Crucian et al. 2008). Therefore, this chapter aims to summarize the latest progress related to the maintaining and directed differentiation of hematopoietic stem cells under microgravity in recent ten years and the scientific achievements in SJ-10 satellite research.

2 The Effects of Microgravity/Spaceflight on Immune System

Besides impact hematopoietic generation and hematopoietic system, spaceflight and microgravity also extensively altered various immune parameters and immune response. Changes in resistance to bacterial and viral infections in Apollo crew members have stimulated interest in the study of immunity and space flight. Results of studies from several laboratories in both humans and rodents have indicated alterations after space flight that include the following immunological parameters: thymus size, lymphocyte blastogenesis, interferon and interleukin production, natural killer cell activity, cytotoxic T-cell activity, leukocyte subset population distribution, response of bone marrow cells to colony stimulating factors, and delayed hypersensitivity skin test reactivity. The interactions of the immune system with other physiological systems, including muscle, bone, and the nervous system, may play a major role in the development of these immunological parameters during and after flight (Sonnenfeld 2002). There are studies about direct effects of space flight on immune responses. Data collected before and after 11 Shuttle space flights show that absolute lymphocyte numbers, lymphocyte blastogenic capability, and eosinophil percent in the peripheral blood of crewmembers are generally depressed postflight. 11 astronauts on shuttle flight 41B and 41D showed decreased circulating monocytes and B lymphocytes in peripheral blood post flight (Taylor et al. 1986). Researchers investigated spaceflight and microgravity on immune responses of rats flown on Biosputnik Cosmos 1887 and Cosmos 2044. The response to macrophage-colony stimulating factor (M-CSF) and granulocyte/monocyte colony-stimulating factor (GM-CSF) of rat bone marrow cells from Cosmos 1887 and 2044 were detected, respectively. The results are similar, which indicated that bone marrow cells from flown rats showed a decreased response to M-CSF and GM-CSF. Meanwhile, researchers also detected surface antigenic markers of immunocytes and they found that the percentages of suppressor T cells and helper T cells in spleens of flown rats on Cosmos 1887 and 2044 both increased (Sonnenfeld et al. 1990, 1992). Bone marrow cells from flown rats on Cosmos 2044 showed an increase in the percentage of cells expressing markers for helper T-cells in the myelogenous population and increased percentages of anti-asialo granulocyte/monocyte-1-bearing interleukin-2 receptor-bearing pan T- and helper T-cells in the lymphocytic population (Sonnenfeld et al. 1992).

During the nine-day spaceflight on the Space lab Life Science 1 (SLS-1) mission on the shuttle Columbia in 1991, experiments including 29 spaceflight male rats and 30 ground controls were conducted to research the effects of microgravity on the total and absolute leukocyte counts of flight rats and assess the lymphocyte subset immune competence in flight rats. Allebban et al. found there was a significant decrease in the number of total leukocytes ($P < 0.0001$) and absolute counts of lymphocytes ($P < 0.0001$) and monocytes ($P < 0.0001$) of flight animals compared with ground controls at the landing day. Meanwhile, there was a slight decrease in the absolute number of eosinophils and a slight increase in the number of neutrophils of flight animals at landing compared with the preflight count. However, the observed decrease in the number of leukocytes and lymphocytes at landing returned to the control levels after a nine-day recovery phase. Immunophenotyping of the peripheral blood and spleen lymphocytes of flight and control animals indicated that, on the day of landing, there was a decrease in the absolute number of $CD4^+$ and $CD8^+$ T cells and B lymphocytes. However, the relative percentages of peripheral blood $CD4^+$, $CD8^+$, and B cells were not found to be depressed. There were no differences in the percent reactivity of spleen lymphocytes of flight animals compared with controls (Allebban et al. 1994). Based on the different responses of peripheral blood and spleen lymphocyte to spaceflight, it seems that there is a compartmentalized response to microgravity, and this was consistent with previous study revealed microgravity effects on individual lymphatic tissues had tissue-specific effect (Nash and Mastro 1992).

Further, researchers carried out experiments more scientific on SLS-2 mission, the second flight of SLS series. Analyses on rats were performed prior to the flight, on recovery and at intervals following recovery. Meanwhile, unlike all other previous spaceflight missions, a group of rats on SLS-2 was killed and dissected by astronauts in space. The main objective of the SLS-2 study is to determine the effects of spaceflight on the hematopoietic system. Lchiki et al. analyzed the white blood cell (WBC) compositions and the bone marrow myeloid progenitor cell populations to ascertain adaptation to microgravity and subsequent readaptation to microgravity and subsequent readaptation to 1 G in rats flown on the 14-day SLS-2 mission. Researcher found that except neutrophilia, the WBC level in flight rats was normal at landing compared to ground control rats. Compared with ground control rats, numbers of colony forming units-granulocyte (CFU-G), colony forming units-granulocyte macrophage (CFU-GM) and colony forming units-macrophage (CFU-M) from flight rats at day 13 in flight were decreased when incubated with recombinant rat interleukin-3 (rrIL-3) alone or in combination with recombinant human erythropoietin (rhEpo). However, on recovery, flight rats had decreased numbers of total leukocytes and absolute numbers of lymphocytes and monocytes with elevated neutrophils compared with control rats. Meanwhile, flight rats had lower numbers of CD4, CD8, CD2, CD3 and B cells in the peripheral blood than ground controls, but no differences in spleen lymphocytes (Ichiki et al. 1996).

3 The Effects of Microgravity/Spaceflight on Hematopoietic Cells

Human have been exploring the space for more than 50 years. Compared to the normal earth environment, short- and long-duration spaceflight provides an abnormal environment for us. During a spaceflight, astronauts and laboratory animals are exposed to outer space environments which contain various factors harmful for organisms, and these factors include specific and unspecific factors. Specific factors are permanent factors of outer space, including microgravity, ionizing radiation, background radiation created by high-energy particles and factor influence circadian rhythms. While unspecific factors are produced in the process of spaceflight mission-launching and landing, including hypergravity, noise, vibrations and G force shock (Domaratskaya et al. 2002). Both the specific and unspecific factors are important for the health of astronauts. Microgravity is the largest effect in spaceflight, which affects physiological systems of human and experimental animal.

Short- and long-duration spaceflight could produce complex physiological changes, including fluid redistribution, neuro vestibular effects, muscle changes, bone demineralization and loss, immune dysregulation, and psychosocial changes in human (Williams et al. 2009). Similarly, spaceflight and microgravity also altered physiological systems of animal. Experiment carried on 45 rats also demonstrated microgravity could cause physiological, biochemical and morphological changes in the animal body in a 22 day's spaceflight on biosatellite Cosmos-605 (Ilyin et al. 1975).

Lots of experimentations and studies have indicated that short- and long-duration spaceflight could alter a wide variety of hematopoietic and immunological responses, including decreased plasma and blood cell mass, altered blood flow, lymphocyte and eosinophil numbers, increased immunoglobulin A and M levels (Graebe et al. 2004; Vernikos 1996).

In order to better understand the effects of spaceflight on bone morrow and hemopoietic system, lots of study and experiments has been studied on the satellite, space shuttle and spaceship. Astronauts always showed anemia and extent of changes on hematopoietic system after experience shot- or long-during spaceflight, including thrombocytopenia, and abnormalities in red blood cell structure (Davis et al. 1996). Numerous studies have proved that exposure aboard a spacecraft leads to lots of changes in the peripheral blood of astronauts. Researchers detected red-cell mass of astronauts on two Skylab missions. The results showed there was a 14% mean decrease in red-cell mass after the 28-day mission and a 12% mean decrease after the 59-day mission. Meanwhile, plasma volume decreases after each mission, and it decreased greater after the 59-mission (Johnson et al. 1975). Iliukhin et al. observed cytokinetic and morphological changes in erythropoiesis of crews experienced 96-, 140- and 175-days spaceflight. The number of circulating erythrocytes decreased in flight and their life time reduced postflight (Iliukhin and Burkovskaia 1981).

Mercury, Gemini, and Russian manned orbital flights gave us the first opportunity to evaluate the actual effects of spaceflight on human being. Various blood indices including plasma volume, red blood cell mass and erythrocyte survival were detected on the Gemini astronauts before and after Gemini orbital flights IV (1965), V (1965) and VII (1965). Though the three spaceflight were affected by different stresses, investigators found plasma volume changes associated with the shorter flights, and it may have been compensated for in the longer Gemini VII flight. At the same time, the survival of erythrocytes and red blood cell mass in Gemini V and VII decreased and there was no compensation for the RBC mass even in the longer flight (Fischer et al. 1967). However, the mechanistic and the cause is unknown.

Because some data could not be obtained in human studies, there also carried out animal experiments during spaceflight to thoroughly study the effects of spaceflight and microgravity. Lots of experiments have proved that spaceflight and microgravity could change the hemopoietic system of rats. On the Soviet biosatellite Cosmos 782, which was launched in 1972, rats experienced a 19.5 day of weightless spaceflight. Based on the output of radioactive CO, survival parameters of erythrocytes were evaluated upon return from orbit. The results indicated that all survival factors and indexes of erythrocytes were altered in flight rats when compared to the ground control rats. Compared to vivarium control rats, the mean potential lifespan, measured size of erythrocytes in flight rats decreased. Meanwhile, random hemolysis was increased three-fold in the flight rats (Leon et al. 1978). During the 18–22 day's spaceflight aboard on Cosmos biosatellites, Shvets et al. investigated the histogenesis of the hemopoietic tissue at the level of stem cells, the results showed microgravity could inhibit the erythropoiesis in various skeletal sites (Shvets et al. 1984). A life science module housing young and mature rats was flown on shuttle mission Spacelab 3 (SL-3) to research the effects of spaceflight and microgravity on blood. The results of hematology studies of flight and control rats indicated the hematocrit, red blood cell counts, and hemoglobin determinations were significantly increased in flight animals. Meanwhile, the flight rats also accompany with a mild neutrophilia and lymphopenia. Lange et al. first performed the erythropoietin assays and clonal studies. There were no significant changes in bone marrow and spleen cell differentials or erythropoietin determinations. Clonal assays demonstrated an increased erythroid colony formation of flight animal bone marrow cells at erythropoietin doses of 0.02 and 1.0 U/ml but not 0.20 U/ml (Lange et al. 1987).

The recovery of normal blood count and the maintenance of hemopoiesis at a constant level are provided for by clonogenic hemopoietic cells of the stem cell and the committed progenitor cell compartments. Hence, changes observed in the peripheral blood can reflect more profound processes occurring in the hemopoietic tissues under the effect of spaceflight factors. In order to study the effects of microgravity on physiological parameters of organisms, Spacelab Life Sciences-1 (SLS-1) was launched aboard Space Shuttle Orbiter Columbia (STS-40) by NASA in 1995. During the spaceflight on SLS-1 mission, researches conducted a comprehensive examination of erythropoiesis and blood volume regulation in rats during space travel. Researchers assessed RBCM (red blood cell mass), PV (plasma volume), reticulocyte counts, marrow erythropoietin levels, iron utilization and storage, RBC survival,

and RBC shape. On landing day (R^+0), they found RBCM and PV adjusted for body mass were significantly lower in the flight animals than controls. Their results also suggested the decrease in RBCM exposure to microgravity during spaceflight was not due to hemolysis or splenic sequestration. The flight animals had lower reticulocyte counts during early recovery, which indicated diminished erythropoiesis during the post-flight study period. Meanwhile, researchers also conducted clonal assays to determine the hematopoietic generating capacity. The flight animals had a significantly decreased number of BFU-e's and CFU-e's recovered from their morrows on landing day at various levels of exogenous EPO, which indicated the numbers of bone morrow erythroid progenitors were decreased in flight animals. However, the result is contradict with the experiments on SL-3 (Lange et al. 1987). Besides the experiments above-mentioned, researchers also detected the RBC counts, Hgb, the number of RBC with atypical shapes and serum EPO, while there were no significant differences in these indexes between spaceflight and ground control animals (Udden et al. 1995). Further, there are study investigate the effects of microgravity and increased gravity on bone marrow of rats. Experiments were carried out in microgravity on rats flown on Soviet Biosatellite 2044 and in hypergravity by centrifugation at 2 × g. Lange et al. investigated bone marrow cell differential counts, clonal studies of RBC colony formation, and plasma erythropoietin determinations of spaceflight rats and ground control rats. The results showed bone marrow cells of spaceflight rats formed fewer CFU-e than ground control rats, which is consistent with previous results conducted on SLS-1 but contradict with the experiments on SL-3 (Lange et al. 1987; Udden et al. 1995). Furthermore, rats in hypergravity formed more CFU-e than ground control rats, which suggested that the decreased proliferative potential directly produced by microgravity could be reversed by hypergravity (Lange et al. 1994).

Consistently, Vacek et al. found the decreased colony forming of hematopoietic cells during spaceflight was caused by specific factor, mainly microgravity. To prove and differentiate the effects of specific and unspecific spaceflight factors on the hemopoietic tissue, researches designed three groups of animals, including the flight group (F), the synchronous control group (SC) and the vivarium ground control group (VC). The flight group was exposed to the entire spaceflight factors (specific and unspecific) aboard the satellite; the synchronous control group was exposed to unspecific spaceflight factors simulated on land; the vivarium control group was kept under normal laboratory conditions. Researchers found the number of CFU-s decreased significantly in bone marrow, spleen, and liver of flown rats on Cosmos-1129, Cosmos-1514, Cosmos-1667 and Cosmos-1887, and the phenomenon was irrespective of sex of rats (Vacek et al. 1985; Domaratskaya et al. 2002). These results revealed that the numbers of CFU-s in bone marrow of flight group rats significantly decreased compared to that of SC and VC group rats. Therefore, it was the effect of specific spaceflight factors lead to the decrease of CFU-s content in the bone marrow. Meanwhile, the numbers of CFU-s contents in the spleen of flight group rats were comparable to those in SC rats. So, the changes of CFU-s content in the spleen of flight group to vivarium control group were caused by unspecific factors. It also demonstrated the decrease of CFU-s content in the main hemopoietic organ

of adult animals-bone marrow, was not because of the redistribution of these cells to the spleen or liver. Vacek et al. also found that a significant decrease was revealed in the contents of progenitor cells of the granulocyte and erythrocyte lineages in the rat bone marrow after a 14-days spaceflight. The number of CFU-gm was about 3–6-fold lower, and the numbers of BFU-e and CFU-e was about of 2.5 and 1.5-fold lower, respectively, than in rats of the VC and SC groups. Vacek et al. also found in the bone marrow of F rats, the number of CFU-f (progenitors of stromal fibroblasts) became almost 15-fold lower than in SC and VC rats, and no differences in this parameter between the two control groups were revealed (Vacek et al. 1990). These data suggest that bone marrow CFU-f is sensitive to the specific spaceflight factors. Hodgson et al. thought that the number of CFU-s naturally decreases because of their differentiation into more "advanced" cell forms, and it appears that the loss of CFU-s during spaceflight is also not counter balanced by the input of "younger" and more potent cells from the stem cell compartment (Hodgson and Bradley 1979).

Spaceflight/microgravity both impacts the proliferation and differentiation of hematopoietic progenitor cells. Davis et al. found that spaceflight/microgravity reduced proliferation and differentiation. During the space shuttle missions STS-63 (Discovery) and STS-69 (Endeavour), researchers investigated the in vitro effects of spaceflight on hematopoietic cell proliferation and differentiation (Davis et al. 1996). $CD34^+$ bone marrow progenitor cells were cultured in a culture system with hematopoietic supportive stromal cells under microgravity/spaceflight or normal gravity, respectively. After 11–13 days of culture, they found the total cell number under microgravity/spaceflight was significantly less than that under normal gravity (57–84% decrease). As for the specific progenitor cell types, microgravity/spaceflight significantly decreased the number of myeloid progenitor cell number and erythroid progenitor cell number, especially erythroid progenitor cell number. These results indicate that spaceflight has a direct effect on hematopoietic progenitor cell proliferation and differentiation and those specific aspects of in vitro hematopoiesis, particularly erythropoiesis.

Besides human and rats, the effects of spaceflight/microgravity on hemopoietic tissues and cells have also been proved on lower vertebrates. Michurina et al. adapted the method of hemopoietic cell transplantation into irradiated recipients for analyzing the effect of spaceflight factors on clonogenic hemopoietic cells of newts. On the biosatellites Bion-10 and Bion-11, they first transplant hemopoietic cell into irradiated recipients for analyzing the effect of spaceflight factors on clonogenic hemopoietic cells. After newts were exposed on board the Bion 11 satellite, the hemopoietic cells from these news were transplanted into irradiated recipients and were analyzed after 22 days. Histological analysis results revealed the number and size of the foci of poorly differentiated hemopoietic cells in the spleens of recipients received and the liver hemopoietic cells of flight group newts were significantly smaller compared to that in spleens of recipients received the liver hemopoietic cells of SC group newts. The absence of hemopoietic recovery in the liver, and the decreased size and number of spleen colonies in the recipients of hemopoietic cells was reported from newts of the group flown. This suggest that spaceflight factors have a specific effect on colony-forming (clonogenic) hemopoietic cells of newts (Michurina et al. 1996).

Analysis of morphologically unrecognizable clonogenic hemopoietic cells in lower vertebrates is possible to perform and newts can be adequately used as experimental animals for studying the effects of spaceflight factors on hemopoiesis on board a biosatellite.

Nevertheless, there are studies showed spaceflight and microgravity didn't impact the properties of hematopoietic cells and the hematopoietic generating potential. Kozinets et al. use morphological, interferometric and electron microscopic techniques examined the morphofunctional properties of peripheral blood cells of Cosmos-936 rats and found the changes of microgravity on rat bone morrow cell composition; cell structure and function were reversible. Rats showed symptoms of a stress reaction immediately at landing and disappeared after three days. The percentage of bone marrow cell distribution was shifted towards enhanced myelopoiesis and diminished erythropoiesis. However, after the readaptation period the ratio of bone marrow cell composition returned to the normal level, which seems spaceflight and microgravity seems doesn't intrinsically change properties of hematopoietic system (Kozinets et al. 1983).

Besides the effects of spaceflight/microgravity on bone marrow and hemopoietic system, researchers also investigated the effects of non-specific spaceflight factors on HSCs. An experiment conducted onboard the biosatellite Cosmos-1514 demonstrated that the effects of spaceflight on the proliferative capacity of HSCs also partly owing to the non-specific flight factors, such as launching effect and landing effect (Vacek et al. 1985). After a 5-day stay under microgravity onboard Cosmos-1514, Vacek et al. found synchronous rats also exhibited a decrease in the number of haemopoietic stem cells (CFUs) in bone marrow and spleens compared to ground control rats. This suggested that non-specific flight factors also decrease the number of CFU-s in the spleens of flight in the experiments conducted onboard the Cosmos-2044 Biosatellite of 14-day flight, Vacek et al. investigated the effects of microgravity on the proliferation ability of progenitors in bone marrow. The results of clonal assay demonstrated that the number of progenitors of erythrocytes (erythroid burst-forming units, BFU-e) and of granulocytes and macrophages (colony forming units-granulocyte macrophage, CFU-GM) in bone marrow was decreased in flight rats exposed to microgravity during a 14-day flight onboard the Cosmos-2044 biosatellite when compared to ground control rats. However, the number of progenitors of both lineages of haemopoiesis was also decreased in synchronous control rats, thus suggesting that the pool of progenitors is influenced also by the action of the nonspecific space flight factors (Vacek et al. 1991). The results are similar with previously results conducted on biosatellite Cosmos-1514 (Vacek et al. 1985).

However, there are fewer studies about the mechanisms of the effects of spaceflight/microgravity on hematopoietic system and cells. The reasons that lead to the suppression of hemopoiesis in animals during the post flight period can be attributed to not only the decreased number of different clonogenic hemopoietic cells, but also to changes in the stroma of hemopoietic organs, such as bone marrow, which provide suitable environment for hemopoiesis (Davis et al. 1996). For spaceflight/microgravity could decrease in the number of fibroblast progenitor cells

(CFU-f) was accompanied by a simultaneous reduction in the number of hemopoietic progenitors of granulocytic and macrophagal lineages, which depend on the cytokine (CSF-gm) produced by fibroblasts. Therefore, spaceflight factors may have an adverse effect on the stem cells of both hemopoietic and stromal tissues.

4 The Effects of Simulated Microgravity on Hematopoietic Cells

Human space flight missions have resulted in some hematologic anomalies. Therefore, the effects of microgravity on the hematologic function have drawn the attention of researchers to the health of astronauts. However, because of the rare less chances and very expensive price of spaceflight experiments, researchers imagining conduct experiments to simulate the microgravity effects in spaceflight on ground. NASA designed a rotating wall vessel (RWV) bioreactor that could produce simulated microgravity on ground. Researchers always adopt NASA's RWV bioreactor to investigate the effects of microgravity on cells. The RWV bioreactor rotates the vessel wall and cell culture media at the same speed, which continuously randomized the gravitational vector and maintaining the cells relatively motionless in the fluid and produced the effect of simulated microgravity (Schwarz et al. 1992; Tsao et al. 1992). Simulated microgravity provides a methodology for researching the effects of microgravity on various kinds of cells. Over the past few decades, there are many studies targeting the effects of simulated microgravity on these properties of hematopoietic cells. These researches revealed that simulated microgravity extensively impact the properties of hematopoietic cells, not only the proliferation capacity, but also the differentiation and migration.

CD34 antigen is surface glycophospho protein expressed on developmentally early lymph hematopoietic stem and progenitor cells and is known as hematopoietic progenitor cell antigen (Krause et al. 1996). Bone marrow $CD34^+$ cells contain hematopoietic stem and progenitor cells and they could differentiate into all the various blood cell types. Plett et al. cultured adult human BM $CD34^+$ cells in RWV bioreactors under either stationary state ($1 \times g$ control) or rotated-produced simulated microgravity for 4–6 days. They examined cellular expansion, hematopoietic potential, retention of primitive cell phenotype, apoptotic cell content and adhesion molecule status of these BM $CD34^+$ cells. The results showed that the number of $CD34^+$ cells nearly didn't increased when cultured under simulated microgravity, while cells cultured under normal gravity proliferated up to 3 fold, which demonstrated that simulated microgravity could significantly decreased the proliferative ability of BM $CD34^+$ cells. One possible explanation maybe that simulated microgravity decreased the exit G0/G1 phase of cell cycle and made these BM $CD34^+$ cells at a greater degree of hematopoietic potential. Meanwhile, compared cells cultured under normal gravity, BM $CD34^+$ cells under simulated microgravity condition produced greater numbers of cells and progenitors, and these cells keep survival for a

longer time. However, simulated microgravity did not affect expression of adhesion molecules and induction of apoptosis of BM $CD34^+$ cells (Plett et al. 2001). Further, they also investigated the effects of simulated microgravity on the migration potential, cell-cycle kinetics and progenitor differentiation of BM $CD34^+$ cells and found that simulated microgravity significantly inhibits the migration potential, cell-cycle progression, and differentiation patterns of primitive BM $CD34^+$ cells (Plett et al. 2004). BM $CD34^+$ cells were cultured under simulated microgravity (μg) by using rotating wall vessels (RWV) or under normal gravity in control cultures for 2–18 days. Simulated microgravity significantly decreased the migration potential and this effect may be caused by a significant reduction of stromal cell-derived factor 1 (SDF-1α), which correlated with decreased expression of F-actin and important for cell-directed migration. Simulated microgravity also altered cell-cycle kinetics by prolonged S phase and reduced cyclin A expression. Compared to be cultured under normal gravity, BM $CD34^+$ cells cultured under simulated microgravity condition favored differentiated into more $CD33^+$ myeloid cells (65.8% vs. 6.9%) and less Gly-A^+ erythroid cells (26.0% vs. 61.4%). Chiu et al. investigated the effects of simulated microgravity on the differentiation and proliferation human umbilical cord blood stem cells (CBSC). $CD34^+$ mononuclear cells were isolated from waste human umbilical cord blood samples and stimulated with vascular endothelial growth factor (VEGF) under simulated microgravity for 14 days. Simulated microgravity significantly increased cellular proliferation with three-dimensional (3D) tissue-like aggregates. Meanwhile, $CD34^+$ cells cultured under microgravity without microcarrier beads (MCB) developed vascular tubular assemblies and exhibited endothelial phenotypic markers. These results suggest that $CD34^+$ human umbilical cord blood progenitors are capable of trans-differentiation into vascular endothelial cell phenotype and assemble into 3D tissue structures (Chiu et al. 2005).

Simulated microgravity also significantly influences properties of erythroid progenitor-like K562 leukemia cells. Yi et al. investigated effects of simulated microgravity on proliferation, cell death, cell cycle progress and cytoskeleton of erythroid progenitor-like K562 leukemia cells. The results showed the cell densities cultured in Rotary Cell Culture System (RCCS) were only 55.5%, 54.3%, 67.2% and 66.4% of the flask-cultured control cells when cultured for 24 h, 48 h, 72 h, and 96 h, respectively. RCCS culture induced an accumulation of cell number at S phase and a decrease at G0/G1 and G2/M phases at 12 h, which concomitant with the changes of intercellular cyclins levels that with a decrease in cyclin A and a decrease in cyclin B, D1 and E. However, simulated microgravity seemed didn't impact apoptosis in their experiments (Yi et al. 2009). Consistently, Long et al. found simulated microgravity environment significantly decreased the proliferation rate of K562 cells. Consistently, simulated microgravity environment also significantly inhibited cell cycle progression and made the cell cycle arrested in G0/G1 phase. Further mechanism study suggested that the decreased proliferation rate and the cell cycle arrested in G0/G1 phase under simulated microgravity environment may be caused by decreased expression of ERK1/2 phosphorylation (Long et al. 2011). These results demonstrated that simulated microgravity inhibit proliferation and cell cycle of K562 leukemia cells.

Migration, proliferation, and differentiation of bone marrow (BM) hematopoietic stem cells (HSC) are important factors in maintaining hematopoietic homeostasis. Besides impact the proliferation, differentiation and migration of BM HSCs and erythroid progenitor-like K562 leukemia cells, simulated microgravity also change the properties of erythroid lineage. Arthur J. Sytkowski and Kerry L. Davis reported simulated microgravity significantly inhibit erythroid growth and erythropoietin (Epo)-induced differentiation. Logarithmic growth of rauscher murine erythroleukemia cells was observed when cultured under normal gravity or simulated microgravity condition by using RWA bioreactor (Sytkowski and Davis 2001). Cells in simulated microgravity grew more slowly and its doubling time was nearly two times of cells cultured under normal gravity (24 h vs. 14.4 h). The percentage of Epo-induced cell differentiation under simulated microgravity was significantly lower than cells cultured under normal gravity (25% vs. 12%). However, simulated microgravity didn't impact cell apoptosis, which are consistent with the result that simulated microgravity had no effect on apoptosis of BM $CD34^+$ cells (Plett et al. 2001). Zou et al. found simulated microgravity not only significantly inhibit cellular proliferation rate but also induced cell apoptosis of the human erythropoietin (EPO)-dependent megakaryoblastic leukemia cell line UT-7/EPO. Meanwhile, simulated microgravity could downregulated the expression of erythropoietin receptor (EPOR), which is crucial for the survival, proliferation, and differentiation of erythroid progenitors (Sytkowski and Davis 2001). Further, when transferred human EPOR gene into UT-7/EPO cells, which increased the expression (approximately 61%) of EPOR on the surface of UT-7/EPO cells, they found that simulated microgravity-induced apoptosis markedly decreased in these UT-7/EPO-EPOR cells (Zou et al. 2011).

Migration, proliferation, and differentiation of bone marrow (BM) hematopoietic stem cells (HSC) are important factors in maintaining hematopoietic homeostasis. Simulated microgravity have a board impact on hematopoietic homeostasis. The results obtained from simulated microgravity may partly reflect the effects of microgravity/spaceflight on hemopoietic cells and hemopoietic system. Simulated microgravity provides an effective alternative method to carry out microgravity experiments for majority of researchers. All these results provided some possible explanation of the hematologic abnormalities observed in humans during space flight. However, the mechanistic of simulated microgravity on hemopoietic system has not been clarified and further researches are needed.

5 Regulation of HSCs Self-renewal in BM

5.1 Stem Cells

Stem cells are a kind of undifferentiated biological cells. They possess two primary characteristics: self-renew and differentiation. They can both experience indefinite cycles of cell division while maintaining the undifferentiated state and differenti-

ate into one or more kinds of functionally mature cells of particular tissues, such as cardiomyocytes, haematopoietic cells, chondrocytes, adipocytes and endothelial cells. Based on the differentiation potential, also known as the number of mature cell types to which they can give rise, stem cells can be divide into totipotent stem cells, pluripotent stem cells, multipotent stem cells, oligopotent stem cells and unipotent cells (Hans 2007). Totipotent stem cells can differentiate into embryonic and extraembryonic cell types. Pluripotent stem cells are the descendants of totipotent cells and can differentiate into nearly all cells. Multipotent stem cells can differentiate into a number of cell types. Oligopotent stem cells can differentiate into only a few cell types. Unipotent cells are cells with lowest differentiation capacity, which can produce only one cell type, their own. However, they have the property of self-renewal, which distinguishes them from non-stem cells, such as progenitor cells. According to the developmental stages, stem cells could be divided into two types in mammals: embryonic stem cells and adult stem cells. Embryonic stem (ES) cells are isolated from the inner cell mass of pre-implantation blastocyst of mammals, the properties of ES cells identified them as being highly suitable for the generation in vitro of specific cell lineages. While adult stem cells, also named tissue-specific stem cells, are existed in various niches throughout the body, such as bone marrow, brain, liver and skin. Adult stem cells including neural stem cells, hematopoietic stem cells, mesenchymal stem cells, epidermal stem cells and so on. They primarily perform functions as tissue maintenance, growth and repair in later life (Rippon and Bishop 2004; Bishop et al. 2002). Because stem cells process plasticity, so theoretically, adult stem cells could be obtained from patients, then differentiated in vitro and transplanted back to the same individual for tissue repair without the need for immunosuppression (Hans 2007). Stem cells can provide appropriate cell source for tissue engineering and therapeutic application.

5.2 Hematopoietic Stem Cells

Hematopoietic stem cells (HSCs) are a kind of pluripotent stem cells, which can give rise to all the other blood cells through the process of haematopoiesis and maintain the homeostasis of organism. HSCs can produce adequate production of blood cells, including all myeloid lineages blood cells (monocytes, macrophages, neutrophils, basophils, eosinophils, erythrocytes, dendritic cells, and megakaryocytes or platelets) and lymphoid lineages blood cells (include T cells, B cells, and natural killer cells). Most blood cells have relatively short lifespans after birth, from several hours like granulocytes to several years like memory T cells. Hence, in order to maintain haematopoiesis, HSCs continuously differentiate into multiple lineages of different types of blood cell and are responsible for blood cell renewal. HSCs are rare in organism. In adult mammals, most of these cells are derived from mesoderm

and located in the red bone marrow (BM), which is contained in the core of most bones. In bone marrow, HSCs are at a very low percentage, generally from 0.01 to 0.05%. In fetal, HSCs predominantly reside in fetal liver (FL). Besides, a small number of HSCs can also be found in the peripheral blood (PB) and umbilical cord blood (UCB).

5.3 Types of HSCs

Generally, HSCs can be divided into three types: long-term self-renewing HSCs (LT-HSCs), short-term self-renewing HSCs (ST-HSCs) and multipotent progenitors (MPPs). In the three types of HSCs, LT-HSCs are thought to self-renew for the whole lifespan of an organism, which have an ability to engraft and repopulate a host hematopoietic system. ST-HSCs and MPPs have a shorter duration, and are able to restore hematopoiesis in a lethally irradiated mouse only for up to four months. Meanwhile, MPPs are not with the ability to self-renewing (Reya et al. 2001). When LT-HSCs differentiated to ST-HSCs and then to MPPs, the ability of self-renewal lost gradually and the ability of mitotic activity increased slowly. After LT-HSCs becomes the non-self-renewing MPPs, these cells continue differentiated to either one of the two hematopoietic lineages, including common lymphoid progenitor (CLP) and common myeloid progenitor (CMP). During the process of differentiation, HSCs first loses self-renewal capacity, and then lose lineage potential step-by-step. CLP finally give raise to mature functional lymphoid lineage cells, including mature nature killer (NK) cells, B cells, T cells and dendritic cells (DCs). Meanwhile, CMP finally differentiated into functional myeloid lineage cells, including eosinophils, basophils, neutrophils and monocytes/macrophages, erythrocytes, megakaryocytes and platelets (Forsberg et al. 2006; Cabrita et al. 2003). CMP can also differentiated into mature DCs (Seita and Weissman 2010). Through differentiation, HSCs can give raise to all kinds of blood cells (Fig. 1). With the advancement of new technologies of multi-color fluorescence flow cytometry, the phenotypes of these cells in the process of HSCs differentiation are defined by lots of specific surface molecular markers, which make it possible to identify and separate them from organism, and these molecular markers are listed in Table 1.

5.4 Molecular Mechanisms Regulating HSCs Self-renewal in BM

In order to maintain the life-long haematopoiesis and homeostasis of mammalian organism, HSCs must replicate themselves to maintain the constant HSCs pool in BM. The process of HSCs replication through mitosis is called self-renewal. Recently, lots of advanced have been achieved about the molecular signature to define

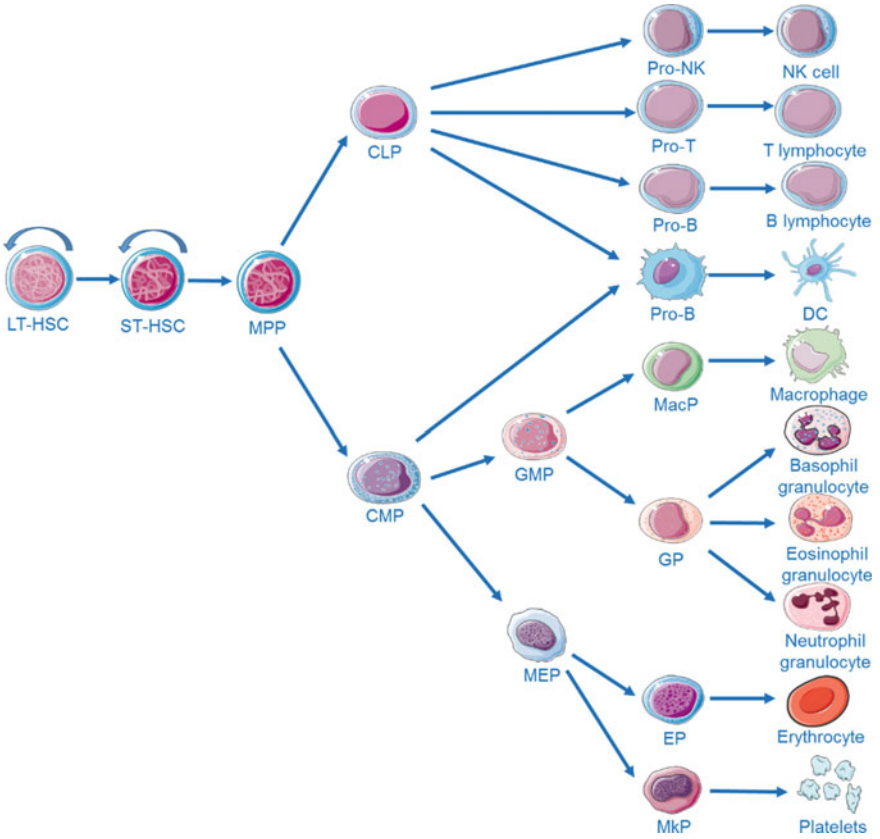

Fig. 1 The hematopoietic lineages of differentiation. The curved arrow indicated self-renewing ability. The LT-HSCs resides at the top of the hierarchy, which are defined as the cells that have both the self-renewal capacity and the potential to give rise to all other hematopoietic cell types. Through differentiation, HSCs first lose self-renewal capacity, then loses lineage potential step-by-step as them commit to become all mature functional blood cells. CLP: common lymphoid progenitor, CMP: common myeloid progenitor, MEP: Megakaryocyte/erythrocyte progenitor, GMP: granulocyte/macrophage progenitor, MkP: Megakaryocyte progenitor, EP: erythrocyte progenitor, GP: granulocyte progenitor, MacP: macrophage progenitor, DC: dendritic cell, NK: natural killer

Table 1 The phenotypes of HSCs and other cells in the process of HSCs differentiation

Populations	Mouse HSCs markers	Human HSCs markers
LT-HSC	$Lin^-cKit^+Sca1^+Flk2^-CD34^-Slamf1^+$	$Lin^-CD34^+CD38^-CD90^+CD45RA^-$
ST-HSC MPP	$Lin^-cKit^+Sca1^+CD34^-$	$Lin^-CD34^+CD38^-CD90^-CD45RA^-$
CLP	$Lin^-Flk2^+IL7Ra^+CD27^+$	$Lin^-CD34^+CD38^+CD10^+$
CMP	$Lin^-cKit^+Sca1^{-/low}CD34^+FcgR^{low}$	$LinCD34^+CD38^+IL3Ra^{low}CD45RA^-$
MEP	$Lin^-cKit^+Sca1^-CD34^-FcgR^-$	$Lin^-CD34^+CD38^+IL3Ra^-CD45RA^-$
GMP	$Lin^-cKit^+Sca1^-CD34^+FcgR^+$	$Lin^-CD34^+CD38^+IL3Ra^+CD45RA^-$

Note Lin stands for lineage markers

the stemness and self-renewal of stem cells and HSCs. The fate choice of HSCs to either self-renew or differentiate is determined by a complex interplay between intrinsic mechanisms and extrinsic signals from the surrounding environment or stem cell niches (Moore and Lemischka 2006).

In adult BM, the number of HSCs stays relatively constant and BM HSCs are retaining quiescent under normal conditions. Previous results showed the majority of BM HSCs slowly, constant incorporation of nucleotide analogues, and demonstrated that the majority of these cells divide regularly (Bradford et al. 1997; Cheshier et al. 1999). It seems that the cell-cycle state of HSCs correlates to their multipotency. When LT-HSCs were engrafted to irradiated recipients, these cells are in the G0 phase of the cell cycle (Passegue et al. 2005). It is widely assumed that the dividing HSCs in BM undergo asymmetric cell division, in which an individual HSC gives rise to a non-identical daughter cell (keeping the HSC identity) and the other becoming a differentiated progenitor cell.

External environmental signals integrate with intrinsic molecular pathways controlled the fates of HSCs. Gain and loss of functional studies have found several transcription factors are implicated in there gulation of HSCs self-renewal. The transcription factor translocation Ets leukemia (Tel) has been demonstrated to be required HSCs self-renewal. Inactivation of Tel leads to the depletion of HSCs in BM without influencing their committed progenitors (Hock et al. 2004b). HoxB4, a member of the homeobox gene family, encodes a set of transcription factors which usually regulate embryonic body patterning and organogenesis. Sauvageau has proved that both in vitro and in vivo, overexpression of HoxB4 in HSCs has been shown to enhance the self-renewal of HSCs (Sauvageau et al. 2004). Furthermore, it has been described that there is a remarkable growth advantage in HoxB4-transduced HSCs over untransduced ones when cultured in vitro (Antonchuk et al. 2002). While HoxB4 knockout mice only exhibit a mild defect in the proliferative potential of HSCs and normal hematopoiesis. The discrepancy may due to the redundant function of other Hox family members (Brun et al. 2004). Two studies independently identified Growth factor independence 1 (Gfi1), which is a zinc finger-containing transcriptional repressor, as a positive regulator of HSCs self-renewal that functions by restraining HSC proliferation. Gfi1 knockout HSCs exhibit increased proliferation and decreased capability for repopulation of irradiated recipients (Zeng et al. 2004; Hock et al. 2004a). Gfi1 might function through upregulating the cell-cycle inhibitor p21, since p21 expression is greatly decreased in Gfi1 knockout HSCs. Consistent with this hypothesis is the observation that p21-deficient HSCs also show impaired repopulation capability compared to wild-type HSCs (Cheng et al. 2000). p18, which is another cell-cycle inhibitor, has an opposite effect on HSCs self-renewal compared to p21. Compared to wild-type HSCs, p18-deficient HSCs increased their repopulation capability (Yuan et al. 2004; Yu et al. 2006). c-Myc protein plays an important role in the homeostasis of HSCs. Conditional decreased the activity of c-Myc in the bone marrow (BM) results in severe cytopenia and accumulation of HSCs in situ, which were caused by HSCs couldn't initiate their normal differentiation. While enforced c-Myc expression in HSCs leading to loss of self-renewal activity at the expense of differentiation (Wilson et al. 2004). Gain and loss of function studies have shown that both Stat5

and Stat3 are important to HSCs self-renewal. They are positive regulator and can promote the ability of self-renewal of HSCs (Kato et al. 2005; Chung et al. 2006). These results indicate that HSCs self-renewal is delicate controlled by lots of transcription factors and molecular pathways regulating cell proliferation and cell-cycle repression.

Besides transcription factors, other proteins also have been found can regulate HSCs self-renewal. Bmi-1, which is polycomb group (PcG) protein that forms the Polycomb repression complex 1 (PRC1) with other members of the PcG family and can modulate gene expression, have been reported could regulate HSCs self-renewal. Bmi1-deficient mice have exhibited the progressive hematopoietic defect with increase of age (Lessard and Sauvageau 2003). In BM HSCs, knockout Bmi-1 can destruct the long-term proliferate ability, while overexpress of Bmi-1 can strengthen the expansion ability of HSCs in vitro and enhance the proliferate ability in vivo (Iwama et al. 2004; Park et al. 2003). All this demonstrated Bmi1 plays a crucial role in maintenance of proliferation capacities of HSCs and progenitors.

Environmental signals, such as Notch, Wnt, BMP and Sonic hedgehog (Shh) signals, also play important roles in regulate the gene expression related with HSCs self-renewal. Duncan reported that Notch signaling is active in HSCs, and its expression was downregulated after HSCs differentiation. It has been reported Notch signaling played important role in lymphoid lineage commitment between T cell and B cell. Notch signaling pathway is always active in HSCs, and the activity is attenuated when HSCs differentiate. When HSCs was treated with Notch signaling inhibitor, the differentiation ability of HSCs was increased and the number of HSCs was decreased (Duncan et al. 2005). Besides, overexpress Notch1 in HSCs increased self-renewal capability (Stier et al. 2002). However, who found that the self-renewal ability of HSCs was not affected when Notch1 signaling was deficient in BM-HSCs (Mancini et al. 2005). Wnt signaling has also been found in the regulation of HSCs self-renewal. Wnt family includes several secreted protein and the receptors of Wnt proteins are the Frizzled family and LDL-receptor-related proteins. Several Wnt proteins have been successfully purified and Wnt3a protein has thus been shown to act on HSCs as a growth factor (Willert et al. 2003). β-catenin is one of the most target molecular downstream of Wnt signal. Reya found that overexpression of activated β-catenin in HSCs lead to expansion of the pool of immature cells in vitro, which can reconstitute irradiated recipients (Reya et al. 2003). The in vivo repopulation capability of HSCs was lost when treated with Wnt signaling inhibitor. Wnt3A has been found to promote self-renewal of HSCs (Willert et al. 2003). However, who found that β-catenin-deficient mice had no defects on HSCs and the self-renewal capability of β-catenin-deficient HSCs was normal (Cobas et al. 2004).

6 Molecular Mechanisms Regulating Differentiation of HSCs to Microphage

Besides the potent proliferative and self-renewal capacity to produce new hematopoietic cells, HSCs can give raise to various lineages of function cells of blood. As showed in Fig. 1, HSCs differentiated macrophages should experience a few selections. The first choice should be experienced is to differentiate into myeloid or lymphoid lineage cells. After they have become CMPs, they will face the second choice that whether to differentiate into GMPs or MEPs. Only when they have differentiate into GMPs, then they can finally differentiate into macrophage. Before they eventually become macrophages, they should experience the stages of CMPs and GMPs. During this process, several transcription factors and molecular pathways have been reported played important roles in this process: the commitment of monocytes/macrophages from HSCs.

During the process of differentiation, primitive HSCs continuously divide and give raise to differentiated daughter cells, and these cells will become a single lineage that possess a fixed genetic program. Differential expression of transcription factors triggers the determination of HSCs fate: commitment to either CLPs or CMPs. With the development of lots of biotechnologies, several candidate transcription factors determine the initial destiny of primitive HSCs have been found, including. But these transcription factors have not been tested in clearly interpretable in vivo models.

PU.1, which is an Ets family transcription factor, plays an important role in both innate and adaptive immune system, it can control the development of granulocytes, macrophages, B cells and T cells in a cell-intrinsic manner. PU.1 is highly expressed in HSCs, CLPs and a part of CMPs (Nutt et al. 2005), which is accordance with its important roles in the development and differentiation of HSCs.

The transcription factor PU.1 is the most studied transcription factor during the initial differentiation of primitive HSCs. In all the studied transcription factors during this process, the most studied transcription factor is PU.1. The expression of PU.1 is one of the earliest events controlling HSCs to lineage commitment. Conditional disruption of PU.1 in bone marrow HSCs inhibit the transition of HSCs to CLP and CMPs, which means PU.1 is important for the generation of initial myeloid and lymphoid progenitors from HSCs (Iwasaki et al. 2005). HSCs upregulated PU.1 and GATA-1 will differentiate into CMPs. Meanwhile, PU.1 is also vital for CLPs for it is consistently expressed in CLPs (Scott et al. 1994). Further, PU.1 can regulate the mRNA expression of IL-7 receptor and M-CSF receptor, which are important for normal developments of lymphoid and myeloid lineages, respectively (DeKoter and Singh 2000; DeKoter et al. 1998). Overexpression of PU.1 in HSCs has been shown to be able to commit multipotent hematopoietic progenitors to monocytic/granulocytic direction (Nerlov and Graf 1998). It seems that expression level of PU.1 determine the differentiation of HSCs. DeKoter found that PU.1 controlled the lineage commitment of HSCs to myeloid or lymphoid cells are dosage-related, for a higher concentration favoring HSCs commitment to myeloid cells (DeKoter and Singh 2000). However, the molecular mechanisms regulating the expression of key transcription factors PU.1

are nearly unknown. The 'extrinsic theory' consider that the stable expression of transcriptional programs might be subject to instruction from outside signals, which has been proved that exogenous anti-TGF-β1 antibody could significantly upregulate PU.1 and GATA-1 expression level in the in vitro culture system of human CLRPP (cytokine low-responding proliferating progenitors) cells.

Kondo found low but detectable level of GM-CSF receptors were expressed on HSCs but not CLPs. It seems that the expression of GM-CSF receptor was down-regulated during the process of HSCs differentiated into CLPs. When GM-CSF or M-CSF receptor was overexpressed in CLPs, these cells were reprogramed to monocytes or granulocyts by GM-CSF or M-CSF in vitro (Kondo et al. 2000). Further, Evans found that signals mediated by cytoplasmic domain of GM-CSFR induced multipotent FDCP-mix cells differentiated into granulocytic/monocytic cells (Evans et al. 1999).

Meanwhile, during the differentiation process, how these differentiation-inducing transcription factors predominate over self-renewal-maintaining factors is also unknown. The expression of intrinsic transcription factors controlling the differentiation of HSCs might be instructed by outside signals. Kondo found low but detectable levels of GM-CSF receptor were expressed on HSCs but not CLPs. During the process of HSCs differentiated into CLPs, the expression of GM-CSF receptor was down-regulated. When GM-CSF or M-CSF receptor was overexpressed in CLPs, these cells were reprogramed to monocytes or granulocyts by GM-CSF or M-CSF in vitro (Kondo et al. 2000).

After the cells have differentiated into CMPs, these cells will experience the second choice that differentiated into MEPs or GMPs. PU.1 and GATA-1 play important roles in controlling this process, for they are co-expressed in CMPs and one of them exclusively expressed will determine the direction of differentiation. It has been proved that PU.1 is vital for monocytic and B lymphocytic development. During the process of CMPs differentiated to GMPs, PU.1 can inhibit the transcriptional activity of GATA-1, which predominately regulate CMPs differentiate into erythroid and megakaryocytic development. Overexpress of PU.1 could inhibit the binding of GATA-1 to its target gene promoter (Zhang et al. 2000). Matsumura found ectopic express PU.1 in erythroid/megakaryocytic leukemia cell K562 could redirect them to differentiate into granulocytes and monocytes, while overexpression of GATA-1 in granulocytic progenitor 32D cells redirects them to megakaryopoiesis (Matsumura et al. 2000). Similarly, Iwasaki found disruption of PU.1 in CMPs blocks myelomonocytic differentiation in vitro (Iwasaki et al. 2005). PU.1 functions may through regulate the expression of M-CSF/M-CSFR or GM-CSF/GM-CSFR, for it has been reported that PU.1 can regulate the expression of M-CSFRα and GM-CSFR (DeKoter et al. 1998; Anderson et al. 1998). Further, M-CSF receptor ectopically expressed in murine multiple-potent EML cells can increase their differentiation potential to granulocyte/monocyte and decrease their differentiation potential to erythroid lineage (Pawlak et al. 2000). However, other transcription factors may also function in this process. Overexpression of c-Myb could reprogram the K562 cells differentiate to granulocytic/monocytic lineage (Matsumura et al. 2000). Egr-1 (early growth response gene-1) was found to promote macrophage production in the expense of ery-

throid and granulocytic development (Krishnaraju et al. 2001). However, SCL could promote productions of erythroid and megakaryocytic colonies when expressed in $CD34^+$ cells (Elwood et al. 1998). TGF-β1 signal could enhance the commitment of erythroid while inhibit the development of granulocyte/monocyte (Drexler et al. 1998; Krystal et al. 1994).

After CMPs have differentiated into GMPs, these bipotent precursor will choice whether to differentiate into granulocytes or monocytes/macrophages. Several transcription factors have been found play important roles in this process. PU.1 plays important regulatory roles in the HSCs differentiation. Rodney et al. found mutation of PU.1 gene could cause a severe reduction in myeloid (granulocyte/macrophage) progenitors. PU.1-deficiency myeloid progenitors can proliferate in vitro in response to the multilineage cytokines interleukin-3 (IL-3), IL-6 and stem cell factor but are unresponsive to the myeloid-specific cytokines granulocyte-macrophage colony-stimulating factor (GM-CSF), G-CSF and M-CSF. PU.1-deficiency myeloid progenitors could not induce detectable macrophage differentiation. Retroviral transduction of PU.1 into mutant progenitors restores responsiveness to myeloid-specific cytokines and development of mature granulocytes and macrophages (DeKoter et al. 1998). PU.1 disruption in GMPs resulting in only myeloblast colony formation, and these myeloblast colonies did not express CD11b (Iwasaki et al. 2005).

Overexpress Egr-1 (early growth response gene-1), also known as Zif268, in myeloid-enriched cells could promote macrophage differentiation and inhibit granulocyte differentiation (Krishnaraju et al. 2001). The interferon consensus sequence binding protein (ICSBP/IRF-8), which can interact with PU.1, was found could inhibit the production of neutrophils from GMCSF-dependent $ICSBP^{-/-}$ cell line Tot2 and granulocytic progenitor 32D cells (Tamura et al. 2000). Meanwhile, express of ICSBP into Tot2 cells could also upregulate the expression of transcription factor Egr-1. $ICSBP^{-/-}$mice developed granulocytosis along with atypical macrophages, which resemble a chronic myelogenous leukemia (CML) -like disease (Holtschke et al. 1996). Furthermore, overexpress ICSBP also could inhibit myelo proliferation both in vitro and in vivo (Hao and Ren 2000; Schmidt et al. 1998).

When multipotent progenitor cells differentiated to macrophage, Maf B, the bZip transcription factor, was upregulated successively. Meanwhile, overexpress Maf B in transformed myeloblasts could lead to the differentiation of monocytes/macrophages independent of overexpression of PU.1 (Kelly et al. 2000).

Tamura et al. found a specific protein FMIP, which could interact with the cytoplasmic domain of M-CSF receptor c-fms and inhibit the c-fms signaling. Overexpression of FMIP in bipotent FDC-P1Mac11 could prevent the M-CSF-induced monocytic differentiation and made all cells differentiated into granulocytes (Tamura et al. 1999). They also found ICSBP could induce macrophage differentiation (Tamura et al. 2000). HoxA10 have been proved could regulate monocytic differentiation. When HoxA10 was overexpressed in U937 cells, it could activate p21 and induced cell cycle arrest, which could promote monocytic differentiation from U937 cells (Bromleigh and Freedman 2000). Overexpression of GATA-2 in FDCP cell line could also induce these cells to monocytic differentiation and accompanied with cell cycle arrest (Heyworth et al. 1999).

Besides, DNA methyltransferases Dnmt3a and Dnmt3b have been proved that they could promote the differentiation of embryonic stem cells. Recently, Grant et al. found Dnmt3a played an important role in HSCs self-renewal and differentiation. *Dnmt3a* loss progressively impairs HSCs differentiation over serial transplantation, while simultaneously expanding HSCs number in the bone marrow. Meanwhile, Dnmt3a-null HSCs upregulate multipotency genes and downregulate differentiation factors (Dnmt3a is essential for hematopoietic stem cell differentiation).

7 The Scientific Achievements in SJ-10 Satellite Research

SJ-10 recoverable satellite is the first microgravity scientific satellite of China, which was launched on April 6, 2016 and mainly carries out microgravity science and space life science. During the 12 days spaceflight, we studied the effects and mechanisms of spaceflight/microgravity on the proliferation of HSPCs and macrophage differentiation. Meanwhile, we also investigated the effects and simulated microgravity of simulated microgravity on the proliferation and macrophage differentiation by using the RWV bioreactor (Fig. 2). About the proliferation of murine hematopoietic stem/progenitor cells, we found that both spaceflight/microgravity and simulated microgravity inhibited the proliferation of HSPCs. Meanwhile, cell

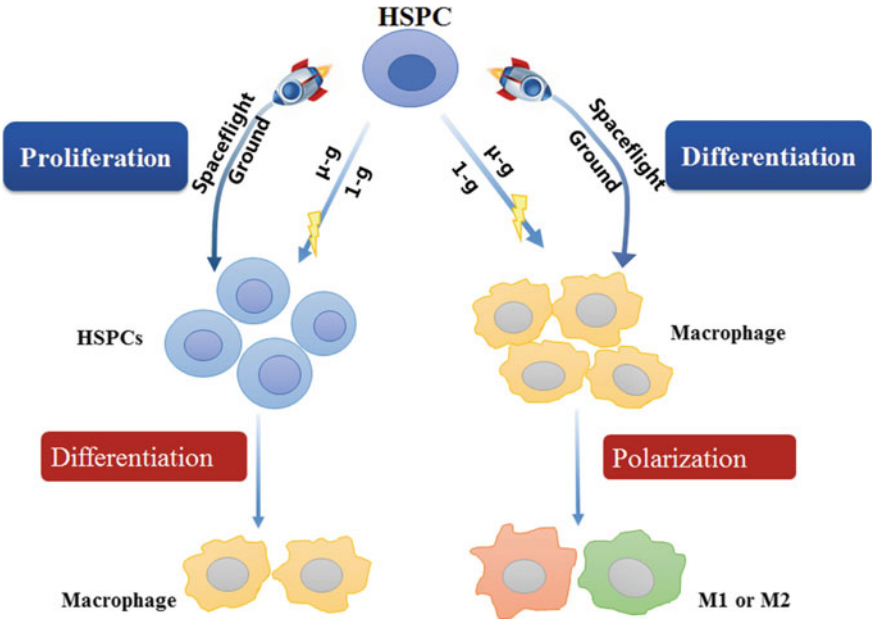

Fig. 2 Diagram of experimental design

cycle analysis demonstrated simulated microgravity inhibited the G1/S transition. RNA-seq and bioinformatics analysis revealed microgravity inhibited proliferation of HSPCs through regulating cell proliferation and cell apoptosis signaling pathway. Further, we also found that HSPCs proliferated under simulated microgravity for 12 days could re-differentiate into more macrophages. About macrophage differentiation, we elucidate the cellular and molecular mechanism of microgravity-affected macrophage differentiation. We found that microgravity significantly inhibits maturation of macrophages and impedes their further M1/2 polarization after in vitro differentiation comparing with the normal gravity. We firstly propose that the two microgravity-driven signaling pathways and metabolic alteration are important in macrophage differentiation affected by microgravity (Fig. 5).

7.1 Spaceflight/Microgravity Decreased the Proliferation of Murine Hematopoietic Stem/Progenitor Cells

Exposure to spaceflight/microgravity can cause a series of physiological and psychological changes, such as bone loss, cardiovascular dysfunction, and immune dysfunction. Anemia and hematopoietic disorder are always observed in astronauts when experienced short- or long-duration of spaceflight. Hematopoietic stem and progenitor cells (HSPCs), which could self-renew and give rise to all the other blood cells, play vital role in the haematopoiesis and homeostasis. However, the effects and mechanism of microgravity on the proliferation of HSPCs are remaining unclear. To study the effect and mechanism of spaceflight/microgravity and simulated microgravity on the proliferation of HSPCs, HSPCs were cultured in incubator which experienced a 12-days spaceflight on SJ-10 satellite (with cell unit in Fig. 3a) and Tianzhou-1 cargo ship (with cell unit in Fig. 3b), and in rotating wall vessel (RWV) bioreactor, respectively. Both spaceflight and simulated all significantly decreased the number of proliferated HSPCs (Fig. 4). Simulated microgravity blocked the cell cycle of HSPCs at G1/S transition and promoted cell apoptosis. RNA-Seq and bioinformatics analysis revealed that microgravity inhibited proliferation and promote apoptosis of HSPCs through regulating cell proliferation and cell apoptosis signaling pathways-associated genes. Meanwhile, microgravity through CSF and cAMP pathways regulated cell proliferation and cell cycle. Furthermore, HSPCs proliferated under simulated microgravity had the same the ability to re-differentiated into macrophages as that cultured under normal gravity. These results directly proved the inhibitory effect of microgravity on proliferation of HSPCs in vitro and preliminary revealed the regulatory mechanism of inhibition of microgravity on proliferation of HSPCs.

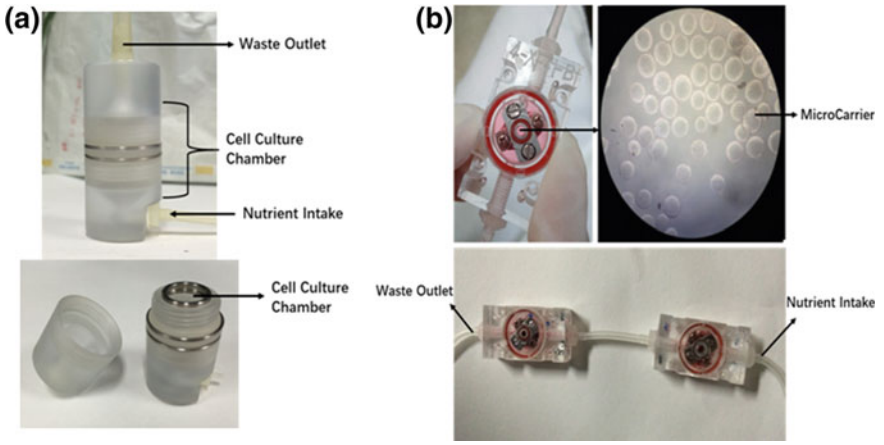

Fig. 3 Cell culture systems during space flight and control experiment. **a** Cell culture unit used in SJ-10 satellite, in which 2×10^6 cells with 2.5 ml medium were placed in the cell culture chamber separated by two pieces of polycarbonate filter membrane in each end of the unit. The nutrient solution enters the culture unit from the nutrient bag connected at one end, infiltrates the filter membrane, enters the cell culture chamber, and then passes from the other end of the culture unit to the waste liquid bag. The cells cultured in this unit will eventually return to the ground for recycling and further analysis. **b** Cell observation unit used in Tianzhou-1 cargo ship, in which cells attached to micro-carriers were cultured with 1.8 ml medium in the middle cell culture chamber of the unit. The camera photographed cells from the glass observation window in the unit and collected the image information. Two units are connected in series, one is 10× magnifications of cells for images collection, and the other is 20×. The nutrient flows from one end of the nutrient solution bag to the other end of the waste liquid bag, and provides nutrient for cells in the cell culture chamber

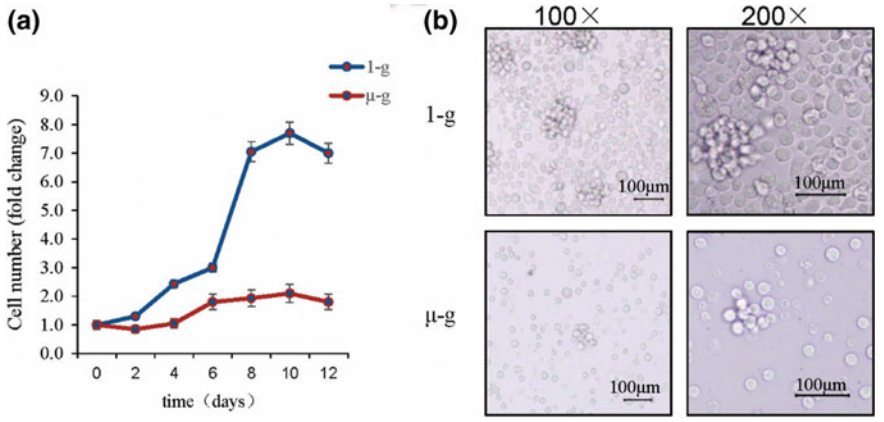

Fig. 4 Cell number and morphology of hematopoietic stem cells (HSPCs) after culturing in different gravity conditions for 12 days. **a** The number change of HSPCs in 12 days culturing in normal gravity and modeled microgravity. **b** Cell morphology of HSPCs after culturing in normal gravity and modeled microgravity for 12 days, observed in microscope at low magnification and magnification

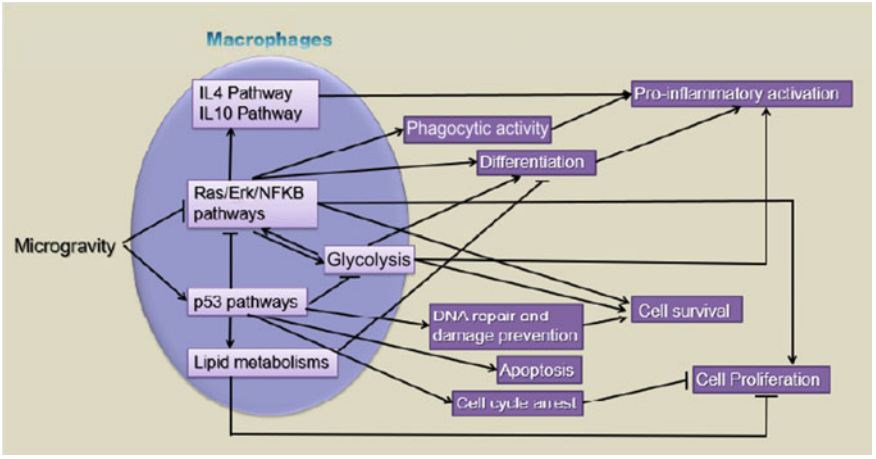

Fig. 5 Schematic view for the relationship and influence of all microgravity-response signaling pathways. The blue circle shows a macrophage under microgravity. White words indicate the important microgravity-response signaling pathways and black words indicate their consequence

7.2 Microgravity Suppresses Macrophage Differentiation

Space flight-associated immune system weakening ultimately precludes the expansion of human presence beyond the Earth's orbit, so it is an urgent need to understand the relevant mechanisms caused by microgravity. To figure out the effect of microgravity on the microgravity-caused changes of cell state and transcriptome profiling during the differentiation of macrophages, we differentiated hematopoietic progenitor cells (HPCs) of mouse bone marrow in the presence of macrophage colony stimulating factor (M-CSF) for 12 days under spaceflight and simulated microgravity conditions, respectively, and performed gene expression analysis by next-generation sequencing (NGS). Results showed that microgravity significantly reduced the proliferation and differentiation of macrophages and even potentially impaired functional polarization of those macrophages. RNA-Seq data indicated that the genes related cell proliferation and macrophage differentiation were down-regulated while the genes related apoptosis and repair process were up-regulated under microgravity. Among paramount gene signature, we identified the major microgravity-regulated pathways during macrophage development (Fig. 5).

Acknowledgements The authors sincerely thank Dr. Shujin Sun from Institute of Mechanics, Chinese Academy of Sciences for free helping and supporting in the supply of microgravity instruments, and Prof. Enkui Duan and Dr. Xiaohua Lei from Institute of Zoology, Chinese Academy of Sciences for valuable opinions and suggestions in the design of our experiment and manuscript. The authors also appreciated Dr. Lu Shi from Institute of Zoology, Chinese Academy of Sciences for proofreading and editing our manuscript. This work was supported by grant from the National Natural Science Foundation of China (NSFC U1738111).

References

Allebban Z, Ichiki AT, Gibson LA et al (1994) Effects of spaceflight on the number of rat peripheral blood leukocytes and lymphocyte subsets. J Leukoc Biol 55(2)a: 209–213

Anderson KL, Smith KA, Conners K et al (1998) Myeloid development is selectively disrupted in PU.1 null mice. Blood 91(10): 3702–3710

Antonchuk J, Sauvageau G, Humphries RK (2002) HOXB4-induced expansion of adult hematopoietic stem cells ex vivo. Cell 109(1):39–45

Bishop AE, Buttery LD, Polak JM (2002) Embryonic stem cells. J Pathol 197(4):424–429

Blaber E, Marcal H, Burns BP (2010) Bioastronautics: the influence of microgravity on astronaut health. Astrobiology 10(5):463–473

Bradford GB, Williams B, Rossi R et al (1997) Quiescence, cycling, and turnover in the primitive hematopoietic stem cell compartment. Exp Hematol 25(5):445–453

Bromleigh VC, Freedman LP (2000) p21 is a transcriptional target of HOXA10 in differentiating myelomonocytic cells. Genes & Dev 14(20):2581–2586. https://doi.org/10.1101/Gad.817100

Brun AC, Bjornsson JM, Magnusson M et al (2004) Hoxb4-deficient mice undergo normal hematopoietic development but exhibit a mild proliferation defect in hematopoietic stem cells. Blood 103(11):4126–4133

Cabrita GJ, Ferreira BS, da Silva CL et al (2003) Hematopoietic stem cells: from the bone to the bioreactor. Trends Biotechnol 21(5):233–240

Cheng T, Rodrigues N, Shen H et al (2000) Hematopoietic stem cell quiescence maintained by p21cip1/waf1. Science 287(5459):1804–1808

Cheshier SH, Morrison SJ, Liao X et al (1999) In vivo proliferation and cell cycle kinetics of long-term self-renewing hematopoietic stem cells. Proc Natl Acad Sci USA 96(6):3120–3125

Chiu B, Wan JZ, Abley D et al (2005) Induction of vascular endothelial phenotype and cellular proliferation from human cord blood stem cells cultured in simulated microgravity. Acta Astronaut 56(9–12):918–922

Chung YJ, Park BB, Kang YJ et al (2006) Unique effects of Stat3 on the early phase of hematopoietic stem cell regeneration. Blood 108(4):1208–1215

Cobas M, Wilson A, Ernst B et al (2004) Beta-catenin is dispensable for hematopoiesis and lymphopoiesis. J Exp Med 199(2):221–229

Crucian BE, Stowe RP, Pierson DL et al (2008) Immune system dysregulation following short- vs long-duration spaceflight. Aviat Space Environ Med 79(9):835–843

Davis TA, Wiesmann W Kidwell W et al (1996) Effect of spaceflight on human stem cell hematopoiesis: suppression of erythropoiesis and myelopoiesis. J Leukoc Biol 60(1):69–76

DeKoter RP, Singh H (2000) Regulation of B lymphocyte and macrophage development by graded expression of PU.1. Science 288(5470):1439–1441

DeKoter RP, Walsh JC, Singh H (1998) PU.1 regulates both cytokine-dependent proliferation and differentiation of granulocyte/macrophage progenitors. EMBO J 17(15):4456–4468

Domaratskaya EI, Michurina TV, Bueverova EI et al (2002) Studies on clonogenic hemopoietic cells of vertebrate in space: problems and perspectives. Adv Space Res 30(4):771–776

Drexler HG, Meyer C, Zaborski M et al (1998) Growth-inhibitory effects of transforming growth factor-beta 1 on myeloid leukemia cell lines. Leuk Res 22(10):927–938

Duncan AW, Rattis FM, DiMascio LN et al (2005) Integration of Notch and Wnt signaling in hematopoietic stem cell maintenance. Nat Immunol 6(3):314–322

Elwood NJ, Zogos H, Pereira DS et al (1998) Enhanced megakaryocyte and erythroid development from normal human CD34(+) cells: consequence of enforced expression of SCL. Blood 91(10):3756–3765

Evans CA, Pierce A, Winter SA et al (1999) Activation of granulocyte-macrophage colony-stimulating factor and interleukin-3 receptor subunits in a multipotential hematopoietic progenitor cell line leads to differential effects on development. Blood 94(5):1504–1514

Fischer CL, Johnson PC, Berry CA (1967) Red blood cell mass and plasma volume changes in manned space flight. J Am Med Assoc 200(7):579

Forsberg EC, Bhattacharya D, Weissman IL (2006) Hematopoietic stem cells: expression profiling and beyond. Stem Cell Rev 2(1):23–30
Graebe A, Schuck EL, Lensing P et al (2004) Physiological, pharmacokinetic, and pharmacodynamic changes in space. J Clin Pharmacol 44(8):837–853
Grigor'ev AI (2007) Physiological problems of manned mission to Mars. Ross Fiziol Zh Im I M Sechenova 93(5):473–484
Hans RS (2007) The potential of stem cells: an inventory. In: Human biotechnology as social challenge, England. Ashgate Publishing, Ltd., p 28
Hao SX, Ren R (2000) Expression of interferon consensus sequence binding protein (ICSBP) is downregulated in Bcr-Abl-induced murine chronic myelogenous leukemia-like disease, and forced coexpression of ICSBP inhibits Bcr-Abl-induced myeloproliferative disorder. Mol Cell Biol 20(4):1149–1161
Heyworth C, Gale K, Dexter M, May G, Enver T (1999) A GATA-2/estrogen receptor chimera functions as a ligand-dependent negative regulator of self-renewal. Genes & Dev 13(14):1847–1860. https://doi.org/10.1101/gad.13.14.1847
Hock H, Hamblen MJ, Rooke HM et al (2004a) Gfi-1 restricts proliferation and preserves functional integrity of haematopoietic stem cells. Nature 431(7011):1002–1007
Hock H, Meade E, Medeiros S et al (2004b) Tel/Etv6 is an essential and selective regulator of adult hematopoietic stem cell survival. Genes Dev 18(19):2336–2341
Hodgson GS, Bradley TR (1979) Properties of haematopoietic stem cells surviving 5-fluorouracil treatment: evidence for a pre-CFU-S cell? Nature 281(5730):381–382
Holtschke T, Lohler J, Kanno Y et al (1996) Immunodeficiency and chronic myelogenous leukemia-like syndrome in mice with a targeted mutation of the ICSBP gene. Cell 87(2):307–317
Hughes-Fulford M, Chang TT, Martinez EM et al (2015) Spaceflight alters expression of microRNA during T-cell activation. FASEB J 29(12):4893–4900
Hwang SA, Crucian B, Sams C et al (2015) Post-spaceflight (STS-135) mouse splenocytes demonstrate altered activation properties and surface molecule expression. PLoS ONE 10(5):e0124380
Ichiki AT, Gibson LA, Jago TL et al (1996) Effects of spaceflight on rat peripheral blood leukocytes and bone marrow progenitor cells. J Leukoc Biol 60(1):37–43
Iliukhin AV, Burkovskaia TE (1981) Cytokinetic evaluation of erythropoiesis on prolonged orbital flights. Kosm Biol Aviakosm Med 15(6):42–46
Ilyin EA, Serova LV, Portugalov VV et al (1975) Preliminary results of examinations of rats after a 22-day flight aboard the Cosmos-605 biosatellite. Aviat Space Environ Med 46(3):319–321
Iwama A, Oguro H, Negishi M et al (2004) Enhanced self-renewal of hematopoietic stem cells mediated by the polycomb gene product Bmi-1. Immunity 21(6):843–851
Iwasaki H, Somoza C, Shigematsu H et al. (2005) Distinctive and indispensable roles of PU.1 in maintenance of hematopoietic stem cells and their differentiation. Blood 106(5):1590–1600
Johnson PC, Kimzey SL, Driscoll TB (1975) Postmission plasma volume and red-cell mass changes in the crews of the first two Skylab missions. Acta Astronaut 2(3–4):311–317
Kato Y, Iwama A, Tadokoro Y et al (2005) Selective activation of STAT5 unveils its role in stem cell self-renewal in normal and leukemic hematopoiesis. J Exp Med 202(1):169–179
Kelly LM, Englmeier U, Lafon I et al (2000) MafB is an inducer of monocytic differentiation. EMBO J 19(9):1987–1997
Kondo M, Scherer DC, Miyamoto T et al (2000) Cell-fate conversion of lymphoid-committed progenitors by instructive actions of cytokines. Nature 407(6802):383–386
Kozinets GI, Korol'kov VI, Britvan II et al (1983) Morphofunctional properties of the peripheral blood and bone marrow cells of rats following a flight on board the Kosmos-936 biosatellite. Kosm Biol Aviakosm Med 17(2):61–65
Kraemer WJ, Mastro AM, Gordon SE et al (2004) Responses of plasma proenkephalin peptide F in rats following 14 days of spaceflight. Aviat Space Environ Med 75(2):114–117
Krause DS, Fackler MJ, Civin CI et al (1996) CD34: structure, biology, and clinical utility. Blood 87(1):1–13

Krishnaraju K, Hoffman B, Liebermann DA (2001) Early growth response gene 1 stimulates development of hematopoietic progenitor cells along the macrophage lineage at the expense of the granulocyte and erythroid lineages. Blood 97(5):1298–1305
Krystal G, Lam V, Dragowska W et al (1994) Transforming growth factor beta 1 is an inducer of erythroid differentiation. J Exp Med 180(3):851–860
Lange RD, Andrews RB, Gibson LA et al (1987) Hematological measurements in rats flown on Spacelab shuttle, SL-3. Am J Physiol 252(2 Pt 2):R216–R221
Lange RD, Gibson LA, Driscoll TB et al (1994) Effects of microgravity and increased gravity on bone marrow of rats. Aviat Space Environ Med 65(8):730–735
Leon HA, Serova LV, Cummins J et al (1978) Alterations in erythrocyte survival parameters in rats after 19.5 days aboard Cosmos 782. Aviat Space Environ Med 49(1 Pt 1):66–69
Lessard J, Sauvageau G (2003) Bmi-1 determines the proliferative capacity of normal and leukaemic stem cells. Nature 423(6937):255–260
Long XX, Zhong TY, Ping BH (2011) Impacts of simulated microgravity on proliferation of K562 Cell. Chin J Microcirc 1:010
Mancini SJ, Mantei N, Dumortier A et al (2005) Jagged1-dependent Notch signaling is dispensable for hematopoietic stem cell self-renewal and differentiation. Blood 105(6):2340–2342
Matsumura I, Kawasaki A, Tanaka H et al (2000) Biologic significance of GATA-1 activities in Ras-mediated megakaryocytic differentiation of hematopoietic cell lines. Blood 96(7):2440–2450
Michurina TV, Domaratskaya EI, Nikonova TM et al (1996) Blood and clonogenic hemopoietic cells of newts after the space flight. Adv Space Res 17(6–7):295–298
Moore KA, Lemischka IR (2006) Stem cells and their niches. Science 311(5769):1880–1885
Nash PV, Mastro AM (1992) Variable lymphocyte responses in rats after space flight. Exp Cell Res 202(1):125–131
Nerlov C, Graf T (1998) PU.1 induces myeloid lineage commitment in multipotent hematopoietic progenitors. Genes Dev 12(15):2403–2412
Nutt SL, Metcalf D, D'Amico A et al (2005) Dynamic regulation of PU.1 expression in multipotent hematopoietic progenitors. J Exp Med 201(2):221–231
Park IK, Qian D, Kiel M et al (2003) Bmi-1 is required for maintenance of adult self-renewing haematopoietic stem cells. Nature 423(6937):302–305
Passegue E, Wagers AJ, Giuriato S et al (2005) Global analysis of proliferation and cell cycle gene expression in the regulation of hematopoietic stem and progenitor cell fates. J Exp Med 202(11):1599–1611
Paulsen K, Tauber S, Dumrese C et al (2015) Regulation of ICAM-1 in cells of the monocyte/macrophage system in microgravity. Biomed Res Int 2015:538786
Pawlak G, Grasset MF, Arnaud S et al (2000) Receptor for macrophage colony-stimulating factor transduces a signal decreasing erythroid potential in the multipotent hematopoietic EML cell line. Exp Hematol 28(10):1164–1173
Plett PA, Frankovitz SM, Abonour R et al (2001) Proliferation of human hematopoietic bone marrow cells in simulated microgravity. Vitro Cell Dev Biol Anim 37(2):73–78
Plett PA, Abonour R, Frankovitz SM et al (2004) Impact of modeled microgravity on migration, differentiation, and cell cycle control of primitive human hematopoietic progenitor cells. Exp Hematol 32(8):773–781
Reya T, Morrison SJ, Clarke MF et al (2001) Stem cells, cancer, and cancer stem cells. Nature 414(6859):105–111
Reya T, Duncan AW, Ailles L et al (2003) A role for Wnt signalling in self-renewal of haematopoietic stem cells. Nature 423(6938):409–414
Rippon HJ, Bishop AE (2004) Embryonic stem cells. Cell Prolif 37(1):23–34
Sauvageau G, Iscove NN, Humphries RK (2004) In vitro and in vivo expansion of hematopoietic stem cells. Oncogene 23(43):7223–7232
Schmidt M, Nagel S, Proba J et al (1998) Lack of interferon consensus sequence binding protein (ICSBP) transcripts in human myeloid leukemias. Blood 91(1):22–29

Schwarz RP, Goodwin TJ, Wolf DA (1992) Cell culture for three-dimensional modeling in rotating-wall vessels: an application of simulated microgravity. J Tissue Cult Methods 14(2):51–57
Scott EW, Simon MC, Anastasi J et al (1994) Requirement of transcription factor PU.1 in the development of multiple hematopoietic lineages. Science 265(5178):1573–1577
Seita J, Weissman IL (2010) Hematopoietic stem cell: self-renewal versus differentiation. Wiley Interdiscip Rev Syst Biol Med 2(6):640–653
Shvets VN, Vatsek A, Kozinets GI et al (1984) Hemopoietic status of rats exposed to weightlessness. Kosm Biol Aviakosm Med 18(4):12–16
Sonnenfeld G (2002) The immune system in space and microgravity. Med Sci Sports Exerc 34(12):2021–2027
Sonnenfeld G, Mandel AD, Konstantinova IV et al (1990) Effects of spaceflight on levels and activity of immune cells. Aviat Space Environ Med 61(7):648–653
Sonnenfeld G, Mandel AD, Konstantinova IV et al (1992) Spaceflight alters immune cell function and distribution. J Appl Physiol (1985) 73(2 Suppl):191S–195S
Stier S, Cheng T, Dombkowski D et al (2002) Notch1 activation increases hematopoietic stem cell self-renewal in vivo and favors lymphoid over myeloid lineage outcome. Blood 99(7):2369–2378
Stowe RP, Sams CF, Pierson DL (2011) Adrenocortical and immune responses following short- and long-duration spaceflight. Aviat Space Environ Med 82(6):627–634
Sytkowski AJ, Davis KL (2001) Erythroid cell growth and differentiation in vitro in the simulated microgravity environment of the NASA rotating wall vessel bioreactor. Vitro Cell Dev Biol Anim 37(2):79–83
Tamura T, Mancini A, Joos H, Koch A, Hakim C, Dumanski J et al (1999) FMIP, a novel Fms-interacting protein, affects granulocyte/macrophage differentiation. Oncogene 18(47):6488–6495. https://doi.org/10.1038/sj.onc.1203062
Tamura T, Nagamura-Inoue T, Shmeltzer Z, Kuwata T, Ozato K (2000) ICSBP directs bipotential myeloid progenitor cells to differentiate into mature macrophages. Immunity 13(2):155–165
Tauber S, Lauber BA, Paulsen K et al (2017) Cytoskeletal stability and metabolic alterations in primary human macrophages in long-term microgravity. PLoS ONE 12(4):e0175599
Taylor GR, Neale LS, Dardano JR (1986) Immunological analyses of U.S. Space Shuttle crewmembers. Aviat Space Environ Med 57(3):213–217
Taylor GR, Konstantinova I, Sonnenfeld G et al (1997) Changes in the immune system during and after spaceflight. Adv Space Biol Med 6:1–32
Tsao YD, Goodwin TJ, Wolf DA et al (1992) Responses of gravity level variations on the NASA/JSC bioreactor system. Physiologist 35(1 Suppl):S49–S50
Udden MM, Driscoll TB, Gibson LA et al (1995) Blood volume and erythropoiesis in the rat during spaceflight. Aviat Space Environ Med 66(6):557–561
Vacek A, Serova LV, Rotkovska D et al (1985) Changes in the number of haemopoietic stem cells (CFUs) in bone marrow and spleens of pregnant rats after a short space flight onboard the Cosmos-1514 biosatellite. Folia Biol (Praha) 31(5):361–365
Vacek A, Bueverova EI, Michurina TV et al (1990) Decrease in the number of progenitors of fibroblasts (CFUf) in bone marrow of rats after a 14-day flight onboard the Cosmos-2044 biosatellite. Folia Biol (Praha) 36(3–4):194–197
Vacek A, Michurina TV, Serova LV et al (1991) Decrease in the number of progenitors of erythrocytes (BFUe, CFUe), granulocytes and macrophages (GM-CFC) in bone marrow of rats after a 14-day flight onboard the Cosmos-2044 Biosatellite. Folia Biol (Praha) 37(1):35–41
Vernikos J (1996) Human physiology in space. BioEssays 18(12):1029–1037
Wichman HA (2005) Behavioral and health implications of civilian spaceflight. Aviat Space Environ Med 76(6 Suppl):B164–B171
Willert K, Brown JD, Danenberg E et al (2003) Wnt proteins are lipid-modified and can act as stem cell growth factors. Nature 423(6938):448–452
Williams D, Kuipers A, Mukai C et al (2009) Acclimation during space flight: effects on human physiology. CMAJ 180(13):1317–1323

Wilson A, Murphy MJ, Oskarsson T et al (2004) c-Myc controls the balance between hematopoietic stem cell self-renewal and differentiation. Genes Dev 18(22):2747–2763

Yi ZC, Xia B, Xue M et al (2009) Simulated microgravity inhibits the proliferation of K562 erythroleukemia cells but does not result in apoptosis. Adv Space Res 44(2):233–244

Yu H, Yuan Y, Shen H et al (2006) Hematopoietic stem cell exhaustion impacted by p18 INK4C and p21 Cip1/Waf1 in opposite manners. Blood 107(3):1200–1206

Yuan Y, Shen H, Franklin DS et al (2004) In vivo self-renewing divisions of haematopoietic stem cells are increased in the absence of the early G1-phase inhibitor, p18INK4C. Nat Cell Biol 6(5):436–442

Zeng H, Yucel R, Kosan C et al (2004) Transcription factor Gfi1 regulates self-renewal and engraftment of hematopoietic stem cells. EMBO J 23(20):4116–4125

Zhang P, Zhang X, Iwama A et al (2000) PU.1 inhibits GATA-1 function and erythroid differentiation by blocking GATA-1 DNA binding. Blood 96(8):2641–2648

Zou LX, Cui SY, Zhong J et al (2011) Upregulation of erythropoietin receptor in UT-7/EPO cells inhibits simulated microgravity-induced cell apoptosis. Adv Space Res 48(2):390–394

Three-Dimensional Cell Culture and Tissue Restoration of Neural Stem Cells Under Microgravity

Jin Han, Yi Cui, Bai Xu, Weiwei Xue, Sumei Liu and Jianwu Dai

Abstract On April 6, 2016, the SJ-10 recoverable microgravity experimental satellite (SJ-10 satellite) was launched from Jiuquan in China, which conducted a mission of space microgravity experiments. As a recoverable satellite, the SJ-10 satellite provided an effective, open, and comprehensive platform to study space life and microgravity science. The SJ-10 satellite program consisted of 27 experiments including both fields of microgravity and space life sciences. Among the experiments, "three-dimensional (3D) cell culture and tissue restoration of NSCs under microgravity" proposed by Dr. Jianwu Dai and his staff was selected from more than 200 applications. This project was characterized by two aspects: neural stem cells and 3D culture. It was the first time that in vitro-cultured NSCs experienced a microgravity environment in space. 3D culture provided a specialized environment to benefit the in vitro tissue constructs. NSC-based therapy has attracted attention in recent years, which may be a promising treatment for many neurological diseases such as spinal cord injury, Alzheimer's disease, stroke, and Parkinson's disease. The 3D culture of NSCs under microgravity may provide valuable data for tissue reconstruction of the nervous system. To communicate the background and progress of this research, this review focuses on the key points of NSCs, 3D culture, and microgravity.

Abbreviations

3D	Three-dimensional
2D	Two-dimensional
BDNF	Brain-derived neurotrophic factor

J. Han · B. Xu · W. Xue · S. Liu · J. Dai (✉)
Key Laboratory of Molecular Developmental Biology, Institute of Genetics and Developmental Biology, Chinese Academy of Sciences, Beijing 100190, China
e-mail: jwdai@genetics.ac.cn

Y. Cui
Reproductive and Genetic Center of National Research Institute for Family Planning, Beijing 100081, China

E. Duan and M. Long (eds.), *Life Science in Space: Experiments on Board the SJ-10 Recoverable Satellite*, Research for Development,
https://doi.org/10.1007/978-981-13-6325-2_10

bFGF	Basic fibroblast growth factor
bHLH	Basic helix-loop-helix
BMP	Bone morphogenetic protein
BMSCs	Bone marrow stromal cells
CNS	Center nervous systems
CREB	CAMP response element-binding protein
DE	Differentially expressed
DEGs	Differentially expressed genes
DG	Dentate gyrus
ECM	Extracellular matrix
EGF	Epidermal growth factor
EGFR	Epidermal growth factor receptor
ESCs	Embryonic stem cells
EWS	Ewing sarcoma
FDA	Fluorescein diacetate
FPKM	Fragments per kilobase of transcript per million mapped reads
GFAP	Glial fibrillary acidic protein
GO	Gene Ontology
HDP	Hanging drop plates
HGF	Hepatocyte growth factor
hiPSC-NSs	HiPSC-derived neurospheres
HUCB-NSCs	Human umbilical cord blood-derived NSCs
IGF-1R	Insulin-like growth factor-1 receptor
IL	Interleukin
KEGG	Kyoto Encyclopedia of Genes and Genomes
MAG	Myelin-associated glycoprotein
Map2	Microtubule-associated protein-2
MEFs	Mouse embryonic fibroblasts
mESCs	Mouse embryonic stem cells
MSCs	Mesenchymal stem cells
mTOR	Mammalian target of rapamycin
NSCs	Neural stem cells
NPCs	Neural progenitor cells
OMGP	Oligodendrocyte myelin glucoprotein
PBS	Phosphate buffered saline
PDGF	Platelet growth factor
PI	Propidium iodide
PLG	Poly(lactide-co-glycolide)
PNS	Peripheral nervous system
RG	Radial glial-like
RMS	Rostral migratory stream
SJ-10 satellite	SJ-10 recoverable microgravity experimental satellite
SGZ	Subgranular zone
SEM	Scanning electron microscope
SVZ	Subventricular zone

Tuj1	Neuron-specific tubulin III
VEGF	Vascular endothelial growth factor
VZ	Ventricular zone

1 Neural Stem Cells

Neural stem cells are a type of progenitor cell of nervous systems, which self-renew and generate both neurons and glia. They are the source of neurons and glia in the CNS, although the regenerative ability of the CNS is limited. The CNS in mammals including humans consists of neurons and glia.

1.1 Main Cell Types of Nervous Systems

Neurons, a nervous system cell type, function in transmitting information through electronic and chemical signals. Neurons connect to each other through synapses between axons or axons and dendrites to form neural networks. Neurons are responsible for transmitting sensory signals from the whole body to the brain or spinal cord, which are the central processors of nervous systems, and precisely convey the ordered signals of the brain or spinal cord to the whole body. The processes from neuron cells are defined as axons and dendrites by their different shapes, lengths, and functions. Dendrites always taper off and are shorter, whereas axons tend to maintain a constant radius and are relatively long. In terms of functions, axons transmit electrochemical signals and dendrites receive them. The structure of the connection of the axon and dendrite is called a synapse. As the central functional unit of nervous systems, damage to neurons would greatly affect the functions of nervous systems. Furthermore, neurons of the CNS cannot regenerate by themselves, which is the main reason that CNS diseases rarely receive a favorable prognosis.

Astroglia, also called astrocytes, are a subtype of glial cells in the CNS. An important function of astrocytes is supporting the physical structure of the CNS. Neurotrophins secreted by astrocytes facilitate neuron functions. The capability of glycogenesis in astroglia maintains the dynamic balance of glucose to fuel neurons. Upon CNS injury, astrocytes fill the space with a glial scar. On one hand, the glial scar protects neural cells from further cell death, and on the other hand, the glial scar forms a barrier that blocks regenerating axons from crossing the injury site.

Oligodendrocytes are another subtype of glial cell in the CNS. Their main functions are to provide support and insulation to axons in the CNS, which are equivalent to the functions performed by Schwann cells in the PNS. Oligodendrocytes ensheath axons by creating myelin that is 80% lipids and 20% proteins. When separated from Schwann cells, a single oligodendrocyte can extend its processes to up to 50 axons. Schwann cells only wrap around one axon. Because of the close interaction of axons and myelin, several myelin-associated proteins and axon guidance molecules are

expressed by oligodendrocytes to regulate the development of axons. However, once injury occurs in the CNS, oligodendrocytes are destroyed and a large amount of myelin is released in the injury site. Researchers have shown that myelin-associated proteins, such as Nogo, MAG, and OMGP, and axon guidance molecules, such as ephrin B3 and semaphorin 4D, act as strong inhibitors of neurite outgrowth from postnatal neurons in vitro.

1.2 Regulation of Neural Stem Cells

During development, NPCs generate different types of neural cells, such as neurons, astrocytes, and oligodendrocytes, which comprise the nervous system (McConnell 1995; Okano and Temple 2009). NSCs give rise to all neurons of the mammalian CNS (Gotz and Huttner 2005). Neurogenesis, defined as the process of generating functional neurons from precursors, is very important for nervous systems and traditionally seen as occurring only during the embryonic and perinatal stages in mammals (Ming and Song 2005). However, current studies suggest that neurogenesis is not limited to the early stages of embryonic development. Neurogenesis in adults can also occur and is generally believed to be very limited under normal physiological conditions, but can be induced after injury (Gould 2007). Some quiescent neural progenitor cells, which exit the cell cycle, activate and undergo a new cell cycle. These new activated neural progenitor cells proliferate to maintain the neural progenitor cell pool, while some neural progenitor cells carry out differentiation processes to produce new functional neurons. The number of neurons in the mature nervous system is determined by the balance among cell proliferation, differentiation, and death (Fogarty et al. 2016). Before neurogenesis, the neural plate and tube consist of a single layer of neuroepithelial cells, which forms the neuroepithelium (Gotz and Huttner 2005). Mammalian neurogenesis begins on day 10 of embryonic development. Neural epithelial cells begin to undergo asymmetric division starting from embryonic day (E) 10. From E10, asymmetrical divisions begin to induce neurogenesis. Most of these cells are called NPCs. At the same time, increasingly more NPCs finish their self-renewal process and enter into asymmetric divisions, which result in neuron differentiation. Early efforts revealed that cells undergoing mitosis are generally found apically in the VZ, lining the ventricles, whereas differentiating neurons are located basally near the brain surface (Fishell and Kriegstein 2003). Some radial glial cells occupy most of the nerve epithelium in the apical direction, which can undergo interkinetic nuclear migration that is dependent on the cell cycle. Neural precursor cells in the ventricular surface divide to maintain their population and give rise to neurons that migrate to remote areas. After neurogenesis, cells that maintain self-renewal stay in the ventricular zone. However, differentiated cells that have finished the cell cycle prefer to move along the pial fiber to construct the cortical plate. During adult neurogenesis, several types of intermediate cells are located between the cortex and ventricles. These intermediate cells are produced through asymmetrical divisions and then undergo symmetrical divisions to produce neurons (Noctor et al. 2004).

1.3 Neurogenesis in the Brain

Previous studies have demonstrated that NSCs produce functional neurons. In the adult brain, kinetic studies of neurogenesis are still insufficient. A conservative estimate in rats and mice suggests that one neuron is produced among 2000 existing neurons every day (Kempermann et al. 1997). With aging, the neurogenesis rate decreases, while neurogenesis persists in the dentate gyrus at the same time in elderly rodents and humans (Gage 2000). From embryonic day 10 onwards in mice and humans, NPCs divide asymmetrically to renew themselves and generate other neural cell types. After birth, most neurons in the nervous system have been generated. Only a few types of NSCs are maintained in some specialized niches (Fishell and Kriegstein 2003). In the brain, NSCs are mainly located in two regions. The SGZ in the dentate gyrus of the hippocampus, where new dentate granule cells appear (Gage 2000; Kempermann and Gage 2000). During adulthood, neurons can be generated from NSCs in the SGZ (Goncalves et al. 2016). In the adult SGZ, there are two cell types. Type 1 cells can be detected by Nestin, GFAP and Sox2 expression, which is similar to the way that NSCs are detected. Type 2 cells may be derived from type 1 cells. GFAP protein is not expressed in type 2 cells; however, some type 2 cells that only express Sox2 can undergo a self-renewal cycle and then differentiate into neurons and astrocytes. Intermediate progenitors generated from some radial and non-radial precursors give rise to neuroblasts, and intermediate neurons migrate to the granule cell layer and differentiate into DG cells. The DG neurons extend processes into molecular layer and project axons towards CA3. Another region is the SVZ of the lateral ventricles, where new neurons are generated and migrate to the olfactory bulb to become interneurons through the RMS (Gage 2000). In the adult SVZ, there is a population of ependymal cells in the ependyma, which are regarded as unique progenitors during adult neurogenesis. Proliferating radial glial-like cells give rise to transient amplifying cells that in turn generate neuroblasts. In the RMS, neuroblasts form a chain and migrate toward the olfactory bulb through a tube formed under the assistance of astrocytes. These progenitor cells in the SVZ also contribute to constant neurogenesis in the olfactory bulb. Once these progenitors reach the core of the olfactory bulb, immature neurons detach from the RMS and migrate radially toward glomeruli where they differentiate into different subtypes of interneurons (Lledo et al. 2006). In fact, in the early central nervous system, their fates have been determined. There are still three cell types: type A cells are considered as migrating neuroblasts, type B cells are GFAP-positive progenitor cells, and type C cells are a class of transit amplifying cells. All of these cells constitute the basis of adult brain neurogenesis.

Adult brain neurogenesis regions are the SGZ in the dentate gyrus of the hippocampus and SVZ of the lateral ventricles. Neurons generated in the SVZ migrate through the rostral migratory stream and reach the olfactory bulb. In the SGZ, intermediate progenitors are generated from radial and non-radial glia, and intermediate neurons migrate into the DG zone. During adult neurogenesis, many factors are involved in regulating the niche. In the SGZ region, mature neurons, newborn neu-

rons, astrocytes, and oligodendroglial cells construct a complex microenvironment that is vital for CNS development, especially adult neurogenesis. Astrocytes in the hippocampus promote the occurrence of hippocampal neurons and the integration of newborn neurons, which may be achieved through the Wnt pathway. In addition, astrocytes from the hippocampus, which are not derived from the spinal cord, promote neural progenitor proliferation and neuronal fate determination of multipotent adult NSCs in culture (Lim and Alvarez-Buylla 1999; Song et al. 2002). Neurogenesis regulation by astrocytes results from some membrane-attached factors being expressed by astrocytes. These factors play a key role in regulating neural precursors, such as migration and synapse formation (Barkho et al. 2006). Microglia play a positive role by enriching the neurogenesis environment in the SGZ region. They recruit T cells to function to the most extent (Ziv et al. 2006). In the SVZ region, there is a class of ventricular cells with high Noggin expression, which promotes neurogenesis through bone morphogenetic protein signaling pathways. Ventricular cells facilitate neural stem cell self-renewal together with pigment epithelium-derived factors. Some dopamine fibers in SVZ progenitors promote NSC proliferation by dopamine receptors (Lim et al. 2000; Platel et al. 2010). In the brain, factors regulating neurogenesis are complex and diverse. Calcium channel agonists increase adult hippocampal neuron differentiation. Neurogenesis regulation also requires the Sonic hedgehog pathway. Better regulation of the microenvironment is essential for the occurrence of nerves in the brain.

1.4 Neurogenesis in the Spinal Cord

In the last decade, NSCs have been found in specialized zones of the nervous system during adulthood. These endogenous NSCs are capable of constantly differentiating into neurons (Shihabuddin 2008). However, studies have generally concentrated on the activation and recruitment of brain endogenous neurogenesis, whereas few reports concern spinal cord endogenous neurogenesis. Thus far, studies have not only identified NSCs in the subgranular zone of the dentate gyrus and the subventricular zone of the lateral ventricles in brain, but also among ependymal cells of the central canal in the spinal cord (Coskun et al. 2008; Gage 2000; Gross 2000). In the spinal cord, the ependymal cell is the only cell type with a potential differentiation ability. The ependymal cell originates from embryonic day 14–16 radial glial cells. At 1 week postnatally, these ependymal cells begin to differentiate and appear to form two distinct subpopulations. The first subpopulation is derived from radial glial progenitor cells during embryonic development. The second subpopulation forms postnatally, and the first ventricular tube occurs in the first 8–15 days after birth (Delgehyr et al. 2015). However, it is unclear whether these astrocytes and oligodendroglia originate from the same cell clone or different ependymal subpopulations. Ependymal cells are ciliated cells lining the ventricular system of the central spinal canal. They are responsible for moving cerebrospinal fluid and forming a barrier in the brain and spinal cord parenchyma. In the intact spinal cord, few ependymal cells

divide. Once cultured in vitro, they vigorously divide and produce astrocytes, oligodendrocytes, and neurons (Burda and Sofroniew 2014). There are three dividing cell subpopulations in the adult mammalian spinal cord. Eighty percent of proliferating cells are oligodendrocyte progenitors. These cells maintain a strong ability to proliferate. Their major function is to generate myelinated oligodendrocytes in the adult spinal cord, especially after spinal cord injury (Barnabe-Heider et al. 2010). Less than 5% of cells are astrocytes. These populations divide infrequently to maintain their population. Upon spinal cord injury, astrocytes participate in glial scar formation (Barnabe-Heider et al. 2010; Lee-Liu et al. 2013). In addition, ependymal cells occupy less than 5%, but they are a class of cells with cilia. They are the only cell type with multipotency in the spinal cord, which allows differentiation and the three types of cells to appear. All of these factors contribute to spinal cord neurogenesis and functional recovery.

1.5 Neurogenesis After Injury

Neurogenesis in other adult CNS regions is generally believed to be very limited under normal physiological conditions, but can be induced after injury (Gould 2007). After spinal cord injury, ependymal cells begin fast divisions by self-renewal and generate a large number of astrocytes that participate in scar formation. In addition, they generate a small number of oligodendrocytes capable of myelinating axons. Therefore, ependymal cells in the adult spinal cord represent a potential NSC population (Burda and Sofroniew 2014). After injuries including peripheral injury, some specialized genes are highly expressed. The appearance of their gene products around the central process periphery promotes regeneration of the central nervous system. ATF3 is expressed in injured neurons and combines with promoters together with C-Jun to promote neuron regeneration. Sox11b also regulates neural progenitor cell proliferation and promotes neural stem cell differentiation to neurons.

1.6 Regulation of Neurogenesis

During adult neurogenesis, a superior neurogenesis microenvironment is regarded as the center where neurogenesis occurs easily. Increasingly more scientists have begun to focus on research of neurogenesis microenvironments (Schofield 1978). In the adult brain, reactive NSCs are restricted by the microenvironment components. Some cellular factors have been identified (Inghilleri and Iacovelli 2011; Riquelme et al. 2008). Mature neurons, such as interneurons, release GABA that regulates the proliferation of sporadic neural stem cells. The process of neuron maturation, dendritic development, and newborn neuron integration is also regulated (Ge et al. 2006). Newborn neuron survival is affected by glutamate, and the NMDAR is involved in such regulation (Tashiro et al. 2006). To investigate mechanisms of adult neurogenesis, many scientists have investigated transcription factors, cytoplasmic factors,

epigenetic regulators, and niche receptors (Ma et al. 2010). In terms of the NSC differentiation mechanism, previous studies have reported two pathways. First, there is self-regulation including negative and positive regulation. The Notch signaling pathway directs NSCs to divide symmetrically and increase NSC numbers, which allows neural stem cells to maintain stem cell traits. Therefore, notch plays a negative role during neural differentiation. However, the bHLH transcription factor family plays an important role in positive regulation. The bHLH transcription factor family includes Mash1, NeuroD, Ngn1/Ngn2, and Math. These factors induce NSCs to undergo asymmetric division and produce new neurons. In addition, transcription inhibitor N-CoR prevents NSCs from differentiating into glial cells (Imayoshi and Kageyama 2014). Wnt also plays a key role during neural stem cell proliferation and differentiation. Wnt3 promotes neuronal fate commitment and proliferation of neural precursors in the adult SGZ (Kleber and Sommer 2004; Lie et al. 2005). Shh is activated in RG cells (Ahn and Joyner 2005) and required for their maintenance and establishment in the SVZ and SGZ of the adult brain (Bonaguidi et al. 2005). Second, exogenous signal regulation is also necessary, which includes cytokines and the niche. EGF and bFGF are involved in maintenance of NSC self-renewal, whereas PDGF, BDNF, IL-1, and LIF function during NSC differentiation. Regarding the niche, many classes of cells exist around neural stem cells. Some neural cells, glial cells, and matrix, including all kinds of glycoproteins and mucoproteins, construct a complex regulation network through crosslinked connections. Interestingly, the Notch signaling pathway also prefers to regulate niche components to prevent ependymal cells from differentiating into niche astrocytes through EphB2 in the adult SVZ region (Nomura et al. 2010). Further research is still necessary. In contrast, BMPs tend to promote NSC differentiation into glial cells rather than neurons in the adult brain (Bonaguidi et al. 2005; Lim et al. 2000). The BMP negative function can be antagonized by noggin and ngn-1 that are expressed by ependymal cells in the SVZ, and astrocytes and granule cells in the SGZ, respectively (Lim et al. 2000; Ueki et al. 2003). Inhibition of BMP signaling in adult SGZ neural precursors may result in their activation and an increase in neurogenesis. However, it can also lead to a decrease in precursors and loss of neurogenesis. Therefore, regulation of the BMP equilibrium is very important. Methamphetamine reduces dentate gyrus stem cell self-renewal by delaying the cell cycle, inducing more neural differentiation. During this process, it may rely on the NMDA signaling pathway. Sox2-positive cells are also decreased (Baptista et al. 2014). Hepatocyte growth factor promotes fibroblast proliferation and survival of cortical neurons, and regulates the maturation of neurons. Factors involved in the regulation and control of neuron occurrence are diverse, complex, and mutually connected, and more research should be performed for further exploration.

1.7 Prospects

Over the past several years, the field of adult neurogenesis has turned its focus from depicting the neurogenesis phenomenon and its regulation to explaining molecular mechanisms of neuronal development, stem cell regulation, and functional contributions. Previous studies have shown tremendous progress in understanding adult neurogenesis. The discovery of continuous neurogenesis in the adult nervous system has overturned a century old dogma and provided us with a new opinion on the plasticity of adult neurogenesis. Currently, we know the neural progenitor cell locations and their occurrence processes. However, it is unclear whether we know all progenitor cell locations. If a new progenitor cell pool was found, it may guide us to perform deeper research for more progress. Although many factors have been demonstrated to regulate adult neurogenesis, the relationship between factor regulation and functional recovery is still being determined. Proving the theory that the regulation mechanism guides regeneration after injury is our ultimate aim. Cognitive testing has provided a good method to understand human DG functions, which may indicate a possible relationship between neurogenesis and behavioral pattern separation. However, new methods are needed to evaluate neurogenesis in vivo (Tamura et al. 2016). More information about neurogenesis after injury will facilitate solving the problem from a new perspective. Gene expression advances have already provided us with a new insight into the molecular mechanisms and signaling cascades involved in neural differentiation and newborn neuron functional integration. Our goal is to search for more effective treatment strategies against neurological disease and further resolve our healthcare difficulties.

2 3D Culture

Cell culture plays important roles in biological research, drug discovery, and industrial applications. As the first cell line, Hela cells are an established cell culture and tool of biology. Traditional cell cultures are 2D, in which cells are grown on flat dishes as a monolayer. However, failures of 2D-cultured cells are due to the lack of natural microenvironments. Recently, increasing evidence has indicated that 3D cell culture systems more accurately represent the actual microenvironment compared with 2D culture systems. Thus, the 3D-cultured cell behavior is more reflective of in vivo cellular responses. In fact, studies have shown that the morphology and physiology of 3D-cultured cells are different from those of cells in 2D culture environments.

With the increase in the number of cell lines, parallel advancement in cell culture techniques, imaging, data acquisition, and analysis methods is being applied to 3D cell culture. Using such systems, the cells are co-cultured in different material structures with a variety of different types of cells in vitro. Cells in a vector with a 3D spatial structure can migrate, grow, and perform many functions. 3D culture meth-

ods mimic in vivo conditions and have become increasingly important in biological research and tissue regeneration.

2.1 3D Culture Methods

Traditional 2D culture usually grows cells as a monolayer on glass plates or, more commonly, polystyrene tissue culture flasks. However, 3D cell cultures grow cells as 3D aggregates or spheroids using a scaffold/matrix or in a scaffold-free manner as shown in Fig. 1 (Edmondson et al. 2014). 3D culture provides a biological microenvironment for cell proliferation, differentiation, and specific extracellular matrix secretion, which can be potentially used in many applications. 3D scaffolds are generated using various natural materials (e.g. collagen, gelatin, elastin, chitosan, chitin, fibrin, and fibrinogen) and synthetic substances (e.g. polystyrene, PCL, and 2-hydroxyethyl methacrylate). The most commonly used scaffolds are collagen, gelatin, agarose, fibronectin, and laminin, especially collagen. In 3D culture systems, a type I collagen matrix is commonly used because of many advantages such as easy processing, flexibility for live cell manipulation, and low cost. By changing the collagen concentration or introducing chemical cross-linking compounds, we can vary the pore sizes of collagen scaffolds, as well as the ligand density and stiffness, making it easy to change the gel structural properties (Baker et al. 2009).

2.2 3D Cultures Models and Scaffolds

A wide variety of techniques are currently applied to culture cells in 3D structures. These techniques can be classified into two main categories: scaffold based and non-scaffold based. Scaffold-based methods include biological scaffolds, polymeric hard scaffolds, and micropatterned microplate surfaces. Non-scaffold-based 3D culture

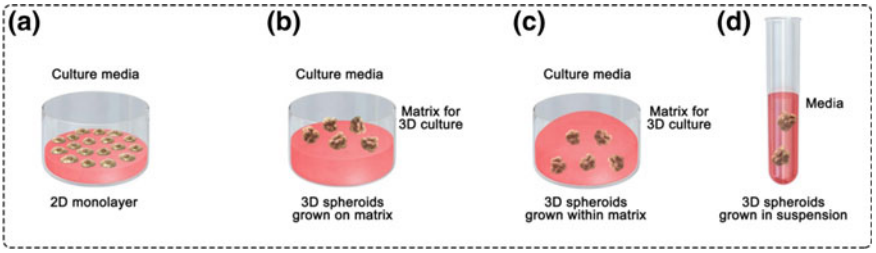

Fig. 1 Schematic diagrams of traditional 2D culture (**a**) and 3D culture of cell spheroids or aggregates grown on a matrix (**b**), cells embedded within a matrix (**c**), or scaffold-free cell spheroids in suspension (**d**)

methods include the hanging drop method, microfluidic 3D cell culture, and spheroids (Ravi et al. 2015).

2.2.1 Scaffold-Based 3D Cell Culture

Biological Scaffolds

Scaffolds can be made of natural or biological components such as proteins commonly found in in vivo microenvironments. They resemble in vivo microenvironments such as exposure to soluble growth factors, hormones, and other molecules that cells interact with in vivo, which can alter gene and protein expression. Biological scaffolds are advantageous compared with polymeric scaffolds, because the latter lack endogenous factors that act mainly to permit cell functions, but not promote appropriate cell behaviors. For example, the viability and proliferation of numerous cell types grown in hydrogels are increased because they are derived from natural sources, which promote many cellular functions (Caliari and Burdick 2016).

Polymeric Hard Scaffolds

3D tumor and tissue models designed to mimic in vivo environments can be created by seeding cells on pre-fabricated scaffolds or matrices. 3D cultures form because cells attach, migrate, and fill the interstices within the polymeric hard scaffold (Erickson et al. 2009). These scaffolds provide a physical support system for cell culture in vitro and have shown utility in in vivo tissue regeneration, because they have the potential to recreate the natural physical and structural environment of living tissue. Polymeric hard scaffolds are used for regenerative medicine and preclinical testing.

Micropatterned Microplate Surfaces

Micropatterned plate surfaces contain micrometer compartments regularly arrayed on the bottom of each well. Wells are square or round. The plate wells allow reduced consumption of culture medium in conventional cell culture. The well materials are mostly rigid and impermeable, and facilitate long term cell culture. They allow precise control of the size, shape, and location of the cultured cell in the micropattern combined with microtechnology as microengineered templates. Micropatterned cell culture provides numerous cell samples for subsequent analysis, which are cultured under the same condition.

2.2.2 Non-scaffold-Based 3D Cell Culture

Hanging Drop Method

HDP takes advantage of natural cell attachment by lacking surfaces to which cells can attach. The cells assemble spontaneously into a 3D structure. The method can be used to co-culture two or more different cell populations, elucidating the role of cell-cell or cell-matrix interactions in specifying spatial relationships between cells. It facilitates studies of embryonic development and tumor-stromal cell interactions in malignant invasion, and applications in tissue engineering. This simple method provides a tool to generate tissue-like cellular aggregates for molecular and biochemical analysis in a physiologically relevant model.

Spheroids

Microplates used for spheroids can be optically clear round bottomed with a black opaque body and have a covalent ultralow attachment surface to reduce cellular adhesion to the well surface. It is easy to exchange medium or apply drugs. The 3D spheroid cellular model can better simulate natural cellular interactions and mimic in vivo microarchitecture for more biologically relevant information. This method promotes formation of single spheroids by robust circular formation.

Microfluidic 3D Cell Culture

Microfluidic techniques allow spatial control of fluids in micrometer-sized channels, which have been explored to extend the physiological relevance of 3D culture models. Microfluidic 3D cell culture using microfluidic perfusion plates enables high quality cell culture in a 3D matrix. Cells in microfluidic platforms can be overlaid or embedded in the gel for long term perfusion culture and be used to create similar heterogeneous models. Multiple 3D ECM experiments can be performed at a fraction of the time. It also provides an additional level of complexity to the cellular environments in which cells have continuous nutrition and oxygen as well as waste removal through culture medium.

2.3 3D Culture Advantages

In 2D cell culture, cells are grown on flat polystyrene dishes. The unnatural material is very stiff. This stiffness may affect cell functions including cell-to-cell and cell-to-matrix attachments, as well as cell proliferation and differentiation (Ravi et al. 2015). Some important areas for which 3D cell culture systems are excellent models include studies involving drug discovery, cytotoxicity, genotoxicity, cell growth,

apoptosis, survival, gene and protein expression, differentiation, and developmental changes. Similarly, co-cultures in 3D systems provide a better understanding of the cell interactions.

2.3.1 Cell Attachments

Cells adhere and spread on a surface and form unnatural cell attachments on a synthetic surface in conventional 2D culture. In contrast, cells attach to another cell and form natural cell-to-cell attachments in 3D cell culture. The cells synthesize and secrete extracellular matrix in three dimensions, which is the natural material to which cells attach. It is flexible and soft like natural tissues. It consists of native complex proteins and provides important biological cues to the cells. In 3D cell culture environments, cells exert forces on one another, move, and migrate. These cell-to-cell interactions in 3D cell culture include gap junctions that directly couple one cell to another. Gap junctions are much more widespread in 3D cell culture. Cells in a 3D system are closely proximate that enables surface adhesion molecules and surface receptors to bind to surface adhesion molecules. In addition, 3D culture maximizes cell-to-cell communication and signaling critical for cell functions. The phenotype or functions of 3D-cultured cells are more complex and similar to the functions of native tissues than those of 2D-cultured cells. For example, liver cells perform more active functions in 3D versus 2D. Muscle cells perform more muscle cell functions in 3D cell culture than 2D cell culture. Moreover, cartilage cells form more differentiated cartilage tissue in 3D compared with 2D.

2.3.2 Cell Proliferation

The proliferation of 3D cultured cells is rapid. The characteristics of 3D-cultured stem cells can be regulated by growth factors to direct differentiation to the desired lineage in a specific 3D environment. The physical, chemical and biological characteristics of a scaffold can be modulated by the features of the materials. In addition, cells cultured in a 3D environment show a different status from those in traditional 2D culture. Currently, 3D culture is used for stem cell research, cancer research, and drug screening. 3D culture has a huge potential for applications in scientific research as well as clinical applications.

2.4 Applications of 3D Cell Cultures

3D culture approaches facilitate better understanding of in vivo conditions. Cells in 3D environments are good models as “near-to-in vivo” systems and provide useful insights in various manners (Cukierman et al. 2001). The major advantage of 3D over 2D systems is the decrease in the gap between the cell culture system and cellular physiology. In conventional 2D conditions, some interactions are lost, including

extracellular matrix components, cell-to-cell attachments, and cell-to-matrix interactions, which are important for cell proliferation, differentiation, and cellular functions in vivo. In addition, the integration of signaling pathways is mutual when cells are grown in basement membrane-like gels (Lee et al. 2007). 3D cell culture systems are applied to differentiation studies. For example, 3D systems are useful to understand the mechanisms of human osteoblast differentiation into osteocytes (Mc Garrigle et al. 2016) and study the role of osteocytes in bone metastasis and tissue engineering, as well as cancer research, gene and protein expression studies, drug discovery, and pharmacological applications.

2.4.1 Cell Function Applications

Cell Morphology Studies

Distinct differences in the morphology of cells have been found when grown as monolayers or in 3D cultures. A panel of breast cancer cell lines exhibited similar morphology as monolayers. However, in 3D culture, their morphologies could be classified into four types. For example, cell lines that formed grape-like morphology (e.g. MDAMB-361, AU565, and CAMA-1) become loosely associated with reduced cell-cell adhesion, which might explain why they have a highly metastatic potential as the tumor progresses.

Cytoskeleton Studies

The compositions of the cytoskeleton and extracellular matrix are very different in cells grown as monolayers or in 3D scaffolds. For example, smooth muscle cells on a 3D matrix have fewer focal adhesions, actin stress fibers, and a reduced cell surface area because of restriction by the surrounding matrix.

Cell Proliferation Studies

Some studies indicate that physiological stiffness is a well conserved inhibitor of mitogenesis at the elastic moduli range of 600–4,300 Pa in tissues isolated from mammary glands, thoracic aortae, and femoral arteries of mouse (Klein et al. 2009).

Cell Adhesion and Signaling Studies

In multicellular organisms, cells are surrounded by various other cells and a well-structured matrix. When grown in a complex environment, communication and adhesion to diverse elements appear to control cell behaviors. For example, morphology of the A549 cell line significantly differs in conventional monolayers and laminin-

enriched 3D cultures. For the first 4 days, the cell doubling times are similar. During the next 4 days, resistance to X-rays increases. Global gene expression of cells in monolayers and 3D cultures is different. The genes may be involved in biological adhesion, cell adhesion, immune responses, or organ development. Cancer biologists and clinicians are increasingly interested in signaling pathways because of their roles in tumor development and influence on therapeutic modalities. For example, mTOR and tIGF-1R signaling cascades are activated in EWS patients because of their roles in chemotherapy resistance. When 2D EWS monolayers and 3D scaffolds are compared, 3D cultures cells show a high amount of phosphorylated IGF-1R, indicating abnormal IGF-1R/mTOR gene expression (Fong et al. 2013).

Cell Apoptosis and Motility Studies

Interactions of the cytoskeleton and the extra materials in 3D have important effects on various cell activities, including inhibition or acceleration of apoptosis.

The movement of cells into biomaterial scaffolds is a prerequisite for tissue repair and regeneration. There is a requirement for engineered biomaterials to optimize 3D-cultured cell migration.

Cell Physiology and Microenvironment Studies

3D cell cultures facilitate expounding the various cell functions, such as proliferation, adhesion, viability, morphology, and microenvironment, and responses to drugs. The environments surrounding cells play a key role in deciding cell differentiation fates and biological functions. Tumor microenvironments have been extensively studied, which, along with abnormal conditions, emphasizes the importance of a healthy milieu for cell behaviors. When oral squamous cell carcinoma cells were cultured on synthetic PLG scaffolds, major changes occurred. A study showed increases in secretion of bFGF, VEGF, and IL-8 by 23-, 2-, and 98-fold, respectively. Certain factors secreted in 3D cultures important for IL-8 expression are lost in 2D models.

Tumor Models and Cancer Biology Studies

3D cultures have gained attention in the field of regenerative medicine for their usefulness as in vitro models of solid tissues. Many cell types grown as 3D tumor spheroids have three layers, inner quiescent, central necrotic, and outer proliferating layers, which mimic the microenvironment of human solid tumors. In terms of tumorigenesis mechanisms, several studies show that 3D cell organizations are more novel, unanticipated visions, and represent an integral missing component in in vitro cancer studies.

2.4.2 Gene and Protein Expression

It will be interesting when we compare gene and protein expression in 3D cultures. Studies show significant differences in gene and protein expression of cells in 3D cultures compared with that of in vivo cancers.

2.4.3 Drug Discovery and Drug Response Studies

Apart from studies on direct drug effects, 3D systems have proven to be efficient models to study the synergistic effects of biologically important substances on cells. A 3D approach is simple but effective. Researchers treated oral squamous cell carcinomas in 3D PLG and 2D monolayers with the cytotoxic PI3-kinase inhibitor LY294002. The monolayers were sensitive to the drug, whereas 3D-cultured tumor cells with their microenvironment had significant resistance (Fischbach et al. 2007). Numerous drug candidates fail in clinic trials every year because of low efficacy, adverse events, and other reasons. Such failures indicate that the results obtained from 2D cultures may not predict in vivo results. For example, studies have failed to reach the primary endpoint of Zalutumumab, a fully human EGFR monoclonal antibody that has been demonstrated clinical benefit in refractory head and neck cancer (Luca et al. 2013). The differences in cellular responses of 2D and 3D cultures are possibly due to five aspects. First, there are some differences in the physical and physiological properties of 3D and 2D cultures. 2D-cultured cells are stretched out on an unnatural flat surface, but cells maintain normal morphology when cultured in scaffold regardless of biological or synthetic materials. Furthermore, therapeutic agents are often designed to target specific cell surface receptors. However, there are differences in the structure, localization, and arrangement of cell surface receptors on 2D- and 3D-cultured cells, which will affect the binding efficiency and their expression. The quantity and position of surface receptors in the same cell type are also different in the two culture environments. Third, gene and protein expression profiles are distinct between 2D- and 3D-cultured cells. 2D-cultured cells grow as a monolayer that is completely different from the in vivo environment, and their reactions to drugs are not accurate. Fourth, 2D-cultured cells are all in the same proliferation stage, whereas 3D-cultured cells are in different stages. Studies show that large spheroids are usually heterogeneous: the outer region is proliferating cells and the inner region is quiescent cells because of the lack of nutrients and gas exchange. Activation of cell proliferation may be needed for reactions to some drugs. Fifth, differences appear in the drug distance to cells and local pH. In a 2D monolayer, drugs diffuse to cells equally, but in a spheroid, the drug diffusion to cells may lead to variable concentrations. This effect depends on how deep the cells are from the surface. The depth of a cell is also related to the local pH.

2.5 Prospects

With the high demand for scientific research, cell culture systems have advanced rapidly over the past decades. As 3D culture systems emerge, they are exhibiting many features that better mimic those of in vivo environments. 3D culture systems are closer to animal models in many aspects (Yamada and Cukierman 2007). 3D culture systems have also been successfully introduced into translational medicine. To date, 3D culture systems have been reported to be appropriate for more than 380 cells lines. The 3D structure provides the possibility to analyze complex cell interactions, which was unable to be fulfilled by traditional 2D culture systems. 3D culture systems have good prospects for both basic and applied research. They have attracted broad interest to develop new support materials. It is evident that 3D cell culture models are better models than traditional 2D monolayer cultures, because 3D cultures improve cell-cell and cell-extracellular matrix interactions, and cell populations and structures resemble in vivo architectures. This approach provides an environment that mimics the in vivo environment. In the past several years, a number of 3D cell culture systems have been developed as experimental tools for diverse research purposes. Certainly, 3D culture systems have very high potential for application in many fields of cell research, disease modeling, and drug discovery.

In summary, 3D systems mimic in vivo conditions compared with 2D systems, making 3D culture more useful for studies of real cell functions and drug applications. 3D cell culture technologies generate more healthy cells and promote cell proliferation, which provide convenient approaches for further studies.

3 3D Neural Stem Cell Culture

Since Reynolds et al. first successfully isolated NSCs from the adult mammalian CNS and induced them to proliferate and differentiate into neurons and astrocytes, NSCs have been defined as self-renewing cells that generate neurons and glia of the nervous systems of all animals during embryonic development (Brent and Reynolds 1992). NSCs differentiate into neurons, astrocytes, and oligodendrocytes (Gage 2000). The classical method for isolating and culturing NSCs is to isolate cells from a particular region of neural tissue in the brain or spinal cord, or from embryonic and neonatal neural tissues. Conventional NSC isolation and culture methods can be divided into two types according to the NSC growth mode: the neurosphere culture method (three-dimensional culture) and monolayer culture method (two-dimensional culture) (Reynolds and Weiss 1992).

3.1 Overview of 3D NSC Culture

The earliest 3D NSC culture appeared in 1992. Reynolds et al. first used a neurosphere assay to promote NSC proliferation in vitro. The striata of adult mice were enzymatically dissociated, and cells were seeded in a culture dish in the absence of a supplementary substrate or adhesion factors (Fig. 2).

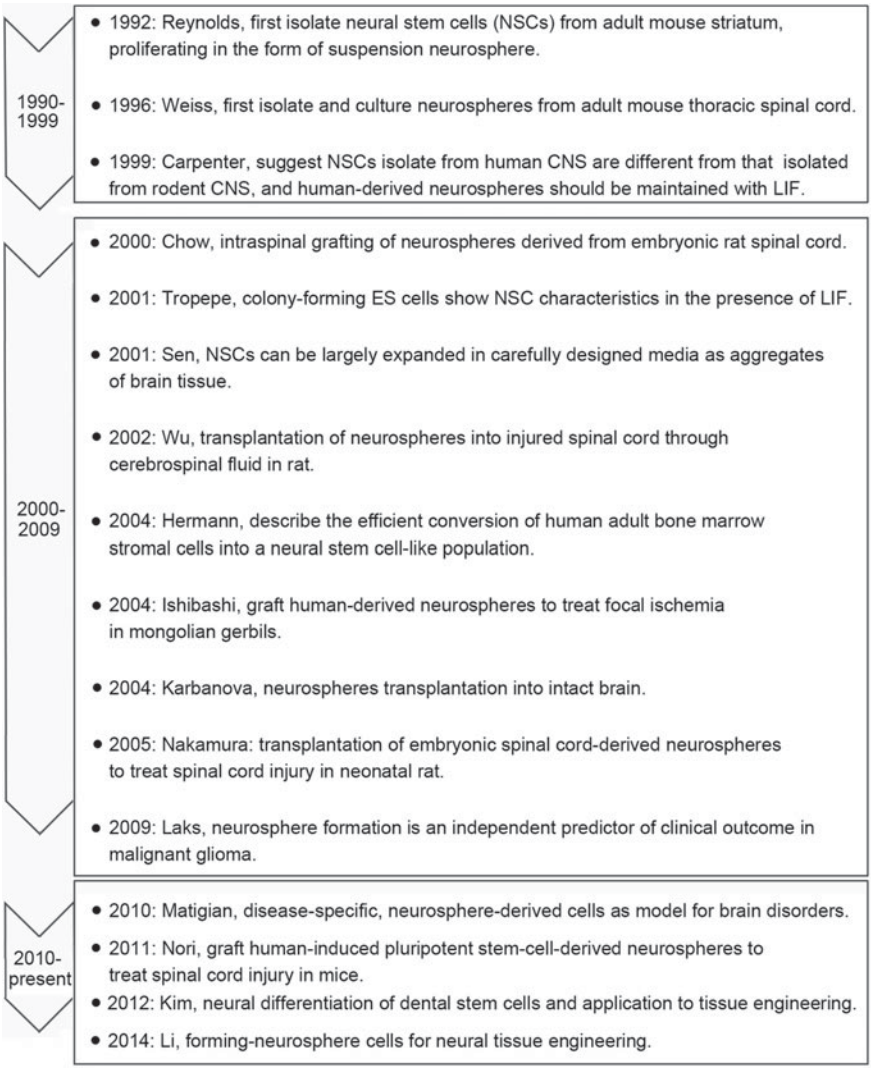

Fig. 2 Graphical summary of events in 3D neurosphere culture and applications in neural tissue engineering

After 2 days in vitro, most cells had died, a few cells were undergoing cell division, and proliferating clusters of cells detached and formed a sphere of nestin-positive cells. This neurosphere culture method is simple to perform and the most common method for isolating, propagating, and studying embryonic and adult NSCs. However, in the neurosphere assay, both NSCs and NPCs proliferate and form clonal spheres. Therefore, to discriminate NSCs from NPCs in the suspension neurosphere assay, Louis et al. established the neural colony-forming cell assay in 2008 (Louis et al. 2008).

3D NSC culture is an artificially created environment in which NSCs are allowed to grow and interact with their surroundings in all three dimensions. Unlike a 2D environment, 3D cell culture permits cells to branch out in all directions in vitro, which is similar to how they would behave in vivo. In addition to the abovementioned neurosphere assay, there are commercially available culturing tools that claim to provide advantages for 3D NSC culture in vitro (Fig. 3).

In general, 3D NSC-culturing platforms can be classified as two types: scaffold-free and scaffold techniques (Cheng et al. 2013). Scaffold-free techniques apply another approach independent from using scaffolds, including the use of low adhesion plates, rotating bioreactors, magnetic levitation, and magnetic 3D bioprinting (Cheng et al. 2013; Souza et al. 2010). Scaffold techniques include the use of solid scaffolds, hydrogels, collagen, and other natural or artificial materials (Yang et al. 2012). Pivotal design requirements for polymer scaffolds used to 3D culture NSCs can be categorized as physical (e.g. rigidity and degradation rate), biochemical (e.g. biological activity), and practical (e.g. cost and reproducibility). Soft matrices are needed because they facilitate cell attachment and axon regrowth. They also demonstrate mimetic mechanical properties observed in vivo, which are required for neural tissue engineering. Scaffolds can be artificially modified for better binding of neurotrophic factors or NSCs. For example, in our previous study, a porous collagen scaffold was modified with chemical moieties for covalent crosslinking with cetuximab, an anti-EGFR antibody. When the functionalized collagen scaffold was implanted into a rat complete transection model, it promoted grafted NSCs to differentiate into neuronal lineages rather than astrocytes (Li et al. 2013). In addition, the anti-EGFR antibody in the collagen scaffold bound to EGFR expressed on the surface of NSCs. As a result, the functionalized collagen scaffold retained grafted NSCs at an injury site, preventing them from diffusing into cerebrospinal fluid.

In vitro 2D and 3D culture models of NSCs show differences in cell morphology, gene expression, cell-cell interactions, cell-matrix interactions, proliferation, migration, and differentiation (Knowlton et al. 2016; Prewitz et al. 2012). For example, outgrowth of axons from NSCs demonstrates a more aligned profile in a biomaterial scaffold, because it provides an aligned ECM structure that controls neurite morphology (Han et al. 2010). A significant difference is noted in gene expression between 2D and 3D NSC cultures, specifically for genes encoding cytoskeleton, ECM, and neuronal function proteins. Cells connected to surrounding cells through intercellular signaling and cell-cell interactions are regulated by the extracellular matrix (ECM). A great advantage of changing from traditional 2D monolayer culture to 3D culture is that the 3D condition stimulates these complicated cell-cell and cell-ECM

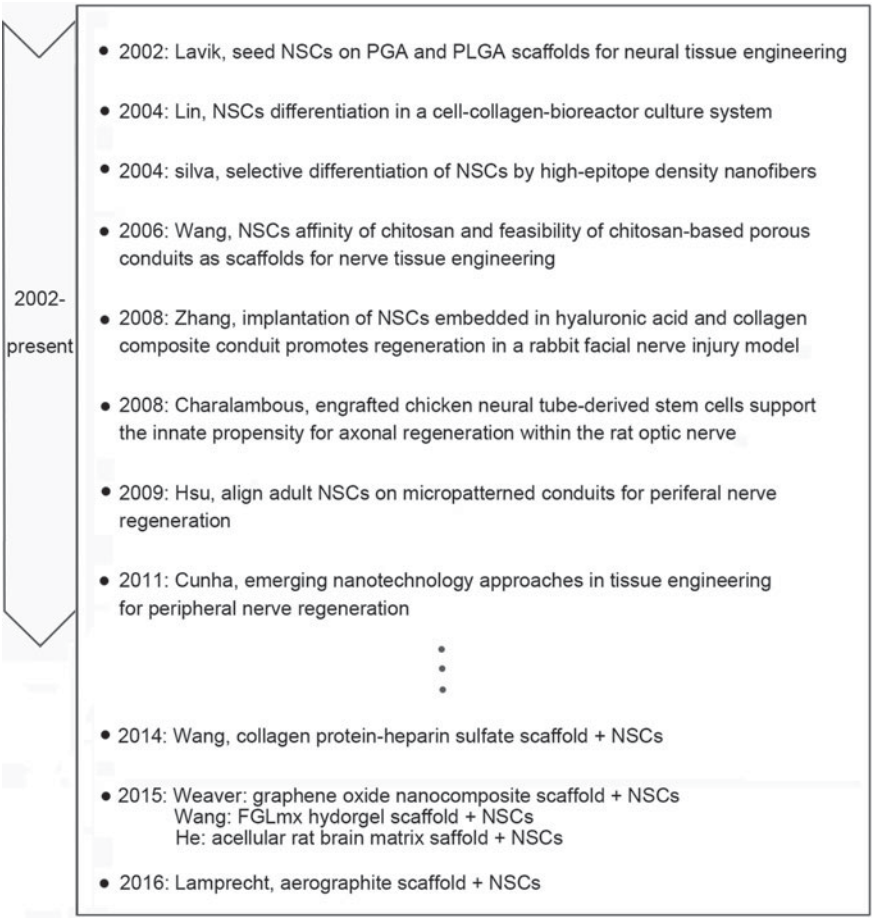

Fig. 3 Graphical summary of events in 3D neural stem cell culture and applications in neural tissue engineering

interactions more than the 2D condition. Cell-cell and cell-ECM signaling define the tissue specificity and drives homeostatic maintenance. According to the organizing principle proposed by Bissell and colleagues, cell-cell and cell-ECM interactions regulate progression of a cell's life cycle, including proliferation, migration, and apoptosis. These interactions are also vital for precise tissue formation during developmental stages (Gibbons et al. 2013). In general, compared with 2D culture, 3D NSC cultures as in vitro models aim to fill the gap between 2D NSC studies and the in vivo environment, especially for neural tissue regeneration therapies where there is little regenerative possibility. These 3D culture models are indispensable to support NSCs, allowing a natural flow of oxygen, nutrients, and growth factors, and possibly favoring neural cell regrowth (Cunha et al. 2011). Applications of these

3D cultures may be very useful for basic research of neural tissue structures and functions, designing disease models, engineering tissue for drug development, and generating replacement tissues with a patient's genetic makeup.

3.2 Applications

The mammalian CNS has little capability for self-repair, and mature neurons are not able to proliferate after severe injury. Recent progress in the field of neural biology and tissue engineering offers a deeper understanding of CNS diseases. A primary example of the intersection between biology and tissue engineering is neural tissue engineering, a domain that gains a great deal from implementing the recent progress in 3D NSC culture in vitro. However, the demand for biomimetic neural tissue models and effective therapies remains unmet. The recent promotion of expanding 2D neural tissue engineering to the third dimension shows great potential to advance the field. Here, we present several of the most representative achievements in 3D culture of NSCs, which is classified into scaffold-free and scaffold techniques (Fig. 4).

3.2.1 Applications of 3D NSC Aggregates

NSCs tend to proliferate and form neurospheres when cultured under scaffold-free conditions. The applications of neurosphere culture in vitro include transplantation for the treatment of CNS diseases and constructing CNS disease models for diagnosis and screening potential drugs by acting as a predictor of clinical outcomes.

Transplanting Neurospheres for the Treatment of Neural Diseases

Studies have reported that functional recovery can be induced after transplantation of neurospheres into the injured brain or spinal cord of rodents. After transplantation in vivo, grafted neurospheres survive, migrate, and differentiate into three neural lineages at the injured site. Furthermore, they enhance angiogenesis to ameliorate hypoxic and ischemic conditions in brain disease or promote axonal regeneration and synapse formation with host tissue neurons in spinal cord injury. A previous study introduced the method of supplying neurospheres to the injured spinal cord through injection into the cerebrospinal fluid from the fourth ventricle or cisterna magna. The results showed that a large quantity of injected cells migrated to the lesion site and integrated with the host spinal cord tissue for repair. In another study, the authors transplanted hiPSC-NSs into a mouse Th10 lesion epicenter at 9 days after inducing the impact injury. The grafted hiPSC-NSs survived and migrated into the host spinal cord tissue. Moreover, they differentiated into neurons, astrocytes, and oligodendrocytes at 2 weeks post-surgery. About 50% of the grafted hiPSC-NSs had differentiated into neurons of which half were mature. The authors also

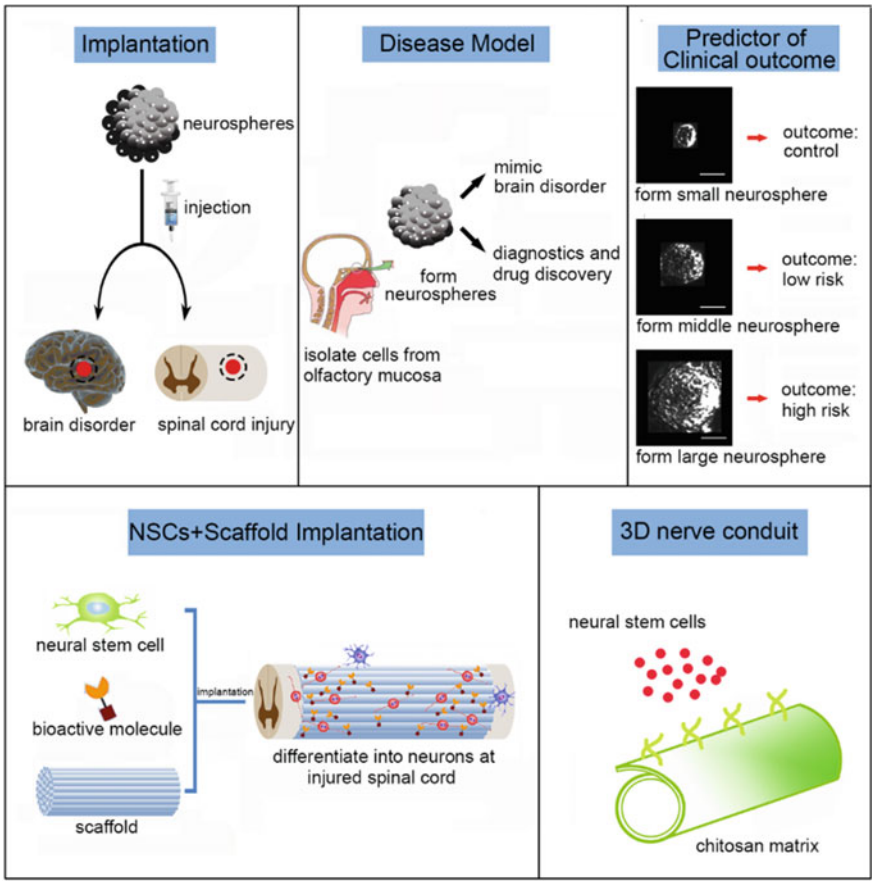

Fig. 4 Example applications of 3D neural stem cell culture

observed synapse formation between hiPSC-derived neurons and host neurons as well as enhanced axonal regrowth and angiogenesis after injury. The transplanted hiPSC-NSs promoted motor functional and electrophysiological recovery after spinal cord injury (Nori et al. 2011).

Constructing CNS Disease Models for Diagnosis and Drug Screening

Recent progress in modeling CNS diseases from patient-derived cells, which are robust enough to produce large quantities of relevant cells, has greatly advanced clinical molecular and functional analyses. For example, Matigian et al. designed schizophrenia and Parkinson's disease models based on patient-derived cells from the olfactory mucosa, which are regenerated from NSCs throughout life. Mucosa biop-

sies from patients and control subjects grew as neurospheres in vitro, and cell lines derived from neurospheres were obtained to analyze gene expression, protein expression, and cell functions including neurodevelopmental pathways in schizophrenia, and xenobiotic metabolism, oxidative stress and mitochondrial functions in Parkinson's disease. The authors claimed to have identified new candidate genes and pathways for future investigation, and the disease model created from patient-derived neurospheres may provide better understanding of the disease etiology, diagnostics, and drug discovery (Matigian et al. 2010).

Neurospheres as a Predictor of Clinical Outcomes

Considering that formation of renewable neurospheres cultured in vitro could be a defining characteristic of certain CNS diseases, such as brain glioma, studies have been designed to evaluate the relationships among neurosphere formation, tumorigenic capacity of patient-derived glioma, and clinical outcomes. Tumor samples were cultured under neurosphere conditions and transplanted into mouse brains to examine whether they were tumorigenic. The authors observed that renewable neurosphere formation and tumorigenic capacity both predicted an increased risk of rapid tumor progression and patient death. In general, this study suggested that the ability of neural stem-like cells from patient-derived brain glioma to form neurospheres in vitro showed potential as a predictor of clinical outcomes (Laks et al. 2009).

3.2.2 Application of NSC-Loaded Scaffolds to Neural Tissue Engineering

Although the development of tissue engineering approaches for nervous systems is in its infancy, a growing number of important applications have emerged. NSCs encapsulated or adhered to natural or artificial scaffolds can be used in the field of modeling and treating nervous system diseases. They can also be used to fabricate biomimetic neural tissue to replace damaged tissue in patients.

Injured Neural Tissue Interacts Reciprocally with NSC-Seeded Scaffolds for Repair

There are several advantages of NSC-seeded scaffold transplantation over NSC aggregate grafts for treating neurological disorders. For example, scaffolds can be designed to incorporate the extracellular matrix composition of neural tissue, which provide mechanical properties for cell attachment. When the scaffold is transplanted in vivo, it will have good biocompatibility with host neural tissue and guide cells to grow in an ordered direction. In addition, scaffolds can be functionalized with different kinds of bioactive molecules to regulate adverse niches caused by injury, facilitating neuronal differentiation of NSCs at injury sites. Park et al. seeded NSCs

onto a polyglycolic acid polymer scaffold and implanted the scaffold into infarction cavities of the mouse brain injured by hypoxia-ischemia. The authors observed that an intricate meshwork of many highly branched neurites of endogenous and grafted NSC-derived neurons emerged, and some anatomical connections appeared to be reconstituted. The results showed that transplantation of NSC-seeded scaffolds may gradually augment the constitutive reparative response by improving a series of interactions between grafted and host NSCs, including promotion of neurogenesis, connectivity, and reformation of injured cortical tissue.

Generation of Functional Artificial Neural Tissue to Replace Damaged or Diseased Tissues

Among the various neural regenerative procedures, one of the most promising is filling the injury site with artificial neural tissue. Lin et al. designed a multicomponent and micropatterned conduit seeded with NSCs and transplanted the nerve guidance conduit into a 10 mm-long defect of the sciatic nerve in male SD rats. The authors found that the biodegradable nerve guidance conduit provided both physical and biological guidance for axon regeneration at the injured site and offered an alternative for repairing sciatic nerve injury. Another study combined HUCB-NSCs and biodegradable scaffolds to form artificial neural tissue and transplanted the HUCB-NSC-seeded scaffold for hypoxic/ischemic brain injury repair. The results indicated that the 3D environment facilitated HUCB-derived NSC maturation and could be considered as a promising regenerative medicine application for nervous system repair (Jurga et al. 2009).

3.3 Challenges

Although it has been reported that NSC aggregates and NSC-loaded scaffolds can be successfully applied to neural tissue engineering, some challenges related to the transition from 2D to 3D culture systems still exist. For example, when NSCs are grown as spheroids in suspension culture, cells in the innermost layer have little access to nutrients and oxygen, and it is inconvenient to expel waste and CO_2. Therefore, the growth of NSCs is suppressed in the center, and large neurospheres are unable to grow past a certain size in standard culture environments, which makes it difficult to research the later stages of development in vitro. The lack of sufficient vascularization is a crucial factor of 3D neural tissue engineering to be considered in future work (Novosel et al. 2011). An abundant blood supply will transport nutrients for NSC metabolism and provide enough oxygen to expel waste and CO_2. Furthermore, formation of new blood vessels in and around grafted artificial neural tissue may contribute to integration of the transplant with host tissue.

Future work in this field will aim at improving long-term survival in 3D-cultured tissue by introducing vasculature. Current techniques include promoting the for-

mation of new blood vessels from existing vessels (Chen et al. 2012). Other novel strategies for enhancing vasculature are electrospinning fibrous meshes, encapsulating blood vessels into synthetic scaffolds, or making use of existing blood vessels in natural scaffolds. Efforts should be directed to allowing mass delivery of oxygen and nutrients to achieve long term viability in neural tissue engineering.

3.4 Prospects

A long-term aim of using 3D culture models of NSCs is the application of personalized neural regenerative tissue engineering. Using a patient's own NSCs to replace an impaired or diseased tissue or organ will decrease issues associated with limited donor supply. Moreover, implementation of 3D fabrication techniques will aid in the formation of biomimetic structures in neural tissue. Therefore, biomimetic tissue could be transplanted into the injured site and replace destroyed neural tissue, thereby ultimately ameliorating the quality of life for patients with developmental neurodegenerative disorders.

4 Microgravity of 3D-Cultured Neural Stem Cells

Recently, increasingly more attention has been focused on the influence of microgravity in tissue engineering. One of the most important characteristics of space is microgravity, i.e. the absence of gravity. There is universal gravity on Earth, which greatly affects cellular metabolism, morphology, signaling pathways, and secretion. It is of great importance to explore how microgravity affects physical, chemical, and biological processes during the exploration and interpretation of space.

Under microgravity, a large variety of fundamental physical phenomena are significantly changed or even eliminated completely. Spaceflight provides a real microgravity environment, but spaceflight opportunities are very rare and the costs are very high. Technical limitations of spaceflight studies seriously restrict tissue engineering research for space biomedicine. Spaceflight studies require perfect technical simulation systems to mimic the microgravity in space. To satisfy research needs, many instruments have been designed to simulate microgravity by the NASA Johnson Space Center for cell culture, such as the slow turning lateral vessel, high aspect ratio vessel, rotating wall bioreactor, and rotary cell culture system. The more widely used bioreactor machines imitate microgravity (Nickerson et al. 2004).

The principle of these microgravity-simulating rotation bioreactors is dependent on the balance between gravitation and the centrifugal force. These devices are commercially available to generate simulated microgravity and conveniently provide a good platform for microgravity studies. A great deal of microgravity-related experiments in cell biology have been performed using these instruments. Simulated microgravity provides a better approach for space studies concerned with biomedical

research on Earth. Using these instruments, we may better understand the effect of microgravity on the functions of stem cells.

4.1 Effect of Microgravity on the Structure and Functions of Stem Cells

Stem cells are widely used in tissue engineering and cell therapies to treat or prevent many diseases. They might play an important role in guiding and shaping the future of clinical medicine. Stem cell technologies are used to induce directed differentiation and maintain stem cell self-renewal. Proper exploitation of these methods may lead to the generation of 3D human tissue models that have great potential for future medical therapies. It has been reported that stem cells tend to gradually lose their polarity and differentiation ability in long term 2D culture. In vitro 3D cultures are emerging as novel systems to study tissue development, organogenesis, and stem cell behavior in vitro. Understanding the effect of microgravity on stem cell functions will provide important information for treatment and preventive strategies to deal with medical problems during space exploration.

In comparison with traditional static adherent culture, microgravity provides a very specialized environment for cell culture. Many researchers have pointed out that microgravity switches 2D cell culture to 3D. In microgravity, cells will not settle at the bottom of the culture dish. They float freely in the culture medium, which contributes to interacting each other and assembly together to form multicellular 3D spherical structures without a scaffold in microgravity. Dissociated cells tend to assemble together for tissue-like self-organization. Microgravity provides an opportunity for dissociated floating cells to self-aggregate and interact with each other freely. Cells are inclined to float in the culture medium and not sediment in a low shear-modeled microgravity environment. In particular, 3D cell aggregates formed under microgravity are larger than those engineered in conventional bioreactors or 2D cultures.

Recent studies have shed light on some molecular mechanisms concerning how microgravity affects the morphology and function of cells. A thorough understanding of gene expression is important to reveal the molecular mechanisms driving microgravity-induced alterations. Various cell types alter their gene expression profiles when exposed to microgravity, but the underlying mechanism has not been clearly elucidated yet. Revealing the molecular mechanisms of stem cells in microgravity will contribute to understanding the intricate regulation of cell growth and functions. Understanding the molecular and cellular mechanisms of alterations in microgravity is urgently needed to meliorate space medicine. It will cause a profound biotechnological effect on regenerative medicine. Many studies have shown that microgravity alters the global expression profile of genes. When murine bone marrow stromal cells were cultured in osteo-inducing medium during spaceflight, microarray results revealed changes in the expression of 1,599 genes. The expres-

sion of most cell cycle-related genes was decreased, suggesting that cell proliferation was inhibited in microgravity. Moreover, the cells tended to express neural associated genes (Monticone et al. 2010). The same conclusion was reached by Professor Ma and his team. Their results indicated that rat mesenchymal stem cells tend to differentiate into neurons in simulated microgravity (Chen et al. 2011). Further studies revealed that the gene expression of EBs during differentiation was changed in microgravity compared with normal conditions. The results of quantitative real-time PCR indicated that expression of most differentiation-related genes was changed (Blaber et al. 2015).

Studies of stem cells in microgravity have made some progress. It is well known that microgravity affects the cell proliferation rate, metabolism, and physiology. Previous studies have shown that microgravity promotes the proliferation of stem cells by sustaining their differentiation ability (Yuge et al. 2006). Cells will not settle at the bottom of a culture dish and float freely in the culture medium, which contributes to interactions each other and assembly together to form multicellular 3D spherical structures without a scaffold in microgravity (Grimm et al. 2014). mESCs were the first ESCs applied to study biological effects of microgravity using a multidirectional G force generator device that simulates microgravity. The major changes of mESCs in microgravity were a decrease of adhesion, increased apoptosis, and delay in the DNA repair process (Wang et al. 2011). The differentiation of ESCs is also significantly affected by microgravity. The formation speed of embryoid bodies was faster in simulated microgravity than in conventional culture, which was accompanied by multidirectional differentiation into hepatocyte-like cells, heart muscle cells, endothelial cells, blood vessel cells, and various other cells types. Furthermore, rat embryonic stem cells form spheres that grow in cultivation medium without LIF, serum, or a feeder layer in microgravity. LIF and a feeder layer of MEFs play pivotal roles in maintaining the pluripotency of ESCs. The results indicated that simulated microgravity may provide a better environment for ESC culture (Kawahara et al. 2009). These findings provide valuable information on ESC-related regenerative medicine. 3D aggregates may be grown to form tissue-like structures in the future. When grown in a 3D environment, ESCs self-organize and differentiate into various cell types of the three germ layers, such as endoderm- and ectoderm-derived cells, mimicking their in vivo counterparts.

As another extensively studied type of adult stem cell, MSCs are widely used in tissue engineering. MSCs can be induced to differentiate into various cell types such as myocardial cells, osteocytes, adipocytes, and hepatocytes. When dog MSCs were cultured under microgravity conditions, both the morphology and growth rate of the cells were better than those of cells cultured under normal conditions. Microgravity decreased the proliferation potential of murine BMSCs in the KUBIK aboard space mission ISS 12S (Soyuz TMA-8 + Increment 13) from March 30 to April 8, 2006 (Monticone et al. 2010). Several studies have demonstrated that the differentiation of MSCs is strongly affected by gravity. Osteogenic differentiation is suppressed by microgravity, whereas differentiation of adipocyte, cartilage, nerve, and endothelial lineages was improved in microgravity. Directed differentiation of MSCs into the cartilage phenotype is significantly enhanced by microgravity com-

pared with normal gravity (Wang et al. 2007). When MSCs were cultured in microgravity, the osteogenic differentiation-related gene RUNX2 was suppressed, whereas adipocyte differentiation-related genes, such as glucose transporter 4, adipsin, leptin, and PPARγ2, were upregulated. Neural differentiation-related genes, such as those involved in neural development, neuron morphogenesis, transmission of nerve impulses, and synapses, were also activated during spaceflight (Monticone et al. 2010). The changes in the differentiation potential of MSCs under microgravity indicated that microgravity is expected to facilitate the clinical application of MSCs.

Neural stem cells play pivotal roles during CNS development by differentiating into multiple cell types such as neurons, astrocytes, and oligodendrocytes. The proliferation of human neural stem cells is also affected by microgravity. Expression of β-adrenoreceptor is induced by microgravity. Furthermore, the formation of cAMP upregulates CREB pathways, and PKA is activated by microgravity. The amount of mitochondrial mass and the ATP level are both elevated by microgravity, demonstrating that microgravity promotes proliferation of neural stem cells by improving the function of mitochondria (Chiang et al. 2012).

The microenvironment of stem cells is formed by the interaction among cells and the relationship between cells and the extracellular matrix. Under microgravity conditions, stem cell niches are apparently different from those under traditional 2D conditions. Stem cell niches play pivotal roles in maintaining the balance of self-renewal and differentiation of stem cells, which determines the fate of stem cells. Currently, scientists have begun focus on the effect of simulated or real microgravity on the structure and function of stem cells.

4.2 Effect of Microgravity on Tissue Engineering

Tissue engineering has provided a broad clinical prospect to treat tissue or organ defects. The study of tissue engineering in simulated or real microgravity environments is a hot research area in space medicine. Space provides low shearing stress microgravity, and microgravity induces many changes in organisms during spaceflight. Recent spaceflight studies have verified the role of microgravity in modulating stem cell-related tissue regeneration. When EBs were exposed to microgravity conditions for 15 days, their differentiation ability was inhibited, whereas self-renewal was maintained. When EB cells cultured in microgravity were returned to normal gravity, they showed greater stemness and more readily differentiated into cardiomyocytes (Blaber et al. 2015). This alteration of the mESC differentiation capacity could have significant implications in the field of human tissue engineering and the use of stem cells to regenerate adult tissues.

In vitro 3D culture has gained a lot of research interest in tissue engineering. As an emerging novel system, 3D culture has been used to study tissue development, organogenesis, and stem cell behavior in vitro. 3D cell culture is widely used in tissue engineering and regenerative medicine. When stem cells are cultured in a 3D environment, they form organoids and can be propagated for a long period in vitro.

To better understand the mechanism of the formation of multicellular 3D structures, we performed analyses from various perspectives, including signal transduction, cell adhesion, apoptosis, and the extracellular matrix induced by altered gravity conditions. Many studies have suggested that the formation of 3D aggregates under microgravity can be divided into three phases of regulation from 2D to 3D growth: (1) cells undergo changes in interactions with the ECM; (2) under microgravity conditions, the expression of proapoptotic factors increases, which increases the apoptosis rate; (3) many signaling and kinase-dependent pathways are altered during the transition from 2D to 3D (Grimm et al. 2014). Wnt signaling can be altered under microgravity conditions. The majority of Wnt pathway-related genes are downregulated by microgravity (Lin et al. 2009). Many kinds of signaling pathways form a complicated network to govern cell actions. Numerous signaling pathways are influenced by microgravity in the interior of the cell (Puca et al. 2012).

Tissues such as 3D constructs can be maintained for long periods in simulated microgravity created by RWV bioreactors. Potential advantages of using a simulated microgravity environment for tissue engineering have been demonstrated by several studies. Devices that generate simulated microgravity are widely used in tissue engineering, which provide better in vitro model systems for spaceflight studies. Various cell types exposed to real space or simulated microgravity conditions can be grown in the form of 3D tissues. Primary porcine hepatocytes gathered spontaneously to form high density 3D aggregates and maintained important metabolic functions when cultured in the NASA rotary bioreactor for 21 days (Nelson et al. 2010). The random positioning machine system produces simulated microgravity, which can be used to engineer cartilage grafts with less cells (Stamenkovic et al. 2010).

Space medicine research can facilitate development of new strategies for tissue engineering. The increasing scientific and medical relevance of such research is evidenced by the growing number of reports in which advanced bioreactors are used for in vitro studies in physiologically relevant cell and tissue models. Tissue engineering in microgravity has had a tremendous effect on space research, biomedical sciences, and its applications on Earth.

5 Systematic Analysis of Molecular Mechanisms Involved in the Proliferation and Differentiation of NSCs During Spaceflight

The SJ-10 satellite provided a platform to elucidate the molecular mechanisms of cell alterations in biological, physical and chemical processes in space. The recovery cabin maintained orbit for 12 days in space. The aim of the SJ-10 satellite was to understand the effect of spaceflight on the growth and differentiation of NSCs. 3D cell culture systems have advantages by providing more physiologically relevant information and predictive data, which closely mimic in vivo conditions compared

with traditional 2D cell culture systems. A biomaterial-based 3D culture system was adopted for differentiation analysis during spaceflight.

5.1 Cell Culture and Harvesting

Rat NSCs were isolated from telencephalon tissue and cultured in proliferation or differentiation media for 12 days during spaceflight of the SJ-10 satellite. Simultaneously, cells were cultured on the ground under similar culture conditions as the control group (Fig. 5). During spaceflight, the cells were cultured in fully automated bioreactors designed by the Shanghai Institute of Technical Physics of the Chinese Academy of Sciences. The automatic cell culture device changed the culture medium, collected images, and fixed cell automatically. When the recovery cabin of the satellite returned to Earth, some cells were fixed by RNA ladder stabilization reagent or paraformaldehyde, while live cells were used to detect cell viability.

5.2 Preparation of 3D Cell Cultures

A collagen sponge scaffold was chosen for 3D NSC culture, which was prepared from bovine collagen. The diameter of the round collagen sponge sheet was approximately 5 mm and its thickness was about 1 mm. Our previous studies had shown that cells maintain a good condition when attached on collagen sponge scaffolds by SEM. Therefore, the collagen sponge scaffold had good biocompatibility with NSCs. Before departure of the satellite, a cell suspension (3×10^5 cells per collagen scaffold) was seeded on the scaffold for cell attachment and then cultured in differentiation medium.

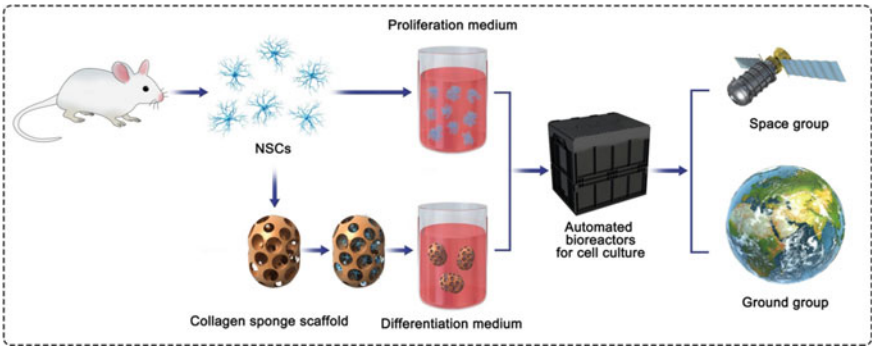

Fig. 5 Schematic diagram of NSC culture in space and ground groups

5.3 Remote Sensing Data of Cell Proliferation

For proliferation analysis, the single cell suspension grew as spheroids in the proliferation medium without outside interference. The diameter and size of the spheroids can be used as key indicators of cell proliferation. During the spaceflight, real-time image data, which reflected the dynamics of cell proliferation, were acquired by the automated imaging system at regular times, and then the images were instantly transmitted back to the telemetry data center on the ground. Based on the images, the size of neurospheres in the space group was smaller than those in the ground group cultured in the same system on Earth. The smaller volume of the neurospheres indicated that the growth rate of NSCs was inhibited in space.

5.4 Cell Viability Analysis

The viability of cells after spaceflight was evaluated by FDA/PI staining, a fluorescence-based universal method. Cells were incubated with the staining solution (100 μg/ml FDA and 60 μg/ml PI) for about 5 min and then transferred to PBS. In the staining process, living cells are stained with FDA, while dead cells are stained with PI. The results of FDA/PI staining indicated that both the proliferative cells of neurospheres and differentiated cells cultured on the scaffold exhibited high cell viability after returning from space.

5.5 Analysis of Immunofluorescence Staining

Immunofluorescence staining was performed by a slightly modified version of published procedures (Cui et al. 2016). Three pivotal differentiation-related markers, Tuj1 (neuron-specific tubulin III, early neuron marker), GFAP (astrocyte marker), and Map2 (mature neuron marker), were chosen as the evaluation indicators of differentiation. First, the cells were incubated with primary antibodies overnight at 4 °C and then incubated with the secondary antibodies for 1 h at room temperature. Fluorescence images were obtained by a scanning laser confocal fluorescence microscope. In the space group, the expression of Map2 was significantly increased compared with the ground group. In contrast, the expression of GFAP was decreased during spaceflight. Nevertheless, the spaceflight had no effect on the expression of Tuj1. The expression of Tuj1 was steady in both space and ground groups. These results led us to speculate that NSCs tended to differentiate into neurons, while the differentiation of NSC to astrocytes was inhibited in space.

5.6 RNA-Seq Preparation and Sequencing

To understand the molecular mechanism driving the differentiation and proliferation of NSCs in space, we performed RNA-seq to understand the alteration of the genome-wide transcription profile caused by spaceflight. Total RNA was extracted using Trizol reagent (Sigma Chemical, St. Louis, MO) from all groups of NSCs. Each group included three biological replicates. An RNeasy Plant Mini Kit (Qiagen Sciences, Valencia, CA) was used to purify the RNA extracts. The quality of RNA was assessed by agarose gel electrophoresis and the ND-1000 NanoDrop spectrophotometer 2000 (NanoDrop Technologies, Wilmington, DE). The concentration and integrity of RNA indicated that the RNA quality of all samples was high. The Illumina X Ten platform was chosen to construct RNA libraries and perform RNA-seq of cell samples cultured in space and ground groups. Transcriptome libraries were constructed from 1 μg total RNA with the TruSeq Stranded mRNA LT Sample Prep Kit (Illumina, San Diego, CA).

Numerous studies have shown that the Illumina platform offers significantly increased sequencing depth, and it may generate millions of 150 bp paired-end high quality sequence reads. In the proliferation group of NSCs, we obtained 46,081,266 and 46,759,526 paired-end reads from space and ground group libraries, respectively. We also obtained 48,036,974 and 48,395,940 paired-end reads for space and ground group libraries in the differentiation group of NSCs, respectively. Low quality reads were filtered and removed. Filtered data were logarithm-transformed and normalized by the quantile method. Clean reads resulting from a filter step were pooled together and then mapped to the reference genome. The matching rates of the read pairs, which were mapped to the rat reference genome in the Ensembl database, release 82, in the four groups were 89%, 85.46%, 89.46%, and 87.69%, respectively. The reference genome sequence of 22,268 Rattus norvegicus genes and annotation data were downloaded from the UCSC website (http://genome.uscs.edu). The relative expression of differentially expressed genes between space and ground groups was measured in fragments per kilobase of transcript per million mapped reads, and represented as the FPKM unit. Based on expected number of fragments per kilobase of transcript sequence per million base pairs sequenced (FPKM) with a false discovery rate (FDR)-adjusted p-value of ≤ 0.05 and |log2 ratio|, ≥ 1, 3279 annotated differentially expressed genes were identified in the differentiation group of NSCs. Moreover, 1589 differentially expressed genes were screened in the proliferation group of NSCs between space and ground groups.

The original sequencing reads were processed by several steps. First, the quality of sequencing data was checked by the NGS QC Toolkit, and then low quality reads, which contained ploy-N regions, were removed. Tophat was used for mapping these clean reads to a reference rat genome to identify known and novel splice junctions and generate read alignments for each sample (Kim et al. 2013). Next, cufflinks was used to calculate and normalize the FPKM value of each gene (Trapnell et al. 2012). The read counts of genes were processed and analyzed by htseq-count (Anders et al. 2015). The gene fusions from the RNA-Seq data were identified by the

deFuse program (McPherson et al. 2011). The identification of DEGs was analyzed by functional estimator SizeFactors and nbinomTest (Anders et al. 2012). The thresholds used to screen the significantly differentially expressed genes were set as p-value < 0.05 and absolute fold change >2.

5.7 Hierarchical Clustering Analysis

Hierarchical clustering analysis of major DEGs was performed using the FPKM values of proliferating or differentiated NSCs in space and ground groups. In the proliferation group, the heatmap of hierarchical clustering showed that the differential gene expression patterns of selected DEGs were related to stemness, the cell cycle, or proliferation (fold-change >2 or $P < 0.5$) using the FPKM values. The expression of cell proliferation marker Ki67, cell cycle regulators (CDKN2a, CDKN2b. and CDK1), and the transcription factor Pax6 was significantly changed during spaceflight. As important cell cycle regulators, the expression of cyclin-dependent kinase CDK1 was downregulated, while the expression of negative cell cycle regulators CDKN2a and CDKN2b was upregulated in the space group. The alteration of cell cycle regulators may induce cell cycle arrest and influence cell proliferation. The expression of cell proliferation marker Ki67 was downregulated in the space group. In addition to these genes, many self-renewal- and neurogenesis-related genes, such as Pax6, Rest, and Klf4, were upregulated in the space group (Fig. 6a). In the differentiation group, the heatmap indicated that the expression of differentiation-related genes and many epigenetic regulator genes in the space group was also significantly altered. The expression of two neuron markers, Map2 and Tuj1, was elevated, while expression of astrocyte marker GFAP was downregulated. In line with the expression of neuron markers, the expression of PTEN, HDAC2, Wnt5A, Neurog2, and Ezh2 genes was also upregulated in the space group (Fig. 6b). Previous studies have demonstrated that these genes may facilitate neural differentiation of NSCs (Barton and Fendrik 2013; Bengoa-Vergniory and Kypta 2015; Chen et al. 2015; Lange et al. 2006; Sher et al. 2012; Sun et al. 2011). Considering that Id3 partly determines neural stem cell differentiation into astrocytes, the downregulation of Id3 shown in the heatmap of the space group may explain why the astrocyte marker GFAP was downregulated.

5.8 Gene Ontology and KEGG Enrichment Analysis

Considering that functional and pathway analyses are powerful tools to gain insights into the underlying biology of differentially expressed genes, GO enrichment and pathway analyses of DEGs were performed using the GO website and KEGG. The Entrez IDs of differentially expressed genes were entered into the R package cluster Profiler to perform GO enrichment analysis (Yu et al. 2012). Functional annotation analysis of DEGs was performed using the DAVID tool (http://david.abcc.ncifcrf.gov/) for biological interpretation (Huang et al. 2009). GO analysis was carried out

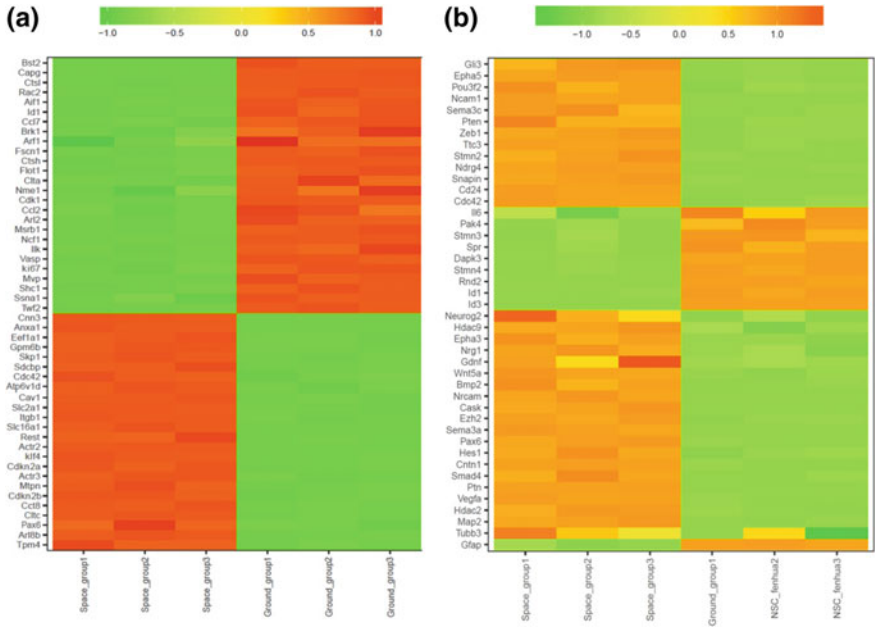

Fig. 6 Hierarchical clustering analysis. Hierarchical clustering analysis of expression profiles of neuron differentiation-related genes in the differentiation group of NSCs. Red indicates a high z-score, while green indicates a low z-score

using the DAVID functional annotation tool, according to the enrichment scores. KEGG enrichment analysis was also used to analyze the pathways of DEGs. Cluster Profiler was used to perform KEGG enrichment analysis after establishing the parameters. Optional interaction genes were extracted among the screened DEGs using BioGrid and String databases (Chatr-Aryamontri et al. 2017; Szklarczyk et al. 2015).

In the proliferation group of NSCs, GO enrichment analysis showed that the DEGs were enriched in the terms of cell proliferation, calcium ion binding, apoptotic process, cell junction, cytoskeleton, and microtubule. Pathway analysis based on the KEGG database showed that these genes were significantly enriched in MAPK, Rap1, and Ras signaling pathways. Additionally, GO enrichment and KEGG pathway analyses showed that DEGs in the proliferation group of NSCs were remarkably enriched in the cell cycle, apoptosis, cytoskeleton, and cell adhesion (Fig. 7).

In the differentiation group of NSCs, GO enrichment analysis showed that the DEGs were most enriched in oxidative stress, apoptosis, cell adhesion, and some signaling pathways. Moreover, KEGG enrichment analysis revealed that the enriched pathways were Wnt signaling, cell adhesion, and TNF and NF-κB signaling pathways (Fig. 8).

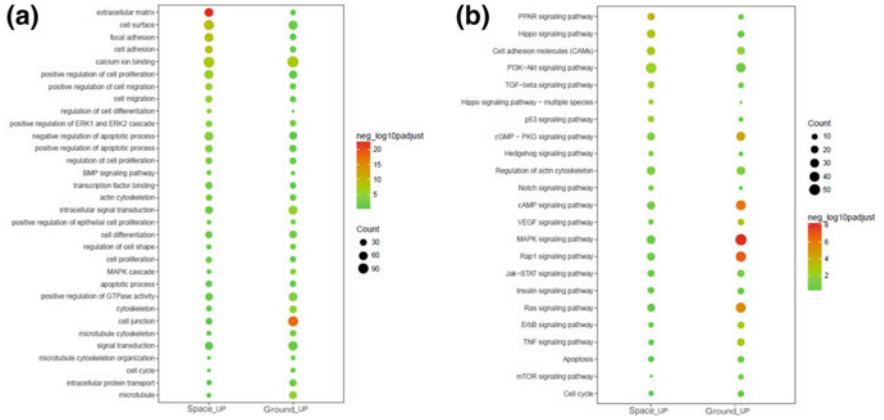

Fig. 7 GO and KEGG analyses of DEGs in space and ground groups of the proliferation group of NSCs

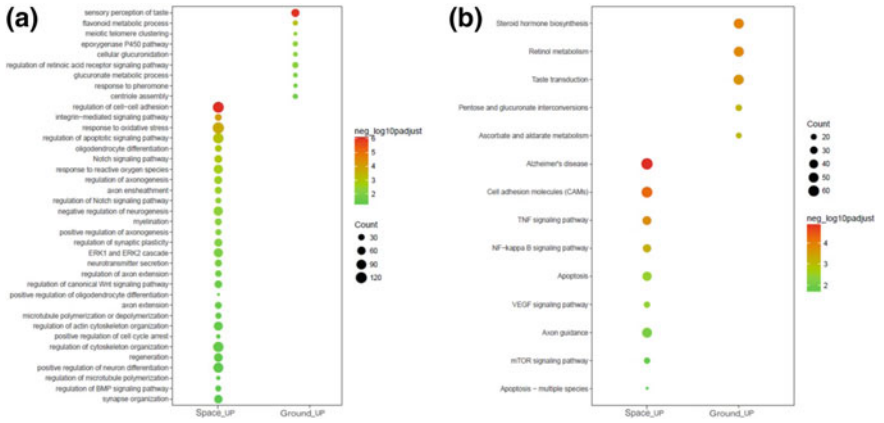

Fig. 8 GO and KEGG analyses of DEGs in space and ground groups of the differentiation group of NSCs

The analyses indicated that many biological processes and signaling pathways were affected by space. The GO terms and KEGG classifications served as indications of significantly different biological processes in NSCs between space and ground environments, which could guild further studies to determine their functions in space. Among the variable cell signaling pathways, Wnt and mTOR signaling pathways have attracted much more attention, because the expression of many important genes involved in the Wnt signaling pathway varied in the space group of NSCs (Fig. 9).

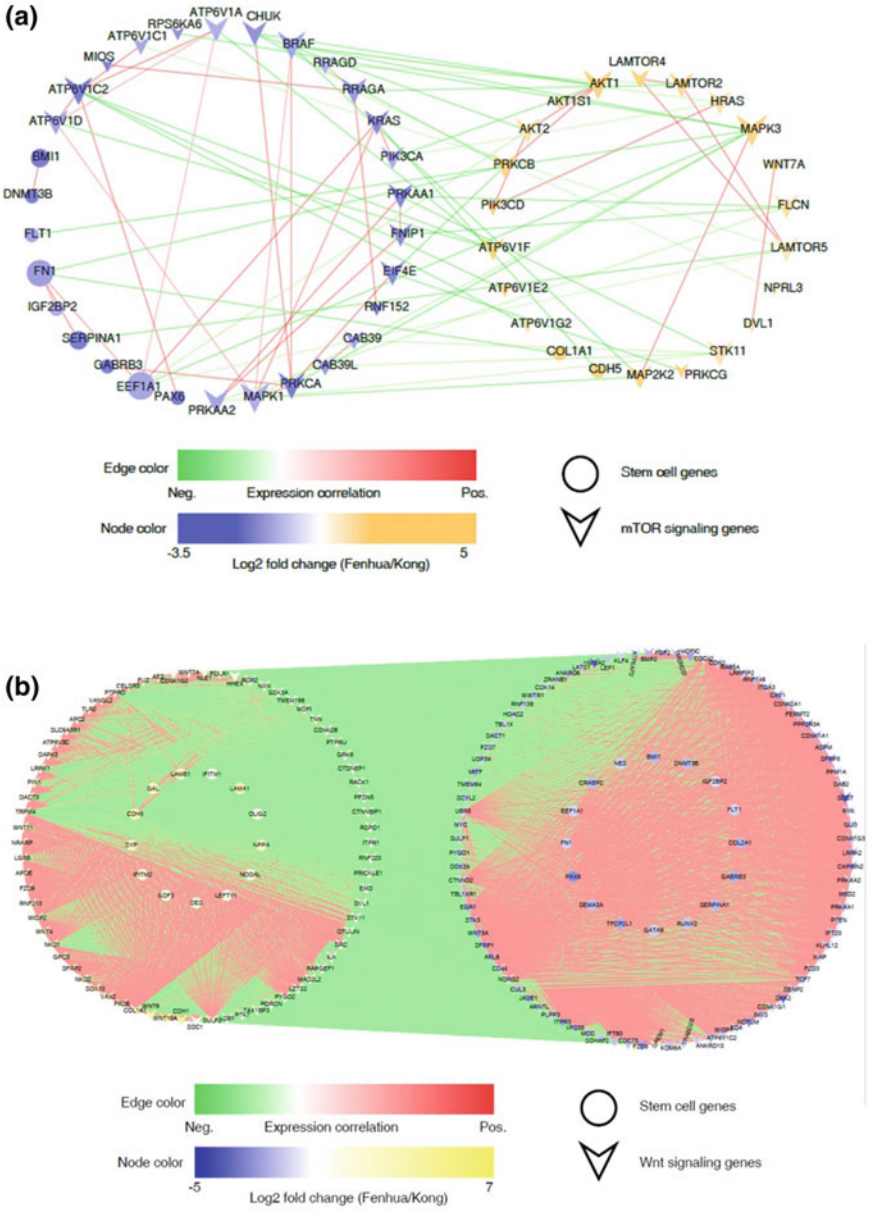

Fig. 9 Interaction regulatory network of NSCs during spaceflight. **a** Interaction regulatory network of mTOR signaling and neural stem cell development-related genes. **b** Interaction regulatory network of Wnt signaling and neural stem cell development-related genes

5.9 Real-Time PCR Analysis of DEGs

To confirm the accuracy of RNA-Seq data, we performed qRT-PCR on 16 randomly selected DEGs to validate the RNA-Seq results. All 16 genes were related to self-renewal and differentiation. First, HiScript II Q RT SuperMix for qPCR System (Vazyme, R223-01) was used to reverse transcribe RNA into cDNA. Then, amplification was performed in 96-well optical reaction plates (Applied Biosystems, Darmstadt, Germany) using a StepOnePlus amplification and detection system (Applied Biosystems Inc., Foster City, CA). The standard reaction mixture contained 100 ng cDNA, a pair of primers, and the SYBR Green I PCR master mix (Applied Biosystems) in a total volume of 25 μl. The standard conditions used for real-time PCR were 10 min at 95 °C, followed by 40 cycles of 15 s at 95 °C for denaturation and 30 s at 55 °C for annealing and elongation. Data were analyzed using StepOne v2.0 software (Applied Biosystems). Data of each sample were normalized to ACTB as an internal control. In accordance with RNA-seq data, the results of qRT-PCR showed that the expression of six genes (Sox2, Notch1, Pax6, Cdkn2b, Cdkn2a, and Cdk1) in the proliferation group was upregulated in the space group. In addition, the expression of proliferation marker ki67 in the proliferation group was downregulated in the space group. Seven genes (Pten, Hdac2, Wnt5a, Neurog2, Ezh2, Ncam1, and Id3) involved in neural differentiation were selected to perform Q-PCR. The expression of these seven genes was elevated in the space group, which has been reported to facilitate neural differentiation of NSCs (Barton and Fendrik 2013; Bengoa-Vergniory and Kypta 2015; Chen et al. 2015; Lange et al. 2006; Sher et al. 2012; Sun et al. 2011). The Q-PCR results validated the accuracy of RNA-seq data.

5.10 Differential Expression and Variation Analysis of miRNAs

As a critical post-transcriptional regulator of gene expression, miRNA plays pivotal roles in regulating differentiation of NSCs. Because numerous gene targets can be regulated by a single miRNA, miRNAs are now considered as important regulators in the proliferation and differentiation processes of NSCs. We also performed small RNA sequencing to gain a large amount of information about the microRNA transcriptome. Differentially expressed miRNAs were screened using DESeq 2 with the thresholds of a multiple hypothesis-corrected p-value of <0.05 and absolute fold change of >2. Quantitative analysis of the differentially expressed miRNAs and systematically organizing the miRNA-target interactions are the basis for thoroughly understanding miRNA-mediated regulatory networks and the underlying molecular mechanisms. In the proliferation group of NSCs, 93 miRNAs were downregulated, which was accompanied by 90 upregulated miRNAs in the space group compared with the ground group. A total of 51 miRNAs were upregulated and 91 miRNAs were downregulated in the differentiation group of NSCs in the space group com-

pared with the ground group. A large number of differentially expressed miRNAs mainly regulated the proliferation, migration, and differentiation of cells. Furthermore, the target genes of these differentially expressed miRNAs were involved in the cell cycle, cell adhesion, and many cell signaling pathways such as Notch and Wnt, indicating that miRNAs serve as important regulators by regulating downstream target genes related to the cell cycle, cell growth, metabolic processes, and cell signaling in the differentiation and proliferation of NSCs.

Among these differentially expressed miRNAs, the expression of let-7, miR-128, miR-378, miR-138, miR-338, and miR-330 was increased in the space group of NSCs which has been reported to have the an inhibitory effect on the proliferation of NSCs (Godlewski et al. 2008; Zhao et al. 2010; Barca-Mayo and Lu 2012; Choi et al. 2016; Cimadamore et al. 2013; Huang et al. 2015). In addition, the expression of differentiation-related miRNAs miR-125, miR-124, miR-134, miR-17, and miR-21 was elevated in the space group of NSCs (Cui et al. 2012; Xu et al. 2012; Gioia et al. 2014; Jiang et al. 2016; Mao et al. 2016).

5.11 Functional Enrichment Analysis of DEG miRNAs and Construction of the miRNA-mRNA Regulatory Network

To predict the potential functions and target genes of differentially expressed miRNAs identified in the space group of NSCs, functional enrichment of predicted target genes was performed. The systematic analysis results of miRNA-mRNA regulatory functions contributes to exploring the possible molecular mechanisms involved in spaceflight. The expression of differentially expressed miRNAs and their target genes was diverse. miRNA target prediction software miRanda and TargetScan were used to obtain information about target genes of these miRNAs. The principle of screening was to satisfy two conditions: matching score >150 and binding energy <−30 kcal/mol. The data were further filtered using expression correlation. Following preliminary analysis of differentially expressed genes, integrated analysis of miRNA and mRNA expression profiles involved in the proliferation or differentiation of NSCs was performed. A core miRNA-mRNA regulatory network that participated in the proliferation or differentiation of NSCs was constructed. The miRNA-mRNA network-based analysis could be useful to reveal the regulating relationships of DE miRNAs and their target genes. The systematic analysis of the expression and functional interaction involving miRNA and mRNA enables identification of the predicted miRNA-target gene network pattern and functional candidates of miRNA-mRNA pairs associated with spaceflight. The miRNA-target gene regulatory network was constructed with the miRNA-target gene pairs by Cytoscape software with the prefuse force directed layout algorithm (Fig. 10). This network may contribute to better understanding of the roles of spaceflight in regulating the proliferation and differentiation processes of NSCs.

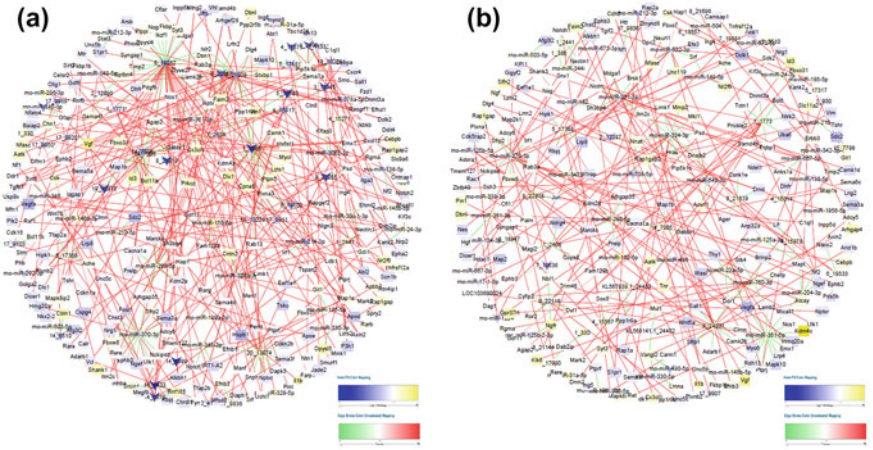

Fig. 10 miRNA-target gene network of self-renewal (**a**) and differentiation-related (**b**) DE miRNAs during spaceflight

Differentially expressed miRNA genes between space and Earth groups were analyzed by databases such as GO and KEGG for functional enrichment analysis. The gene expression data of these genes were extracted and imported into Cytoscape, and then the ExpressionCorrelation plugin computed the coexpression network based on chosen genes (Shannon et al. 2003). By integrating large scale analysis of the transcriptome, miRNAome data and bioinformatics analysis, the GO and KEGG analyses indicated that the proliferation, cell cycle, differentiation, adhesion, apoptosis, and migration of NSCs are affected by spaceflight. Furthermore, the GO analysis of DEGs combined with mRNA-miRNA regulatory network analysis indicated that many pivotal genes, miRNAs, and signaling pathways were involved in the proliferation or differentiation of NSCs during spaceflight. In the proliferation group of NSCs, many target genes involved in regulating the proliferation of NSCs were regulated by these differentially expressed miRNAs between space and ground groups, such as cyclin D1, Ccnd2, Lin28b, E2F2, Hmga1, and Hmga2. Moreover, several neural differentiation-related genes, such as Nestin, Smad4, Stat3, and sp1, were regulated by some differentially expressed miRNAs in the differentiation group of NSCs between space and ground groups. The results also showed that Pax6 and RunX2 genes involved in self-renewal of NSCs were elevated in the space group. In contrast, the expression of oligodendrocyte markers Gal and Olig2 was decreased.

Apart from direct regulation of target genes involved in the differentiation or proliferation of NSCs, miRNAs may also regulate differentiation or proliferation processes via regulating cell signaling pathways. For example, the neural differentiation-related genes Plxna1, Myo6, and Lif are downstream targets of miR-125. Moreover, the Wnt signaling pathway can be regulated by miR-125 in the differentiation group of NSCs. In addition, many target genes of the differentially expressed miRNAs are involved in this pathway. Using bioinformatics analysis, we constructed a network

among stem cell- and Wnt signaling-related genes to further elucidate the role of Wnt signaling during spaceflight. The correlation analysis indicated that certain Wnt signaling-related genes, which have been demonstrated to facilitate neuron differentiation, were significantly upregulated in the space group of NSCs (Lange et al. 2006). Taken together, the mRNA-miRNA networks supported the presumption that exposure to space caused alterations of proliferation and differentiation processes via different regulatory mechanisms in NSCs. Neural differentiation of NSCs was facilitated in space, whereas cell proliferation was suppressed during spaceflight.

6 Summary

As a recoverable satellite, the recovery cabin of the SJ-10 satellite maintained orbit for 12 days in space. The satellite provided an effective, open, and comprehensive platform to study space life and microgravity science, which allows elucidation of the molecular mechanisms of cell alterations in biological, physical and chemical processes in space. When NSCs are exposed to space, the cells maintained self-renewal in the proliferation medium despite a decrease in their growth rate. In addition, the cells were inclined to differentiate into neurons when cultured in differentiation medium in space. Detailed genomic analyses of NSCs after spaceflight may help us to reveal the molecular mechanisms of their differentiation and proliferation states in space environments.

Acknowledgements This work was supported by the "Strategic Priority Research Program of the Chinese Academy of Sciences" (XDA04020000) and National Science Foundation of China (U1738109 and 81601084).
We are greatly thankful to everyone who helped us to complete the SJ-10 satellite project. We thank Prof. Zhang Tao and his staff of the Shanghai Institute of Technical Physics (Chinese Academy of Sciences, CAS) for designing and manufacturing the fully automated bioreactors for 3D-cultured NSC survival in space. We thank Prof. Suo Guangli and his graduate student Zhou Yuanshuai of the Suzhou Institute of Nano-tech and Nano-Bionics (CAS) and Prof. Wu Xianming of the Institute of Genetics and Developmental Biology (CAS) for processing the bioinformatics data.

References

Ahn S, Joyner AL (2005) In vivo analysis of quiescent adult neural stem cells responding to Sonic hedgehog. Nature 437:894–897
Anders S, Reyes A, Huber W (2012) Detecting differential usage of exons from RNA-seq data. Genome Res 22:2008–2017
Anders S, Pyl PT, Huber W (2015) HTSeq—a Python framework to work with high-throughput sequencing data. Bioinformatics 31:166–169
Baker EL, Bonnecaze RT, Zaman MH (2009) Extracellular matrix stiffness and architecture govern intracellular rheology in cancer. Biophys J 97:1013–1021
Baptista S, Lasgi C, Benstaali C et al (2014) Methamphetamine decreases dentate gyrus stem cell self-renewal and shifts the differentiation towards neuronal fate. Stem Cell Res 13:329–341

Barca-Mayo O, Lu QR (2012) Fine-tuning oligodendrocyte development by microRNAs. Front Neurosci 6:13
Barkho BZ, Song H, Aimone JB et al (2006) Identification of astrocyte-expressed factors that modulate neural stem/progenitor cell differentiation. Stem Cells Dev 15:407–421
Barnabe-Heider F, Goritz C, Sabelstrom H et al (2010) Origin of new glial cells in intact and injured adult spinal cord. Cell Stem Cell 7:470–482
Barton A, Fendrik AJ (2013) Sustained vs. oscillating expressions of Ngn2, Dll1 and Hes1: a model of neural differentiation of embryonic telencephalon. J Theor Biol 328:1–8
Bengoa-Vergniory N, Kypta RM (2015) Canonical and noncanonical Wnt signaling in neural stem/progenitor cells. Cell Mol Life Sci 72:4157–4172
Blaber EA, Finkelstein H, Dvorochkin N et al (2015) Microgravity reduces the differentiation and regenerative potential of embryonic stem cells. Stem Cells Dev 24:2605–2621
Bonaguidi MA, Mcguire T, Hu M et al (2005) LIF and BMP signaling generate separate and discrete types of GFAP-expressing cells. Development 132:5503–5514
Brent A, Reynolds SW (1992) Generation of neurons and astrocytes from isolated cells of the adult mammalian central nervous system. Science 255:1707–1710
Burda JE, Sofroniew MV (2014) Reactive gliosis and the multicellular response to CNS damage and disease. Neuron 81:229–248
Caliari SR, Burdick A (2016) A practical guide to hydrogels for cell culture. Nat Methods 13:405–414
Chatr-Aryamontri A, Oughtred R, Boucher L et al (2017) The BioGRID interaction database: 2017 update. Nucleic Acids Res 45:D369–D379
Chen J, Liu R, Yang Y et al (2011) The simulated microgravity enhances the differentiation of mesenchymal stem cells into neurons. Neurosci Lett 505:171–175
Chen YC, Lin RZ, QiH et al (2012) Functional human vascular network generated in photocrosslinkable gelatin methacrylate hydrogels. Adv Funct Mater 22:2027–2039
Chen X, Wang W, Zhang J et al (2015) Involvement of caspase-3/PTEN signaling pathway in isoflurane-induced decrease of self-renewal capacity of hippocampal neural precursor cells. Brain Res 1625:275–286
Cheng TY, Chen MH, Chang WH et al (2013) Neural stem cells encapsulated in a functionalized self-assembling peptide hydrogel for brain tissue engineering. Biomaterials 34:2005–2016
Chiang MC, Lin H, Cheng YC et al (2012) Beta-adrenoceptor pathway enhances mitochondrial function in human neural stem cells via rotary cell culture system. J Neurosci Methods 207:130–136
Choi I, Woo JH, Jou I et al (2016) PINK1 deficiency decreases expression levels of mir-326, mir-330, and mir-3099 during brain development and neural stem cell differentiation. Exp Neurobiol 25:14–23
Cimadamore F, Amador-Arjona A, Chen C et al (2013) SOX2-LIN28/let-7 pathway regulates proliferation and neurogenesis in neural precursors. Proc Natl Acad Sci USA 110:E3017–3026
Coskun V, Wu H, Blanchi B et al (2008) CD133+ neural stem cells in the ependyma of mammalian postnatal forebrain. Proc Natl Acad Sci USA 105:1026–1031
Cui Y, Xiao Z, Han J et al (2012) MiR-125b orchestrates cell proliferation, differentiation and migration in neural stem/progenitor cells by targeting Nestin. BMC Neurosci 13:116
Cui Y, Han J, Xiao Z et al (2016) The miR-20-Rest-Wnt signaling axis regulates neural progenitor cell differentiation. Sci Rep 6:23300
Cukierman E, Pankov R, Stevens DR et al (2001) Taking cell-matrix adhesions to the third dimension. Science 294:1708–1712
Cunha C, Panseri S, Villa O et al (2011) 3D culture of adult mouse neural stem cells within functionalized self-assembling peptide scaffolds. Int J Nanomed 6:943–955
Delgehyr N, Meunier A, Faucourt M et al (2015) Ependymal cell differentiation, from monociliated to multiciliated cells. Methods Cell Biol 127:19–35
Edmondson R, Broglie JJ, Adcock AF et al (2014) Three-dimensional cell culture systems and their applications in drug discovery and cell-based biosensors. Assay Drug Dev Technol 12:207–218

Erickson IE, Huang AH, Chung C et al (2009) Differential maturation and structure-function relationships in mesenchymal stem cell- and chondrocyte-seeded hydrogels. Tissue Eng Part A 15:1041–1052
Fischbach C, Chen R, Matsumoto T et al (2007) Engineering tumors with 3D scaffolds. Nat Methods 4:855–860
Fishell G, Kriegstein AR (2003) Neurons from radial glia: the consequences of asymmetric inheritance. Curr Opin Neurobiol 13:34–41
Fogarty LC, Song B, Suppiah Y et al (2016) Bcl-xL dependency coincides with the onset of neurogenesis in the developing mammalian spinal cord. Mol Cell Neurosci 77:34–46
Fong EL, Lamhamedi-Cherradi SE, Burdett E et al (2013) Modeling Ewing sarcoma tumors in vitro with 3D scaffolds. Proc Natl Acad Sci USA 110:6500–6505
Gage FH (2000) Mammalian neural stem cells. Science 287:1433–1438
Ge S, Goh EL, Sailor KA et al (2006) GABA regulates synaptic integration of newly generated neurons in the adult brain. Nature 439:589–593
Gibbons MC, Foley MA, Cardinal KO (2013) Thinking inside the box: keeping tissue-engineered constructs in vitro for use as preclinical models. Tissue Eng Part B Rev 19:14–30
Gioia U, Di Carlo V, Caramanica P et al (2014) Mir-23a and mir-125b regulate neural stem/progenitor cell proliferation by targeting Musashi1. RNA Biol 11:1105–1112
Godlewski J, Nowicki MO, Bronisz A et al (2008) Targeting of the Bmi-1 oncogene/stem cell renewal factor by microRNA-128 inhibits glioma proliferation and self-renewal. Cancer Res 68:9125–9130
Goncalves JT, Schafer ST, Gage FH (2016) Adult neurogenesis in the hippocampus: from stem cells to behavior. Cell 167:897–914
Gotz M, Huttner WB (2005) The cell biology of neurogenesis. Nat Rev Mol Cell Biol 6:777–788
Gould E (2007) How widespread is adult neurogenesis in mammals? Nat Rev Neurosci 8:481–488
Grimm D, Wehland M, Pietsch J et al (2014) Growing tissues in real and simulated microgravity: new methods for tissue engineering. Tissue Eng Part B Rev 20:555–566
Gross CG (2000) Neurogenesis in the adult brain: death of a dogma. Nat Rev Neurosci 1:67–73
Han Q, Jin W, Xiao Z et al (2010) The promotion of neural regeneration in an extreme rat spinal cord injury model using a collagen scaffold containing a collagen binding neuroprotective protein and an EGFR neutralizing antibody. Biomaterials 31:9212–9220
Huang DW, Sherman BT, Lempicki RA (2009) Systematic and integrative analysis of large gene lists using DAVID bioinformatics resources. Nat Protoc 4:44–57
Huang Y, Liu X, Wang Y (2015) MicroRNA-378 regulates neural stem cell proliferation and differentiation in vitro by modulating Tailless expression. Biochem Biophys Res Commun 466:214–220
Imayoshi I, Kageyama R (2014) bHLH factors in self-renewal, multipotency, and fate choice of neural progenitor cells. Neuron 82:9–23
Inghilleri M, Iacovelli E (2011) Clinical neurophysiology in ALS. Arch Ital Biol 149:57–63
Jiang D, Du J, Zhang X et al (2016) miR-124 promotes the neuronal differentiation of mouse inner ear neural stem cells. Int J Mol Med 38:1367–1376
Jurga M, Lipkowski AW, Lukomska B et al (2009) Generation of functional neural artificial tissue from human umbilical cord blood stem cells. Tissue Eng Part C Methods 15:365–372
Kawahara Y, Manabe T, Matsumoto M et al (2009) LIF-free embryonic stem cell culture in simulated microgravity. PLoS ONE 4:e6343
Kempermann G, Gage FH (2000) Neurogenesis in the adult hippocampus. Novartis Found Symp 231:220–235; discussion 235–241, 302–226
Kempermann G, Kuhn HG, Gage FH (1997) Genetic influence on neurogenesis in the dentate gyrus of adult mice. Proc Natl Acad Sci USA 94:10409–10414
Kim D, Pertea G, Trapnell C et al (2013) TopHat2: accurate alignment of transcriptomes in the presence of insertions, deletions and gene fusions. Genome Biol 14:R36
Kleber M, Sommer L (2004) Wnt signaling and the regulation of stem cell function. Curr Opin Cell Biol 16:681–687

Klein EA, Yin L, Kothapalli D et al (2009) Cell-cycle control by physiological matrix elasticity and in vivo tissue stiffening. Curr Biol 19:1511–1518
Knowlton S, Cho Y, Li XJ et al (2016) Utilizing stem cells for three-dimensional neural tissue engineering. Biomater Sci 4:768–784
Laks DR, Masterman-Smith M, Visnyei K et al (2009) Neurosphere formation is an independent predictor of clinical outcome in malignant glioma. Stem Cells 27:980–987
Lange C, Mix E, Rateitschak K et al (2006) Wnt signal pathways and neural stem cell differentiation. Neurodegener Dis 3:76–86
Lee GY, Kenny PA, Lee EH et al (2007) Three-dimensional culture models of normal and malignant breast epithelial cells. Nat Methods 4:359–365
Lee-Liu D, Edwards-Faret G, Tapia VS et al (2013) Spinal cord regeneration: lessons for mammals from non-mammalian vertebrates. Genesis 51:529–544
Li X, Xiao Z, Han J et al (2013) Promotion of neuronal differentiation of neural progenitor cells by using EGFR antibody functionalized collagen scaffolds for spinal cord injury repair. Biomaterials 34:5107–5116
Lie DC, Colamarino SA, Song HJ et al (2005) Wnt signalling regulates adult hippocampal neurogenesis. Nature 437:1370–1375
Lim DA, Alvarez-Buylla A (1999) Interaction between astrocytes and adult subventricular zone precursors stimulates neurogenesis. Proc Natl Acad Sci USA 96:7526–7531
Lim DA, Tramontin AD, Trevejo JM et al (2000) Noggin antagonizes BMP signaling to create a niche for adult neurogenesis. Neuron 28:713–726
Lin C, Jiang X, Dai Z et al (2009) Sclerostin mediates bone response to mechanical unloading through antagonizing Wnt/beta-catenin signaling. J Bone Miner Res 24:1651–1661
Lledo PM, Alonso M, Grubb MS (2006) Adult neurogenesis and functional plasticity in neuronal circuits. Nat Rev Neurosci 7:179–193
Louis SA, Rietze RL, Deleyrolle L et al (2008) Enumeration of neural stem and progenitor cells in the neural colony-forming cell assay. Stem Cells 26:988–996
Luca AC, Mersch S, Deenen R et al (2013) Impact of the 3D microenvironment on phenotype, gene expression, and EGFR inhibition of colorectal cancer cell lines. PLoS ONE 8:e59689
Ma DK, Marchetto MC, Guo JU et al (2010) Epigenetic choreographers of neurogenesis in the adult mammalian brain. Nat Neurosci 13:1338–1344
Mao S, Li X, Wang J et al (2016) miR-17-92 facilitates neuronal differentiation of transplanted neural stem/precursor cells under neuroinflammatory conditions. J Neuroinflammation 13:208
Matigian N, Abrahamsen G, Sutharsan R et al (2010) Disease-specific, neurosphere-derived cells as models for brain disorders. Dis Model Mech 3:785–798
Mc Garrigle MJ, Mullen CA, Haugh MG et al (2016) Osteocyte differentiation and the formation of an interconnected cellular network in vitro. Eur Cell Mater 31:323–340
Mcconnell SK (1995) Strategies for the generation of neuronal diversity in the developing central nervous system. J Neurosci 15:6987–6998
Mcpherson A, Hormozdiari F, Zayed A et al (2011) deFuse: an algorithm for gene fusion discovery in tumor RNA-Seq data. PLoS Comput Biol 7:e1001138
Ming GL, Song H (2005) Adult neurogenesis in the mammalian central nervous system. Annu Rev Neurosci 28:223–250
Monticone M, Liu Y, Pujic N et al (2010) Activation of nervous system development genes in bone marrow derived mesenchymal stem cells following spaceflight exposure. J Cell Biochem 111:442–452
Nelson LJ, Walker SW, Hayes PC et al (2010) Low-shear modelled microgravity environment maintains morphology and differentiated functionality of primary porcine hepatocyte cultures. Cells Tissues Organs 192:125–140
Nickerson CA, Ott CM, Wilson JW et al (2004) Microbial responses to microgravity and other low-shear environments. Microbiol Mol Biol Rev 68:345–361
Noctor SC, Martinez-Cerdeno V, Ivic L et al (2004) Cortical neurons arise in symmetric and asymmetric division zones and migrate through specific phases. Nat Neurosci 7:136–144

Nomura T, Goritz C, Catchpole T et al (2010) EphB signaling controls lineage plasticity of adult neural stem cell niche cells. Cell Stem Cell 7:730–743
Nori S, Okada Y, Yasuda A et al (2011) Grafted human-induced pluripotent stem-cell-derived neurospheres promote motor functional recovery after spinal cord injury in mice. Proc Natl Acad Sci USA 108:16825–16830
Novosel EC, Kleinhans C, Kluger PJ (2011) Vascularization is the key challenge in tissue engineering. Adv Drug Deliv Rev 63:300–311
Okano H, Temple S (2009) Cell types to order: temporal specification of CNS stem cells. Curr Opin Neurobiol 19:112–119
Platel JC, Dave KA, Gordon V et al (2010) NMDA receptors activated by subventricular zone astrocytic glutamate are critical for neuroblast survival prior to entering a synaptic network. Neuron 65:859–872
Prewitz M, Seib FP, Pompe T et al (2012) Polymeric biomaterials for stem cell bioengineering. Macromol Rapid Commun 33:1420–1431
Puca A, Russo G, Giordano A (2012) Properties of mechano-transduction via simulated microgravity and its effects on intracellular trafficking of VEGFR's. Oncotarget 3:426–434
Ravi M, Paramesh V, Kaviya SR et al (2015) 3D cell culture systems: advantages and applications. J Cell Physiol 230:16–26
Reynolds BA, Weiss S (1992) Generation of neurons and astrocytes from isolated cells of the adult mammalian central nervous system. Science 255:1707–1710
Riquelme PA, Drapeau E, Doetsch F (2008) Brain micro-ecologies: neural stem cell niches in the adult mammalian brain. Philos Trans R Soc Lond B Biol Sci 363:123–137
Schofield R (1978) The relationship between the spleen colony-forming cell and the haemopoietic stem cell. Blood Cells 4:7–25
Shannon P, Markiel A, Ozier O et al (2003) Cytoscape: a software environment for integrated models of biomolecular interaction networks. Genome Res 13:2498–2504
Sher F, Boddeke E, Olah M et al (2012) Dynamic changes in Ezh2 gene occupancy underlie its involvement in neural stem cell self-renewal and differentiation towards oligodendrocytes. PLoS ONE 7:e40399
Shihabuddin LS (2008) Adult rodent spinal cord-derived neural stem cells: isolation and characterization. Methods Mol Biol 438:55–66
Song H, Stevens CF, Gage FH (2002) Astroglia induce neurogenesis from adult neural stem cells. Nature 417:39–44
Souza GR, Molina JR, Raphael RM et al (2010) Three-dimensional tissue culture based on magnetic cell levitation. Nat Nanotechnol 5:291–296
Stamenkovic V, Keller G, Nesic D et al (2010) Neocartilage formation in 1 g, simulated, and microgravity environments: implications for tissue engineering. Tissue Eng Part A 16:1729–1736
Sun G, Fu C, Shen C et al (2011) Histone deacetylases in neural stem cells and induced pluripotent stem cells. J Biomed Biotechnol 2011:835968
Szklarczyk D, Franceschini A, Wyder S et al (2015) STRING v10: protein-protein interaction networks, integrated over the tree of life. Nucleic Acids Res 43:D447–452
Tamura Y, Takahashi K, Takata K et al (2016) Noninvasive evaluation of cellular proliferative activity in brain neurogenic regions in rats under depression and treatment by enhanced [18F]FLT-PET imaging. J Neurosci 36:8123–8131
Tashiro A, Sandler VM, Toni N et al (2006) NMDA-receptor-mediated, cell-specific integration of new neurons in adult dentate gyrus. Nature 442:929–933
Trapnell C, Roberts A, Goff L et al (2012) Differential gene and transcript expression analysis of RNA-seq experiments with TopHat and Cufflinks. Nat Protoc 7:562–578
Ueki T, Tanaka M, Yamashita K et al (2003) A novel secretory factor, Neurogenesin-1, provides neurogenic environmental cues for neural stem cells in the adult hippocampus. J Neurosci 23:11732–11740

Wang H, Zhang Z, Xin W (2007) Microgravity resulted from 3D dynamic culture induces compounding of bone morrow-derived mesenchymal stem cells with Pluronic F-127 scaffold used for repairing of cartilage defects. Chin Tissue Eng Clin Recov 11:2609–2613

Wang Y, An L, Jiang Y et al (2011) Effects of simulated microgravity on embryonic stem cells. PLoS ONE 6:e29214

Xu W, Li P, Qin K et al (2012) miR-124 regulates neural stem cells in the treatment of spinal cord injury. Neurosci Lett 529:12–17

Yamada KM, Cukierman E (2007) Modeling tissue morphogenesis and cancer in 3D. Cell 130:601–610

Yang K, Lee JS, Kim J et al (2012) Polydopamine-mediated surface modification of scaffold materials for human neural stem cell engineering. Biomaterials 33:6952–6964

Yu G, Wang LG, Han Y et al (2012) clusterProfiler: an R package for comparing biological themes among gene clusters. OMICS 16:284–287

Yuge L, Kajiume T, Tahara H et al (2006) Microgravity potentiates stem cell proliferation while sustaining the capability of differentiation. Stem Cells Dev 15:921–929

Zhao C, Sun G, Li S et al (2010) MicroRNA let-7b regulates neural stem cell proliferation and differentiation by targeting nuclear receptor TLX signaling. Proc Natl Acad Sci USA 107:1876–1881

Ziv Y, Ron N, Butovsky O et al (2006) Immune cells contribute to the maintenance of neurogenesis and spatial learning abilities in adulthood. Nat Neurosci 9:268–275

Advances of Mammalian Reproduction and Embryonic Development Under Microgravity

Xiaohua Lei, Yujing Cao, Ying Zhang and Enkui Duan

Abstract The development of life beyond the earth is a dream of human being. Human long duration orbital spaceflight, exploration of Mars and other new space frontiers, colonization of the Moon will require understanding of fundamental of embryogenesis and reproductive function in space environment. It is therefore important to study the effect of microgravity environment on the reproductive system of mammals and to determine whether embryos can develop normally in without gravitational cue. It is important to look at the entire process of fertilization, the cleavage of pre-implantation embryos and blastocyst lineage formation under microgravity in space. It is important to investigate the potential mechanisms and at which point the effected stages regulate back to producing normal embryos. This chapter reviews both others and our lab's research progress about the reproductive science and the mammalian early developmental outcomes under simulated microgravity on earth and real microgravity in space. In addition, we describe the latest experimental results of development of mouse pre-implantation embryos from China's SJ-10 recoverable microgravity experimental satellite (SJ-10 satellite). Finally, this chapter conclude with perspectives of necessary space research in the area of embryonic development and mammalian reproduction in the future.

Abbreviations

Amotl2	Angiomotin-like 2
bp	Blastopore
EPI	Epiblast
FAs	Focal adhesions
HARV	High Aspect Ratio Vessel
ICM	Inner cell mass

X. Lei · Y. Cao · Y. Zhang · E. Duan (✉)
State Key Laboratory of Stem Cell and Reproductive Biology, Institute of Zoology, Chinese Academy of Sciences, Beijing, China
e-mail: duane@ioz.ac.cn

E. Duan and M. Long (eds.), *Life Science in Space: Experiments on Board the SJ-10 Recoverable Satellite*, Research for Development,
https://doi.org/10.1007/978-981-13-6325-2_11

IF	Intermediate filaments
MF	Microfilaments
miRNA	MicroRNAs
MT	Microtubules
NRB	Natural radiation background
PrE	Primitive endoderm
PKC	Protein kinase C
RCCS	Rotating Cell Culture System
SJ-10 satellite	SJ-10 recoverable microgravity experimental satellite
TE	Trophectoderm
3D	Three-dimensional
UV	Ultraviolet

1 Introduction

In mammals, the beginning of early embryonic development is mainly devoted to the generation of the gametes (Sperm and Oocyte). When the oocyte is fertilized, the zygote, derived from two terminally differentiated gametes, is formation and continued undergo the sequential mitotic cell divisions. The first cleavage division of the fertilized egg forms the symmetric 2-cell embryo. Three to four rounds of cleavage produce an 8–16 cells embryo, which is prepared for compaction and polarization (Cockburn and Rossant 2010; Kojima et al. 2014). The compaction of the blastomeres was considered as the first recognizable morphogenetic event during pre-implantation development. Through compaction, 8–16 cells embryo will give rise to two distinct cell types by asymmetric division rounds: the trophectoderm (TE), which will form placenta and the embryonic ectoderm/endoderm inner cell mass (ICM). When the embryo has 8–16 cells (or blastomeres), its shape resembles that of a blackberry and is therefore called morula. Following cavitation, the morula forms a cavity within through the accumulation of fluid in the intercellular spaces, which is called as the blastocyst (Chazaud and Yamanaka 2016; Piliszek et al. 2016). The cells of the ICM differentiates into epiblast (EPI), which contributes to all fetal cells, and primitive endoderm (PrE), which produces mostly the extra-embryonic yolk sac.

Mammalian pre-implantation development is controlled stringently by the regulatory of gene and protein expression during the cell division and differentiation, including transcriptional regulation, epigenetic modification, microRNAs (miRNA), and signal transduction (Frum and Ralston 2015; Guo et al. 2010; Morris et al. 2013). In mammals, the developmental potential and viability of preimplantative embryos are also sensitive to the growth environment. Previous studies have shown that changes in environment can alter epigenetic modification (Dey et al. 2004; Fleming et al. 2004). Regarding the formation of the blastocyst, several questions remain undefined or controversial, such as how is the developmental potential of cells regulated during the transition from the zygote to the pluripotent ICM cells and the multipotent TE cells? How are the fates of cells determined?

Due to the fact that blastomeres are able to sense environmental cues, changed gravity condition can affect cell division, compaction and blastocyst formation. Previous studies have demonstrated successful reproduction by sea urchins, fish, amphibians and birds in microgravity conditions (also called weightlessness) (Crawford-Young 2006; Ogneva 2015), while the potential effect of weightlessness on the reproductive system in mammalian is still limited and controversial. Several reports on successful experiments concerning the prenatal development of mammals under spaceflight conditions mostly did not concern the earliest developmental stages (Ronca et al. 2008). Since the space experiments are expensive and complicated, experiments that were performed at the earliest stages of development were largely unsuccessful, including fertilization and development of preimplantation embryo under the space environment.

In 2016, China launched the SJ-10 satellite, which carried thousands of 2-cell embryos in incubator to reach preset orbit. Researchers successfully received high-resolution pictures of embryos cultured in image unit. The data showed that some of the embryos developed into advanced blastocysts in four days. This study represents a crucial step in mammalian reproduction and firstly proves that the early embryo development is possible in outer space. This also represents an important milestone in human space exploration, although it is a one small step for mouse embryos, but one giant leap for human reproduction in space. However, it will further still study the possibility of mammalian embryo implantation and subsequent post-implantation development as well as human pregnant ability in outer space.

In this chapter, we highlight examples of developmental events during the fertilization to early pre-implantation development in mammal that appear to progress consistently according to a timeline. In addition to a brief review of the previous work that carried by others and our laboratory about reproductive science and development biology under microgravity environment, we also describe the latest experimental results of development of mouse early embryos from China's SJ-10 satellite. Finally, this chapter concludes with perspectives of necessary space research in the area of embryonic development and mammalian reproduction for the future.

2 Timing of Pre-implantation Developmental

In the mammal, studies of the timing mechanism have been focused on the morphogenetic events in pre-implantation development such as the fertilization, the cleavage, the compaction of blastomeres and the formation of the blastocyst (see Fig. 1). Fertilization is the fusion of haploid gametes, oocyte and sperm, to form the diploid zygote, which is totipotent, can developing into not only the fetus but also the placenta. Once the egg is fertilized, the zygote continues to encompass a series of events including cleavage, compaction, and differentiation into blastocyst. In this regard, the zygote gradually loses its developmental potential. At 2-cell stage embryo, each blastomere is also maintained totipotency, which can give rise to an adult animal. Individual blastomere decreases the developmental potential, when the embryo develops fur-

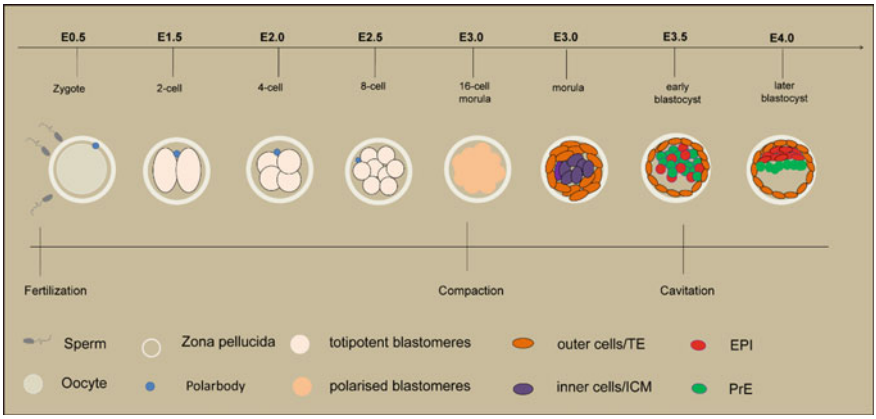

Fig. 1 Schematic of the early stages of development in mouse, with corresponding names of the subsequent stages. The timeline below indicates the embryonic days. The main timing of morphogenetic events is showed during pre-implantation development. Colour legend describes respective embryonic cells and lineages. TE, trophectoderm; ICM, inner cell mass; EPI, epiblast; PrE, primitive endoderm

ther. Until now, no mouse has been derived from single blastomere at the 4-cell stage or later. However, single 4- and 8-cell stage blastomeres are pluripotency, which are able to contribute to all the tissues of the embryo (Chung et al. 2006; Van de Velde et al. 2008). During the transition from eight cell stage to blastocyst, blastomeres start the first cell fate decision in embryogenesis that are differentiated into two distinct lineages, cell positioned inside (the ICM) retain pluripotency and cell on the outside develop into the TE, which are able to form the extraembryonic cell types of the placenta (Chazaud and Yamanaka 2016; Kuckenberg et al. 2011). In the second fate decision, cells of the ICM that are in contact with the blastocyst cavity are set aside to form the second extraembryonic tissue, the PrE. While cells of the ICM that are in contact with the TE are develop into EPI, which gives rise to the embryo itself (Zernicka-Goetz et al. 2009).

2.1 Fertilization

Fertilization, the process by which female and male gametes fuse, occurs in the ampullary region of the uterine tube. The first significant event in fertilization is the fusion of the membranes of the two gametes resulting in the formation of a channel that allows the passage of material from one cell to the other. The activation of the ovum by the fertilizing spermatozoon starts before the enlargement of the head of the spermatozoon which occurs about 1–2 h after penetration. After fertilization, the zona pellucid expands (Calarco 1991). The first polar body can be visible before fertilization, but the second polar body is discharged into zona pellucid within 2 or

3 h after fertilization. After sperm entry into the egg cytoplasm, the spermatozoal nucleus, now called the male pronucleus, begins to swell, and its chromosomal material disperses and becomes similar in appearance to that of the female pronucleus (Coticchio et al. 2015). Both male and female pronucleus may be seen as early as 6 h after mate. The nucleus has a remarkable nucleolus. The two pronuclei synthesize DNA before their fusion and each, with many distinctive acidophilic nucleoli and devoid of RNA, move toward each other, meeting near the center of the ovum. Sometimes, the nucleoli may be found indented into the nuclear membrane. Fertilization is considered to be complete when the pronuclei are come into contact and the spermatozoal centrioles give rise to the first cleavage spindle, which precedes division of the fertilized egg, namely the zygote.

2.2 Cleavage and Compaction

During cleavage the cells are called "Blastomeres". Cleavage of embryo is slow that takes approximately 12–24 h between each blastomere division. The first cleavage begins about 20 h after the egg has been fertilized once the male and the female pronuclei fusion (Abramczuk and Sawicki 1975). Mammalian embryos undergo triple or quartic cleavage to become compact embryo. The first cleavage is normally meridional that the 1-cell embryo divides into two totipotent blastomeres, whereas these blastomeres then divide sequentially, either meridional (parallel) or equatorial (orthogonal) to the initial cleavage plane of the 2-cell embryo. If parallel-oriented division occurs, the 4-cell embryo establishes a planar structure (~20%), whereas if orthogonal division occurs (~80%), a tetrahedron results (see Fig. 2) (Gardner 2002). During cleavage DNA has been synthesized and embryo has double the DNA content of metrocyte. Contrary to normal somatic cell, the mammalian embryo begins development with slow divisions and shows rapid cell cycles. During cleavage G1 and G2 stages are by-passed so cells simply progress from S (DNA synthesis) to M (mitosis) without the intervening growth phases and G2/M phase length is about 3–5 h (O'Farrell et al. 2004; Sikora-Polaczek et al. 2006). It should be noted that, no growth occurs in size as the initial amount of cytoplasm is partitioned to the daughter cells at each cleavage division and the blastomeres display the maximal increased of the nucleo-cytoplasmic ratio in the first 3–4 cleavage divisions. However, the total embryo will always remain ~100 μm in diameter.

After triple cleavage divisions, eight-cell embryo is formed and it subsequently undergoes an increase in intercellular adhesion called compaction. It has been observed that the blastomeres of eight-cell stage embryo quickly come together, maximizing the contact surface, causing all cells to adopt a more flattened morphology and forming a compact globule. In the mouse or human embryo, compaction is associated with the formation of adherens and tight junctions between cells. E-cadherin is a major component of adherens junctions that appears in the cell-cell contact regions at the eight-cell stage (Fierro-Gonzalez et al. 2013). But beyond that, other new molecular components are also being identified as the process of com-

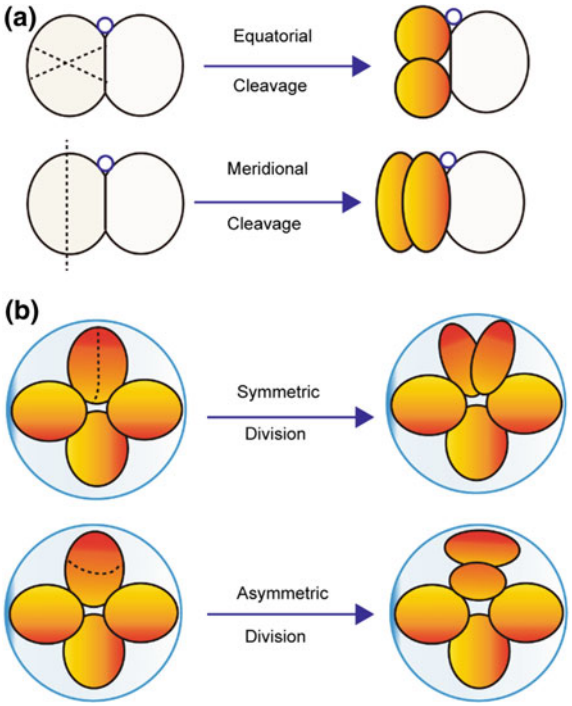

Fig. 2 Schematic illustration for different types of blastomere division. **a** Representative equatorial (E) and meridional (M) cleavages in the two-cell stage embryo. The blue circle is the second polar body. The dashed lines mark the cleavage planes. **b** Symmetric and asymmetric divisions in the eight-cell embryo. Only four blastomeres in the eight-cell embryo are shown. Symmetric division results in two polarized blastomeres with equal position in the embryo, while asymmetric division produces one polarized outer cell and one apolar inside cell (Adapted from Chen et al. 2010.)

paction, such as the Epithin, which is a mammalian transmembrane serine protease that has been found to be co-localized with E-cadherin at both the 8-cell and morula stages in mammal (Khang et al. 2005). Maternal E-cadherin is able to mediate the compaction process at the morula stage, even though loss of E-cadherin in mice (Larue et al. 1994). E-cadherin is regulated post-translationally *via* protein kinase C (PKC) or other signaling pathway. Activation of PKC triggers premature compaction in the four-cell stage embryo; nevertheless, inhibition of PKC, but not inhibitions of other kinases impair compaction during mouse preimplantation embryogenesis (Liu et al. 2013; Pauken and Capco 1999).

2.3 Blastocyst Formation and Cell Fate Specification

Following compaction, the blastomeres become polarized along their apical–basal axis and the cells are allocated to either outside (apical) and inside (basolateral) positions. The outside cells of compacted embryo contribute to the first epithelium, the TE lineage (Tarkowski and Wroblewska 1967), whereas those of cells positioned inside become the ICM of the embryo. The development of cellular polarity is required for correct lineage specification, because interfering with the function of polarity

proteins affects blastocyst morphogenesis and ICM-TE lineage allocation (Alarcon 2010; Thomas et al. 2004). The process of compaction and polarization triggers a series of events during which inside cells transition from totipotent to pluripotent and outside cells commit to TE, losing the ability to contribute to other embryonic lineages between the 32- and 64-cell stages (Szczepanska et al. 2011). In the 32- to 64-cell stage the morula acquires an eccentrically placed, slit-like cavity with a developing fluid-filled, which process is called cavitation. This is the beginning of the blasocoel and the process of blastulation, driving the blastocyst stage, which undergoes normal cell cycle and rapidly expansion.

As above described, the first fate decision in the mouse/human embryo is taken as two populations of cells during the 8–16 cell and 16–32 cell. Cells positioned inside (the ICM) retain pluripotency and cells on the outside develop into extraembryonic TE, which will support the development of the embryo in the uterus. Several transcription factors (e.g., *Oct4*, Nanog and *Sox2*) involved in ICM specification, which are initially expressed in all cells of the morula, with their expression gradually becoming restricted to the ICM (Bedzhov et al. 2014). By contrast, some transcription factors are important for TE specification, such as *Cdx2* (Niwa et al. 2005), *Eomes* (Russ et al. 2000) and *Gata3* (Ralston et al. 2010) are restricted earlier, at the 8- to 16-cell transition. In the second fate decision, cells of the ICM that are in contact with the blastocyst cavity are set aside to form the second extraembryonic tissue, the PrE. Therefore, there is some questions that if ground-level gravity is essential for polarity in the blastocyst, and whether weightlessness or hypergravity condition would be expected to affect the first and second cell fate determination. These questions will be answered by space science researches in the nearly future.

2.4 The Molecular Basis of Pre-implantation Cell Fate Specification

A dominating difference between inside and outside cells is cell–cell contact. When inside cells are generated, they lose polarization and confront uniform cell–cell contacts. By comparison, outside cells remain polarized and have asymmetric cell-cell contacts, with an apical domain forming at the bare patch of membrane that is not in contact with neighbouring cells. Par3 and atypical aPKC are apical factors called Par complex, which accumulate at the apical domain. Downregulation of the function of either Par3 or an aPKC affect cell position and result in an increased contribution of cells to the ICM in the preimplantation mouse embryo (Hirate et al. 2013; Plusa et al. 2005). Notably, the apical polarity complex is upstream of the TE fate scheme because the polarity and cell adhesion are not affected in Tead4$^{-/-}$ embryos (Nishioka et al. 2008). E-cadherin is another molecular mediate cell adhesion, and embryos lacking both maternal and zygotic E-cadherin have more Cdx2-positive cells, indicating that when all cells of the embryo are polarized, the majority will take on a TE fate. In addition, cells with membrane-enriched aPKC show nuclear

localization of Yap and express Cdx2, independent of their position within the embryo (Stephenson et al. 2010). Therefore, cell-cell contact can therefore be considered as an inhibitor of apical domain formation and the internalization of cells by asymmetric divisions as a mechanism by which embryonic cells can be protected from differentiation cues. Amot and angiomotin-like 2 (Amotl2) are homologous membrane-associated Hippo pathway components that are differentially localized in inside and outside cells: in inside cells Amot is present throughout the membrane, whereas in outside cells its localization is apical (Hirate et al. 2013). Above all, how the TE and ICM are specified in a compact embryo containing outside and inside cells can reference a model in Fig. 3 proposed by Bedzhov et al. (2014).

In fact, blastomeres are able to sense environmental cues, which are transduced into cells through signaling pathways. Consequently, many changes within the cells, including transcriptional activity and epigenetic modifications, are directed by the signaling pathways to solidify the cell fate choice. As above described, cell fate determination is associated with changes in transcriptional profiles. Therefore, different sets of proteins are expressed to carry out distinct biological functions in various cells. Transcription of genes is regulated through many mechanisms, including transcription factors, epigenetic modifications, and miRNA. In addition, extracellular environmental cues can be transduced into intracellular compartments through signaling pathways, and regulate transcriptional activities (Chen et al. 2010).

2.5 Changes of Transcriptomic and Epigenetic Evens During Pre-implantation Mouse Development

During the transcriptomic reprogramming, a large number of maternal mRNA are erasure and zygotic genome activity at the maternal-to-zygotic transition. At stage of 2-cell embryo in mouse, approximately 80% of the maternal mRNA was removed and about 4000 new genes are transcribed at the first zygotic genome activation (see Fig. 4). At stage of 8-cell stage embryo, additionally 5000 new genes are transcribed (Puscheck et al. 2015; Ruden et al. 2018). Methylation of DNA is an essential epigenetic control mechanism in embryonic development and preservation of conformable levels of DNA methylation during preimplantation embryo development is require for the viability of embryos (Barton et al. 2001). DNA methylation are subject to periods of dynamic reprogramming in preimplantation embryos (Messerschmidt et al. 2014; Shi and Wu 2009). The 8-cell embryo dispels a lot of epigenetic programs due to DNA demethylation (Yang et al. 2007), while *de novo* methylation occurs after the morula stage and shows distinguishing methylation between the ICM and the TE (see Fig. 5). Notably, many important methylation imprinted genes (~100–200) shows not de- and re-methylated during preimplantation development in unstressed normally embryos (Peters 2014). However, some research have reported that loss of parental imprinting in mouse preimplantation embryo with poor culture condition

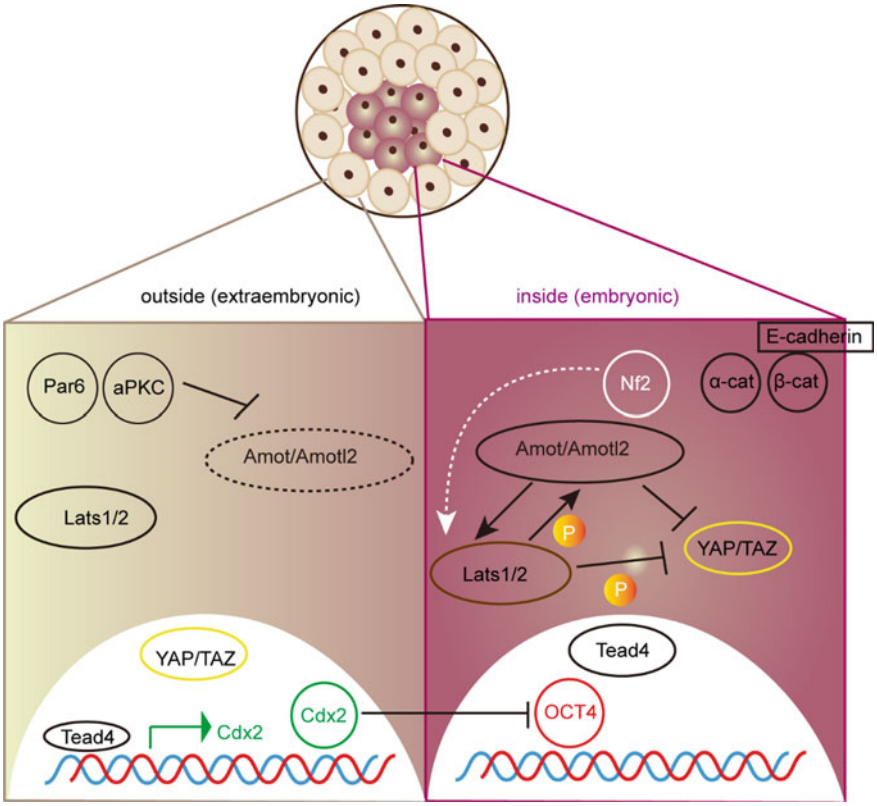

Fig. 3 Cell lineage specification during preimplantation development in mouse. In compacted morula stage, it is the earliest point where blastomeres have differential spatial positioning. Blastomeres on the inside of the embryo endure symmetric cell–cell contact and give rise to the pluripotent ICM. Outside cells have asymmetric cell–cell contact and form the extraembryonic TE. The asymmetry in cell–cell contact leads to accumulation of polarity proteins such as Par6 and aPKC at the apical domain. Par6 and aPKC activity inhibits activity of Amot and the Hippo pathway kinases Lats1/2. Therefore, Taz and Yap are de-repressed, Tead4 transcriptional activity is switched on and Cdx2 expression and the TE cell fate action are activated. In inside cells, symmetric cell–cell contact prevents establishment of an apical domain. Amot is active and is likely related to AJs through a putative Nf2-α-catenin–β-catenin-E-cadherin complex. Amot sequesters Yap/Taz to the cytoplasm as well as activating the Hippo pathway proteins Lats1/2. Lats1/2 can inhibit Yap/Taz activity via the canonical Hippo pathway and can also activate Amot in a positive feedback loop. In the absence of Yap/Taz in the nucleus, Tead4 activity is switched off, Oct4 expression is promoted and the default pluripotent programme is expressed. As a result, positional and polarity cues in these two populations lead to changes in gene regulation and differentiation into their respective lineages (Adapted from Bedzhov et al. 2014.)

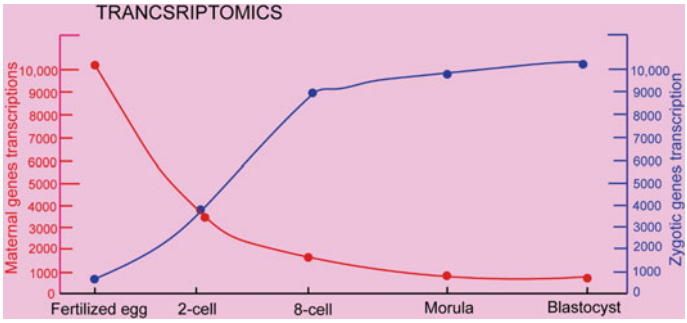

Fig. 4 Changes of transcriptomics in fertilized egg, preimplantation mouse embryos. At the 2-cell stage, about ~80% of maternal transcripts are destroyed (red line) and during zygotic genome activation ~4,000 new transcripts are expressed at the 2-cell stage and another ~5,000 new transcripts are expressed at the 8-cell stage (blue line) (Adapted from Ruden et al. 2018.)

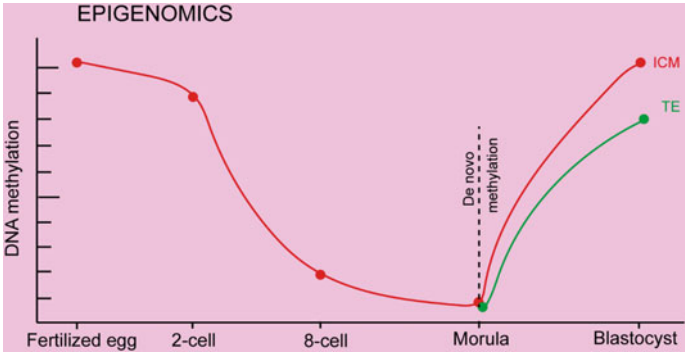

Fig. 5 DNA demethylation dynamics and DNA methylation dynamics in fertilized egg and preimplantation mouse embryo. Global demethylation by the 8-cell stage and remethylation after morula stage (red line indicates that remethylation is higher than in the ICM than the placental trophoblast lineage-green line) (Adapted from Ruden et al. 2018.)

in vitro or early environmental stress due to aberrant demethylation (Doherty et al. 2000; Mann et al. 2004; Market et al. 2012).

3 Fertilization and Pre-implantation Development in Microgravity

As we know, human embryogenesis is similar in many ways to the mouse or rat. However, it has been impossible to study the effects on human early embryo development due to the ethnical issue and the technical difficulties of space missions. Does gravity play an essential role in the normal development of an embryo is issue

of common concern. In fact, several studies investigating the role of microgravity on reproduction and embryo development during spaceflight have been reported that altered gravity has no lethally effects on fertilization or pregnancy in sea urchins, fish, amphibians and birds fertilized (Ijiri 1998; Sabo et al. 1995; Schatten et al. 1999; Souza et al. 1995; Yokota et al. 1992). Inspiringly, some experiments showed that the fertilization rates were similar to the result of ground control. Nevertheless, unlike those animal studied to date, mammalian reproduction is very sensitive to environmental factors. The first space mission reported that rats mated in hypogravity, indicating that female rats ovulated and cycled normally; however, no births resulted and all the fetuses were resorbed, when postflight laparotomies (Serova and Denisova 1982). Thus, it is now no clear indication of that whether exposure to space environment could cause detrimental effects on the development of embryo in mammals, especially preimplantation development.

3.1 Fertilization in Spaceflight or Simulated Microgravity Environment

It is known that exposure to microgravity conditions reduces the number of mature spermatozoa in the epididymis; moreover, this decrease was more significant in simulated microgravity experiments, e.g., with exposure to simulated rotational suspension positioning (Courtine and Pozzo 2004; Kamiya et al. 2003; Serova 1989). There is some question that whether the fertilization might be affected due to the mobility changes of sperm? What is an effect of spaceflight on fertilization of animals? In fact, the bull sperm swim with higher velocity in microgravity has been reported by Tash et al. This increased velocity is owed to changes in phosphorilization of specific flagellar proteins (Tash and Bracho 1999). The sperm motility decreased in the microgravity condition produced by the parabolic flight, but the process of fertilization in vitro is not sensitive to the gravitational vector (Sasaki et al. 2004). Ikeuchi et al. applied clinostat and parabolic flight experiments to examine changes in human sperm motility in a simulated μG environment and found that sperm motility was reduced under μG environment (Ikeuchi et al. 2005).

Two important studies were the amphibian and the vertebrate development in the virtual absence of gravity. In 1994, the Xenopus eggs were successfully fertilized. Despite sagittal sections of gastrulae showing differences between embryos developed on the 1 × g condition and embryos developed at microgravity condition in space (see Fig. 6), some embryos can develop to tadpoles with normal externally in space during the Japanese Spacelab mission STS-47 (Souza et al. 1995). In the second International Microgravity Laboratory mission (IML-2, STS-65) in 1994, four of a small Japanese killifish (Medaka, Oryzias latipes) mated successfully in space and young fish hatched during the 15 days of space travel (Ijiri 1998). Notably, the obtained live offspring did not exhibit any changes in behavior or morphology and produced healthy second-generation (F2) fishes when those fishes back on the

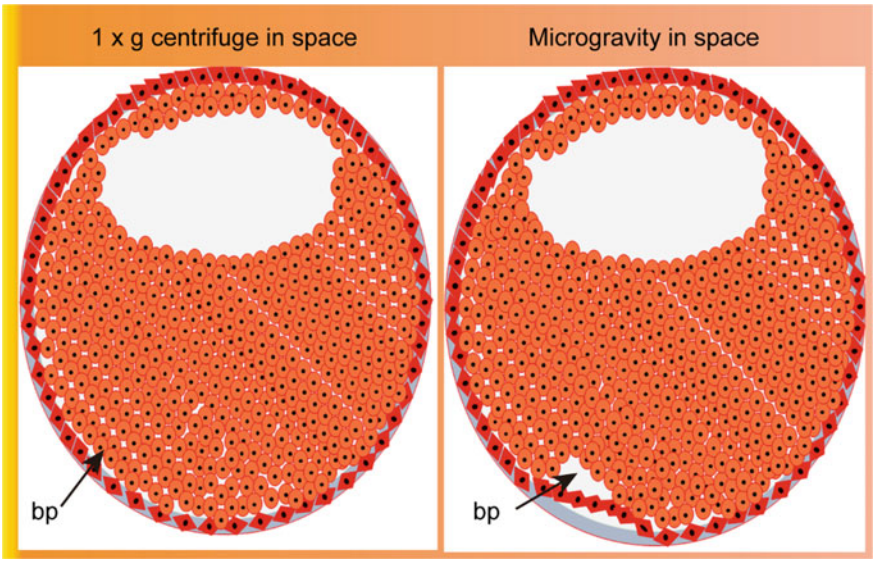

Fig. 6 Sections of gastrulae (stage $10^{1/4}$) in xenopus showing differences between embryos developed on the 1 × g centrifuge (left) and those developed at microgravity (right). The microgravity embryo generally showed thicker blastocoel roofs comprising more cell layers than in the 1 × g controls; and the dorsal lip of the blastopore (bp) formed nearer the vegetal pole than in the 1 × g controls. Embryos were fixed in flight and stained with hematoxylin, eosin-B, phloxine-B, and fast green (Adapted from Souza et al. 1995.)

ground (see Fig. 7). Beyond vertebrates, several other species have been proclaimed to successful natural mating in microgravity. Some study of the effect of space flight factors, particularly of weightlessness and radiation on fertilization of the virgin drosophila melanogaster was performed during the flights of Vostok mission and the biological satellite Cosmos-936. The preliminary results showed that drosophila females were mated to males and occurred normally in-flight because embryos were recovered after landing (Antipov et al. 1965; Parfyonov et al. 1979). Later, *C. elegans* were uploading on board the European facility Biorack during the Spacelab IML-1 mission, experiment results indicated that some animals successfully reproduced twice in space and generated thousands of offspring (Nelson et al. 1994). Above all, so far, viable generations could obtain from nature in-flight fertilization in fruit flies, fish, nematodes and Xenopus. However, unlike the other non-mammalian animals studied to date, mammalian fertilization in microgravity is complicated and highly specialized.

In vivo study, natural mating of rats in a Cosmos 1129 biosatellite experiment was tried. Post flight investigations on the flight animals revealed that 2 out of 5 females had occurred ovulation, copulation, and fertilization in microgravity, but the females failed to keep the pregnancies (Serova and Denisova 1982). Later, some experiments found that space flight of pregnant animals beginning after embryo implantation does

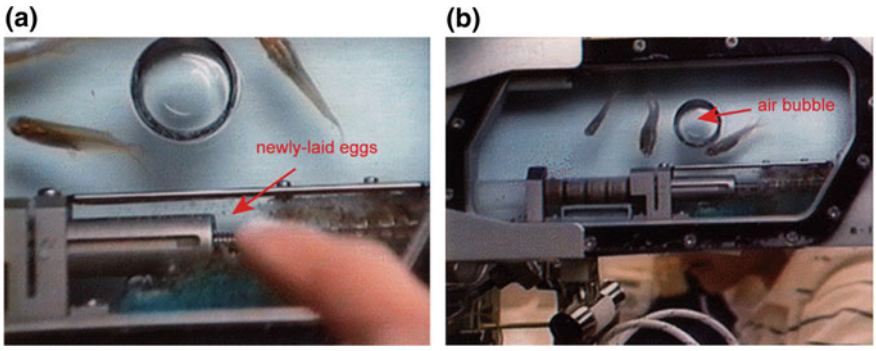

Fig. 7 Mating and laying eggs of Medaka fish in space. **a** Red arrow indicate the newly-laid eggs; **b** Male is embracing female with his fins. See two fish together at the center of the aquarium. At the central of these fish, there is a large air bubble. These pictures were acquired from space in real-time (Reproduced from Ijiri 1998.)

not affect placental structure and selected hormone level parameters (Burden et al. 1997; Macho et al. 1996, 2001).

It is notable that the real microgravity experiments in mammal have been limited due to technical difficulty and financial limitations. Therefore, earth-bound simulated equipment has been used to study the effect of microgravity on fertilization in mammal. A horizontally rotating clinostat has been used to examine the effects of altered gravitational states on mouse fertilization. The process of fertilization in vitro is not sensitive to the gravitational vector (Kojima et al. 2000). Recently, a three-dimensional (3D) clinostat, which faithfully simulates 10^{-3} g has been used to study the effect of microgravity on in vitro fertilization. Expectations, most of these oocytes were fertilized normally, which suggested microgravity appears to have no harmful effects on mouse fertilization in vitro (Wakayama et al. 2009). Another experiment was determined whether simulated microgravity conditions affect in vitro fertilization in bovine using the Rotating Cell Culture System (RCCS) bioreactor with High Aspect Ratio Vessel (HARV) (Synthecon, Houston, Texas). Unfortunately, the results have shown that clinostat rotation resulted in complete inhibition of fertilization compared to controls which had a 77% fertilization rate. From those results, they indicated that there was a negative impact on bovine in vitro fertilization under simulated microgravity environments (Jung et al. 2009). So, the effects of simulated microgravity on mammalian fertilization are still controversial issue.

3.2 Cleavage, Compaction and Embryonic Development in Microgravity

Several flight data on embryogenesis exist as well, indicating that there are some sensitive periods that embryos do not do well during the space flight or weightlessness

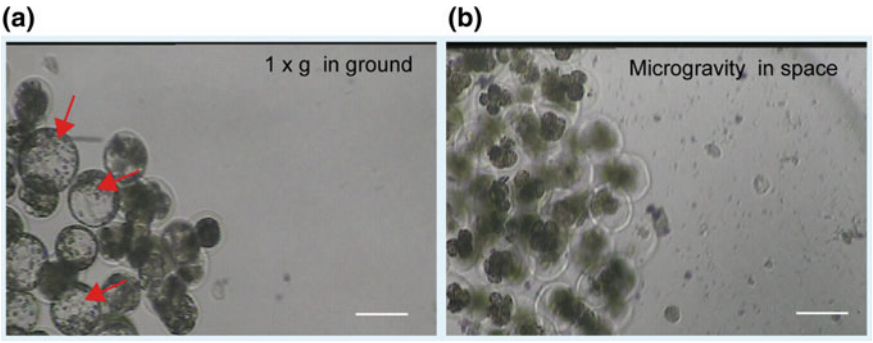

Fig. 8 The embryonic sample images of the culture unit in space experiment and in ground experiment. **a** On the ground experiment, 4-cell mouse embryos could develop to blastocysts and hatched blastocysts (Red arrow indicate). **b** On the space experiment, the embryos did not develop, all of the embryo degenerated. White bar = 100 μm (Adapted from Ma et al. 2008.)

environment. In 1986 in the Kosmos-1514 biosatellite mission, 10 pregnant female rats were delivered to space when at the beginning of the 13th day of pregnancy. According to the experimental design, those rats returned to the earth after 5 days of spaceflight, and on the day of return, 5 female rats of the spaceflight were dissected, providing approximately 60 fetuses for study. The remaining 5 females were allowed to continue their pregnancy to term, and approximately 50 living neonates were obtained from them. These neonates were observed postnatally for several months until to reach sexual maturity (Gazenko 1988). Unfortunately, data concerning the effect of microgravity on the terms of total embryo birth rate, number of live fetuses of the mammalian embryology experiment on Kosmos-1514 was not showed in published articles. To date, only five quail embryos have survived in weightlessness and only one of these embryos survived to the latter stages of development (Bellairs 1994). During the STS-80 Columbia space flight mission, mouse 2-cell embryos were collected on the ground and forty-nine embryos were launched on the CMIX-5 Payload, which were cultured for four days in space environment. However, none of the embryos in space showed any sign of development due to all of the embryos degenerated (Schenker and Forkheim 1998). Actually, in 2006 in SJ-8 Satellite of China, our research group investigated the effect of microgravity on the development of mouse 4-cell embryos (Ma et al. 2008). Unfortunately, no developed embryos were observed during space flight and the real-time image showed all of the embryo degenerated. However, of those embryos on the ground cultured, 4-cell mouse embryos could develop to blastocysts and hatched blastocysts (see Fig. 8). These flight experiments could imply that gravity may be needed during the earliest stages of mammalian embryogenesis, but the failure of these experiments on early development of mammalian embryos may be associated both with the characteristics of pre-implantation development (e.g., the special mitotic divisions or the complexity of the cell fate) and with the conditions of the experiments.

Changes in cell shape and movement as seen in microgravity could cause dysmorphology to occur during development. In many types of cells, the structure of the cortical cytoskeleton was altered when first exposed to microgravity. Cytoskeletal components such as microtubules are changed in microgravity and the orientation and growth of microtubules in microgravity is one process that profoundly affects embryo development (Crawford-Young 2006). Recently, mouse 2-cell embryos were exposed with short-term in mimicking conditions of hypergravity to investigate its influence on the development of early embryo. The development rate of blastocyst formation and actin filament structures were analyzed (see Fig. 9). Those result shows that short-term exposure in hypergravity conditions does not affect the normal development and actin filament structures of mouse embryos (Ning et al. 2015).

According to Yokota et al. reported, altering the position of the first horizontal cleavage furrow of the Xenopus egg in microgravity reduces embryonic survival (Yokota et al. 1992). However, whether decrease of gravity effects the cleavage division of the mammalian embryo is unknown. Therefore, more detail process about the early stage embryonic development in mammal including the cleavage and compaction need to be investigated.

The effect of simulated microgravity on early embryo development and polarization of the ICM and TE components in mice was initially performed using a 3D clinostat. The results suggest that the effects of microgravity might be limited to embryonic cell growth rate or differentiation, but weightlessness environment does not appear to impair cell localization within the blastocyst. The polarization of preimplantation embryos was independent of gravity in this artificial model (Wakayama et al. 2009). There have been experiments carried out using a rotating wall vessel bioreactor with similar results. Simulated microgravity significantly inhibited the development of mouse 8-cell stage embryos cultured in vitro due to producing the higher concentration of NO (a messenger molecule) in the embryos (Cao et al. 2007). However, whether the increased NO concentration was the major reason for affecting the pre-implantation and the mechanism by which it might affect mammalian embryo development in a space or weightlessness environment should be further investigate.

4 Cytoskeleton and Cytoskeletal Changes During Microgravity

Actin is a main component of cytoskeleton in eukaryotic cells and is formed by individual actin proteins known as globular actin (G-actin) and filamentous actin (F-actin or Microfilaments). F-actin filaments consist of multiple G-actin subunits that interact with one another and are constantly assembled and disassembled (Lee and Dominguez 2010; Paoli et al. 2013). Microtubules typically grow (polymerize) into long tubular polymers consisting of alpha- and beta-tubulin dimers bind together

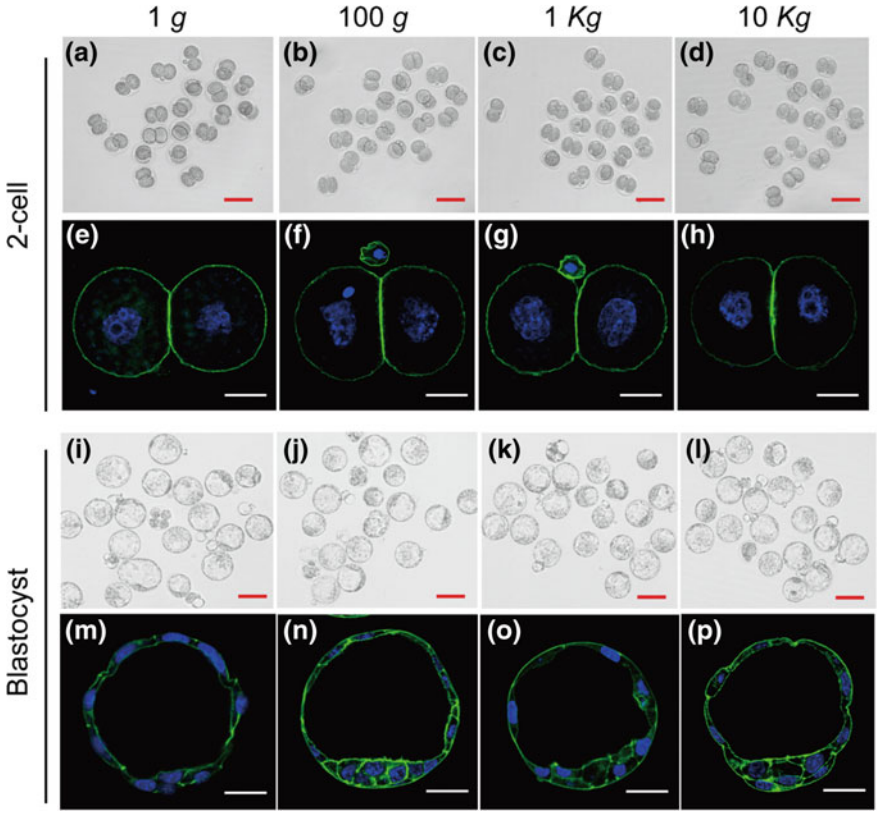

Fig. 9 In vitro development of 2-cell embryos after short-term exposed on different gravity conditions. Morphology of 2-cell embryos after exposed to 1 g (**a**), 100 g (**b**), 1 kg (**c**), 10 kg (**d**) for 20 min and subsequent developed blastocysts 1 g (**i**), 100 g (**j**), 1 kg (**k**), 10 kg (**l**). Red bar = 100 μm. Fluorescence images to illustrate the actin cytoskeletal distribution of hypergravity treated 2-cells embryos (**e** to **h**) and subsequent developed blastocysts (**m** to **p**) using a confocal microscope. The embryos were stained with Alexa Fluor 488-phalloidin (green) to visualize actin filaments and DAPI to stain the cell nuclei (blue). White bar = 20 μm

in a specific orientation. Microfilaments link to the microtubule network in vivo to form a strong stable tensegrity structure (Ingber 2003).

Cell may sense mechanical stresses, including those due to gravity, through changes in the balance of forces that are transmitted across transmembrane adhesion receptors that link the cytoskeleton (involves all three cytoskeletal filament) to the extracellular matrix and to other cells (e.g., integrins, cadherins, selectins) (Ingber 1999). Cells respond to their environment within a three-dimensional tissue structure. The number of adhesive structures in a cell and its resulting cell polarity may change the way it will behave. Developmental arrest appears related to altered cytoskeletal organization. Neganova et al. investigated the role of E-cadherin mediated signaling in cell polarization and the rescue of blocking 2-cell embryos by aggregation, to

answer whether there was a link between the expression of E-cadherin and the distribution of microtubules and mitochondria. They found that E-cadherin-mediated signaling and its downstream effect on cytoskeletal organization are required in the rescue of blocking embryos by aggregation, indicating normal preimplantation development appears to be dependent on the polarized expression of surface E-cadherin and the microtubule-mediated dispersal of mitochondria (Neganova et al. 2000).

It has been proved that microgravity affects both cytoskeleton and cell shape (Gaboyard et al. 2002). All of the cytoskeleton components; microfilaments (MF), microtubules (MT) and intermediate filaments (IF), may become disorganized in microgravity environment. A higher density of filamentous actin and decreased organization in stress fibers was observed after spaceflight (Rijken et al. 1992). The number of stress fibers was reduced and the cytosolic network was density in microgravity (Meloni et al. 2011). Some articles also focus the influence of microgravity on the microtubule structure and the intermediate filaments, in particular on the vimentin and cytokeratin network. Previous studies investigated the changes in focal adhesion (FAs) changes in real microgravity environment, found that there was a significant alteration about the localization of vinculin and a protein linking integrins to the actin network in FAs after 24 h (Vorselen et al. 2014). While another study reported that changes of the cytokeratin network in part of the cells are occurring after 48 h of microgravity (Vassy et al. 2001).

The disorganized of cell cytoskeleton may induced apoptosis. Abnormal patterning may either cause premature cell death or the lack of death at inappropriate times (Zahir and Weaver 2004). Changes in cell architecture will cause changes in the way cells respond to their environment. Alterations in this architecture can be brought about by changes in the way microtubules and other cytoskeletal components behave in microgravity (Sytkowski and Davis 2001). Changes in the position of cell structures such as mitochondria have been investigated (Schatten et al. 2001). Changes observed in mitochondria clustering and the area around the nuclear envelope are likely to be caused by changes in the cytoskeleton (Schatten et al. 2001). Mitochondria clustering may cause an increase in the amount of glucose consumed by cells due to crowding. An increase in cell apoptosis is one significant consequence of the changes in cell structure and function that occur in microgravity (Schatten et al. 2001).

Several cells have been studied under microgravity conditions in recent years. One of the first proves of cytoskeletal changes in a space environment were found by Rijken et al. in 1991 (Rijken et al. 1992). Subsequently, other experiments focusing on the role of actin were performed with various cell types, including Hughes-Fulford and Lewis (1996) and Lewis et al. (1998) studied changes in the actin cytoskeleton of osteoblasts. Marina et al. found microgravity decreased the Tubulin volume density and changes the gene and protein expression. Corydon et al. obtained a fast live-cell imaging under real microgravity by using a compact fluorescence microscope for (Corydon et al. 2016a, b). In recent years, many articles have also reported the changes of cytoskeleton that were observed in simulated condition. Most cells appear to exhibit cytoskeleton changes and alteration of gene expression profile when short term exposed to simulated microgravity (see Table 1). Thus, simulated microgravity studies have also usefulness in confirming some observations and making the imag-

ing more complete by tracking changes at more time points, can revealing that the adaptation to a simulated microgravity environment is a very dynamic process.

5 Radiation and DNA Damage During Microgravity

It is known that high level of radiation in space is another factor different between space and earth environment. Previous study indicated that ultraviolet (UV) space irradiation leaded to lack dorsal and anterior structures in fertilized frog eggs yields embryos. The embryos fail to develop the cortical/cytoplasmic rotation that specifies dorsoventral polarity, thus they lack an array of parallel microtubules associated with the rotation (Elinson and Pasceri 1989). However, some other studies suggested that space radiation from short term orbital flights does not affect fertilization or later embryogenesis in these vertebrates, such as salamander and medaka fish eggs could be fertilized and developed normally during orbital space flight (Aimar et al. 2000; Gualandris-Parisot et al. 2002). For mammals, studies of reproduction and development in space have not progressed as well as in other animals due to the difficulty in maintaining animals and performing experiments in space. More recently,

Table 1 Cytoskeleton changes in cells in microgravity

Type of cell	Microgravity condition	Exposure time	Changes in cell (microgravity vs. ground based control)	References
Human adult retinal epithelium (ARPE-19) cells	Simulated in random positioning machine (RPM)	5 and 10 days	Alterations of F-actin and fibronectin Decrease cell growth and changes gene expression patterns	Corydon et al. (2016a, b)
Rat bone marrow mesenchymal stem cells (BMSC)	Simulated in clinostat	24 h 48 h	Inhibited migration of BMSC Reorganization of F-actin filaments Depolymerized actin cytoskeleton Inhibited osteogenic differentiation	Mao et al. (2016), Chen et al. (2016)

(continued)

Table 1 (continued)

Type of cell	Microgravity condition	Exposure time	Changes in cell (microgravity vs. ground based control)	References
Human umbilical vein endothelial cells (ECs)	Simulated in random positioning machine (RPM)	24 h and 72 h	Reduced the main cytoskeletal components (filaments and microtubules) Alteration in mechanical behavior	Janmaleki et al. (2016)
Rat neural crest stem cells (NCSCs)	Simulated in rotatory cell culture system (RCCS)	24 h	Disrupted organization of filamentous actin Increased globular actin level	Lin et al. (2016)
Human primary cells of nervous glioma tissues	Simulated in rotary culture	7 days or 14 days	Declined the ability of adhesion β-tubulin was highly disorganized	Wang et al. (2016)
Human follicular thyroid cancer cells	Simulated in random positioning machine (RPM)	24 h	Alterations in the F-actin cytoskeleton Changes in gene expression	Riwaldt et al. (2016)
Mouse embryonic stem cells	Simulated in a 2D pipette clinostat Simulated in RCCS	3 days	Cytoskeleton related 19 genes were modulated Deregulated the MAP kinase and focal adhesion Enhanced mesendoderm differentiation Increased the expression of Wnt signaling pathway	Shinde et al. (2016), Lei et al. (2014)

(continued)

Table 1 (continued)

Type of cell	Microgravity condition	Exposure time	Changes in cell (microgravity vs. ground based control)	References
Human FTC-133 cancer cells	Real microgravity in space (live cell imaging)	6 min	Changes the disturbance of F-actin bundles, the appearance of filopodia- and lamellipodia-like structures and cellular detachment	Corydon et al. (2016a, b)
Human osteoblast cells	Real space flight	10 days	Decreased the Tubulin volume density Changes the gene and protein expression	Kapitonova et al. (2013)
A431 (human epidermoid cancer cells)	Spaceflight	6 min	Loss of stress fibers, more F-actin	Rijken et al. (1992)
MC3T3 (osteoblasts)	Spaceflight	4 days	Loss of stress fibers, extended podia, perinuclear localization	Hughes-Fulford and Lewis (1996)

a study reported by Japanese researchers, freeze-dried sperms were cryopreserved on the International Space Station and were exposed to space radiation for 9 months, after returned to earth, these space stored freeze-dried sperms produced healthy offspring. The space-preserved samples showed evidence of slightly increased DNA damage compared with control samples preserved on Earth, but this was found to be largely repaired in embryos following fertilization. In addition, the birth rate of pups derived from the sperm stored in space was comparable to those of pups derived from the control samples (Wakayama et al. 2017). It is remarkable that the authors omit to do the natural radiation background (NRB) experiment, for example, they did not expose their sperm samples to the highest-NRB areas (70 mSv/y, Ramsar, Iran) to verify the measurability of their data before exposing them to space (Ferlazzo and Foray 2017). Thus, although difficulty and limited opportunities in carrying out experiments in space, the effects of space radiation on reproduction may also can be examined under ground-based simulated condition.

Differential sensitivity of mouse embryos in vitro to X-irradiation or UV irradiation. DNA damage induction may delays embryo cleavage kinetics and reduces blastocyst formation. For preimplantation embryos, mouse embryos of different stage

shows discriminating development during in vitro culture after UV irradiation. The UV sensitivity was the highest in 1-cell embryos and it decreased with development towards the morula stage as indicated by the rate of blastulation following UV irradiation. Interestingly, UV irradiation exposure of the in vitro development of the embryos was further impaired by the presence of caffeine in the culture medium at concentration levels which did not influence with the development of nonirradiated embryos. However, 2-cell embryos caffeine treatment was only effective during the first 24 h after irradiation, suggest that early mammalian embryos are able to repair UV-induced DNA damage by the post replication repair mechanism (Eibs and Spielmann 1977). There is also evidence from previous studies indicating that irradiation of early post-implantation embryos with low doses of X-rays does not result in marked cell cycle delay but rather induces a strong p53 and ATM expression, which are key regulators of the embryonic apoptosis pathway (Heyer et al. 2000).

However, some studies suggested that the frequency of DNA damage will increase when biological samples are exposed to irradiation under microgravity environment (Horneck 1999; Wang et al. 2011). Microgravity may impair the early-stage repair of radiation-induced DNA lesions of cells. Thus, results from experiments in space on the interaction of microgravity and radiation should be further special consideration.

6 Goals and Primary Results of the Mammalian Early Embryo Development Experiment on China' SJ-10 Satellite

6.1 The Background and Objectives of the Experiment

Changes in the gravitational field have significant effects on the physiology of living organisms. Does gravity affect the reproductive system and the normal embryonic development? In the past few decades, numerous experiments on reproductive in space environment have been performed using birds, fish, amphibian and sea urchin (Ijiri 1998; Sabo et al. 1995; Schatten et al. 1999; Souza et al. 1995; Yokota et al. 1992). Most of previous results indicated that the process of fertilization is not sensitive to the absence of gravity and finding the fertilization rates were even comparable to that in paralleled controls at normal gravity. However, unlike the other taxa studied to date, mammalian early embryo from different species appears highly sensitive to the environment in which it develops during the cleavage stages (Gardner and Lane 2005; Wale and Gardner 2016), either in vitro or in vivo, for example, in response to outer space environment including cosmic radiation, vibration during space flight. So far, the potential effects of weightlessness on the mammalian development are still unclear and the very possibility of the development of a mammalian embryo in microgravity was not undisputed, particularly studying of preimplantation mammalian embryo cultured in vitro. Actually, the first attempt to develop mammalian early embryos in space was carried out by NASA's STS-80 Spacecraft in 1996. How-

ever, none of the 49 mouse embryos on board successfully developed, while eleven of the fifth ground control 2-cell embryos reached the blastocyst stage (Schenker and Forkheim 1998). Since real space experiments are expensive and complicated, no one attempted to develop embryos again in the decade following NASA's failure. In 2006, China launched the recoverable satellite SJ-8, which carried hundreds mouse embryos in its orbital module. The four-cell embryos were placed in a specially sealed embryonic incubator, and then the incubator was loaded in a space embryonic culture box devised for space-flight. Despite real time high-resolution micrographs of the mouse embryos were obtained, those embryos none grew (Ma et al. 2008). However, the experiment performed on the ground in the same device showed that four-cell mouse embryos could develop to blastocysts and hatched blastocysts. Thus, space biologists have still questioned whether gravity was required for mammalian embryogenesis.

Since the technical difficult and financial limitations for space flight experiments in mammal development, some ground-based facilities for simulation of microgravity have been used to study the effect of microgravity on fertilization and preimplantation development in mammal. Recently, Wakayama et al. reported that using a 3D clinostat, which simulates microgravity via continuous 3D rotation, to study fertilization and the earliest stages of embryonic development under conditions that replicate space travel. Simulated microgravity cultured embryos successfully reached the blastocyst stage and yielded viable offspring upon implantation into female mice, but at a significantly lower the live birth rate than their 1 × g counterpart (Wakayama et al. 2009). The experiment reveals developmental difficulties arising from mammalian reproduction in space and normal preimplantation embryo development might require 1 × g condition. Interestingly, similar conclusions can be drawn from an earlier study that using a horizontal clinostat device to study the effects of simulated microgravity on mammalian fertilization and preimplantation development in vitro (Kojima et al. 2000). In 2016, China launched the country's first microgravity experimental satellite, SJ-10, on April 6. High-resolution photographs were obtained deriving from SJ-10 satellite. The results crucial from experiments aboard China's SJ-10 satellite prove for the first time that early-stage mammal embryos can develop in space.

The basic objective of the mammalian embryology experiment on China' SJ-10 satellite was attempt to detect the developmental status of mouse early embryos in space. To discover whether mammalian preimplantation embryo can developed normally from 2-cell stage to blastocyst in vitro exposed to space environment and whether the space environment affect the fate of cell differentiation and polarization of blastocyst. What are the potential mechanisms that affect the development of mammal preimplantation embryos in space? This experiment will be critical in understanding the beginning of mammalian life, as well as the first step in understanding the entire process of reproduction in space. In addition, understanding the early embryo development process in space will provide an insight into human reproduction in space. This will become increasingly important as humans look to carry out long-duration spaceflights and colonise other planets.

6.2 Preliminary Results and Discussion

6.2.1 The Effect of Vibration at Launch on the Preimplantation Development in Mice

It was previously shown that 2-cell embryo is the most sensitive stage for its easy blockage, which will induce a various adverse impact during the development of preimplantation embryo in mice (Gardner et al. 2013; Whittingham 1971). Prior to the preimplantation development in space, ground-based experiments were carried out on the earth to investigate the effect of vibration, acting at launch on 2-cell stages of mouse embryos development. Hundreds of 2-cell embryos were exposed to the vibration platform with 80–100 Hz for 10 min (see Fig. 10).

After exposed in vibration platform for 10 min, these exposed embryos were further cultured in CO_2 incubator for 72 h and the development of blastocysts were counted. Notably, those embryos with short-term vibration showed similar development capacity to control group (without vibration), and had comparable morphologies to those in the control group (see Fig. 11). Thus, these results suggest that short term vibration did not affect the development of mammalian preimplantation embryos.

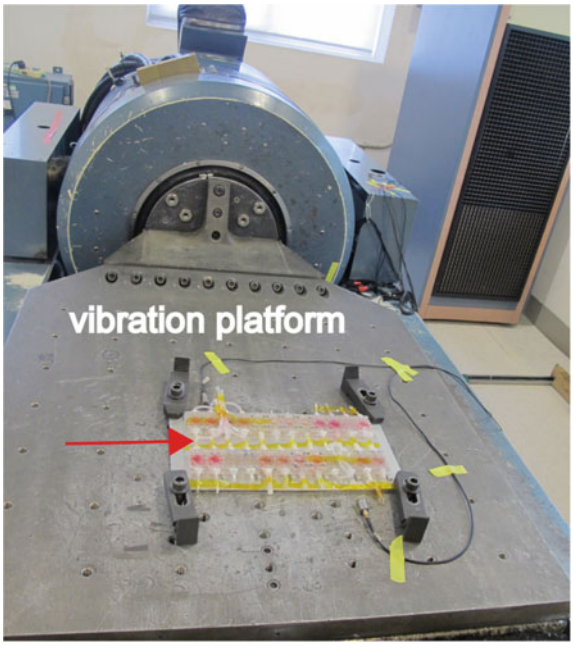

Fig. 10 Vibration platform were provided by the Shanghai Institute of Technical Physics of the Chinese Academy of Sciences. Red arrow indicating the samples were exposed to vibration environment

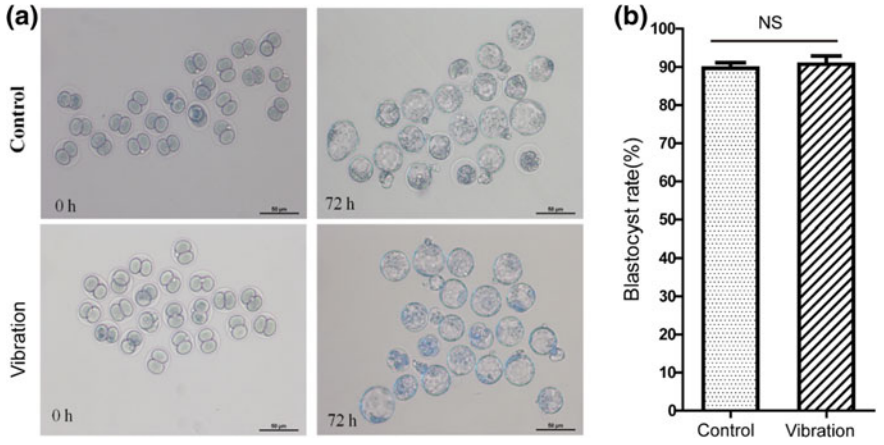

Fig. 11 The in vitro development of 2-cell embryos after short-term exposed on 80–100 Hz vibration conditions. **a** Representative imaging of embryo after 10 min exposed to vibration and subsequent 72 h development in CO_2. Bar = 100 μm. **b** The percentage of blastocyst formation in control group and vibration treated group. Error bars represent s.e.m. from three independent experiments. Two-sided Student's t-test. NS, not significant

6.2.2 The Effect of Hypergravity on the Preimplantation Development in Mice

In addition to the above vibration experiment, which simulated the effect of launch on the development of preimplantation embryo, we also detect whether the 2-cell embryo samples can tolerate the short-term hypergravity produced by the launch process. The centrifuge was used to obtain the desired hypergravity. We exposed mouse 2-cell embryos on centrifuge for 20 min with a speed of 10,000 rpm/min. After 20 min hypergravity exposure, those embryos were cultured in an incubator at 37 °C with 5% CO_2 in air. The percentage of blastocysts developed from hypergravity treated 2-cell mouse embryos after 72 h culture was compared with that of synchronous controls. Interestingly, we found that the mouse 2-cell embryos could tolerate to a very extreme acceleration with normally morphology, and exposed embryos could grow and accomplished the whole process of preimplantation development from 2-cell to blastocyst (see Fig. 12). More importantly, the blastocyst formation rate in hypergravity group showed no significant difference when compared with the without hypergravity treated control. In short, our results showed that short-term exposure to hypergravity environment has no significant effect on preimplantation development of mammals.

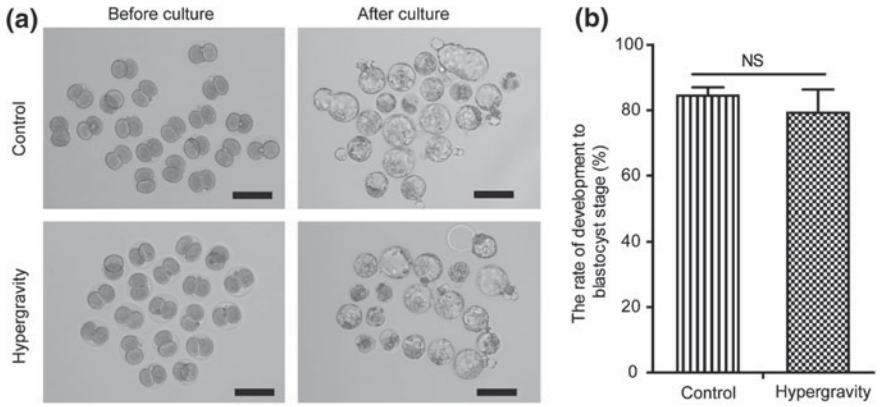

Fig. 12 Effect of short-term simulated hypergravity on mouse preimplantation development. **a** Morphology of 2-cell embryos after short-term exposed on 10,000 rpm/min hypergravity conditions and subsequent development in CO_2 for 72 h. **b** The percentage of blastocyst formation in control group and simulated hypergravity treated group. Error bars represent s.e.m. from three independent experiments. Two-sided Student's t-test. NS, not significant

6.2.3 Seal Culture System and Development of Full-Term Offspring

As we known, mammalian preimplantation embryos are very sensitive to the culture environment, it is important to establish stable culture condition (Itoi et al. 2012; Swain 2011). Currently, CO_2 incubators (air-jacketed/water-jacketed) are commonly used for maintaining an optimal culture environment in terms of gas phase, temperature and humidity, which is called conventional culture system. However, the traditional CO_2 incubator with pressure vessels which contain N_2, O_2 and CO_2 is large, heavy, require considerable installation area and containing a potential risk factor in a vacuum that cannot be used to our SJ-10 satellite study. Therefore, establishment of available culture systems (for example, sealed-culture method) for the embryos development in space is very pivotal.

According to previous studies, we performed some of experiments to establish sealed culture system. We compared two culture system: conventional microdrop culture (control culture) and a novel sealed culture method (sealed culture) to culture 2-cell embryos in vitro (see Fig. 13).

In this study, modified CZB medium and two kinds of embryos (fresh embryos and frozen-thawed embryos) were used to evaluate the flexibility of sealed culture method. As shown in Fig. 14, the majority of embryos reached the blastocyst stage in fresh cultured 2-cell embryo and the development rates of blastocyst did not difference significantly from the conventional culture system (89.2% vs. 84.2%). Similarly, the blastocyst formation rate in the sealed culture system of frozen-thawed 2-cell embryos was also no significantly lower than controls (84.1% vs. 79.1%), which most of those 2-cell embryos reached the morula/blastocyst stage. These results sug-

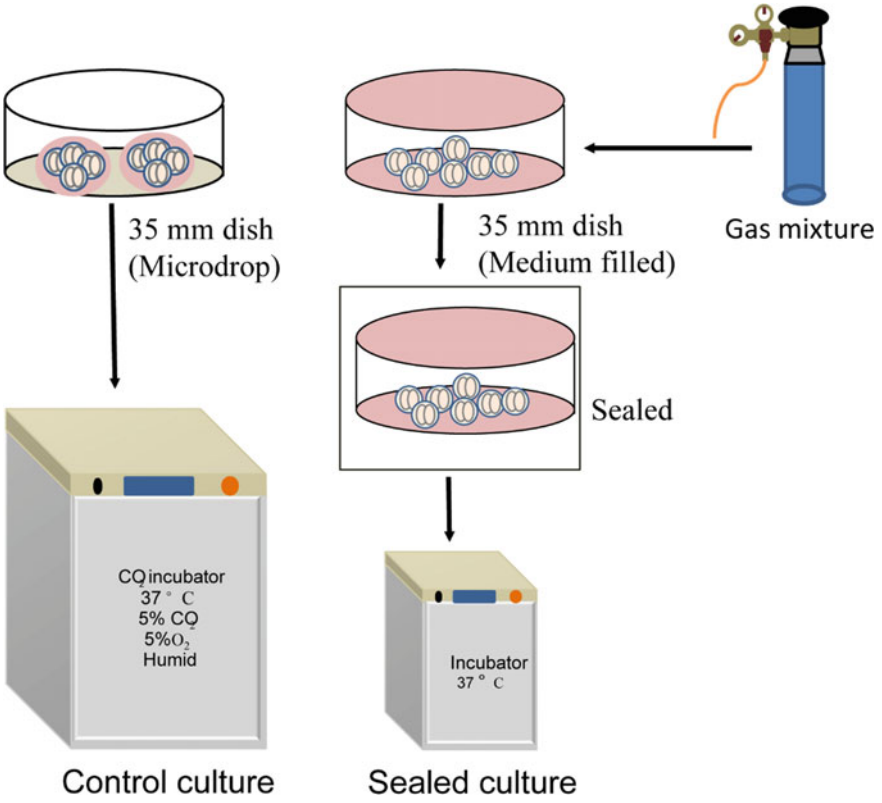

Fig. 13 Schematic diagram of the experimental procedure in two culture system. Control culture: embryos were transfer to 50–100 μL microdrops of CZB medium in 35 mm culture dish and kept in a CO_2 incubator at 37 °C. Sealed culture: the CZB medium was firstly inflated with a gas mixture (5% O_2, 5% CO_2 and 90% N_2) for about 2 h, and then the embryos were transferred to 35 mm culture dish with gas saturated medium. The culture dish was sealed and placed in 37 °C incubator without gas

gest that mouse preimplantation embryos can be cultured in sealed culture system in vitro established by us without the need for a traditional incubator.

We performed additional experiments to investigate whether mouse embryos cultured in the sealed culture system has the potential for full-term development. After 72 h culturing of 2-cell embryos, developed blastocysts were transferred into pseudopregnant ICR strain female mice. The recipient mice were maintained until term pregnancy and the number of pups sired was documented at term pregnancy. As shown in Fig. 15, embryos derived from the sealed culture systems can developed to full term (see Fig. 15a). In addition, the success rates of producing offspring (32% vs. 29.5%) were not significant different between the blastocyst developed derived from fresh and frozen-thawed 2-cell (data not shown). It is note that all of the obtained pups grew to adulthood and were fertile (see Fig. 15b).

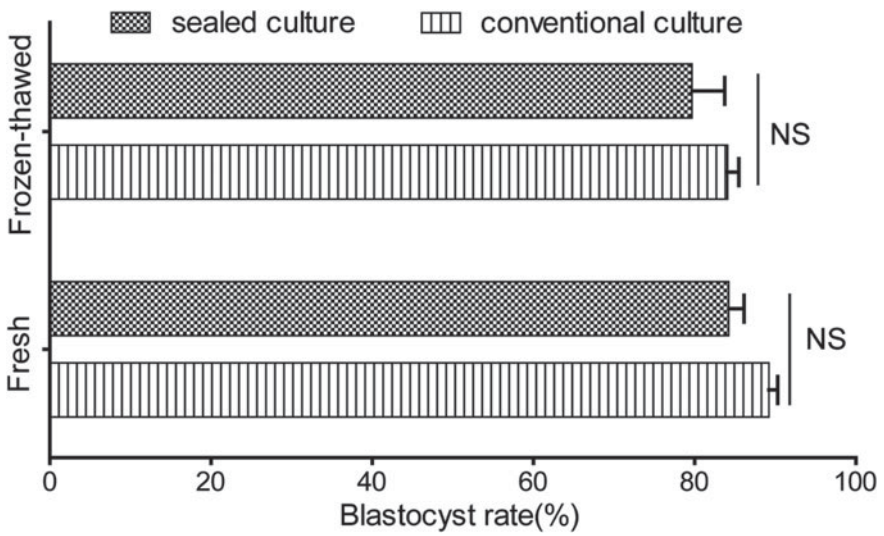

Fig. 14 Blastocyst development rates of 2-cell embryos derived from fresh and frozen-thawed cultured that were cultured under sealed culture and conventional culture system. Error bars represent s.e.m. from three independent experiments. Two-sided Student's *t*-test. NS, not significant

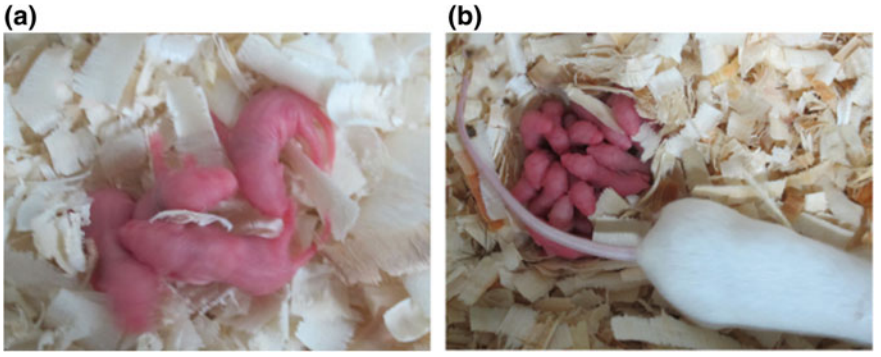

Fig. 15 Development of full-term offspring. **a** Pups derived from embryos cultured in sealed culture system. **b** After seven or eight weeks, these pups grew to adulthood and were proven fertile when randomly selected mice mating

6.2.4 Establish a Sealed Culture System in Automated Embryo Culture Box

Due to resource limitation and the security assurance of the SJ-10 satellite, we designed and developed a multi-functional, enclosed embryo culture box that is about the size of a microwave oven. The embryo culture box was provided power and automatically maintained temperature control, imaging and medium exchange.

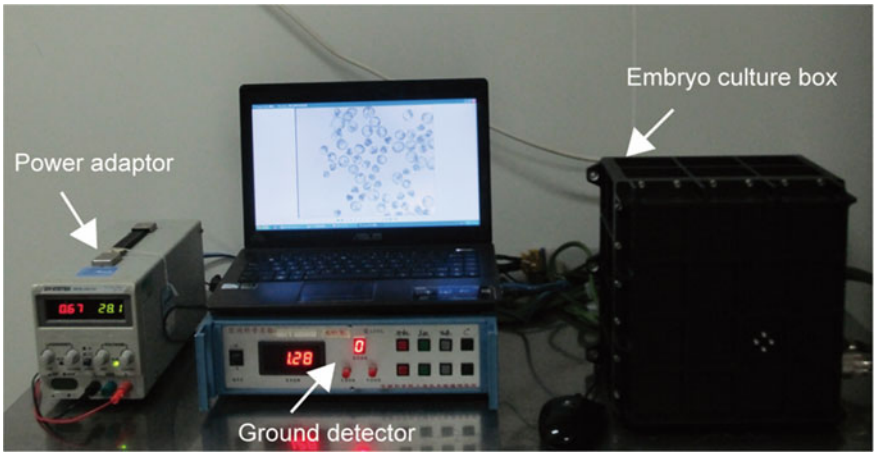

Fig. 16 Testing embryo culture in automated sealed culture box in ground

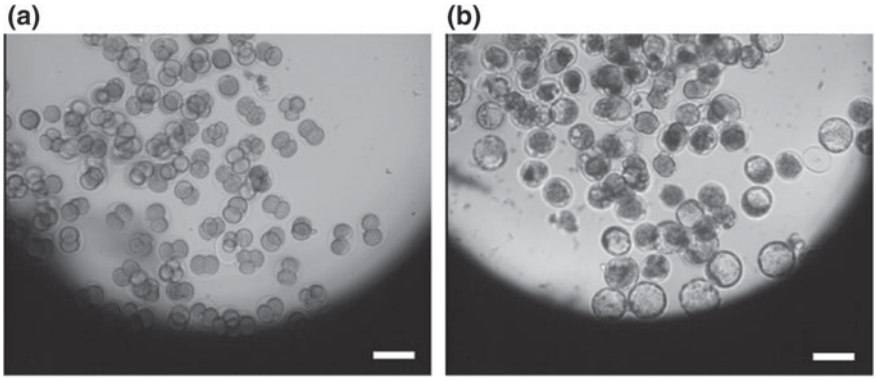

Fig. 17 Preimplantation development in imaging culture unit in automated sealed embryo culture box. **a** Two-cell stage embryo cultured for 0 h in imaging culture unit. **b** Blastocyst cultured for 96 h in imaging culture unit. Bar = 100 μm

The ground test experiments were performed at our laboratory according to the standardized procedure of experiment (see Fig. 16). To determine the feasibility of sealed embryo culture box, we transferred 2-cell embryo in culture units and incubated embryos in the automatic embryo culture box with sealed conditions. During the experiment, our results revealed that images of 2-cell embryo can be automated captured in embryo culture box (see Fig. 17a). After 96 h in culture, many 2-cell embryos were able to develop into blastocyst in imaging culture unit (see Fig. 17b). These results indicate that the automated sealed embryo culture box could be used to culture early embryo for the subsequent spaceflight experiment.

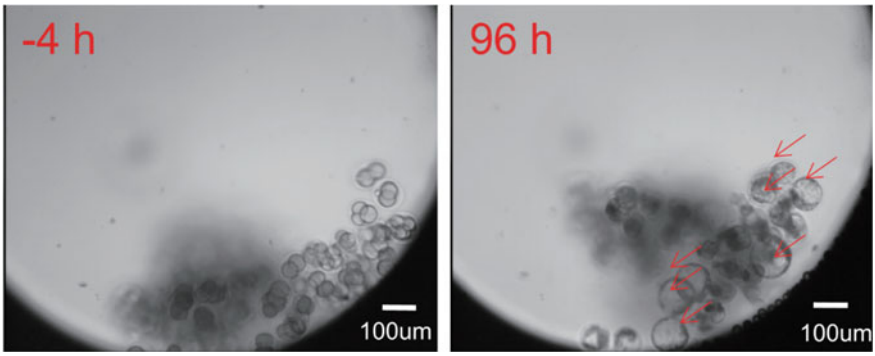

Fig. 18 Representative photograph of mouse preimplantation embryos development in imaging culture chamber during spaceflight (Red arrow: blastocyst). Bar = 100 μm

6.2.5 Development of Mouse Early Embryo During Space Flight

In total, thousands of 2-cell stage embryos were transferred in embryo culture box and the apparatus were laid in satellite in space. The SJ-10 satellite was launched on 6 April by means of a Long March rocket 2D in the Cosmodrome Jiuquan. During the spaceflight experiment, a camera on board the SJ-10 satellite took photographs of the embryos every 4 h, the obtained images were then transmitted back to Earth. We successfully received high-resolution pictures of embryos developing in space. Received images showed some of the 2-cell mouse embryos had completed the developing process that developed into advanced blastocyst in 96 h culturing (see Fig. 18). The results crucial from experiments aboard China's SJ-10 satellite prove for the first time that preimplantation development of mammalian embryo can completed in space. Besides, the development rate of blastocyst of returned embryos has been analyzed and compare it with those of ground cultured embryos. Importantly, the returned blastocysts has been analyzed by single cell DNA whole genome sequencing and single cell methylation sequencing to evaluate the quality of embryos developed in space and a potential mechanisms that affect the development of mammal preimplantation embryos in space. In brief, this finding will be critical in understanding the beginning of mammalian life, as well as the first step in understanding the entire process of reproduction in space and understanding the early embryo development process in space will provide an insight into human reproduction in space in the future.

7 Envisioned Future Opportunities and Challenges

With the development of space science and technology, more and more space programs and exploration activities will be performed. China has announced a program for building manned space station. The planned Chinese space station will be built

in 2022. In the future, it is anticipated that, space travel will include longer missions, and even human can live in space habitats for years, such as, manned space colonization will eventually lead to gestation and birth in outer space. Thus, it is expected that the study of mammalian reproduction will be increased and application of assistant reproduction technology will be used to produce humans in space habitats.

As we known, microgravity and cosmic radiations pose significant health hazards to human body in outer space or during spaceflights. Therefore, understanding the potential risks and hazards associated with mammal reproduction in space is priority. Despite mouse preimplantation embryos have been proved that can be successfully developed in space on board China's SJ-10 satellite, these developed blastocysts in space should further investigate the distinctive characterization, including the diversity of development rate and the changes of gene expression and epigenetic regulation, which might result in long-term effects on offspring well-being.

But for now, it is still very important to study whether space environment on space station or spacecraft causes harmful effects in mammalian preimplantation embryo development. We need to ask whether space developed blastocyst can implantation after transfer into uterus and subsequently develop to full-term offspring. If can, whether these blastocysts developed in space are epigenetic anomalies which may transmitted to progeny of the postnatal generation and transmit into future generations. In addition, on future work must consider the security and provide protection against space environment hazards for mammalian development in space.

Acknowledgements We thank National Space Science Center of the CAS and institute of mechanics of CAS for organizing this program. We are grateful to thank the chief scientist of SJ-10 satellite program, Prof. Wenrui Hu for guiding in science and technology. We also thank Dr. Tao Zhang for providing the embryo culture hardware and vibration platform for our study. This research was supported by the National Natural Science Foundation of China Grants (U1738103, 31600683) and the Strategically Guiding Scientific Special Project from the Chinese Academy of Sciences (XDA04020202-20, XDA15014000).

References

Abramczuk J, Sawicki W (1975) Pronuclear synthesis of DNA in fertilized and parthenogenetically activated mouse eggs. Exp Cell Res 92:361–371

Aimar C, Bautz A, Durand D et al (2000) Microgravity and hypergravity effects on fertilization of the salamander Pleurodeles waltl (urodele amphibian). Biol Reprod 63:551–558

Alarcon VB (2010) Cell polarity regulator PARD6B is essential for trophectoderm formation in the preimplantation mouse embryo. Biol Reprod 83:347–358

Antipov VV, Delone NL, Parfyonov GP et al (1965) Results of biological experiments carried out under conditions of "Vostok" flights with the participation of cosmonauts A.G. Nikolajev, P.R. Popovich and V.F. Bykovsky. Life Sci Space Res 3:215–229

Barton SC, Arney KL, Shi W et al (2001) Genome-wide methylation patterns in normal and uniparental early mouse embryos. Hum Mol Genet 10:2983–2987

Bedzhov I, Graham SJ, Leung CY et al (2014) Developmental plasticity, cell fate specification and morphogenesis in the early mouse embryo. Philos Trans R Soc Lond B Biol Sci 369

Bellairs R (1994) Experiments on embryos in space: an overview. Adv Space Res 14:179–187
Burden HW, Zary J, Lawrence IE et al (1997) Effects of space flight on ovarian-hypophyseal function in postpartum rats. J Reprod Fertil 109:193–197
Calarco PG (1991) Fertilization of the mouse oocyte. J Electron Microsc Tech 17:401–411
Cao YJ, Fan XJ, Shen Z et al (2007) Nitric oxide affects preimplantation embryonic development in a rotating wall vessel bioreactor simulating microgravity. Cell Biol Int 31:24–29
Chazaud C, Yamanaka Y (2016) Lineage specification in the mouse preimplantation embryo. Development 143:1063–1074
Chen L, Wang D, Wu Z et al (2010) Molecular basis of the first cell fate determination in mouse embryogenesis. Cell Res 20:982–993
Chen Z, Luo Q, Lin C et al (2016) Simulated microgravity inhibits osteogenic differentiation of mesenchymal stem cells via depolymerizing F-actin to impede TAZ nuclear translocation. Sci Rep 6:30322
Chung Y, Klimanskaya I, Becker S et al (2006) Embryonic and extraembryonic stem cell lines derived from single mouse blastomeres. Nature 439:216–219
Cockburn K, Rossant J (2010) Making the blastocyst: lessons from the mouse. J Clin Invest 120:995–1003
Corydon TJ, Kopp S, Wehland M et al (2016a) Alterations of the cytoskeleton in human cells in space proved by life-cell imaging. Sci Rep 6:20043
Corydon TJ, Mann V, Slumstrup L et al (2016b) Reduced expression of cytoskeletal and extracellular matrix genes in human adult retinal pigment epithelium cells exposed to simulated microgravity. Cell Physiol Biochem 40:1–17
Coticchio G, Dal Canto M, Mignini RM et al (2015) Oocyte maturation: gamete-somatic cells interactions, meiotic resumption, cytoskeletal dynamics and cytoplasmic reorganization. Hum Reprod Update 21:427–454
Courtine G, Pozzo T (2004) Recovery of the locomotor function after prolonged microgravity exposure. I. Head-trunk movement and locomotor equilibrium during various tasks. Exp Brain Res 158:86–99
Crawford-Young SJ (2006) Effects of microgravity on cell cytoskeleton and embryogenesis. Int J Dev Biol 50:183–191
Dey SK, Lim H, Das SK et al (2004) Molecular cues to implantation. Endocr Rev 25:341–373
Doherty AS, Mann MR, Tremblay KD et al (2000) Differential effects of culture on imprinted H19 expression in the preimplantation mouse embryo. Biol Reprod 62:1526–1535
Eibs HG, Spielmann H (1977) Differential sensitivity of preimplantation mouse embryos to UV irradiation in vitro and evidence for post replication repair. Radiat Res 71:367–376
Elinson RP, Pasceri P (1989) Two UV-sensitive targets in dorsoanterior specification of frog embryos. Development 106:511–518
Ferlazzo ML, Foray N (2017) Space radiobiology needs realistic hypotheses and relevant methodology. Proc Natl Acad Sci USA 114:E6733
Fierro-Gonzalez JC, White MD, Silva JC et al (2013) Cadherin-dependent filopodia control preimplantation embryo compaction. Nat Cell Biol 15:1424–1433
Fleming TP, Kwong WY, Porter R et al (2004) The embryo and its future. Biol Reprod 71:1046–1054
Frum T, Ralston A (2015) Cell signaling and transcription factors regulating cell fate during formation of the mouse blastocyst. Trends Genet 31:402–410
Gaboyard S, Blanchard MP, Travo C et al (2002) Weightlessness affects cytoskeleton of rat utricular hair cells during maturation in vitro. NeuroReport 13:2139–2142
Gardner RL (2002) Experimental analysis of second cleavage in the mouse. Hum Reprod 17:3178–3189
Gardner DK, Lane M (2005) Ex vivo early embryo development and effects on gene expression and imprinting. Reprod Fert Develop 17:361–370
Gardner DK, Hamilton R, McCallie B et al (2013) Human and mouse embryonic development, metabolism and gene expression are altered by an ammonium gradient in vitro. Reproduction 146:49–61

Gazenko OG (1988) Ontogenesis of mammals in microgravity. Nauka Publishers, Moscow
Gualandris-Parisot L, Husson D, Bautz A et al (2002) Effects of space environment on embryonic growth up to hatching of salamander eggs fertilized and developed during orbital flights. Uchu Seibutsu Kagaku 16:3–11
Guo G, Huss M, Tong GQ et al (2010) Resolution of cell fate decisions revealed by single-cell gene expression analysis from zygote to blastocyst. Dev Cell 18:675–685
Heyer BS, MacAuley A, Behrendtsen O et al (2000) Hypersensitivity to DNA damage leads to increased apoptosis during early mouse development. Gene Dev 14:2072–2084
Hirate Y, Hirahara S, Inoue K et al (2013) Polarity-dependent distribution of angiomotin localizes Hippo signaling in preimplantation embryos. Curr Biol 23:1181–1194
Horneck G (1999) Impact of microgravity on radiobiological processes and efficiency of DNA repair. Mutat Res-Fund Mol M 430:221–228
Hughes-Fulford M, Lewis ML (1996) Effects of microgravity on osteoblast growth activation. Exp Cell Res 224:103–109
Ijiri K (1998) Development of space-fertilized eggs and formation of primordial germ cells in the embryos of Medaka fish. Adv Space Res 21:1155–1158
Ikeuchi T, Sasaki S, Umemoto Y et al (2005) Human sperm motility in a microgravity environment. Reprod Med Biol 4:161–168
Ingber D (1999) How cells (might) sense microgravity. FASEB J 13(Suppl):S3–S15
Ingber DE (2003) Tensegrity I. Cell structure and hierarchical systems biology. J Cell Sci 116:1157–1173
Itoi F, Tokoro M, Terashita Y et al (2012) Offspring from mouse embryos developed using a simple incubator-free culture system with a deoxidizing agent. PLoS ONE 7:e47512
Janmaleki M, Pachenari M, Seyedpour SM et al (2016) Impact of simulated microgravity on cytoskeleton and viscoelastic properties of endothelial cell. Sci Rep 6(32418)
Jung S, Bowers SD, Willarda ST (2009) Simulated microgravity influences bovine oocyte in vitro fertilization and preimplantation embryo development. J Anim Vet Adv 8:1807–1814
Kamiya H, Sasaki S, Ikeuchi T et al (2003) Effect of simulated microgravity on testosterone and sperm motility in mice. J Androl 24:885–890
Kapitonova MY, Salim N, Othman S et al (2013) Alteration of cell cytoskeleton and functions of cell recovery of normal human osteoblast cells caused by factors associated with real space flight. Malays J Pathol 35:153–163
Khang I, Sonn S, Park JH et al (2005) Expression of epithin in mouse preimplantation development: its functional role in compaction. Dev Biol 281:134–144
Kojima Y, Sasaki S, Kubota Y et al (2000) Effects of simulated microgravity on mammalian fertilization and preimplantation embryonic development in vitro. Fertil Steril 74:1142–1147
Kojima Y, Tam OH, Tam PP (2014) Timing of developmental events in the early mouse embryo. Semin Cell Dev Biol 34:65–75
Kuckenberg P, Peitz M, Kubaczka C et al (2011) Lineage conversion of murine extraembryonic trophoblast stem cells to pluripotent stem cells. Mol Cell Biol 31:1748–1756
Larue L, Ohsugi M, Hirchenhain J et al (1994) E-cadherin null mutant embryos fail to form a trophectoderm epithelium. Proc Natl Acad Sci USA 91:8263–8267
Lee SH, Dominguez R (2010) Regulation of actin cytoskeleton dynamics in cells. Mol Cells 29:311–325
Lei X, Deng Z, Zhang H et al (2014) Rotary suspension culture enhances mesendoderm differentiation of embryonic stem cells through modulation of Wnt/beta-catenin pathway. Stem Cell Rev 10:526–538
Lewis ML, Reynolds JL, Cubano LA et al (1998) Spaceflight alters microtubules and increases apoptosis in human lymphocytes (Jurkat). FASEB J 12:1007–1018
Lin SC, Gou GH, Hsia CW et al (2016) Simulated microgravity disrupts cytoskeleton organization and increases apoptosis of rat neural crest stem cells via upregulating CXCR56 expression and RhoA-ROCK1-p38 MAPK-p53 signaling. Stem Cells Dev 25:1172–1193

Liu H, Wu Z, Shi X et al (2013) Atypical PKC, regulated by Rho GTPases and Mek/Erk, phosphorylates Ezrin during eight-cell embryo compaction. Dev Biol 375:13–22
Ma B, Cao Y, Zheng W et al (2008) Real-time micrography of mouse preimplantation embryos in an orbit module on SJ-8 satellite. Microgravity Sci Tec 20:127–136
Macho L, Kvetnansky R, Nemeth S et al (1996) Effects of space flight on endocrine system function in experimental animals. Environ Med 40:95–111
Macho L, Kvetnansky R, Fickova M et al (2001) Endocrine responses to space flights. J Gravit Physiol 8:P117–P120
Mann MR, Lee SS, Doherty AS et al (2004) Selective loss of imprinting in the placenta following preimplantation development in culture. Development 131:3727–3735
Mao X, Chen Z, Luo Q et al (2016) Simulated microgravity inhibits the migration of mesenchymal stem cells by remodeling actin cytoskeleton and increasing cell stiffness. Cytotechnology 68:2235–2243
Market VB, Denomme MM, Mann MR (2012) Loss of genomic imprinting in mouse embryos with fast rates of preimplantation development in culture. Biol Reprod 86(143):1–16
Meloni MA, Galleri G, Pani G et al (2011) Space flight affects motility and cytoskeletal structures in human monocyte cell line J-111. Cytoskeleton (Hoboken) 68:125–137
Messerschmidt DM, Knowles BB, Solter D (2014) DNA methylation dynamics during epigenetic reprogramming in the germline and preimplantation embryos. Genes Dev 28:812–828
Morris SA, Graham SJ, Jedrusik A et al (2013) The differential response to Fgf signalling in cells internalized at different times influences lineage segregation in preimplantation mouse embryos. Open Biol 3:130104
Neganova IE, Sekirina GG, Eichenlaub-Ritter U et al (2000) Surface-expressed E-cadherin, and mitochondrial and microtubule distribution in rescue of mouse embryos from 2-cell block by aggregation. Mol Hum Reprod 6:454–464
Nelson GA, Schubert WW, Kazarians GA et al (1994) Development and chromosome mechanics in nematodes: results from IML-1. Adv Space Res 14:209–214
Ning L, Lei X, Cao Y et al (2015) Effect of short-term hypergravity treatment on mouse 2-cell embryo development. Microgravity Sci Tec 27:465–471
Nishioka N, Yamamoto S, Kiyonari H et al (2008) Tead4 is required for specification of trophectoderm in pre-implantation mouse embryos. Mech Dev 125:270–283
Niwa H, Toyooka Y, Shimosato D et al (2005) Interaction between Oct3/4 and Cdx2 determines trophectoderm differentiation. Cell 123:917–929
O'Farrell PH, Stumpff J, Su TT (2004) Embryonic cleavage cycles: how is a mouse like a fly? Curr Biol 14:R35–R45
Ogneva IV (2015) Early development under microgravity conditions. Biofizika 60:1024–1035
Paoli P, Giannoni E, Chiarugi P (2013) Anoikis molecular pathways and its role in cancer progression. Biochim Biophys Acta 1833:3481–3498
Parfyonov GP, Platonova RN, Tairbekov MG et al (1979) Biological experiments carried out aboard the biological satellite Cosmos-936. Life Sci Space Res 17:297–299
Pauken CM, Capco DG (1999) Regulation of cell adhesion during embryonic compaction of mammalian embryos: roles for PKC and beta-catenin. Mol Reprod Dev 54:135–144
Peters J (2014) The role of genomic imprinting in biology and disease: an expanding view. Nat Rev Genet 15:517–530
Piliszek A, Grabarek JB, Frankenberg SR et al (2016) Cell fate in animal and human blastocysts and the determination of viability. Mol Hum Reprod 22:681–690
Plusa B, Frankenberg S, Chalmers A et al (2005) Downregulation of Par3 and aPKC function directs cells towards the ICM in the preimplantation mouse embryo. J Cell Sci 118:505–515
Puscheck EE, Awonuga AO, Yang Y et al (2015) Molecular biology of the stress response in the early embryo and its stem cells. Adv Exp Med Biol 843:77–128
Ralston A, Cox BJ, Nishioka N et al (2010) Gata3 regulates trophoblast development downstream of Tead4 and in parallel to Cdx2. Development 137:395–403

Rijken PJ, de Groot RP, Kruijer W et al (1992) Identification of specific gravity sensitive signal transduction pathways in human A431 carcinoma cells. Adv Space Res 12:145–152
Riwaldt S, Bauer J, Wehland M et al (2016) Pathways regulating spheroid formation of human follicular thyroid cancer cells under simulated microgravity conditions: a genetic approach. Int J Mol Sci 17:528
Ronca AE, Fritzsch B, Bruce LL et al (2008) Orbital spaceflight during pregnancy shapes function of mammalian vestibular system. Behav Neurosci 122:224–232
Ruden D, Bolnick A, Awonuga A et al (2018) Effects of gravity, microgravity or microgravity simulation on early mammalian development. Stem Cells Dev [Epub ahead of print]
Russ AP, Wattler S, Colledge WH et al (2000) Eomesodermin is required for mouse trophoblast development and mesoderm formation. Nature 404:95–99
Sabo V, Boda K, Majek S et al (1995) The second generation of the incubator hardware for studying avian embryogenesis under microgravity conditions. Acta Astronaut 35:421–426
Sasaki S, Ikeuchi T, Kamiya H et al (2004) Male fertility in space. Hinyokika Kiyo 50:559–563
Schatten H, Chakrabarti A, Taylor M et al (1999) Effects of spaceflight conditions on fertilization and embryogenesis in the sea urchin Lytechinus pictus. Cell Biol Int 23:407–415
Schatten H, Lewis ML, Chakrabarti A (2001) Spaceflight and clinorotation cause cytoskeleton and mitochondria changes and increases in apoptosis in cultured cells. Acta Astronaut 49:399–418
Schenker E, Forkheim K (1998) Mammalian mice embryo early development in weightlessness environment on STS 80 space flight. Israel Aerospace Medicine Institute Report
Serova LV (1989) Effect of weightlessness on the reproductive system of mammals. Kosm Biol Aviakosm Med 23:11–16
Serova LV, Denisova LA (1982) The effect of weightlessness on the reproductive function of mammals. Physiologist 25:S9–S12
Shi L, Wu J (2009) Epigenetic regulation in mammalian preimplantation embryo development. Reprod Biol Endocrinol 7:59
Shinde V, Brungs S, Henry M et al (2016) Simulated microgravity modulates differentiation processes of embryonic stem cells. Cell Physiol Biochem 38:1483–1499
Sikora-Polaczek M, Hupalowska A, Polanski Z et al (2006) The first mitosis of the mouse embryo is prolonged by transitional metaphase arrest. Biol Reprod 74:734–743
Souza KA, Black SD, Wassersug RJ (1995) Amphibian development in the virtual absence of gravity. Proc Natl Acad Sci USA 92:1975–1978
Stephenson RO, Yamanaka Y, Rossant J (2010) Disorganized epithelial polarity and excess trophectoderm cell fate in preimplantation embryos lacking E-cadherin. Development 137:3383–3391
Swain JE (2011) A self-contained culture platform using carbon dioxide produced from a chemical reaction supports mouse blastocyst development in vitro. J Reprod Dev 57:551–555
Sytkowski AJ, Davis KL (2001) Erythroid cell growth and differentiation in vitro in the simulated microgravity environment of the NASA rotating wall vessel bioreactor. Vitro Cell Dev Biol Anim 37:79–83
Szczepanska K, Stanczuk L, Maleszewski M (2011) Isolated mouse inner cell mass is unable to reconstruct trophectoderm. Differentiation 82:1–8
Tarkowski AK, Wroblewska J (1967) Development of blastomeres of mouse eggs isolated at the 4- and 8-cell stage. J Embryol Exp Morphol 18:155–180
Tash JS, Bracho GE (1999) Microgravity alters protein phosphorylation changes during initiation of sea urchin sperm motility. FASEB J 13(Suppl):S43–S54
Thomas FC, Sheth B, Eckert JJ et al (2004) Contribution of JAM-1 to epithelial differentiation and tight-junction biogenesis in the mouse preimplantation embryo. J Cell Sci 117:5599–5608
Van de Velde H, Cauffman G, Tournaye H et al (2008) The four blastomeres of a 4-cell stage human embryo are able to develop individually into blastocysts with inner cell mass and trophectoderm. Hum Reprod 23:1742–1747
Vassy J, Portet S, Beil M et al (2001) The effect of weightlessness on cytoskeleton architecture and proliferation of human breast cancer cell line MCF-7. FASEB J 15:1104–1106

Vorselen D, Roos WH, MacKintosh FC et al (2014) The role of the cytoskeleton in sensing changes in gravity by nonspecialized cells. FASEB J 28:536–547
Wakayama S, Kawahara Y, Li C et al (2009) Detrimental effects of microgravity on mouse preimplantation development in vitro. PLoS ONE 4:e6753
Wakayama S, Kamada Y, Yamanaka K et al (2017) Healthy offspring from freeze-dried mouse spermatozoa held on the International Space Station for 9 months. Proc Natl Acad Sci USA 114:5988–5993
Wale PL, Gardner DK (2016) The effects of chemical and physical factors on mammalian embryo culture and their importance for the practice of assisted human reproduction. Hum Reprod Update 22:2–22
Wang Y, An L, Jiang Y et al (2011) Effects of simulated microgravity on embryonic stem cells. PLOS ONE 6(e2921412)
Wang X, Du J, Wang D et al (2016) Effects of simulated microgravity on human brain nervous tissue. Neurosci Lett 627:199–204
Whittingham DG (1971) Culture of mouse ova. J Reprod Fertil Suppl 14:7–21
Yang X, Smith SL, Tian XC et al (2007) Nuclear reprogramming of cloned embryos and its implications for therapeutic cloning. Nat Genet 39:295–302
Yokota H, Neff AW, Malacinski GM (1992) Altering the position of the first horizontal cleavage furrow of the amphibian (Xenopus) egg reduces embryonic survival. Int J Dev Biol 36:527–535
Zahir N, Weaver VM (2004) Death in the third dimension: apoptosis regulation and tissue architecture. Curr Opin Genet Dev 14:71–80
Zernicka-Goetz M, Morris SA, Bruce AW (2009) Making a firm decision: multifaceted regulation of cell fate in the early mouse embryo. Nat Rev Genet 10:467–477

Effects of Space Microgravity on the Trans-differentiation Between Osteogenesis and Adipogenesis of Human Marrow-Derived Mesenchymal Stem Cells

Cui Zhang, Liang Li and Jinfu Wang

Abstract With the development of scientific exploration in deep space, human activities will become more frequent, and activity time will be longer in the deep space. The environment alteration may cause severe bone changes of human in deep space. The changes of bone mass caused by spatial microgravity are related to the decrease of osteoblast formation and development in bone tissue, and the decrease of osteoblast formation is related to the down-regulation of differentiation of human bone marrow mesenchymal stem cells (hMSCs). Therefore, the study for the biological effects of microgravity on bone cell formation and the relative molecular mechanisms at stem cell level is one of the important subjects to explore the effects of spatial microgravity on bone changes. These studies may provide a scientific basis for the development and the related technologies of target drugs research. Based on exploring the flight conditions on the ground and simulating flight experiments with the automated space experimental device, we utilized a real microgravity environment in the SJ-10 recoverable microgravity experimental satellite (SJ-10 satellite) to examine the effects of space microgravity on transcriptome expression and differentiation potentials of hMSCs.

Abbreviations

ALP	Alkaline phosphatase
BMP2	Bone morphogenetic protein-2
ECM	Extracellular matrix
FBS	Heat-inactivated fetal bovine serum

C. Zhang · L. Li
Institute of Cell and Development Biology, College of Life Sciences, Zhejiang University, Zijingang Campus, Hangzhou 310058, Zhejiang, People's Republic of China

J. Wang (✉)
College of Life Sciences, Zhejiang University, Zijingang Campus, Number 866 of Yuhangtang Road, West Lake Dist, Hangzhou, Zhejiang, People's Republic of China
e-mail: wjfu@zju.edu.cn

E. Duan and M. Long (eds.), *Life Science in Space: Experiments on Board the SJ-10 Recoverable Satellite*, Research for Development,
https://doi.org/10.1007/978-981-13-6325-2_12

GADD45	Growth arrest and DNA damage inducible alpha
GO	Gene ontology
hBMSCs	Human bone marrow mesenchymal stem cells
LSM	Lymphocyte separation medium
MMP1	Matrix metallopeptidase 1
MSCs	Mesenchymal stem cells
NG	Normal ground gravity
PBS	Phosphate buffer saline
PLGA	Synthetic poly (D, L-lactide-co-glycolide)
qRT-PCR	Quantitative real-time PCR
RNA-SEQ	RNA sequence
RPM	Random positioning machine
SEM	Scanning electronic microscope
SMG	Simulated microgravity
α-MEM	A-minimum essential medium

1 Summarization

1.1 Introduction for Mesenchymal Stem Cells

Stem cells are a population of undifferentiated cells with the potentials of self-renewal and multidirectional differentiation (Cedar 2006). Stem cells can produce two identical stem cells by symmetry splitting or differentiate into terminal cells by asymmetric splitting. In addition, the committed differentiation is regulated by the inherent mechanisms and the microenvironments.

According to their source and development potentials, stem cells can be classified into embryonic stem cells and adult stem cells. Embryonic stem cells derived from animal embryonic cell clusters or primordial reproductive crests can differentiate into all the cell types needed for fetal development. Adult stem cells can produce various types but not all the cell types required for fetal development. Adult stem cells play an important role in repair and regeneration of tissues and organs in adult animals, such as epidermal and hematopoietic systems. Under some conditions, adult stem cells can be proliferated into new stem cells, or form functional cells in accordance with a certain differentiation process to maintain the balance of growth and decay of tissues and organs.

Mesenchymal stem cells (MSCs), one of the pluripotent stem cells, originate from the mesoderm and ectoderm in the early stages of development and are initially found in the bone marrow and subsequently found in other tissues of human body. MSCs can differentiate into hematopoietic cells as well as osteoblasts, chondrocytes, adipose tissue cells, cardiomyocytes, nerve cells, hepatocytes, and other types of cells in vitro or in vivo (Pereira et al. 1995; Tuan et al. 2003; Wang 2008; Pereira et al. 1995; Wang et al. 2007; Fu et al. 2006). For their source, MSCs can be obtained

from the donor under certain conditions without involving in ethical issues, which is superior to other stem cells. The superior characteristics of MSCs can be reduced as: (1) MSCs can be easily extracted from cord blood, peripheral blood, adipose tissue, placenta, muscle especially myocardium, and other tissues and organs (Lee et al. 2004; O'Donoghue et al. 2003; Chen et al. 2004; In't Anker et al. 2004; Warejcka et al. 1996; Nasef et al. 2008). (2) MSCs are easy to be cultured and passaged several times in vitro, and their genetic characteristics is still stable after several passages. Therefore, a large number of MSCs can be obtained in a short time. All the above characteristics meet the needs for tissue engineering and treatment of disease based on stem cells. (3) MSCs have a high efficiency of gene transfection in vitro, and the foreign genes have the capacity of stable and efficient expression in MSCs. (4) MSCs have low immunogenicity and portability (Nasef et al. 2008; Sotiropoulou and Papamichail 2007) and can be delivered to various tissues or organs in the body in a variety of ways and repair the damaged tissues or organs without immune rejection. Because MSCs have the above-mentioned advantages, they have been widely used in experimental and clinical studies in recent years. Bone marrow is an important source of MSCs, MSCs from bone marrow are easier to be isolated, cultured and purified than MSCs from other sources, and this advantage brings a wider prospect of research and treatment of the bone marrow-derived MSCs. In this project, human bone marrow mesenchymal stem cells (hMSCs) were used as cell material to study the potentials of committed differentiation of hMSCs, the signal pathways and the key signal molecules specific for this committed differentiation under space microgravity.

1.2 Microgravity and Bone Loss

1.2.1 Effects of Microgravity on Bone Loss

Due to the disappearance of gravity force, a variety of tissues and organs in the body may produce a series of adaptive changes, which leads to space medical problems and thereby becomes an important obstacle to human long-term space exploration.

As an important inherit sensor organ of gravity, bone is one of organs affected by microgravity. Bone loss caused by long-term space flight mainly performs the reduced bone mineral salt content and sedimentation efficiency as well as the declined bone substance density and biomechanics function, thus gives rise to the symptoms of osteoporosis. Bone loss caused by microgravity exists continuously in the whole space flight progress. Astronauts lose their bone densities at the rate of 1–2% average each month (Tilton et al. 1980) and need a longer time for recovery after they return to earth (Lang et al. 2006) found that the amount of bone cells in astronauts decreased about 12% after space flight from four to six months and was unable to restore completely one year after they returned to earth. Another report also showed that the bone mass of astronauts was still less than preflight even five years later after astronauts had a long-term space flight and returned to earth (Schneider et al. 1995). Many symptoms accompanied with bone loss, such as the increased urine

calcium excretion, the elevated blood calcium concentration and the increased risk of kidney stones or vascular sclerosis. In a word, bone loss induced by microgravity environment damages seriously the physical health and the abilities of task execution and re-flight of astronauts.

Although astronauts can adopt some effective measures, such as physical exercise, nutritional supplements and drug prevention, to against the damages caused by microgravity during space flight, bone loss cannot not be prevented completely. Therefore, the study of molecular mechanism of bone loss under microgravity environment and the design of effective countermeasures have the great significance for the health of astronauts in long-term space residence.

1.2.2 Mechanisms of Bone Loss Caused by Microgravity

Bone tissue consists mainly of cells and bone matrix, and the cells in bone include bone mesenchymal cells, bone progenitor cells, osteoblasts, bone cells, and osteoclasts. The bone has been maintained in a dynamic balance between bone resorption and bone formation to accommodate the mechanical environment. On the one hand, osteoclasts migrate to the old bone surface, and then secrete acidic substances to dissolve minerals and secrete protease to digest bone matrix, finally result in the formation of bone resorption lacunae. On the other hand, bone mesenchymal stem cells can differentiate into bone progenitor cells and osteoblasts in turn, and the bone progenitor cells and osteoblasts migrate to bone resorption site and secrete bone matrix, and further differentiate into the mature bone cells to repair the bone tissue. These bone cells can mineralize and finally form new bones (Hill 1998). Combination of bone resorption and bone formation maintains a dynamic balance to keep a normal bone mass under normal circumstances. However, this balance of bone reconstruction may be broken due to the change of mechanical environment, and the destroyed balance may result in microgravity-relative bone loss.

Effects of Microgravity on Mesenchymal Stem Cells

Osteoblasts are derived from bone marrow stem cells. Bone formation includes two progresses: (1) Mesenchymal stem cells differentiate into osteoblasts, and (2) osteoblasts differentiate into to the mature bone cells. In vitro, bone mesenchymal stem cells (BMSCs) can be firstly induced to the directional differentiation of bone progenitors and osteoblasts, and finally induced toward the differentiation of bone cells. Differentiation of BMSCs into osteoblasts is a very complex process and regulated by many factors such as cytokines, hormones and mechanical force stimulation. The changes of mechanical force stimulation caused by microgravity may directly affect the function of BMSCs and thereby affect the bone formation.

Previous studies showed that microgravity affects the proliferation ability of BMSCs. BMSCs are harvested from the femur subculture of rats experimented by a seven-day tail hanging and cultured for passage. The results showed that the pro-

liferation of BMSCs under simulated microgravity is slower than that under normal gravity (Pan et al. 2008). Experiments in Cell Rotary have also proved the inhibited effects of simulated microgravity on the proliferation of mesenchymal stem cells (Huang et al. 2009). Furthermore, the mitotic cycle of mesenchymal stem cells was blockaded in G0/G1 stage by microgravity (Dai et al. 2007), which indicates that the proliferation ability of BMSCs was restrained under microgravity environment.

Under specific induction conditions, BMSCs can be induced to differentiate into many types of cells, including osteoblasts, chondrocytes, fat cells, myocardial cells and other kinds of cells, but the differentiation behaviors are changed significantly under microgravity. BMSCs stimulated by microgravity were passaged under normal gravity, and then induced to differentiate into osteoblasts and adipocytes in the conditioned medium. Results showed that the differentiation ability of bone mesenchymal stem cells into adipocytes gradually decreases with the time of microgravity removal, while the differentiation ability into osteoblasts does not increase and remains in a low potential of osteogenesis compared with the control under normal gravity (Pan et al. 2008). Microgravity inhibits the osteogenic differentiation of BMSCs and reduces the expression of RUNX2, COL1A1, ALP and other osteoblast marker genes. At the same time, the expression PPARG2 (peroxisome proliferator activated receptor gamma), a key adipogenic transcription factor, is increased significantly (Huang et al. 2009; Marie and Kaabeche 2006; Zayzafoon et al. 2004) found that PPARG2 can positively regulate the differentiation of BMSCs into adipocytes and negatively regulate the differentiation of BMSCs into osteoblasts. The balance of differentiation into adipocytes and osteoblasts can be restored through foreign importing TGF-β2 to regulate the PPARG2 expression (Lazarenko et al. 2006). RUNX2, a bone specific transcription factor, can activate the expression of osteopontin and osteocalcin, and promote miner deposition. In addition, PPARG2 can inhibit the expression of RUNX2 gene or reduce the concentration of activated RUNX2 by combining with RUNX2 (Platt and El-Sohemy 2009). Therefore, microgravity not only directly weakened the osteogenic ability of BMSCs, but also inhibits the osteogenic differentiation of BMSCs through enhancing their adipogenic differentiation.

Effects of Microgravity on Osteoblasts

The data obtained from some space flight experiments illuminated that microgravity inhibits osteoblast differentiation. Previous study showed that microgravity environment not only obviously suppresses the osteoblast differentiation of MG63 cells cultured on “Photon-10” for a nine-day flight experiment but also decreases their responses to 1, 25(OH)2VD3 and TGF-β (Carmeliet et al. 1997). In addition to the decreased number and declined function of osteoblasts, microgravity also changes the morphology of osteoblasts. After space flight, the microtubules and actin filaments of MC3T3 cells are depolymerized, and the middle fiber shows an abnormal morphology. More detection found that the order of cytoskeleton declines, microtubules become shorter, and the reticular structure appears around the nucleus. All results

proved that microgravity destroys the morphological characteristics of osteoblasts (Hughes-Fulford et al. 1998)

Gravity plays a key regulatory role in the osteogenic differentiation through changing chemical signals in cells. Dai et al. (2013) found that microfilament cytoskeleton is involved in regulating the response of osteoblasts to BMP2, and microgravity inhibits the response of RUNX2 to BMP2 by promoting depolymerization of microfilaments in osteoblasts, while the promoting effect of BMP2 on osteoblast differentiation can be restored partly after adding the skeleton stabilizer. Another study showed that the mechanical stimulation and cytokines can allegedly regulate the osteoblast differentiation. Membrane surface protein integrin αVβ3 in osteoblasts, one of important molecules in response to gravity, can regulate the osteogenic differentiation through PI3K signaling pathway with cooperating with IGF-1 (Dai et al. 2014). miRNAs also play an important role in regulating the bone loss caused by microgravity. MIR-103 has been proved as a miRNA associated with bone loss caused by microgravity environment. Zuo et al. (2015) found that the expression of MIR-103 significantly increases in mouse during the tail hanging experiment and the expression of RUNX2 significantly decreases. Further study showed that MIR-103 directly targets RUNX2 and inhibits its protein expression, thus exhibits regulatory function on the bone loss caused by microgravity. Injection of MIR-103 inhibitor can reduce the bone loss caused by tail hanging experiment. In addition, Sun et al. (2015a, b) simulated the microgravity effects using a cell rotary system and found that the expression of MIR-103 significantly increases in MC-3T3 cells under cell rotary system. It suggests that microgravity may suppress the expression of Cav1.2, one calcium ion channel, and then inhibit the proliferation of MC-3T3 cells.

MIR-214 is also related with the bone loss caused by microgravity. Wang et al. (2013) found that the expression of OCN and ALP decreases and the bone formation index such as bone volume (BV), bone mineral density (BMD) declines in tail hanging mice models, while the expression of MIR-214 increases. MIR-214 can suppress the bone formation through inhibiting the expression of ATF4. The delivery of MIR-214 antagonists to osteoblasts using osteoblast specific delivery system can significantly inhibit the bone loss caused by tail hanging.

Effects of Microgravity on Osteoclasts

Osteoclasts are derived from mononuclear cells, and RANKL secreted by osteoblasts can induce mononuclear cells to differentiate into osteoclasts. In FOTON-M3 space mission, Tamma et al. (2009) inoculated osteoclasts and osteoclast precursors on cow bone chips to examine the differentiation of osteoclasts. They found that the expression of genes specific for osteoclasts are significantly increased, and bone resorption lacunaes are also increased after space flight. These findings suggest that microgravity enhances the osteoclasts activity. Ground experiments showed that simulated microgravity can activate signaling molecules specific for osteoclastic differentiation, such as ERK, P38, PLC2 and NFATc1, and the activated molecules make osteoclast precursors more sensitive to the RANKL-mediated osteoclastic differen-

tiation. After the osteoclasts are cultured in a rotary system for 24 h and treated with RANKL for 3–4 days, the formation of TRAP-positive multinucleated osteoclasts can be enhanced, and the osteoclast marker genes TRAP and cathepsin K raise significantly (Saxena et al. 2011). In addition, the expression of RANKL/OPG significantly increases in osteoblasts under simulated microgravity, and the medium supernatant from this simulated microgravity experiment can promote the differentiation of osteoclasts (Rucci et al. 2007).

1.3 Methods and Techniques of Cell Research in Space

At present, microgravity biology mainly includes two aspects: space flight experiment and ground simulation experiment. Space flight experiment is the most obvious way to obtain a low gravity by space vehicles, such as space shuttle and return satellite. However, flight experiments are expensive and have limited opportunities (Krikorian et al. 1992; Mesland et al. 1996; Katembe et al. 1998a, b). Therefore, the following methods can also be used to reduce or offset 1-g gravity (Claassen et al. 1994; Mesland et al. 1996), drop towers, parabolic flights (tens of microseconds), and sounding rockets (microgravity for a few minutes). However, the duration of microgravity experiment provided by these methods is too short for biological experiments. The device used widely to simulate "weightlessness" in ground is called as the clinostat, which is based primarily on the time required for gravity stimulation by plants (Claassen and Spooner 1994; Hoson et al. 1997).

1.3.1 Parabolic Flights

Various types of aircraft, ranging from small propeller-powered aerobatics to large KC-135 turbojet airliners, have been used for parabolic flight to create a gravity-reducing environment. A small propeller can produce microgravity for 5–8 s. A small non-military helicopter such as a learner jet, the Nagoya Mu-300, can produce $2 \times 10^{-2} \times$ g microgravity for more than 20 s. Parabolic aircraft modified by the European Space Agency (ESA), the Canadian Space Agency and the United States Aeronautics and Space Administration (NASA) are capable to produce 1-3 $\times 10^{-2} \times$ g microgravity for 20–30 s. Boeing KC-135 and supersonic F-104 helicopters are used for parabolic flight aircraft in United States. The F-104 parabolic flight, which flight path is from 25,000 to 65,000 feet, produces $3 \times 10^{-2} \times$ g for 30 s or less than $1 \times 10^{-1} \times$ g for 60 s. The parabolic trajectory of the KC-350 (NASA-930) flight is similar to F-104 parabolic flight and the path was from 26,000 to 34,000 feet. Before the 90s, NASA's parabolic flight was designed to train astronauts and pilot space flight hardware, and it could be used to carry out scientific experiments for 5–6 times one year.

1.3.2 Sounding Rocket Flights

Sounding rockets are suborbital vehicles which normally lands on the area about 100 miles far from the launch site and provides a microgravity of $1 \times 10^{-5} \times g$ for 7–14 min (Gurkin 1992). The cellular biology study by using sounding rocket is similar to those by using parabolic flight. However, the sounding rockets can supply a longer time and a higher level of microgravity, and thereby study extensively the cytology.

1.3.3 Orbital Spaceflights

Orbital aircrafts such as bio-satellites, space crafts and space shuttles, can provide several days to tens of days, as well as higher and more stable level of microgravity.

1.3.4 Space Stations

More than 10 space stations have been established since 1971, such as "Salute" series and Mir Space Stations established by the former Soviet Union, and Sky Laboratory set up by Unite States. In recent years, International Space Station, the biggest space station, which was jointly established by Unite States, ESA, Russia, Canada, has brought a series of opportunities for the development of space life science. Temple Space Station, prepared by China, has completed partial assembly.

1.3.5 Ground Simulators

Gyrator is a device that rotates a biological sample around an axis (usually a horizontal axis), where the organism is still in the gravitational field and is subjected to a constant gravitational vector. However, the direction of organism and gravity is continuously changing in a gyrator. Whenever the relative direction of gravity changes, the biological effects have not yet time to show before the next direction has changed. Since the direction of gravity vector cannot be kept constant for this minimum time, the effect of gravity is always too late to behave as if there is no gravitational force, and this phenomenon is similar to microgravity. Thus, the biological effect under microgravity condition is demonstrated (Wang et al. 2015). The gravity vector is of constant size and continuous change of directions from a reference coordinate system fixed on a biological sample. However, the object is always in a constant gravity role in a rotor. Strictly, gyrator only simulates the effect of microgravity, but not simulates microgravity. The performance of organisms on the gyroscope is just qualitatively similar to the samples under the space microgravity conditions, but not in quantitative level.

1.4 Scientific Significance of This Space Experiment

After performing a variety of experiments under simulated microgravity and developing multiple comparisons with experiments under normal gravity, we have determined the biological effects, molecular mechanisms and key cell signaling molecules specific for these effects during the osteogenic differentiation. Else, we performed the experiments of regulation with small molecule drugs in view of the key signaling molecules, thus identified the feasibility of reversing the effects of microgravity on the osteogenic differentiation. However, any simulated experiment has its limitation and controversy. The effective solution for this problem is to perform scientific experiments in the real space microgravity, so as to truly reflect the biology effects and molecule mechanisms of microgravity on osteogenic differentiation.

The Recoverable Science Satellite SJ-10 of China provided a true microgravity and pressure sealing environment for us to develop biological experiments in space. Two-week flight cycle is just suitable for our experimental period in space, and the timely returned space cell samples can provide a guarantee for analysis on the effects of microgravity. The experiment for committed differentiation of hMSCs was performed in satellite recoverable capsule. Therefore, it is necessary to develop the automatic space experiment equipment that can carry out the stable and meticulous cell culture operation. This space equipment should meet the requirements of space experiment process involving culture, differentiation and fixing of cells and samples preservation at low temperature.

The objective of this space experiment is to study the effects of microgravity on the osteogenic differentiation potentials and molecule mechanisms as well as the key cell signaling molecules specific for osteogenic differentiation. These studies may provide scientific basis for overcoming the bone loss during space exploration and developing the targeted drugs. This project is the first research on the molecule mechanisms specific for osteogenic differentiation of mesenchymal stem cells under real microgravity.

2 Space Culture Device

2.1 Research Basis for Space Culture Device

Due to the disappear of convection, sedimentation and hydrostatic pressure caused by microgravity in the space environment, the limitation of space resources (such as volume, weight, power consumption etc.) and the maneuverability of cells culture in space, the cultivation vessels and devices used on the ground cannot be used in the space experiments. It is necessary to develop a cell bioreactor that is specifically adapted for operation in the space environment. The space cell bioreactor should meet the requirements of loading bearing, temperature controlling, culture fluid supplication, gas exchanging and pH buffering functions as the cell culture device on the

ground, and the realization of various functions must be taken account of the mechanical characteristics in the space microgravity environment, especially the change in the fluid mechanics behavior. Else, the bioreactor should substantially depend on the automatic operation.

The space experiment for the committed differentiation of hMSCs is designed as two programs (experiment I and experiment II) according to the arrangement of scientific mission for SJ-10 satellite. The culture proposal included: (1) MSCs in experiment I were induced for two days with osteogenic induction medium (Levis-15 medium supplement with 10% of FBS, 50 μg/mL L-ascorbic acid, 10 mM β-sodium glycerol-phosphate, 10^{-7} M dexamethasone, 100 U/mL penicillin, and 100 μg/mL streptomycin), then the induction medium was replaced with washing buffer-PBS, finally RNAlater was added after wiping off PBS. Then the cell samples were stored for ten days under ~6 °C until the satellite returned to the ground. After satellite returns to the ground, space samples were harvested, RNA and proteins in samples were extracted, and the effects of microgravity on the expression of genes and the activity of proteins specific for osteogenic or adipogenic differentiation were analyzed. (2) hMSCs in experiment II were induced for seven days with osteogenic induction medium, refreshing induction medium every two days. Then the induced program was terminated, cells were fixed with 4% formaldehyde after being washed with PBS for one time. The fixed sample was kept in ~9 °C until satellite returned to the ground. Samples in experiment II was harvested and detected by histochemistry and immunohistochemistry to analyze the osteogenic differentiation potentials of hMSCs.

According to the object of this space experiment, the automatic device controlled by software must satisfy the following requirement. Firstly, this device should contain the cell culture unit and the liquid storage unit. Moreover, the device can provide airtight environment and suitable temperature for cell culture as well as the lower temperature for storage of cell samples and liquids. Furthermore, the device can timely replace the liquid in cell culture unit, including the induction medium, washing buffer and reagents. The device can also adjust and control the volume and rate of liquid replacement. Finally, the device is able to automatically monitor the humidity, pressure and other conditions inside the device.

2.2 Principle of Space Culture Device

On the basis of the above design requirements, the National Space Science Center of Chinese Scientific Academy designed and prepared an automatic device for culture and induction of hMSCs. In this device, the cultivate unit consists of two cultivation vessels respectively for experiment I (two days) and experiment II (seven days), and three PLGA three-dimensional scaffolds with hMSCs are cultured in each cultivation vessel. The cultivate unit can provide 37 ± 1 °C temperature environment controlled by semiconductor thermostat. hMSCs are cultured in the normal culture medium (α-MEM culture medium supplemented with 10% of FBS, 100 U/mL penicillin,

100 μg/mL streptomycin and 5 ng/mL BFGF) before the orbital implantation, and the normal culture medium is taken out after the orbital implantation, and then the induction medium is injected into cultivation vessels to start the induction program. At the end of induction, the induction medium is aspirated into the washing buffer. Finally, RNAlater (for 2 days) or 4% formaldehyde (for 7 days) is injected into the cultivation vessel to treat cells. Then, the thermostat is switched to cryogenic storage state until the satellite returns to the ground.

The liquids required for space experiment are stored in their respective containers. Induction medium, RNAlater and cell fixing solution are stored at low temperature controlled by a semiconductor thermostat for seven days, and the temperature of washing buffer and waste liquid is not controlled overall the space experiment process. The fluid circuit system containing of the syringe pump and the fluid dispenser implements the liquid withdrawal and injection. In order to prevent the liquid to reflux, three electromagnetic valves are connected with the fixing solution, RNAlater and waste liquid task separately and then connected with the corresponding piping of the fluid distributor, and the liquids are distributed into the cultivation vessel inlets and outlets. Solenoid valve opens only when necessary to prevent fixing solution or waste liquid mixing to the cultivation vessel when the channel switch opens during medium replacing, which can avoid any impact on the normal cell culture. Load system principle is shown as Fig. 1 in chapter "Study on Bone Marrow Box, Radiation Gene Box and Integrated Electrical Control Boxes".

The measurement and control circuit with regarding a FPGA logic controller as the core completes the process of operation, data detection and storage in the space experiment. Data transformation and command reception are run through a 422 serial port and an integrated electronic control box. Integrated electronic control box controls the experimental process and provides power required by the load according to the present or injection instructions. Load electric control schematic diagram is shown in Fig. 1.

2.3 The Structure and Performance Index of Space Culture Device

2.3.1 Whole and Internal Structure of Space Culture Device

As shown in Fig. 2, the space culture device includes five parts: an external three-stage airtight chassis, 2 cultivation vessels, 6 liquid storage units, 1 automatic liquid change system, and 1 electronic control system. The fluid system tubing is connected by silicone rubber.

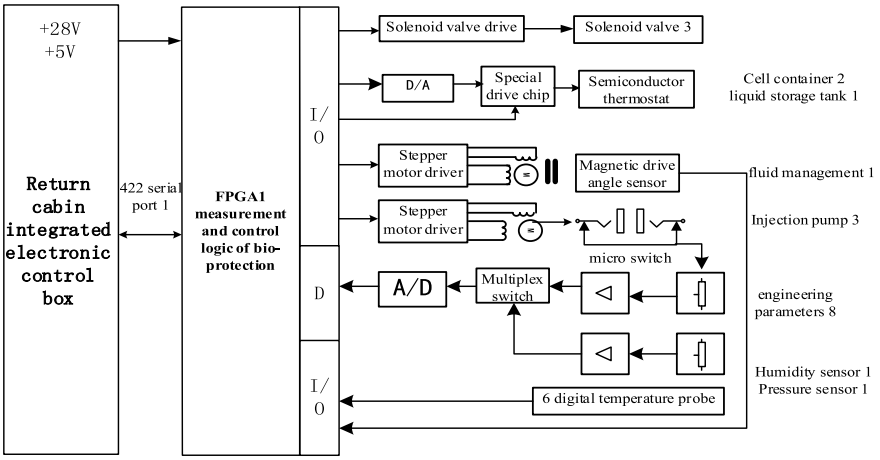

Fig. 1 Load electric control schematic diagram. The measurement and control circuits with regarding a FPGA logic controller as the core complete the space experiment processes and the data transformation and command reception are run through a 422 serial port and an integrated electronic control box

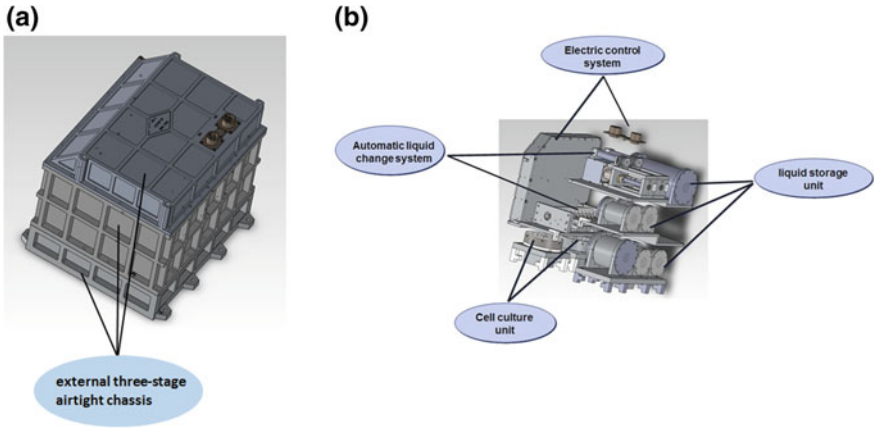

Fig. 2 Space culture device for hMSCs. The external of space culture device is an three-stage airtight chassis, and the internal structure of device contains 2 cultivation vessels, 6 liquid storage units, 1 automatic liquid change system, and 1 electronic control system

2.3.2 The Main Indicators of Space Culture Device

The internal structure designing of space culture device is not only necessary to meet the requirement of scientific experiment and adapt to the characteristic of microgravity environment, but also limited to the satellite space, energy, air pressure and thermal control and other resource. The main performance indicators are showed as Tables 1 and 2.

Table 1 Load overall indexes

Index	Parameter
Overall volume (size)	250 mm × 300 mm × 270 mm
Total mass	16 kg
Power consumption	Peak power consumption: 40 W; average power consumption: 17 W
Internal pressure	0.01 MPa (outside pressure: vacuum ~0.01 MPa)
Internal atmosphere	Air
Experiment cycle in orbit	~12 days and 12 h

Table 2 Load component indexes

Index		Parameter
Cell culture conditions	Cultivation vessel	Area: ϕ55 mm; volume: 25 ml/group; containing three PLGA scaffolds; two groups
	PLGA scaffold	25 mm (diameter) × 1 mm (thickness)
	Emission and on-orbital culture temperature	37 °C
	Keeping temperature in RNAlater	6 ± 2 °C
	Keeping temperature after fixation	8 ± 2 °C
Liquid storage temperature	Induction fluid reservoir	Volume: 125 ml; number: one; storage temperature: 8 ± 2 °C
	Fixation liquid reservoir	Volume: 40 ml; number: one; storage temperature: 8 ± 2 °C
	RNAlater reservoir	Volume: 40 ml; number: one; storage temperature: 8 ± 2 °C
	Washing buffer reservoir	Volume: 40 ml; number: two; storage temperature: uncontrolled
	Waste liquid reservoir	Volume: 240 ml; number: one; storage temperature: uncontrolled
Liquid system indexes Injection pump	Fluid distributor	Volume: 5 ml; Flow rate: 1–3 ml/min
		Ten channels, positioning accuracy ±1°

3 Ground Preparation and Scientific Matching Experiments

Due to the limitation of space, environment, loading capacity and flight program of the satellite, the space experiments are different from the ground experiments. Therefore, many experimental conditions should be improved and optimized on the ground to meet the requirement of the space experiments. A multi-stage and multi-round matching experiment should be performed on the ground to ensure that the cells are kept in a relative good condition of growth and differentiation in the space culture device. The matching experiment is divided into four stages: the matching experiment phase for the component testing of device, the matching experiment phase for preliminary device, the matching experiment phase for the official device, and the matching experiment phase for launching preparation. Each stage had its definite experimental target, process and time node. A systemic matching experiment of osteogenic differentiation is formed through the connection of different processes involving induction of differentiation, washing, fixation and lysis of induced cells in the space culture device.

3.1 Preparation of hMSCs

hMSCs were extracted from healthy donors sponsored by the First Affiliated Hospital of Zhejiang University. The purification of hMSCs is referred to the previous literature (Shi et al. 2010). Briefly, 5 mL human bone marrow was added to the DMEM medium containing heparin to prevent blood coagulation, and then transported to the laboratory at low temperature. Mononuclear leucocytes were isolated using lymphocyte isolation liquid Fillco by centrifuging at 1800 rpm for 10 min. Cells were seeded in the culture dish with a density of 10^6 cells/mL. hMSCs could be purified through the adherent culture, and the cells at passage 3 or 4 were used for the matching experiment. The properties of hMSCs were determined by detecting the cell surface markers using flow cytometry. hMSCs showed the following phenotype: $CD34^-$, $CD14^-$, $CD19^-$, $CD45^-$, HLA-DR^-, $CD73^+$, $CD105^+$, $CD90^+$, which make sure that these cells are MSCs (Fig. 3).

3.2 Preparation of PLGA Scaffold

In order to simulate the three-dimensional environment in vivo, PLGA three-dimensional scaffold was used for cell culture. The preparation of porous poly-lactic-co-glycolic acid (PLGA) scaffold was described previously (Zong et al. 2010). Briefly, the gelatin particles were bound together to form a three-dimensional assembly through a water vapor treatment before the polymer solution was cast. The PLGA

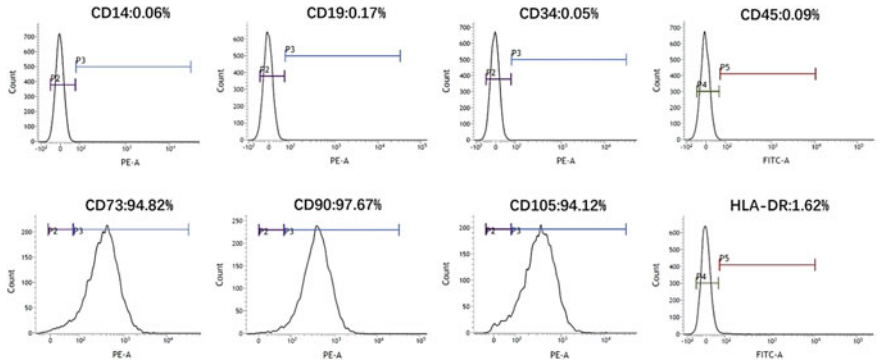

Fig. 3 Flow cytometric analysis of surface markers in hMSCs. hMSCs at passage 4 tested positive for CD73, CD90, and CD105 and negative for CD34, CD19, CD45, CD14, and HLA-DR

scaffolds were prepared as cylinders (ϕ 25 $\times$ 1 mm) and had porosity of 85%. The pore diameter was 280–450 μm.

3.3 Culture and Osteogenic Induction of hMSCs in the Condition Without Carbon Dioxide

Gas involving O_2 and CO_2 is one of the necessary conditions for survival of mammalian cells cultured. O_2 is mainly involved in tricarboxylic acid cycle, resulting in production of the energy required for growth and proliferation of cells and synthesis of various components required for cell growth. CO_2 is not only one of cell metabolites, but also one of components required for cell growth and reproduction, and its major role in cell culture is to maintain the pH value of medium. Culture medium pH is generally kept between 7.0 and 7.4. Most of culture mediums are based on a balanced salt solution (BSS), which acts as a buffer solution and can greatly stabilize the pH when a small amount of acid, base or water is added. The pH buffer system plays an important role in maintaining the normal pH value of the organism and the normal physiological environment. Most of cells can only be operated in a very narrow pH range, and need a buffer system to counteract the changes of pH that may occur during their metabolic processes. Since the carbonate pH buffering system is a physiological pH buffering system, which is the most important pH buffer system in human blood, this system is used in most of culture mediums to maintain a stable pH value. A given amount of sodium bicarbonate is often added in the preparation of powder culture medium. For carbonate regarding as the basis pH buffering system in most of cell cultures, the concentration of CO_2 in the incubator needs to be kept between 2 and 10% to maintain a stable pH value, and the CO_2 concentration at 5% in the open culture can maintain the concentration of dissolved carbon dioxide in the medium. In addition, a certain degree of ventilation in the cultivation vessel is needed

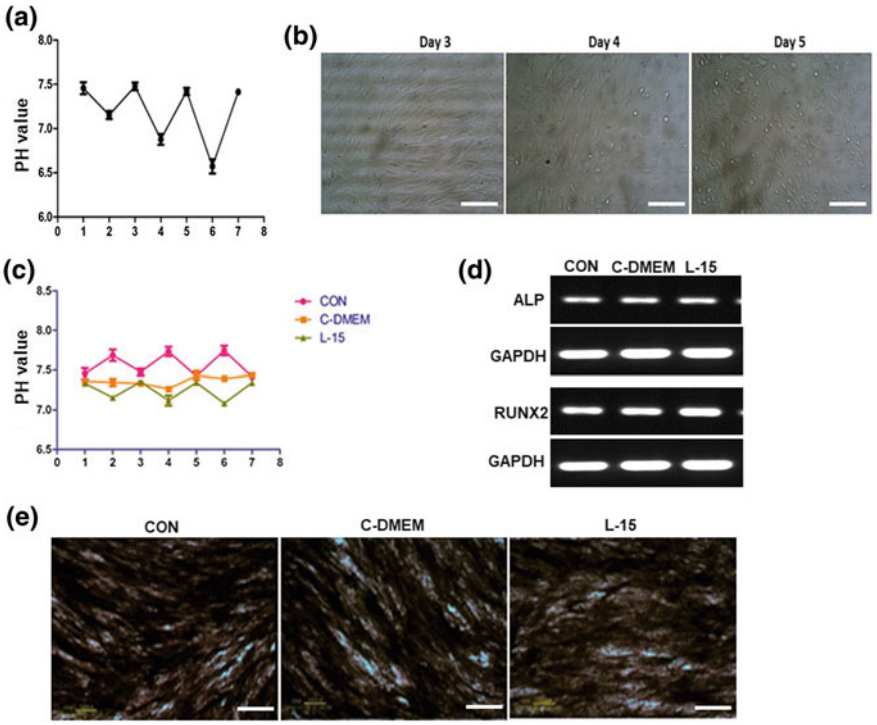

Fig. 4 The influence of Levis'-15 and C-DMEM induction media on the osteogenic differentiation of hMSCs. **a** The PH valve in the culture of hMSCs with the traditional induction medium for 7 days in the condition without carbon oxygen. **b** The morphology of hMSCs cultured with the traditional induction medium in the condition without carbon oxygen for 3, 4 and 5 days. **c** The PH valve in the culture of hMSCs in the traditional induction condition (traditional induction media with 5% carbon oxygen) for 7 days and the PH valve in the culture of hMSCs with Levis'-15 and C-DMEM induction media in the condition without carbon oxygen. **d** The expression of ALP and RUNX2 mRNA in hMSCs cultured in the traditional induction condition and in Levis'-15 and C-DMEM induction media in the condition without carbon oxygen for 2 days; **e** ALP staining of hMSCs cultured in the traditional induction condition and in Levis'-15 and C-DMEM induction media in the condition without carbon oxygen for 7 days. Scale: 100 μm. CON: hMSCs cultured in the traditional induction condition; C-DMEM: hMSCs cultured with C-DMEM induction medium; L-15: hMSCs cultured with Levis'-15 induction medium

to facilitate the exchange of gas. It has been found that HCO_3-depletion in the culture medium is accelerated if the cells are not incubated in a carbon dioxide incubator due to the low concentration of carbon dioxide in the air and thereby may reduce the proliferation of cells. Therefore, most of animal cells need to be cultured in the carbon dioxide incubator. In the space science experiment, however, CO_2 storage tanks could not be loaded due to the constraints for satellite space, payload, device design and safety in SL-10 satellite. Therefore, how hMSCs can normally grow and differentiate in the condition without carbon dioxide is the primary problem we should resolve.

In the previous experiment, we explored whether hMSCs could be induced toward to osteogenic differentiation in the condition without carbon dioxide. Experimental protocol was as following: hMSCs were cultured in the induction medium of osteogenic differentiation for 2 days and 7 days in a cell incubator without carbon dioxide, and the induction medium was changed every 2 days. We collected the cell culture supernatant and measured the pH valve of the supernatant, and found that the pH valve of the cell culture supernatant decreased very rapidly, and this decrease in pH valve became more rapid as the induction time increased (Fig. 4a). The morphological changes were not observed on day 2. However, the cells became rounded on day 4 and cells death occurred on day 5 (Fig. 4b). It is concluded that hMSCs cannot be cultured for normal growth more than 7 days in the condition without carbon dioxide. Therefore, this experimental conditions need to be optimized to meet the requirement of this space experiment.

When the permeable cultivation vessel is taken out of the CO_2 incubator, the carbonate buffer system in the culture medium is lost its buffer effects due to the low concentration of carbon dioxide in the air. Therefore, additional pH buffering systems, such as HEPES buffer systems, are often added to the culture medium to increase pH buffering capacity. HEPES has a strong buffering capacity between pH 7.2 and 7.4. We increased the concentration of HEPES buffer system components in the traditional induction medium (L-DMEM medium supplement with 10% of FBS, 50 μg/mL L-ascorbic acid, 10 mM β-sodium glycerol-phosphate, 10^{-7} M dexamethasone, 100 U/mL penicillin, and 100 μg/mL streptomycin) to study whether the PH valve of induction medium can be maintained in the physiology range for 7 days in the condition without carbon dioxide. However, we found that the HEPES buffer system could stabilize the pH valve of induction medium for a short term but not for a long-term in the condition without carbon dioxide. Therefore, we used a phosphate buffer system to replace the carbonate buffer system in the traditional induction medium. Sodium bicarbonate was added to L-DMEM culture medium without $NaHCO_3$. Sodium dodecahydrate, potassium dihydrogen phosphate, and sodium chloride were used to adjust the osmotic pressure, and then the pH valve of medium was adjusted to 7.2. This medium was designed as Table 3 and named as C-DMEM medium.

In addition, Levis'-15 (hereinafter referred to as L-15 medium) is a commercial medium suitable for cell growth in the condition without carbon dioxide. We performed the experiments of osteogenic differentiation in Levis'-15 and C-DMEM induction media (Levis'-15 or C-DMEM medium supplement with 10% of FBS, 50 μg/mL L-ascorbic acid, 10 mM β-sodium glycerol-phosphate, 10^{-7} M dexamethasone, 100 U/mL penicillin, and 100 μg/mL streptomycin) in the condition without carbon oxide. As shown in Fig. 4c, no significant difference of cell morphology was detected between cells cultured in these carbon dioxide-free induction media (Levis'-15 and C-DMEM induction media) and the traditional induction medium. During the induction, both carbon dioxide-free induction media maintained the normal physiological PH valve.

In order to investigate the effects of these carbon dioxide-free induction media on the osteogenic differentiation of hMSCs, we examined the genes expression of

Table 3 The specific formula of C-DMEM

Number	Element	Content (mg/L)
1	Glycine	30
2	L-arginine hydrochloride	84
3	L-cystine cysteine	63
4	L-glutamine	584
5	L-histidine hydrochloride	42
6	L-isoleucine	105
7	L-leucine	105
8	L-lysine hydrochloride	146
9	L-methionine	30
10	Phenylalanine	66
12	L-serine	42
12	L-threonine	95
13	L-tryptophan	16
14	L-tyrosine sodium salt	104
15	Glycine	94
16	L-arginine hydrochloride	4
17	L-cystine cysteine	4
18	L-glutamine	4
19	Nicotinamide	4
20	Vitamin B6	4
21	Riboflavin	0.4
22	Vitamin B1	4
23	No optical inositol	7.2
24	Calcium chloride	200
25	Iron nitrate	0.1
26	Magnesium sulfate	97.67
27	Potassium chloride	400
28	Sodium chloride	8170
29	Sodium dihydrogen phosphate monohydrate	125
30	Potassium dihydrogen phosphate	70
31	Disodium hydrogen phosphate dodecahydrate	1500
32	Sodium bicarbonate	410
33	D-glucose	1000
34	Sodium pyruvate	110
35	Phenol red	15

RUNX2 and ALP specific for osteogenesis after induction for 2 days (Fig. 4d) and the activity of ALP after induction for 7ays (Fig. 4e). The results showed that these carbon dioxide-free induction media can significantly promote the osteogenic differentiation of hMSCs, and there is no difference of differentiation potentials between cells cultured in the carbon dioxide-free induction media and the traditional induction medium.

The above results indicated that both C-DMEM and L-15 induction media are able to maintain the normal PH value for 7 days, and does not change the properties of the cells. These features can meet the requirement for osteogenic induction of hMSCs in the condition without carbon dioxide.

3.4 Storage of Induction Medium in Low Temperature

L-Glutamine is important in cell culture. L-glutamine can be used as the energy source of cells, and participates in protein synthesis and nucleic acid metabolism. However, glutamine is an amino acid particularly easy to be deteriorated. Previous studies have shown that the half-life of glutamine is about 2 weeks at 4 °C, and the stability of glutamine is related with the storage temperature and the PH value. The degradation of glutamine will increase as the increase of temperature.

Cell contamination, usually including bacterial and fungal contamination, is a common problem in cell culture, especially in space experiments of cells. The complexity of operation for cell culture in space is far greater than that on the ground, which may increase the probability of contamination. Therefore, the addition of antibiotics can effectively prevent the contamination of bacterial and fungal in cell culture. Conventional antibiotics, penicillin and streptomycin, are two broad-spectrum bacterial antibiotics used commonly, and amphotericin B is another anti-fungal antibiotics. But these antibiotics have lower stability. The antibiotics diluted in the culture medium can be usually stored at 4 °C for more than 2 weeks. Subsequently, the antibiotic effect of antibiotics will decrease obviously as the time and temperature increase.

Generally, the optimal storage conditions for cell culture media supplemented with glutamine and antibiotics are 2–8 °C on the ground. In the SJ-10 satellite, however, the lowest temperature in the liquid storage tank of space culture device can be only kept 10 ± 1 °C due to the limitation of energy consumption in the satellite. In order to verify whether the induction medium and other solutions stored at this temperature is still effective for induction of osteogenic differentiation, the prepared L-15 induction medium was placed in 4 °C low-temperature refrigerator and 12 °C incubator respectively. The osteogenic differentiation of hMSCs was induced for 7 days with the stored L-15 induction medium, and the induced cells were subjected to ALP staining. As shown in Fig. 5a, the induction medium stored at 11 °C could induce the osteogenic differentiation of hMSCs, and the expression of ALP was positive. There was no difference of osteogenic potentials between cells induced with the induction medium stored at 11 °C and the induction medium stored at 4 °C.

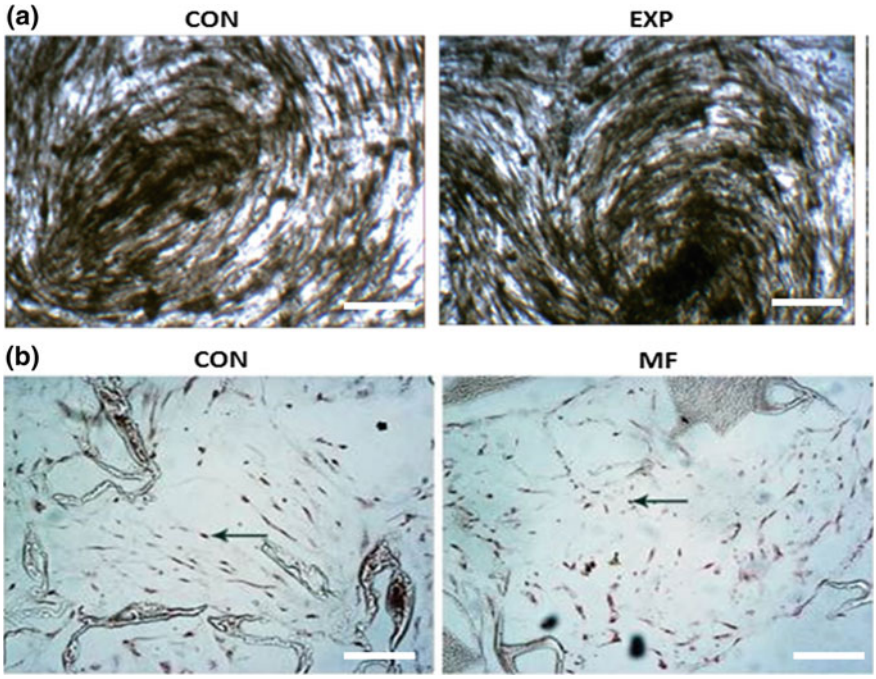

Fig. 5 ALP staining of hMSCs. **a** ALP staining of hMSCs cultured for 7 days with Levis'-15 induction medium stored at 4 °C or 11 °C; CON: Levis'-15 induction medium stored at 4 °C; EXP: Levis'-15 induction media stored at 11 °C. **b** ALP staining of hMSCs cultured for 7 days with Levis'-15 induction medium after the mechanical simulation experiments. Scale: 100 μm. CON: control; MF: the mechanical simulation experiment

Results showed that 10 ± 1 °C of liquid storage provided by space culture device can meet the scientific requirement for this space experiment.

3.5 Simulation Experiment of Mechanic Environments

During launching and flying, the satellite must be subjected to the dynamic loads such as vibration, shock and noise generated during rocket launching, satellite-rocket separating and orbiting. The animal cells are sensitive to mechanic force. In order to ensure the smoothness of the space experiment, therefore, it is necessary to simulate the mechanic environment caused by dynamic loads to examine the effects of mechanical environment during the satellite launching and flying on the adhesion, growth and differentiation of hMSCs.

We performed the experiments to study the effects of shock, oscillation, and acceleration on cells cultured in the space culture device. The experimental parameters

Table 4 Mechanical environmental simulation parameters

Mechanical environmental simulation project	Parameters
Impact test	Size: 600 g Direction: X, Y, Z three directions
Oscillation test	Size: sine experiment: 0–500 Hz; random experiment: 10–2000 Hz Direction: X, Y, Z three directions
Acceleration experiment	X, Y, Z three directions the size of 9 g – X direction size of 16 g

are shown in Table 4. We treated the three-dimensional scaffold surface with gelatin and matrix glue to increase the adhesion of cells. The cells were seeded into the scaffolds, and then the scaffolds were placed in the cultivation vessels. The cultivation vessels were fixed in a culture apparatus before mechanical simulation experiments. After the mechanical simulation experiment, cells in the cultivation vessels were examined. We did not find any floating cells, which showed the good adherence of cells in scaffolds. In addition, the mechanical simulation experiment indicated that the mechanical simulation has no effect on the osteogenic potentials of hMSCs (Fig. 5b). Therefore, our results suggested that hMSCs could withstand the loading of satellite during launching and flight.

4 Space Flight Experiments

4.1 Space Flight Experiments Programs

The above-mentioned matching experiment on the ground solved several major problems that may be encountered in the space experiment, which ensured the smooth running of this space experiment. On this basis, we developed the process for space experiment. The specific process is shown as Fig. 6. The space experiment consisted of two phases: the ground preparation phase pre-launching and the flight phase post-launching. The process for ground preparation was run by manual operation of the inspection device on the ground, and the process for space experiment in flight stage was run by the integrated electronic control program set prior to the operation of the flight sequence. If the process of space experiment program is abnormal, the procedure of operation will be changed by sending the immediate command from the ground.

To better simulate the in vivo environment of hMSC growth and differentiation and reflect the real microgravity environment, a three-dimensional scaffold was used to culture hMSCs instead of regular cell culture. The core diameter and porosity were shown in Sect. 3.2 and hMSCs seeding density was 4×10^5/scaffold.

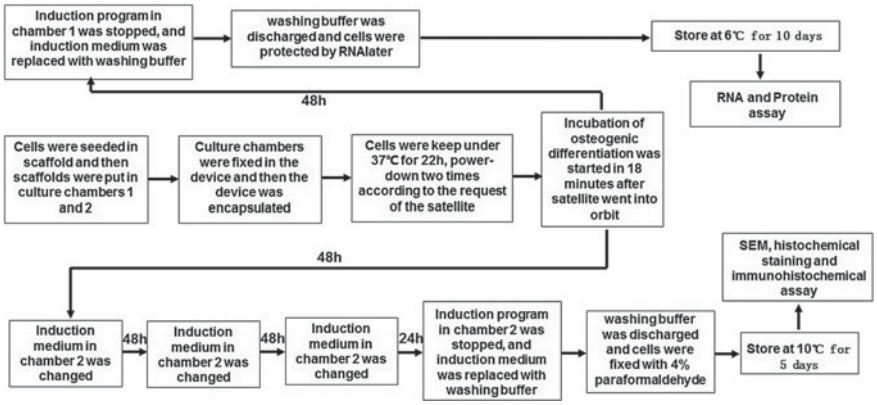

Fig. 6 The induction program of cells. Two treatments were designed in this space experiment: osteogenic differentiation of hMSCs was induced for 2 days and 7 days respectively. Induction of osteogenic differentiation was started in 18 min after the satellite went into the preconcerted orbit

The space experiment started at 2 am April 6, 2016, and stopped at 2 pm April 18, 2016. The space experiment was lasted for 12 days and 12 h. At 18 min after injection, the induction procedure of osteogenic differentiation was started by the integrative electric control program. The culture medium was extracted from the cultivation vessel, and then the induction medium was injected into the cultivation vessel. After 2 days of space osteogenic induction, cells induced in one of cultivation vessels were lysed, and then the temperature was switched to 6 °C until satellite returned to the ground. After 7 days of space osteogenic induction, cells induced in another cultivation vessel were fixed, and then the temperature was switched to 6 °C until satellite returned to the ground. The temperature in the liquid storage unit was set as 8 ± 2 °C during ground preparation and maintained for 7 days after launching, and then the control of temperature was stopped. The process of space experiment consisted of 13 procedures and the temperature-controlling were shown as Table 5 and Fig. 7.

4.2 Overviews of Returned Space Culture Device

After the satellite returned to the ground, the external appearance of space culture device dismantled from satellite was intact by visual viewing. Two cultivation vessels were filled with RNAlater and fixative liquids respectively, and the amount of liquids in other tanks was also normal. Two cultivation vessels were confirmed to be free of contamination. The results showed that the space experiment programs were completed satisfactorily and the required cell samples in the space experiment were obtained from the space culture device. Disassembly of space culture device is showed as Fig. 8.

Table 5 Temperature-controlling data in the space culture device

Time	Temp in cultivation vessel 1 (°C)	Temp in cultivation vessel 2 (°C)	Temp in storage tank (°C)	Markers
On Track Day 1	37.0625	37.0625	9.6875	Meet the requirements
On Track Day 2	37.25	37.25	9.75	Meet the requirements
On Track Day 3	5.9375	36.93755	9.6875	Meet the requirements
On Track Day 4	6.0	37.0625	9.6875	Meet the requirements
On Track Day 5	5.9375	37.25	9.75	Meet the requirements
On Track Day 6	5.9375	36.93755	9.6875	Meet the requirements
On Track Day 7	6.0	37.0625	9.6875	Meet the requirements
On Track Day 8	5.9375	9.125	21.25	Meet the requirements
On Track Day 9	5.9375	9.25	21.25	Meet the requirements
On Track Day 10	5.9375	9.25	21.25	Meet the requirements
On Track Day 11	6.0	9.125	21.125	Meet the requirements
On Track Day 12	5.8125	9.0	21.125	Meet the requirements
On Track Day 13	5.755	8.9375	20.1875	Meet the requirements

The space experiment samples were brought back to the laboratory at low temperature. At the same time of space experiment, we performed the ground-based control experiments. The cells, reagents, culture device and experimental programs used in the ground-based control experiments were same as the space experiments. Afterwards, the samples from space experiments and ground-based control experiments were analyzed as followings.

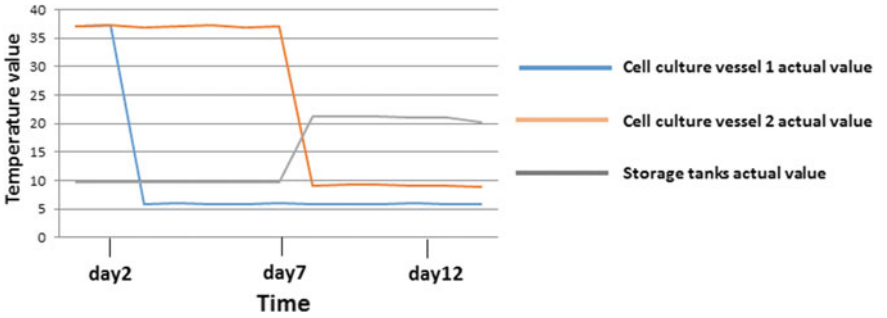

Fig. 7 Temperature curve in space culture device. The temperature in cultivation vessel 1 was maintained at ~37 °C for the first 2 days and then remained at ~6 °C for another 10 days. The temperature in cultivation vessel 2 was maintained at ~37 °C for the first 7 days and then remained at ~9 °C for another 5 days. The temperature in storage tanks was maintained at ~10 °C for the first 8 days and then uncontrolled for the remaining time

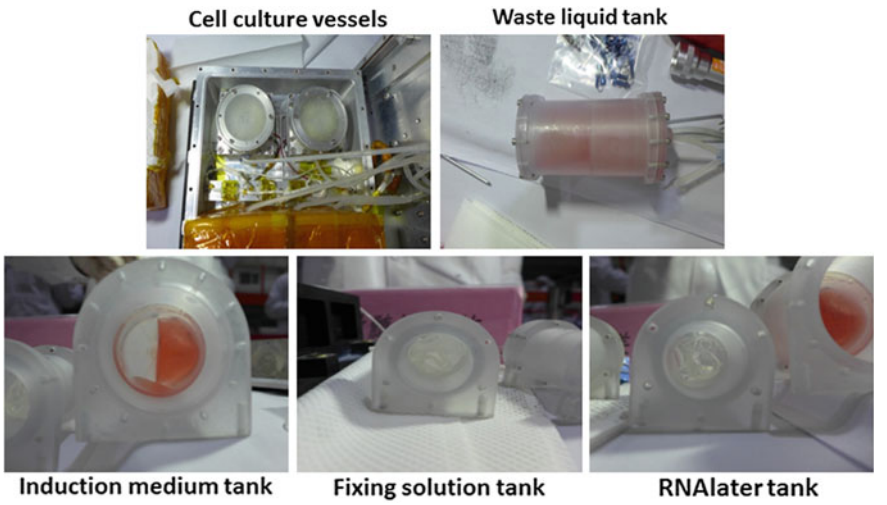

Fig. 8 Disassembly of space culture device at the recycling station. Two cultivation vessels were filled with RNAlater and fixative liquids respectively and the amount of liquids in other tanks was also normal

4.3 Materials and Methods for Analysis of Induced Cells

4.3.1 RNA Isolation

After RNA samples lysed with RNALater were collected, RNALater was removed by centrifugation at 1000 g for 3 min, and the pellet was then washed three times with PBS. RNA extraction was performed using TRIzol (Sigma). Following a phenol/chloroform extraction and isopropanol precipitation, RNA samples were treated

with DNase I using the DNA-free TM kit (Ambion). The prepared RNA samples were subjected to deep sequencing and real-time (reverse transcriptase) polymerase chain reaction (PCR) assays.

4.3.2 Real-Time Polymerase Chain Reaction (PCR) Assays

The PCR assay was performed to determine the expression of genes specific for osteogenesis or adipogenesis in cells under normal gravity or space microgravity. After a lysate from each cell culture compartment was collected, RNALater was removed by centrifugation at 1000 g for 3 min, and then the pellet was washed with PBS three times. RNA extraction was performed using the TRIzol reagent. Reverse-transcription was conducted using 1 μg of total RNA with the RevertAid First Strand cDNA Synthesis kit. Primers were designed using the Primer Premier 6.0 Demo and Oligo 7.36 Demo Software as shown in Table 6. Quantitative real-time PCR reactions were run in triplicate on a Roche 480 II Real-Time PCR Detection System using the 480 SYBR Green qPCR Supermix. The cycling conditions of the real-time PCR were as follows: 40 cycles at 95 °C for 15 s and 60 °C for 1 min. GAPDH served as the reference gene of classical real-time PCR.

Table 6 Primer sequences for real time-PCR

Gene name	Primer sequences	Product size (bp)
ALPL	5′-AACATCAGGGACATTGACGTG-3′(F) 5′-GTATCTCGGTTTGAAGCTCTTCC-3′(R)	159
COL1A1	5′-GTGCGATGACGTGATCTGTGA-3′(F) 5′-CGGTGGTTTCTTGGTCGGT-3′(R)	119
RUNX2	5′-CCGCCTCAGTGATTTAGGGC-3′(F) 5′-GGGTCTGTAATCTGACTCTGTCC-3′(R)	132
BMP2	5′-ACTACCAGAAACGAGTGGGAA-3′(F) 5′-GCATCTGTTCTCGGAAAACCT-3′(R)	118
PPARG2	5′-TACTGTCGGTTTCAGAAATGCC-3′(F) 5′-GTCAGCGGACTCTGGATTCAG-3′(R)	141
Adipsin	5′-GACACCATCGACCACGACC-3′(F) 5′-GCCACGTCGCAGAGAGTTC-3′(R)	128
Glut4	5′-ATCCTTGGACGATTCCTCATTGG-3′(F) 5′-CAGGTGAGTGGGAGCAATCT-3′(R)	90
LEP	5′-TGCCTTCCAGAAACGTGATCC-3′(F) 5′-CTCTGTGGAGTAGCCTGAAGC-3′(R)	164

(continued)

Table 6 (continued)

Gene name	Primer sequences	Product size (bp)
CEBPA	5′-GGTGCGTCTAAGATGAGGGG-3′(F) 5′-CATTGGAGCGGTGAGTTTGC-3′(R)	140
CEBPB	5′-ACCCACGTGTAACTGTCAGC-3′(F) 5′-GCCCCCAAAAGGCTTTGTAA-3′(R)	237
GAPDH	5′-GGAGCGAGATCCCTCCAAAAT-3′(F) 5′-GGCTGTTGTCATACTTCTCATGG-3′(R)	197
GADD45B	5′-TGCTGTGACAACGACATCAAC-3′(F) 5′-GTGAGGGTTCGTGACCAGG-3′(R)	135
PDK4	5′-GGAAGCATTGATCCTAACTGTGA-3′(F) 5′-GGTGAGAAGGAACATACACGATG-3′(R)	169
RNF5	5′-GCCAGAACGGCAAGAGTGT-3′(F) 5′-GGCTCCCTCGCCCATAAAG-3′(R)	80
TK1	5′-GTTTTTCCCTGACATCGTGGA-3′(F) 5′-CGAGCCTCTTGGTATAGGCG-3′(R)	133
TK2	5′-TGTCGGAATGGTTTGACTGGA-3′(F) 5′-TGGTCAGCCTCAATCACCAGA-3′(R)	200
IL1A	5′-AGATGCCTGAGATACCCAAAACC-3′(F) 5′-CCAAGCACACCCAGTAGTCT-3′(R)	147
GANI1	5′-GCTCAACCAAATTACATCCCGA-3′(F) 5′-TCGTAGTCACTCAGTGCTACAC-3′(R)	206
CDC6	5′-GCCGAACTAGAACAGCATCTT-3′(F) 5′-GGGCTGGTCTAATTTTTCCTGC-3′(R)	246
CDC25B	5′-ACGCACCTATCCCTGTCTC-3′(F) 5′-CTGGAAGCGTCTGATGGCAA-3′(R)	195
CDKN1C	5′-GCGGCGATCAAGAAGCTGT-3′(F) 5′-GCTTGGCGAAGAAATCGGAGA-3′(R)	152
TNFAIP1	5′-GGGCAGAGTTGGATACCCC-3′(F) 5′-TGCGTGTGGGTTGTAGCAATA-3′(R)	130
NFKB2	5′-GGGCCGAAAGACCTATCCC-3′(F) 5′-CAGCTCCGAGCATTGCTTG-3′(R)	136
CASP3	5′-GAAATTGTGGAATTGATGCGTGA-3′(F) 5′-CTACAACGATCCCCTCTGAAAAA-3′(R)	164

4.3.3 RNA-Sequencing Assay

Adaptor ligation and PCR amplification were performed using a TruSeq RNA sample prep kit (Illumina, San Diego, CA, USA). SPRI beads (Ampure XP, Beckman, Brea, CA, USA) were used in each purification step after RNA fragmentation for size selection. All libraries were analyzed for quality and concentration using a TBS380 PicoGreen (Invitrogen). Sequencing was performed using a HiSeq 4000 SBS Kit (Illumina). RNA-seq reads were mapped to the human reference genome

using TopHat2. Gene expression analysis and measurement was performed with FeatureCount software and FPKM. Genes with FDR < 0.05 and $|\log_2 (\text{fold})| \geq 1$ were marked as significant.

4.3.4 Whole-Cell Protein Extraction and Western Blot Analysis

Cells osteogenically induced under normal gravity or space microgravity for 2 days were used for analysis of activity of proteins. Lysates were prepared by sonication of the scaffold in lysis buffer containing 1 mM NaF, 1% Nonidet P-40, 0.25% sodium deoxycholate, 1 mM Na_3VO_4, 1 mM EDTA, 150 mM NaCl, 1 mM phenylmethylsulfonyl fluoride (PMSF), and a phosphatase inhibitor. Protein concentration was determined using the BSA protein assay kit. The expression levels of Runx2 or p-Runx2, were determined by western blotting. Proteins from each sample were subjected to SDS-PAGE in a 10% gel, and then transferred to a 4.5-μm PVDF membrane. The membrane was blocked with a BLOTTO solution, and then incubated with anti-Runx2, anti-tyrosine antibody or with anti-GAPDH antibody at 4 °C overnight. Afterwards, the membrane was reprobed with appropriate secondary antibodies (conjugated with horseradish peroxidase) for 1 h. Next, the immunoreactive proteins were visualized using ECL Western blotting detection reagents, and light emission was quantified with a Tanon 6600 Luminescence Imaging Workstation.

4.3.5 Histochemical and Immunohistochemical Analyses

Cells osteogenically induced under normal gravity and space microgravity for 7 days and fixed with 4% formaldehyde were embedded in paraffin and then sectioned at 3-μm thickness. Alkaline phosphatase activity was visualized using the ALP Gomori Staining Kit.

To determine the expression levels of ALP, COL1A1 and Runx2 in cells osteogenically induced under normal gravity or space microgravity for 7 days, paraffin-embedded slices were incubated with anti-ALP, anti-COL1A1 and anti-Runx2 antibodies at a dilution of 1:100 overnight at 4 °C. Slides were washed with PBS three times and then incubated in the REAL EnVision Detection System.

4.3.6 Scanning Electronic Microscope (SEM) Assay

To examine the effect of microgravity on the morphology of cells in the scaffold, the sample fixed with 4% formaldehyde was used for the SEM assay. After the 4% formaldehyde was discarded, the sample was fixed in 2.5% glutaraldehyde (Sigma-Aldrich, Shanghai, China) in PBS at 4 °C overnight. The sample was then washed with PBS for 15 min and post-fixed in 1% OsO4 in PBS for 2 h. The sample was washed with PBS again for 15 min and then dehydrated with a graded ethanol series for 15 min. After being dehydrated two times in 100% ethanol, the sample was

transferred into isoamyl acetate for 1 h, dehydrated with liquid CO_2 in a Hitachi HCP-2 critical point dryer, coated with gold-palladium in a Hitachi E-1010 ion sputter for 5 min, and examined under a Hitachi SU8010 SEM. The cells were randomly selected in five fields of the same magnification, and the length of bipolar cells in the microgravity group and the gravity group was compared.

4.3.7 Statistical Analysis

The images of western blots were semi-quantitatively analyzed in the ImageJ software (NIH, USA). Statistical analyses involved Student's t test and significance was assumed at P values < 0.05.

4.4 The Effects of Space Microgravity on the Transcriptome Expression of hMSCs

4.4.1 Global RNA-Seq Data Analysis and Gene Ontology of Genes and Genomes Enrichment Analysis of Differentially Expressed Genes

hMSCs under osteogenic induction for 2 days both in space and on the ground was fixed with RNAlater and saved for 10 days at 4 °C. Then we prepared RNA samples and quantified expression level of transcriptome of space flight and ground cells by RNA-sequence technology. Using a moderately stringent cut-off (log2 (fold change) ≥ 1 and FDR < 0.05) 548 genes (302 genes upregulated and 246 genes downregulated) significantly change their expression levels. Using a higher stringency cut-off (log2 (fold change) ≥ 1 and FDR < 0.01) only 162 of the quantified genes were considered significantly altered (Fig. 9a).

4.4.2 Gene Ontology of Genes and Genomes Enrichment Analysis of Differentially Expressed Genes

Although at a different level, genes with many biological processes displayed significant altered expression. Using GO significant enrichment analysis, it was found that these altered genes were mainly involved in response to stress, cell proliferation, regulation of cell proliferation, inflammatory reaction and so on. Top10 of GO term enrichment list was shown in Fig. 9b.

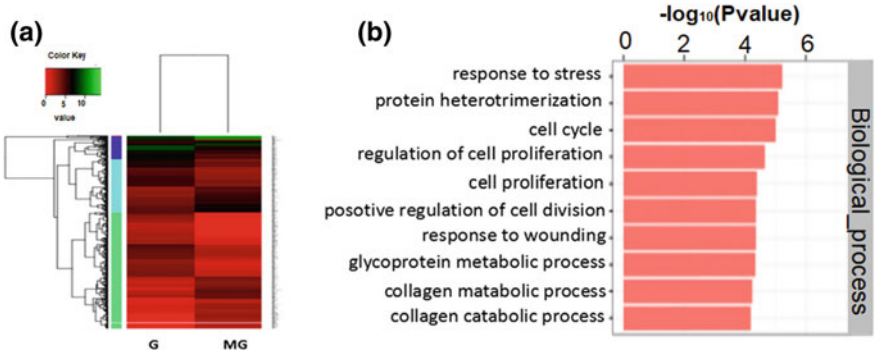

Fig. 9 Global analyze of the effects of space microgravity on the transcriptome expression of hMSCs. **a** The Heat map and cluster analysis of gene expression profiles. **b** Go function analysis of differentially expressed genes between hMSCs under microgravity and gravity

Stress Response-Related Genes

After a two-day space flight, stress response-related genes are the largest number group of the changed genes. Of 548 changed genes, 127 genes were associated with stress response. Among them, genes involved in endoplasmic reticulum stress response, DNA-damage response and oxidative stress response occupy the most, and some other stress response genes also changed under SF environment.

The stress response GADD45 family of genes are rapidly induced by a wide variety of endogenous and exogenous stress stimuli (Yang et al. 2009) and they are implicated in cell cycle arrest, DNA demethylation and repair, apoptosis, cell survival, genomic stability, inflammation, and in response to physiological (Jung et al. 2007; Smith et al. 2000; Barreto et al. 2007). In the present study, two isoforms of GADD45, GADD45B and GADD45G, exhibited apparently up-regulated expression after exposure to 2-days space flight, which suggested space flight may cause DNA damage and cycle arrest of osteogenic-induced hMSCs. MMP1, also induced by DNA damage, is significantly increased under space flight (Leiros et al. 2017). CHAF1A, which participate into DNA replication and repair (Rodriges et al. 2016), was also increased. Pyruvate dehydrogenase kinase 4 (PDK4), encodes a mitochondrial protein and regulates of glucose metabolism by inhibiting the pyruvate dehydrogenase complex, was also increased by space flight. In addition, a large number of altered genes response to oxidative stress, involving SOD2, PARP1, TXNIP, HDAC2, HFE, HSPA6, HMGA1 and BIRC3 all increased under space flight environment.

Space flight also inhibited the expression of some stress-stress related genes. RNF5, one E3 ubiquitin ligase that has been implicated in motility and cellular stress response (Didier et al. 2003), was inhibited under SF. In addition, the most obvious reduction genes class was associated to endoplasmic reticulum stress. Some proteins associated with protein folding and transport in the endoplasmic reticulum were significantly decreased, such as HYOU1, at the same time, some endoplasmic

reticulum stress induced genes increased, involving HSPA6, ATF3 and YOD1. The TK1 and TK2, which were involved in DNA synthesis, was also significantly reduced after space flight.

Space Flight Promoted Inflammation Response

Space flight was associated with significant shifts in expression of mRNAs involved with the inflammation response. Levels of mRNA of the chemokine family members CCL3 (3.76-log fold), CCL20 (3.63-log fold), CXCL2 (3.50-log fold), CXCL3 (2.70-log fold), CXCL5 (1.77-log fold), CXCL6 (1.70-log fold); inflammatory cytokines IL1A (2.64-log fold), IL1B (3.23-log fold) genes were significantly increased in space flight compared with ground control. And the expression of BCL6, a factor known to be important in resolving inflammatory responses, was also increased 2.56 log fold. GNAI (1.88-log fold), which expression is promoted by chemokine, was also increased after space flight. Conversely, GNG2, which expression is inhibited by GNAI, mRNA level was significantly decreased 2.62-log fold) after space flight.

Space Flight Inhibited Cell Cycle

Biological process enriches analyze showed that of expression changed 528 genes, 68 genes was relative to cell cycle. RNA-sequence revealed the down regulation of CDC6, CCNB1 and CDK1 genes at 2.75, 2.29 and 1.85 log fold respectively when hMSCs were osteogenic induced after space flight. Similarly, CDC25B, which activates complex of CDK1/Cyclin B and is required for entry into mitosis (Forrest et al. 1999; Lincoln et al. 2002; Nilsson and Hoffmann 2000), was decreased 2.07 log fold. CDCA8 (2.62-log fold), an essential regulator of mitosis and cell division, was also inhibited by space flight. On the other hand, CDKN1C, which is capable of inhibiting several CDK with demonstrated roles in the G1/S-phase transition (Lopez-Abad et al. 2016), the expression of which was increased at 2.58-log fold by SF. GADD45B and GADD45G, whose transcript level is increased following stressful growth arrest conditions, was also increased 2.22-log fold under space environment. All the changed genes revealed that space flight arrest cell cycle and inhibited mitosis of hMSCs under osteogenic differentiation.

hMSCs Differentiation Potential

According to the RNA-Seq assay, we found a significant difference in the expression of 21 osteogenesis-related genes in space samples compared to ground samples (Table 7). The expression of seven members of the collagen family was significantly reduced, including that of COL1A1, COL1A2, COL3A1, COL4A1, COL5A1, and COL18A1. In addition, the expression of ALP, a marker of early osteogenesis, and Runx2, a key transcription factor in early osteoblasts, was also significantly

Table 7 Osteogenic and adipogenic differentiation relative genes changed in RNA-SEQ

Function	Gene ID	log2(fold)	FDR
Genes relative to osteogenic differentiation of hMSCs	COL1A1	−7.02	0.0005
	COL1A2	−2.75	0.037
	COL3A1	−2.81	0.0075
	COL4A1	−2.49	0.0433
	COL5A1	−3.86	0.016
	COL6A1	−4.63	0.024
	COL18A1	−3.65	0.011
	ALPL	−2.55	0.0039
	RUNX2	−2.59	0.0118
	BMP2	−4.4	0.00195
	BMP4	−2.38	0.028
	ID3	−6.13	0.0045
	HTRA1	−4.82	0.00365
	TNC	−3.43	0.0086
	RBP4	−3.03	0.00375
	COMP	−1.54	0.0023
	BCAP29	2.34	0.023
	MMP1	2.29	0.0359
	CCL3	3.86	0.0003
	CSF2	4.979	0.0277
	ANGPT1	−2.34	0.00645
Genes relative to adipogenic differentiation of hMSCs	LEP	2.47	0.03295
	CFD	2.55	0.01277
	CEBPB	3.8	0.00155
	PPARG	1.56	0.0431
	MEDAG	3.42	0.0002
	ZFP36	2.06	0.0207
	BBS4	2.07	0.0374
	ACSL4	1.67	0.03255
	NR1D1	2.03	0.0212
	LRRC8C	1.97	0.0245
	TRIB3	−5.92884	0.00145
Genes relative to the balance of osteogenic and adipogenic differentiation of hMSCs	ROS1	−2.23	0.0152
	SAT1	4.3	0.00015
	LEPR	1.32	0.031515
	HDAC2	1.58	0.04405
	NAMPT	2.56	0.00195

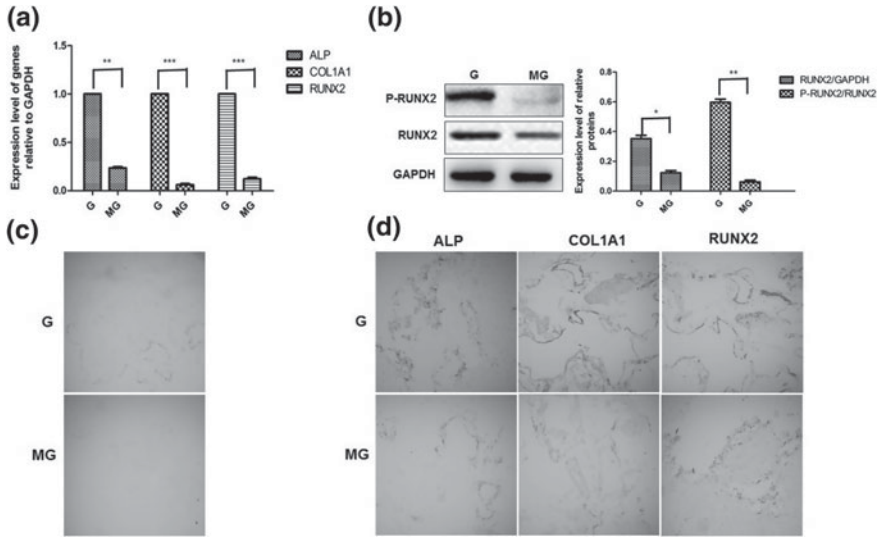

Fig. 10 Effects of space microgravity on the expression of mRNA and proteins specific for osteogenesis. **a** The mRNA expression of ALP, COL1A1, and Runx2 in cells osteogenically induced for 2 days. The quantitative data were obtained by real-time PCR (n = 3). **b** The expression and activity of the Runx2 protein in cells osteogenically induced for 2 days (n = 3). The band intensity was quantified in triplicate by means of the ImageJ software for each protein, and the data were normalized to a corresponding *GAPDH* value. **c** The histochemical detection of ALP in cells osteogenically induced for 7 days. **d** Immunohistochemical detection of ALP, COL1A1, and Runx2 in cells osteogenically induced for 7 days. $*P < 0.05$, $** P < 0.01$, $***P < 0.005$. G: normal gravity, MG: space microgravity (Reprinted from Zhang et al. 2018)

decreased under the microgravity environment. Teal-time PCR results confirmed that the expression levels of Runx2, ALP and COL1A1 mRNA in the cells osteogenically induced under space microgravity declined remarkably as compared to those in cells osteogenically induced under normal gravity, especially COL1A1, a highly expressed bone-specific gene in early osteoblasts (Fig. 10a) We also measured the activation of the Runx2 protein in cells osteogenically induced for 2 days. The results showed that space microgravity inhibited both mRNA expression and activity of the Runx2 protein (Fig. 10b); these data indicated that space microgravity inhibited early genes specific for osteogenesis of hMSCs by decreasing the expression and activity of Runx2.

Analysis of ALP, COL1A1, and Runx2 expression in cells osteogenically induced for 2 days revealed that space microgravity decreased the expression of genes specific for osteogenesis. Therefore, we inferred that space microgravity could inhibit the osteogenic potential of hMSCs. By SEM assay of cells osteogenically induced for 7 days, we found that space microgravity resulted in obvious changes of cell morphology compared with normal gravity, including polygonal retraction and shorter cell spindle (Fig. 11a). In addition, H&E staining indicated that the cell shape became

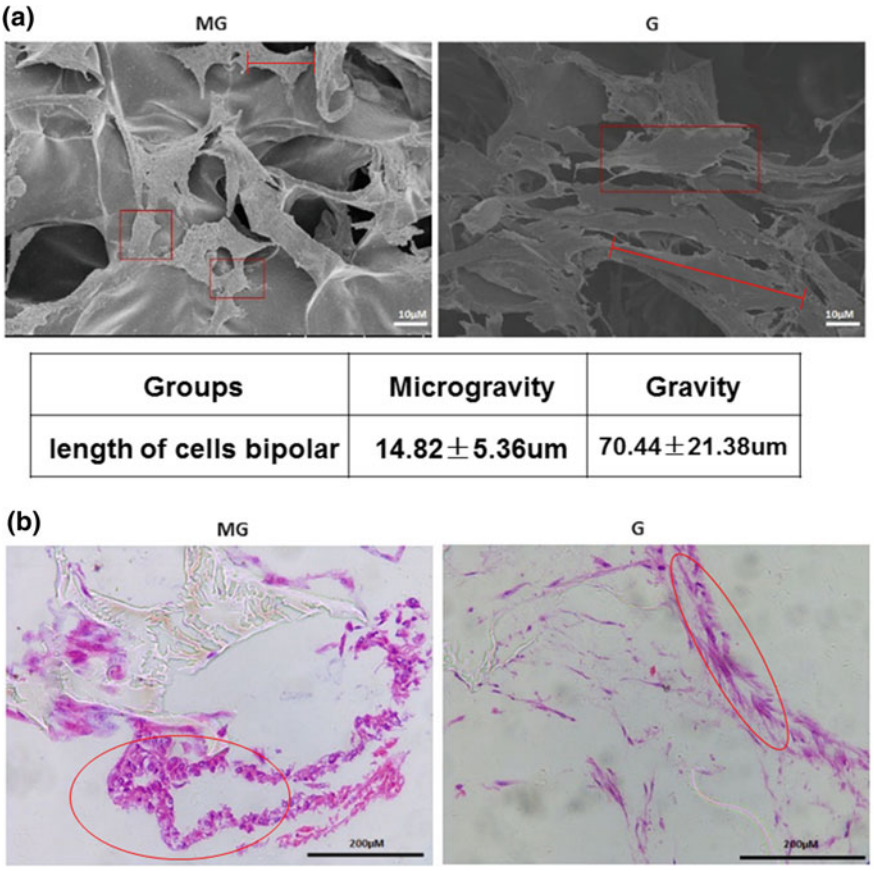

Fig. 11 Effects of space microgravity on hMSCs morphology. **a** Morphology of cells osteogenically induced for 7 days under microgravity and normal gravity was analyzed by SEM. Bipolar cell length was measured, and the actual length was calculated according to scale. **b** H&E staining of cells osteogenically induced for 7 days under microgravity and normal gravity. H&E staining was performed to locate the cells and observe the cells' morphology on the scaffold. G: normal gravity, MG: space microgravity (Reprinted from Zhang et al. 2018.)

round, as opposed to the triangular or fusiform shape of cells induced in normal gravity (Fig. 11b). Histochemical staining of ALP in cells osteogenically induced for 7 days confirmed this hypothesis. hMSCs could be induced to differentiate into osteoblasts with positive ALP staining under normal gravity (Fig. 11c). In contrast, the positive staining decreased in cells osteogenically induced for 7 days under space microgravity. Immunohistochemical analysis was also used to detect the protein expression of COL1A1 and Runx2 in the cells osteogenically induced for 7 days. In agreement with our hypothesis, few cells with positive staining for COL1A1 and Runx2 were found among the cells osteogenically induced under space microgravity (Fig. 11d).

It has been demonstrated that simulated microgravity increases adipogenesis of hMSCs, and activation of transcription factor PPARγ2 plays a crucial role in the expression of marker genes specific for adipogenesis (Zayzafoon et al. 2004). To identify the effects of space microgravity on the adipogenesis of hMSCs, we analyzed the expression of genes specific for adipogenesis. Figure 12a shows that expression of adipocyte markers, such as adipsin, leptin, and glucose transporter 4 (Glut4), was increased in cells osteogenically induced for 2 days under space microgravity. Meanwhile, space microgravity promoted expression of PPARγ2 (Fig. 12b), suggesting that space microgravity stimulates adipogenic differentiation even under osteogenic induction conditions.

CEBPA and CEBPB are key early regulators of adipogenesis. CEBPB directly induces the expression of PPARγ2, and PPARγ2 in turn activates the transcription of CEBPA (Barlier-Mur et al. 2003). Therefore, we analyzed the expression of CEBPA and CEBPB as shown in Fig. 12b. The results revealed that mRNA and protein levels of CEBPB increased in cells osteogenically induced for 2 days under space microgravity as compared with the cells osteogenically induced under normal gravity. In contrast, the level of CEBPA expression was not significantly different between cells osteogenically induced under normal gravity and space microgravity. One of the reasons may be that osteogenic induction for only 2 days is not enough to cause PPARγ2 to switch to activation of the CEBPA expression.

Dysregulation of Genes Involved with Signaling Pathway

TNF-α/NF-KB is involved in a variety of cellular physiological responses, such as cell growth, differentiation, apoptosis, immune, inflammation, stress response, and many other physiologic processes (Barnes and Karin 1997; Karin and Greten 2005). As one of inflammatory response regulation pathway, we selected genes involved in the TNF-α/NF-KB signaling system. The TNF-α downstream target TNF-α-induced protein 6 (TNFAIP6) mRNA was significantly increased in SF hMSCs (3.27-log fold). REL, a subunit of NF-KB family, was also increased under SF (1.91-log fold). However, TNFRSF1A associated via death domain (TRADD) mRNA decreased (3.02-log fold). P53 pathway was also changed significantly by KEGG pathway. GADD45B, GADD45G, CCND2 were all involved in P53 pathway and related to gene damage, and other gene involved in P53 pathway was CASP3, an apoptosis-related gene.

Validation of Gene Expression by qRT-PCR

Quantitative real-time PCR (qRT-PCR) was performed to validate the differentially expressed genes involved in the RNA-seq data (Fig. 13). The results showed that the expression patterns of these thirteen genes were highly in agreement with the RNA-seq results.

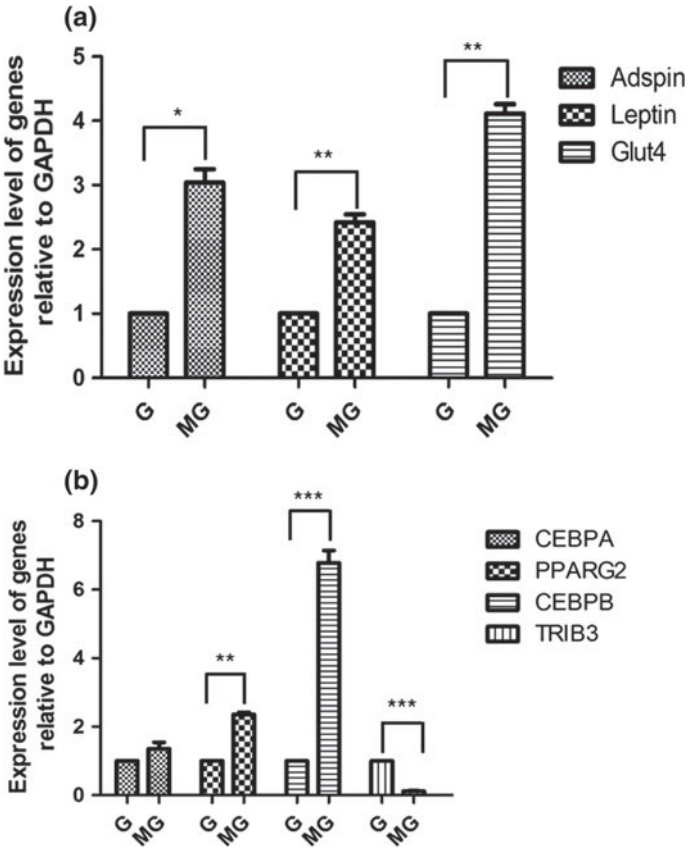

Fig. 12 Effects of space microgravity on the mRNA expression of genes specific for adipogenesis. **a** The mRNA expression of adipsin, glut4, and leptin in cells osteogenically induced for 2 days. The quantitative data were obtained by real-time PCR (n = 3). **b** The mRNA expression of PPARγ, CEBPA, CEBPB, and TRIB3 in cells osteogenically induced for 2 days. The quantitative data were obtained by real-time PCR (n = 3). The data were normalized to the corresponding GAPDH value. $*P < 0.05$, $** P < 0.01$, $***P < 0.005$. G: normal gravity, MG: space microgravity (Reprinted from Zhang et al. 2018)

4.4.3 Discussion

Expose to the space stresses, including microgravity, radiation, hypoxia and other factors, the physical condition of astronauts changed greatly, including bone loss, muscular atrophy and impaired immune system function and cardiovascular deconditioning (Atkov 1992; Basso et al. 2005; Bucaro et al. 2004; Heer et al. 1999; Leach 1992). The changes of physiological function were ultimately caused by changes in the biological process of cells. The effect of space environment on different types of cells is complex and varied. Space flight has been shown to result in suppression of

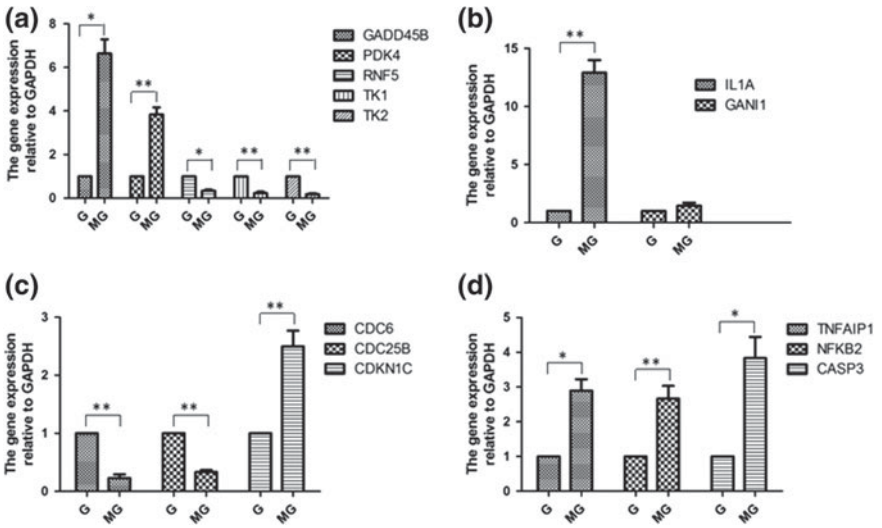

Fig. 13 Quantitative PCR was used to verify gene expression. **a** q-PCR detection of genes associated with stress response GADD45B, PDK4, RNF5, TK1 and TK2; **b** The expression of inflammation-related genes IL1A and GANI1; **c** Expression of cell cycle related genes: CDC6, CDC25B and CDKN1C; D: Expression of NFKB2 and CASP3, TNFAIP1 in the signaling pathway.. *$P < 0.05$, ** $P < 0.01$. G: normal gravity; MG: space microgravity

antigen-specific T cell function, inducing a sustained vascular endothelial cell dysfunction, promoting human fibroblast cells proliferating (Fritsch-Yelle et al. 1996; Leach 1992; Mehta et al. 2000; Zhang et al. 2016). The main purpose of this article was to explore mRNA expression change of osteogenic induced hMSCs in response to microgravity in space. By RNA-sequence assay, we found that a series of biological processes mRNA expression level significantly changed, including response to stress, cell cycle and inflammation response. Moreover, space flight may affect TNF-α/NF-KB signaling system of osteogenic-induced hMSCs.

When stimulated by internal and external factors, cells will produce overmuch ROS and other free radicals and then result in cell oxidative stress through destructing the balance of oxidation and antioxidant system (Reuter et al. 2010; Pi et al. 2010). Overexpression of ROS can regulate many oxidizing substances and antioxidant-related gene expression by activating NRF2, NF-KB and MAPK pathways (Kanninen et al. 2011; Sykiotis et al. 2011; Pantano et al. 2006). It has been reported that space flight can induce oxidative stress response (Mao et al. 2014; Gambara et al. 2017). In this study, we also found that space flight increased the expression of a mass of genes related to oxidative stress. TXNIP, as an oxidative stress biomarker, inhibits the antioxidative function of thioredoxin resulting in the accumulation of reactive oxygen species and cellular stress. Hypoxia, availability of glucose or radiation can induce TXNIP expression and it has also been reported that space environment can induce TXNIP expression (Yu et al. 2010; Li et al. 2015; Hoshikawa et al. 2011; Versari et al.

2013). In the present study, space flight promoted TXNIP expression. SOD2 is one of the markers of oxidative stress response and it has been reported that simulated microgravity or radiation increased SDO2 gene expression and increased expression of SOD2 can reduce cellular ROS (Chen et al. 2016; Zhang et al. 2017; Oscarsson et al. 2017; Qiu et al. 2010). HSPA4, which is often called Hsp70 and known as the major heat shock protein that prevents stress-induced apoptosis, was upregulation under space flight environment in many kind of cells (Gritsyna et al. 2015; Cui et al. 2010), while some others considered that space flight inhibited Hsp70 expression (Cubano and Lewis 2001; Amann et al. 1992; Ishihara et al. 2008). In the present study, HSPA6, a member of Hsp70 family, was promoted by space flight. Survival related gene, HMGA1(Mahajan et al. 2013) and anti-apoptotic gene, BIRC3(Gressot et al. 2017), expression was also promoted by space flight. Together these data support the hypothesis that space flight cause cell oxidative stress and the cells adapted to this stress response by changing the expression of related genes.

Exogenous high temperature and pressure, ultraviolet, strong acid and alkali and other physical and chemical factors and endogenous oxidative stress, DNA replication and transmission errors can cause DNA damage. Cells can maintain genome integrity through the activation effector proteins of DNA repair, apoptosis and cell cycle arrest (Girardi et al. 2012; Hoshino et al. 2007; Lu et al. 2017a, b). We found that SF decreased the TK1, TK2 expression. TK genes catalyze cytosolic and mitochondrial deoxy thymidine phosphorylation and all the three synthases are necessary for DNA replication (Munch-Petersen 2010). The TK1 and TK2 deficiency could prevent DNA replication process and then increase cellular sensitivity to DNA damage. In addition, under SF environment, the DNA repair related genes GADD45B, GADD45G, PARP1, and HDAC2 (Lu et al. Lu et al. 2017a, b; Huang et al. 2016; Liu et al. 2009) was increased. SF also inhibited some cell cycle essential genes expression. CCNB/CDK1 protein complex form the key substrate phosphorylation and translate the cell cycle from the G2 to M period (Sherr 1996). It is necessary to start the cell cycle factor. CDC6, CDC25B and CDCA8 also play a key role in the smooth progress of the cell cycle. The inhibition effect of SF on these cell cycle related genes could cause cell cycle arrest. Apoptosis is essential for the development and survival of most multicellular animals by preventing growth of cells mutation due to DNA damage. CASP3, as a biomarker of apoptosis, was increased by SF. The high expression of CASP3 was also indicated by other space flight (Novoselova et al. 2015). However, besides to CASP3, the expression of other members of the CASP family did not change significantly. CCND2, CASP3, GGDD45B, and GGAD45G are all involved in P53 pathway and P53 pathway was significantly change by KEGG pathway analyze. BCL2L11 belongs to BCL2 family and acts as an apoptotic activator by interacting with other members of the BCL-2 protein family (Concannon et al. 2010; Fischer et al. 2007). SF also promoted the expression of BCL2L11 in our study. The above results show that SF may inhibit DNA replication by decreasing the synthesis of thymine and then result in DNA damage and the DNA damage would induce DNA repair-related genes expression, cycle arrest and cell apoptosis, and P53 pathway played an important role in it.

Some studies have shown that simulated microgravity inhibits proliferation and osteogenesis of hMSCs and increases their adipogenesis (Orlic et al. 2001; Zayzafoon et al. 2004; Dai et al. 2007). On the other hand, these simulation methods involving clinostats, random positioning machine (RPM) and rotating wall vessel (RWV) bioreactors, cannot actually remove the force of gravity. The constant rotation of a sample may result in the g-vector being time-averaged to near-zero (Klaus 2001) and the controversy still exists regarding these experiments. Thus, the effects of real space microgravity on the osteogenic differentiation of hMSCs should be examined in a real space environment. In this study, we analyzed the effects of space microgravity on the osteogenic differentiation of hMSCs exposed to space microgravity for 2 days and 7 days by detecting the expression of ALP, a marker of early osteogenesis. We demonstrated that space microgravity reduced the osteogenic potential of hMSCs by inhibiting the expression of ALP. This finding is consistent with other data indicating downregulation of the markers of osteoblastic function and differentiation under simulated microgravity (Nakamura et al. 2003). We next analyzed another protein osteoblastic marker, COL1A1, a major ECM component secreted by osteoblasts during differentiation (Ontiveros and McCabe 2003; Owen et al. 1990). We detected reduced expression of COL1A1, which confirmed that space microgravity inhibits osteogenesis of hMSCs. In addition, space microgravity increased the expression of marker genes specific for adipogenesis, such as leptin, adispin, and GLUT4 mRNA, even under osteogenic induction conditions. In agreement with these data, the expression of PPARγ2, a key transcription factor involved in adipogenic differentiation (Tontonoz et al. 1994), was increased under space microgravity, and the increased expression of PPARγ2 resulted from increased CEBPB expression. Therefore, we concluded that gene expression in hMSCs shifts toward adipogenesis instead of osteogenesis under space microgravity.

Many articles have reported that space flight can cause the animal or cell immune dysfunction and inflammatory response (Chang et al. 2015; Strewe et al. 2015; Crucian et al. 2014; Kizilay et al. 2017). By RNA-sequence results and real-time PCR validation, we found that space flight induced the expression of some chemokine family members and inflammatory cytokine family members in osteogenic-induced hMSCs. The ground simulated microgravity experiments also showed that simulated microgravity contributed to intracellular inflammatory responses of hMSCs under osteogenic differentiation (Gershovich et al. 2013). It has also been reported that hMSCs isolated from elder patients secreted high levels of inflammatory cytokines, therefore, we speculate that cell cycle arrest and apoptosis caused by space flight may lead to elevated expression of inflammatory factors. Inflammation stress may hinder the normal physiological function of hMSCs, such as differentiation potential.

Acknowledgements We much thank the opportunity of space experiment supplied by SJ-10 Recoverable Scientific Satellite. This study was supported by the grants from Strategically Guiding Scientific Special Project from Chinese Academy of Sciences (XDA04020202-23), Chinese National Nature Science Foundation (U1738102, 81570932).

References

Amann RP, Deaver DR, Zirkin BR et al (1992) Effects of microgravity or simulated launch on testicular function in rats. J Appl Physiol (Bethesda, Md.: 1985) 73(2 Suppl):174s–185s

Atkov O (1992) Some medical aspects of an 8-month's space flight. Adv Space Res Off J Comm Space Res (COSPAR) 12(1):343–345

Barlier-Mur AM, Chailley-Heu B, Pinteur C et al (2003) Maturational factors modulate transcription factors CCAAT/enhancer-binding proteins alpha, beta, delta, and peroxisome proliferator-activated receptor-gamma in fetal rat lung epithelial cells. Am J Respir Cell Mol Biol 29(5):620–626

Barnes PJ, Karin M (1997) Nuclear factor-kappaB: a pivotal transcription factor in chronic inflammatory diseases. N Engl J Med 336(15):1066–1071

Barreto G, Schafer A, Marhold J et al (2007) Gadd45a promotes epigenetic gene activation by repair-mediated DNA demethylation. Nature 445(7128):671–675

Basso N, Bellows CG, Heersche JN (2005) Effect of simulated weightlessness on osteoprogenitor cell number and proliferation in young and adult rats. Bone 36(1):173–183

Bucaro MA, Fertala J, Adams CS et al (2004) Bone cell survival in microgravity: evidence that modeled microgravity increases osteoblast sensitivity to apoptogens. Ann N Y Acad Sci 1027:64–73

Carmeliet G, Nys G, Bouillon R (1997) Microgravity reduces the differentiation of human osteoblastic MG-63 cells. J Bone Miner Res Off J Am Soc Bone Miner Res 12(5):786–794

Cedar SH (2006) The function of stem cells and their future roles in healthcare. Br J Nurs (Mark Allen Publishing) 15(2):104–107

Chang TT, Spurlock SM, Candelario TL et al (2015) Spaceflight impairs antigen-specific tolerance induction in vivo and increases inflammatory cytokines. FASEB J Off Publ Fed Am Soc Exp Biol 29(10):4122–4132

Chen XJ, Lin F, Qiao C (2004) Isolation, culture and osteogenic potential of human adipose stromal cells and [J]. J Pract Stomatol 20:12–15

Chen H, Lv K, Dai Z et al (2016) Intramuscular injection of mechano growth factor E domain peptide regulated expression of memory-related sod, miR-134 and miR-125b-3p in rat hippocampus under simulated weightlessness. Biotech Lett 38(12):2071–2080

Claassen DE, Spooner BS (1994) Impact of altered gravity on aspects of cell biology. Int Rev Cytol 156:301–373

Claassen DE, van Twest JS, Spooner BS (1994) Formation and vesiculation of biomembranes during spaceflight. Adv Space Res Off J Comm Space Res (COSPAR) 14(8):111–114

Concannon CG, Tuffy LP, Weisova P et al (2010) AMP kinase-mediated activation of the BH3-only protein Bim couples energy depletion to stress-induced apoptosis. J Cell Biol 189(1):83–94

Crucian BE, Zwart SR, Mehta S et al (2014) Plasma cytokine concentrations indicate that in vivo hormonal regulation of immunity is altered during long-duration spaceflight. J Interf Cytokine Res Off J Int Soc Interf Cytokine Res 34(10):778–786

Cubano LA, Lewis ML (2001) Effect of vibrational stress and spaceflight on regulation of heat shock proteins hsp70 and hsp27 in human lymphocytes (Jurkat). J Leukoc Biol 69(5):755–761

Cui Y, Zhou J, Li C et al (2010) Effects of simulated weightlessness on liver Hsp70 and Hsp70mRNA expression in rats. Int J Clin Exp Med 3(1):48–54

Dai ZQ, Wang R, Ling SK et al (2007) Simulated microgravity inhibits the proliferation and osteogenesis of rat bone marrow mesenchymal stem cells. Cell Prolif 40(5):671–684

Dai Z, Wu F, Chen J et al (2013) Actin microfilament mediates osteoblast Cbfa1 responsiveness to BMP2 under simulated microgravity. PLoS ONE 8(5):e63661

Dai Z, Guo F, Wu F et al (2014) Integrin alphavbeta3 mediates the synergetic regulation of core-binding factor alpha1 transcriptional activity by gravity and insulin-like growth factor-1 through phosphoinositide 3-kinase signaling. Bone 69:126–132

Didier C, Broday L, Bhoumik A et al (2003) RNF5, a RING finger protein that regulates cell motility by targeting paxillin ubiquitination and altered localization. Mol Cell Biol 23(15):5331–5345

Fischer SF, Bouillet P, O'Donnell K et al (2007) Proapoptotic BH3-only protein Bim is essential for developmentally programmed death of germinal center-derived memory B cells and antibody-forming cells. Blood 110(12):3978–3984
Forrest AR, McCormack AK, DeSouza CP et al (1999) Multiple splicing variants of cdc25B regulate G2/M progression. Biochem Biophys Res Commun 260(2):510–515
Fritsch-Yelle JM, Charles JB, Jones MM et al (1996) Microgravity decreases heart rate and arterial pressure in humans. J Appl Physiol (Bethesda, Md.: 1985) 80(3):910–914
Fu Y, Wang T, Liang WW (2006) Isolation, culture and differentiation of rat bone marrow-derived mesenchymal stem cells into neuron-like cells. Lingnan J Emerg Med 11:1–3
Gambara G, Salanova M, Ciciliot S et al (2017) Gene expression profiling in slow-type calf soleus muscle of 30 days space-flown mice. PLoS ONE 12(1):e0169314
Gershovich PM, Gershovich IuG, Buravkova LB (2013) The effects of simulated microgravity on the pattern of gene expression in human bone marrow mesenchymal stem cells under osteogenic differentiation. Fiziol Cheloveka 39(5):105–111
Girardi C, De Pitta C, Casara S et al (2012) Analysis of miRNA and mRNA expression profiles highlights alterations in ionizing radiation response of human lymphocytes under modeled microgravity. PLoS ONE 7(2):e31293
Gressot LV, Doucette T, Yang Y et al (2017) Analysis of the inhibitors of apoptosis identifies BIRC3 as a facilitator of malignant progression in glioma. Oncotarget 8(8):12695–12704
Gritsyna YV, Abdusalamova ZR, Vikhlyantsev IM et al (2015) Changes in gene expression and content of Hsp70 and Hsp90 in striated muscles of mice after 30-day space flight on the biosatellite Bion-M1. Dokl Biochem Biophys 463:199–202
Gurkin LW (1992) The NASA sounding rocket program and space sciences. ASGSB Bull Publ Am Soc Gravit Space Biol 6(1):113–120
Heer M, Kamps N, Biener C et al (1999) Calcium metabolism in microgravity. Eur J Med Res 4(9):357–360
Hill PA (1998) Bone remodelling. Br J Orthod 25(2):101–107
Hoshikawa H, Indo K, Mori T, Mori N (2011) Enhancement of the radiation effects by D-allose in head and neck cancer cells. Cancer Lett 306(1):60–66
Hoshino T, Nakaya T, Araki W et al (2007) Endoplasmic reticulum chaperones inhibit the production of amyloid-beta peptides. Biochem J 402(3):581–589
Hoson T, Kamisaka S, Masuda Y et al (1997) Evaluation of the three-dimensional clinostat as a simulator of weightlessness. Planta 203(Suppl):S187–197
Huang Y, Dai ZQ, Ling SK et al (2009) Gravity, a regulation factor in the differentiation of rat bone marrow mesenchymal stem cells. J Biomed Sci 16:87
Huang R, Langdon SP, Tse M et al (2016) The role of HDAC2 in chromatin remodelling and response to chemotherapy in ovarian cancer. Oncotarget 7(4):4695–4711
Hughes-Fulford M, Tjandrawinata R, Fitzgerald J et al (1998) Effects of microgravity on osteoblast growth. Gravit Space Biol Bull Publ Am Soc Gravit Space Biol 11(2):51–60
In't Anker PS, Scherjon SA, Kleijburg-van der Keur C et al (2004) Isolation of mesenchymal stem cells of fetal or maternal origin from human placenta. Stem Cells (Dayton, Ohio) 22(7):1338–1345
Ishihara A, Fujino H, Nagatomo F et al (2008) Gene expression levels of heat shock proteins in the soleus and plantaris muscles of rats after hindlimb suspension or spaceflight. J Physiol Sci JPS 58(6):413–417
Jung HJ, Kim EH, Mun JY et al (2007) Base excision DNA repair defect in Gadd45a-deficient cells. Oncogene 26(54):7517–7525
Kanninen K et al (2011) Targeting glycogen synthase kinase-3 for therapeutic benefit against oxidative stress in Alzheimer'S disease: involvement of the Nrf2-ARE pathway. Intem J Alzheimer's Dis 15:56–64
Karin M, Greten FR (2005) NF-kappaB: linking inflammation and immunity to cancer development and progression. Nat Rev Immunol 5(10):749–759
Katembe WJ, Edelmann RE, Brinckmann E et al (1998a) Development of spaceflight experiments with Arabidopsis as a model system in gravitropism studies. J Plant Res 111:463–470

Katembe WJ, Edelmann RE, Brinckmann E, Kiss JZ (1998b) The development of spaceflight experiments with Arabidopsis as a model system in gravitropism studies. J Plant Res 111(1103):463–470
Kizilay Mancini O, Lora M, Shum-Tim D et al (2017) A proinflammatory secretome mediates the impaired immunopotency of human mesenchymal stromal cells in elderly patients with atherosclerosis. Stem Cells Transl Med 6(4):1132–1140
Klaus DM (2001) Clinostats and bioreactors. Gravit Space Biol Bull: Publ Am Soc Gravit Space Biol 14(2):55–64
Krikorian AD, Levine HG, Kann RP et al (1992) Effects of spaceflight on growth and cell division in higher plants. Adv Space Biol Med 2:181–209
Lang TF, Leblanc AD, Evans HJ et al (2006) Adaptation of the proximal femur to skeletal reloading after long-duration spaceflight. J Bone Miner Res Off J Am Soc Bone Miner Res 21(8):1224–1230
Lazarenko OP, Rzonca SO, Suva LJ et al (2006) Netoglitazone is a PPAR-gamma ligand with selective effects on bone and fat. Bone 38(1):74–84
Leach CS (1992) Biochemical and hematologic changes after short-term space flight. Microgravity Q MGQ 2(2):69–75
Lee OK, Kuo TK, Chen WM et al (2004) Isolation of multipotent mesenchymal stem cells from umbilical cord blood. Blood 103(5):1669–1675
Leiros GJ, Kusinsky AG, Balana ME et al (2017) Triolein reduces MMP-1 upregulation in dermal fibroblasts generated by ROS production in UVB-irradiated keratinocytes. J Dermatol Sci 85(2):124–130
Li Y, Miao LY, Xiao YL et al (2015) Hypoxia induced high expression of thioredoxin interacting protein (TXNIP) in non-small cell lung cancer and its prognostic effect. Asian Pac J Cancer Prev APJCP 16(7):2953–2958
Lincoln AJ, Wickramasinghe D, Stein P et al (2002) Cdc25b phosphatase is required for resumption of meiosis during oocyte maturation. Nat Genet 30(4):446–449
Liu B, Suyeoka G, Papa S, Franzoso G et al (2009) Growth arrest and DNA damage protein 45b (Gadd45b) protects retinal ganglion cells from injuries. Neurobiol Dis 33(1):104–110
Lopez-Abad M, Iglesias-Platas I, Monk D (2016) Epigenetic characterization of CDKN1C in placenta samples from non-syndromic intrauterine growth restriction. Front Genet 7:62
Lu T, Zhang Y, Wong M et al (2017a) Detection of DNA damage by space radiation in human fibroblasts flown on the International Space Station. Life Sci Space Res 12:24–31
Lu Y, Kwintkiewicz J, Liu Y et al (2017b) Chemosensitivity of IDH1-mutated gliomas due to an impairment in PARP1-mediated DNA repair. Can Res 77(7):1709–1718
Mahajan L, Pandit H, Madan T et al (2013) Human surfactant protein D alters oxidative stress and HMGA1 expression to induce p53 apoptotic pathway in eosinophil leukemic cell line. PLoS ONE 8(12):e85046
Mao XW, Pecaut MJ, Stodieck LS et al (2014) Biological and metabolic response in STS-135 space-flown mouse skin. Free Radical Res 48(8):890–897
Marie PJ, Kaabeche K (2006) PPAR gamma activity and control of bone mass in skeletal unloading. PPAR Res 2006:64807
Mehta SK, Stowe RP, Feiveson AH et al (2000) Reactivation and shedding of cytomegalovirus in astronauts during spaceflight. J Infect Dis 182(6):1761–1764
Mesland DA, Anton AH, Willemsen H et al (1996) The Free Fall Machine—a ground-based facility for microgravity research in life sciences. Microgravity Sci Technol 9(1):10–14
Munch-Petersen B (2010) Enzymatic regulation of cytosolic thymidine kinase 1 and mitochondrial thymidine kinase 2: a mini review. Nucleosides Nucleotides Nucleic Acids 29(4–6):363–369
Nakamura H, Kumei Y, Morita S et al (2003) Suppression of osteoblastic phenotypes and modulation of pro- and anti-apoptotic features in normal human osteoblastic cells under a vector-averaged gravity condition. J Med Dent Sci 50(2):167–176
Nasef A, Ashammakhi N, Fouillard L (2008) Immunomodulatory effect of mesenchymal stromal cells: possible mechanisms. Regen Med 3(4):531–546
Nilsson I, Hoffmann I (2000) Cell cycle regulation by the Cdc25 phosphatase family. Prog Cell Cycle Res 4:107–114

Novoselova EG, Lunin SM, Khrenov MO et al (2015) Changes in immune cell signalling, apoptosis and stress response functions in mice returned from the BION-M1 mission in space. Immunobiology 220(4):500–509

O'Donoghue K, Choolani M, Chan J et al (2003) Identification of fetal mesenchymal stem cells in maternal blood: implications for non-invasive prenatal diagnosis. Mol Hum Reprod 9(8):497–502

Ontiveros C, McCabe LR (2003) Simulated microgravity suppresses osteoblast phenotype, Runx2 levels and AP-1 transactivation. J Cell Biochem 88(3):427–437

Orlic D, Kajstura J, Chimenti S et al (2001) Mobilized bone marrow cells repair the infarcted heart, improving function and survival. Proc Natl Acad Sci USA 98(18):10344–10349

Oscarsson N, Ny L, Molne J et al (2017) Hyperbaric oxygen treatment reverses radiation induced pro-fibrotic and oxidative stress responses in a rat model. Free Radic Biol Med 103:248–255

Owen TA, Aronow M, Shalhoub V et al (1990) Progressive development of the rat osteoblast phenotype in vitro: reciprocal relationships in expression of genes associated with osteoblast proliferation and differentiation during formation of the bone extracellular matrix. J Cell Physiol 143(3):420–430

Pan Z, Yang J, Guo C et al (2008) Effects of hindlimb unloading on ex vivo growth and osteogenic/adipogenic potentials of bone marrow-derived mesenchymal stem cells in rats. Stem Cells Dev 17(4):795–804

Pantano C, Reynaert NL, van der Vliet A et al (2006) Redox-sensitive kinases of the nuclear factor-kappaB signaling pathway. Antioxid Redox Signal 8(9–10):1791–1806

Pereira RF, Halford KW, O'Hara MD et al (1995) Cultured adherent cells from marrow can serve as long-lasting precursor cells for bone, cartilage, and lung in irradiated mice. Proc Natl Acad Sci USA 92(11):4857–4861

Pi J, Zhang Q, Fu J et al (2010) ROS signaling, oxidative stress and Nrf2 in pancreatic beta-cell function. Toxicol Appl Pharmacol 244(1):77–83

Platt ID, El-Sohemy A (2009) Regulation of osteoblast and adipocyte differentiation from human mesenchymal stem cells by conjugated linoleic acid. J Nutr Biochem 20(12):956–964

Qiu X, Brown K, Hirschey MD et al (2010) Calorie restriction reduces oxidative stress by SIRT3-mediated SOD2 activation. Cell Metab 12(6):662–667

Reuter S, Gupta SC, Chaturvedi MM, Aggarwal BB (2010) Oxidative stress, inflammation, and cancer: how are they linked? Free Radic Biol Med 49(11):1603–1616

Rodriges Blanko E, Kadyrova LY et al (2016) DNA mismatch repair interacts with CAF-1- and ASF1A-H3-H4-dependent Histone (H3-H4)2 tetramer deposition. J Biol Chem 291(17):9203–9217

Rucci N, Rufo A, Alamanou M et al (2007) Modeled microgravity stimulates osteoclastogenesis and bone resorption by increasing osteoblast RANKL/OPG ratio. J Cell Biochem 100(2):464–473

Saxena R, Pan G, Dohm ED, McDonald JM (2011) Modeled microgravity and hindlimb unloading sensitize osteoclast precursors to RANKL-mediated osteoclastogenesis. J Bone Miner Metab 29(1):111–122

Schneider V, Oganov V, LeBlanc A et al (1995) Bone and body mass changes during space flight. Acta Astronaut 36(8–12):463–466

Sherr CJ (1996) Cancer cell cycles. Science (New York, N.Y.) 274(5293):1672–1677

Shi D, Meng R, Deng W et al (2010) Effects of microgravity modeled by large gradient high magnetic field on the osteogenic initiation of human mesenchymal stem cells. Stem Cell Rev 6(4):567–578

Smith ML, Ford JM, Hollander MC et al (2000) p53-mediated DNA repair responses to UV radiation: studies of mouse cells lacking p53, p21, and/or gadd45 genes. Mol Cell Biol 20(10):3705–3714

Sotiropoulou PA, Papamichail M (2007) Immune properties of mesenchymal stem cells. Methods Mol Biol 407:225–243

Strewe C, Crucian BE, Sams CF et al (2015) Hyperbaric hyperoxia alters innate immune functional properties during NASA Extreme Environment Mission Operation (NEEMO). Brain Behav Immun 50:52–57

Sun Z, Cao X, Hu Z et al (2015a) MiR-103 inhibits osteoblast proliferation mainly through suppressing Cav1.2 expression in simulated microgravity. Bone 76:121–128
Sun Z, Cao X, Zhang Z et al (2015b) Simulated microgravity inhibits L-type calcium channel currents partially by the up-regulation of miR-103 in MC3T3-E1 osteoblasts. Sci Rep 5:8077
Sykiotis GP, Habeos IG, Samuelson AV et al (2011) The role of the antioxidant and longevity-promoting Nrf2 pathway in metabolic regulation. Curr Opin Clin Nutr Metab Care 14(1):41–48
Tamma R, Colaianni G, Camerino C et al (2009) Microgravity during spaceflight directly affects in vitro osteoclastogenesis and bone resorption. FASEB J Off Publ Fed Am Soc Exp Biol 23(8):2549–2554
Tilton FE, Degioanni JJ, Schneider VS (1980) Long-term follow-up of Skylab bone demineralization. Aviat Space Environ Med 51(11):1209–1213
Tontonoz P, Hu E, Spiegelman BM (1994) Stimulation of adipogenesis in fibroblasts by PPAR gamma 2, a lipid-activated transcription factor. Cell 79(7):1147–1156
Tuan RS, Boland G, Tuli R (2003) Adult mesenchymal stem cells and cell-based tissue engineering. Arthritis Res Ther 5(1):32–45
Versari S, Longinotti G, Barenghi L et al (2013) The challenging environment on board the International Space Station affects endothelial cell function by triggering oxidative stress through thioredoxin interacting protein overexpression: the ESA-SPHINX experiment. FASEB J Off Publ Fed Am Soc Exp Biol 27(11):4466–4475
Wang T (2008) 2007 annual meeting of American Heart Association and the latest results of cardiac resuscitation. Chin Emerg Med 28:112–113
Wang T, Fu Y, Fang XS (2007) Differentiation and identification of bone marrow mesenchymal stem cells into cardiomyocytes in vitro. J Sun Yat-Sen Univ 28:S9–11
Wang X, Guo B, Li Q et al (2013) miR-214 targets ATF4 to inhibit bone formation. Nat Med 19(1):93–100
Wang T, Sun Q, Xu W et al (2015) Modulation of modeled microgravity on radiation-induced bystander effects in Arabidopsis thaliana. Mutat Res 773:27–36
Warejcka DJ, Harvey R, Taylor BJ et al (1996) A population of cells isolated from rat heart capable of differentiating into several mesodermal phenotypes. J Surg Res 62(2):233–242
Yang Z, Song L, Huang C (2009) Gadd45 proteins as critical signal transducers linking NF-kappaB to MAPK cascades. Curr Cancer Drug Targets 9(8):915–930
Yu FX, Chai TF, He H, Hagen T, Luo Y (2010) Thioredoxin-interacting protein (Txnip) gene expression: sensing oxidative phosphorylation status and glycolytic rate. J Biol Chem 285(33):25822–25830
Zayzafoon M, Gathings WE, McDonald JM (2004) Modeled microgravity inhibits osteogenic differentiation of human mesenchymal stem cells and increases adipogenesis. Endocrinology 145(5):2421–2432
Zhang Y, Lu T, Wong M et al (2016) Transient gene and microRNA expression profile changes of confluent human fibroblast cells in spaceflight. FASEB J Off Publ Fed Am Soc Exp Biol 30(6):2211–2224
Zhang Z, Lang J, Cao Z et al (2017) Radiation-induced SOD2 overexpression sensitizes colorectal cancer to radiation while protecting normal tissue. Oncotarget 8(5):7791–7800
Zhang C, Li L, Jiang Y et al (2018) Space microgravity drives transdifferentiation of human bone marrow-derived mesenchymal stem cells from osteogenesis to adipogenesis. FASEB J Off Publ Fed Am Soc Exp Biol 32(8):4444–4458
Zong C, Xue D, Yuan W et al (2010) Reconstruction of rat calvarial defects with human mesenchymal stem cells and osteoblast-like cells in poly-lactic-co-glycolic acid scaffolds. Eur Cells Mater 20:109–120
Zuo B, Zhu J, Li J et al (2015) microRNA-103a functions as a mechanosensitive microRNA to inhibit bone formation through targeting Runx2. J Bone Miner Res Off J Am Soc Bone Miner Res 30(2):330–345

Facilities and Techniques of Space Life Science

Meimin Zhang, Weibo Zheng, Guanghui Tong, Zengchuang Xu, Yin Zhang, Yongchun Yuan, Hao Sun, Fangwu Liu, Kun Ding and Tao Zhang

Abstract The life science research facility is an important technical means and basic condition guarantee for the development of space life science and biotechnology. Silkworm Culture Apparatus (SCA), Stem Cell Culture Apparatus (SCCA), Embryo Culture Apparatus (ECA), Plant Culture Apparatus (PCA) and Higher Plant Culture Apparatus (HPCA) are customized space life science experiment facilities, developed to carry out several different life science experiments in space microgravity condition, which are on board SJ-10 recoverable science experimental satellite (SJ-10 satellite). In this chapter, the composition, structure, function and space experiment process of ECA, SCCA, SCA, APCA, and PCA are introduced. The common key technologies of each apparatus are summarized and the feasibility of each apparatus in preflight and space flight stage are analyzed.

Abbreviation

ABRS	Advanced Biological Research System
ADSEP	Advanced Separations Processing Facility
BS	Bioculture System
ECA	Embryo Culture Apparatus
HPCA	Higher Plant Culture Apparatus
ISPR	International Standard Payload Rack
ISS	International Space Station
PCA	Plant Culture Apparatus
SCA	Silkworm Culture Apparatus
SCCA	Stem Cell Culture Apparatus
SJ-10 satellite	SJ-10 recoverable microgravity experimental satellite

M. Zhang · W. Zheng · G. Tong · Z. Xu · Y. Zhang · Y. Yuan · H. Sun · F. Liu · K. Ding · T. Zhang (✉)
Shanghai Institute of Technical Physics, Chinese Academy of Sciences, Shanghai, China
e-mail: haozzh@sina.com

E. Duan and M. Long (eds.), *Life Science in Space: Experiments on Board the SJ-10 Recoverable Satellite*, Research for Development,
https://doi.org/10.1007/978-981-13-6325-2_13

1 Introduction

Silkworm Culture Apparatus (SCA), Stem Cell Culture Apparatus (SCCA), Embryo Culture Apparatus (ECA), Plant Culture Apparatus (PCA) and Higher Plant Culture Apparatus (HPCA) are customized space life science experiment facilities, developed to carry out several different life science experiments in space microgravity, which are loaded on China recoverable science experiment satellite (Table 1). SCA is used for space radiation biology research with silkworm embryos. SCCA is used for 3D cell culture and biotechnology experiment in microgravity with two kinds of different stem cells. ECA is used for embryonic development research in space with mice embryos. PCA is used for signal transduction mechanism research in Arabidopsis seedlings. HPCA is used for researching effect of illumination cycles on higher plant.

2 International Progress of Space Life Science Experiment Facilities

With development of space science and technology, the space life science experiment and research has gradually formed a new subject, and the research content has involved widely, which covers the biological effects of space environment factors, effects of gravity on the evolution of life and physiological activities, space biotechnology of producing significant biological products, space controlled ecological protection technology such as energy/material cycle model on long-term orbit, space medicine of human being's physiological and psychological state and astrobiology for origin of life and detection of extraterrestrial life traces and so on. All of these research work get further at both micro cell molecular level and macro comprehensive level. As a result, there are higher demands for the complexity, advancement and completeness of the experimental equipment.

Table 1 Five space life science experiment facilities developed by Shanghai Institute of Technical Physics

Facility	Space experiment
Silkworm Culture Apparatus (SCA)	Effects of space environment on silkworm embryo development and mechanism of mutation
Plant Culture Apparatus (PCA)	Biological effects and the signal transduction of microgravity stimulation in plants
Higher Plant Culture Apparatus (HPCA)	Photoperiod-controlling flowering of Arabidopsis and rice in microgravity
Stem Cell Culture Apparatus (SCCA)	Three-dimensional cell culture of neural stem cells in space
Embryo Culture Apparatus (ECA)	Development of mouse early embryos in space

It is possible to establish and use various kinds of advanced space experiment system on large spacecraft platform and reciprocating spacecraft. Advanced space biology experiment system provides superior environmental conditions and support capabilities for space life science experiments and research: more adequate volume, weight and power consumption in terms of resources; more appropriate temperature, humidity and air pressure in terms of environmental conditions; more refined imaging, spectroscopy and interference technology in terms of detection means; many types of work mode including automatic, manual, remote science and others in terms of the experimental operation method.

The establishment and application of the International Space Station (ISS) marks a great breakthrough in the space science experiments. ISS provides a special laboratory for exploring the basic problems of many disciplines. It is an effective test platform to verify the research results which cannot be verified on the ground, making ISS a new starting point of deep space exploration. A variety of experimental facilities developed for ISS research such as biomedicine, basic biology, biotechnology and other fields of life science development reflect the level of the current international space life science experiment facilities and technology.

The features of design, function and operation of ISS science experiment equipment are mainly in the following aspects.

(1) "Top-to-Down" design

The top layer of ISS major research facilities is device-level payloads—international standard payload rack (ISPR), which is a key part for development of next level basic laboratory instrument ISS experiment system; the second layer is a standard special drawer-style laboratory cabinet installed in ISPR; the third layer is experiment instrument in the special laboratory cabinet and the bottom layer is all kinds of standard components for specific function within the instrument for the experiment. Using this top-down design method to develop the entire equipment and instrumentation system can make the best use of the space experiment resources that the ISS environment can provide.

(2) Unified standard design

From the ISPR design of hardware modules to achieve special function, the same specifications and standards are widely used. ISPR has standardized ISIS (International Subrack Interface Standard) interfaces, including mechanical interfaces with standard guide rails and slide guide mechanisms, and blind with the power supply and data transmission electrical interface, the next level of experimental equipment can be easily installed in the ISPR. Different hardware modules with different functions are also standardized, so that each module has standardized external dimensions, standard mechanical interfaces, and electrical interfaces. The replacement between modules is simple and easy to operate. For example, the Advanced Separations Processing Facility (ADSEP) device developed by Space Hardware Optimization Technology, Inc. in the United States contains six modules with standardized design for cell dynamics, space pharmacy development, and space bimolecular separation techniques. The standardized design provides technical basis for the exchange of

research equipment and resource sharing between different countries or research institutions in the ISS.

(3) System design maintains good compatibility and continuous advancement

The ISPR design aims at multi-users. Under the premise of adopting the standard modular design, the secondary drawer standard special experiment cabinet provides flexible design and installation conditions, allowing researchers to design unique and dedicated research components to meet the needs of special experiments. The experimental device can be designed as an independent and complete instrument, installed on a platform with a locking function cabinet, or the experimental device can be designed as several components or components, and assembled into experimental instruments in a standard dedicated experimental cabinet, with good compatibility. At the same time, the development of system hardware adopts continuous supplementing, perfecting, and improving design methods, so that it is always on the basis of inheriting the original technology and has the rising space for continuous development, ensuring that the experimental system has continuous advancement. The life science experiment facilities on ISS are shown in Table 2.

Table 2 Life science experiment facilities on ISS

Facility	Space experiment
The Advanced Biological Research System (ABRS)	Space biology of plant growth or other small biological samples
Advanced Plant Experiment (APEX)	Plant growth genetics research
The Transgenic Arabidopsis Gene Expression System (TAGES)	The transgenic arabidopsis gene expression
Biological Laboratory (BioLab)	Support biological experiments on micro-organisms, cells, tissue cultures, small plants and small invertebrates
The Bioculture System (BS)	Workbench and storage cabinet
The Vegetable Production System (VEGGIE)	Plant growth and development
Autonomous Biological System (ABS)	Highly self-regulating environment allows controlled proliferation of aquatic samples
Aquatic Habitat (AQH)	Aquatic habitat
NanoRacks Astrium Centrifuge (NRAC)	Biological and microbiological experiments
European Modular Cultivation System (EMCS)	Life science and biotechnology
Astro Garden (Astro Garden)	Plant growth
Portable Astroculture Chamber (PASC)	Life science and biotechnology
X-ray Crystallography Facility (XCF)	Dedicated experimental system for analyzing crystal growth process of macromolecular proteins
Fluorescence Based Biosensor (FBB)	Space microbiological monitoring

(4) Advanced observation, measurement and analysis technologies

The ISS experiment system is equipped with many advanced observation, measurement and analysis equipment, making it easy for researchers to operate the ISS space science experiments as it is at the ground laboratory. ISPR's standard video signal interface stores image information formed in various locations of experimental instruments in real-time through optical fibers and transmitted to ground laboratories. Optical detection technologies (such as laser light scattering, optical interference, X-ray diffraction, etc.) are increasingly used. On the one hand, on-site measurement and real-time analysis of important and unstable biological product components has been realized, changing only the results at an early stage without knowing the status of the process; on the other hand, the quantitative analysis of the change process of space experiment is realized, and create conditions for obtaining scientific significance research results.

(5) Flexible and diverse space experimental operation method

On the one hand, the existence of astronauts makes the operation of space experiments more flexible, and the space operation methods can be divided into several categories, such as astronaut operation, non-astronaut operation, automatic and remote operation. On the other hand, the operation of space experiment contains a multidisciplinary research content, and the professional level is high. Therefore, ISS has established extensive communication, such as voice, image, telemetry and transmit the real-time/delay data, so that the ground professional researchers can fully evaluate the status of the orbit test, and adjust the experimental process. Within the resource constraints, ISS designed a flexible way to enhance the scientists to control the experimental process. First, the ground scientists carefully analyze the previous experimental data and experimental methods, then submit a detailed operation plan in a week before the operation of space experiments, so the effect and quality of the whole space experiment is improved.

(6) Networked control and management

Networked control management Distributed management of payload through automatic data switching. Three data communication network modes are used in this management mode: MIL-STD-1553B payload bus; 802.3 Ethernet; high speed optical data transmission network. All payloads are associated with these three networks. The main control module manages each functional module through addressing and communication. Due to the uniqueness of the instrument control identification, no matter which cabin it is installed in, it can be accurately operated and controlled by a unique equipment identification, including power supply, switch and other operations, acquisition, storage and transmission of the telemetry parameters in various functional modules (such as: temperature, device status, etc.), the functional modules share the data bus, forming a complete network management system.

3 Progress of Space Life Science Experiment Facilities in China

In the past, Chinese space industry has achieved rapid development. Under the support of the national "863" program and the "921" project, China's space science has been greatly developed. A large number of space flight and ground simulations have been carried out, and a series of research results have been obtained. "Shenzhou" series of spacecraft have been equipped with a general biological incubator, protein crystallization device, animal and plant cell fusion device and other space life science experimental equipment, conducting a large number of space biology experimental research.

The crystal growth observation device uses transparent oxide crystals of lithium tetraborate and potassium niobate as experimental materials on the Shenzhou-2 spacecraft. The correlation between the fluid effect and the material preparation has been successfully studied. Figure 1 shows observations of crystal growth observed on satellites and spacecrafts in China in 1996 and 2000. The magnification is 1.5 times and the focusing accuracy is 0.1 mm. It can be saved by tape recording and image transmission.

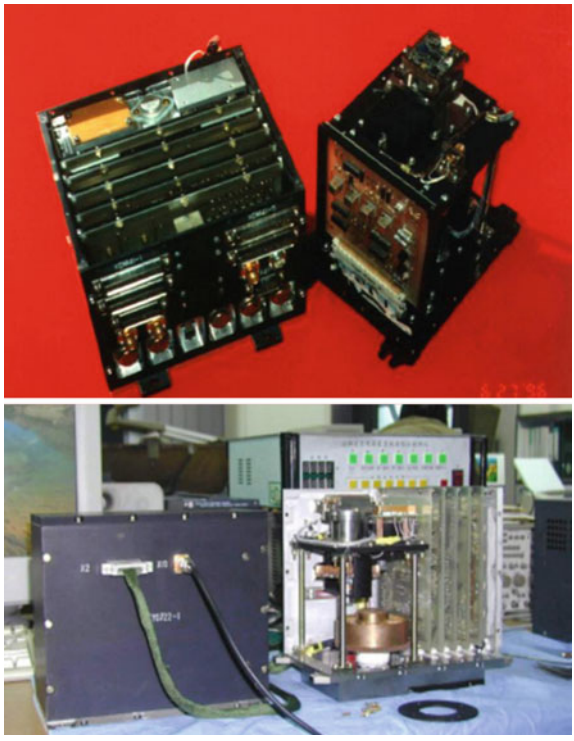

Fig. 1 Crystal growth observation device

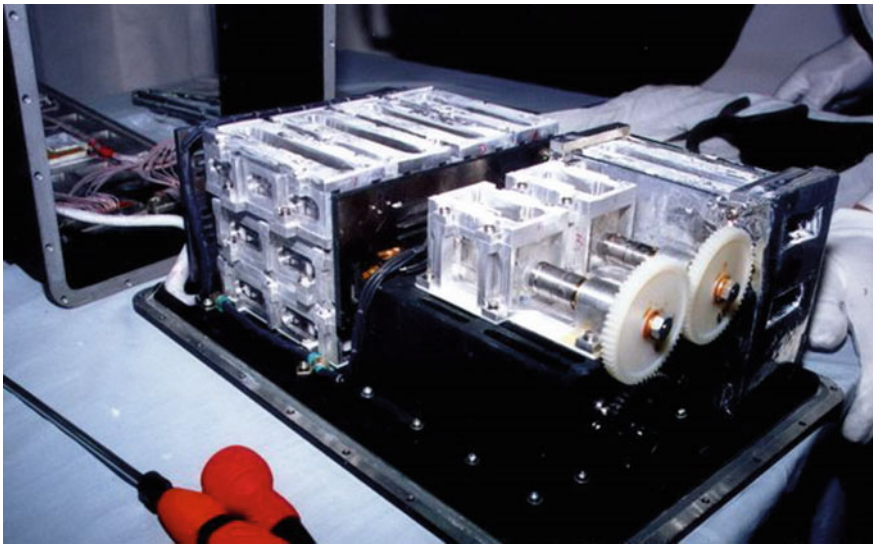

Fig. 2 Space protein crystallization device on Shenzhou-2 and 3 spacecraft

Experimental facilities for life science research in manned space missions mainly include space protein crystallization devices, cell bioreactors, space cell electrofusion devices, space continuous free flow electrophoresis devices, and space biological incubators.

The space protein crystallization device is shown in Fig. 2. The active temperature control is used to control the crystallization temperature to 20 ± 1 °C and 4 ± 1 °C, respectively; the crystallization method is vapor phase diffusion and liquid-liquid diffusion; the crystallization chamber is in the form of a skateboard and cock-style two. The experimental device can perform 60 component sample experiments in one flight, and the sample is recovered with the device. A total of 120 samples of 30 proteins were subjected to crystallization experiments. The crystallization rate reached 70%, and several high-quality crystals that could be used for crystal structure analysis were obtained. The human dehydroisandone sulfotransferase protein crystals obtained in the Shenzhou-3 spacecraft experiment are one of the best growing protein crystals in the space experiments to date.

Cell reactors are used to culture human tissue lymphoma cells, human granulocyte lymphocytes, anti-Chlamydia protein mouse lymphocyte hybridoma cells, and anti-anthrax protein mouse lymphocyte hybridoma cells, which focus on current major human diseases, and on the research of special biological effects in space. The drug cell culture experiment was a complete success, as shown in Figs. 3 and 4. With active temperature control, a device containing two independent experimental groups is suitable for spatial electrofusion experiments of animals and plants. Samples are recovered with the device. Space cell electrofusion devices are used to study the method of space cell fusion and to open up new methods for cell engineering. Cell fusion

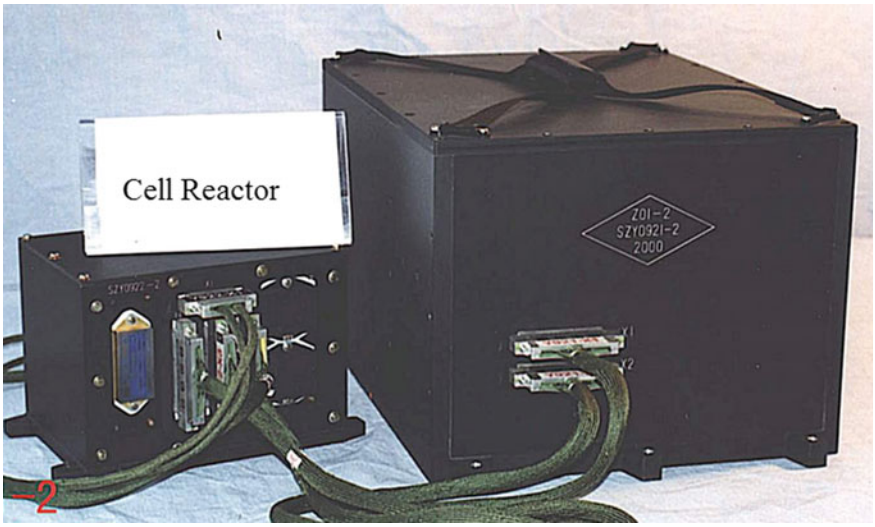

Fig. 3 Cell reactor on Shenzhou 3 spacecraft

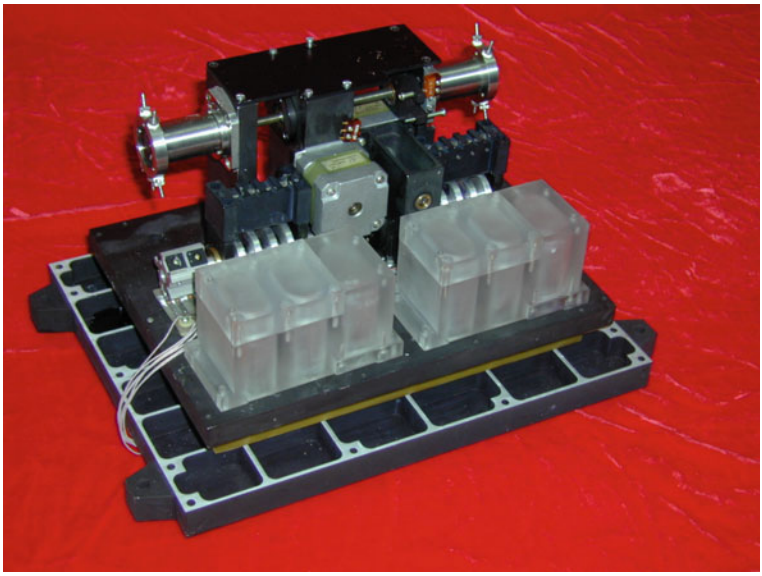

Fig. 4 Space cell fusion apparatus

Fig. 5 Embryonic culture observation system

is a new approach to biopharmaceuticals based on the principle of "complementary advantages", selecting biological cells with different advantages, conducting asexual hybridization, and acquiring and nurturing bioengineering of new species. Taking advantage of space microgravity conditions can increase the yield of hybrid cells.

In 2006, observation experiments on the cultivation of mouse embryos and observation experiments on vegetative growth and reproductive growth of higher plants were carried out on SJ-8 satellite (Lu et al. 2008). The embryo culture observation system realized automatic searching, capturing and microscopic imaging of mouse embryos with a spatial distribution of 60–100 μm in three dimensions in the culture unit (Fig. 5). The supported microscope objective magnification was from 4× to 40×, and the automatic search and capture range was 10.3 mm and the micro displacement control accuracy is 2.5 μm. The space higher plant culture observation system realized real-time image monitoring of the whole process of seedling germination, seedling growth, and flowering of the experimental plants in a space-tight environment, as well as the whole process real-time microscopic image monitoring of flower buds, blooming, and fading of the sample plant flowers (Fig. 6).

Fig. 6 Higher plant culture observation system

The Chinese Academy of Sciences and the German Space Agency collaborated to carry out a common biological incubator experimental study (Peter and Markus 2014). The BIOBOX general biological incubator experiment (Jin et al. 2014; Zhang et al. 2015) was completed on the Shenzhou-8 spacecraft from November 1st to 17th, 2011.

4 Goals and Primary Results of Space Life Science Experiment Facilities on SJ-10 Satellite

4.1 Silkworm Culture Apparatus (SCA)

4.1.1 Preface

SCA (Fig. 7) is used for radiation biology research in space with silkworm embryos on China recoverable science satellite.

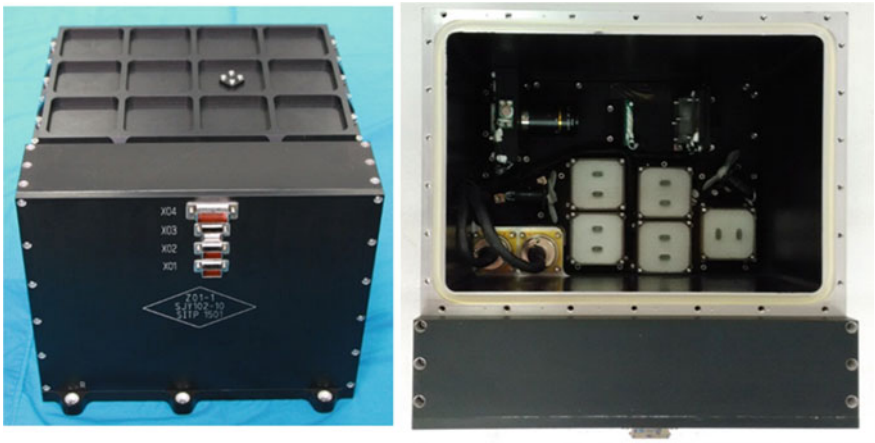

Fig. 7 Silkworm culture apparatus (SCA)

The main functions of SCA are as follows: (1) Suitable for the resource and constraint conditions of recoverable satellite platform such as volume, mass, power; Meeting the needs of the biological research under the condition of existing resources on satellite; (2) Providing the required environment for continuous culture silkworm for more than 12 days in space flight; (3) Providing monitoring and control of temperature and other life support conditions; (4) Fixing biological samples in stages according to the growth cycle of biological samples.

The batch fixing technology of biological samples and the silkworm culture technology in a space enclosed environment are the main technical difficulties and key points of SCA. SCA successfully completed the space flight experiment, and achieved low-temperature fixation of silkworm. The first successful acquisition of images of the silkworm embryo development process provided good support for scientific research.

4.1.2 System Components

There are 6 experiment units (Fig. 8) in SCA, each experiment unit has two experiment containers. Experiment unit 1 to experiment unit 5 can be fixed below 6 °C. Experiment Unit 6 is not fixed at a low temperature, the temperature is kept at a temperature of 23 ± 4 °C, and imaging observation is available. Life support unit provides the required environment for the silkworm experiment including a controlled thermal environment, atmospheric environment and enough oxygen. Fixation unit fixes silkworm eggs in stages according to the growth cycle of biological samples. Camera associate with a LED light is used to observe the silkworm hatch and record the experimental images; Electrical control unit is core control module of the facility, including secondary power conversion, temperature comparison and control,

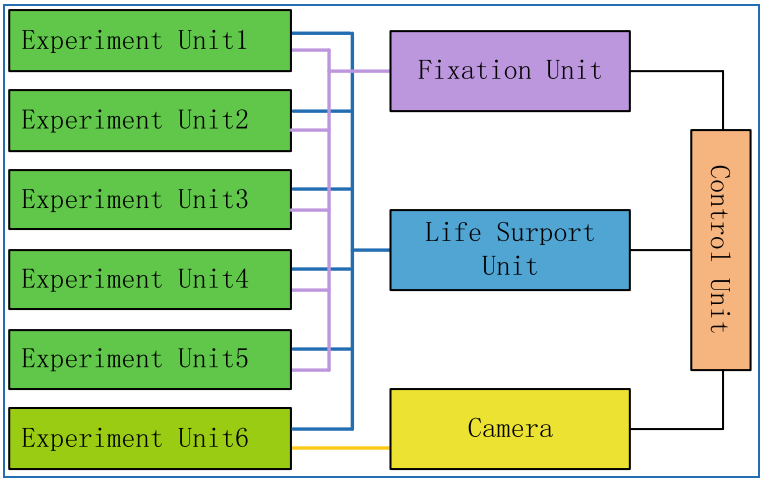

Fig. 8 SCA function composition

control of the experimental process, and reception remote control/program control commands and data exchange with satellite measurement and control systems.

4.2 Main Technical Indicators

The main technical indicators of SCA are shown in Table 3.

Table 3 Main technical indicators of SCA

Parameter	Numerical value
Weight	13.5 ± 0.2 kg
Size	300 mm × 300 mm × 250 mm
Power dissipation	≤15 W
Period	12d
Specimen quantity	6 groups
Culture temperature	23 ± 4 °C
Fixation	Low temperature fixation, 5 groups
Storage temperature	≤6 °C
Imaging	Image, 1 group

4.3 Key Technologies

(1) Closed culture of silkworm eggs in space

The key technology for silkworm culture is to provide appropriate life support conditions, including temperature, air pressure, and oxygen supply. The development of this project fully utilized the experimental basis of the ground-based silkworm culture, combined with the existing space biological culture technology and the development experience of the culture device, and multiple matching experiments (Fig. 9) to solve the space closed culture technology of silkworm. The oxygen supply of the culture unit is a passive method, which is mainly achieved through the exchange of gas between the culture unit and the SCA. In order to ensure the oxygen supply required by the biological sample during the cultivation process, the SCA must maintain enough space inside the incubator for storage the required air.

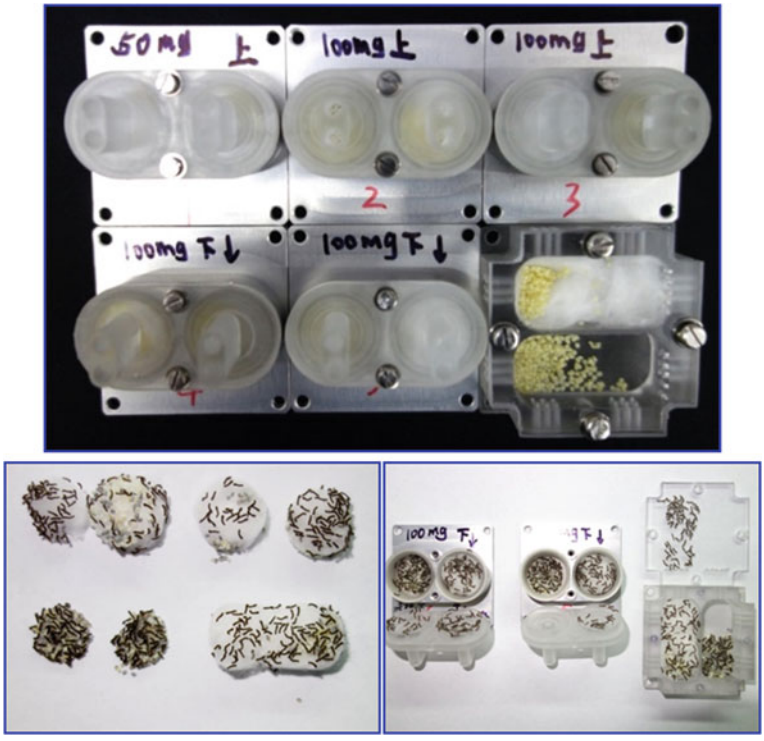

Fig. 9 Closed culture experiment (12d on ground)

(2) Multi-zone low temperature fixation

The method of independent temperature zone design combined with semiconductor rapid cooling technology is used to achieve the cryogenic fixation and preservation of biological samples. According to the demands of biological research, the biological samples are fixed in batches during the experimental process; using a low-temperature fixing method, a semiconductor chiller integrated with the silkworm culturing unit is started for cooling, and the temperature of the biological sample is reduced to fixed requirements (fixed, unit temperature is below 6 °C).

4.4 Space Flight Experiment

SCA conducted space flight experiments for 12 days and 14.5 h according to the on-orbit experimental procedure. The closed culture of silkworm eggs in space and multi-zone low temperature fixation technology was verified.

All the components and parts of SCA functioned properly. Through the analysis of the downlink data, the culture temperature was 20–22 °C, and the fixed temperature was 2–4 °C. For the first time, the image of the space development process of the silkworm embryo was successfully obtained. The obtained images of silkworm embryo development are shown in Fig. 10.

4.5 Facility and Specimen Recovery

On April 18, 2016, SCA was recovered successfully in Siziwangqi along with the returned SJ-10 satellite. After returning, the equipment was working properly. The facility and sample status of the recycling equipment are shown in Fig. 11. The recovered silkworm samples were in good condition and met the needs of scientific applications for further study.

5 Plant Culture Apparatus (PCA)

5.1 Preface

PCA (Fig. 12) is designed for the comparative analysis about different research material, which are plant hormone metabolism and signaling pathways interference genetically modified rice and their wild type, in microgravity environment.

Plant chemical fixing method and low temperature storage are the main technical difficulties and key points of PCA. The PCA successfully completed the space flight experiment, and achieved the first application of technologies and methods such as

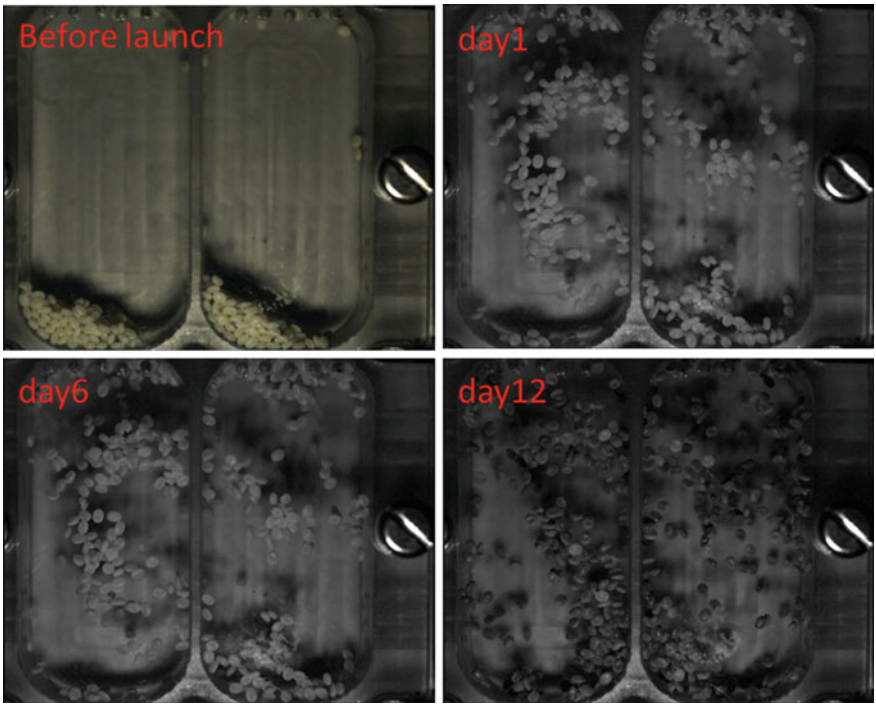

Fig. 10 Silkworm image in space flight

Fig. 11 SCA recovery

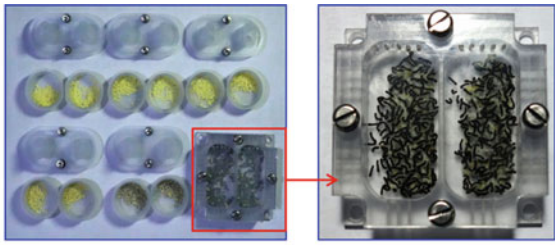

seedling chemical fixed storage and 3D printing special functional components in space life science experiments, which provided good support for scientific research.

On April 6, 2016, the PCA carrying the *Arabidopsis thaliana* seedlings was launched with the SJ-10 satellite and began a space flight test for approximately 12 days and 14.5 h. During the orbital operation, PCA successfully achieved chemical fixation and low-temperature storage of Arabidopsis seedlings. A total of 101 visible light images of the plant growth process in real time were obtained, as well as all in-orbit engineering parameters and scientific parameters. On April 18, 2016,

Fig. 12 Plant Culture Apparatus (PCA)

equipment and sample recovery operations were successfully performed at the recycling site, and satisfactory data and sample results were obtained.

5.2 System Components

Six independent experiment units are designed to cultivate plants for this space experiment, each experiment unit contains four to six plants (Fig. 13). After 12 days culture, plants in five experiment units are fixed with reagent. All fixed plants are kept in low temperature until they return to the lab for detailed analysis.

The experiment unit in PCA is designed as airtight box. All conditions that plants need to grow up will be supplied in PCA, such as water, air and nutrient, etc. Five of the six experiment units are temperature adjustable, each experiment unit connect with liquid management system. A camera is used to monitor the status of the plants while it growing up; the sixth experiment units are set in a normal temperature area with a spectrum camera to analysis spectrum character of the plants.

5.3 Main Technical Indicators

The main technical indicators of PCA are shown in Table 4.

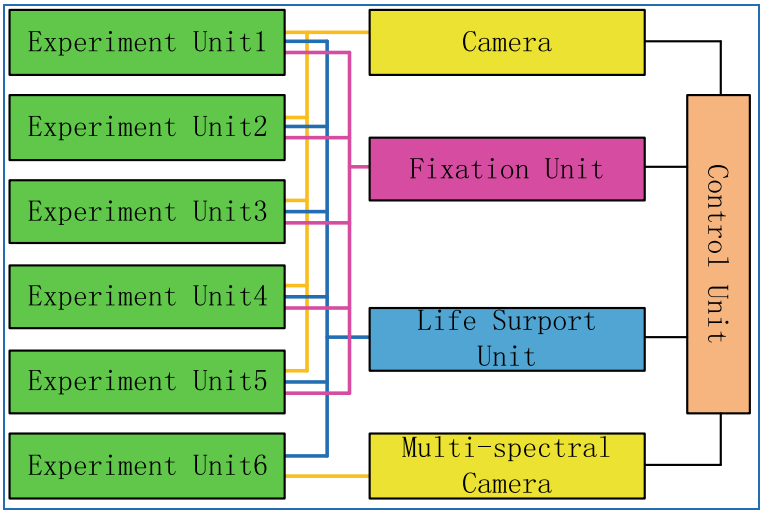

Fig. 13 PCA function composition

Table 4 Main technical indicators of PCA

Parameter	Numerical value
Weight	17.5 ± 0.2 kg
Size	350 mm × 350 mm × 250 mm
Power dissipation	≤25 W
Period	12d
Specimen quantity	6 groups
Culture temperature	22 ± 2 °C
Fixation	Chemical fixation, 5 groups
Storage temperature	≤10 °C
Imaging	1 group

5.4 Key Technologies

(1) Plant chemical fixing method and low temperature storage technology

The implementation of plant fixation under microgravity requires two steps: injecting the fixative solution into the plant cultivating unit and lowering the temperature of the culturing unit. Fixed-solution injection technology is realized by special design methods of transport pump injection of fixed fluid combined with culture unit structure. Ground injection test is used to verify the effective injection of fixed fluid; cooling preservation technology is implemented using a semiconductor refrigerator combined with an independent temperature zone design method; ensuring plant samples fixed effect. The fixed unit (Fig. 14) consists of a liquid reservoir, a check valve, an infusion pump and pipeline. According to the needs of biological experimental,

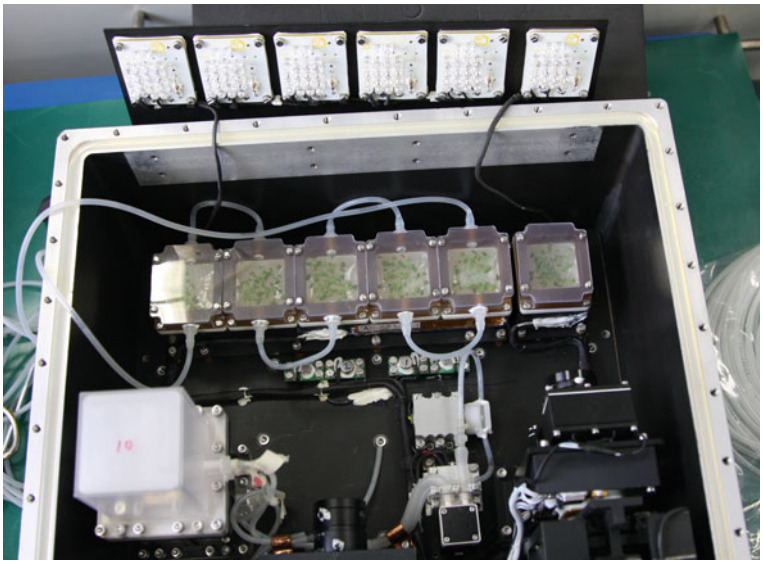

Fig. 14 Fixed unit

program-controlled instructions can be used for low-temperature fixation of plant biological samples during the experiment.

(2) Micro-spectral imaging analysis

The micro-multi-spectral fluorescence camera adopts the new technology of integrated optical splitter spectroscopy proposed by the Shanghai Institute of Technical Physics of the Chinese Academy of Sciences which is significantly reducing the volume and weight of the multi-spectral fluorescence camera. The technology was verified in space.

(3) The culture unit uses 3D printing (Fig. 15) to achieve special design

The culture unit adopts 3D printing to achieve special design and realizes the first application of technologies and methods such as 3D printing special function components in space life science experiments.

PCA successfully completed the space flight experiment, and achieved the first application of technologies and methods such as seedling chemical fixed storage and 3D printing special functional components in space life science experiments, which provided good support for scientific research.

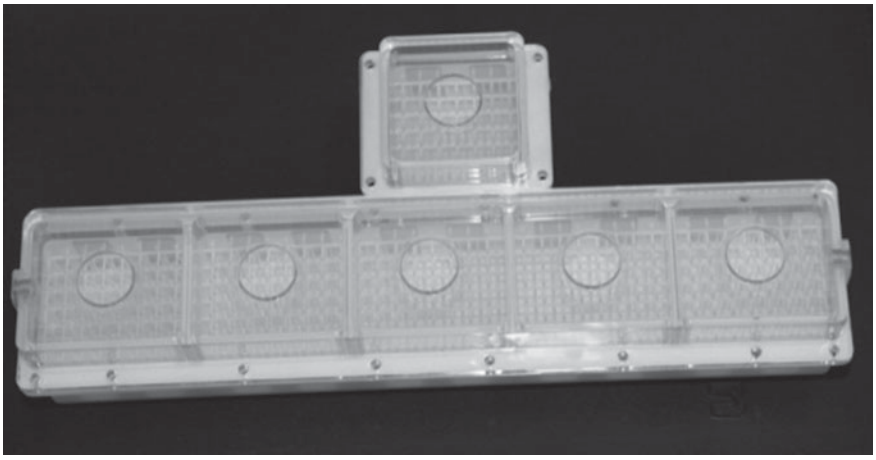

Fig. 15 The culture unit uses 3D printing

5.5 Space Flight Experiment

On April 6, 2016, the PCA carrying the *Arabidopsis thaliana* seedlings was launched with the SJ-10 satellite and began a space flight test for approximately 12 days and 14.5 h. During the orbital operation, PCA successfully achieved chemical fixation and low-temperature storage of Arabidopsis seedlings. A total of 101 visible light images of the plant growth process in real time were obtained, as well as all in-orbit engineering parameters and scientific parameters.

PCA worked properly in space. Culture temperature was 20–24 °C. Fixation storage temperature was 5–9 °C. Illumination was 6000–7000 lx. Arabidopsis was developed normally in space. Arabidopsis was fixed with chemical fixative in space (Figs. 16 and 17).

5.6 Facility and Specimen Recovery

On April 18, 2016, equipment and sample recovery operations were successfully performed at the recycling site, and satisfactory data and sample results were obtained (Fig. 18).

Fig. 16 Culture circumstance

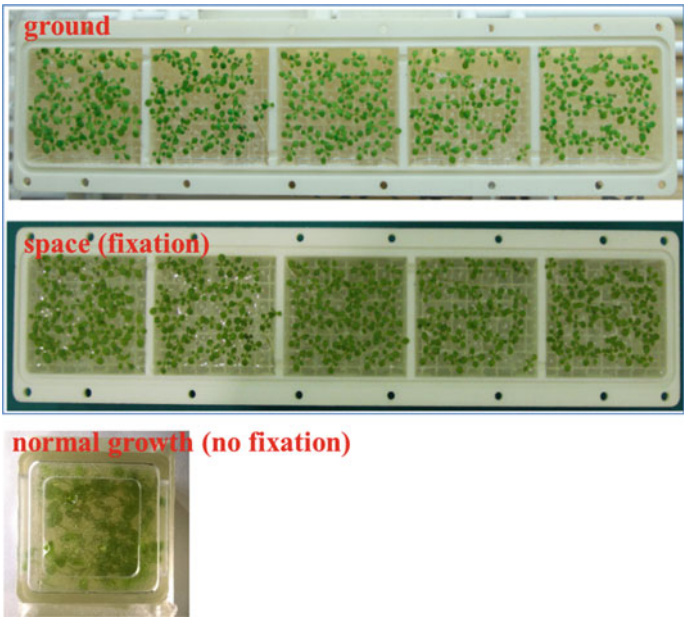

Fig. 17 Arabidopsis in space

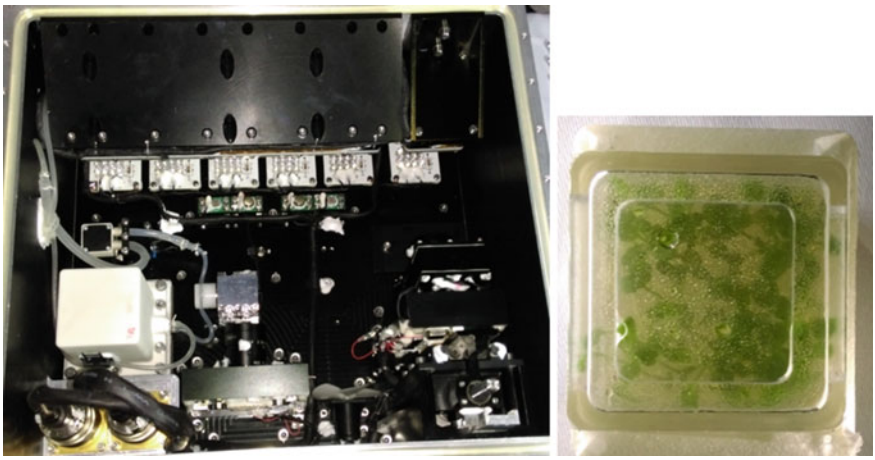

Fig. 18 PCA recovery

6 Higher Plant Culture Apparatus (HPCA)

6.1 Preface

HPCA (Fig. 19) is designed to research the effects of the microgravity on long day and short day photoperiod inducing flowering of plants and its molecular mechanism research of the influence of space experiments, using *Arabidopsis thaliana* and rice as the research materials.

The functions of the equipment include: adapting to the constraints of SJ-10 satellite platform, detection and controlling cultivating environmental temperature, providing lighting and on-line detection, acquisition of real-time color image information and fluorescence of the target sample during the space experiment process, image information, removal of harmful gases, etc.

The key point technologies of HPCA include activation of flowering gene expression in transgenic plant in space by heating and observed GFP gene expression in real-time through fluorescence imaging technology. HPCA successfully completed the space flight experiment. The first time the on-orbit track was successfully used to activate gene expression by thermal control and GFP fluorescence imaging technology of transgenic plants, which provided good support for scientific research.

On April 6, 2016, HPCA containing *Arabidopsis thaliana* and rice was launched with the SJ-10 satellite, and began a space flight experiment for about 12 days and 14.5 h. HPCA successfully achieved heat shock induced gene expression and GFP fluorescence imaging technology for transgenic plants for the first time on track. The long-day visible light image 101, short-day visible light image 48 and fluorescence were obtained. On April 18, 2016, equipment and sample recovery operations were

Fig. 19 Higher plant culture apparatus (HPCA)

successfully performed at the recycling site, and satisfactory data and sample results were obtained.

6.2 System Components

The units of HPCA (Fig. 20) main contains: cultivate unit, camera and electronic control unit. Training unit is mainly composed of rice cultivation box and Arabidopsis box. The cultivate unit mainly includes: Arabidopsis, paddy box of long-day; Arabidopsis, paddy box of short-day. Control unit mainly includes: Fluorescent camera, light unit, life support unit and camera.

Higher plant culture modules are divided into long-day light culture units and short-day light culture units. Shading partitions are used between long and short daylight culture units. Each culture unit contains two culture areas (*Arabidopsis thaliana* and rice). Each culture area is relatively Separation, air, moisture and light are shared. A short-day heat-activated start-up control unit (temperature controlled at 37° C for about 1 h) was set up in the *Arabidopsis thaliana* culture area for experimental studies of heat shock initiation gene expression.

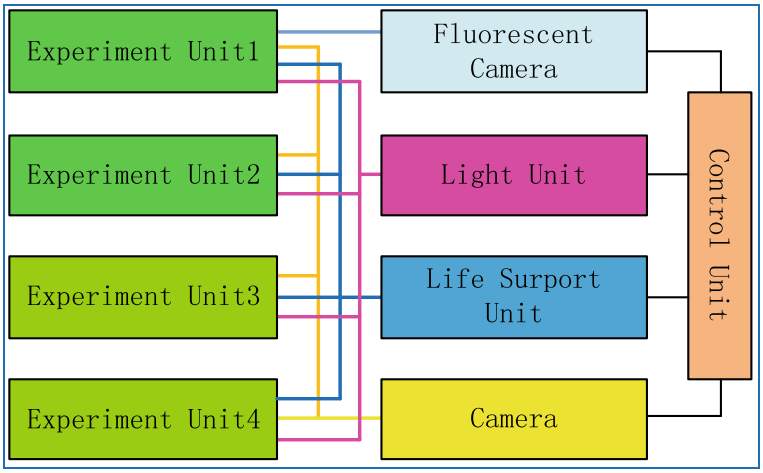

Fig. 20 HPCA function composition

Table 5 Main technical indicators of HPCA

Parameter	Numerical value
Weight	17.5 ± 0.2 kg
Size	370 mm × 270 mm × 270 mm
Power dissipation	≤45 W
Period	12d
Specimen quantity	4 groups
Culture temperature	18–28 °C
Light cycle	Long day (16 h light/8 h dark)/Short day (8 h light/16 h dark)
Light intensity	200 μmol/m^2 s
imaging	Fluorescent image

6.3 Main Technical Indicators

The main technical indicators of HPCA are shown in Table 5.

6.4 Key Technologies

(1) Gene expression thermal activation control of transgenic plant

The heat shock induction technology for gene expression of transgenic plants was successfully achieved for the first time in orbit; the heat shock temperature required for scientific samples was 37 °C. Heater and specially-designed fan structure were

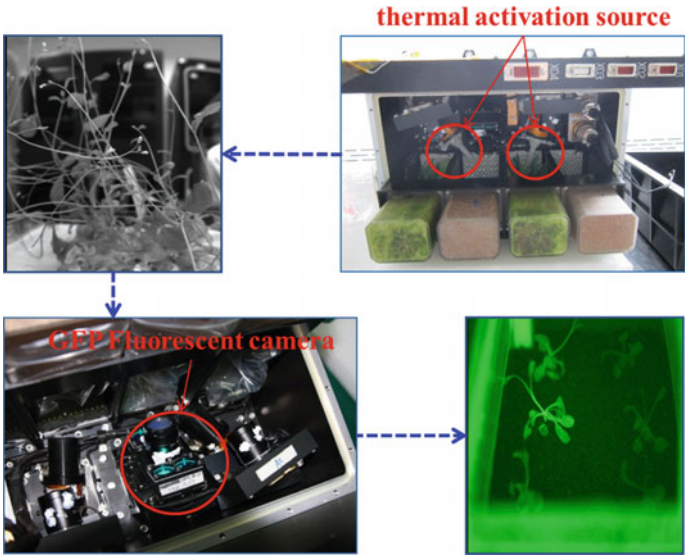

Fig. 21 Fluorescent image with GFP labeling technique

used to perform heat shock on transgenic Arabidopsis and rice plant samples. So, it is required to control the temperature accurately to 37 °C and to ensure the process of heat shock in the transgenic Arabidopsis and rice plants can completed effectively.

(2) GFP Fluorescent Image

HPCA successfully achieved heat shock induced gene expression and GFP fluorescence imaging (Fig. 21) technology for transgenic plants for the first time on track. The long-day visible light image 101, short-day visible light image 48 and fluorescence were obtained in real time for the growth and development of the downstream plants. With 48 images and all on-orbit engineering parameters and scientific parameters, the work is stable and reliable.

6.5 Space Flight Experiment

On April 6, 2016, HPCA containing *Arabidopsis thaliana* and rice was launched with the SJ-10 satellite, and began a space flight test for about 12 days and 14.5 h. HPCA successfully achieved heat shock induced gene expression and GFP fluorescence imaging technology for transgenic plants for the first time on track. The long-day visible light image 101, short-day visible light image 48 and fluorescence were obtained. On April 18, 2016, equipment and sample recovery operations were successfully performed at the recycling site, and satisfactory data and sample results were obtained.

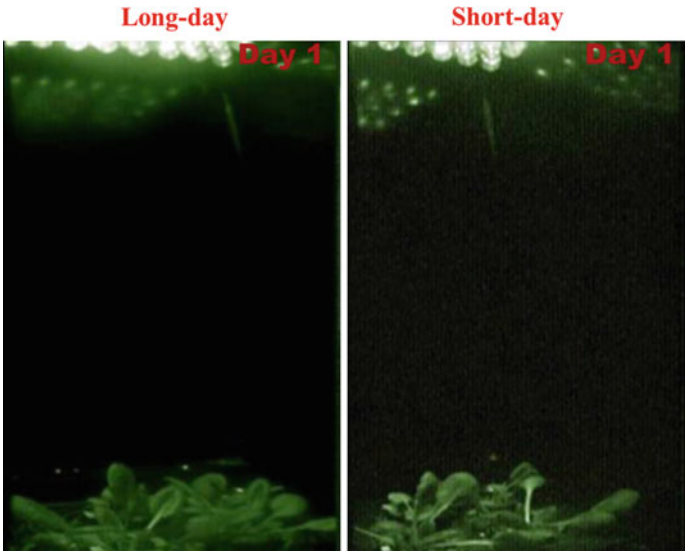

Fig. 22 HPCA images

All the components and parts of HPCA functioned properly. Through the analysis of the downlink data, the culture temperature was 20–23 °C, Rice illumination was 11,000–12,000 lx, Arabidopsis illumination was 6000–7000 lx. Observed specimen every 2 h and fluorescent imaged 48 times (Figs. 22 and 23).

6.6 Facility and Specimen Recovery

On April 18, 2016, equipment and sample recovery operations were successfully performed at the recycling site, and satisfactory data and sample results were obtained (Fig. 24).

7 Stem Cell Culture Apparatus (SCCA)

7.1 Preface

SCCA (Fig. 25) was used for 3D cell culture and biotechnology experiment in microgravity with 2 kinds of different stem cells. SCCA successfully completed the space flight experiment and the recovery of equipment and samples. Microscopic images

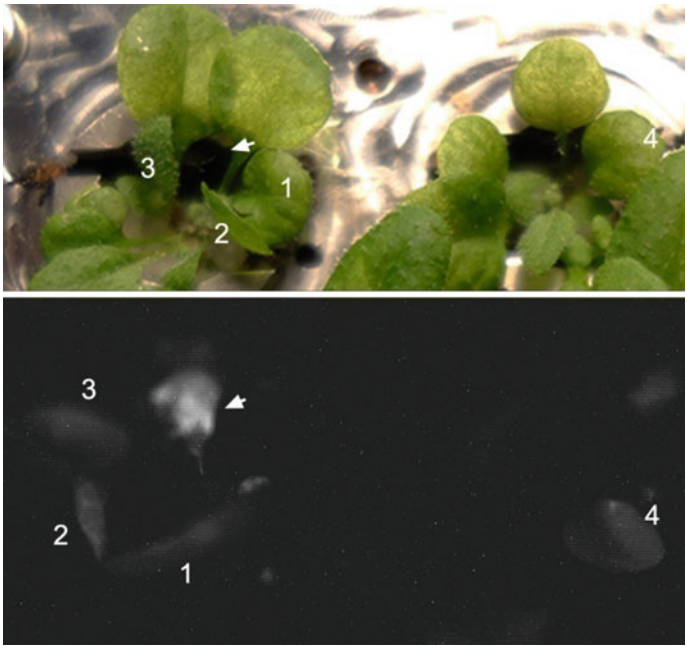

Fig. 23 Fluorescent image after thermal activation

of the proliferation and differentiation process of neural stem cells and hematopoietic stem cells were obtained, laying a very important foundation for further research.

The complicated liquid transportation, auto-focus microscope, multi-zone temperature control and two different chemical fixation methods are key technologies of SCCA.

7.2 System Components

SCCA (Fig. 26) consists of experiment units, auto-focus microscope, control unit, fixation units and life support unit. Sixteen experiment units in SCCA are divided into 4 groups, each group contains 4 experiment units. The group 1 is used for long term culturing, the group 2 and 3 are used for fixation with different chemical fixation liquid after culturing, the group 4 is used for imaging with auto-focus microscope during culturing.

SCCA consists of 3 layer structure within 16 cells, 16 sets of liquid line, 2 sets of 8-channel peristaltic pumps, 8 one-way valves, 4 liquid storage chambers, 4 liquid waste storage chambers, 8 membrane pumps, 4 culture solution and 2 stationary liquid.

Fig. 24 HPCA recovery

Fig. 25 Stem Cell Culture Apparatus (SCCA)

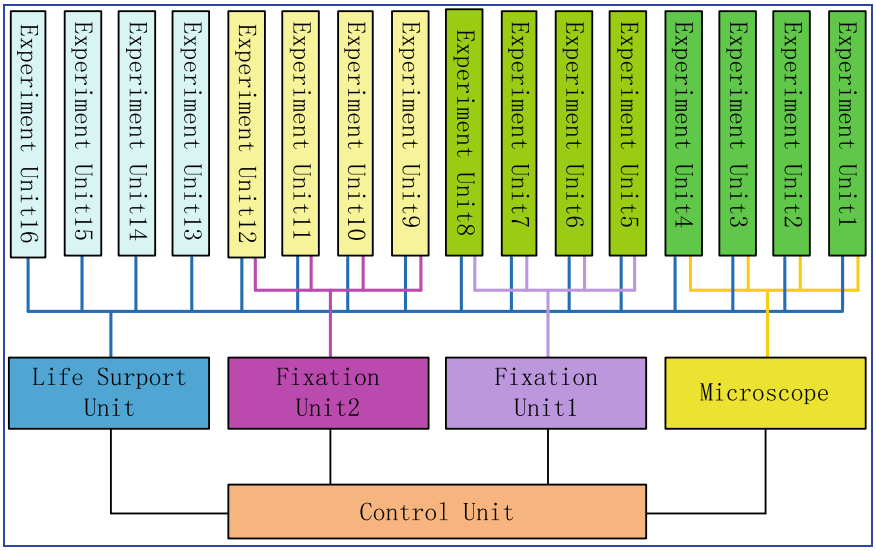

Fig. 26 SCCA function composition

7.3 Main Technical Indicators

The main technical indicators of SCCA are shown in Table 6.

Table 6 Main technical indicators of SCCA

Parameter	Numerical value
Weight	36 ± 0.33 kg
Size	400 mm × 300 mm × 400 mm
Power dissipation	≤28 W
Period	12d
Specimen quantity	4 groups
Culture temperature	36.5 ± 1 °C
Liquid transportation	16 channel, flow 0.5 ml/h ch
Fixation	Chemical fixation, 2 groups
Storage temperature	≤10 °C
imaging	Microscope, 1 group

7.4 Key Technologies

(1) Complicated 16-channel liquid transfer and control system, chemical fixation of stem cells and low temperature storage

The method of chemical fixation and cryopreservation is used for the fixed preservation of space stem cells. Through a combination of a fixed pump and a valve, the fixed solution is injected into the culture chamber, and the temperature control point of the temperature area is switched to achieve chemical fixation of the cell sample.

Under space microgravity conditions, through the use of a fully automatic perfusion culture method and the application of complex fluid pathway management techniques, the culture of stem cells for up to 12 days and the chemical fixation and cryogenic storage of on-orbit stem cells have been successfully achieved.

(2) In situ auto-searching and capturing microscopic image of stem cells

There are two kinds of hematopoietic stem cells and neural stem cells in SCCA. The target characteristics and scales of the two stem cells are different. The neural stem cells will aggregate and the hematopoietic stem cells do not aggregate. The microscope imaging design is compatible with stem cells at different scales. The microscopic imaging system (Fig. 27) consists of microscopic optics, illumination and autofocus components, image sensing components, and information processing. It is mainly used to obtain cell morphology and growth process.

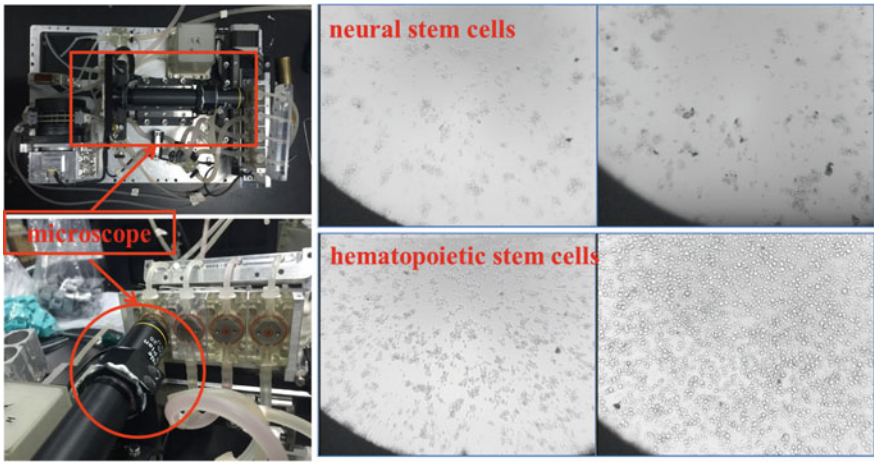

Fig. 27 Microscope of SCCA

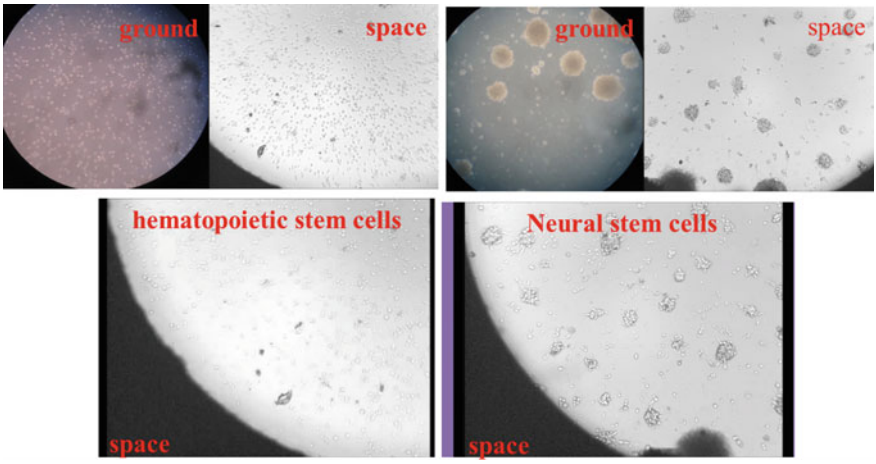

Fig. 28 Microscopic image of stem cells

7.5 Space Flight Experiment

On April 6, 2016, SCCA carrying hematopoietic stem cells and neural stem cells was launched with the SJ-10 satellite and began a space flight test for approximately 12 days and 14.5 h. SCCA successfully achieved perfusion culture and chemical immobilization of the sample. Real-time acquisition of 1184 microscopic images (Fig. 28) of the proliferation and differentiation process of the downstream neural stem cells and hematopoietic stem cells.

All the components and parts of SCCA functioned properly. Culture temperature was 36.5 ± 1 °C. Fixation liquid temperature was 5–6 °C. Fixation storage temperature was 5–6 °C. Microscope imaged 37 times.

7.6 Facility and Specimen Recovery

On April 18, 2016, equipment and sample recovery operations were successfully performed at the recycling site, and satisfactory data and sample results were obtained (Fig. 29).

Fig. 29 SCCA recovery

8 Embryo Culture Apparatus (ECA)

8.1 Preface

ECA (Fig. 30) is a space life science experiment instrument developed by the Shanghai Institute of Technical Physics of the Chinese Academy of Sciences and suitable for SJ-10 satellite in China. ECA is used to develop early embryonic development of mammals under microgravity conditions. The research meets the culture conditions for the growth and development of mouse embryos in a spaceflight environment. It has automatic searching, capturing, and microscopic imaging capabilities for mouse embryos with three-dimensional distribution in the culture unit and transmits the image data.

On April 6, 2016, ECA carrying the mouse embryo was ejected with the launch of SJ-10 satellite. SCA successfully achieved two chemical fixations of the embryonic sample, real-time acquisition of 2368 images of the entire process of early embryonic development in the down-scale space, as well as all on-orbit engineering parameters and scientific parameters, and the work is stable and reliable.

On April 18, 2016, equipment and sample recovery work was successfully performed at the recycling site. The recovered samples were in good condition and satisfactory data and sample results were obtained.

The embryo culture device successfully completed the space flight experiment and equipment and sample recovery work. SCA functioned properly on the track, the data was completely downloaded, and the recovered samples were in good condition. This project achieved embryo culture for the first time in a spaceflight environment

Fig. 30 Embryo culture apparatus (ECA)

and acquired microscopic images of the entire process of early mouse embryonic development in space.

8.2 System Components

ECA (Fig. 31) is used for embryonic development research in space with mice embryos. ECA consists of experiment units, auto-focus microscope, fixation units, life support unit and control box. In the ECA, ten experiment units are divided in 3 groups. The group 1 contains 4 experiment units, used for imaging with auto-focus microscope, the group 2 and 3, each contains 3 experiment units, used for fixation with different chemical fixation liquid after culturing. The fixative fluid is stored in the fixation units. After the fixed instruction is received, the fix fluid is injected into the incubator through the transport pump and 6 samples are fixed at a time.

8.3 Main Technical Indicators

The main technical indicators of ECA are shown in Table 7.

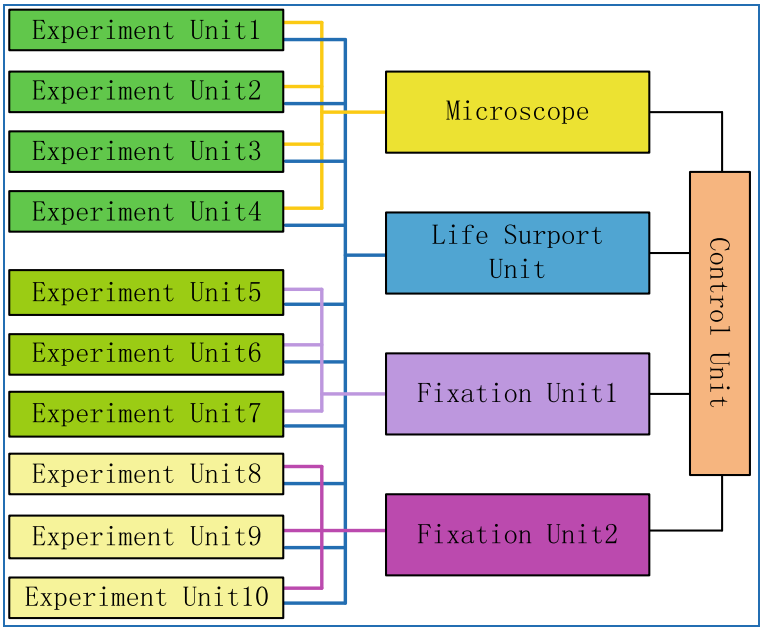

Fig. 31 ECA function composition

Table 7 Main technical indicators of ECA

Parameter	Numerical value
Weight	≤20 kg
Size	270 mm × 250 mm × 200 mm
Power dissipation	≤30 W
Period	4d
Specimen quantity	3 groups
Culture temperature	36.5–37.2 °C
Fixation	Chemical fixation, 2 groups
Storage temperature	≤10 °C
imaging	Microscope, 1 group

8.4 Key Technologies

(1) Embryo culture techniques in space-tight environment

The key technology for mouse embryo culture in space-enclosed environment is to provide appropriate life support conditions, including precise culture temperature control (accurate culture temperature control at 36.5–37.2 °C), nutrient solution supply and CO_2 environment and aseptic environment protection, etc.

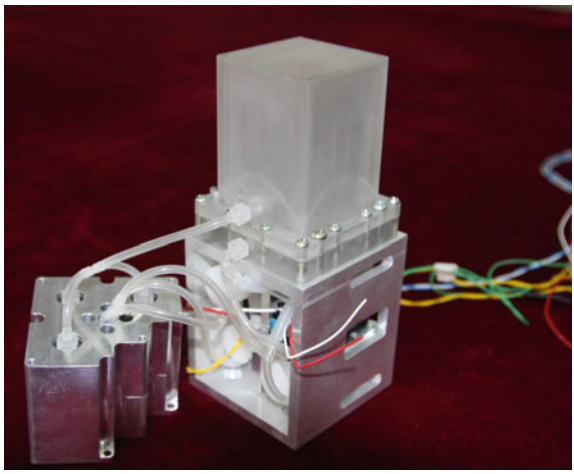

Fig. 32 Chemical fixation and low temperature storage cells

The project is based on the experimental basis of mouse culture and combined with the existing space embryo culture technology and culture device development experience to solve the embryo culture technology in the space closed environment.

SCA successfully completed the space flight experiment and realized embryo culture for the first time in a space flight environment. For the first time, microscopic images of the early development of the space mouse embryo were obtained.

(2) Chemical fixation of embryos and low temperature storage

Chemical fixation and cryopreservation methods were used for the fixed storage of mouse embryos. Through a combination of a fixed pump and a valve, the fixed solution was injected into the culturing chamber, and the temperature control point in the temperature zone was switched to achieve chemical fixation of the cell sample.

Chemical samples are used to fix biological samples, and chemical fixatives are injected into each culture unit through a transport pump to fix the sample. The sample fixing unit is shown in Fig. 32 and consists of the fixed fluid chamber, the transport pump, the culturing chamber, and the valve. This project is to achieve the chemical fixation of six kinds of samples. Six kinds of biological samples are respectively installed in two groups of culture modules for cultivation, in which one group of samples of the culture module is cultured and fixed, and the temperature of the fixed compartment is preserved; the other group of samples of the culture modules is cultured, fixed, and cryopreserved after fixation.

(3) In situ auto-searching and capturing microscopic image of embryos with low density unpredictable distribution

The size of mouse embryos is small and have to be observed with a microscope. However, the depth of field of the microscope is small, and the focusing mechanism have to be used for searching and capturing the target for imaging. The four embryo culture chambers are arranged on the linear displacement platform along the direction

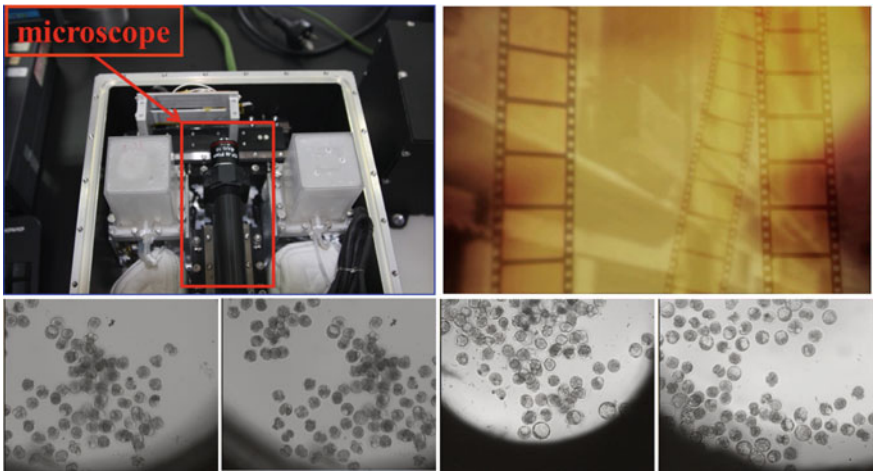

Fig. 33 Microscopic imaging of embryos on ground test

of movement of the platform, and the arrangement of the microscope considers the direction in which the optical axis is perpendicular to the linear motion. The support platform of the microscope also requires a linear motion, and the movement of the microscope is controlled by the translation stage to control its movement to obtain a clear image (Fig. 33).

8.5 Space Flight Experiment

SCA successfully completed the space flight experiment and successfully achieved two chemical fixations of the embryonic sample. The real-time acquisition of 2368 images of the entire process of early embryonic development in the down-scale space was achieved undersealed environment in space and embryo culture was obtained for the first time. The microscopic images of the whole process of early mice embryonic development in space provide good support for scientific research and have been highly recognized by international counterparts.

ECA worked properly in space. Culture temperature was 36.0–37.5 °C. Low temperature storage was 2–4 °C. Normal temperature storage was 21–23 °C. Several embryos were fixed in space and in good condition.

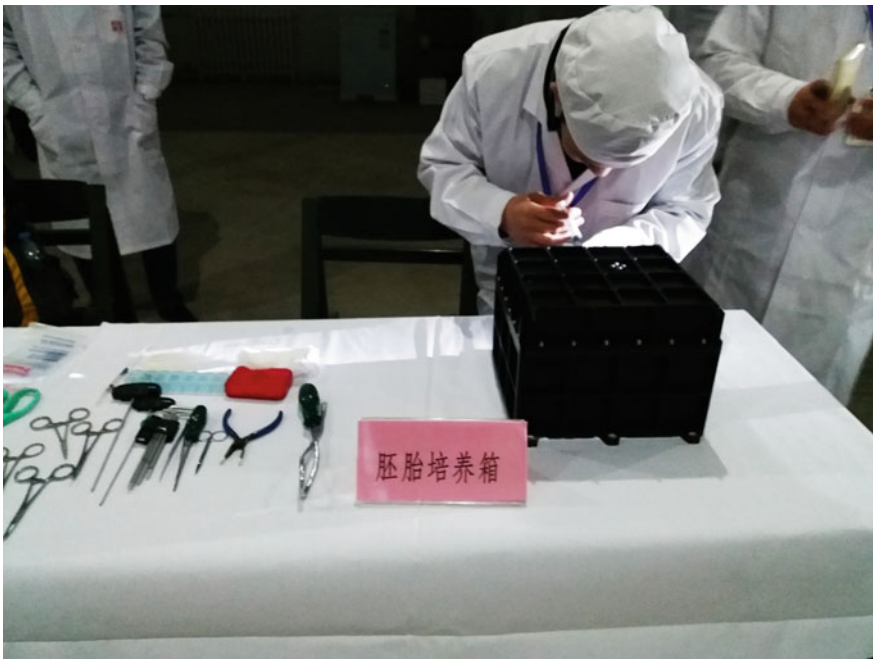

Fig. 34 ECA recovery (picture provided by Xiaohua Lei)

8.6 Facility and Specimen Recovery

On April 18, 2016, ECA and sample recovery operations were successfully performed at the recycling site, and satisfactory data and sample results were obtained (Fig. 34).

9 Conclusion

Five space-based life science experimental devices developed by Shanghai Institute of Technical Physics were successfully launched into orbit with SJ-10 satellite, and the space flight mission was successfully completed according to the experimental procedure. SCA realized the high-density cultivation of silkworm embryos in a space-contained manner and the multi-temperature discrimination batches of silkworm embryos in five culture units. At the same time, for the first time, the images of the embryonic development process of the silkworm were successfully obtained. PCA achieved the first application of technologies and methods such as chemical fixing of Arabidopsis seedlings for low temperature storage and 3D printing of special functional components in space life science experiments; HPCA successfully achieved heat shock induced gene expression and GFP fluorescence imaging

technology for transgenic plants for artificially controlling plant flowering in space; SCCA successfully realized perfusion culture and chemical immobilization of samples, and real-time acquisition of downstream data 1184 microscopic images of the proliferation and differentiation processes of space-derived neural stem cells and hematopoietic stem cells, as well as all on-orbit engineering parameters and scientific parameters, were the first to achieve spatially confined environmental stem cell culture in the country, and the first time in the world was the proliferation and differentiation of neural stem cells and hematopoietic stem cells. SCA successfully achieved two chemical fixations of the embryonic sample, real-time acquisition of 2368 images of the entire process of early embryonic development in the downscale space, and the first realization of embryo culture in a space-tight environment, obtained the microscopic images of early mouse embryonic during spaceflight.

All of these apparatuses worked properly in space. Some new techniques have been applied in space experiments:

(1) Thermal activation and fluorescent imaging;
(2) In situ auto-searching and capturing microscopic image;
(3) Complicated multi-channel liquid transfer and control.

Some important life science research results have been found:

(1) GFP fluorescent images reveal gene expression in space;
(2) Microscopic images reveal mouse embryos and stem cells development process in space.

10 Perspectives of Space Life Science Experiment Facilities in the Future

After decades of hard work and development, Chinese space life science and technology research has achieved a certain technological foundation and a place in the world today. The hardware development work in this phase was based on the exploration of basic experimental technical problems, mainly solving the basic experimental methods and technical support conditions for conducting space life science research, and testing the reliability and practicality of space experimental hardware for future science and the innovative research of technology laid a solid foundation.

However, there is still a big gap between Chinese space life science experimental devices and technology from the international advanced level. The main reason is that most life science payload devices are single devices, and the type of scientific research supported is limited. In-orbit detection methods have a relatively simple ability to cultivate environmental support, and collaborative experiments between various payloads have not yet been conducted. The development of space-based large-scale life science research and technology devices still lacks sufficient experience and there is still a long way to go compared to the level of the International Space Station.

This is also a major factor restricting Chinese ability to carry out multi-type and multi-domain life science research and collaborative experiments. It is urgent to develop the large-scale load of experimental cabinets with the help of Chinese Space Station construction. Therefore, the development of a life science experiment platform such as an experimental cabinet that is highly integrated, modular, and complex in terms of system relationships places high demands on the capabilities of the participating research units. It must be widely developed within the United Nations to carry out common research and increase research efforts. The simultaneous innovation of knowledge and technology was carried out, and efforts were made to narrow the gap with the international advanced level.

References

Jin J, Chen H, Cai W (2014) Growth of rice cells in Shenzhou 8 under microgravity and transcriptome analysis. Manned Spacefl 20(9):480–485

Lu J, Zhang T, Zheng W (2008) Advanced space facilities for higher plant culture and animal embryo culture in microgravity. Microgravity Sci Technol 20(2):121–126

Peter P, Markus B (2014) German SIMBOX on Chinese mission Shenzhou-8: Europe's first bilateral cooperation utilizing China's Shenzhou programme. Acta Astronaut 94:584–591

Zhang Y, Wang L, Xie J et al (2015) Differential protein expression profiling of Arabidopsis thaliana callus under microgravity on board the Chinese SZ-8 spacecraft. Planta 241(2):475–488

Study on Bone Marrow Box, Radiation Gene Box and Integrated Electrical Control Boxes

Yuanda Jiang, Yanqiu Wang, Xunfeng Zhao and Xingzhu Cui

Abstract This chapter introduces the working principle, development, on-orbit operation and recovery of three scientific experimental payloads in SJ-10 recoverable microgravity experimental satellite (SJ-10 satellite) mission, which include the bone marrow box, the radiation gene box and their integrated electric control box. The electric control box, consisting of two units, belongs to the application sub-system of SJ-10 satellite and provides the functions of power supply, operation command, and data transmission and storage for the scientific experimental load of the return cabin and the sealed cabin of SJ-10 satellite. These instruments are developed by the National Space Science Center of Chinese Academy of Sciences.

Abbreviations

FPGA	Field Programmable Gate Array
DA	Digital to Analog
PID	Proportional Integral differential
PWM	Pulse Width Modulation
LED	Light Emitting Diode
RGB	Radiation Gene Box
SRD	Space Radiation Detector
ADC	Analog to Digital Converter
RC-IECB	Return cabin integrated electric control box
SC-IECB	Sealed cabin integrated electric control box
MRAM	Magnetic Random Access Memory
CCSDS	Consultative Committee for Space Data Systems
LVDS	Low-Voltage Differential Signaling

Y. Jiang (✉) · Y. Wang · X. Zhao
National Space Science Center, Chinese Academy of Sciences, Beijing, China
e-mail: jzmz@vip.sina.com

X. Cui
Institute of High Energy Physics, Chinese Academy of Sciences, Beijing, China

E. Duan and M. Long (eds.), *Life Science in Space: Experiments on Board the SJ-10 Recoverable Satellite*, Research for Development,
https://doi.org/10.1007/978-981-13-6325-2_14

CPU	Central Processing Unit
UDCB	Universal Drive Control Box
CCD	Charge Coupled Device

1 Design and Operation of Bone Marrow Box and Radiation Gene Box

1.1 Study of Bone Marrow Box

1.1.1 Background Introduction

Committed differentiation of human bone marrow stem cells (hMSCs) is one of the research projects on the SJ-10 recoverable scientific experimental satellite, which aims to study the effects of microgravity on the osteogenic differentiation potentials and molecular mechanisms as well as the key cell signaling molecules specific for osteogenic differentiation, to evaluate the bone variability of space occupants in space travel, and to provide scientific basis for the development of target drugs. The experimental instrument (referred to as the bone marrow box) is developed for the scientific task. Because the cell samples need to be returned to the ground for analysis, the instrument s arranged in the satellite return capsule.

The space experimental task lasts for 12 days (from launching to returning). The experimental samples are divided into two groups: (1) hMSCs are induced for two days with osteogenic induction medium in orbit, then replacing the induction medium with PBS, finally fixing cells with RNAlater. The fixed cell samples are stored at low temperature until being returned to the ground. The effects of microgravity on the expression of genes and the activity of proteins specific for osteogenic or adipogenic differentiation are analyzed. (2) hMSCs are induced for 7 days with osteogenic induction medium, refreshing induction medium every 2 days. Then the cells are washed with PBS and fixed with 4% formaldehyde. The fixed samples are kept at low temperature until being returned to the ground. Samples of this group are detected by histochemistry and immunohistochemistry to analyze the osteogenic differentiation potentials of hMSCs comparing with ground controls.

1.1.2 Working Principle

hMSCs are cultured in a three-dimensional scaffold (microporous matrix material), and divided into two groups (two-day and seven-day culture) according to the on-orbit experimental procedure. The three wafer skeletons are placed in one culture container, and a separate semiconductor (two-way temperature control) thermostat provides a (37 °C) temperature environment for cell culture. The cells are in normal culture state before being launched into the orbit. After the satellite was launched

into the orbit, the culture solution was changed to the osteogenic induction medium. After the end of the inducing culture, the medium is washed out with PBS and the lysate or fixative is injected to fix the cells on orbit. Then the thermostat is switched to a low temperature (8 °C) state until the satellite returns to the ground.

The liquids used in the experiment are stored in different containers. The induction liquid, lysate liquid and fixing liquid are stored at a low temperature (8 °C) for 7 days controlled by a semiconductor thermostat and the temperature control is stopped after fixation. The cleaning solution does not need temperature control in the whole flight. The liquid discarded during the experiment is collected in a single waste tank.

The fluid circuit driven by the syringe pump and the fluid dispenser conducts liquid extraction and injection. The fluid interface of the fixative, lysing and waste tanks is first connected to the solenoid valve, and then connected to the corresponding pipeline of the fluid distributor, different liquids distributed to the inlet and outlet of the culture vessel through the manifold. The solenoid valve is opened only when needed to prevent the fixed liquid or waste liquid from being mixed into the culture vessel when the channel is switched. The principle of the load system is shown in Fig. 1.

The space experiment is controlled by an FPGA (Field Programmable Gate Array) logic controller as the core measurement and control circuit to complete various operations, and process data detection and storage. Data transmission and command reception are performed through a 422 serial port and an integrated electric control box. The integrated electric control box controls the experimental process of the

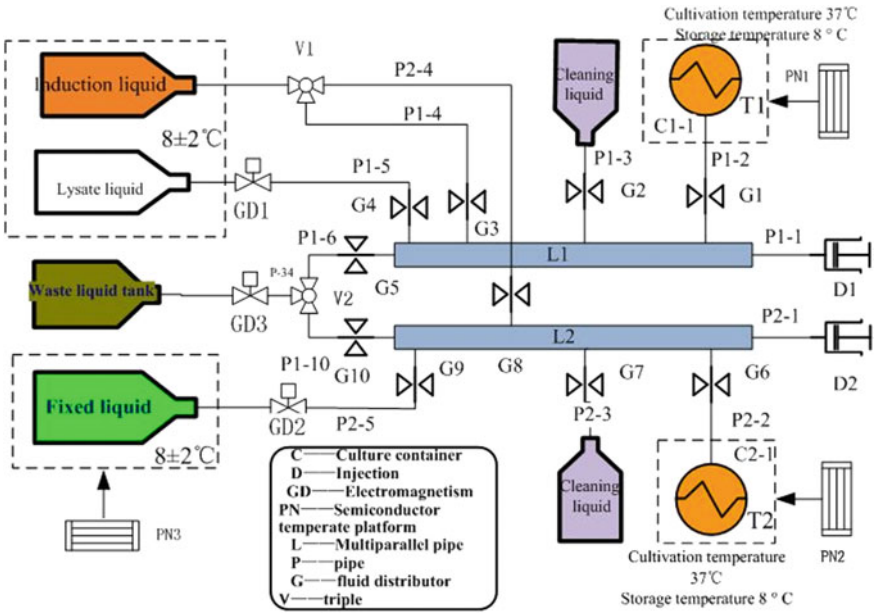

Fig. 1 Schematic diagram of the bone marrow box system

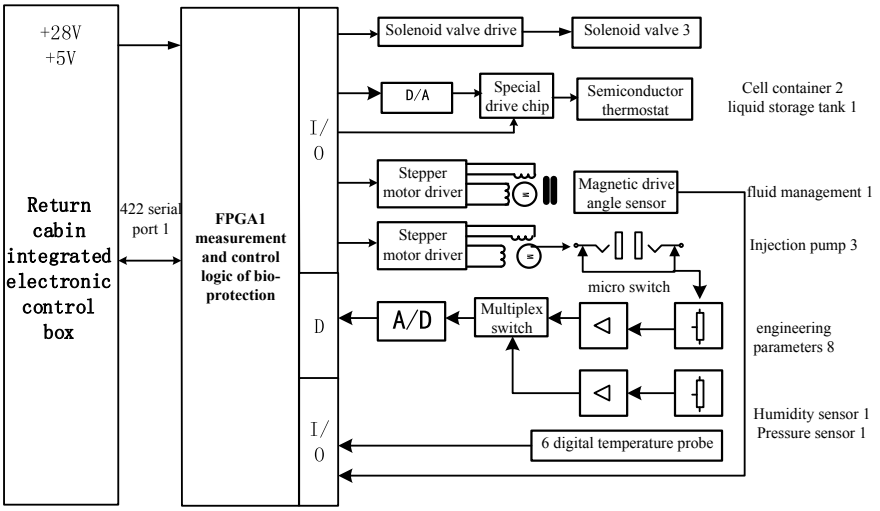

Fig. 2 Schematic diagram of the bone marrow box electronic control system

load according to preset instructions or injected instructions, and provides the power required for the load. The schematic diagram of the load electronic control is shown in Fig. 2.

1.1.3 System Composition

Overall System Composition

The exterior and the internal structures of bone marrow culture box are shown in Figs. 3 and 4, consisting of a cell culture vessel, a temperature control platform, a liquid storage tank, a syringe pump, a fluid dispenser, a solenoid valve assembly, a temperature and humidity pressure three-in-one sensor assembly, a biosafety measurement and control FPGA, a three-stage airtight chassis and other components. The parts of fluid system are connected with silicone rubber tubes.

Main Indicators

The internal components and structure design of the bone marrow box must meet the requirements of scientific experiments, adapt to the characteristics of the microgravity environment, and be constrained by resource conditions such as satellite space, energy, air pressure and thermal control. Its main performance parameters are as follows:

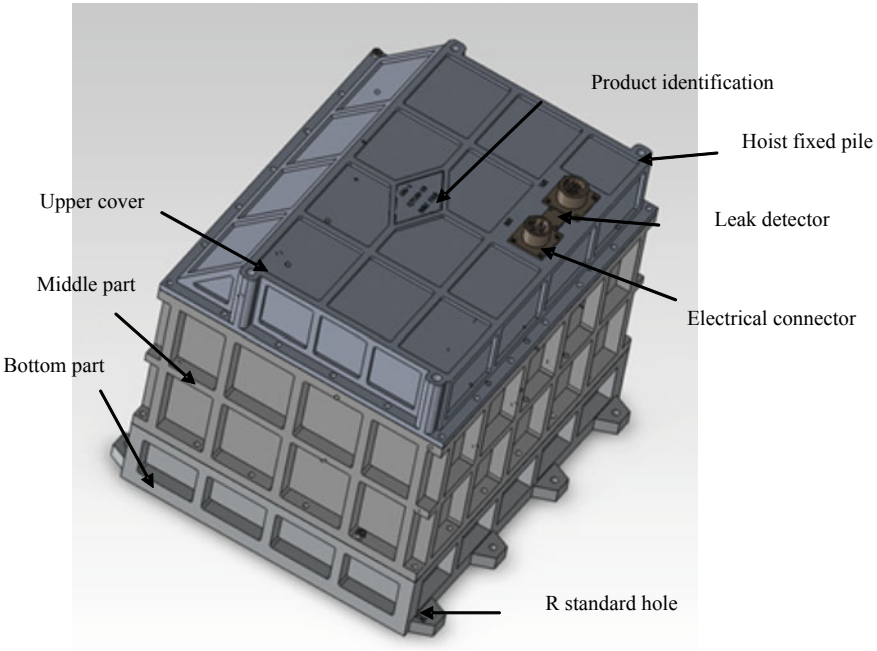

Fig. 3 Overall structure schematic of bone marrow culture box

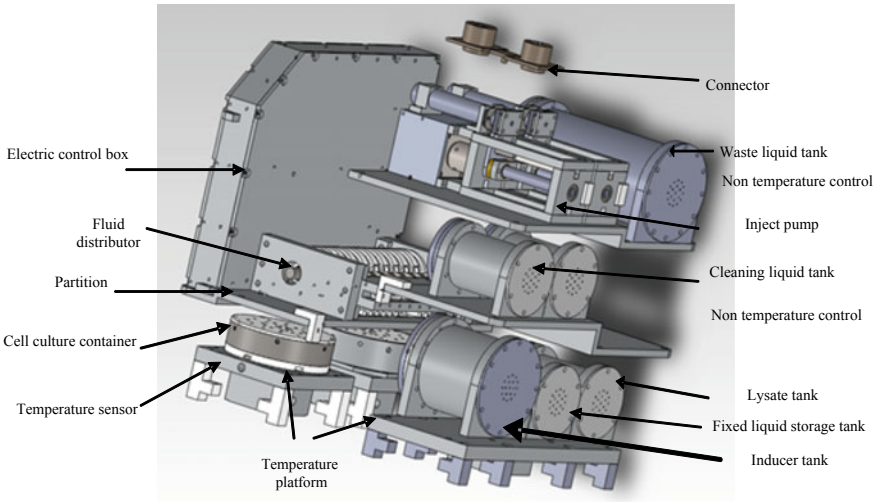

Fig. 4 Internal structure schematic of bone marrow culture box

(1) Overall load index:

The overall volume (size): 250 × 300 × 270 mm; Total mass: 16 kg.
Power consumption: peak power 40 W, average power 17 W; Internal air pressure: 0.1 MPa (external pressure: vacuum ~0.01 MPa);
Internal atmosphere: air.
On-orbit test cycle: full course, about 14 days.

(2) Cell culture conditions:

Cell culture container: area ϕ55 mm and volume 25 ml/piece, containing 3 three-dimensional culture scaffolds; a total of 2 sets;
Three-dimensional culture scaffold: ϕ25 × 1 mm;
Cell culture temperature: 37 ± 1 °C;
Maintain temperature after cell lysing: 8 ± 2 °C;
Maintain temperature after cell fixing: 8 ± 2 °C.

(3) Liquid storage conditions:

Induction liquid storage tank: volume ~125 ml, 1 set, storage temperature: 8 ± 2 °C;
Fixative liquid storage tank: volume ~40 ml, 1 set, storage temperature: 8 ± 2 °C; Lysate storage tank: volume ~40 ml, 1 set, storage temperature: 8 ± 2 °C;
Cleaning liquid storage tank: volume ~40 ml, a total of 2 sets, without temperature control;
Waste tank: volume ~240 ml; without temperature controlled.

(4) Fluid system indicator:

Syringe pump: volume ~5 ml, flow rate ~1–3 ml/min.
Fluid distributor: 10 channels, positioning accuracy ±1°.

Components

(1) **Cell culture container (CCC)**

The cell culture container is constructed as shown in Fig. 5, in which the three-dimensional culture scaffold inoculated with the cells is embedded in the base slot, and the circular groove of the partition plate is aligned with the circular groove of the bottom plate and fastened by the hollow connector to prevent culture scaffold moving. The partition plate blocks the inverted film from touching the cell when the inverted film is turned over, and the small hole of the partitioning plate provides a path for the liquid to enter or discharge from the container; the basin-shaped inverted film (flexible material) is installed between the base and the middle section, and is squeezed and fastened by the external screw. The inverted film has a 3-mm flipping edge, which is used for sealing. The upper cover has breathable holes to limit and protect the inverted film.

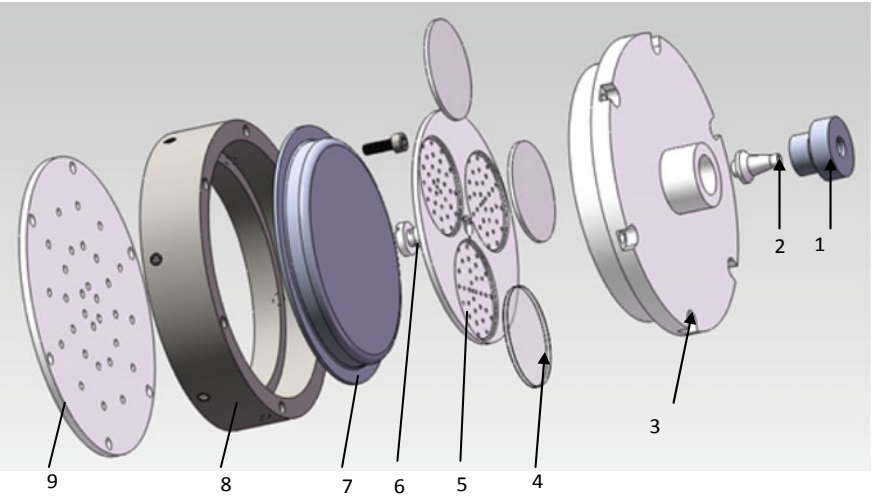

Fig. 5 Three-cell cell culture device mold diagram. 1. Pipe fixing; 2. pipe core; 3. bottom of container; 4. three-dimensional culture scaffold; 5. partition plate; 6. hollow connector; 7. inverted film; 8. middle of container; 9. upper cover

The liquid enters firstly from the bottom fluid interface, then the interior of the inverted film through the hollow connector, the three-dimensional culture scaffold, and the small hole of the partition plate. When the inverted film is turned upside down, the air outside the inverted film is removed by the small hole of the upper cover plate until it is full. When the liquid is removed, it flows through the hollow connector, the small hole of the partition plate, the three-dimensional culture scaffold, and the bottom fluid interface. Then the inverted film is turned down, and the air outside the inverted film is sucked through the small hole of the upper cover until the liquid is drained. The gas-liquid separation of the inverted film enables a variable volume of a cell culture container, which is suitable for adherent cell culture and liquid replacement in microgravity environment.

(2) **Cell culture temperature control components**

Cell culture temperature control components include heat transfer platform, culture container fixed ring, heat insulation pillar, semiconductor temperature control sheet, temperature sensor and other components, as shown in Fig. 6. The lower heat transfer platform (heat-conducting material) is fixed on the bottom plate of the box chassis through the heat-insulating pillars. The proper gap ensures that the heat-conducting surface of the semiconductor temperature control sheet embedded in the bottom of the heat transfer platform is closely attached to the bottom plate of the chassis, and that the temperature-control sheet is coated with thermal grease on both sides. To improve heat transfer efficiency, the semiconductor temperature control sheet is coated heat-conducting silicone grease on the both sides. The temperature sensor is embedded in the reserved hole of the lower heat transfer station, and the spot thermal

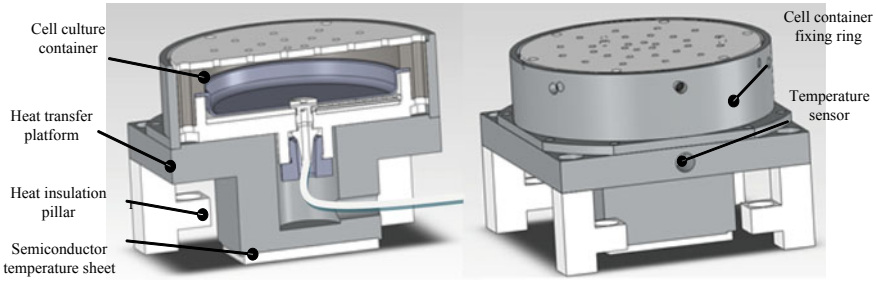

Fig. 6 Cell culture temperature control component diagram

silica gel is solidified. The cell culture container is a movable component, which is fixed on the base component by screws, functioning as a heat transfer relay. The cell culture container is fixed on the bottom of the box and then covered with insulation material.

Temperature control is defined as follows: During the cell culture process, the semiconductor thermostat is kept in a heated state. After the end of the culture and the on-orbit treatment (such as lysing or fixing), the semiconductor thermostat is switched to the cooling state for low temperature storage. The insulation material covering is used for reducing heat dissipation.

(3) **Liquid storage and temperature control**

The liquid storage tank (LST) is designed in the same manner as the cell culture vessel, except that there are no hollow parts such as cell culture sheets and porous plates. The temperature control and the installation of the radiation are similar to the temperature control method of the cell culture, but it is only used for cooling.

(4) **Fluid transport and management**

A syringe pump (Figs. 7 and 8) is used to transport various liquids required for cell culture. With a full capacity of 5 ml, the total amount and flow rate of the injected liquid can be accurately controlled, and the shear force of the liquid flow on the cells can be reduced. The fluid transport consists of two syringe pumps and one fluid distributor (Figs. 9 and 10). Each culture vessel is equipped with a syringe pump. The pipeline connection is shown in Fig. 1. The electrical control box is in accordance with the integrated electronic control. The actions of fluid injection, extraction, and collection are conducted under the instructions of the electrical control box.

The fluid distributor is composed of several cams in different position (angle). The drive shaft is connected in series by a motor, the position signal is read and positioned by the spindle end magnetic encoder, and the corresponding liquid conveying pipe (silicon rubber tube) is pressed by the cam. The pipe opens when the cam notch moves towards it, while it is closed due to being squeezed when the cam notch moves to other direction, thereby realizing multi-channel fluid management. The cam notch opening angle is related to the number of fluid pipes in accordance with the expression (1):

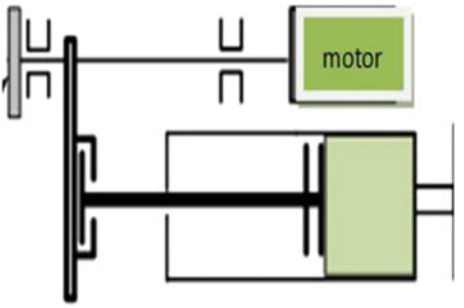

Fig. 7 Schematic diagram of the syringe pump

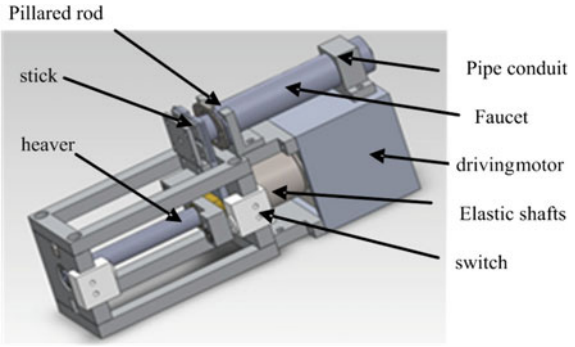

Fig. 8 Injection pump

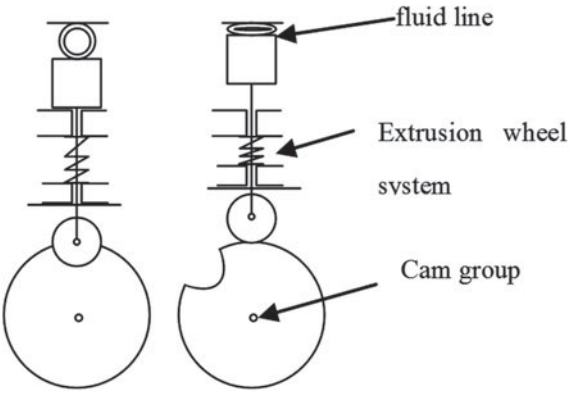

Fig. 9 Schematic diagram of the fluid dispenser mechanism

$$n = \frac{360^\circ}{\theta 1 + \theta 2} = \frac{360^\circ}{2\theta} \tag{1}$$

Here n is the number of pipelines, $\theta 1$ is the opening angle of the pipeline, and $\theta 2$ is the opening angle of the pipeline. Generally $\theta 1 = \theta 2$.

The opening angle is determined by the pipe size and margin. When $\theta = 15.5^\circ$, 10 channels can be managed. The 12-bit encoder is used with a positioning accuracy of $\pm 1^\circ$, ensuring accurate cam position. The direction of the cam notch can be arranged

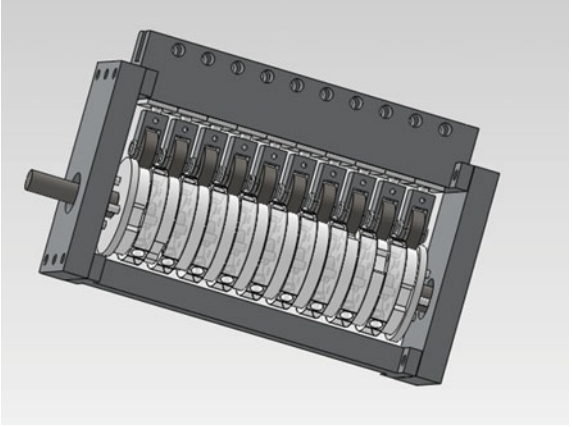

Fig. 10 Design drawing of the fluid dispenser mechanism

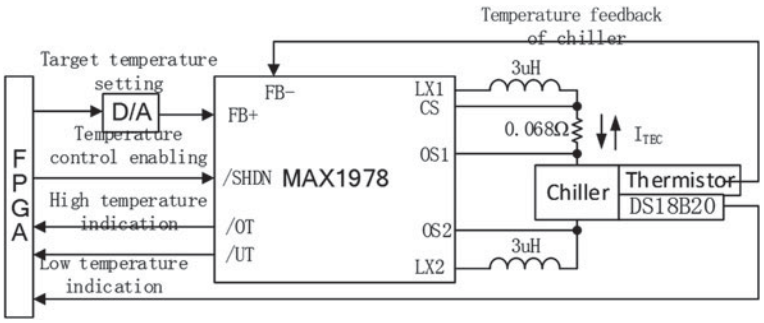

Fig. 11 Semiconductor temperature control chip drive circuit diagram

according to actual needs. The loaded fluid pipeline needs 10 channels, all work in series, and the cam notches are arranged according to the circumference to meet the experimental needs.

(5) **Life support measurement and control circuit**

Cell culture temperature control circuit:
The bio-protection FPGA on the drive control box sets the target temperature through the D/A (Digital to Analog), and collects the actual temperature of the cooling fin through the partial pressure of the thermistor and a fixed resistor. The MAX1978 (part no.) features bidirectional control that compares the difference between the target temperature and the actual temperature to determine whether it is cooling or heating. The internal amplifier and the external resistor container form a hardware PID (Proportional Integral differential) operation circuit, so that the output circuit completes the PWM (Pulse Width Modulation) drive to achieve precise temperature (Figs. 11 and 12).

Fig. 12 Semiconductor temperature control sheet

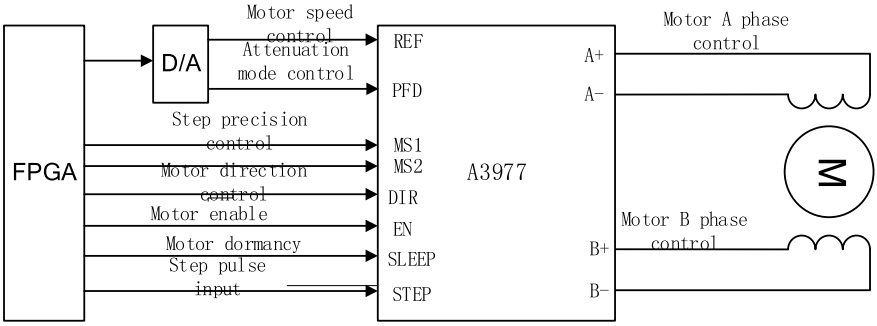

Fig. 13 Step motor drive circuit

Syringe pump and fluid dispenser drive circuit:
The syringe pump and fluid distributor are driven by the same type of step motor. The step motor drive chip is A3977 (part no.), and the motor drive circuit is shown in Fig. 13. The chip is subdivided, enabled and commutated by the FPGA to realize the forward and reverse, stop and speed control of the step motor. Injection pump body strokes two limit switch control. When the FPGA acquisition motor near the end limit switch is closed, the motor is rotating and the liquid is inhaled into the pump. When the remote limit switch is closed, the motor is reversed and the liquid is squeezed out of the pump tube. The limit switch spacing determines the amount of liquid transport in one action.

The fluid management action is also controlled by the A3977. The step motor drives the cam group to rotate, so that the squeeze wheel moves up and down to lock or release the fluid line to achieve multi-channel fluid distribution. The spindle top

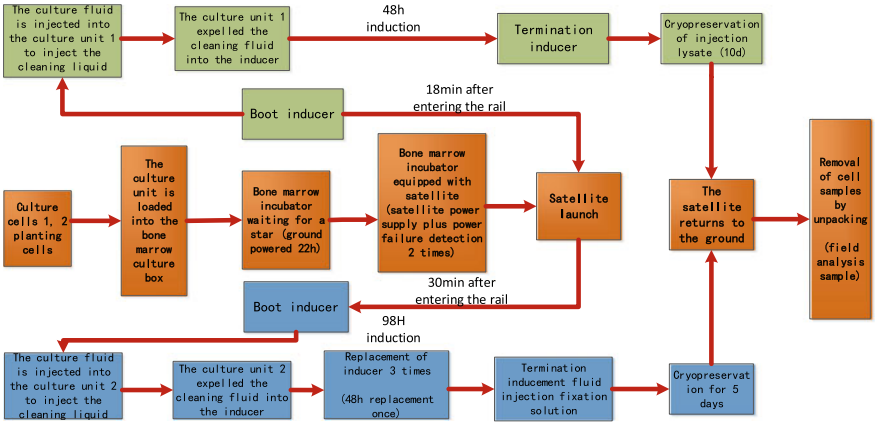

Fig. 14 On-orbit experimental flow chart

magnetic encoder output signal corresponds to the cam notch (10 positions) angle and is fed back to the main control circuit (FPGA) to turn the cam group to the predetermined position.

Experimental Procedure

According to the content and requirements of the project track, the on-orbit experimental process design is shown in Fig. 14.

1.1.4 Operation of the Bone Marrow Box on Orbit

Temperature requirements for all aspects of scientific experiments:
Temperature requirement cell culture stage in orbit: 37 ± 1 °C;

Cryopreservation temperature requirements after in-orbit sample processing (lysing, fixing):

Cell culture tank 1 storage temperature: 6 ± 2 °C;
Cell culture tank 2 storage temperature: 8 ± 2 °C;
Cell culture solution, lysate, f ixative storage temperature: 8 ± 2 °C.

There is no temperature control for the cell culture solution, the lysate, and the fixative after the experiment;

There is no temperature control for the cleaning solution and the recovery solution.

Analysis of temperature control in orbit operation:
The temperature control raw data of each link in the orbital experimental process is shown in Fig. 15, and the data analysis is shown in Table 1.

The bone marrow box is operated in orbit according to the instruction node to complete cell culture fluid replacing, on-orbit sample processing (cracking, fixing) and waste liquid recovering. The cell culture units 1, 2 and the liquid storage tank temperature control meet the requirements of scientific experiments.

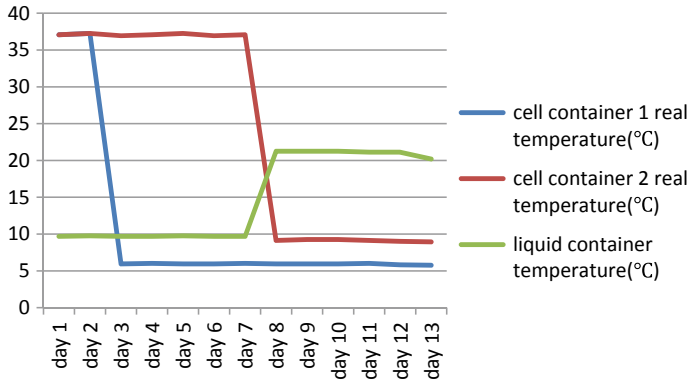

Fig. 15 Temperature control curve of cell unit in bone marrow box

Table 1 Temperature control data of in-orbit operation of bone marrow box

On-orbit time (day)	CCC 1 temp (°C)	CCC2 temp (°C)	LST (°C)	Remarks
1th	37.0625	37.0625	9.6875	OK
2th	37.25	37.25	9.75	OK
3th	5.9375	36.93755	9.6875	OK
4th	6	37.0625	9.6875	OK
5th	5.9375	37.25	9.75	OK
6th	5.9375	36.93755	9.6875	OK
7th	6	37.0625	9.6875	OK
8th	5.9375	9.125	21.25	OK
9th	5.9375	9.25	21.25	OK
10th	5.9375	9.25	21.25	OK
11th	6	9.125	21.125	OK
12th	5.8125	9	21.125	OK
14th	5.755	8.9375	20.1875	OK

1.1.5 Installation and Recovery of Bone Marrow Box Samples

- Sample installation before launching

The process of inoculating the cell sample into the culture vessel, injecting the culture solution, fixing the container, connecting the fluid network, and re-balancing the atmosphere in the box is operated by the scientific team. The sealing and testing are operated by the technical team and supervised and cooperated with each other. The overall unit is tested and proved to be qualified for acceptance by satellite systems. The sample and reservoir installation results are shown in Fig. 16, and the fluid network installation results are shown in Fig. 17.

- Sample disassembly after recycling

After the satellite return cabin is landed, the results of the unpacking inspection of the bone marrow box indicate that all the culture fluid (pink) injected is transferred to the waste liquid tank and the lysate and the fixative are all transferred to the cell culture vessel (colorless). There is no abnormality such as leakage or looseness in the box. The running data analysis shows that the on-track temperature control data meets the design requirements, the cell samples recovered are well preserved and can be used for subsequent detection and analysis and the orbital science experiment is carried out successfully (see Figs. 18 and 19).

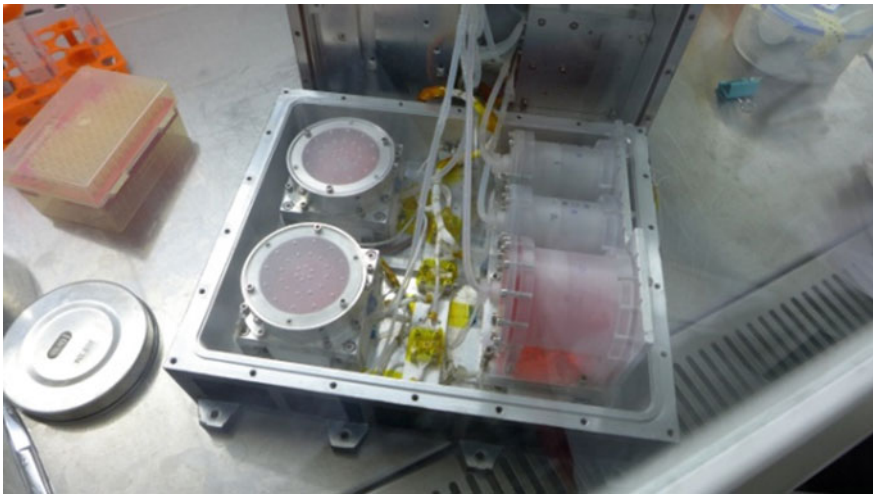

Fig. 16 Culture unit and liquid storage unit

Fig. 17 Fluid transport unit

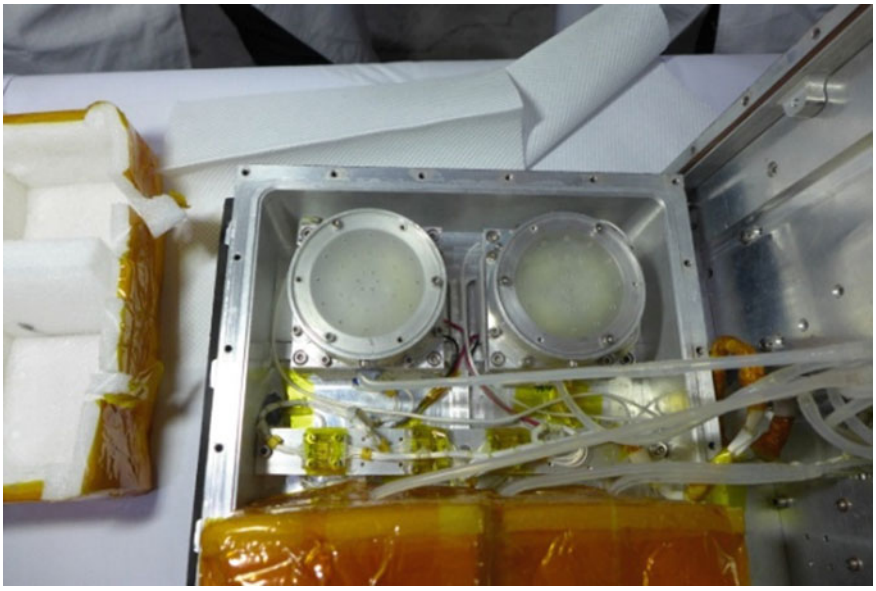

Fig. 18 Recovery unit after recovery

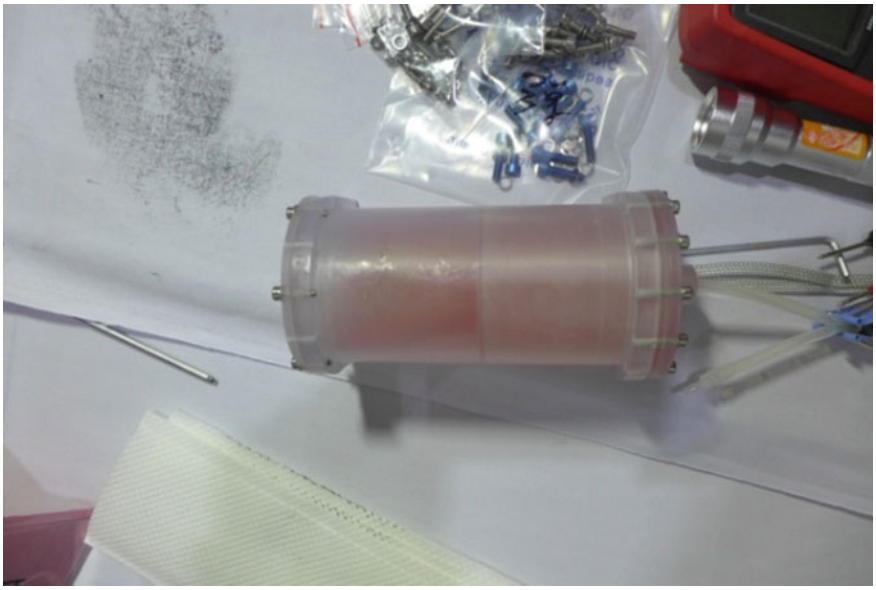

Fig. 19 Recovery solution

1.2 The Research of Radiation Gene Box (RGB)

1.2.1 Scientific Backgrounds

The role of spatial radiation on genomic stability and genetic effects is one of the projects of the SJ-10 recoverable scientific experimental satellite. The goal is to study the combined influence of spatial radiation and weightlessness at animal cellular and individual level. Genomic radiation effect experimental device (refer as radiation gene box) is designed for the task of this space experiment.

This space experiment includes two species. One is the mouse cells cultured for 1 day and 5 days in space. At the end of cell culture in space, the cells are fixed and stored at the temperature of 8 ± 2 °C till they are returned to the ground. Another is the drosophila culture during whole procedure of the flight. The drosophila samples are collected after the satellite is returned. The spatial experimental effects on the recovered samples are analyzed by comparing with ground control samples.

1.2.2 Working Principle

Mouse cells are cultured in an adherent manner and divided into two groups (1-day and 5-day culture). Two culture vessels in each group are placed in two stacks respectively and controlled by two independent semiconductor thermostats,

which provides a 37 °C temperature (Cultivation Temperature: CT) environment. After the experiment, the cells are fixed by perfusing the fixative into the culture vessel and driving the culture solution into the waste liquid tank using the syringe pump and the fluid dispenser, then the thermostat is switched to low temperature (Saving Temperature: ST) (8 °C) control till returning. The inlets of liquid storage tank and the waste liquid tank are firstly connected with the electromagnetic valve, and then connected with the fluid distributor to prevent the fixing liquid or the waste liquid from being mixed into the culture container, so as to avoid affecting the normal culture of the cells.

The drosophila culture adopts a light-transmissive airtight container, and the food is placed in one time. These experiments are divided into 4 groups, the drosophila sample is installed before launching. The external LED (Light Emitting Diode) lights of the container provide the required illumination for the cultivation of drosophila. The temperature control is carried out by means of thermal contact between the payload bottom plate and the satellite to ensure that the ambient temperature of the drosophila culture is maintained at 18–28 °C.

The radiation detector measures the radiation particles (electrons, protons, alpha particles, and gamma rays) in the internal space of the box, providing the data for bio radiation analysis.

The payload is managed by two FPGA logic controllers for various operations of the experimental process, including data detection and radiation detection data acquisition. Through two 422 serial ports, data transmission and command reception are performed respectively by the integrated electric control box. The integrated electric control box controls the space experiment process of the payload according to preset instructions or injected instructions, and provides the power for the payload. The principle of the payload system is shown in Fig. 20. The schematic diagram of the payload electronic control is shown in Fig. 21.

1.2.3 System Composition

Overall System Composition

The radiation gene box consists of cell culture containers, drosophila culture containers, a temperature control platform, a liquid storage tank, syringe pumps, a fluid dispenser, electromagnetic valves, a temperature, a humidity and pressure three-in-one sensor assembly, a radiation detector, a bio-control measurement and control FPGA, a radiation detection data acquisition FPGA, and a three-part airtight case. The fluid system is connected with silicone rubber tubes. As shown in Fig. 22, the internal layout and structure are shown in Fig. 23.

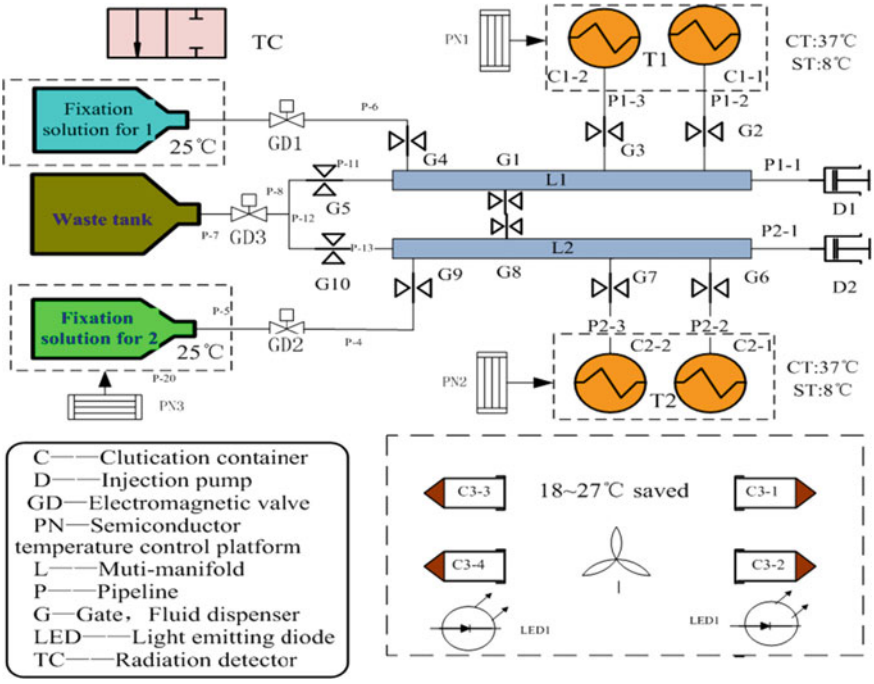

Fig. 20 The principle of RGB

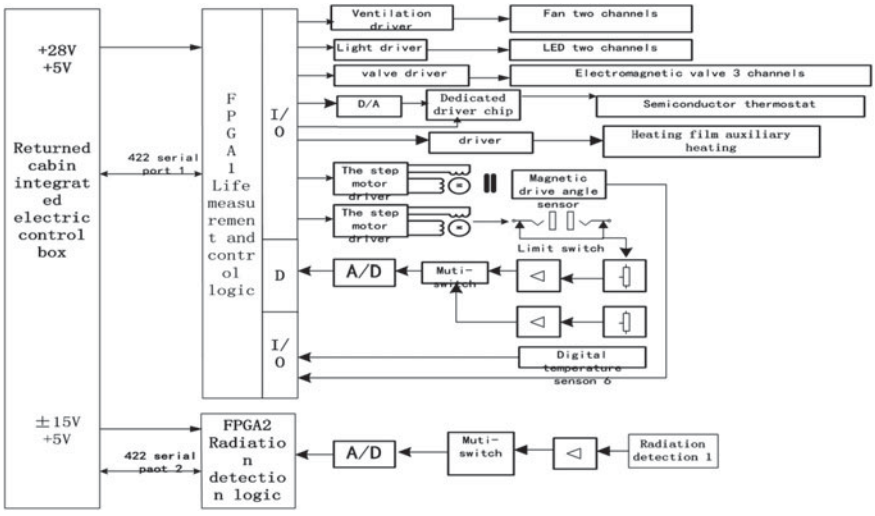

Fig. 21 The schematic diagram of RGB

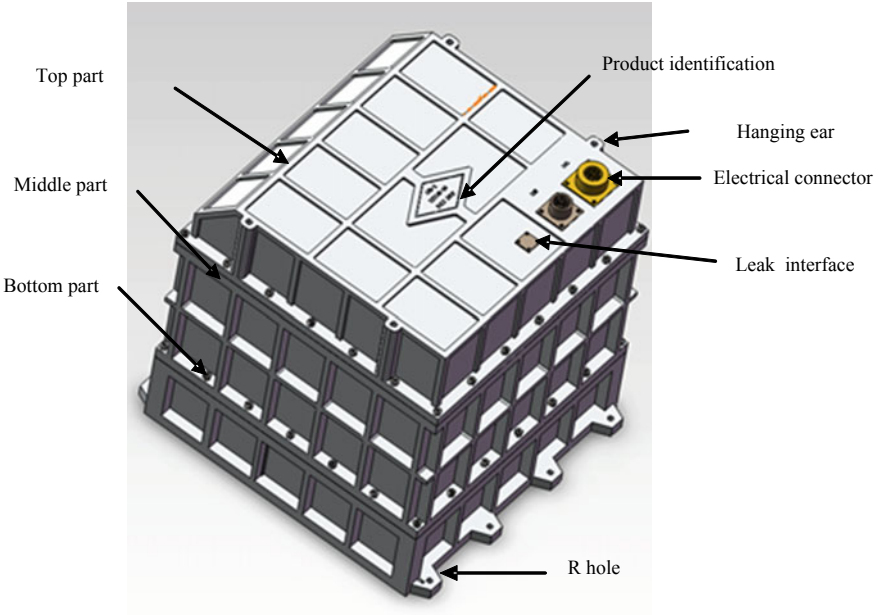

Fig. 22 The radiation gene box overall structure

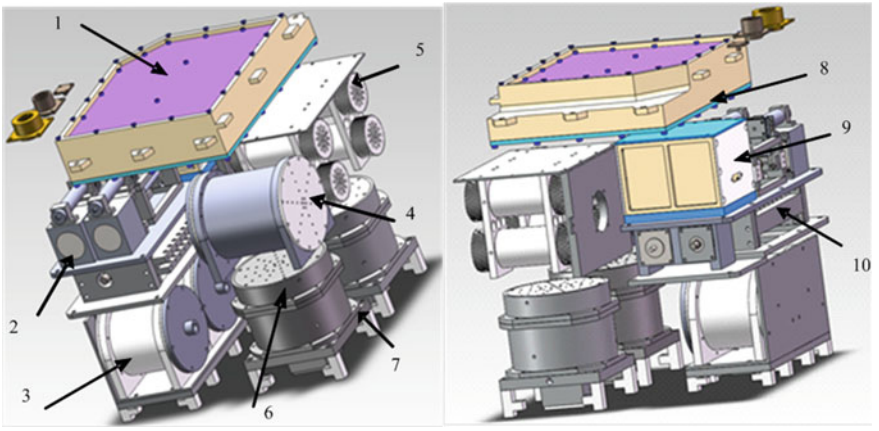

Fig. 23 The internal layout and structure of the radiation gene box. 1. Life support FPGA; 2. injection pump; 3. liquid storage tank; 4. waste tank; 5. drosophila culture tank; 6. cell culture container; 7. temperature control platform; 8. detector FPGA; 9. radiation detector; and 10. fluid dispenser

Main System Indicator

The internal components and structure design of the radiation gene box must meet the requirements of scientific experiments, adapt to the characteristics of the microgravity environment, and be constrained by resource conditions such as satellite space, energy, air pressure and thermal control. Its main performance parameters are shown as follows:

(1) Overall indicators of payload:

Total volume (size): 300 mm × 300 mm × 320 mm;
Total weight: 22 kg
Power consumption: Peak power 40 W, average power 23.5 W
Internal pressure: 0.1 MPa (External pressure of box: vacuum ~0.01 MPa)
Internal atmosphere: air (including 5% CO_2)
Process cycle On-orbit: 14 days

(2) Cell culture conditions:

Cell culture container: area: ϕ75 mm; volume: 50 ml/piece, 4 sets, divided into two groups, two in each group;
Launch and on-orbit culture temperature: 37 ± 1 °C;
Maintain temperature after fix: 8 ± 2 °C.

(3) Liquid storage conditions:

Fixative liquid storage tank: volume: 200 ml, 2 sets, storage temperature: 20 ± 5 °C;
Waste tank: Volume: 40 ml; without temperature control.

(4) Drosophila culture conditions:

Culture vessel: 4 (airtight structure), volume: ϕ 35 × 80 mm, containing food 2 ml
Internal atmosphere: air, 0.1 MPa
Ambient temperature: 18–27 °C
Fluid system indicator
Syringe pump: volume: 5 ml, flow rate: 1–3 ml/min
Fluid distributor: 10 channels, positioning accuracy ±2°

(5) Radiation detector:

4 types of particle detection, 15 channels of energy
Gamma Ray: 0.5–2 MeV
Electronics: 0.5–10 MeV, 3 channels (maximum counting flux: ~10^4 cps)
Proton: 5–200 MeV, 8 channels (maximum counting flux: ~10^4 cps)
Alpha particles: 30–300 MeV, 3 channels (maximum counting flux: ~10^2 cps).

Components

(1) Cell culture container

The container is composed of a cell culture sheet, a bottom cover, a middle section, an orifice plate, a hollow connecting piece, a flipping film, an upper cover plate, a pipe connecting piece and a lock nut, wherein the cell culture piece is designed as a $\phi 75 \times 1$ mm disk. The cells are attached to the sheet; the culture piece is embedded in the base groove, and the porous plate is covered, and then the hollow piece is fastened to the base to prevent the culture piece from moving. The basin-shaped inverted film made of flexible material is installed between the bottom part and the middle part, and fixed and pressed by the external screws. The inverted film is pushed up when the liquid is injected, and turned down when the liquid is removed, which functions as a variable-volume cell culture container with separating capacity between the internal liquid and the outside air. The inverted film has a 3-mm flipping edge, which acts as a liquid seal. The perforated plate blocks the inverted film to touch the cells, and provides a passage for air when liquid entering or discharging from the container. The top part has a venting hole which protects the inverted film. The liquid enters and exits from the bottom interface. The cell culture container is suitable for cell cultivation and liquid replacement in microgravity environments. As shown in Fig. 24.

(2) Double unit stacking cell cultivation and temperature controlling components

The cell temperature controlling component comprises an underlying heat transfer station, an upper heat transfer station, a culture vessel fixed ring, an adiabatic pillar, a semiconductor temperature control chip, a temperature sensor, and a resistance heating film (see Fig. 25).

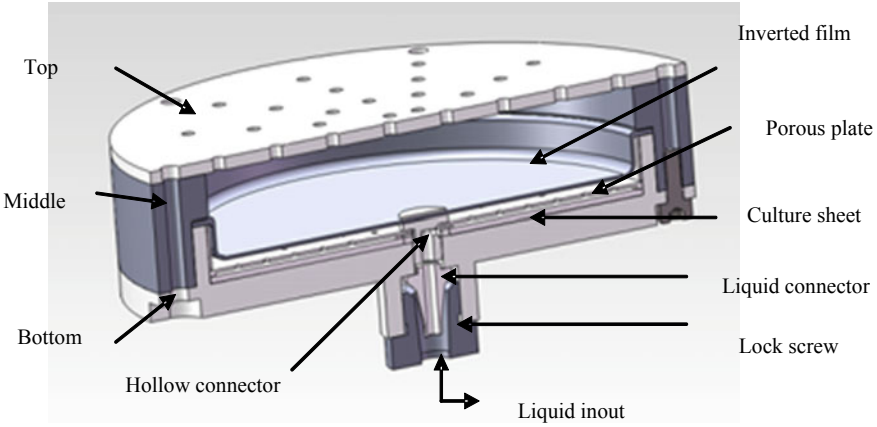

Fig. 24 Cell culture container assemble model

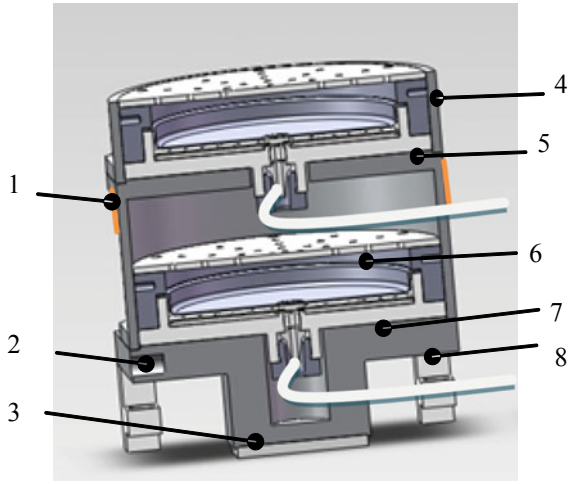

Fig. 25 Double unit stacking cell cultivation container assemble model. 1. Resistance heating film; 2. temperature sensor slot; 3. semiconductor temperature controller; 4. culture container fixed ring; 5. upper layer heat transfer platform; 6. cell culture container; 7. lower layer heat transfer platform; and 8. insulation pillar

The lower heat transfer table (heat-conducting material) is fixed on the bottom plate through the heat-insulating pillar, and the appropriate gap ensures that the heat-conducting surface of the semiconductor temperature control sheet embedded in the bottom of the heat transfer platform is closely attached to the bottom plate of the chassis, and the heat-control film is coated on both sides with heat-conductive silicone grease. The above structure together constitutes a fixed base component of the temperature control system, functioning as main heating and cooling unit. The temperature sensor is embedded in the reserved hole of the lower heat transfer station. The upper basin-shape heat transfer table (heat conductive material) is a movable component, which is fixed on the base component by screws, and functions as a heat transfer relay. The resistance heating film is attached to the side wall of the upper heat transfer station to assist heating, so that the temperature the upper and lower cells containers keeps uniform during cultivation.

Temperature control process: During the cell culture process, the semiconductor thermostat and the heating film work simultaneously to ensure that the temperature for the cells in the upper and lower containers is same. After the cultivation process is finished and fixed, the heating film stops working, and the semiconductor thermostat switches to the cooling state, and the fixed cells are stored in low temperature state. The insulation material covering is used for reducing heat dissipation and power consumption.

(3) Liquid storage and temperature control

The design of the liquid storage tank is similar to that of the cell culture vessel. The temperature control and installation are similar to the temperature control of the cell culture unit, and there is no auxiliary heating but only the refrigeration process.

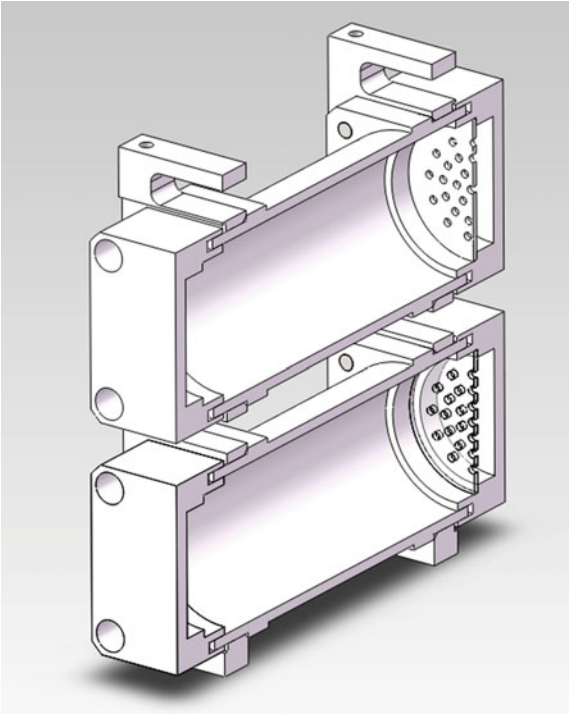

Fig. 26 Drosophila container assemble model

(4) Cell culture fluid transport and management

See section "Components" for cell culture fluid transport and management.

(5) Drosophila cultivation

Since the drosophila culture environment is not compatible with the cell culture environment, the drosophila culture container is designed to be airtight and isolated from the cell culture environment. The container is composed of a sealing cover, a middle section of the container, a physical baffle, a bracket and a sealing ring, and is made of transparent polycarbonate. The inner wall of the middle section of the container is shallowly threaded so that the drosophila can inhabit in a microgravity environment. The sealing ring is placed in the end cover groove and fastened into the middle section by screws to achieve airtightness. The drosophila food is filled in a shallow groove of an end cover, covered by a porous baffle, and leaked through the hole for the drosophila to eat. The drosophila sample is installed before the launching. Its structural design is shown in Fig. 26.

(6) The life support measurement and control circuit

See section "Components" for the life support measurement and control circuit.

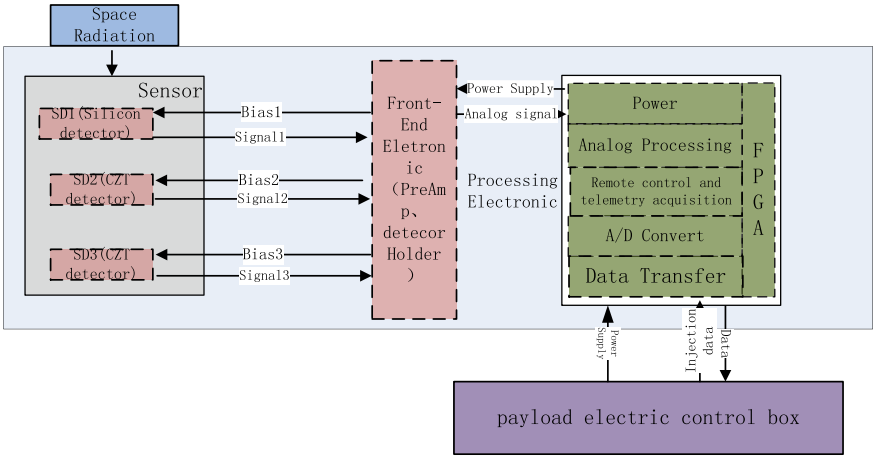

Fig. 27 The schematic diagram of the SRD

(7) Radiation detector (Cui et al. 2018)

To measure the fluxes, spectra and elemental composition of the main particles inside the RGB, the SRD (Space Radiation Detector) is designed as a ΔE-E solid state telescope. The energy loss of charge particle in the detector can be determined by the Bethe formula:

$$\left(\mathrm{e}^{dE/dx}\right)_{ion} \times E \propto MZ^2 \tag{2}$$

where $(\mathrm{d}E/\mathrm{d}x)_{\mathrm{ion}}$ is the energy loss per unit distance, M is the mass of incident particle, Z is the charge of incident particle, while E is energy of the incident particle. The measure of discriminating the particles by the energy deposited in the three subdetectors had been described by Liu (2014).

As shown in Fig. 27, the SRD apparatus is composed of three parts, which are the sensor, the cables and the processing electronic. Energy deposited by space radiation in the sensor will be converted to electronic signals and amplified, and then the signals are transferred to the processing electronic through the cables, where they are converted into digital signals and transferred to the payload electric control box.

The sensor is designed as a classical charge-particle telescope with three solid state detectors. The first layer (SD1) is a silicon diode with thickness of 80 μm, followed by the other two layers (SD2 and Sd3) which are cadmium Zinc Telluride (CZT) detectors of 2-mm thickness. The sensitive areas of all the three detectors are 1 cm^2. An aluminum foil of 100 μm is placed in front of the first layer as entrance window, which keeps the sensor from interference of visible light and isolate the sensor from the moisture environment inside the RGB. The lower threshold of the incident particle is determined by the material and thickness of window. The distance

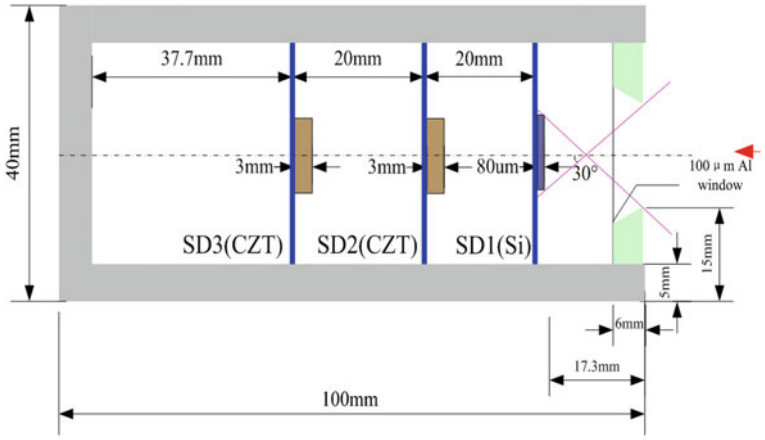

Fig. 28 The telescope architecture of the SRD sensor

between the window and the first layer is 11.3 mm. Both the distance between SD1 and SD2 and that between SD2 and SD3 are 20 mm. As shown in Fig. 28.

The solid angels of three sub-detectors are derived by considering both the geometrical factors of the sub-detectors and the energies of charge particles, which are 0.81 cm^2 Sr, 0.33 cm^2 Sr and 0.33 cm^2 Sr, respectively.

The cables are designed to supply the biases for the three detector of the sensor and to transfer the analog amplified signals of the three detector to the processing electronic. The cables are twisted in pairs to reduce interference effectively.

The electronic processing consists of shaping amplifier, ADC, power supply module and FPGA. The amplified signals from the sensors are transformed to Gaussian pulse signals by the shaping amplifier, and then the pulse is converted to digital signal by the Analog to Digital Converter (ADC) The digital signals are integrated to a spectrum and stored in the data storage area in FPGA every 10 s. The data uploading and telemetering are also accomplished by the FPGA. The appearance of the three parts described above is shown in Fig. 29.

Experimental Flow Control

- Cell on-orbit experimental contents:

(1) Cell culture: Provide 37 °C temperature control for four cell culture units, and culture for 1 day and 5 days in orbit respectively;
(2) Cell fixation: After the cells are cultured on orbit for a specified number of days, the waste liquid is discharged, and the fixative solution is injected;
(3) The fixed cells are stored at a low temperature, and the cells after the fixative solution is added are subjected to low temperature control to keep the storage temperature at $8 \pm 2°$ C.

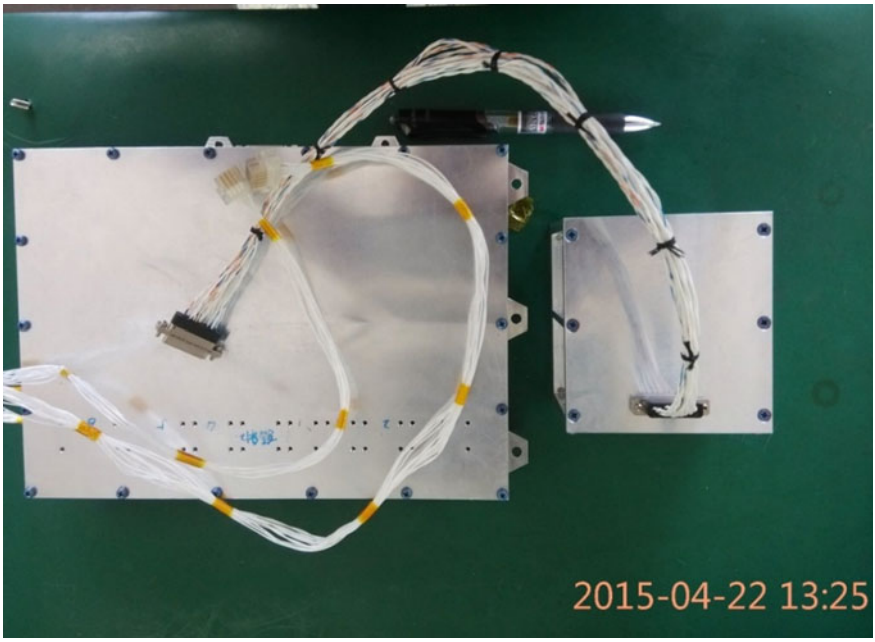

Fig. 29 The appearance of SRD instrument. The sensor is in the right side, and the electronic processing is in the left side. The two ends of the cables are jointed to the sensor and electronic processing respectively with screws

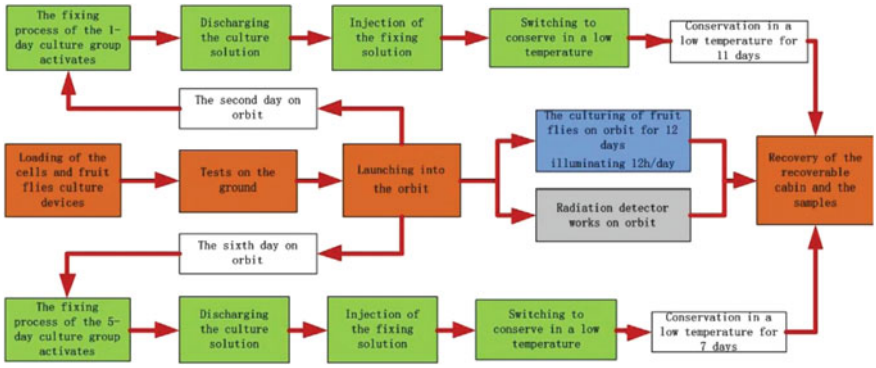

Fig. 30 The diagram of experimental flow

- Drosophila in-orbit experimental contents:

To study whether the early chrysalises of both wild-type and mutant Drosophila can survive and normally feather in a space environment. The diagram of Experimental flow described above is shown in Fig. 30.

1.2.4 Operation on Orbit

The temperature control of radiation gene box is shown in Table 2.

The radiation gene box has a total of 17 experimental procedures in the orbit. Among them, 14 experimental procedures are cell culture experiments that require temperature control and liquid exchange, and 4 experimental procedures (LED on, LED off, fan on, fan off) are drosophila experiments. During the on-orbit flight phase, the experiment is performed one by one according to the on-orbit flight timing, and the operation is normal. Complete cell culture fluid replacement, on-orbit sample processing (fixation) and waste liquid recovery, cell culture unit 1, 2 and drosophila and liquid storage tank temperature control meet the requirements of scientific experiments (see Fig. 31). On-orbit: stage motors, syringe pumps, fluid distributors, fans, LEDs, and heating membrane modules work properly.

After the radiation detector was launched, the detector was powered on and worked at all the flight time.

The three subdetectors are calibrated using ^{241}Am+^{238}Pu radioactive source before launching to determine the up and low thresholds of them. The calibration results are listed in Table 3.

As it can be seen from the tables, the low energy electron is the most intensity charge particle inside the RGB, however the Helium ion with energy above 60 MeV make more contribution to total dose (Table 4).

Based on the discussion above, we can draw a conclusion that the gamma ray flux is higher than any other particle flux inside the RGB and the electron is the most intense charge particle, while the Helium ion is the most harmful radiation to the cells inside the RGB. The dose rate inside the Radiation Gene Box is much higher than the

Table 2 Temperature control data of in-orbit operation of bone marrow box

On-orbit time (day)	CCC 1 temp (°C)	CCC2 temp (°C)	Drosophila temp (°C)	LST (°C)	Remarks
1th	37.75	37.7	21.25	24.0625	OK
2th	37.7	37.75	22	24.0625	OK
3th	7.3125	37.5625	22.625	24	OK
4th	7.375	37.5	21.25	24.0625	OK
5th	7.4375	37.5625	22.375	24.0625	OK
6th	7.375	37.5625	21.625	24.0625	OK
7th	7.375	7.875	21.25	21.375	OK
8th	7.375	7.875	21.25	21.5	OK
9th	7.4375	7.875	22.375	21.5	OK
10th	7.4375	7.9375	22.125	21.4375	OK
11th	7.3125	7.8125	21.25	20.4375	OK
12th	7.25	7.6875	20.4375	20.5	OK
14th	7.1875	7.6	18.375	18.5625	OK

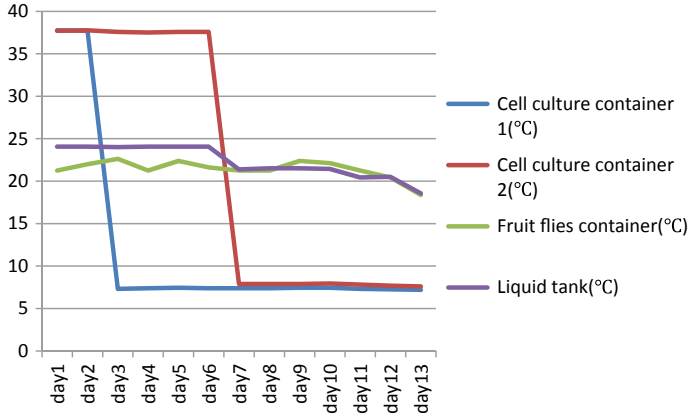

Fig. 31 On-orbit temperature control curve

Table 3 The calibration results of the three subdetectors

Subdetector	Channel for 5.4 MeV α particle	Voltage for 5.4 MeV α particle (V)	Noise channel	Up threshold[a] (MeV)	Low threshold[b] (keV)
SD1 (Si)	680	4.9	26	8.14	250
SD2 (CZT)	45	0.43	1	125	120
SD3 (CZT)	58	0.55	1	95	93

[a]Corresponding to 10 V voltage which is the maximum output voltage of multi-channel analyzer
[b]Corresponding to pedestal of the energy spectrum

ground, but the integral dose of 12 days inside the RGB is about 2.14 mSv. It seems unlikely to have obvious biological effects on the tissues of mice and drosophila (Cui et al. 2018).

1.2.5 Sample Installation and Recycle

The process of inoculating the cell sample, placing the culture vessel, injecting the culture solution, fixing the container, connecting the fluid line, exhausting and balancing the atmosphere, and packing the drosophila are completed by the scientific team. The sealing and testing are completed by the technical team and supervised and coordinated. The overall unit is tested and proved to be qualified for acceptance by satellite systems. The sample and reservoir installation results are shown in Fig. 32. The fluid pipeline installation results are shown in Fig. 33. The recovered cell samples are shown in Fig. 34. The drosophila recovery is shown in Figs. 34 and 35. Among them, the cell samples are well preserved and can be used for subsequent research and analysis. Drosophila samples are all feathered but failed to survive.

Table 4 The dose of all the particle bins (Cui et al. 2018)

Particle bin	Total counts[a]	Conversion coefficient[b] (pSv cm^2)	Dose (pSv)
E1 (0.5–1 MeV)	3140909^{+1596}_{-4}	1.80	$5.63\text{E}+6^{+2874}_{-7.2}$
E2 (1–2 MeV)	33649^{+17}_{-4}	4.96	$1.67\text{E}+5^{+85}_{-20}$
E3 (2–10 MeV)	99461^{+51}_{-2193}	25.5	$2.54\text{E}+6^{+1293}_{-5.59E+4}$
P1 (5–7 MeV)	48186^{+1161}_{-37}	20.5	$9.88\text{E}+5^{+2.38E+4}_{-751}$
P2 (7–10 MeV)	16731^{+403}_{-41}	30.67	$5.14\text{E}+5^{+1.24E+4}_{-1246}$
P3 (10–15 MeV)	12788^{+308}_{-33}	63.97	$8.18\text{E}+5^{+1.97E+4}_{-2088}$
P4 (15–35 MeV)	378774^{+9128}_{-33}	194.09	$7.35\text{E}+7^{+1.77E+6}_{-6335}$
P5 (35–50 MeV)	8970^{+216}_{-714}	382.54	$3.43\text{E}+6^{+8.27E+4}_{-2.73E+5}$
P6 (50–85 MeV)	15444^{+372}_{-1605}	649.02	$1.00\text{E}+7^{+2.42E+5}_{-1.04E+6}$
P7 (85–150 MeV)	32399^{+781}_{-6014}	1495	$4.52\text{E}+7^{+1.09E+6}_{+8.39E+6}$
P8 (150–200 MeV)	58657^{+1414}_{-967}	1882	$1.10\text{E}+8^{2.66E+6}_{1.82E+6}$
G (0.5–2 MeV)	5951998_{-1853}	2.46	$1.46\text{E}+7^{0}_{-4556}$
A1 (30–60 MeV)	1482^{+738}_{-49}	15779	$2.34\text{E}+7^{+1.17E+7}_{-7.67E+5}$
A2 (60–140 MeV)	29942^{+14920}	42337	$1.27\text{E}+09^{+6.31E+8}_{0}$
A3 (140–300 MeV)	8578^{+4274}	67067	$5.75\text{E}+08^{+2.87E+8}_{0}$
Total dose (mSv)	$2.14^{-0.94}_{+1.30E-4}$		

[a]The systematic uncertainties were calculated from the misjudging rate derived from Geant4 simulation by Liu (2014)

[b]The conversion coefficients are taken as interpolations of mean values of the lower limits and upper limits of the energy ranges

1.3 Summary

The satellite ambient temperature is consistent with expectations and match the experimental simulation temperature. The energy support and microgravity levels are consistent with expectations. The command upload and telemetry information downlink are consistent with expectations, and there is no difference between satellite parameter requirements and expectations.

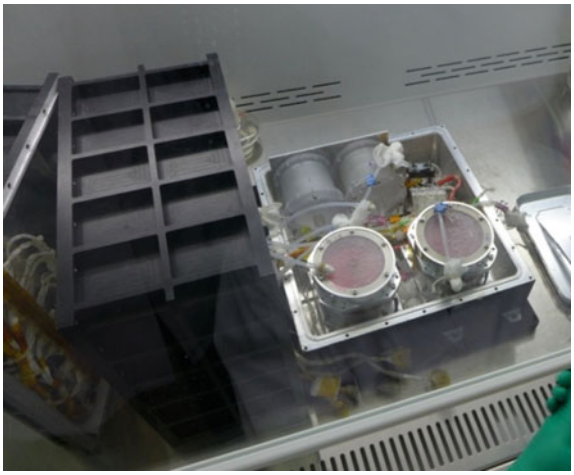

Fig. 32 Assembly before launching

Fig. 33 State of fixed cell after returning

The on-orbit experiment of the bone marrow box is successfully carried out according to the experimental procedure. The temperature control of different time periods meets the experimental requirements, and the recovered cell samples are well preserved and can be subsequently tested and analyzed.

The radiation gene box is performed on the orbit in accordance with the on-orbit flight time sequence, and all experimental procedures are performed normally. The two scientific experiments of cell and drosophila culture are conducted successfully. After recovery, the mouse cell in the four culture units are in good condition and

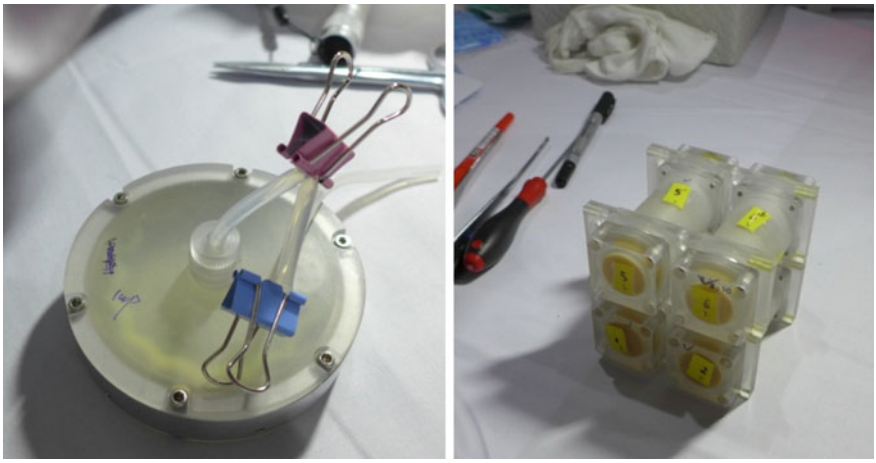

Fig. 34 Unit of cell cultivation after returning

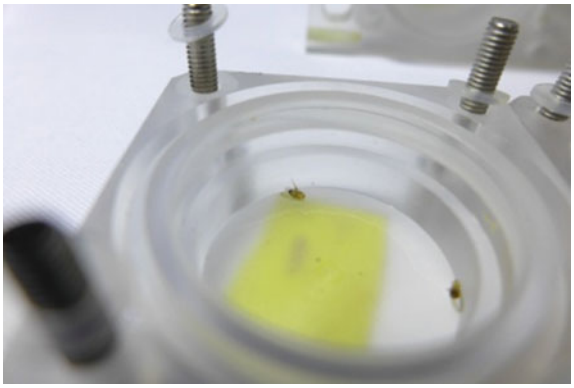

Fig. 35 Drosophila after returning

can be used for subsequent detection and analysis. The obtained orbital irradiation data meets the needs of scientific application analysis. The on-orbit experiment is successfully completed.

After the bone marrow box and the radiation gene box are recycled, the equipment is airtight, the pressure value and humidity value are within the normal range. The data collection and transmission are consistent with expectations, the operation is still normal, and the 1:1 space and ground comparison experiment is completed.

2 Research on Integrated Electrical Control Box

2.1 Design of IECB for Recovery Cabin

Due to the limited resources available by satellites, the distributed control method is adopted, that is, multiple experimental devices for power supply, image processing, data communicating, data processing, and experimental procedures (programmed instruction sets) are collectively provided with one electronic control box. A unified design of the drive control circuit is arranged in the experimental device. The image acquisition, temperature control, fluid transfer, station switching, engineering and scientific parameters are transmitted and stored in the big memory device under the command of the program control.

According to the structural characteristics of the SJ-10 return satellite, two IECB are developed. These two electrical boxes are RC-IECB (Return cabin integrated electric control box) and SC-IECB (Sealed cabin integrated electric control box). RC-IECB controls the multi-function furnace, radiation gene box and bone marrow incubator, and a universal drive circuit is designed for the three experimental devices; SC-IECB has 4 experimental devices under its jurisdiction, that is, a coal combustion box, a wire characteristic box and an evaporation convection box, and a unified designed drive control circuit is arranged for the four experimental device. Two integrated electric control boxes support the detection, control and management of the on-orbit scientific experiments of seven effective experimental devices. This solution reduces volumetric weight, power consumption, and improves reliability.

2.2 System Composition Principle

The IECB is a comprehensive measurement and control management equipment, which should have higher reliability requirements than the single unit of the experimental device. Therefore, the design adopts the technical methods of single-unit cold standby, intelligent monitoring of key parameters, data verification and intelligent error correction. It ensures that the experimental process of each experimental device is working well.

2.2.1 The Principle of the SC-IECB of the Sealed Cabin

The SC-IECB is composed of a power distribution unit, a computer and interface unit, a colloid image processing unit, a coal combustion image processing unit, a wire burning image processing unit and an evaporative convection image processing unit. The structural and the physical diagrams are shown in Fig. 36 and Fig. 37, respectively.

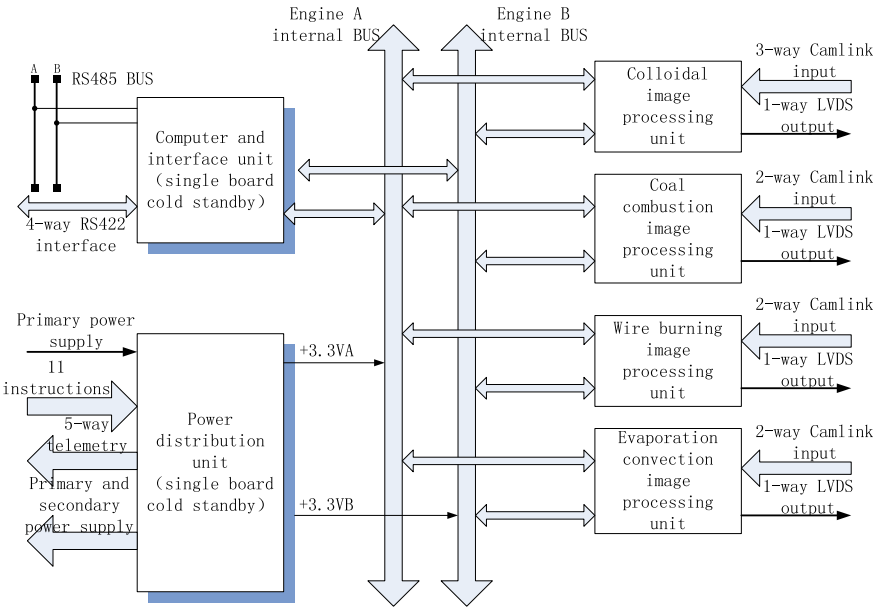

Fig. 36 SC-IECB block diagram

Fig. 37 SC-IECB appearance

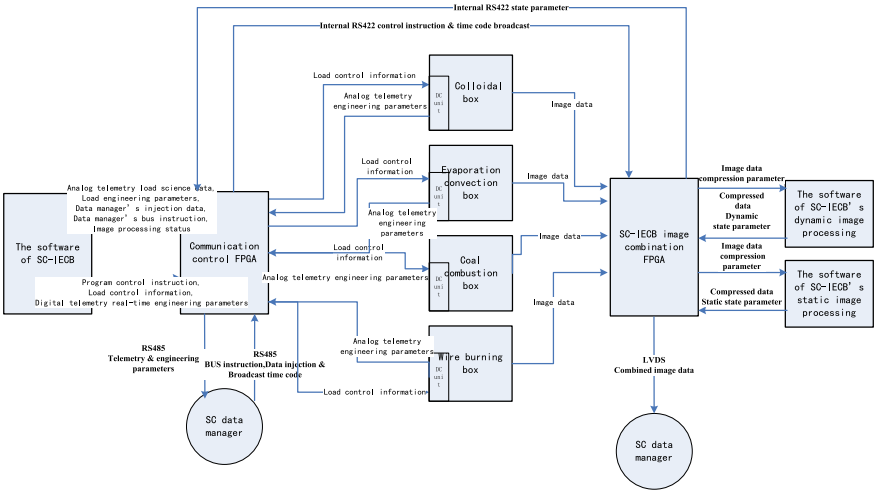

Fig. 38 SC-IECB system information flow diagram

Experimental device working mode setting and parameter setting:

The workflow table (Fig. 38; the structure of the flow table shown in Fig. 39) of each experimental device managed by SC-IECB is stored in the non-volatile memory MRAM. The memory stores three identical workflow tables for each experimental device. When the content in the MRAM is read, the three-to-two check is performed, and then the software program sends control information according to the experimental flow chart, and transmits it to the driving circuit of the experimental device via the RS422 interface, so that the experimental device performs the experimental operation. The integrated electric control box forwards a 120-byte engineering telemetry parameter data block to the experimental device support subsystem every 3 s to reflect the working status of each experimental device and itself. After receiving the remote control instruction forwarded by the experimental device support subsystem, the current working mode of the experimental device is set according to the content of the remote control instruction, and the experimental device experimental parameters are modified.

2.2.2 RC-IECB Composition Principle

The RC-IECB consists of two functional units: the power distribution unit and the computer and the interface unit. The block diagram is shown in Fig. 40. The structural and the physical diagrams are shown in Fig. 41. The system information flow chart is shown in Fig. 42.

The experimental device operating mode settings and parameter settings are as described in the previous section.

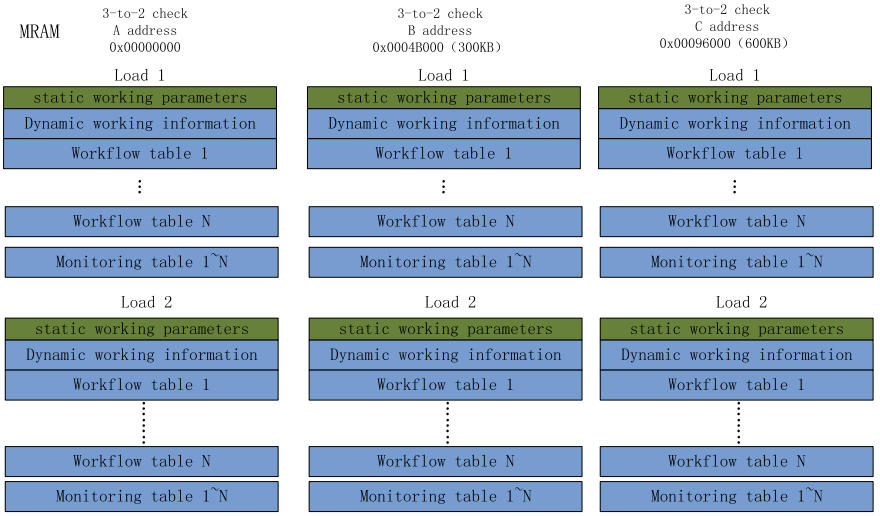

Fig. 39 Experimental device experimental flow chart structure

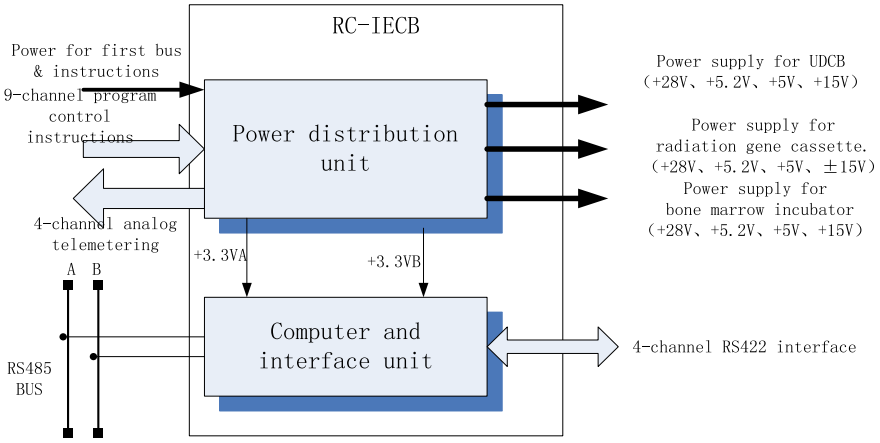

Fig. 40 RC-IECB block diagram

2.3 System Functions

2.3.1 Main Functions of the IECB

(1) Experimental device power distribution function:

- Receiving a primary power supply from the experimental device support subsystem to realize power supply to seven experimental device devices, including primary and secondary power supply;

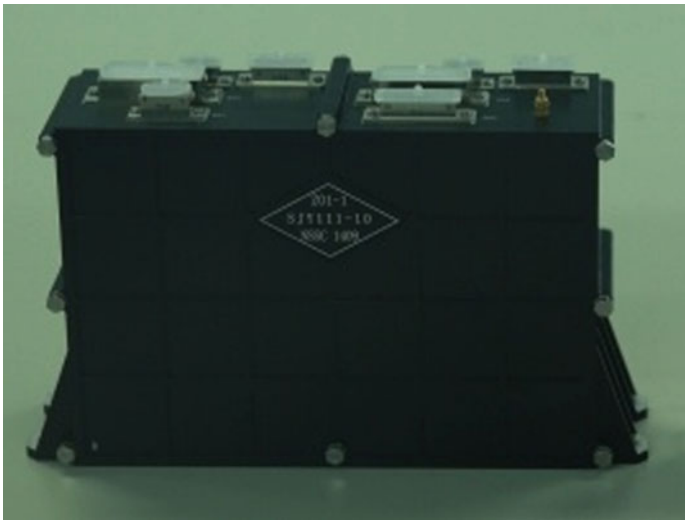

Fig. 41 RC-IECB assembly composition structure and physical appearance

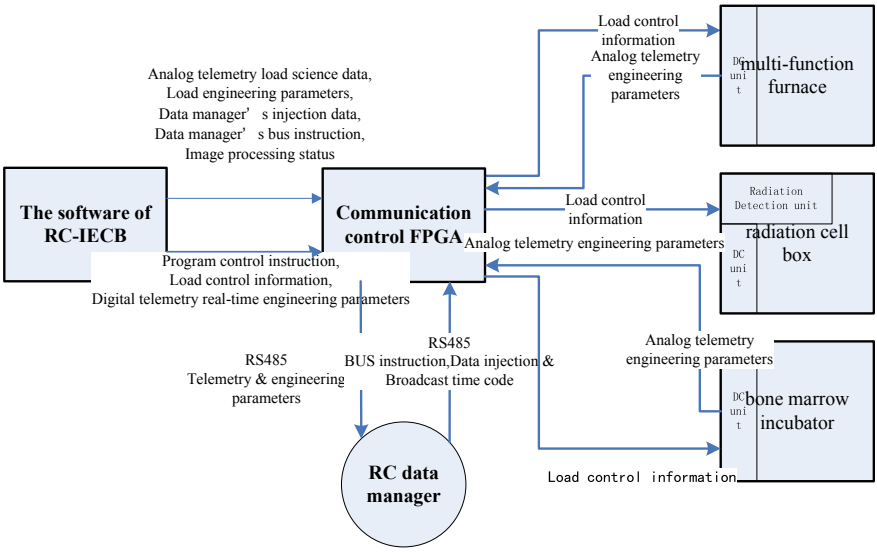

Fig. 42 RC-IECB information flow diagram

- The power distribution function of the experimental device is implemented according to the program control command of the experimental device support subsystem.

(2) Scientific data collection and organization functions:

- The sealed cabin integrated electrical control box receives the image or video data of the experimental device through the Camera Link interface, which is compressed and combined to form a CCSDS (Consultative Committee for Space Data Systems) source packet format according to the respective application process identifiers, and sent to the sealed cabin experimental device manager through the LVDS (Low-Voltage Differential Signaling) interface;
- Recycling cabin integrated electrical control box. The scientific data of the experimental device received through the RS422 interface is organized into CCSDS source packet format according to the respective application process identifiers and sent to the recovery cabin experimental device manager through the RS485 bus.

(3) Engineering parameter collection and organization function:
The working state parameters of the experimental device are obtained through the RS422 interface, and organized into an engineering parameter telemetry source package.

(4) Bus communication function:

- Communicating with the experimental device manager through the RS485 bus, send the engineering parameters and scientific data of the experimental device, and receive the time code and data injection of the experimental device manager.

(5) Experimental device operation management and control functions:

- Data injection analysis and execution function: receiving data injection instructions of the experimental device through the RS485 bus and parsing, and executing data injection instructions of the relevant experimental device;
- Completing the operation management and control of the corresponding experimental device according to the preset program, the ground vertical remote injection and the operating state of the experimental device;
- Effective experimental device health management: monitoring telemetry parameters, scientific data and other operational status, online monitoring according to pre-set conditions when the effective experimental device is abnormal, and to achieve effective experimental device fault isolation, recovery and system reconstruction.

2.3.2 Main Functions of the IECB Application Software

(1) RS485 bus communication management: receiving and parsing the bus command and data injection sent by the digital tube, transmitting the telemetry data and engineering parameters of the integrated electric control box and each experimental device, performing bus maintenance and broadcasting time;
(2) Effective experimental device operation management: controlling the operation of the experimental device according to the preset program, the operating state of the experimental device, and the ground data injection forwarded by the satellite number tube, and forwarding the experimental device data injection control command;
(3) Collecting the analog quantity and engineering parameters and scientific data of the experimental device;
(4) Collecting the comprehensive electronic control box telemetry and engineering parameters, and organizing into the integrated electrical control box telemetry and engineering parameter data package together with the telemetry and engineering parameters of the experimental device;
(5) Comprehensive electrical control box health management and operation and maintenance.

2.3.3 The Main Functions of the SC-IECB Image Processing Software

(1) Image compression processing: compressing the received colloidal material box, coal combustion box, wire characteristic box and evaporation convection box image data according to data injection or experimental device management requirements;
(2) The processed image is sent to the image combining FPGA through the internal bus, waiting for the combined transmission;
(3) Receiving a compression command or a compression parameter;
(4) Collecting and feedback the compressed state;
(5) Health management and operation and maintenance.

2.3.4 The Main Functions of the Image-Integrated FPGA of the SC-IECB

(1) The internal bus communication function of the sealed compartment, that is, the data exchange with the integrated electrical control box application software through the internal bus;
(2) Image compression bypass function, which can directly output single or multiple image data through CPU control. The default state is image compression enable;
(3) After the integrated electronic control box application software completes the setting, the data packing function of multiple input code streams can be realized;
(4) Output function of combined image data.

Table 5 Main technical indicators of the RC-IECB

No	Indicator item	Design requirement	Actual value
1	Weight (kg)	3.25 ± 0.065	3.272
2	Body size (mm)	$242 \pm 1 \times 78 \pm 1 \times 168 \pm 1$	242.18 ×78.22 × 168.05
3	Primary power supply	28^{+4}_{-3} V	32.04–25.02 V
4	Experimental device (28 V)	(V)28^{+4}_{-3} V	27.911 V
5	Experimental device (15 V)	(V)+15 ± 1%	15.004 V
6	Experimental device(−15 V)	(V)−15 ± 1%	−15.001 V
7	Experimental device (5 V)	(V)+5 ± 1%	5.0012 V
8	Experimental device (5.25 V)	(V)5.25 ± 1%	5.2528 V
9	Surge	<7.2 A/5 ms	2.84 A/5 ms (A), 2.88 A/5 ms (B)
10	Number of asynchronous RS422 serial communication interfaces	4	1 marrow culture incubator, 2 radiation cell boxes, multi-function furnace 1
11	RS422 Bus speed	115,200 ±3% bps	116,279 bps
12	RS485 Bus speed	115,200 ±3% bps	116,279 bps

2.3.5 The Main Technical Indicators of the IEBC

See Tables 5 and 6.

2.3.6 Working Mode

RC-IECB and SC-IECB have two identical modes of operation: standby mode and experimental mode.

(1) Standby mode

The main task of IECB in standby mode, the bus communication task, receives bus data from the load manager: including bus commands, data injection, and others. Organization and transmission tasks of engineering telemetry parameters. Clock management tasks and system maintenance tasks.

(2) Experimental mode

The IECB enters the experimental mode after receiving a data injection or bus command. The experimental procedure of each experimental device is performed in

Table 6 Main technical indicators of the SC-IECB

No	Indicator item	Design requirement	Actual value
1	Weight (kg)	5.9 ± 0.15 kg	5.992 kg
2	Body size (mm)	$242 \pm 1 \times 166 \pm 1 \times 168 \pm 1$	242.18 ×165.49 × 168.14
3	Primary power supply	28^{+4}_{-3} V	32.04–25.02 V
4	Experimental device (28 V)	28^{+4}_{-3} V	27.852 V
5	Experimental device (15 V)	14.85–15.15 V	14.981 V
6	Experimental device (−15 V)	−15.15 to −14.85 V	−14.982 V
7	Experimental device (5 V)	4.95–5.05 V	4.9866 V
8	Experimental device (12 V)	12.474–12.726 V	12.535 V
9	RS422 Bus speed	115,200 ±3% bps	115,279 bps
10	RS485 Bus speed	115,200 ±3% bps	115,279 bps
11	LVDS Bus	Clock 20 MHz, IDS Table requirement	OK
12	Image data interface	Sealed cabin integrated electric control box image input interface	Camera link image input interface 9 channels, parallel code rate does not exceed 40 Msps, meets the requirements
13		Colloid observation image input interface	Colloid observation image input 3 way, the frame rate is 5 fps, 1 fps and 1 f/30 min, image pixels are 1620 × 1236 × 8 bit, 659 × 494 × 8 bit, 659 × 494 × 24 bit, LVDS output clock rate ≤20 MHz, fulfill requirements
14		Coal combustion image input interface	Coal combustion image input 2 way, the frame rate is 75 fps and 50 fps, image pixels are 640 × 480 × 24 bit and 320 × 256 × 8 bit, LVDS output clock rate ≤20 MHz, fulfill requirements

(continued)

Table 6 (continued)

No	Indicator item	Design requirement	Actual value
15		Wire characteristic image input interface	Wire characteristic image input 2 way, the frame rate is 1 fps/25 fps and 1 fps/25 fps, image pixels are 1024 × 776 × 8 bit, LVDS output clock rate ≤20 MHz, fulfill requirements
16		Evaporation convection image input interface	Evaporation convection image input 2 way, the frame rate 1 fps/25 fps and 1 fps/25 fps, image pixels are 1024 × 776 × 8 bit, LVDS output clock ≤20 MHz, fulfill requirements

sequence according to the settings of the experimental flow chart. Each experimental device in the recovery compartment can perform experimental work simultaneously; each experimental device in the sealed compartment performs experimental work in a time sharing manner.

In the experimental mode, the IECB is mainly used to control the experimental device for scientific experiments, including:

- Controlling the motor, wire, cooling film, heating film, solenoid valve, needle valve, fan, LED lamp, temperature sensor, pressure sensor, humidity sensor, camera, and others according to the experimental procedure, and receiving the scientific data from the transmission of the experimental device data and engineering status parameters;
- Monitoring the state of the experimental device and performing corresponding fault handling when the experimental device is abnormal;
- Bus communication tasks: receiving bus data such as bus instructions and data injection, organization and transmission of engineering telemetry parameters, clock management, and system maintenance.

2.3.7 IECB in Rail Power Supply and Distribution Operation

The orbital operation data shows that the IECB power supply is normal, the engineering telemetry acquisition function is normal, and the operational data of the orbital experimental equipment is obtained. It can be seen that the assignment of the program control instructions of the experimental device and that the working mode setting and the operating parameter setting are correct.

2.4 Universal Drive Control Box (UDCB)

IECB uses a distributed control method for experimental devices. The relevant experimental device is equipped with a drive control box and corresponding FPGA software. The drive control circuit (UDCB) and its FPGA software use a universal maximum envelope design and are connected to the IECB via the RS422 interface. The IECB uniformly configures and stores the workflow tables required for the relevant experimental equipment, and implements related experimental operations through the FPGA software embedded in the UDCB. UDCB is divided into two categories, namely the physical experiment class UDCB and the life experiment class UDCB. Physical UDCB is used in multi-function furnaces, wire boxes, evaporative convection boxes, colloidal material boxes, and coal combustion chambers. The life-based UDCB serves the bone marrow incubator and the radiation gene cassette.

2.4.1 Physical UDCB Design, Working Principle and Function

The physical drive control circuit is mainly divided into two parts: the FPGA board and the drive board. The FPGA board collects and processes the secondary power signal and communicates with the IECB. The FPGA board sends a signal according to the workflow meter, and the UDCB performs power amplification to operate the electronic components in the experimental device to perform related experimental work. UDCB has 8 main functional units: power supply unit, FPGA control unit, communication unit, digital acquisition unit, analog acquisition unit, motor drive unit, switch quantity control unit, and heating unit. When applied, it can be assembled as needed. The block diagram of UDCB working principle is shown in Fig. 43.

The main functions of the physical class UDCB are:

(1) Communicating with IECB, uploading engineering parameters and scientific data, receiving and executing from IECB instructions;
(2) Analogue acquisition and processing of heat flow, thermocouple, Hall signal, pressure, humidity, atmosphere, and telemetry voltage;
(3) Digital signal acquisition and processing such as DS18B20, encoder, limit switch and photoelectric switch;
(4) Switching control of CCD, LED, piezoelectric ceramics, fan, solenoid valve, needle valve and laser;
(5) Motor drive control;
(6) Heating control of furnace wire, heating film, heating sheet and wire.

2.4.2 Life-Based UDCB Design, Working Principle and Function

The bio-UDCB serves the bone marrow culture box and the radiation gene cassette in the recovery compartment. Integrates all the functions of the above two experimental

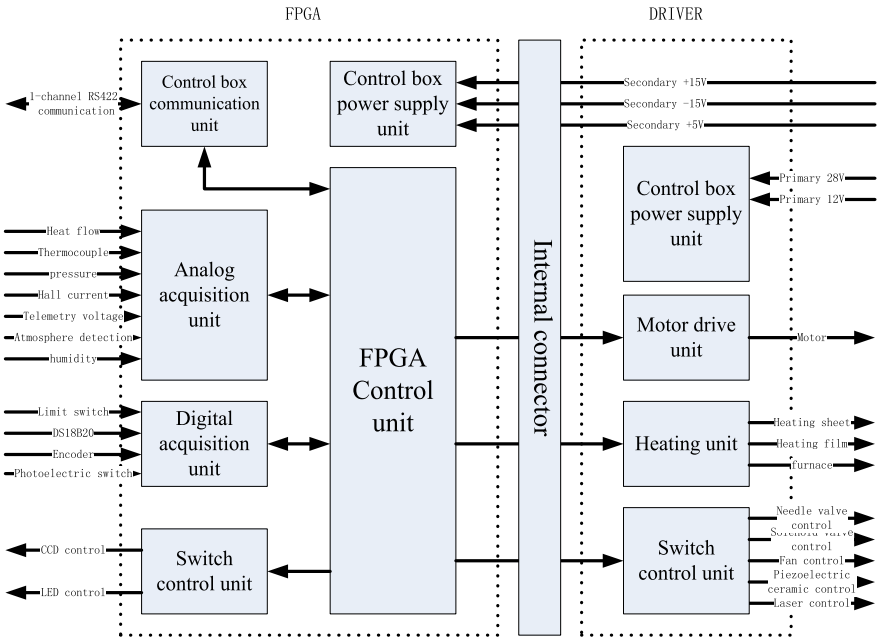

Fig. 43 Schematic diagram of the physical class UDCB

devices, and customizes the assembly according to the requirements of each experimental device. There are five main functional units: temperature control drive unit, liquid transport unit, biological characteristic parameter analog quantity acquisition unit, FPGA circuit unit, and temperature detection unit. The working principle block diagram is shown in Fig. 12. The main drive circuits are shown in Figs. 11, 12, and 14.

The main functions of Bio-UDCB are:

(1) Communicating with IECB, uploading engineering parameters and scientific data, and receiving IECB instructions to issue an execution signal;
(2) Analog and digital acquisition processing: voltage telemetry signal acquisition and processing, digital temperature sensor (DS18B20), magnetic encoder and limit switch and other digital signal acquisition and processing;
(3) Switching quantity control such as solenoid valve;
(4) Motor drive control;
(5) Heater heating and cooling control.

3 Conclusion

In summary, the bone marrow box and radiation gene box designed by the National Space Science Center (NSSC) of the Chinese Academy of Sciences function

well in SJ-10 satellite mission. After the satellite recovery module returns to the ground, the recovered biological samples are well preserved and can be used for subsequent analysis. The experimental device still works normally after recycling. The RC-IECB, SC-IECB and UDCB designed by NSSC are in normal working condition, supporting the on-orbit operation of seven experimental devices related to space life and microgravity physics on satellite.

Acknowledgements The bone marrow box, the radiation gene box, and the integrated comprehensive electric control box are successfully completed. The SJ-10 satellite on-orbit scientific experiments are inseparable from the hard work and effort of the development team. First of all, we would like to thank Prof. Wenrui Hu, the chief scientist of the SJ-10 Science Experiment Satellite, for his correct guidance. Secondly, we would like to thank the China Academy of Space Technology for providing a platform that is the basis for our payloads to achieve their functions. Once again, thanks to the supervision and support of the NSSC. Thanks to the general manager of the payload, Changbin Xue, Liangqing Lv, and Hao Geng for their help with the three payloads. The success of the payload development is inseparable from the NSSC's researchers. Thanks to the developers of the integrated electric control box: electronic research department: Changbin Xue, Lin Guo, Linlin Wang, Feng Man, Wentao Dong, Yuyin Tan, Li Zhou's hard work. Thanks to the designers of the radiation gene box and the bone marrow box, for their persistence and dedication, and the hard work of Zhiyuan Zhang, Xiaoqing Wang, Baoming Geng, Zhibin Sun, Handong Yang and Weining Li. Thanks to the designers of radiation detector Yaqing Liu, Yunlong Zhang. Thanks again to all the contributions of those involved in the three payloads' development missions.

References

Cui X, Liu Y, Peng W et al (2018) Radiation detection technology and methods. 2:43. https://doi.org/10.1007/s41605-018-0071-1

Liu Y (2014) Design of space particle detector system onboard SJ-10. PhD thesis, University of Chinese Academy of Sciences

National Space Science Center of the Chinese Academy of Sciences (2016) The summary of SJ-10 satellite payload radiation gene box task. SJY109-10-SB-18

National Space Science Center of the Chinese Academy of Sciences (2016) The summary of SJ-10 satellite payload bone marrow incubator task. SJY108-10-SB-18